# MINERALIZED TISSUES AND THE OROFACIAL REGION: MORPHOLOGY, COMPOSITION AND DISEASE

**ERICH J. RAUBENHEIMER MChD**
**FC Path(SA) Oral Pathology PhD**

**PUBLISHED WORK SUBMITTED TO THE UNIVERSITY OF PRETORIA FOR THE DEGREE OF DOCTOR OF SCIENCE IN ODONTOLOGY (ORAL AND MAXILLOFACIAL PATHOLOGY)**

**PROMOTER:** **PROFESSOR A. J. LIGTHELM**
**DEAN**
**SCHOOL OF DENTISTRY**
**FACULTY OF HEALTH SCIENCES**
**UNIVERSITY OF PRETORIA**

**July 2003**

**EXAMINERS:** **PROFESSOR DR W. H. BINNIE**
**Dallas, Texas, USA**
**PROFESSOR DR T. SOLHEIM**
**Oslo, Norway**

**DECLARATION**

I, the undersigned, declare that the work contained in this presentation of publications is my own original work, as set forth in the statements which precede the published articles, and has not previously in its entirety or in part been submitted to any University for a degree.

.....

E J RAUBENHEIMER

I certify that on the 7th day of Nov 2003 Erich Johann Raubenheimer signed this declaration in my presence.

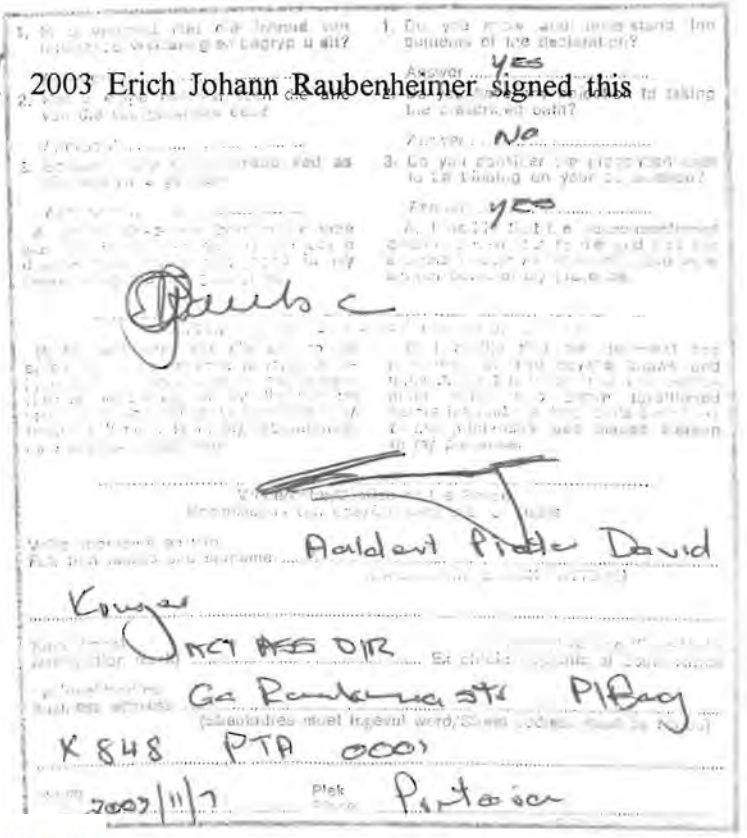


.....

COMMISIONER OF OATH

# DEDICATION

To my wife Claudia and our children for sustained encouragement, love and support

## INTRODUCTION

My interest in research was initially stimulated by Prof J C G Slabbert, the then Head of Prosthodontics at the University of Pretoria, who supervised a study for which a fellow undergraduate student and myself won the Middleton Shaw award for undergraduate research at the annual meeting of the South African Division of the International Association for Dental Research. Upon completion of my undergraduate studies, Prof L M Jonck offered me a research position in the Department of Oral Pathology at the University of Pretoria, in anticipation of my then fiancée, and later wife, Claudia Noffke, to complete her studies in Dentistry. During that year I was exposed to both the practice of Dentistry on a part time basis and academic Dentistry, and I had no difficulty in deciding that my future would be in the latter. My decision to specialize in Oral Pathology was based on an observation that no other discipline in Dentistry serves as a more appropriate basis for research, a step that I have never regretted. Profs I W Simson and L Dreyer of the Department of Anatomical Pathology provided me with an exceptional training program in Histopathology, an aspect that I appreciate daily in my research and service-rendering program. Although specialization in Oral Pathology is academically more demanding than any other post graduate program in Dentistry, the first two Oral Pathologists to qualify from the University of Pretoria, Dr J Prinsloo and Dr A J Ligthelm (now Professor and Dean of the School of Dentistry at the same University) served as role models and proof that it was indeed possible to master the course.

Over the past 20 years in a diagnostic histopathologic service rendering capacity at a tertiary health center I have found myself at the rock face of a rapidly changing

discipline. Developments that revolutionized diagnostic histopathology, which was in the earlier years based on morphology, histochemistry and ultra structure only, have, although advancing accuracy, compounded the practice of the specialty. These developments include amongst others immunohistochemistry, histomorphometry and molecular pathology. Fruitful research cooperation with a more recently qualified colleague, Prof WFP Van Heerden, made my transition to molecular techniques easier. A fair representation of these techniques as well as many papers co-authored by Prof van Heerden are included in the list of publications submitted.

The morphology of normal tissues in and around the oral cavity is influenced by a multitude of local and systemic disease states. Through my diagnostic histopathologic service-rendering program that is focused on the orofacial region, a thorough understanding of the morphology of normal tissue types as well as localized- and systemic diseases afflicting this complex anatomical region has developed. The hardest tissue type and most difficult to prepare from an analytical point of view, namely teeth, are found in this region. Unlike most other laboratories dealing with microscopic techniques, those serving Oral Pathology departments are generally well acquainted with the preparation of mineralized tissue samples for analytical purposes. I am furthermore fortunate (from a researchers point of view) to be involved in the diagnosis of advanced pathology that is the result of patient ignorance and neglect, rendering our material the envy of many Oral Pathologists internationally. My wife, who qualified as a Dentomaxillofacial Radiologist joined our institution, and her enthusiasm for her subject resulted in several collaborative studies encompassing histopathology and radiology.

Many of the studies on large mammals were facilitated by South Africa's wealth in animals as well as the positive predisposition of the managers of our national parks towards research. The support services provided by the small staff component of the Department as well as the level of equipment in our laboratory are noteworthy. These positive factors in my working environment provided an opportunity to focus research programs on studies of normal and diseased mineralized- and soft tissues in man and animal.

The papers are grouped into four sections. Section 1 deals with multiple myeloma, its characteristic oral manifestations and complications. Section 2 encompasses several studies on mineralized tissues, teeth and bone. It includes histomorphometric studies on metabolic bone diseases as well as several projects that focus on human teeth and elephant ivory. Section 3 reflects studies on the normal structure- and neoplastic proliferations involving salivary glands. The role of the controversial myoepithelial cell in health and disease is highlighted and several diagnostic principles added to the study of salivary neoplasia. Section 4 is on diagnostic interpretation of jaw tumors and cysts. Contributions are made to the histopathologic and radiological interpretation of cysts and tumors of the jaws and in particular the late manifestations thereof.

# ACKNOWLEDGEMENTS

1. My parents for their love and support and investing their hard earned money in my education.
2. My wife, Claudia for the sacrifices she has made to her career in order to facilitate my academic progress.
3. My children, Simon, Johann, Annika and Daniel for providing me with a reason to give my best.
4. My Secretary, Mrs. C S Begemann for typing and editing every manuscript generated during my career.
5. The laboratory staff of the Department of Oral Pathology at Medunsa and in particular Mr. J Hangelbroek, Mrs. Vorster and Mrs. E Mathibe for providing me with technological support.
6. The research management at Medunsa for their role in facilitating the funding of most of my research projects.
7. Prof. Willie van Heerden, a colleague and friend with whom I have co-authored many scientific papers.
8. The late Prof. J Dauth for introducing me to the art of preparing a scientific manuscript.
9. Mr. M J Dreyer of the Department of Chemical Pathology at Medunsa for his unselfish contributions to the biochemical analyses presented in this document.

10. The management of the National Parks Board for allowing our research team to harvest tissue during the culling program in the Kruger Park.

# SUMMARY

This presentation consists of 50 selected publications that appeared in national and international peer reviewed journals over the past 19 years (1984 – 2003). The presentations are summarized under the following headings: Studies on multiple myeloma; Studies on mineralized tissues: Bone and teeth; Salivary glands: Normal structure and neoplastic proliferations and Diagnostic interpretation of jaw tumors and cysts.

**Studies on multiple myeloma**

In this section 7 publications are presented. The publications reported on the solitary tumorous orofacial presentation of multiple myeloma, ultrastructural appearance of neoplastic plasma cells as well as myeloma- associated amyloidogenesis with particular reference to deposits in the tongue. A theory on the cytogenesis of the distended endoplasmic reticulum in a case of non-secretory myeloma is presented. A unique study on salivary immunoglobulin concentrations in myeloma patients concludes this section.

**Studies on mineralized tissues: Bone and teeth**

Fourteen publications are presented in this section, four of which deal with static and dynamic histomorphometric studies on metabolic diseases of bone. The four publications include a review article on the histopathologic changes in metabolic bone disease states. In a series of cases of rickets a sub classification with therapeutic implications was proposed. Three publications reported on aspects of biochemical analyses of human

dentin. In the first study two new amino acids were discovered in dentin. The other two publications recorded the inorganic composition of opaque and translucent dentin and inorganic composition of tubular and inter tubular areas in dentin respectively. The last seven publications of this section deal with elephant ivory. Geographic variations in the composition ivory were established as well as a theory on the histogenesis of the unique chequered pattern thereof presented. Two manuscripts recorded the early development of the tush (or deciduous tusk) and tusk as well as tusklesness, and a theory on the latter phenomenon is presented. The morphology of the tush was established and one publication highlighted the importance of tusklessness as an indicator for the effect of ivory harvesting on the ivory bearing genome. The last publication demonstrated the value of trace elements in sourcing the origin of ivory.

**Salivary glands: Normal structure and neoplastic proliferations**

In this section, ten publications are presented. Embryology, functions and proliferative aspects of myoepithelial cells were analyzed in an invited review and aspects thereof emphasized in a manuscript which focused on salivary gland myoepithelium. A paper is presented on the structure of the salivary gland and composition of the saliva of the elephant. In a scanning electron microscopic study, aspects of the distribution of myoepithelium in the elephant salivary glands were reported. The remaining six publications deal with diagnostic aspects of series and case studies of salivary gland neoplasms in humans.

**Diagnostic interpretation of jaw tumors and cysts**

Nineteen publications are presented in this section. The uniqueness of most publications lies in the population sample studied. Most series on jaw tumors and cysts recorded internationally are on population samples in the northern hemisphere. Except for two publications that reported on jaw pathology recorded in Germany, all manuscripts in this section deal with pathology in a black South African population sample. Most studies analyzed histopathologic and radiological features of jaw tumors and emphasized the late manifestations thereof. A rare syndrome involving the development of enamel, absence of teeth and tumorous fibrous proliferations in the jaw was described and a molecular study identified a viral infection in an odontogenic tumor.

# OPSOMMING

Hierdie voorlegging bestaan uit 50 geselekteerde publikasies wat in nasionale en internasionale wetenskaplike joernale oor die afgelope 19 jaar (1984 – 2003) gepubliseer was. Die voorlegging word opgesom onder die volgende hoofde: Studies van veelvuldige mïelomatose; Studies van gemineraliseerde weefsels: Been en tande; Speekselkliere: Normale struktuur en neoplastiese proliferasies; Diagnostiese interpretasie van kakebeen tumore en siste.

**Studies van veelvuldige mïelomatose**

Sewe publikasies word in hierdie seksie aangebied. Hierdie publikasies beskryf die solitêre orofasiale kliniese presentasie van mïeloom, ultrastrukturele voorkoms van neoplastiese plasmaselle en mïeloom geassosieerde amiloidose met spesifieke verwysing na die tong. 'n Teorie oor die sitogenese van die uitgesette endoplasmiese retikulum in 'n geval van nie- sekreterende mïeloom word ingesluit. 'n Unieke studie wat handel oor die speeksel immunoglobulien inhoud van mïeloom pasiente sluit hierdie seksie af.

**Studies van gemineraliseerde weefsel: Been en tande**

Veertien publikasies word in hierdie seksie aangebied waarvan vier oor statiese en dinamiese histomorfometriese analieses van been handel. Hierdie vier publikasies sluit 'n oorsigsartikel oor die histologiese veranderinge van metaboliese been siektes in. In 'n reeks pasiente met ragitis word 'n histologiese subklassifikasie, wat terapeutiese waarde het, voorgestel. Drie publikasies handel oor aspekte van die biochemiese samestelling

van menslike dentien. In die eerste hiervan word twee nuwe aminosure vir die eerste keer in dentien aangetoon. Die ander twee publikasies handle oor analieses van die anorganiese samestelling van opaak en deursigtige dentien asook die verskille in die anorganiese samestelling van tubulêre en intertubulêre dentien. Die laaste sewe publikasies in die seksie het betrekking op olifant ivoor. Geografiese variasies in die samestelling van ivoor asook 'n teorie oor die histogenese van die unieke patroon in olifant ivoor word bespreek in twee voorleggings. 'n Verdere twee artikels handel oor die vroeë ontwikkeling van die primêre en permanente ivoortand asook tandloosheid en 'n teorie oor laasgenoemde verskynsel word aangebied. Die morfologie van die primêre ivoortand word vasgestel en in een publikasie word bespiegel oor die invloed van ivoor jag op die genoom van die Afrika olifant. Die laaste artikel in hierdie seksie toon die waarde van spoorelementele analieses in die bepaling van die oorsprong van ivoor van die Afrika olifant.

**Speekselkliere: Normale struktuur en neoplastiese proliferasies**

In hierdie seksie word tien publikasies aangebied. Die embriologie, funksies asook proliferatiewe aspekte van die mioepiteelsel word ondersoek in 'n genooide oorsigsartikel en verdere aspekte daarvan word beklemtoon in 'n artikel wat fokus op mioepiteelselle in speekselkliere. Die struktuur van die parotis speekselklier asook die samestelling van die speeksel van die olifant word aangebied. In 'n aftaselektronmikroskopiese studie word aspekte van die distribusie van mioepiteelselle in die speekselkliere van olifante bespreek. Die laaste ses publikasies in hierdie seksie handel oor diagnostiese aspekte van speekselklier tumore in mense.

**Diagnostiese interpretasie van kakebeen tumore en siste**

Negentien publikasies word aangebied in die seksie. Hierdie studies is uitsonderlik daarin dat almal, met die uitsondering van twee, gevorderde kaakpatologie in swart Suid Afrikaanse pasiente rapporteer. Die meeste publikasies analieseer die histopatologiese en radiologiese kenmerke van kaaktumore en presenter die laat manifestasies daarvan. 'n Raar sindroom, wat die ontwikkeling van emalje, afwesigheid van tande en tumureuse bindweefsel vergroeisels insluit word beskryf en 'n molekulere studie rapporteer 'n virus infeksie in 'n odontogene tumor.

## CONTENTS

## LIST OF PUBLISHED SUBMISSIONS

**SECTION 1: Studies on multiple myeloma**



**SECTION 2: Studies on mineralized tissues: bone and teeth**

**SECTION 3: Salivary glands: Normal structure and neoplastic proliferations**

**SECTION 4: Diagnostic interpretation of jaw tumors and cysts**

# 1. STUDIES ON MULTIPLE MYELOMA

## Declaration

Seven studies are submitted in this division, six of which (2 –7) were initiated by myself and one by the late Professor J Dauth (1). I was responsible as fifth author in the first study (1) for the microscopic analyses and relevant discussion only. In the second study (2), I collected the data and performed the evaluation of the light microscopic and ultrastructural features and prepared the manuscript, Dauth and de Coning did the biochemistry, Jordaan performed the biopsy and du Toit did the autopsy. I prepared the manuscript in study (3) and Lello and Fayman took the biopsies and assisted with the writing of the paragraph on the surgical management of the cases. Dauth, Dvornak and Senekal performed the biochemical analyses and provided inputs on the evaluation thereof. The ultrastructural interpretation in study (4) was done by myself, Dauth assisted with the biochemical interpretation and van Wilpe performed the electron microscopy. Study (5) was written edited by me, Dauth provided inputs on the biochemical- and Pretorius the clinical manifestations of the cases. I collected the data and prepared the manuscripts in studies (6) and (7). In both, Dauth contributed to the biochemical analyses of the cases whereas in study (7) van Heerden performed the statistical analysis and van der Walt performed the salivary immunodiffusion analytic technique.

**Abstract**

The orofacial manifestations of multiple myeloma in an African population sample had never been reported in the literature. Study (1) stimulated the authors interest in the unique and up to that stage unreported tumorous orofacial manifestation of multiple myeloma. Another two patients with the same orofacial features were subsequently recorded in study (3) and the principles in the management thereof established. The structural crystalline inclusions in the nuclei of the neoplastic plasma cells in study (2) formed the basis of an ultrastructural investigation of 10 cases of multiple myeloma presented in study (4). Ultrastructural diagnostic features, which characterize neoplastic plasma cells, were described including nuclear-cytoplasmic asynchrony and erythrophagocytosis. Distention of the rough endoplasmic reticulum with accumulation of colloid was shown in the plasma cells of a non-secretor myeloma in study (5) and a hypothesis on the pathogenesis thereof presented. Amyloidosis, a complication of multiple myeloma, was investigated with light- and electron microscopic techniques in tongue biopsies of 30 patients suffering multiple myeloma (6). The findings established the tongue as a common site for amyloidogenesis. It was not possible to show a positive correlation between the percentage of plasma cells in bone marrow aspirates or the presence of urinary light chains and amyloidogenesis in multiple myeloma. Study (6) did not support the reported higher amyloidogenic potential of lambda light chains. Study (7) compared immunoglobulin concentrations in mixed saliva and blood of 24 myeloma patients (the largest series on immunoglobulin related proteins in saliva of myeloma patients reported). The authors failed to confirm depressed salivary immunoglobulin concentrations despite circulatory humoral immunoparesis. This study added an

interesting parameter to the debate on multiple myeloma induced selective immunoparesis and partially explains the paucity of opportunistic oral infections in patients suffering this disease.

## 2. STUDIES ON MINERALIZED TISSUES: BONE AND TEETH

### Declaration

Fourteen publications are submitted in this section all of which were initiated and planned by myself. In study (8) Dauth and I wrote the manuscript, De Villiers prepared the graphics and Potgieter provided the clinical data and radiographs. Van Heerden and I prepared the manuscript of study (9) and Potgieter and Golele provided clinical information and radiographs. I analyzed the data and prepared the manuscripts in studies (10) and (11). In studies (12), (13) and (14) Nkhumeleni prepared the specimen for analyses and executed the literature reviews and Dauth, Van Heerden and myself analyzed the data and wrote the manuscripts. Smith performed and Pitout interpreted the amino acid analyses in study (12) and Turner and Dreyer performed the inorganic analyses in study (13) and Turner in study (14) respectively. I prepared the manuscript in study (15), Rama and Dreyer performed the inorganic analyses, Dauth assisted with the interpretation thereof and Brown and Smith interpreted and performed the organic analyses respectively. I wrote the manuscripts of studies (16), (17) and (18). Studies (15) and (16) are based on my PhD thesis. Bosman and Noffke edited the manuscript of study (16) and Vorster prepared the micrographs. The results of study (19) were partially used by Van Niekerk for the dissertation of his masters degree. Van Heerden, Van Niekerk and myself prepared the publication, De Vos provided the material and Turner

executed the ultra structural examination. I prepared the manuscript of study 20 and provided the material for study 21. I assisted with the writing of the latter manuscript.

**Abstract**

Technical difficulties encountered during the preparation of specimen of mineralized bone and teeth for analytical purposes are responsible for the paucity in the literature on the morphology, composition and metabolic induced changes affecting these tissue types. The abundance of material available to the author prompted this research program. Study (8) served as an introduction to the techniques employed in dynamic labeling of bone and the histomorphometric measurement thereof. After demonstrating that it was indeed possible to monitor osteoblastic-, osteoclastic- and mineralization activities in bone accurately, a histomorphometric diagnostic service was introduced. Study (9) emanated from service rendering in this field and established the value of histomorphometry in the diagnoses and management of rickets. Based on histomorphometric findings, rickets was devided in hypertrophic- and atrophic types, with specific diagnostic and prognostic implications. Study (10) propagated the use of histomorphometry in the diagnoses and monitoring of the responses to therapy of other metabolic bone disease states. A need for a review on the histopathologic changes in metabolic bone diseases arose which prompted study (11). This review was presented as invited guest speaker at the 10th International Association of Oral Pathology meeting in Guatemala, 2000.

Analytical studies on human teeth were initiated concomitantly. The amino acid composition of dentin was investigated in study (12) and two amino acids, identified for

the first time in human dentin, were recorded. In study (13) it was shown that there is a significant difference in the magnesium, fluoride and zinc contents between opaque and translucent dentin. Study (14) proved higher levels of mineralization of the tissue that occlude dentinal tubules than that between the tubules in translucent human dentine.

The potential of determining the geographic origin of elephant ivory (dentin) on the inorganic composition thereof was illustrated with the aid of atomic absorption spectrometry, inductively coupled plasma optical emission spectroscopy and ion selective electrodes in study (15). The histology of elephant ivory was described in study (16) and a theory on the histogenesis of the unique chequered pattern proposed. Studies (17) and (18) are detailed histologic descriptions of the intrauterine development of the tush (deciduous tusk) and tusk of the elephant. The analyses of data obtained on elephant tusklessness in the Kruger Park resulted in study (18), which proposed an explanation for differences reported in the incidence rates of tusklessness amongst different elephant populations in Africa. In study (19) the morphologic characteristics of the tush were recorded for the first time in the scientific literature. Study (20) demonstrated the weak tusks of the Kaokoveld elephant to be the result of a probable vitamin C deficiency. This hypothesis was based on the low level of hydrolyzed lysine found in Koakoveld ivory. Results obtained through nuclear microprobe analyses for trace elements in ivory validated the potential use of this technique for the determination of the geographic origin of ivory (21).

# 3. STUDIES ON SALIVARY GLANDS: NORMAL STRUCTURE AND NEOPLASTIC PROLIFERATIONS

## Declaration

Ten publications are submitted in this section. Studies (22) to (25) and (30) were initiated and designed by me and studies (27) to (29) and (31) by Van Heerden. I collected the material, interpreted the light- and electron micrographs and prepared the manuscripts of studies (22) and (23). All authors were involved in the collection of specimen analyzed in study (22). Dreyer performed the biochemical analyses, Dauth assisted with the interpretation thereof and I prepared the manuscript. In study (25) I collected the material and prepared the manuscript with Van Niekerk, who also performed the electron microscopy. Thein provided some of the cases in study (26) and Van Heerden and I reviewed the microscopic sections and prepared the manuscript. In studies (27), (28) and (29) I participated in the analyses of the data and preparation of the manuscripts. Van Heerden and I prepared the manuscript of study (30) whereas I contributed to the material and participated in editing the manuscript of study (31).

## Abstract

Study (22) followed on an invitation from the editor of Critical Reviews in Clinical Laboratory Sciences to prepare a review article on the myoepithelial cell. The manuscript was written at a stage when developments pertaining to myoepithelial cells

revolutionized the understanding of their involvement in pathologic processes. The manuscript was illustrated with, amongst others, micrographs of tissues collected from exocrine glands of the African elephant and buffalo. Study (23) focused on salivary myoepithelium and their differentiation in neoplasms of salivary gland origin.

The structure of the homocrine seromucinous parotid salivary gland of the African elephant and the composition of its saliva was established in study (24). Unique biochemical characteristics of elephant saliva, the first time reported on, include the absence of amylase and elevated concentrations of potassium, urea, calcium and phosphorus. In study (25) the influence of secretory pressure on myoepithelial development in the salivary system of the elephant was illustrated with the aid of scanning electronmicroscopy after enzymatic digestion of the basement membranes of the secretory apparatus.

Studies (26) to (31) investigated aspects of salivary gland neoplasia. In study (26) a polymorphous low grade adenocarcinoma with tyrosine crystalloids had been reported, refuting the claim that these deposits are unique to benign mixed tumors of salivary gland origin. The overlapping AgNOR count between various salivary gland neoplasms demonstrated in study (27) mitigated against the use of this technique as an absolute criterion in the diagnosis of this group of neoplasms. The largest series on intraoral salivary gland neoplasms reported in an African population sample at the date of publication appears under study (28). This study showed significant differences in the pattern and pathology of intraoral salivary gland neoplasms when compared with findings

in studies performed at other geographic locations. In a study encompassing DNA flow cytometry and AgNOR staining (29) a statistically insignificant but positive correlation was found between these techniques. The AgNOR technique, which is fast and cost effective, was recommended above flow cytometry to determine the proliferative activities of tissue of salivary gland neoplasms imbedded in wax.

During the early nineties new approaches to the diagnosis and classification of salivary gland neoplasms created confusion. This precipitated study (30) that attempted to clarify misconceptions and establish uniform diagnostic principles. In study (31) the clinico-pathologic features, immunohistochemistry and DNA ploidy status of a series of intraoral salivary duct carcinomas were reported. The tumors were found to be composed predominantly of ductal cells with prominent cytokeratin expression and the majority was found to be aneuploid. The value of the ploidy status in determining the prognosis of salivary duct carcinomas will however require a follow-up study of the patients presented.

## 4. DIAGNOSTIC INTERPRETATION OF JAW TUMORS AND CYSTS

### Declaration

Studies (32), (34), (37), (38), (41), (46), and (48) were initiated and planned by me. In study (30) Van Heerden and I prepared the manuscript, Turner performed the sections for microscopic analyses and Mare provided the material. I was involved in the evaluation of the cases and preparation of the manuscript in study (33) and Weir and Kreidler

provided clinical data and radiographs. In study (34) Van Heerden assisted me in analyzing the data and preparing the manuscript whereas Seeliger interpreted the radiographs and Dreyer provided clinical data and treated the case. I contributed towards the preparation of the manuscripts in studies (35) and (36) and collected data and prepared the manuscript of study (37). Noffke interpreted the radiographs in the latter study. Van Heerden and myself analyzed the data and prepared the manuscripts in studies (38) and (39), Sitzman and Heymer provided clinical data and Turner performed the microscopic techniques. I participated in the analyses of the data and the preparation of the manuscript in study (40). Van Heerden and I analyzed the data and prepared the manuscript in study (41) and Kreidler provided the clinical information and radiographs. I translated the manuscripts of studies (42) and (43) from German into English and together with Van Heerden analyzed the pathological specimen and edited the final versions of both manuscripts. I participated in the analyses of the data and preparation of the manuscript in study (44). My role in study (45) was limited to the microscopic analyses of the case. Van Heerden and I analyzed the microscopic slides and prepared the manuscript in study (46) and Noffke interpreted the radiographs. I participated in the microscopic analyses and preparation of the manuscript in study (47). The microscopic appearances of the tumors in studies (48) and (49) were analyzed by me, Lello provided the clinical data in study (48), Noffke performed the radiographic analyses in study (49) and all the authors contributed to the preparation of the manuscripts. I did the microscopic examination and assisted in the preparation of the manuscript in study (50).

**Abstract**

Descriptions of odontogenic tumors in large mammals are unusual. Study (32) described the features of an odontoma in the mandible of an African elephant. The tumor was at the stage of publication the largest odontoma reported in the literature.

Studies (33) and (35) described the clinico-pathologic features of extremely large examples of ossifying fibroma and adenomatoid odontogenic tumor respectively. In study (33) a shift towards a greater fibrous tissue component at the expense of bone as well as an increased incidence of aneurysmal bone cyst formation in large ossifying fibromas were demonstrated. The large adenomatoid odontogenic tumors in study (34) proved unrestricted growth potential, thereby negating the hypothesis that they are hamartomatous rather than neoplastic in nature.

Studies (35), (36) and (37) described hitherto unreported syndromes, which exhibit multiple hamartomatous odontogenic fibroma-like proliferations. Studies (35) and (37) demonstrated the unique association between multiple unerupted teeth, enamel malformation and central odontogenic fibroma-like lesions. At the time of reporting, study (38) represented the fourth case of true peripheral dentinogenic ghost cell tumour reported in the English literature.

Studies (39) and (40) analyzed the clinico-pathologic features of glandular odontogenic cysts. Electron microscopy employed in study (39) showed a process morphologically similar to apoptosis in the epithelial lining of these cysts. Study (40) analyzed nine cases

of glandular odontogenic cyst, bringing the total number reported in the literature to 54. This study represents the most detailed radiological description of these cysts thus far and proposes a histopathologic overlap with the central type mucoepidermoid carcinoma.

Studies (41), (42) and (43) reported on the classification, differential diagnosis of dentigerous-like cysts and relative frequencies of cysts-like lesions affecting the jawbones. In study (41) new developments in the classification of odontogenic cysts of the jaws were reported. Pitfalls in the clinical diagnosis of dentigerous cyst-like lesions were highlighted in study (42). It was demonstrated that a significant percentage of lesions with a dentigerous appearance were in fact unicystic ameloblastomas or odontogenic keratocysts. This study emphasized the need for microscopic examination in order to establish an accurate diagnosis. In the extensive review of jaw cyst-like lesions in a German population sample (43), the presentation of unicystic ameloblastomas in a significantly higher age category than is generally reported, was demonstrated. The relative frequencies of jaw cysts in this population sample differ in many respects from our experience.

Ameloblastomas were analyzed in studies (44), (45) and (46). A retrospective study of 30 unicystic ameloblastomas (44) revealed their aggressive behavior as well as a need for thorough microscopic examination of the cyst wall in order to determine the extent of surgical removal. HPV type 18 DNA was found in a verrucous lesion within the lining of a locule in a polycystic ameloblastoma in study (45). Identification of the virus, which was considered to represent a secondary infection, was the first description of its kind in

an ameloblastoma. A detailed microscopic investigation of a series of 108 ameloblastomas (46) demonstrated clinico-pathological diversity in a significant number of tumors. The association of ameloblastomas with adenomatoid odontogenic tumor-like proliferations, ameloblastic fibroma- like areas, melanocytes, mucous- and squamous cell metaplasia and stromal desmoplasia amongst others were reported.

Study (47) reviewed the literature and reported a case of calcifying epithelial odontogenic tumor with intracranial extension. This study demonstrated the serious complications following neglect of a benign maxillary odontogenic neoplasm. Studies (48) and (49) highlighted the potential pitfalls in the diagnosis of low-grade osteosarcomas and extra nodal Hodgkins lymphomas of the jaws respectively. Study (50) reported on a rare case of tumoral calcinosis involving the temporomandibular joint, emphasizing the differential diagnosis thereof.

# Unusual presentation of multiple myeloma

## A report of 2 cases

J. DAUTH, J. P. DE CONING, W. M. POLITZER, T. ROBERTSON, E. J. RAUBENHEIMER

**Summary**

The diagnosis of multiple myeloma (overt plasma cell dyscrasia) is usually not considered in patients under 30 years of age. Furthermore, multiple myeloma with coexistent megaloblastic and iron deficiency anaemia is very uncommon. Within 6 months we encountered 2 patients under 30 years of age who had multiple myeloma, one with advanced secondary amyloidosis and the other with severe megaloblastic and iron deficiency anaemia.

*S Afr Med J* 1984; 65: 968 - 971

At the time of diagnosis of multiple myeloma the mean age of patients is reported to be 62 years.[1] Less than 2% of patients with multiple myeloma are below the age of 40 years, and very few well-documented cases in patients below the age of 30 years have been reported.[2]

The pathological features of multiple myeloma or overt plasma cell dyscrasia include the following:[3] (*i*) local or widespread proliferation of B-type lymphocytes; (*ii*) excessive production of one of the monoclonal types of immunoglobulin or its subunits, viz. heavy or light chains; and (*iii*) often decreased production of normal immunoglobulins. These factors have to be considered in the diagnosis of multiple myeloma or overt plasma cell dyscrasia when an abnormal band is detected on serum protein electrophoresis. Special investigations such as bone marrow aspiration, biopsy, comprehensive radiographic skeletal studies and relevant biochemical determinations on blood and urine samples will then establish the diagnosis.

## Case reports

### Case 1

A 25-year-old Black man (Fig. 1) was referred from a rural hospital complaining of having had painless swellings below the tongue and over both parotid glands for 'many years'. On examination bilateral enlargement of the parotid and submandibular salivary glands and submental lymph nodes was noted. The tongue was hard and enlarged with limited mobility, and an epulis was present in the anterior mandibular sulcus.

**Departments of Chemical Pathology, Haematology and Oral Pathology and Oral Biology, Medical University of Southern Africa and Ga-Rankuwa Hospital, Pretoria**
J. DAUTH, M.B. CH.B., M.MED (PATH.), D.P.H., D.I.H.
J. P. DE CONING, B.SC.
W. M. POLITZER, M.D. (PRAGUE)
T. ROBERTSON, A.I.M.L.S., M.T.
E. J. RAUBENHEIMER, B.CH.D., M.CH.D.

Radiographic studies showed destruction of T7 and lytic lesions in the right parietal area of the skull, the posterior part of the right sixth rib and right ischium and pubis. There was also erosion of the anterior surface of L4. In view of the radiographic findings the following differential diagnoses were considered: lymphoma with bony and soft-tissue infiltration, multiple myeloma and histiocytosis X. The relevant biochemical and haematological findings are shown in Tables I and II respectively.

Serum protein electrophoresis showed a faint monoclonal peak in the early $\gamma$ area with normal IgG, IgA and IgM levels. Bence Jones protein was present in the urine. The serum and urine immuno-electrophoretic patterns are shown in Fig. 2. IgG,

**TABLE I. RELEVANT BIOCHEMICAL FINDINGS IN CASE 1**

| | Patient's values | Normal ranges |
|---|---|---|
| **Serum** | | |
| Urea (mmol/l) | 4,1 | 2,5 - 6,7 |
| Creatinine ($\mu$mol/l) | 70 | 53 - 97 |
| Uric acid (mmol/l) | 0,42 | 0,1 - 0,5 |
| Total protein (g/l) | 67 | 60 - 80 |
| Albumin (g/l) | 38 | 26 - 52 |
| Magnesium (mmol/l) | 0,65 | 0,75 - 1,25 |
| Total calcium (mmol/l) | 1,94 | 2,25 - 2,70 |
| IgG (g/l) | 12,0 | 6,4 - 13,5 |
| IgA (g/l) | 1,2 | 0,7 - 3,12 |
| IgM (g/l) | 0,75 | 0,56 - 3,5 |
| **Urine** | | |
| Total protein (g/l) | 42 | < 0,08 |

**TABLE II. RELEVANT HAEMATOLOGICAL FINDINGS IN CASE 1**

| | Patient's values | Normal ranges (males) |
|---|---|---|
| WBC | $7,8 \times 10^9$/l | $7,5 \pm 3,5 \times 10^9$/l |
| RBC | $4,2 \times 10^{12}$/l | $5,8 \pm 1,0 \times 10^{12}$/l |
| Hb (g/dl) | 12,2 | $16,4 \pm 2,5$ |
| MCV (fl) | 91,0 | $85,0 \pm 8,0$ |
| MCH (pg) | 29,0 | $29,5 \pm 2,5$ |
| Differential count (%) | | |
| Polymorphs | 40 | 40 - 75 |
| Lymphocytes | 58 | 20 - 45 |
| Monocytes | 2 | 2 - 10 |
| Platelets | $365 \times 10^9$/l | $150 - 400 \times 10^9$/l |
| Reticulocytes (%) | 4,0 | 0 - 2 |
| ESR (mm/h) | 45 (Wintrobe) | 0 - 20 |

WBC = total white cell count; RBC = red cell count; Hb = haemoglobin concentration; MCV = mean corpuscular volume; MCH = mean corpuscular haemoglobin; ESR = erythrocyte sedimentation rate.

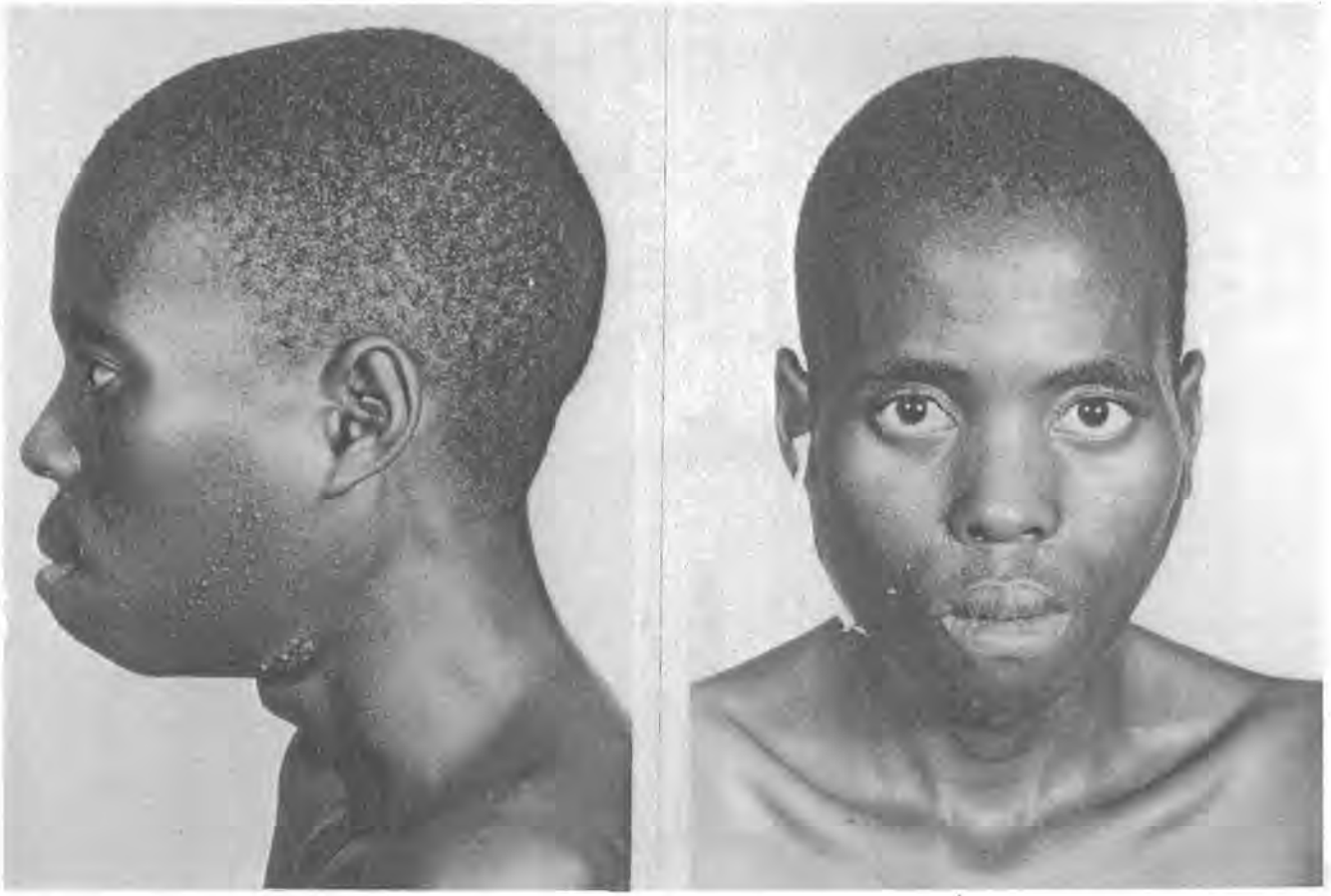

**Fig. 1. Patient 1 — frontal and lateral views showing enlargement of the parotid and submandibular salivary glands.**

IgA and IgM as well as $\kappa$ and $\lambda$ light chains were present in the serum, while immuno-electrophoresis of the urine showed the presence of $\kappa$ chains identical to those in the serum and also a smaller number of $\lambda$ chains.

Microscopic examination of both bone marrow aspirate and a biopsy specimen showed a 40% diffuse infiltrate of pleomorphic plasmacytoid cells. Immunoperoxidase staining (Immunolok Histoset, Immunolok Inc.; Carpinteria, USA) of bone marrow sections showed the presence of $\kappa$ light chains in the cytoplasm of the plasma cells.

The tongue, parotid gland and intra-oral epulis showed extensive deposits of amyloid, this reacting positively with methyl violet and Congo red stains. Numerous dilated capillaries and patchy infiltrates of foamy histiocytes and giant cells were present in the deposits.

On the basis of the radiological, haematological and biochemical findings the diagnosis of multiple myeloma with secondary amyloidosis was made and a course of chemotherapy was instituted.

## Case 2

A 26-year-old Black male patient was seen in the casualty department of Ga-Rankuwa Hospital, Pretoria, in a comatose condition with generalized oedema. Since 1981 he had been treated at an outside clinic with thioridazine hydrochloride for a 'psychiatric condition'. On examination the patient responded to pain only. The pulse rate was 100/min and the blood pressure was 90/50 mmHg. The patient had deep, sighing breathing with bilateral rhonchi. Multiple petechial haemorrhages were present all over the body. The patient was then admitted to the intensive care unit.

A full blood count revealed severe macrocytic normochromic anaemia and a leuco-erythroblastic reaction, and blood gas analysis showed the presence of metabolic acidosis (Tables III and IV). On the basis of the haematological findings bone marrow aspiration was performed before packed red blood cells

**TABLE III. RELEVANT HAEMATOLOGICAL FINDINGS IN CASE 2**

| | Patient's values | Normal ranges (males) |
|---|---|---|
| **WBC** | 6,1 x $10^9$/l (corrected) | 7,5 ± 3,5 x $10^9$/l |
| **RBC** | 0,43 x $10^{12}$/l | 5,8 ± 1,0 x $10^{12}$/l |
| **Hb (g/dl)** | 1,9 | 16,4 ± 2,6 |
| **MCV (fl)** | 156 | 85 ± 8 |
| **MCH (pg)** | 46 | 29,5 ± 2,5 |
| **Differential count (%)** | | |
| **Polymorphs** | 60 | 40 - 75 |
| **Lymphocytes** | 26 | 20 - 45 |
| **Monocytes** | 1 | 1 - 10 |
| **Eosinophils** | 1 | 1 - 6 |
| **Promyelocytes** | 5 | |
| **Myelocytes** | 2 | |
| **Metamyelocytes** | 2 | |
| **NRBC/100 WBC** | 18 | |
| **Megaloblasts present** | | |
| **Platelets** | 10 x $10^9$/l | 150 - 400 x $10^9$/l |
| **Reticulocytes (%)** | 1,5 | 0 - 2 |

NRBC/100 WBC = nucleated red blood cells/100 WBC.

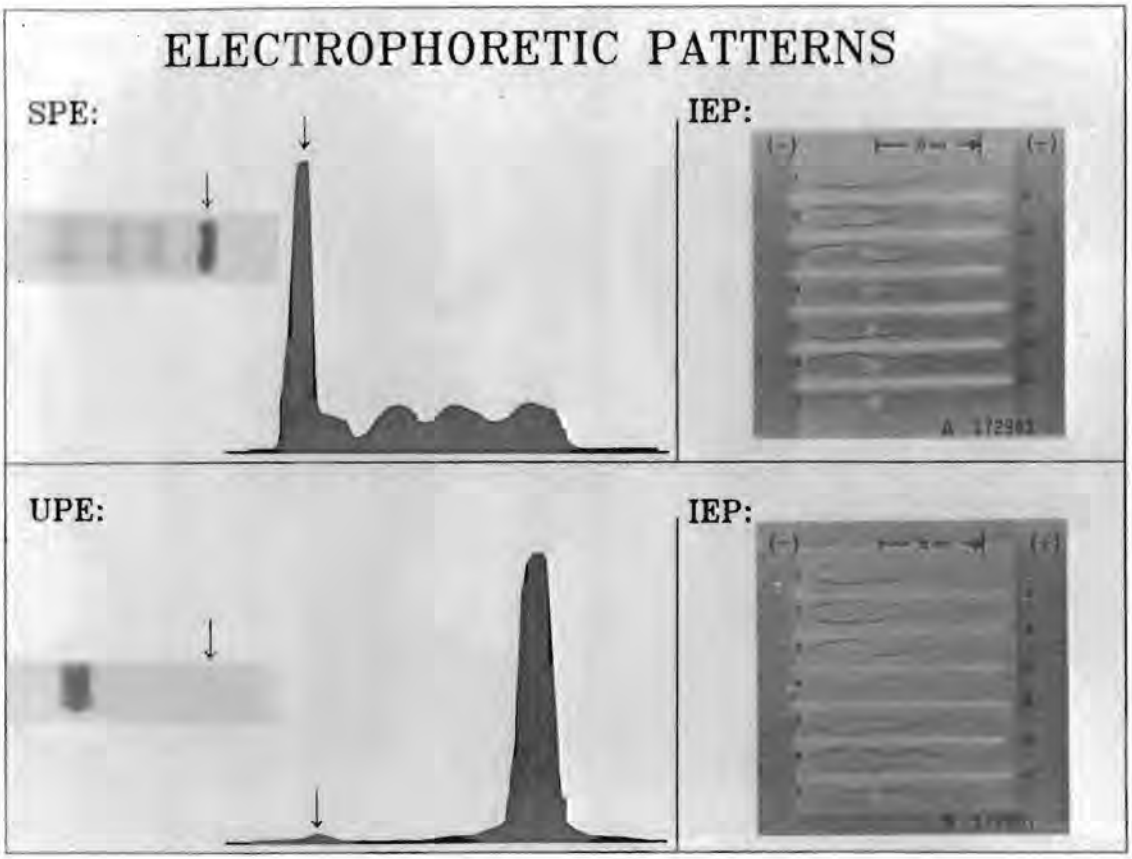


**Fig. 2. Serum and urine electrophoretic patterns (SPE and UPE respectively) as well as densitrometric scans of case 1 appear on the left. The peaks (arrows) reflect albumin. On the right, immuno-electrophoretic membranes on both serum (top) and urine (bottom) are shown. In both cases the patients' specimens were put in the wells with even numbers, while control serum was used in the unevenly numbered wells. Antisera were placed in the troughs as follows: A = polyvalent; B = anti-IgG; C = anti-IgA; D = anti-IgM; E = anti-κ; F = anti-λ.**

**TABLE IV. BIOCHEMICAL FINDINGS AVAILABLE IN CASE 2**

| | Patient's values | Normal ranges |
|---|---|---|
| **Serum** | | |
| Urea (mmol/l) | 11,4 | 2,5 - 6,7 |
| Creatinine (μmol/l) | 172 | 53 - 97 |
| **Arterial blood** | | |
| pH | 7,45 | 7,35 - 7,45 |
| $P_{CO_2}$ (kPa) | 2,09 | 4,67 - 6,00 |
| $P_{O_2}$ (kPa) | 10,09 | 10,00 - 13,33 |
| $HCO_3$ (mmol/l) | 10,9 | 20 - 26 |
| Total $CO_2$ (mmol/l) | 11,3 | 24,5 - 30,0 |
| Base excess (mmol/l) | −12,0 | −3,0 - +1,0 |
| $O_2$ saturation (%) | 94,5 | 96 - 100 |
| IgG (g/l) | 58,4 | 6,4 - 13,5 |
| IgA (g/l) | 0,17 | 0,7 - 3,12 |
| IgM (g/l) | 0,47 | 0,56 - 3,5 |

were transfused. Despite treatment for cardiac failure and pulmonary oedema the patient never regained consciousness and died within a few hours. Consent for performance of an autopsy could not be obtained.

The bone marrow showed marked hypercellularity without stainable iron and decreased erythropoiesis and granulopoiesis. The majority of the red cell precursors were megaloblastic and there was a 50% plasma cell infiltrate. On account of the bone marrow findings the small amount of serum available was used for serum protein electrophoresis. An abnormal monoclonal band was found in the early γ area with immunoparesis. The immunoglobulin levels are shown in Table IV. Immuno-electrophoresis of the serum showed the presence of IgG and κ light chains. The diagnosis of megaloblastic and iron deficiency anaemia with multiple myeloma was made.

## Discussion

Case 1 demonstrated that serum protein electrophoresis has certain pitfalls, since the faint monoclonal band could be mistaken for an oligoclonal gammopathy.[4] Furthermore, there was no immunoparesis and the age of the patient was far below the expected mean age of 62 years. It was only after examination of the urine for Bence Jones protein, radiographic studies and bone marrow aspiration and biopsy that the diagnosis of multiple myeloma could be made.

The amyloid deposits were suggestive of a pattern I distribution;[3] this principally involves the tongue, gastro-intestinal tract, skin, nerves, muscles and carpal ligaments and is frequently seen in multiple myeloma-related amyloidosis. κ light chains were demonstrated in the plasma cells, serum and urine of this patient. Isobe and Osserman[5] found λ light chains in 50 patients with pattern I amyloid distribution.

The demonstration of multiple myeloma in case 2 was unexpected. A leuco-erythroblastic reaction is rare and is seen in association with heavy infiltration of the bone marrow by neoplastic disease, including multiple myeloma.[6] The patient's sudden death prevented us from establishing the cause of the

megaloblastic anaemia. Larsson[7] has described the coexistence of multiple myeloma and pernicious anaemia, and Di Bisceglie and Hodkinson[8] have reported a similar occurrence in a Black patient aged 72 years. However, our patient was not of that age group. Hoffbrand *et al.*[9] described mild megaloblastic changes in patients with myeloma due to vitamin $B_{12}$ or folate deficiency, but none of his patients showed 'florid megaloblastic changes seen in severe megaloblastic anaemia'. Since our patient had severe megaloblastic anaemia, he may have had a combined deficiency.

In conclusion, the fact that 2 patients below the age of 30 years with multiple myeloma were encountered within a period of 6 months suggests that this disease may occur at a much earlier age in Black patients.

We are indebted to Drs J. M. C. Hoog and R. Meek and the Audiovisual Department of MEDUNSA for assistance with these 2 cases.

REFERENCES

1. Kyle RA. Multiple myeloma: review of 869 cases. *Mayo Clin Proc* 1975; **50:** 29.
2. Hewell GM, Alexanian R. Multiple myeloma in young persons. *Ann Intern Med* 1976; **84:** 441-443.
3. Farhangi M, Ossermann EF. Biology, clinical patterns and treatment of multiple myeloma and related plasma-cell dyscrasias. In: Twomey JJ, Good RA, eds. *The Immunopathology of Lymphoreticular Neoplasms, Comprehensive Immunology.* New York: Plenum Medical Books, 1978: 641-716.
4. Ritzmann SE. Immunoglobulin abnormalities. In: Ritzman SE, Daniels JC, eds. *Serum Protein Abnormalities: Diagnostic and Clinical Aspects.* 1st ed. Boston: Little, Brown, 1975: 351-485.
5. Isobe T, Osserman EF. Patterns of amyloidosis and their association with plasma cell dyscrasia, monoclonal immunoglobulins and Bence-Jones proteins. *N Engl J Med* 1974; **290:** 473-477.
6. Weick JK, Hagendorn AB, Linman JW. Leukoerythroblastosis;: diagnostic and prognostic significance. *Mayo Clin Proc* 1974; **49:** 110.
7. Larsson SO. Myeloma and pernicious anaemia. *Acta Med Scand* 1962; **172:** 195-205.
8. Di Bisceglie AM, Hodkinson HJ. Multiple myeloma and pernicious anaemia. *S Afr Med J* 1982; **62:** 535-536.
9. Hoffbrand AV, Hobbs JR, Kremenchuzky S, Mollin DL. Incidence and pathogenesis of megaloblastic erythropoiesis in multiple myeloma. *J Clin Pathol* 1965; **20:** 699-705.

# Tumours of accessory parotid glands

## Case reports

A. T. RICHARDS, L. A. CHAIT, R. B. SKUDOWITZ

**Summary**

Tumours arising in accessory parotid glands are a distinct entity and a pitfall for the unwary. The diagnosis is made on the basis of clinical examination and a high index of suspicion is essential. Treatment is by wide exposure and careful dissection because of the relationship of the accessory parotid gland to the facial nerve and parotid duct. Four cases are described.

S Afr Med J 1984; 65: 971 - 972

The accessory parotid gland is recognized as a distinct entity in the *Nomina Anatomica.* It can be described as salivary tissue adjacent to the parotid duct (Stensen's duct) and separate from the main body of the gland[1] to distinguish it from an anterior facial process, which is parotid tissue extending anteriorly from the main gland but remaining in continuity with it.

Lesions arising in accessory parotid tissue are well described, not all that uncommon, and very often misdiagnosed. During the past 2 years we have treated 4 patients with such lesions.

**Park Lane Clinic, Johannesburg**
A. T. RICHARDS, M.B. B.CH., F.C.S. (S.A.), F.R.C.S., F.A.C.S.
L. A. CHAIT, M.B. B.CH., F.R.C.S.
R. B. SKUDOWITZ, M.B. B.CH., D.T.M. & H., F.F. PATH. (S.A.)

## Case reports

All the lesions occurred in adult patients between the ages of 25 and 35 years; 2 patients were male and 2 female. The patients presented with a mid-cheek, painless nodule about 1 - 2 cm in diameter and lying deep to the skin just below the zygomatic arch, and easily felt against the tensed masseter muscle. Sialography performed on 3 patients did not demonstrate a lesion.

## Anatomy

In order to prevent damage to vital structures at operation it is important to understand the anatomy of the accessory parotid gland. It always lies between the zygomatic (buccal) branch of the facial nerve (above) and the parotid duct (below). One or more fine ducts drain the accessory gland and enter the parotid duct (Fig. 1).

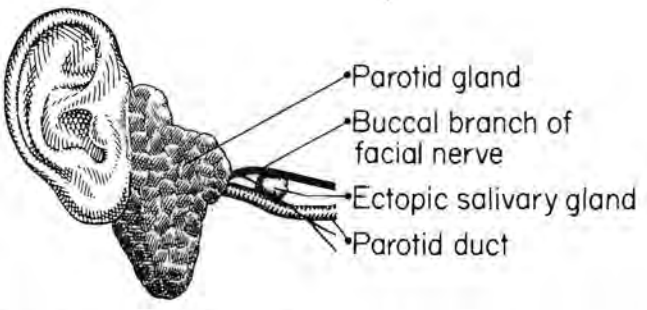


**Fig. 1. Anatomical relations of the accessory parotid gland.**

# MULTIPLE MYELOMA PRESENTING AS A SOLITARY EXPANSILE MANDIBULAR TUMOR

Erich J. Raubenheimer, M.Ch.D., Oral, Path.,[1] Joseph Dauth, M.Med, Path.[2]
Johann B. Jordaan, M.Ch.D., M.F.O.S.,[3] Lourens M. du Toit, M.B.Ch.[4]
Johannes P. de Coning, B.Sc., Med., Hons.[5]

[1,2,3,4,5]Medical University of Southern Africa

SUMMARY

A case of multiple myeloma of the mandible presenting as a solitary expansile lesion is reported. Factors influencing the diagnosis and prognosis of the disease are discussed and a multidisciplinary approach to the diagnosis of suspected cases emphasized. The unexpected finding of crystalline inclusions in the nuclei of neoplastic plasma cells demonstrated by ultrastructural examination is considered.

## INTRODUCTION

Mutliple myeloma (M.M.) is characterized by a neoplastic proliferation of one or more clones of plasma cells. The disease occurs most frequently in the 6th and 7th decades of life[1,2] and the neoplastic plasma cells synthesize monoclonal immunoglobulins or subunits thereof (heavy or light chains) which may be detected in serum even before lesions become clinically apparent.[1,3] If abnormal light chains are produced they are excreted in urine as Bence Jones proteins, causing renal tubular damage and eventually renal failure.[2] Additional laboratory findings include normocytic normochromic anemia,[2] raised erythrocyte sedimentation rate (ESR), thrombocytopenia[4] and immunoparesis.[2] Furthermore, excessive light chain production leads to amyloid deposits in soft tissues and organs[5] in 6-16% of patients with M.M.[6]

[1]Professor, Department of Oral Pathology
[2]Associate Professor, Department of Chemical Pathology
[3]Professor, Department of Maxillo-Facial Surgery
[4]Registar, Department of Anatomical Pathology
[5]Medical Natural Scientist, Department of Chemical Pathology

### *Oral Manifestations of M.M.*

In a radiographic and case record survey of 59 cases, Bruce and Royer[7] found jaw involvement in 17 patients with M.M. A more recent study showed that the incidence of jaw involvement may even be higher.[8] Jaw lesions are more commonly found in the mandible[7,9] and are associated with areas of hemopoiesis, namely the premolar- and molar regions and the ascending ramus.[7,9,10]

The typical radiographic appearance is that of multiple radiolucent lesions with round, well defined, non-corticated borders.[11] Rarely, diffuse involvement of the jaws occur with a radiographic appearance of osteoporosis. Root resorbtion of associated teeth is characteristically absent[12] and mandibular lesions may be associated with pathologic fractures.[13] Common oral symptoms include pain, swelling, numbness of the jaw, mobility of teeth and soft tissue tumors.[10] Enlargement of the tongue and salivary glands are the result of amyloid deposits.[12]

We report a case with multiple myeloma of the mandible which presented as a solitary expansile tumor.

## CASE PRESENTATION

A female patient, 70 years of age, was admitted from a rural hospital with a history of a rapid increasing swelling and paresthesia of the lower jaw. She was in a poor systemic condition with a hemoglobin value of 6 g/d$\ell$ for which whole blood infusion was administered.

A soft swelling was present over the lower third of her face. (Fig. 1). A large indurated tumor (10 x 6 cm) extended along the length of the corpus of the mandible breaking the lip seal and protruding extra-orally. Displaced teeth and consequent traumatic ulcerations were present on the mucosa

*Fig. 1:* Clinical appearance of mandibular tumor.

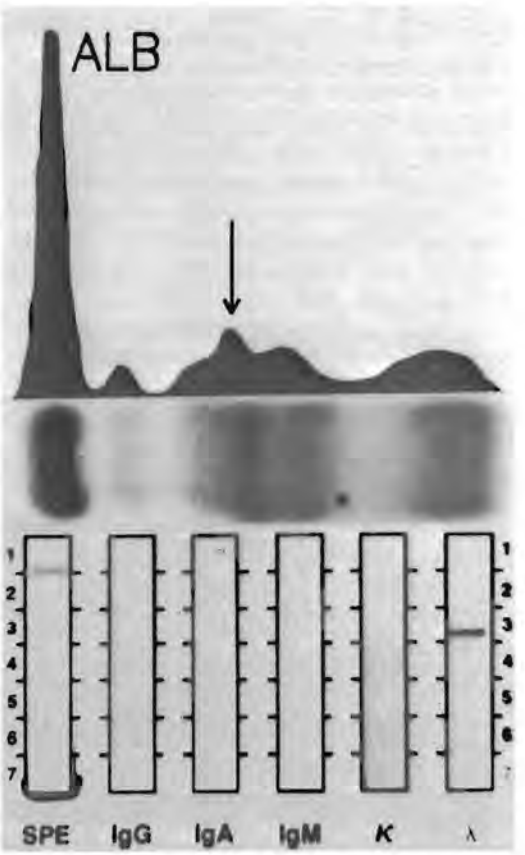


*Fig. 2:* Serum protein electrophoretogram and densitometric scan (top) showing an abnormal band in the inter $\beta$ — $\alpha_2$ region (arrow). Serum immunofixation (bottom) demonstrates the presence of λ-light chains.

overlying the tumor. The size of the lesion made satisfactory radiographs difficult, but a poorly defined osteolytic lesion with cortical expansion and destruction extending from the 33 to 47 region was identified. Teeth 44 and 45 were displaced without any sign of root resorbtion. The differential diagnoses of an ameloblastoma, osteogenic sarcoma or metastatic deposit from an unknown primary malignancy were made. The patient bled profusely from the tumor 2 weeks after admittance. Local hemostatic measures and a further whole blood infusion were needed to stabilize her condition.

Serum protein electrophoresis (SPE) showed a paraprotein band in the inter-$\beta$ — $\alpha_2$ area. With immunofixation (Beckman Paragon™ I.F.E., Beckman Instruments, Inc. Immuno Systems Operations Brea, C.A.) this band proved to be a monoclonal light chain of the λ-type (Fig. 2). Other stigmata of multiple myeloma included impairment of renal function, normocytic normochromic anemia and a raised erythrocyte sedimentation rate (ESR) (Table I). Unfortunately, urinalysis was not done after the provisional diagnosis of Bence Jones lambda light chain multiple myeloma had been established due to the patient's sudden exitus caused by acute renal failure.

Microscopic examination of the ante mortem biopsy of the tumor and post mortem tissue removed from the mandible and sixth rib showed extensive infiltration of immature plasma cells (plasmablasts) (Fig. 3a). There was a marked reduction of hemopoietic tissue and fat and immunoperoxidase stains (Immunolok Histoset, Immunolok Inc.; Carpinteria, USA) demonstrated the presence of λ-light chains in the cytoplasm

**Table 1**
**THE RELEVANT BIOCHEMICAL AND HEMATOLOGICAL FINDINGS IN THE PATIENT**

| | PATIENT'S VALUES | REFERENCE RANGES |
|---|---|---|
| SERUM | | |
| Total Protein (g/ℓ) | 57 | (60 - 80) |
| Albumin (g/ℓ) | 28 | (26 - 52) |
| Urea (mmol/ℓ) | 28,9 | (2,5 - 6,7) |
| Creatinineaμmol/ℓ) | 477 | (53 - 97) |
| IgG (g/ℓ) | 9,61 | (6,4 - 13,5) |
| IgA (g/ℓ) | 1,60 | (0,7 - 3,12) |
| IgM (g/ℓ) | 0,70 | (0,56 - 3,50) |
| HEMATOLOGY | | |
| WBC (x10⁹/ℓ) | 9,89 | (7,5 ± 3,5) |
| RBC (x10¹²/ℓ) (Females) | 2,69 | (4,8 ± 0,6) |
| Hb (g/dℓ) (Females) | 8,9 | (14,0 ± 2,0) |
| MCV (fℓ) | 90,0 | (85,0 ± 8,0) |
| ESR (mm/h Wintrobe) (Females) | 64 | (0 - 20) |
| Platelets (x10⁹/ℓ) | 338 | (150 - 400) |

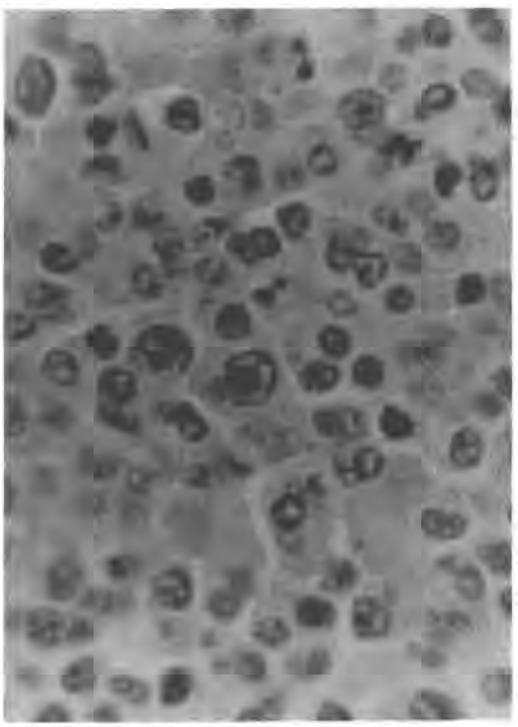

*Fig. 3(a, left):* Photomicrograph showing infiltration of the bone marrow by plasmablasts. (Hematoxylin and eosin stain. Magnification, x400)

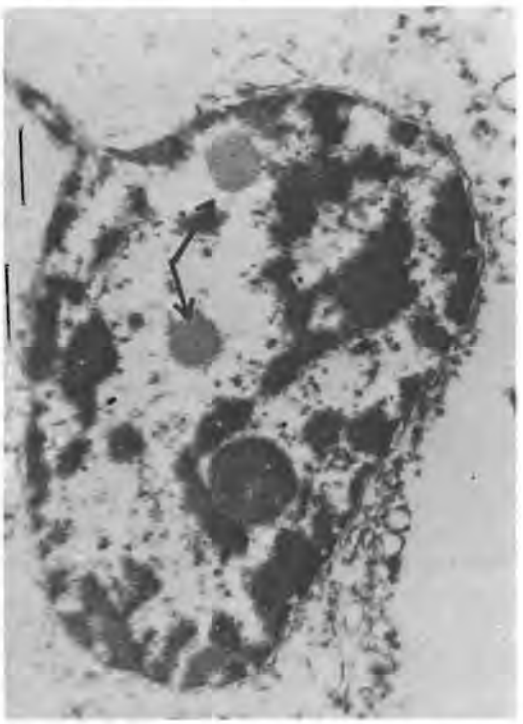

*Fig. 3(b, right):* Electronmicrograph of a plasmacell nucleus containing crystalline inclusions (arrows). (Magnification, x7 500.)

of the plasma cells. Congo-red stains failed to demonstrate amyloid deposits. In addition to the expected features of plasmablasts, electronmicroscopy showed intranuclear inclusions in some cells. These inclusions were not membrane bound, had a diameter of 400-700 nanometer(nm.) and a lattice-like crystalline structure. (Fig. 3b).

## DISCUSSION

The large, solitary expansile tumor of the mandible and absence of immunoparesis are not characteristic features of multiple myeloma. On the other hand, the age of the patient,[1,2] anemia with raised ESR,[2] absence of tooth resorbtion,[12] paresis of the jaw,[10] hemorrhagic diathesis[6] and renal complications[1] are features commonly found in patients with M.M.

Anemia is present in 80% of cases and correlates with the extent of plasma cell infiltration in the bone marrow, erythrophagocytosis by myeloma cells, folate and vitamin $B_{12}$ deficiency or chronic blood loss due to a hemorrhagic diathesis.[2,6,13] Chronic blood loss was probably responsible for the low hemoglobin levels in our patient as erythrophagocytosis could not be demonstrated microscopically and the extent of systemic red bone marrow displacement was not sufficient to account for her anemia. Fur-

thermore, a megaloblastic anemia, secondary to Vitamin $B_{12}$ or folate deficiency was absent. The mechanisms by which M.M. contribute to hemorrhagic disorders are numerous and complex. It could be the result of a thrombocytopenia secondary to the obliteration of bone marrow, interaction between myeloma proteins and coagulation factors, improper platelet function due to the "coating action" of the abnormal proteins or the hyperviscosity syndrome.[2] This syndrome has been reported in a small percentage of myelomas[14] and is the direct result of the high concentration of circulating immunoglobulin components. The increased viscosity of plasma may lead to an increased resistance to blood flow in capillaries[2] which predisposes to hemorrhages from the gingiva, mucous membranes of the gastro-intestinal tract and sites of minor surgery or trauma.[4] The bleeding tendency in our patient was not associated with a thrombocyopenia or the hyperviscosity syndrome as the platelet count and total serum protein values were normal. Impaired platelet function and interaction between coagulation factors and abnormal circulating proteins therefore seem to be the most likely cause of our patient's hemorrhagic diathesis.

A multidisciplinary approach in the diagnosis of M.M. is essential as biochemical, radiographic and microscopic parameters are not only useful in the diagnosis of suspected cases, but also provide valuable information regarding classification, stage of progression, complications and prognosis of the disease.[2,15,16]

Microscopically, a myelomatous infiltrate is classified as either plasmacytic or plasmablastic.[2] The former is characterized by small, normal appearing plasma cells with a low mitotic index and is associated with a longer survival time. The plasmablastic type shows infiltration by immature nucleolated plasma cell precursors and has a less favourable prognosis.[2,16] The diagnosis of M.M. on bone marrow plasmacytosis alone is unreliable as numerous other common conditions, like chronic inflammation, malignancies unrelated to plasma cells and autoimmune diseases often cause a plasma cell infiltrate in excess of 50 volume percent.[17,18] However, periarterial and endosteal accumulations of plasma cells, which are characteristic of M.M.,[16] were also present in our microscopic preparations. Concomitant hypoplasia of haemopoietic tissue and increased osseous remodelling are also more in favour of a neoplastic lesion rather than reactive bone marrow plasma cell infiltrate.[19] The extent of the lytic bone lesions and degree of plasmacytosis of uninvolved bone marrow adds valuable information regarding the stage of progression of disease.[16]

Immunochemical typing is helpful in predicting complications and prognoses of patients with M.M. It has been shown that light chain secreting myelomas are frequently associated with amyloidosis[4,20-23] and that they also have the highest mitotic rate.[2,24] Furthermore, the median survival time of patients with λ-light chain disease is reported to be significantly less than in κ-light chain disease.[1,24] The plasmablastic cell type and λ-light chain secretory activity placed our patient in a low prognostic category. This is supported by the rapid deterioration of her renal function which was the cause of death, a complication often encountered in patients with M.M.[25]

The absence of macroglossia and our inability to demonstrate amyloid histochemically supports Smith's observation that amyloid deposits of the tongue are not associated with M.M. of the jaws.[26] However, Smith's conclusion may be incorrect as most patients with amyloidosis present with systemic complications for which rectal, and not tongue biopsies are performed.

Detailed reports on the ultrastructure of plasma cells in M.M. have appeared in the medical[27-33] and dental[34] literature. In addition to the normal ultrastructural features of plasma cells,[28] the cells in M.M. may exhibit phagocytic vacuoles containing iron,[33] erythrocytes[20,30,33] platelets[31] and lymphocytes.[30] Perinuclear microfilaments may be responsible for cell mobility and phagocytosis.[33] Intracytoplasmic crystalline inclusions in neoplastic plasma cells have been studied extensively[28,32] and based on histochemical and ultrastructural features, these cytoplasmic inclusions are fibrillar, proteinaceous in nature and often sur-

rounded by a smooth limiting membrane.[32] Brilliant staining of the inclusions with acid phosphatase- and glucoronidase techniques suggest that they are essentially lysosomal in nature.[32] The origin of intranuclear inclusions, however, is poorly understood.[28] Absence of a membrane surrounding the intranuclear inclusions in the case under study, negates the possibility of these being located in cytoplasmic-nuclear invaginations. A transmissible agent, probably a virus, was isolated from multiple myelomas in mice,[35] mink,[36] and humans.[37] Passenger viruses, finding optimal growth conditions in the milieu of myeloma cells, have recently been reported.[29] The latticelike structure of the inclusions and the diameter of the individual crystals in our case do not resemble the shape and size of any known virus. It is therefore possible that the inclusions represents crystallization of a protein formed within the nucleus of the neoplastic plasma cells.

## CONCLUSION

The presentation of the myelomatous tumour as a large, solitary expansile jaw lesion adds an interesting aspect to the reported clinical features of M.M. A multidisciplinary approach, including biochemical- and microscopical parameters is helpful in the diagnosis, prediction of complications and determination of the prognosis. Furthermore, intranuclear crystalline inclusions, as seen in this case, are probably accumulations of unknown proteins in the nuclei of the neoplastic plasmacells. This phenonemon requires further ultrastructural and biochemical investigation.

*Reprints: Professor E.J. Raubenheimer Department of Oral Pathology and Oral Biology Medical University of Southern Africa, P.O. Medunsa 0204, Republic of South Africa.*

**ACKNOWLEDGEMENT**

We are indebted to Miss. M. Holtzhausen and Mr. C. Lourens for their assistance during the preparation of the manuscript.

**REFERENCES**

1. Farhangi, M., Osserman, E.F.: Biology, Clinical Patterns and Treatment of Multiple Myeloma and Related Plasma-cell Dyscrasias. In: Twomey, J.J., Good, R.A. eds. The Immunopathology of Lymphoreticular Neoplasma. Comprehensive Immunology, New York, 1978, Plenum Medical Books, pp. 641-716.
2. Wintrobe, M.M., Lee, R.G., Boggs, D.R., Bithell, T.C., Foerster, J., Athens, J.W., Lukens, J.N.: Clinical Hematology ed. 8, Philadelphia, 1981, Lea and Febiger, pp. 1726-1760.
3. Stevens, S., Alexander, R.: Evaluation of Multiple Myeloma. Arch. Int. Med. 115:90-93, 1965.
4. Gross, P.D., Roth, N.A., Koudelka, B.M.: Multiple Myeloma presenting as a hemorrhagic diathesis. J. Oral Maxillofac. Surg. 41:129-132, 1983.
5. Glenner, G.G., Ein, D., Eanes, E.D., Bladen, H.A., Terry, W., Page, D.L.: Creation of "Amyloid" fibrils from Bence Jones proteins in vitro. Sciences 174:712-714, 1971.
6. Cranin, A.N., Gross, E.R.: Severe oral perioral amyloidosis as a primary complication of Multiple Myeloma. Report of a case. Oral Surg. 23:158-163, 1967.
7. Bruce, K.W., Royer, R.Q.: Multiple Myeloma occurring in the Jaws: A Study of 17 cases. Oral Surg. 6:729-744, 1953.
8. Cataldo, E., Meyer, I.: Solitary and multiple plasma-cell tumors of the jaws and oral cavity. Oral Surg. 22:628-639, 1966.
9. Smith, D.B.: Multiple Myeloma involving the jaws: Review with report of an additional case. Oral Surg. 10:910-919, 1957.
10. Lewin, R.W., Cataldo, E.: Multiple Myeloma discovered from oral manifestations: Report of case. J. Oral Surg. 25:68-72, 1967.
11. Worth, H.M.: Principles and Practice of Oral Radiographic Interpretation, Chicago, 1969, Year Book Medical Publishers, pp. 582-584.
12. Epstein, J.B., Voss, N.J.S., Stevenson-Moore, P.: Maxillo-facial manifestations of Multiple Myeloma. An unusual case and a review of the literature. Oral Surg. 57:267-271, 1984.
13. Sippel, H.W., Natiella, J.R., Greene, G.W.: Multiple Myeloma: Review and report of case. J. Oral Surg. 27:808-819, 1969.
14. Pruzanski, W., Watt, J.G.: Serum viscosity and hyperviscosity syndrome in IgG Multiple Myeloma. Ann. Intern. Med. 77:853-858, 1972.
15. Hobbs, J.R.: Immunochemical classes of myelomatosis, including data from a theurapeutic trial conducted by a medical research council working party. Brit. J. Haemat. 16:599-606, 1969.
16. Bartl, R., Frisch, B., Burkhardt, R., Fateh-Moghadam, A., Mahl, G., Gierster, P., Sund, M., Kettner, G.: Bone marrow histology in myeloma: its importance in diagnosis, prognosis, classification and staging. Brit. J. Haemat. 51:361-375, 1982.
17. Canale, D.D., Collins, R.D.: Use of bone marrow particle sections in the diagnosis of Multiple Myeloma. Am. J. Clin. Path. 61:383-392, 1974.
18. Huyn, B.H., Kwa, D., Gabaldon, H., Ashton, J.K.: Reactive plasmacytic lesions of the bone marrow. Am. J. Clin. Path. 65:921-928, 1975.
19. Hansen, O.O.: Bone marrow studies in Myelomatosis. Scan. J. Haematol. 21:265-272, 1978.
20. Glenner, G.G.: Amyloid deposits and Amyloidosis: The β-Fibrilloses (First of two parts). N. Engl. J. Med. 302:1283-1292, 1980.
21. Glenner, G.G.: Amyloid deposits and Amyloidosis: The β-Fibrilloses (Second of two parts). N. Engl. J. Med. 302:1333-1343, 1980.

22. Scheinberg, M.A., Cathcart, E.J.: New concepts in the pathogenesis of primary and secondary amyloid disease. Clin. Exp. Immunol. 33:185-190, 1978.
23. Glenner, G.G., Page, D.L.: Amyloid, amyloidosis and amyloidogenesis. In: Richter G.W., Epstein, M.A. eds: International Review of Experimental Pathology. Vol. 15, New York, 1976, Academic Press, pp. 1-92.
24. Shustik, C., Bergsagel, D.E., Pruzanski, W.: κ and λ Light Chain Disease: Survival rates and clinical manifestations. Blood 48:41-51. 1976.
25. Maldonado, J.E., Velosa, J.A., Kyle, R.A., Wagoner, R.D., Holley, K.E., Salassa, R.M.: Fanconi Syndrome in adults. A manifestation of a latent form of Myeloma. Am. J. Med. 58:354-364, 1975.
26. Smith, D.B.: Multiple Myeloma involving the jaws. Review with report of an additional case. Oral Surg. 10:910-919, 1957.
27. Maldonado, J.E., Brown, A.L., Jr., Bayrd, E.D., Pease, G.L.: Ultrastructure of the myeloma cell. Cancer 19:1613-1627, 1966.
28. Maldonado, J.E., Brown, A.L., Jr., Bayrd, L., Bayrd, E.D., Pease, G.L.: Cytoplasmic and intranuclear electron-dense bodies in the myeloma cell. Light and electron microscopy observations. Arch. Path. 81:484-500, 1966.
29. Tavassoli, M., Baughan, M.: Virus like particles in human myeloma without paraproteinemia. Arch. Pathol. 96:347-349, 1973.
30. Fitchen, J.H., Lee, S.: Phagocytic myeloma cells. Am. J. Clin. Path. 71:722-723, 1979.
31. Ludwig, H., Pavelka, M.: Phagocytic plasma cells in a patient with Multiple Myeloma. Blood 56:173-176, 1980.
32. Raman, S.B.K., van Slyck, E.J.: Nature of intracytoplasmic crystalline inclusions in myeloma cells (morphologic, cytochemical, ultrastructural, and immunofluorescent Studies). Am. J. Clin. Path. 80:244-228, 1983.
33. Wirt, D.P., Grogan, T.M., Payne, C.M., Kummet, T.D., Durie, B.G.M., Finley, P.R., Rollins, D.: Phagocytic, Lambda Light* Chain Plasma Cell Myeloma. Am. J. Clin. Path. 80:75-84, 1983.
34. Chen, S.Y.: Ultrastructure of a plasma-cell myeloma in the mandible. Oral Surg. 48:57-63, 1979.
35. Howatson, A.F., McCulloch, E.A.: Virus-like bodies in a transplantable mouse plasma cell tumour. Nature 181:1213-1214, 1958.
36. Porter, D.D., Dixon, F.J., Larsen, A.E.: The development of a myeloma-like condition in mink with Aleutian Disease. Blood 25:736-742, 1965.
37. Mitchell, D.N., Rees, R.J.W., Salsbury, A.J.: Possible transmissibility of human myelomatosis in immunologically deficient mice. Lancet, ii:1009-1012, 1971.

# Multiple myeloma presenting as localized expansile jaw tumour

**E. J. Raubenheimer[1], G. E. Lello[2], J. Dauth[3], M. S. Fayman[2], N. Dvornak[3] and J. C. Senekal[3]**

[1]Department of Oral Pathology; [2]Department of Maxillofacial and Oral Surgery; [3]Department of Chemical Pathology, Medical University of Southern Africa, Medunsa

*E. J. Raubenheimer, G. E. Lello, J. Dauth, M. S. Fayman, N. Dvornak and J. C. Senekal: Multiple myeloma presenting as localized expansile jaw tumour. Int. J. Oral Maxillofac. Surg. 1988; 17: 382–385.*

*Abstract.* Myelomatous involvement of the maxilla is an exceptionally rare occurrence, and the presentation of the lesion as an expansile jaw bone tumour has not been reported. 2 cases, one with a maxillary lesion, the other with a mandibular lesion are presented, both of which illustrate gross bone expansions. Additionally, 1 case presented with a rare biclonal IgG kappa and IgG lambda light chain secreting myeloma. Relevant clinical, immunological, histological, biochemical and histochemical features are presented and discussed, and suggestions pertaining to surgical management made.

Key words: myeloma; jaw tumours.

Accepted for publication 25 June 1988

Multiple myeloma is a malignant neoplastic condition characterized by uncontrolled proliferation of a clone of abnormal plasma cells. The clinical features of the disease may be directly due to the proliferating process itself and/or indirectly to substances released by the neoplastic cells. The former results in bone marrow displacement and multiple osteolytic lesions with pathologic fractures and pain, while the latter results in the elaboration of high levels of circulating monoclonal immunoglobulins, osteoclast-activating factor and other regulating substances. The circulating monoclonal immunoglobulins or their sub-units may lead to proteinuria, renal tubular damage and amyloid deposits. Stimulation of osteoclasts may result in hypercalcaemia and bone loss.

Myelomatous infiltrates have a predilection for areas of haemopoiesis and commonly involve the calvaria and mandible[1], pelvis, ribs, sternum, clavicles and proximal portions of the humerus and femur. Multiple myeloma is usually not associated with extraskeletal lesions, but occasionally lymph nodes, liver, spleen, and other organs are involved. The preliminary clinical diagnosis often relies on the identification of multiple, punched-out, lytic bone lesions. Involvement of the maxilla is regarded as exceptional[4, 9] and the clinical presentation of myeloma as an expansile jaw bone tumour is a rarely-described feature[10]. Myeloma as an expansile bone tumour in other skeletal regions has been adequately covered in the literature. 2 cases are presented, illustrating features of expansile jaw bone tumours.

## Case histories

### Case no. 1

A 40-year-old black man presented with a swelling in the region of the right zygomatic eminence. The swelling had been present for a few months, and had progressively enlarged during this period. Although the patient reported some recent, unexplained weight loss, a more detailed history was unobtainable. He was a known schizophrenic for which he had received treatment for the past 3 years.

On examination, a 4 × 3 cm bony hard, painless, fixed mass was palpable in the region of the right zygomatic eminence, with softer, more nodular and slightly mobile extensions beneath the right lower eye lid, lateral to the right nasal ala, and in the right temporal region. The margins of the lesion were poorly delineated (Fig. 1a). No neck lymphnodes were palpable.

Infra-orbital nerve sensation was diminished, and intra-orally, the occlusion was unimpaired despite some expansion of the lateral wall of the sinus into the maxillary buccal vestibulum. Orbital movements were full, and gross vision intact. Although a physical examination was normal, the patient was disoriented in time and place. X-rays showed an ostcolytic lesion involving the frontal and zygomatic processes of the maxilla and the right zygoma. The antero-lateral wall of the right maxillary sinus was expanded and eroded, as was the right inferior orbital margin (Fig. 1b). A computer tomographic scan confirmed the invasion of the tumour into the inferior turbinate bone, maxillary sinus, right infratemporal space, orbital floor and palatine bone. Technetium phosphate bone scans revealed no lesions in the rest of the skeleton. A differential diagnosis of a carcinoma of the maxillary sinus, an osteogenic sarcoma or odontogenic myxoma was made at this stage. Serum protein electrophoresis showed a monoclonal band in the gamma region which on immunofixation electrophoresis (IFE) was shown to be distinct monoclonal IgG bands, one with kappa and the other with lambda light chains (Fig. 2a); IFE of urine showed low concentrations of IgG kappa only. Bradshaw and boiling tests for Bence-Jones proteinuria were negative. Immunoparesis was absent, but the patient had a slight normocytic normochromic anaemia with a severely raised erythrocyte sedimentation rate (ESR). Other relevant biochemical and haematologic findings shown in Table I were normal.

Microscopic examination of a maxillary biopsy showed a diffuse infiltrate of plasma cells. Endosteal invasion with extensive osteoclastic activity was noted (Fig. 2b) and scattered foci of tumour necrosis were associated with an infiltrate of eosinophils. Immunoperoxidase stains (Immunolok Histoset, Immunolok Inc.; Carpinteria, USA) were distinctly positive for IgG and kappa light chains and scattered neoplastic cells also reacted positively for lambda light chains, confirming the biclonal nature of the infiltrate.

A diagnosis of a biclonal IgG kappa and IgG lambda light chain-secreting myeloma with only mid-facial involvement was established and a course of radiotherapy was given.

### Case no. 2

A female patient, approximately 70 years of age, was admitted from a rural hosptial with

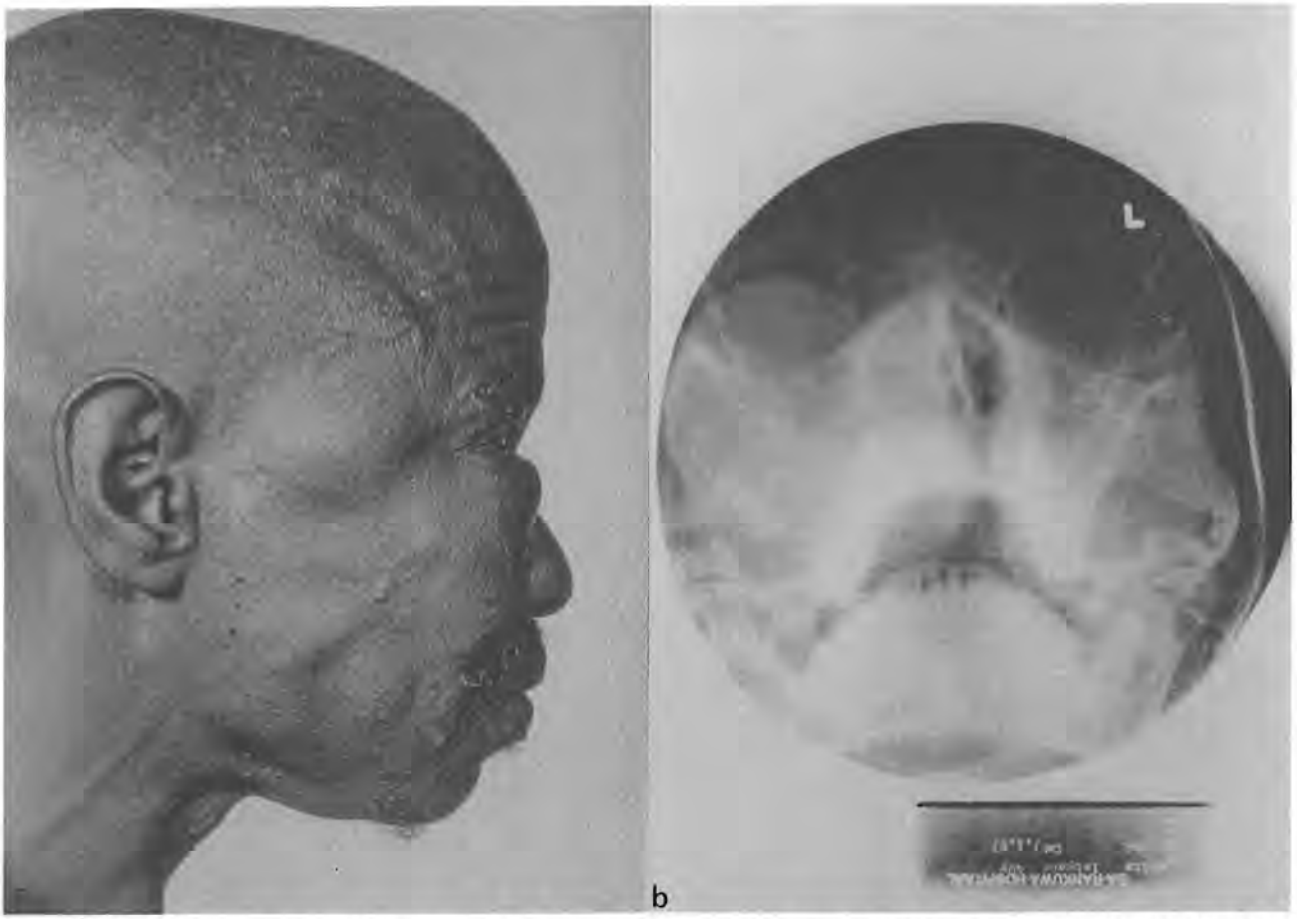


*Fig. 1.* (a). 40-year-old male (case no. 1) with myelomatous tumours above the right zygomatic arch, beneath the orbit, lateral to the ala and overlying the zygomatic eminence. (b) Radiograph of the case depicted in (a), showing destruction of the right maxillary sinus, inferior orbital margin, zygoma and lateral wall of the nose.

a history of painful mandibular teeth associated with a rapidly enlarging swelling. On external examination, a 10 × 6 cm tumour appeared to extend from the right mandibular second premolar area to the angle of the jaw on the left side. The tumour protruded extraorally, preventing lip closure, and sensory function of the left and right mandibular nerve was lost. Intraoral examination revealed traumatic mucosal ulcerations and severe displacement of teeth. A lipoma, 15 cm in diameter, was present in her right scapular region and she was severely anaemic. Radiographs of the mandible showed a poorly-defined lytic lesion with cortical bone destruction and extension into the symphysis of the left mandible. Full body radiographic examination revealed no further abnormalities. A clinical differential diagnosis of an odontogenic myxoma or osteogenic sarcoma was made.

Serum protein electrophoresis and immunofixation techniques showed a monoclonal lambda light chain band in the inter beta-region. Other findings included impairment of renal function, normocytic normochromic anaemia and a raised ESR (Table 1). Urinalysis was not done due to the patient's sudden exitus caused by acute renal failure. Microscopic examination of the mandibular tumour revealed a diffuse infiltrate of plasmablasts. Many cells were severely pleomorphic and extensive bone resorption was observed. All neoplastic cells stained positive with immunoperoxidase techniques for lambda light chains only. At autopsy, an interstitial nephritis with renal tubular damage, and a 1 × 2 cm lytic lesion of the right 6th rib with a microscopic appearance consistent with myeloma, was revealed. A diagnosis of lambda light-chain-secreting myeloma presenting clinically as a solitary expansible mandibular tumour, was made.

## Discussion

Multiple myeloma should be distinguished from solitary plasmacytoma of bone, a condition which is described as a single plasma cell proliferation in the absence of anaemia[2]. Plasmacytoma of bone has a better prognosis than multiple myeloma and has at least a 3-year disease-free period after adequate radiotherapy. The distinction between solitary plasmacytoma and myeloma, however, is not always clear and both these disease processes probably form part of a continuous spectrum of neoplastic plasma-cell proliferation. Although our cases may have originated as plasmacytomas, we regard both as overt myelomas. Case no. 1 exhibited signs of localized dissemination with involvement of the maxilla, maxillary antrum and zygoma, and case no. 2 had a profound anaemia and a distant neoplastic deposit.

The laboratory diagnosis of multiple myeloma is multidisciplinary and primarily encompasses biochemical identification of a monoclonal peak of immunoglobulin or subunits thereof, and microscopic demonstration of a plasma cell infiltrate in excess of 30 volume % is diagnostic of myeloma[2]. Furthermore, microscopic and biochemical parameters are important in determining the prognosis of the disease. Light-chain-secreting myelomas are said to have

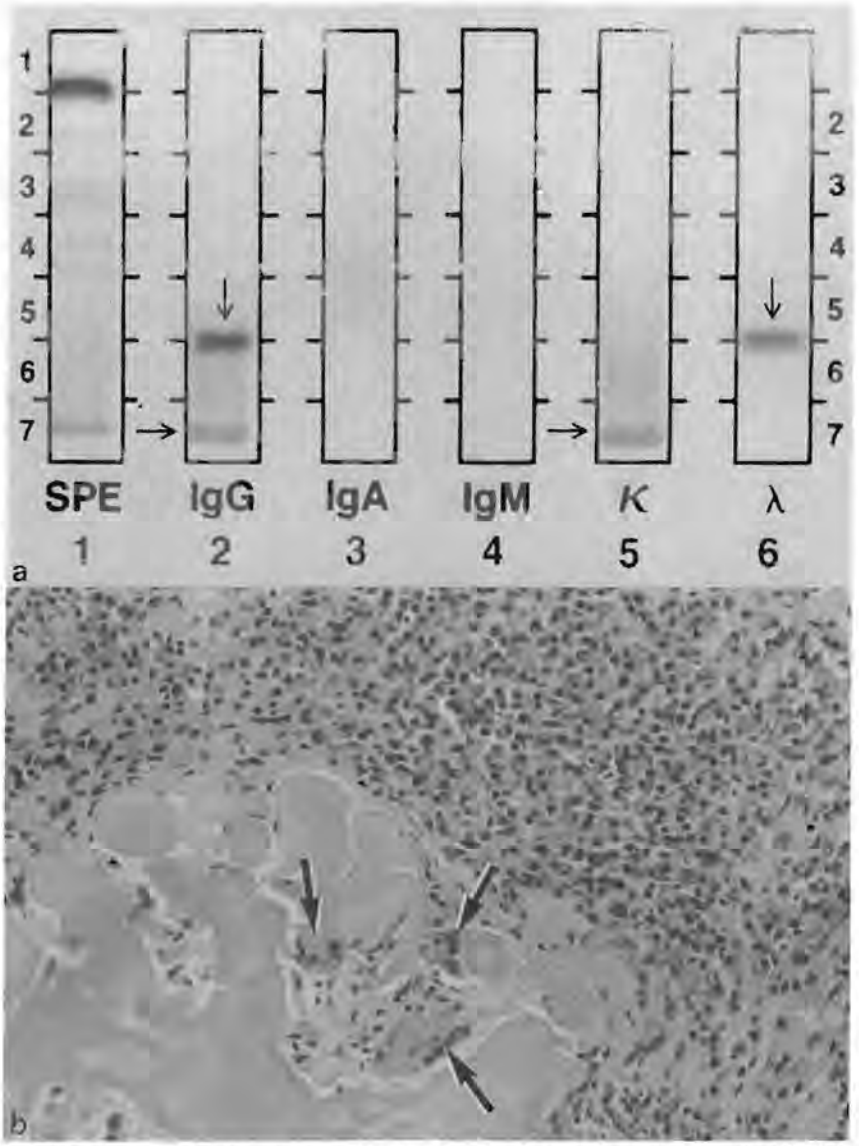


*Fig. 2.* (a) Serum IFE of case no. 1 showing 2 monoclonal IgG bands (arrows) with their corresponding kappa and lambda light chains (arrows). (b) Diffuse infiltrate of plasma cells (case no. 1). Note the disruption of the endosteum and osteoclastic activity (arrows). (HE stain, ×60).

the fastest growth rate and are associated with more osteolytic lesions than other immunochemical varieties[7,12] and typing of the light chain by means of IFE (or other methods), should always be carried out, because the median survival time of lambda light-chain disease is reported to be significantly shorter than kappa-light disease[5]. Plasma cell maturity and the extent of infiltration of myeloma cells in the biopsy is highly significant in predicting the duration of survival[1]. Plasmablastic myelomas are characterized by an infiltrate of nucelolated plasma cells and usually have a grave prognosis which is aggravated by hypercalcaemia and renal insufficiency[1,8].

Biclonal gammopathies, although relatively rare, are well documented[7]. These authors found 57 patients with biclonal gammopathies between 1966 and 1979 and only 6 had 2 IgG components (similar to our case no. 1). The immunoperoxidase stains of plasma cells in our case showed that there were 2 different cell populations synthesizing the para-proteins, and not a single cell population or precursor cells "switching" from one immunoglobulin class to another[6]. Furthermore, in a study of 56 patients with more than one paraprotein, Gore *et al.*[6] found no evidence that multiband myeloma has a worse prognosis than myeloma with a monoclonal protein. Kyle *et al.*[7] also found the clinical features of biclonal gammopathy and its response to therapy similar to those of monoclonal gammopathy.

Although myeloma does not present frequently as a solitary expansile tumour, it should not be excluded from the differential diagnosis of a localized expansile tumour of the jaw. If multiple myeloma is suspected, a multidisciplinary approach towards the diagnosis should always be followed. The physician should obtain a full blood count with differential and platelet counts, biochemical assessment of renal function, calcium status, serum protein electrophoresis, quantification of immunoglobulins, IFE or immunoelectrophoresis, bone marrow biopsy and aspiration, urinalysis which includes IFE and a radiographic skeleton survey[8].

Surgery has few indications in the treatment of lesions within the jaw bones. Decortication of adjacent sections of the mandible or removal of sequestrae when osteomyelitis intervenes as a consequence of impaired and depressed immunity may be necessary.

Pathological fractures of the mandible may require long-term splinting by means of arch bars or metal cap splints in order to minimize patient discomfort when fractured bone ends fail to unite. Small lesions related to pathological fractures could be excised and the gap bridged by an appropriate metal plate and fixation screws, placed well clear of the lesion, in order to splint the mobile bone segments. In this way, the patient with a good prognosis will be afforded the ability to function until such time, should it arise, when graft reconstruction may be contemplated. Immediate reconstruction of resected segments of involved bone should be attempted, particularly when a patient, debilitated only in terms of jaw function but with an otherwise good prognosis, presents for treatment. Less readily excisable lesions may be debulked, especially when encroaching upon such important organs as the eye, and particularly so when the prognosis is good. It must however be borne in mind that although a patient may present with only one detectable lesion, as in our second case, the disease is held by many to be multicentric in origin[13] and thus apparent control of the primary lesion may prove fallacious. The prognosis may be particularly difficult to determine. Furthermore, rapid deterioration and demise may occur as a result of secondary complications, as happened in our 2nd case.

*Table 1.* Relevant biochemical and haematological findings

| | Reference ranges | Case no. 1 | Case no. 2 |
|---|---|---|---|
| total protein (g/l) | 60–80 | 80 | 57 |
| albumin (g/l) | 26–52 | 33 | 28 |
| urea (mmol/l) | 2.5–6.7 | 4.4 | 28.9 |
| creatinine (μmol/l) | 53–97 | 79 | 477 |
| total calcium (mmol/l) | 2.25–2.70 | 2.25 | not done |
| IgG (g/l) | 6.4–13.5 | 33 | 9.61 |
| IgA (g/l) | 0.7–3.12 | 5.67 | 1.60 |
| IgM (g/l) | 0.56–3.50 | 0.66 | 0.70 |
| WBC ($\times 10^9$/l) | 7.5±3.5 | 9.17 | 9.89 |
| RBC ($\times 10^{12}$/l) | 4.8±0.6 (females)<br>5.8±1.0 (males) | 4.33 | 2.69 |
| Hb (g/dl) | 14.0±2.0 (females)<br>16.4±2.8 (males) | 12.6 | 8.9 |
| ESR (mm/h Westergren) | 3–15 (females)<br>1–10 (males) | 104 | 64 |
| platelets ($\times 10^9$/l) | 150–400 | 355 | 338 |

These complications include predominantly renal failure, infection and anaemia. Patients presenting with multiple myeloma lesions have a poor prognosis, with a median survival time of 2–3 years, and surgical considerations should be weighed against this background and the patients' response to radiation and chemotherapy, as surgery can only be comtemplated as a palliative procedure.

*Acknowledgements* – We thank Mrs. L. Boyes, Mrs. B. Lentz, Mr. C. Lourens and Mr. J. P. de Coning for their assistance and Mrs. M. Barnard for secretarial services.

## References

1. Bartl, R., Frisch, B., Burkhardt, R., Fateh-Moghadam, A., Mahl, G., Gierster, P., Sund, M. & Kettner, G.: Bone marrow histology in myeloma: its importance in diagnosis, prognosis, classification and staging. *Br. J. Haematol.* 1982: **51**: 361–374.
2. Corwin, J. & Lindberg, R. D.: Solitary plasmacytoma of bone vs. extramedullary plasmacytoma and their relationship to multiple myeloma. *Cancer* 1979: **43**: 1007–1013.
3. Drurie, B. G. M. & Salmon, S. E.: A clinical staging system for multiple myeloma. *Cancer* 1975: **36**: 842–854.
4. Epstein, J. B., Voss, N. J. S. & Stevenson-Moore, P.: Maxillofacial manifestation of multiple myeloma. An unusual case and a review of the literature. *Oral Surg.* 1984: **57**: 267–271.
5. Farhangi, M. & Osserman, E. F.: Biology, clinical patterns and treatment of multiple myeloma and related plasma cell dyscrasias. In: Twomey, J. J. & Good, R. A. (eds.): *The immunopathology of lymphoreticular neoplasms; comprehensive immunology.* Plenum Medical Books New York 1978, p. 641.
6. Gore, M. E., Riches, P. G. & Kohn, J.: Identification of the paraproteins and clinical significance of more than one paraprotein in serum of 56 patients. *J. Clin. Pathol.* 1979: **32**: 313–317.
7. Kyle, R. A., Robinson, R. A. & Katzmann, J. A.: The clinical aspects of biclonal gammopathies. Review of 57 cases. *Am. J. Med.* 1981: **71**: 999–1008.
8. Kyle, R. E.: Diagnosis and management of multiple myeloma and related disorders. *Progress in Haematol.* 1986: **14**: 257–280.
9. Orlean, S. L. & Blewitt, M. D.: Multiple myeloma with manifestation of a bony lesion in the maxilla. Report of a case. *Oral Surg.* 1965: **19**: 817–824.
10. Prein, J. et al.: *Atlas of tumors of the facial skeleton.* Springer Verlag, 1986.
11. Raubenheimer, E. J., Dauth, J. & Van Wilpe, E.: Multiple myeloma: a study of 10 cases. *J. Oral Path.* 1987: **8**: 383–389.
12. Schustik, C., Bergsagel, D. E. & Pruzanski, W.: Kappa and lambda light chain disease: survival rates and clinical manifestations. *Blood* 1976: **48**: 41–51.
13. Shafer, W. G., Hine, M. K. & Levy, B. M.: *A textbook of oral pathology.* W. B. Saunders Company, Philadelphia 1984, p. 191.

Address:
*E. J. Raubenheimer*
*Department of Oral Pathology and Oral Biology*
*P.O. Box D24*
*Medunsa 0204*
*Republic of South Africa*

# Multiple myeloma: a study of 10 cases

**E. J. Raubenheimer[1], J. Dauth[2], E. van Wilpe[3]**

Departments of [1]Oral Pathology, [2]Chemical Pathology, [3]Anatomical Pathology, Medical University of Southern Africa, Medunsa, South Africa.

Raubenheimer EJ, Dauth J, Van Wilpe E. Multiple myeloma: a study of 10 cases. J Oral Pathol 1987: 16: 383–388.

The clinical, radiographical, biochemical, microscopical and ultrastructural features of 10 cases of multiple myeloma were studied. The skull and jaw regions were frequently involved by the disease and although the diagnosis remains multidisciplinary, microscopical parameters differentiating a myelomatous bone marrow infiltrate from a reactive plasmacytosis are discussed. Biochemical and microscopical factors influencing the prognosis are highlighted and significant ultrastructural findings include erythrophagocytosis, cytoplasmic nuclear asynchrony of plasmablasts and intranuclear viral like inclusions.

Professor E. J. Raubenheimer, Department of Oral Pathology, Medical University of Southern Africa, PO Medunsa 0204, SOuth Africa.

Accepted for publication June 1st, 1987.

Multiple myeloma (MM), a disease of the elderly, is characterized by neoplastic proliferation of a clone of plama cells capable of synthesizing and secreting immunoglobulin (Ig) or its subunits. Common systemic findings include multiple lytic bone lesions with pathologic and compression fractures, hypercalcèmia, anemia, renal tubular disease with renal insufficiency and infections secondary to immunosuppression (1). Frequent oral manifestations of multiple myeloma are pain, swelling, numbnees, mobility of teeth (2) and enlargement of the tongue, salivary glands and soft tissue tumors as a result of amyloid deposits (3). Radiolytic lesions are rarely found in the maxilla (4) and although lytic bone lesions are more frequent in the mandible, MM patients may present with diffuse osteoporosis (3), or even a destructive expansile mandibular tumor (5).

Monoclonal Ig's or fractions thereof secreted by the neoplastic plasma cells can be demonstrated in the serum and urine of the majority of patients and circulating free light chains (Bence Jones proteins) are often associated with amyloid deposits in tissues (1). Only in rare instances are the secretory products absent and these cases are referred to as non-secretory myelomas. The IgG class of MM accounts for approximately 66% while the combined IgA, IgM and Bence Jones types constitute 29% of cases. Rare variations of MM (including the IgD, IgE and heavy chain types) and biclonal and triclonal forms account for the remainder (1).

As a multitude of non-neoplastic conditions can give rise to a bone marrow plasmacytosis, the diagnosis of MM should always follow a multidisciplinary approach encompassing radiographic, biochemical and bone marrow microscopic investigations. A bone biopsy, however, provides useful information on the diagnosis, classification and staging of patients with MM (6).

A limited number of investigations on the ultrastructure of neoplastic plasma cells have been reported in the literature. Characteristically the cells exhibit large amounts of rough endoplasmic reticulum arranged in lamellar patterns, abundant mitochondria in perinuclear locations, prominent Golgi complexes (7, 8) and cytoplasmic microfilaments (9). Occasional erythrophagocytosis and uptake of cells of the myeloid series and even platelets by myeloma cells may result in a hemolytic anemia (9, 10). Intranuclear and intracytoplasmic crystalline inclusions have been suggested to be related to the process of abnormal immunoglobulin synthesis (11), may be of lysosomal origin (12) or may even represent viral inclusions (13).

This study was undertaken to correlate the light and electron microscopical appearances of biopsies of 10 consecutive cases of MM with clinical, radiographical and biochemical findings. Furthermore, the incidence of oral and skull involvement in the group of patients was determined.

## Material and methods

The age and sex incidence, presenting complaints, radiographic distribution of lesions, immunochemical subtype and other relevant biochemical changes of 10 consecutive cases with MM were studied on admission. Serum total protein, albumin, urea and creatinine levels were determined with a continuous flow analyzer (SMA II, Technicon Instruments Corp, Tarrytown, NY 10591) and serum total calcium levels by atomic absorption spectrophotometry (Perkin-Elmer Corp., Norwalk, Connecticut 06856 USA). Quantitation of IgG, IgA and IgM levels were done with rate nephelometry (Auto ICS, Beckman Instruments Inc, Fullerton, USA). Immunochemical typing of the heavy and light chains in serum and concentrated urine was carried out with immunofixation electrophoresis (Paragon™ IFE gels, Beckman Instruments Inc.).

Trephine biopsies were taken of lytic bone lesions and fixed in buffered formalin and glutaraldehyde followed by osmium tetroxide for light and transmission electron microscopy respectively. Biopsies intended for light microscopy were divided into 2 portions. One portion was routinely decalcified (EDTA) and embedded in paraffin wax. Sections 4 μ thick were cut and stained with hematoxylin, eosin, Gomori's stain for reticulin fibres, periodic acid schiff (PAS) for glycoproteins, Berlin Blue stain for iron and immunoperoxidase stains (Immunolok Histo-

Table 1. Biochemical findings.

| Serum | Reference value | Patient (sex and age) | | | | | | | | | |
|---|---|---|---|---|---|---|---|---|---|---|---|
| | | Case 1 (M,25Y) | Case 2 (M,76Y) | Case 3 (M,72Y) | Case 4 (F,56Y) | Case 5 (F,72Y) | Case 6 (F,67Y) | Case 7 (M,65Y) | Case 8 (M,62Y) | Case 9 (M,65Y) | Case 10 (F,70Y) |
| Total protein (g/l) | 60–80 | 67 | 63 | 101 | 97 | 98 | 61 | 97 | 140 | 93 | 57 |
| Albumin (g/l) | 28–52 | 38 | 27 | 24 | 46 | 29 | 43 | 31 | 32 | 31 | 28 |
| Urea (mmol/l) | 2.5–6.7 | 4.1 | 19.5 | 5.6 | 6.2 | 5.5 | 8.8 | 7.5 | 5.6 | 10.1 | 28.9 |
| Creatinine (umol/l) | 53–97 | 70 | 527 | 101 | 61 | 86 | 63 | 99 | 87 | 106 | 477 |
| Total calcium (mmol/l) | 2.25–2.70 | 1.94 | 2.16 | 2.09 | not done | 2.58 | 2.72 | 2.35 | 2.61 | 3.00 | not done |
| Immunochemical type | – | Bence-Jones kappa | IgG lambda | IgG lambda | IgG kappa | IgG kappa | IgA kappa non-secretor | IgA lambda | IgG kappa | IgG kappa | Bence-Jones lambda |
| IgG (g/l) | 6.4–13.5 | 12.0 | 15.9 | 84.9 | 37.9 | 65.0 | 6.05 | 8.3 | 104 | 69.9 | 9.6 |
| IgA (g/l) | 0.7–3.12 | 1.20 | 4.44 | 1.07 | 0.65 | 0.45 | 0.32 | 60.70 | 8.34 | 0.49 | 1.60 |
| IgM (g/l) | 0.56–3.50 | 0.75 | 1.36 | 0.58 | 0.62 | 0.26 | 0.47 | 0.40 | 0.40 | 0.27 | 0.70 |
| Urine Light chain type | | kappa | lambda | lambda | kappa | absent | absent | absent | kappa | absent | lambda |

set, Immunoloc Inc., Carpinteria, California) for IgG, IgA, IgM and kappa and lambda light chains. The other portion of the biopsy was embedded in plastic without decalcification and sections 2 μ thick were cut and stained with hematoxylin, eosin, modified Gomori's stain for reticulin, methyl green pyronine stain for plasma cells and Prussian blue stain for ferric iron. Tissues for electron microscopy were embedded in Araldite and ultrathin sections were cut and examined with a Joel 100 cx II electron microscope.

Four quantitative and 3 semiquantitative parameters were studied light microscopically. The quantitative parameters included the predominant morphologic cell type (plasmablastic or plasmacytic determined by the presence or absence of a nucleolus), the immunochemical subtype (IgA, IgM, IgG, kappa or lambda), the stage of the disease (according to the quantity of plasma cell infiltration in the biopsy: Stage 1 less than 20 volume percent, Stage 2:20 – 50 vol. %, Stage 3 more than 50 vol. %) and trabecular bone volume (expressed as percentage of total surface area of the section as measured with an image analyzer). The semiquantitative parameters included the proliferation pattern of the plasma cells (nodular or diffuse), endosteal invasion, disruption of the reticulin pattern of the bone marrow and the degree of hemopoietic depression which were expressed as absent, slight, moderate or severe.

Ultrastructurally, attention was given to deviations of cytoplasmic and nuclear morphology.

## Results

The series consisted of 4 female and 6 male patients and the age at diagnosis varied from 25–76 years (mean 63 years). Two patients presented with complaints of generalized skeletal pains, 2 with vertebral collapse and paraplegia, 2 with oral and paraoral complications and one with a pathological fracture of the left femur. The presenting symptoms of 3 patients were unknown. Of the 3 with oral complaints, Case 1 had an enlarged tongue, parotid glands and mucosal swellings. Microscopical examination of these lesions revealed extensive amyloid deposits. The other, Case 10, had a large tumour (10×6 cm) consisting of a neoplastic plasma cell infiltrate involving the anterior mandible.

Table 2. Microscopical findings.

| Microscopical parameter | Patients | | | | | | | | | |
|---|---|---|---|---|---|---|---|---|---|---|
| | Case 1 | Case 2 | Case 3 | Case 4 | Case 5 | Case 6 | Case 7 | Case 8 | Case 9 | Case 10 |
| Morphological cell type | Plasma-cytic | Plasma-blastic | Plasma-blastic | Plasma-cytic | Plasma-cytic | Plasma-cytic | Plasma-blastic | Plasma-cytic | Plasma-cytic | Plasma-blastic with bizarre cells |
| Immunochemical cell type | kappa | IgG lambda | IgG lambda | IgG kappa | IgG kappa | IgA kappa | IgA lambda | IgG kappa | negative | negative |
| Stage | 3 | 3 | 3 | 3 | 2 | 1 | 2 | 3 | 2 | 3 |
| Trabecular bone volume | 8.31 | 0.52 | 13.52 | 21.03 | 0.12 | 13.68 | 16.21 | 11 | 10.14 | 18 |
| Proliferation pattern | diffuse | nodular | diffuse | diffuse | diffuse | diffuse | diffuse | diffuse | nodular | nodular |
| Endosteal invasion | absent | present | present | present | absent | absent | present | present | absent | present |
| Reticulin disruption | +++ | ++ | ++ | ++ | + | – | + | +++ | + | +++ |
| Hemopoietic depression | +++ | ++ | +++ | ++ | + | – | – | +++ | – | +++ |

– = absent
+ = slight
++ = moderate
+++ = severe

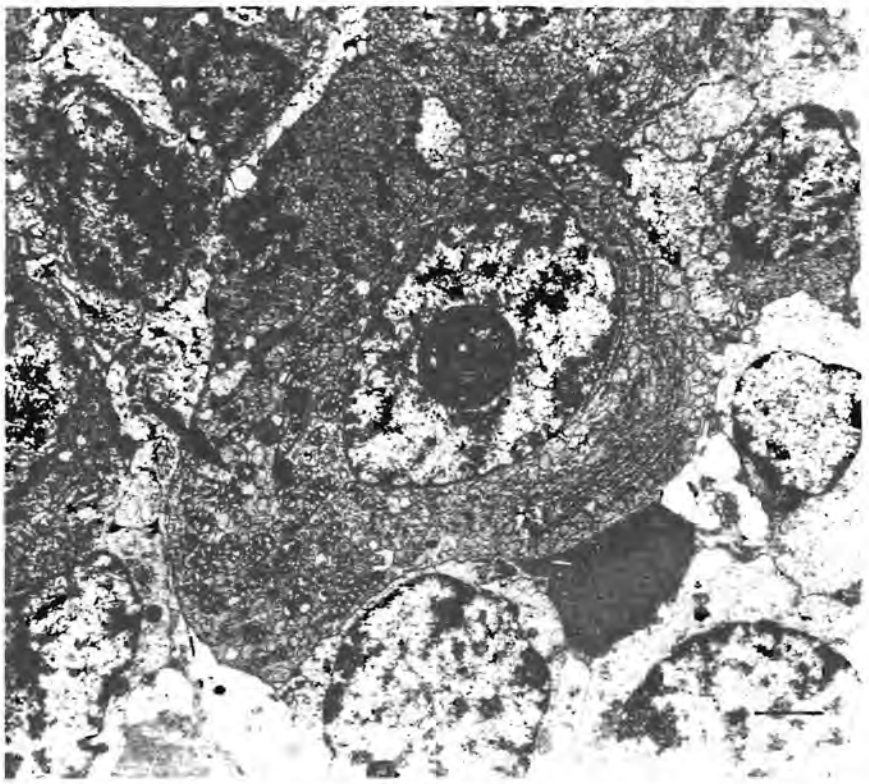

*Fig. 1.* Electron micrograph of a plasmablast. Note the prominent nucleolus and mature cytoplasm with endoplasmic reticulum, mitochondria and lysosomal iron pigment (arrow) (Bar = 2μ).

Multiple radiolytic lesions were present in 5 patients and involved the skull and vertebral bodies (4 cases), pelvic bones (3 cases) ribs and long bones (2 cases) and mandible (1 case). Localized lesions were present in 2 patients, affecting the femur head (Case 9) and mandible (Case 10). Case 6 exhibited diffuse osteoporosis, while one case had no bone lesions (Case 3) and radiographs were unobtainable in Case 2. Post mortem examination of the patient with the expansile mandibular tumor (Case 10) revealed an additional myelomatous deposit in the right sixth rib.

The relevant biochemical findings are shown in Table 1. The most common immunochemical type of MM was IgG kappa followed by IgG lambda. Light chains were absent from urine in 4 cases, one being the IgA non-secretor myeloma. Suppression of the levels of one or more normal (residual) immunoglobulins was found in 6 cases. Three cases had hypocalcemia and severe hypercalcemia was present in one case only (Case 9).

The microscopical findings are reflected in Table 2. Four cases were of the plasmablastic type (Fig. 1) and 6 cases of the plasmacytic type. Gomori stains were particularly helpful in identifying disruption of the reticulin fibre system of the bone marrow and the pattern of proliferation. Endosteal invasion with increased osteoclastic activity was identified in 6 cases (Fig. 2). Of all myelomas, those with multiple lytic lesions exhibited the least bone (9.86% of the total surface area of the section compared to an average 14.07% for cases with one or no lytic lesions). The one case with diffuse osteoporosis and no lytic lesions (Case 5) only had as little as 0.12% trabecular bone in the biopsy. Abundant cytoplasmic colloid, reacting with the PAS technique, was a prominent feature of the neoplastic cells in Case 6 (the non-secretor myeloma) and the immunoperoxidase technique confirmed the presence of intracytoplasmic IgA and kappa light chains in these cells. Immunoperoxidase stains facilitated the identification of the monoclonal nature of the infiltrate and correlated positively with the immunochemical type in 8 cases, the remaining 2 (Cases 9, 10) being negative with this technique.

In contrast to the ultrastructural features of normal plasma cells, electron microscopical investigations revealed a distended endoplasmic reticulum containing colloid in Case 6 (Fig. 3), red blood cell phagocytosis and lysosomal iron pigment in Cases 4 and 8 (Fig. 1), prominent cytoplasmic microfilaments in Cases 3 and 8, and cytoplasmic constrictions suggesting amoeboid movement and numerous microvilli on cell surfaces adjacent to other plasmacells

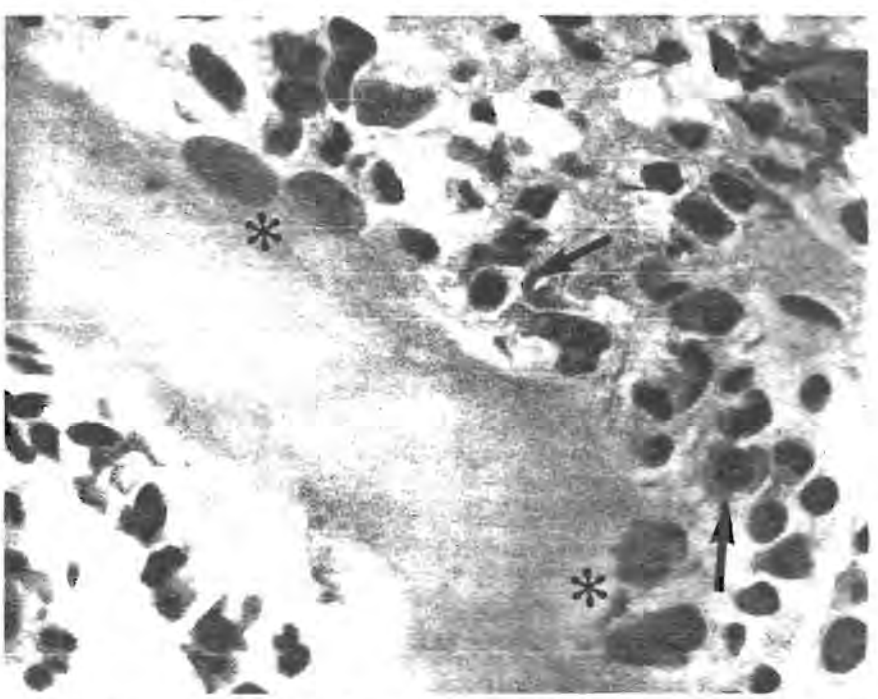

*Fig. 2.* Photomicrogaph showing endosteal invasion by neoplastic plasma cells (arrows) with osteoclastic activation (asterisk) and bone resorption (H&E, ×400).

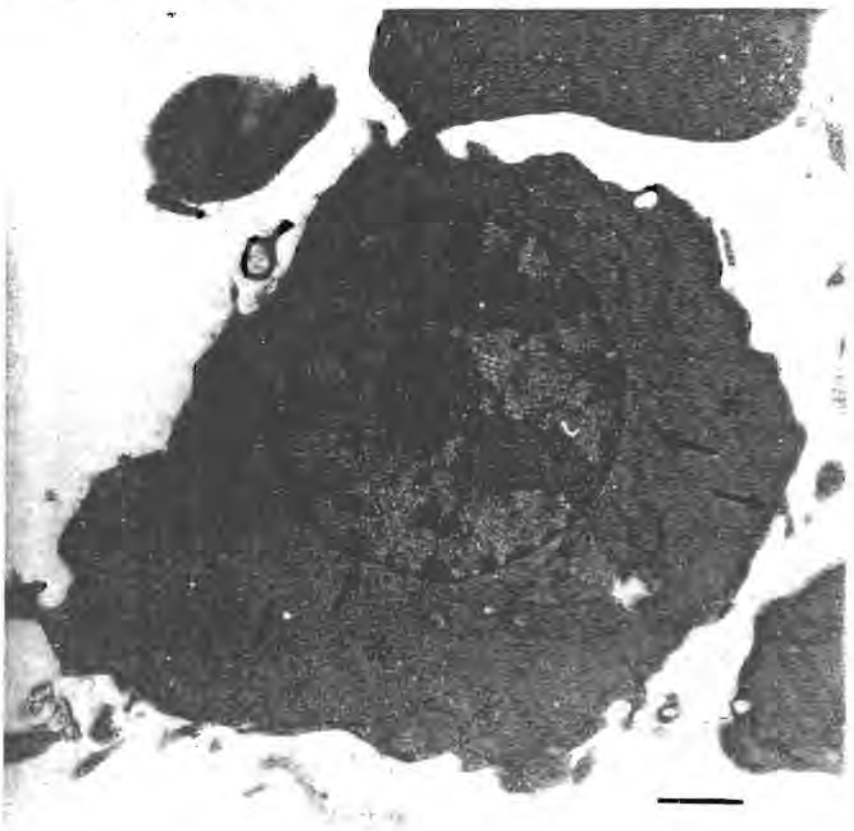

*Fig. 3.* Electron micrograph of a plasma cell in Case 6 showing distended endoplasmic reticulum (arrows) containing colloid (asterisk) (Bar = 2μ).

in Case 8 (Fig. 4). Case 10 showed intranuclear lattice like crystalline inclusions (Fig. 5) and all plasmablastic myelomas exhibited a discrepancy between nuclear and cytyoplamic maturity (Fig. 1).

Three patients (Cases 1, 5 and 10) died within one year of diagnosis. Post mortem examination revealed a chronic interstitial nephritis with renal tubular damage in Cases 1 and 10 and a fulminant opportunistic lung infection in Case 5.

## Discussion

The average age at the time of diagnosis of multiple myeloma is reported to be 62 years with less than 2% of all cases occuring before 40 years (14). These findings are supported by our series except for Case 1 whom should be regarded as exceptionally young for MM.

Involvement of the paraoral tissues, jaw and cranium ranks high as presenting clinical features of multiple myeloma. In a radiographic and case record survey of 59 cases, Bruce and Royer (4) found jaw involvement in 17 patients with MM. A more recent study indicated that the incidence of jaw involvement may even be higher (16). In our series 3 patients had radiographic demonstrable jaw lesions: one had a lytic lesion of the mandibular ramus (as part of multiple skeletal radiolucencies), one presented with a mandibular tumor which proved to be a myelomatous infiltrate and one patient presented with mandibular osteoporosis as part of a generalized osteoporosis. Furthermore, extensive oral and paraoral amyloid deposits in a fourth patient caused us to suspect and to investigate for MM, proving that oral involvement in this disease may be as high as 40%. If cranial involvement is also taken into account, the skull and jaw may be regarded as the region most commonly affected by MM. The extent of hemopoiesis in the calvaria of the skull may serve to explain this phenomenon as myelomatous infiltrates are reported to have a predilection for these areas (2, 4). The low incidence of maxillary involvement in MM (17) is supported by our study.

The occurence of the different immunochemical subtypes of myeloma in our study follows the pattern reported in the literature (1). However, Case 6, being a non-secretory IgA MM did not show any detectable paraprotein in the serum or urine. The final diagnosis was established only after radiographic and microscopic bone marrow investigations with immunoperoxidase staining had been performed. The presence of immune suppression further supported the diagnosis of MM. Non-secretory MM is a rare condition with a reported incidence of 1–5% of cases of MM (18, 19). Although our study indicates that immune suppression with decreased levels of one or more residual immunoglobulins do not occur in as many as the reported 98% of myeloma patients (1),

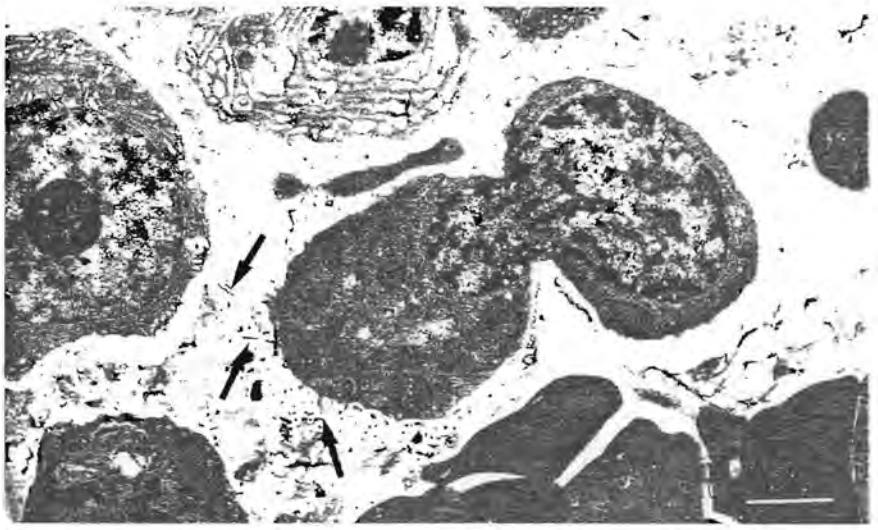

*Fig. 4.* Electron micrograph of plasma cell with a cytoplasmic constriction (centre). Note microvilli on the opposed surfaces of adjacent plasma cells (arrows) (Bar = 4μ).

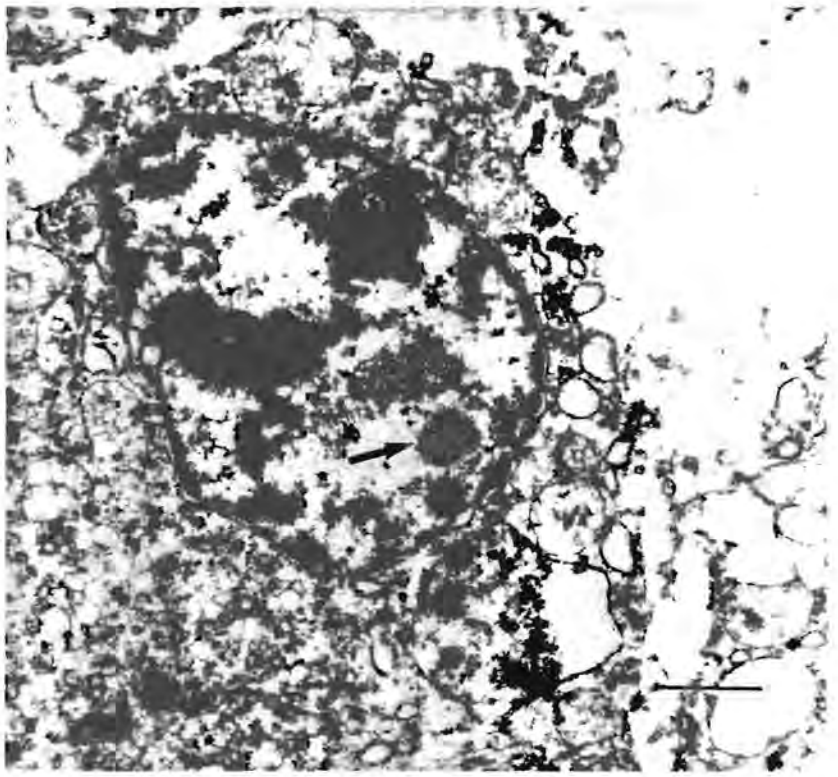

*Fig. 5.* Electron micrograph of tissue removed during autopsy from Case 6. The nucleus of a plasmablast contains a proteinaceous viral-like inclusion (arrow) and the cytoplasm shows autolytic change (Bar = 2μ).

this complication, which was identified in 6 of our cases, may lead to opportunistic infections and death.

Renal involvement due to the excretion of excessive light chains (20) and hypercalcemia (14) are 2 of the most important causes of renal failure and death in patients with myeloma. Light chain secreting myelomas are said to have the fastest growth rate and is associated with more osteolytic lesions than other immunochemical varieties (21). Furthermore, the median survival time of lambda-light chain disease is reported to be significantly shorter than kappa light chain disease (15, 21). Although our series was not large enough to draw definite conclusions on the prognosis of the immunochemical subtypes, both patients with light chain disease died within one year of diagnosis.

Neoplastic plasmacells are capable of inducing bone resorption by secreting osteoclast activating factor (OAF) (22), a phenomenon which is reported to be associated with frequent hypercalcemia (1, 23). Although our study supports the occurence of increased osteoclastic activity and bone loss in MM, a low to normal level of total circulating calcium appear to be more prevelant than hypercalcemia. As approximately one half of the total calcium is bound to albumin (25), hypocalcemia in patients with multiple myeloma may be associated with low levels of albumin which may be secondary to renal damage with albuminuria. However, only Case 2 with hypocalcemia had severe renal function impairment with low albumin levels while Case 1 with the lowest total calcium concentration had a normal serum albumin level. The reason for these findings remain unclear but we feel that the determination of ionized calcium levels in cases with MM may be more helpful as these determinations give a better assessment of the calcemic status especially in patients with renal function impairment (25).

Although microscopical examination of a bone marrow biopsy is reported to be more reliable in the diagnosis of multiple myeloma than aspiration cytology (6), the former technique has its limitations. It is often difficult to distinguish a neoplastic from a reactive bone marrow infiltrate, as the latter could lead to a bone marrow plasmacytosis in excess of 50 volume percent (26). Our study supports the observations of Bartl et al. (6) that microscopic findings such as the monoclonal nature of the infiltrate, plasma cell maturity, endosteal invasion, depression of hemopoiesis, bone resorption and disruption of the reticulin fibre pattern may be helpful in identifying a myematous infiltrate in a bone marrow biopsy. Furthermore, Stage 3 infiltrates in our patients were associated with moderate to severe reticulin fibre disruption and hemopoietic depression and exhibited more frequent endosteal invasion than Stages 1 and 2. With progression of the disease, the significance of the abovementioned microscopic parameters therefore appears to increase. It should be emphasized however, that unless the microscopical changes are convincing, the diagnosis of MM should not be established without biochemical and radiographic support.

Multiple myeloma of the plasmacytic type is characterized by the infiltration of small normal appearing plasma cells. The infiltrate in plasmablastic myelomas, on the other hand, are characterized by nucleolated and often pleomorphic cells. The higher mitotic rate of plasmablasts compared to plasmacytes and the fact that 2 of the 4 patients in our series with plasmablastic myelomas died within one year of diagnosis, support's Bartl's observation (6) that this type is associated with a rapid clinical deterioration.

Ultrastructurally, all plasmablastic infiltrates had a primitive nucleolated nucleus contained in a highly differentiated organelle-rich cytoplasm. The discrepancy in nuclear/cytoplasmic maturity (or nuclear/cytoplasmic asynchrony) may prove helpful in distinguishing neoplastic from reactive plasmablasts, the latter which would be expected to show matching cytoplasmic maturity with nuclear morphology. Cytoplasmic microfilaments may facilitate amoeboid movement and the identification of erythrophagocytosis may serve to explain the occurance of anemia, especially in cases not associated with extensive neoplastic bone marrow displacement. The significance of cytoplasmic microvilli which appeared to make contact with adjacent neoplastic cells remains speculative. Distention of the rough endoplasmic reticulum in the non-secretor myeloma cells may be indicative of an intact synthetic but defective immunoglobulin excretory mechanism. Immunoperoxidase stains support this observation as monoclonal cytoplasmic immunoglobulins of the IgA kappa type could be identified in this case. The lattice-like intranuclear inclusions identified in Case 10 were

not membrane bound and, therefore, do not represent nuclear invagination of crystalline cytoplasmic proteinaceous deposits. The inclusions may either be related to intranuclear protein synthesis (11) or represent 'passenger' virusses (13) finding optimal growth conditions within the milieu of the myeloma cell.

*Acknowledgements* – The authors wish to thank Mrs C. S. Begemann for secreterial assistance and Mr D. P. du Plessis for preparation of immunoperoxidase stains. We are also indebted to Drs N. Dvornak, J. Elias, J. Lottering, J. C. Senekal and P. van der Walt for collection of material and Mrs L. Boyes and Mrs B. Lentz for their assistance with special laboratory techniques.

## References

1. Ritzmann SE. Immunoglobulin abnormalities. In: Ritzmann SE, Daniels JC eds. Serum protein abnormalities. Diagnostic and clinical aspects. Boston: Little, Brown, 1975: 351.
2. Lewin RW, Cataldo E. Multiple myeloma discovered from oral manifestations: report of case. J Oral Surg 1967: *25:* 68.
3. Epstein JB, Voss NJS, Stevens-Moore P. Maxillofacial manifestations of multiple myeloma. An unusual case and a review of the literature. Oral Surg 1984: *57:* 267.
4. Bruce KW, Royer RQ. Multiple myeloma occuring in the jaws. A study of 17 cases. Oral Surg 1953: *6:* 729.
5. Raubenheimer EJ, Dauth J, Jordaan JB, du Toit LM, de Coning JP. Multiple myeloma presenting as a solitary expansile mandibular tumor. J Oral Med (in press).
6. Bartl R, Frisch B, Burkhardt R, et al. Bone marrow histology in myeloma: its importance in diagnosis, prognosis, classification and staging. Br J Haematol 1982: *51:* 361.
7. Chen S. Ultrastructure of plasma-cell myeloma of the mandible. Oral Surg 1979: *48:* 57.
8. Lazarus HM, Kellermeyer RW, Aikawa M, Herzig RH. Multiple myeloma in young men. Clinical course and electron microscopic studies of bone marrow plasma cells. Cancer 1980: *46:* 1397.
9. Wirt DP, Grogan TM, Payne CM, et al. Phagocytic, lambda light chain, plasma cell myeloma. Am J Clin Pathol 1983: *80:* 75.
10. Ludwig H, Pavelka M. Phagocytic plasma cells in a patient with multiple myeloma. Blood 1980: *56:* 173.
11. Muldonado JE, Brown AL, Bayrd ED, Pease GL. Cytoplasmic and intranuclear electron-dense bodies in the myeloma cell. Arch Pathol 1966: *81:* 484.
12. Raman SBK, van Slyck EJ. Nature of intracytoplasmic crystalline inclusions in myeloma cells (morphologic, cytochemical, ultrastructural and immunofluorescent studies). Am J Clin Pathol 1983: *80:* 224.
13. Tavassoli M, Baughan M. Virus-like particles in human myeloma without paraproteinemia. Arch Pathol 1973: *96:* 347.
14. Kyle RA. Multiple myeloma. Review of 869 cases. Mayo Clin Proc 1975: *50:* 29.
15. Farhangi M, Ossermann EF. Biology, clinical patterns and treatment of multiple myeloma and related plasma cell dyscrasias. In: Twomey JJ, Good RA eds. The immunopathology of lymphoreticular neoplasms, comprehensive immunology. New York: Plenum, 1978: 641.
16. Cataldo E, Meyer I. Solitary and multiple plasma cell tumors of the jaws and oral cavity. Oral Surg 1966: *22:* 628.
17. Silverman LM, Shklar G. Multiple myeloma. A report of a case. Oral Surg 1962: *15:* 301.
18. Mancilla R, Davis GL. Non-secretory multiple myeloma. Immunohistologic and ultrastructural observations on two patients. Am J Med 1977: *63:* 1015.
19. Bartoloni C, Flamini G, Logroscino C, et al. IgD (kappa) "non-secretory" multiple myeloma: report of a case. Blood 1980: *56:* 898.
20. Jones DB. Kidney. In: Kissane JM, ed. Anderson's pathology. St. Louis: Mosby, 1985: 730.
21. Shustik C, Bergsagel DE, Pruzanski W. Kappa and lambda-light chain disease: survival rates and clinical manifestations. Blood 1976: *48:* 41.
22. Mundy GR, Luben RA, Raisz LG, Oppenheim JJ, Buell DN. Bone resorbing activity in supernatants from lymphoid cell lines. N Engl J Med, 1974: *290:* 867.
23. Mundy GR, Raisz LG, Cooper RA, Schechter GP, Salmon SE. Evidence for the secretion of an osteoclast stimulating factor in myeloma. N Engl J Med 1974: *291:* 1041.
24. Zilva JF, Pannall PR. Plasma proteins and immunoglobulins: proteinuria. In: Clinical chemistry in diagnosis and treatment. London: Lloyd-Luke, 1979: 305.
25. Cannella G, Cristinelli L, Cancarini GC, Maccagnola S, Sandrini S, Maiorca R. Assessment of calcemic status in dialyzed uraemic patients. Scand J Clin Invest 1983: *43* (Suppl): 105.
26. Huyn BH, Kua D, Gabaldon H, Ashton JK. Reactive plasmacytic lesions of the bone marrow. Am J Pathol 1975: *65:* 921.

*Histopathology* 1991, **19**, 380–382

BRIEF REPORT

# Non-secretory IgA κ myeloma with distended endoplasmic reticulum: a case report

E.J.RAUBENHEIMER, J.DAUTH* & J.C.SENEKAL*

*Departments of Oral Pathology and *Chemical Pathology, Medical University of Southern Africa, Republic of South Africa*

Date of submission 28 February 1991
Accepted for publication 31 May 1991

A case of non-secretory multiple myeloma is presented. Plasma cells showed abundant cytoplasmic colloid contained in distended rough endoplasmic reticulum. Uniform cytoplasmic positivity for IgA heavy- and κ light-chains was demonstrated with the immunoperoxidase staining technique. It is proposed that distension of the endoplasmic reticulum by immunoglobulin-related proteins is indicative of a block in their excretion or of the presence of active synthesis of the immunoglobulins or their subunits.

Keywords: non-secretory myeloma, ultrastructure

## Introduction

Non-secretory myelomas comprise approximately 1% of cases with multiple myeloma[1]. The laboratory diagnosis of this condition is made difficult by the absence of circulating monoclonal protein, and pathologists have to rely on the clinical presentation, radiographs and microscopic findings for the diagnosis and subsequent typing of the infiltrate.

## Case report

A 57-year-old woman presented with generalized bone pains, weight loss and a pathological fracture of the left femur. Radiographic studies showed diffuse osteolytic bone lesions highly suggestive of multiple myeloma. Neither specimens submitted for serum and urine protein electrophoreses nor those submitted for immuno-fixation electrophoreses showed any monoclonal proteins. Other significant biochemical changes were paresis of IgG, IgA and IgM and hypercalcaemia. The erythrocyte sedimentation rate was elevated and the patient had a normocytic, normochromic anaemia.

Address for correspondence: Professor E.J.Raubenheimer, Department of Oral Pathology, Medical University of Southern Africa, PO Medunsa, 0204, Republic of South Africa.

### PATHOLOGICAL FINDINGS

A bone marrow aspiration and needle biopsy showed a diffuse infiltrate of plasma cells in excess of 30% of the total cell count. Most of the plasma cells contained abundant cytoplasmic colloid displacing the nucleus (Figure 1a). Immunoperoxidase staining of bone marrow sections showed the uniform presence of IgA heavy- and κ light-chains in the distended cytoplasm of the plasma cells (Figure 1). Stains for other immunoglobulin heavy and light chains were negative. Electronmicroscopical studies of the plasma cells showed distended endoplasmic reticulum containing colloid (Figure 1b).

On account of the monoclonal plasma cell infiltrate, the clinical, biochemical, haematological and radiographic appearances and an absence of a circulating monoclonal component, the diagnosis of a non-secreting IgA κ myeloma was made.

## Discussion

Failure to detect a monoclonal component in the serum and/or urine of a patient with other clinical signs of myeloma is the characteristic feature of non-secretory myeloma. Significant abnormalities found in our patient and supporting the diagnosis of myeloma were multiple lytic bone lesions, immunoparesis, a raised serum calcium, elevated erythrocyte sedimentation rate, anaemia and a bone marrow plasmacytosis in excess of 30%. Immunoperoxidase stains proved the infiltrate of plasma cells to be a monoclonal IgA κ type.

The term non-secretory, coined for this variety of

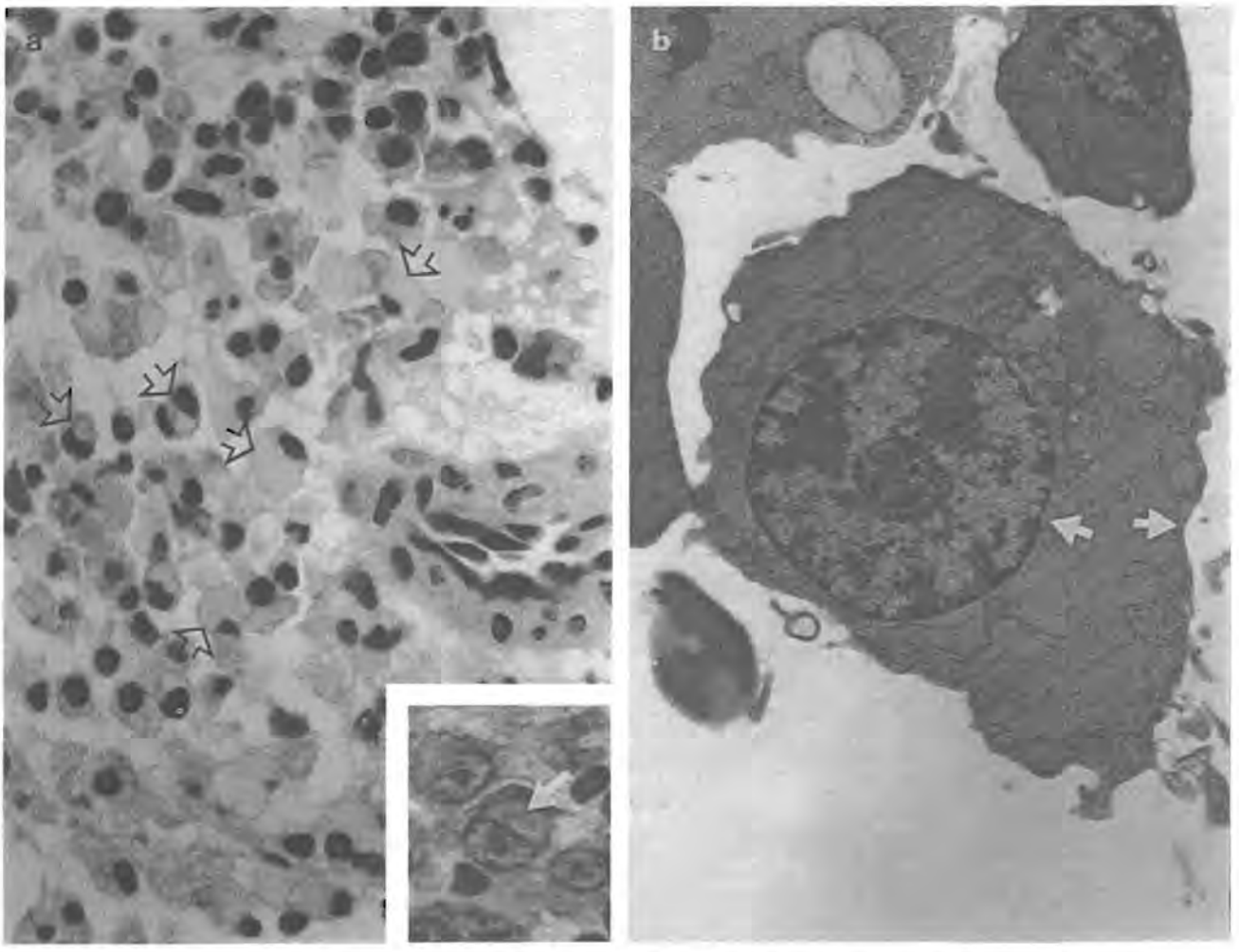


**Figure 1. a** Light microscopy of a bone marrow section, showing plasma cells with abundant cytoplasmic colloid (arrows). *Inset*: positive staining of the cytoplasmic colloid for IgA. **b** Electronmicroscopical view of a plasma cell with distended endoplasmic reticulum (arrows). ×8200.

myeloma, implies that a block in its release rather than in its synthesis accounts for the absence of a paraproteinaemia. The absence of a circulating monoclonal spike associated with the lack of intracellular immunoglobulins, on the other hand, suggests a block in immunoglobulin production[2]. These cases are often referred to as 'non-producers'[3] and immunoperoxidase stains for immunoglobulin typing would be negative.

The phenomenon of non-secretion in multiple myeloma is perplexing. Most studies have failed to reveal plasma cell abnormalities associated with the lack of a circulating monoclonal protein in non-secretory myelomas[2,4]. It is accepted, however, that the degree of distension of the rough endoplasmic reticulum cisternae in plasma cells at any particular time is influenced by the amount of immunoglobulin synthesized and the kinetics of its secretion. The distension of the rough endoplasmic reticulum by immunoglobulin-related proteins in our patient is, therefore, indicative of a block in excretion in the presence of active synthesis of the immunoglobulins or their subunits. It is important to note that plasma cells with distended endoplasmic reticulum are occasionally observed in infiltrates of secretory types of multiple myeloma[5]. It would be interesting to determine whether these cells also exhibit decreased secretory activity.

The signet-ring cell change exhibited by the IgG $\kappa$ myeloma reported by Eyden & Banerjee[6] resembles the infiltrate in our case and was also caused by large cytoplasmic membrane bound vesicles which compressed the nucleus against the cell membrane. Although the authors postulate the phenomenon to represent a membrane re-cycling defect, strong vacuolar staining for IgG and $\kappa$ light-chains is indicative of a process similar to that proposed in our case.

## Acknowledgements

We are indebted to Mrs C.S.Begemann for secretarial assistance and Mr H.Ebrahim for photographic services.

## References

1. Kanoh T, Niwa Y. Nonsecretory IgD (kappa) multiple myeloma. Report of a case and review of the literature. *Am. J. Clin. Pathol.* 1987; 88; 516–519.
2. Mancilla R, Davis GL. Nonsecretory multiple myeloma. Immunohistologic and ultrastructural observations on two patients. *Am. J. Med.* 1977; 63; 1015–1022.
3. Doster DR, Folds J, Gabriel DA. Nonsecretory multiple myeloma. *Arch. Pathol. Lab. Med.* 1988; 112; 147–150.
4. Bartoloni C, Flamini G, Logroscino C, Scuderi, Garnbassi G, Terranova T. IgD (kappa) 'nonsecretory' multiple myeloma: report of a case. *Blood* 1980; 56; 898–901.
5. Maldonado JE, Brown AL, Bayrol ED, Pease GL. Ultrastructure of the myeloma cell. *Cancer* 1966; 19; 1613–1627.
6. Eyden BP, Banerjee SS. Multiple myeloma showing signet-ring cell change. *Histopathology* 1990; 17; 170–172.

---

*Histopathology* 1991, **19**, 382–385

BRIEF REPORT

# So-called cutaneous lymphadenoma: a lymphotropic solid syringoma?

W.Y.W.TSANG & J.K.C.CHAN
*Institute of Pathology, Queen Elizabeth Hospital, Hong Kong*

Date of submission 25 March 1991
Accepted for publication 3 June 1991

Keywords: cutaneous lymphadenoma, syringoma, skin neoplasm

## Introduction

Lymphadenoma is a newly characterized skin neoplasm, occurring mostly in the head and neck region of young and middle-aged adults[1]. The histogenesis of this peculiar tumour is unknown, but it has been suggested to be of possible pilosebaceous derivation. We report one such case, and provide evidence that this represents a sweat duct tumour.

## Case report

A 30-year-old woman presented with a skin nodule over the left upper eyelid. A whitish firm nodule measuring $6 \times 5 \times 3$ mm was excised with the overlying ellipse of skin. There was no recurrence after 2 years.

The lesion was located in the dermis and was non-circumscribed (Figure 1). It was composed of irregular, sometimes anastomosing, epithelial islands of variable sizes and shapes dispersed among a cellular fibrous stroma. Some of the islands assumed a tadpole-shaped configuration. These islands were bounded by one to several layers of vaguely palisaded epithelial cells. Their centres were composed of more loosely arranged cells, including some large polygonal cells with retracted eosinophilic cytoplasm, vesicular nuclei and prominent nucleoli, reminiscent of lacunar cells (Figure 2). There was a variable infiltrate of small lymphocytes possessing slightly irregular or elongated nuclei. Rarely, ductules lined by a single layer of cuboidal cells were found within the epithelial islands (Figure 3a). They were highlighted by immunostaining for carcino-embryonic antigen (Figure 3b), which also stained the surrounding sweat ducts and sebaceous glands. The epithelial nature of the cellular islands, including the large cells, was confirmed by immunostaining for cytokeratin (AE1/AE3, CAM 5.2). Staining with CAM 5.2 was generally weak, whereas staining with AE1/AE3 was more intense, with accentuation in the ductular elements within the epithelial islands. The cellular islands showed weak cytoplasmic staining for epithelial membrane antigen, while the ductules showed strong luminal staining. Immuno-

Address for correspondence: Dr W.Y.W.Tsang, Institute of Pathology, Queen Elizabeth Hospital, Wylie Road, Kowloon, Hong Kong.

# Multiple myeloma and amyloidosis of the tongue

**E. J. Raubenheimer[1], J. Dauth[2], F. J. Pretorius[3]**

Departments of [1]Oral Pathology, [2]Chemical Pathology, [3]Internal Medicine, Medical University of Southern Africa, Republic of South Africa.

Raubenheimer EJ, Dauth J, Pretorius FJ. Multiple myeloma and amyloidosis of the tongue. J Oral Pathol 1988: 17: 554–559.

Tongue biopsies of 30 diagnosed cases of multiple myeloma were examined light and electron microscopically and amyloid deposits were identified in 8 patients. Immunochemical typing of amyloid in kappa and lambda subtypes was performed successfully although positive staining of tissue-associated immunoglobulin light chains made reliable identification of amyloid with this technique difficult. Cells of macrophage lineage appear to play a central role in light chain-associated amyloidogenesis. Our findings do not agree with the reported higher amyloidogenic potential of lambda light chains and we were unable to show a positive correlation between the percentage plasma cells in bone marrow aspirates or the presence of urinary light chains and myeloma-associated amyloidosis.

Professor E. J. Raubenheimer, Department Oral Pathology and Oral Biology, Medical University of Southern Africa, PO Medunsa 0204, Republic of South Africa.

Accepted for publication December 9, 1988

Multiple myeloma (MM) is characterized by a malignant proliferation of plasma cells which, in most instances, secrete large quantities of monoclonal immunoglobulins or subunits thereof. Amyloidosis is frequent in patients suffering from MM and leads to organ dysfunction including cardiac and renal failure, malabsorption syndromes, and peripheral neuropathies (1). It is generally agreed that amyloid fibrils in patients with MM are derived from monoclonal immunoglobulin light chains (Bence Jones proteins) (2). Although the exact mechanism involved in the extracellular depositioned of light chain-associated amyloid is less clear, considerable evidence supports the role

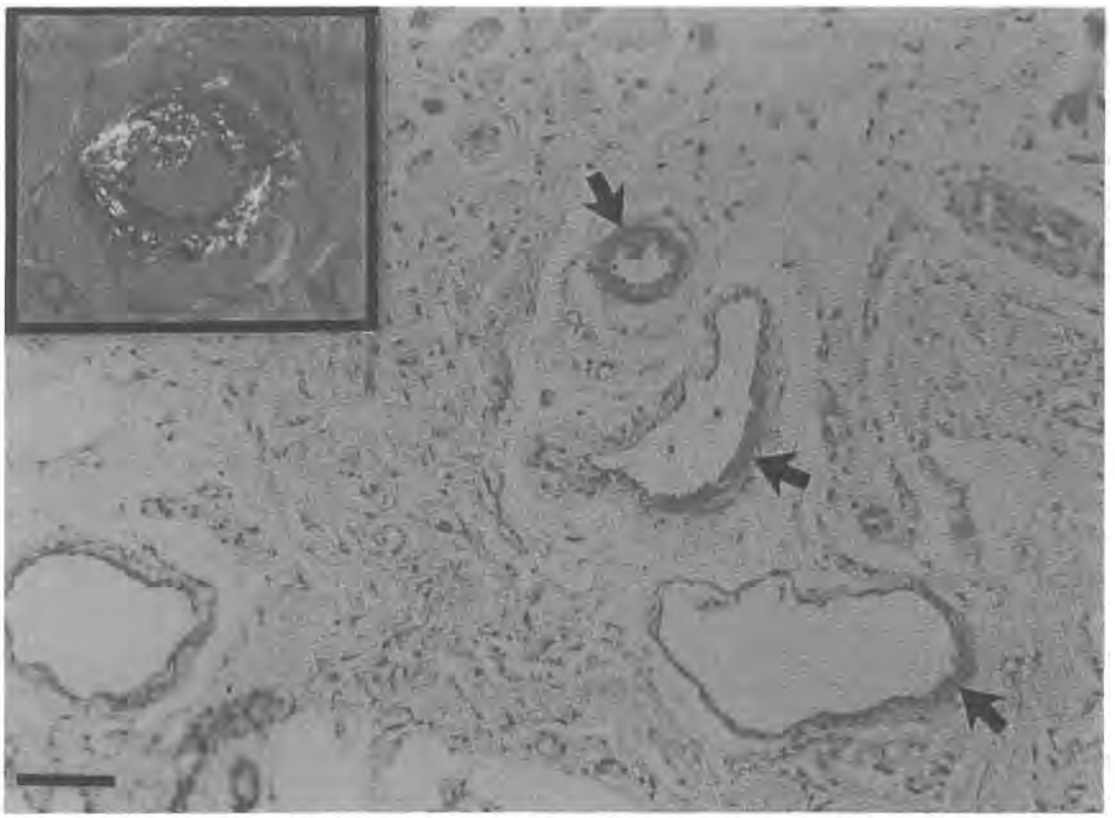

*Fig. 1a.* Mild perivascular amyloid deposits (arrows) in Case 7. (Congo red stain, bar = 50 μ) Inset: Congo red stain viewed with polarized light.

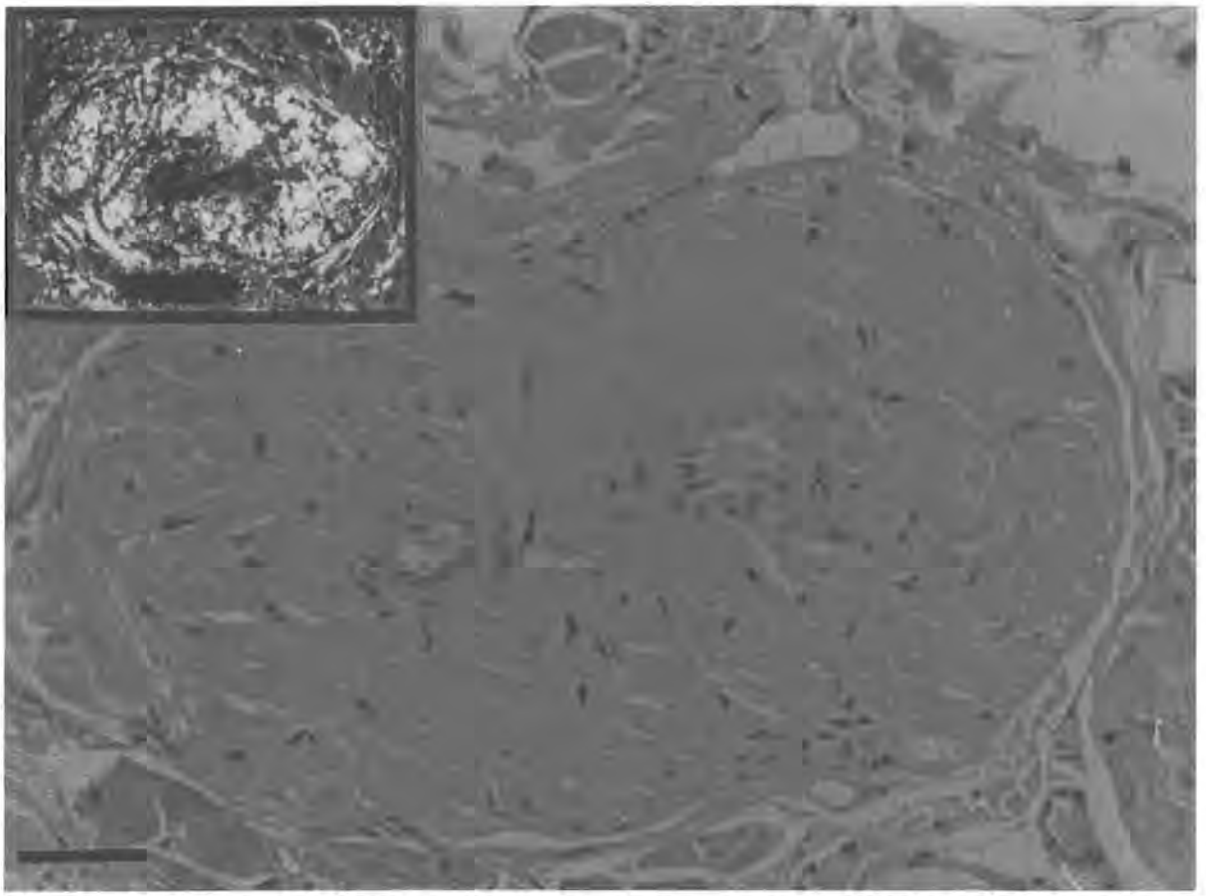

*Fig. 1b.* Severe perivascular amyloid deposits in Case 1. (Congo red stain, bar = 35 μ) Inset: Congo red stain viewed with polarized light.

macrophages play in MM-related amyloidogenesis (3). The light chain class found in amyloidosis in MM is reported to be more commonly of the lambda than the kappa type with a frequency of 2 to 1. This ratio is the reverse of that seen in most cases of monoclonal gammopathy (1). Furthermore, amyloidogenesis in MM appears to be related to the presence of kappa or lambda light chains in urine and a high percentage bone marrow plasma cells (4).

It was previously stressed that primary amyloidosis (including amyloidosis occurring with MM) typically involves such mesodermal tissues as smooth and skeletal muscle, as well as the cardiovascular system, whereas secondary amyloidosis affects the liver, spleen and kidneys (5). An extensive overlap in the distribution of primary and secondary amyloidosis has been reported (6, 7) and differential organ involvement is no longer considered to be a useful basis for the classification of amyloidosis. With increasing acceptance of the role light chains play in amyloidogenesis, the amyloid type associated with MM was designated AL protein (A for amyloid fibril protein and L for immunoglobulin light chain) in recent amyloid classification systems (1).

The purpose of this study was to determine the incidence of amyloidosis of the tongue in patients with MM admitted to the Ga-Rankuwa hospital. Furthermore, immunochemical subtyping of amyloid deposits was performed and the biochemical changes associated with MM-related amyloid deposits noted.

## Material and methods

The tongues of 30 proven cases of MM were examined clinically and incision biopsies were performed on the lateral borders thereof. The tissue was divided and fixed in 3% buffered formalin and 4% glutaraldehyde and processed for LM and TEM, respectively. Sections for LM were stained with H&E, Congo red stain for amyloid and the immunoperoxidase technique (Immunolok Histoset, Immunolok, Carpinteria, CA) was employed for the detection of kappa and lambda light chains and IgG, IgA, or IgM. Heavy and light chains in the serum and urine were typed utilizing immunofixation electrophoresis (Paragon ™ IFE Gels, Beckman Instruments, Fullerton, U.S.A.) and immunoglobulin concentrations, as well as light chain levels in the serum and urine, were quantitated by rate nephelometry (Auto ICS, Beckman). Bone marrow aspirations of the iliac crest or sternum were performed as part of the diagnosis of MM and the volume of plasma cells expressed as a percentage of the total nucleate cell count. The microscopic features were correlated with the percentage plasma cells in the bone marrow aspirates, the secretory type of myeloma and serum and urinary biochemical findings.

## Results

Biopsy wounds of all cases healed without complication or patient complaints except in Case 26 where an unexpected hemorrhage occurred. This complication was, however, readily brought under control by suturing.

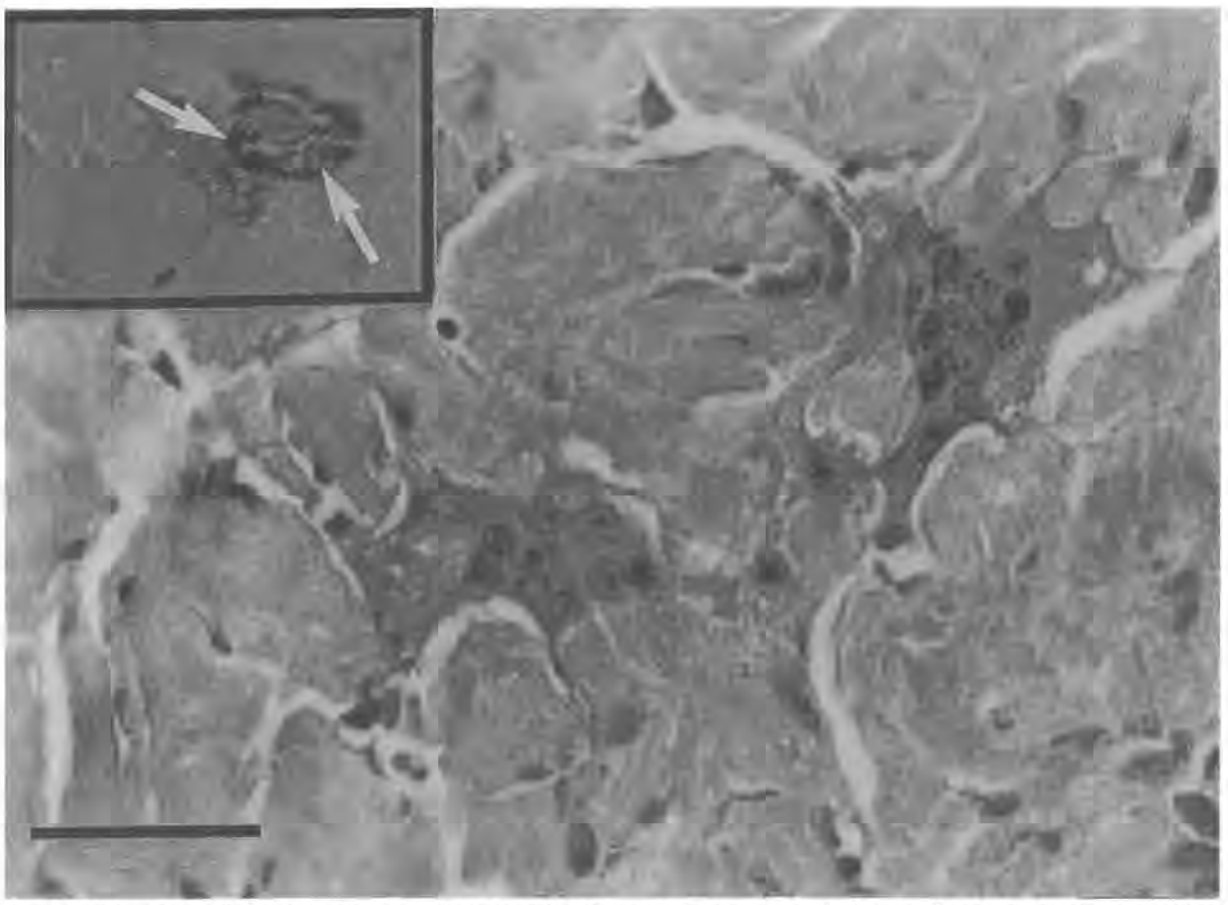

*Fig. 1c.* Diffuse amyloid deposits with giant cells in Case 17. (Congo red stain, bar = 40 μ) Inset: Giant cell containing cytoplasmic kappa chains (arrows) (Immunoperoxidase stain for kappa light chains).

Examination of Congo red stains viewed with polarized light identified amyloid deposits in 7 cases, ranging from mild (4 cases, Fig. 1a) to severe (1 case, Fig. 1b) perivascular deposits. Two cases exhibited diffuse amyloid deposits extending against an atrophic mucous membrane. The amyloid in the latter patients contained large, dilated and thin walled bloodvessels and many macrophages and giant cells (Fig. 1c). Of the positive cases, only 3 exhibited macroglossia, 2 of which had mucosal atrophy, diffuse amyloid deposits and mucosal nodules composed of amyloid. Tongue enlargement was present in 4 patients without amyloidosis (Table 1).

Electron microscopic examination confirmed amyloid in all positive cases and identified in addition, amyloid fibrils in an eighth patient (Fig. 1d).Immunoperoxidase stains for light chains showed kappa or lambda positivity of amyloid which corresponded to the relevant MM light chain type in the serum. Positive staining of tissue associated-monoclonal immunoglobulins and light chains concurring with the MM secretory type, made identification of small amyloid deposits in the immunoperoxidase stained sections difficult (Fig. 2). The relevant MM light chain was present in the cytoplasm of amyloid-associated giant cells in the 2 cases with diffuse mucosal deposits (Fig. 1c). Immunoperoxidase stains further identified in both amyloid-positive and -negative cases the relevant monoclonal immunoglobulin and light chain type in groups of keratinocytes and spindleshaped cells in the basal cell region of the mucous membrane (Fig. 3). The positive epithelial cells corresponded to foci of clear cells observed in hematoxylin- and eosin-stained sections.

Four patients, 2 of whom had amyloid deposits, were under 35 years old, well below the reported mean age of 62 years for MM (8). Case 13, who presented with a solitary maxillary tumor, had a biclonal gammopathy (IgG kappa and IgG lambda). Urinary light chains were absent in 3 cases with amyloidosis. One patient with amyloidosis (Case 13) only had 10% plasma cells in his bone marrow aspirate. Other relevant clinical, biochemical and microscopical findings are in Table 1.

## Discussion

To date there is no accurate non-invasive diagnostic procedure for amyloidosis. Although rectal biopsies have been advocated as more successful than biopsies of the gingiva for the identification of amyloid (9), the risks and patient discomfort are greater than with intraoral biopsy techniques (10). Despite immune suppression which occurs frequently in patients with MM, post biopsy infections were not encountered in our study. The difficulty in controlling hemorrhage and the high risk of infection following rectal biopsy render this procedure less attractive. As amyloid deposits are often limited to the deeper parts of the submucosa (1), tongue biopsies are more appropriate than the more superficial gingival biopsies. This study furthermore indicates that tongue biopsies are probably more

Table 1. Clinical, biochemical, and microscopical data of 30 MM patients.

| Case no | Age | Sex | MM type | Tongue enlargement | Residual Ig levels | Urinary | | % plasma cells | Amyloid | |
|---|---|---|---|---|---|---|---|---|---|---|
| | | | | | | light K | chain λ | | type | distribution |
| 1 | 66 | F | Gκ | Yes | ↓ | − | − | 60 | K | Severe pv. |
| 2 | 34 | M | Gλ | No | ↓ | − | + | 65 | λ | Mild pv. |
| 3 | 60 | F | Gλ | No | ↓ | − | − | 5 | − | − |
| 4 | 69 | M | Aκ | Yes | ↓ | − | − | 70 | − | − |
| 5 | 78 | M | Gκ | No | Normal | + | − | 30 | − | − |
| 6 | 79 | M | Gκ | No | ↓ | − | − | 80 | − | − |
| 7 | 60 | F | Gκ | No | ↓ | + | − | 40 | K | Mild pv. |
| 8 | 60 | M | Aκ | No | ↓ | + | − | 30 | K | Mild pv. |
| 9 | 42 | M | Gλ | Yes | ↓ | − | + | 80 | − | − |
| 10 | 72 | M | Gλ | No | Normal | − | − | 5 | − | − |
| 11 | 36 | M | Gκ | No | Normal | − | − | 3 | − | − |
| 12 | 52 | M | Gκ | | ↓ | + | − | 30 | − | − |
| 13 | 40 | M | Gκ+Gλ | No | Normal | − | − | 10 | N.A. | EM pv. |
| 14 | 45 | M | Aκ | No | ↓ | + | − | 15 | − | − |
| 15 | 40 | F | Aλ | No | ↓ | − | + | 30 | − | − |
| 16 | 60 | F | Aλ | No | ↓ | − | + | N.A. | − | − |
| 17 | 25 | M | κ | Yes | Normal | + | − | 30 | K | Diffuse |
| 18 | 70 | F | λ | No | Normal | N.A. | N.A. | N.A. | − | − |
| 19 | 57 | M | Gλ | Yes | Normal | − | − | 70 | − | − |
| 20 | 33 | M | κ | No | ↓ | + | − | N.A. | − | − |
| 21 | 70 | F | Gλ | No | ↓ | − | + | N.A. | − | − |
| 22 | 55 | M | λ | Yes | ↓ | − | + | 33 | λ | Diffuse |
| 23 | 62 | F | Gκ | No | Normal | − | − | 30 | − | − |
| 24 | 55 | F | Gκ | No | ↓ | + | − | 55 | − | − |
| 25 | 60 | M | Gκ | No | ↓ | + | − | N.A. | − | − |
| 26 | 33 | M | Gκ | No | ↓ | − | − | N.A. | − | − |
| 27 | 35 | M | Gλ | Yes | ↓ | − | + | 40 | − | − |
| 28 | 53 | M | Gκ | No | ↓ | − | − | 2 | − | − |
| 29 | 60 | M | Gκ | No | ↓ | − | − | 30 | K | Mild pv. |
| 30 | 60 | M | Aλ | No | Normal | − | − | 20 | K | − |

N.A. – Not available. pv. – perivascular EM – electron microscopic.

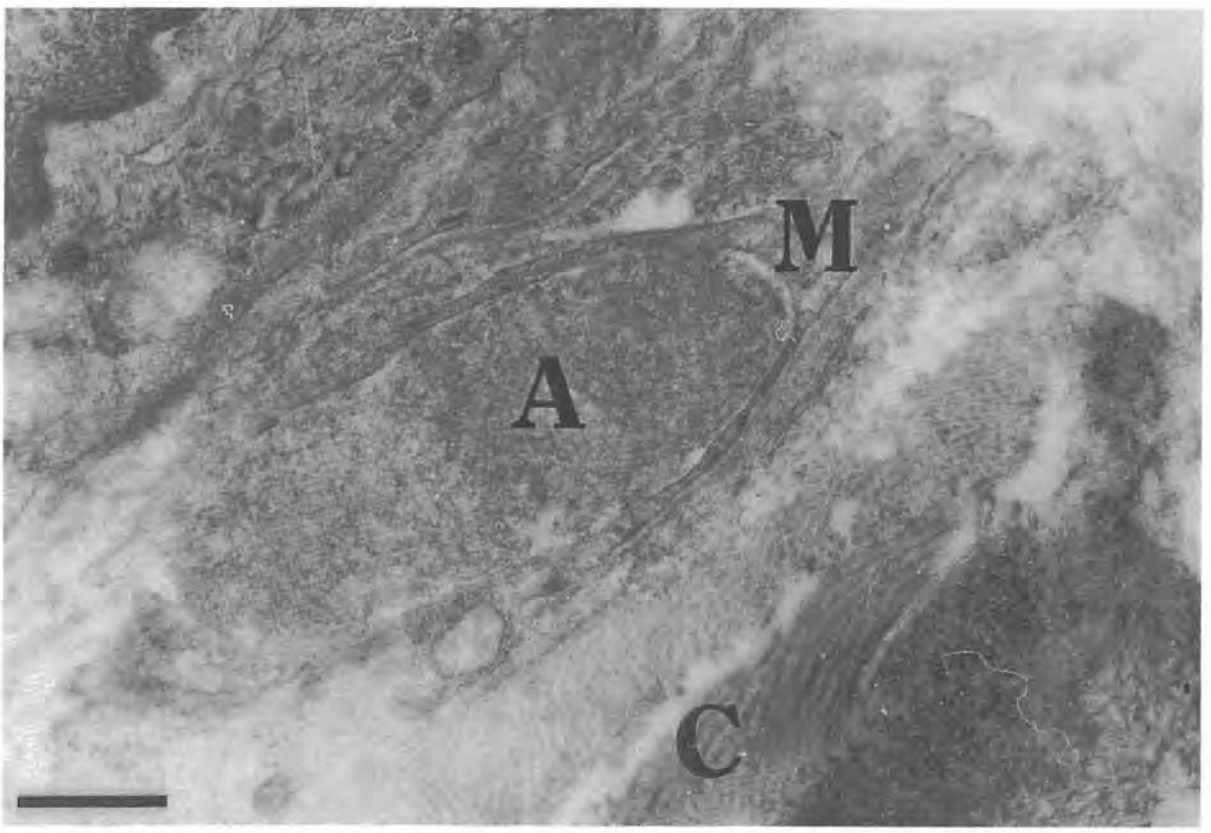


*Fig. 1d.* Transmission electron micrograph of amyloid (A) deposits in Case 13. Note collagen fibres (C) and cytoplasmic process of macrophage (M). (Bar = 2 μ).

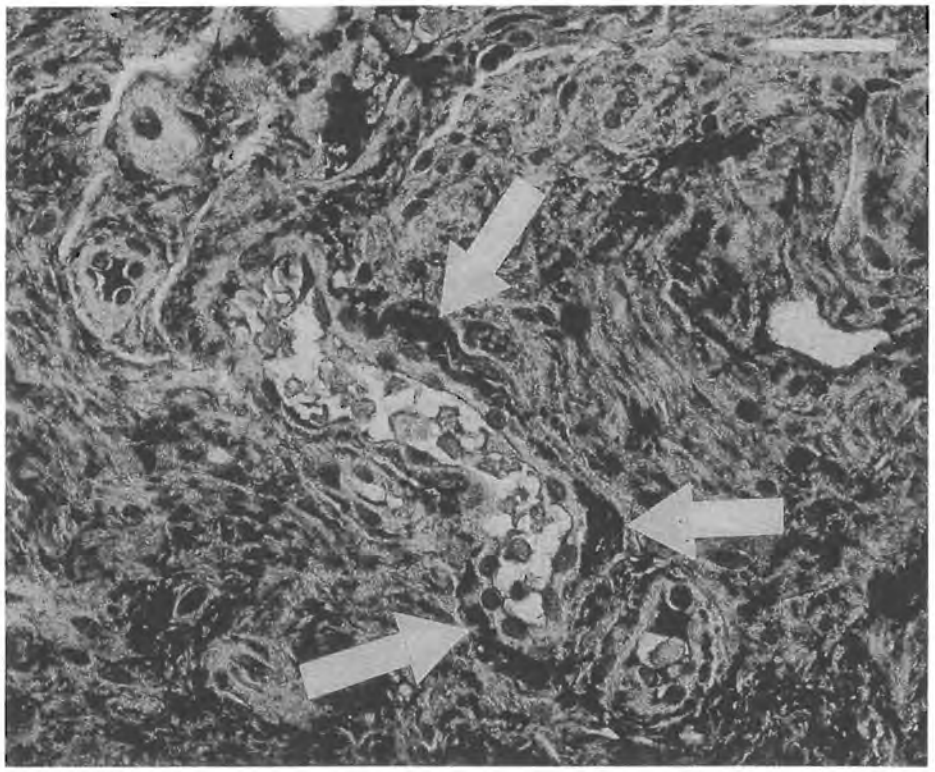

*Fig. 2.* Immunoperoxidase stain for kappa light chains in Case 29. Note pericapillary amyloid deposits (arrows). (Bar = 40 μ).

successful than biopsies of other areas of the gastrointestinal tract for the identification of amyloid as our incidence of MM-associated amyloidosis of 27% is higher than the 6–15% generally reported in the literature (1, 6, 7). It could be argued that the amyloid deposits in some of our positive cases were unrelated to MM and represented senile amyloidosis, a significant percentage of which is of the AL type (1). This seems unlikely as the AL amyloid

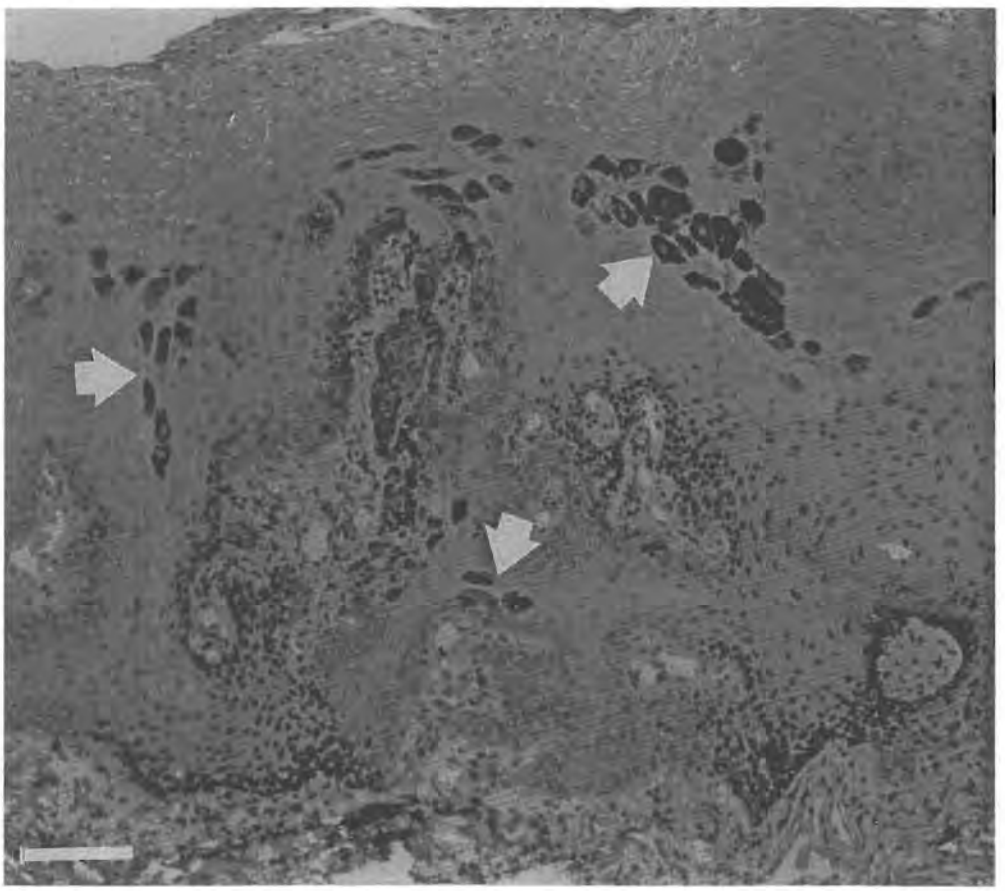

*Fig. 3.* Immunoperoxidase stain for IgG in Case 6. Note positive staining of focal groups epithelial cells (arrows). (Bar = 100 μ).

subtypes in our study corresponded with the patients' MM secretory type. Furthermore, a recent study (11) failed to identify senile amyloid in tongue biopsies of 94 patients beyond the age of 40 years.

Macroglossia is a feature which has been reported in one fifth of patients with MM-associated amyloidosis (1, 12). Our study indicates that although macroglossia does occur more frequently in MM patients with amyloidosis, tongue enlargement can also be encountered in the absence of amyloid (Table 1). The presence of mucosal nodules covered by an atrophic mucous membrane is probably a more specific clinical sign indicative of amyloidosis of the tongue.

Although EM is the technique of choice for the identification of minute amyloid deposits and intracellular fibrils, LM examination of Congo red stains yields acceptable results. Our study supports the feasibility of kappa and lambda subtyping of AL amyloid with the immunoperoxidase method (13). However, the high concentration of tissue-associated monoclonal immunoglobulin chains or fragments thereof in MM makes identification of amyloid in these sections difficult. The presence of amyloid-associated giant cells which contained light chains, supports the role macrophages play in AL type amyloidogenesis.

The relevant MM secretory type immunoglobulin and light chain in focal groups of epithelial cells in the tongue mucosa is a feature not yet described. Preliminary investigations suggest that spindle-shaped cells in the basal region of the tongue mucosa are involved in the presentation of phagocytosed immunoglobulin chains to the basal epithelial cell layer. Although the significance of this phenomenon is speculative, it may form part of a process of trans-mucosal elimination of excessive proteins and the role of Langerhans cells in this process needs to be investigated.

Only 4 patients in our series had Bence Jones (or light chain secreting) MM and 2 of these exhibited amyloid deposits. It is noteworthy that the amyloid in these 2 cases had a diffuse distribution and contained the most striking macrophage and giant cell reaction.

Our study does not support a higher amyloidogenic potential for lambda light chains, as the majority of deposits were of the kappa type. Furthermore, our youngest patient, Case 17, with a kappa light chain secreting MM presented with the most extensive amyloid deposits of all. Three patients with amyloidosis had no urinary light chains even though extremely sensitive immunochemical techniques were employed for the detection thereof. Urinary light chain excretion is dependent on a variety of factors, of which renal tubular function plays an important role: light chains will be absent from the urine while the ability of the renal tubuli to absorb and catabolize light chains are maintained. We detected light chains in the urine of 11 patients without amyloidosis and, therefore, suggest that the presence of urinary light chains as indicative of co-existing amyloidosis be used with caution.

The association between amyloidosis and a high percentage plasma cells in random bone marrow aspirations or biopsies appears to be inconsistant. Both techniques may fail to identify significant plasma cell levels due to the patchy and often atypical distribution of the tumor mass, as illustrated by our Case 13. The absence of amyloid in patients with 70% or more bone marrow plasma cells in our study further supports our scepticism of this correlation.

Amyloidosis is a recognised and grave complication of MM. As no biochemical or hematological parameter appears to be associated with amyloidosis in MM, we suggest that routine tongue biopsies be performed on patients with MM for the identification and immunochemical subtyping af AL type amyloid.

*Acknowledgements* – We are indebted to Mrs C. S. Begemann for secretarial services and Drs. C. Hatting and S. Klebanoff for their assistance.

## References

1. Kyle RA. Amyloidosis. In: Wiernik PH, Canellos GP, Kyle RA, Schiffer CA, eds. Neoplastic diseases of blood. New York: Churchill Livingstone, 1985: 607.
2. Glenner GG. Amyloid deposits and amyloidosis: the betafibrilloses. New Engl J Med 1980: *302:* 1283.
3. Drurie BGM, Persky B, Soehnlen BJ, Grogan TM, Salmon SE. Amyloid production in human myeloma stem-cell culture, with morphologic evidence of amyloid secretion by associated macrophages. New Engl J Med 1982: *307:* 1689.
4. Kyle RA, Greipp PR. Amyloidosis (AL): clinical and laboratory features in 229 cases. Mayo Clin Proc 1983: *58:* 665.
5. Dahlin DC. Secondary amyloidosis. Ann Intern Med 1949: *31:* 105.
6. Cohen AS. Amyloidosis. New Engl J Med 1967: *227:* 574.
7. Limas C, Wright JR, Matsuzaki M, Calkins E. Amyloidosis and multiple myeloma. A re-evaluation using a control population. Am J Med 1973: *54:* 166.
8. Kyle RA. Multiple myeloma: a review of 869 cases. Mayo Clin Proc 1975: *50:* 29.
9. Blum A, Sohar E. The diagnosis of amyloidosis. Ancillary procedures. Lancet 1962: *7:* 721.
10. Schwartz HC, Olson DJ. Amyloidosis: a rational approach to diagnosis by intraoral biopsy. Oral Surg Oral Med Oral Pathol 1975: *39:* 837.
11. Van der Waal N, Henzen-Logmans S, van der Kwast WAM, van der Waal I. Amyloidosis of the tongue: a clinical and postmortem study. J Oral Pathol 1984: *13:* 632.
12. Briggs GW. Amyloidosis. Ann Intern Med 1961: *55:* 943.
13. Fujihara S, Balow JE, Costa JC, Glenner GG. Identification and classification of amyloid in formalin-fixed, paraffin-embedded tissue sections by the unlabelled immunoperoxidase method. Lab Invest 1980: *43:* 358.

Oral Oncol, Eur J Cancer, Vol. 29B, No. 4, pp. 295–297, 1993
Printed In Great Britain

0964–1955/93 $6.00 + 0.00




# Salivary Immunoglobulin Related Proteins in 24 Patients with Multiple Myeloma

**Erich Raubenheimer, Willie van Heerden, Joseph Dauth and Tracy van der Walt**

**Mixed saliva and blood of 24 cases of multiple myeloma (MM) were collected and the immunoglobulin and light chain concentrations compared with that found in the saliva and blood of 16 age matched control patients. The concentrations of salivary IgA, IgG and lambda light chains were significantly increased in IgA-, IgG- and lambda light chain producing MM respectively. Salivary IgA concentration in non-IgA MM and salivary IgG concentration in non-IgG MM were within normal ranges. Despite a significant decrease in circulating normal immunoglobulins, this study fails to support suppression of normal salivary immunoglobulin concentrations in patients suffering MM.**
*Oral Oncol, Eur J Cancer*, Vol. 29B, No. 4, pp. 295-297, 1993.

## INTRODUCTION

In the majority of patients with multiple myeloma (MM) serum protein electrophoresis will disclose the presence of a monoclonal paraprotein which may present as an increase in one of the immunoglobulin classes and/or immunoglobulin-related light chains (Bence-Jones proteins). MM are immunochemically typed according to the circulating monoclonal immunoglobulin and/or light chain type produced by the disseminated neoplastic plasma cells. This typing is helpful in predicting complications and prognosis of patients suffering MM [1]. The decrease in the concentrations of circulating normal immunoglobulins predispose to opportunistic infections, a serious and often terminal complication in MM [2].

Reports on the presence of abnormal immunoglobulin-related proteins in secretions of MM patients are infrequent in the literature. Analysis of saliva of 10 patients with MM [3], identified monoclonal IgA in 5 out of 7 patients with IgA MM and monoclonal IgG in both patients with IgG MM. No free light chains were detected in the saliva of the 1 patient with light chain producing MM. An increased concentration of IgG was present in the saliva of 1 case of IgG MM studied by Brandtzaeg [4].

The purpose of this study was to determine the concentrations of immunoglobulins and light chains in saliva and serum of 24 patients with MM and to compare the values obtained with that found in age matched, systemically healthy patients.

## PATIENTS AND METHODS

Whole saliva and blood of 24 patients with MM and 16 age matched systemically healthy control patients were collected after a thorough clinical oral examination. The saliva was expressed with the aid of a sterile syringe from a cottonwool swab after it had been chewed for 3 min. Patients with overt signs of gingivitis or periodontitis were excluded from the control group of the study. Quantitation of IgA, IgG and IgM levels in serum were done with rate nephelometry (Auto ICS, Beckman Instruments Inc. Fullerton, U.S.A.). Immunochemical typing of the light chains in serum was carried out with immunofixation electrophoresis (Paragon™ IFE gels, Beckman Instruments Inc.).

Salivary immunoglobulins and light chains were quantitated with low concentration radial immunodiffusion plates (LC-Partigen® and M-Partigen®, Behringwerke AG, Marburg, West Germany). The concentrations were expressed in grams per litre (g/l), compared with the respective circulating concentrations and the findings were subjected to statistical analysis using Student's *t*-test for uncorrelated data.

## RESULTS

Clinical examination of the MM patients revealed no signs of oral mucosal infections. 17 patients had IgG MM, 4 IgA MM and 3 light chain producing MM (two kappa- and one lambda MM). The mean concentrations and standard deviations of the major immunoglobulin classes in MM patients and the control group are expressed in Table 1 and the immunoglobulin light chain concentrations in Table 2. The circulating residual immunoglobulin concentrations in MM patients were generally below the normal ranges (Table 3) and that of the control group (Table 1). No significant differences were found between salivary IgA concentrations in non-IgA MM and the control group ($P > 0.05$) and salivary IgG levels in non-IgG MM and the control group ($P > 0.8$). In IgA MM, salivary IgA concentrations were found to be significantly higher than in the control group ($P < 0.01$). A significant increase in salivary IgG in IgG MM ($P < 0.01$ was also present. The concentration of lambda light chains in the saliva of lambda-producing MM was significantly higher than the control group ($P < 0.01$). Although salivary kappa light chain concentrations in kappa-producing MM showed great variations, with single values far above those of control patients, statistical analysis failed to prove a significantly higher concentration of kappa light chains in kappa-producing MM when compared to the control group ($P > 0.05$).

Correspondence to E.J. Raubenheimer
E.J. Raubenheimer and W. van Heerden are at the Department of Oral Pathology; and J. Dauth and T. van der Walt are the Department of Chemical Pathology Medunsa, P.O. Medunsa 0204, Republic of South Africa.
Received 17 Dec. 1992; accepted 19 Feb. 1993.

*Table 1. Concentrations of major immunoglobulin types in MM- and control patients*

| | Saliva g/l | | Serum g/l | | |
|---|---|---|---|---|---|
| | IgG | IgA | IgG | IgA | IgM |
| IgA MM (2 × IgA κ's 2 × IgA λ's) | 0.04 ± 0.03 | 1.1 ± 0.9 | 5.85 ± 4.4 | 41.5 ± 25.3 | 2.0 ± 3.5 |
| IgG MM (12 × IgG κ, 5 × IgG λ) | 0.22 ± 0.16 | 0.05 ± 0.05 | 75.9 ± 32.4 | 0.63 ± 0.6 | 0.57 ± 0.42 |
| Lambda MM ($n$ = 1) | 0 | 0.14 | 5.5 | 0.3 | 0.2 |
| Kappa MM ($n$ = 2) | 0.7 ± 0.01 | 0.04 | 13.1 ± 1.5 | 0.65 ± 0.07 | 0.25 ± 0.07 |
| Control ($n$ = 16 | 0.047 ± 0.03 | 0.081 ± 0.03 | 20.0 ± 6.6 | 3.28 ± 1.3 | 2.16 ± 1.7 |

*Table 2. Light chain concentrations in MM- and control patients*

| | Saliva g/l | | Serum g/l | |
|---|---|---|---|---|
| | κ | λ | κ | λ |
| κ-producing MM ($n$ = 16) | 0.44 ± 1.0 | 0.006 ± 0.01 | 43.5 ± 24.5 | 2.2 ± 1.8 |
| λ-producing MM ($n$ = 8) | 0.03 ± 0.06 | 0.16 ± 0.12 | 4.4 ± 2.9 | 55.1 ± 37.0 |
| Control ($n$ = 16) | 0.03 ± 0.03 | 0.02 ± 0.01 | 13.4 ± 5.3 | 7.04 ± 1.5 |

*Table 3. Normal ranges*

| | |
|---|---|
| Serum | |
| IgG | 14.4—22.7 g/l |
| IgA | 1.9—4.7 g/l |
| IgM | 0.7—2.6 g/l |
| κ | 5.66—13.0 g/l |
| λ | 3.04—7.35 g/l |
| Saliva | |
| IgA | 0.05—0.48 (mean 0.137) g/l* |
| IgG | 0.007—0.037 (mean 0.016) g/l |
| κ | N/A |
| λ | N/A |

*Grönblad 1981 [5].

## DISCUSSION

This study represents the largest series in which the concentrations of immunoglobulin related proteins in saliva of patients with multiple myeloma were determined. Although changes in the circulating immunoglobulin concentrations are well documented [2], little is known of alterations in salivary immunoglobulins and immunoglobulin related proteins in this disease.

A study using immunoelectrophoresis to determine the presence of salivary immunoglobulins in 10 patients suffering MM [3] failed to express the concentrations and the findings can therefore not be compared directly to ours. These authors conclude that although the concentration of monoclonal immunoglobulin is low in saliva, its presence is adequate proof that circulating immunoglobulins can find their way into external secretions. The technique employed in our study is more sensitive and made accurate quantitation of the different immunoglobulin-related proteins possible. All our cases of IgA MM had significantly increased concentrations of IgA in saliva when compared to the salivary IgA concentrations found in the control group. The same applies to salivary IgG in IgG MM and lambda light chain concentrations in the saliva of lambda producing MM. Despite a few kappa producing MM that had high salivary kappa concentrations, statistical analysis failed to support a significant increase in salivary kappa concentrations in kappa producing MM when compared to control values. Although transmission of circulating immunoglobulin related proteins to saliva appears to be enhanced by elevated serum concentrations, no direct correlation could be found between these values.

The occurrence of systemic immune suppression in MM is well documented. This study supports the findings of Coelho *et al.* [3] which failed to identify salivary immunoglobulin impairment in MM. No statistical evidence of a decrease in the concentration of normal salivary IgA in non-IgA MM patients could be found in our study. This was confirmed in that no clinical evidence of an opportunistic infection was seen in the oral cavities of our MM patients. The mechanism by which normal immunoglobulin production is suppressed in MM, is not clearly understood [6]. It has been postulated that neoplastic plasma cells secrete a factor capable of activating suppressor macrophages which in turn inhibit normal B cell function [7]. The observation that salivary gland associated immunoglobulin production is not altered in MM, adds an interesting parameter to the debate on MM-induced immunoparesis.

1. Shustik, C, Bergsagel, DE, Pruzanski, W. Kappa and Lambda light chain disease: survival rates and clinical manifestations. *Blood* 1976, **48**, 41–46.
2. Farhangi, M, Osserman, EF. Biology, clinical patterns and treatment of multiple myeloma and related plasma cell dyscrasias. In Twomey, JJ, Good, RA, eds. *The Immunopathology of Lymphoreticular Neoplasma, Comprehensive Immunology*. New York, Plenum Medical Books, 1978, 641–716.
3. Coelho, IM, Pereira, MT, Virella G. Analytical study of salivary immunoglobulins in multiple myeloma. *Clin Exp Immunol* 1974, **17**, 417–426.

4. Brandtzaeg T. Human secretory immunoglobulins. II. Salivary secretions from individuals with selectively excessive or defective synthesis of serum immunoglobulins. *Clin Exp Immunol* 1971, **8**, 69–85.
5. Grönblad, EA. Concentrations of immunoglobulins in human whole saliva: effect of physiological stimulation. *Acta Odontol Scand* 1982, **40**, 87–95.
6. Brodes, SM, Waldmann, TA. Multiple myeloma and immunodeficiency. In: Wiernik PH, Canellos GP, Kyle RA, Schiffer CA, eds. *Neoplastic Diseases of Blood*. New York, Churchill Livingstone 1985, 483–498.
7. Jacobson DR, Zolla-Pazner S. Immunosuppression in multiple myeloma. *Semin Oncol* 1986, **13**, 282.

**Acknowledgements**—This project was funded by the Medical Research Council (MRC) of South Africa. We are indebted to Mrs CS Begemann for secretarial services.

105 The Relation Between Temporomandibular Joint Internal Derangement, Occlusion and Parafunction. W D SNYMAN*, J C NEL and J DE VRIES, University of Pretoria and Medunsa

Occlusal discrepancies and parafunction have been frequently cited as causes of both condylar and masticatory muscle disorders. It has been postulated that both these factors result in mandibular displacement, causing compression of the intracapsular tissues, micro-trauma, pain, impairment of the blood supply and consequently degenerative changes in the temporomandibular joint. This theory is supported by the fact that alteration to the occlusion is followed by a clinical improvement in a high percentage of patients

The purpose of this study was to determine whether or not an association exists between parafunction, occlusal discrepancies and internal derangement of the temporomandibular joint. A total of 273 patients treated for temporomandibular dysfunction at the TMJ clinic, Department of Restorative Dentisty, University of Pretoria were examined for signs and symptoms of anterior displacement of the menisci, with reduction (ADTMR). The occlusal status was determined by means of an occlusal index previously described. The results indicated a small positive correlation ($r_s$ = + 0.18) between ADTMR and eccentric bruxism ($P < 0.0005$), a higher correlation ($r_s$ = + 0.39) between ADTMR and centric bruxism ($P < 0,0005$), and an even higher correlation between ADMR ($r_s$ = + 0.556) and RC/IC discrepancies ($P < 0,0005$)

It can be concluded that a reasonably high positive correlation exists between internal derangement of the Temporomandibular Joint, occlusal discrepancies and centric bruxism

106 Pilot Study for Comparing two Parallel-sided Root canal Posts, Oval in Diameter with Standard cylindrical posts. N.P.Louw and *I.J.du Toit – University of Stellenbosch, TYGERBERG, 7505.

Standard parallel-sided posts are round in cross section and are difficult to fit into the oval shape of most root canals. Cast posts overcome this problem but cannot be made parallel and therefore suffers from lack of retention. A new commercial product, "Triax" (T), with oval cross-section, was subjected to tensile, shear and torque forces and compared to a commercially available cylindrical post, Parapost Plus (P).

Roots were covered with silicone and mounted in brass containers with acrylic. The root canals of the teeth were prepared for laterally condensed sealing and post-channels were drilled at low speed with the jigs and drills specified by the manufacturers. The different posts with a standardised core was cemented with zinc-phosphate cement according to the A.D.A. specifications and the tooth-post-core assembly tested to failure by means of the three mentioned force variables in a Lloyds Jay-Jay T5001 tensile testing machine.

RESULTS are not statistically significant mainly because an insufficient number of tests could be completed due to problems encountered with jigs and cores.

TENSILE: (P) n=20; force=298,23 N(ewtons) (S.D.=61,75): (T) n=14; force=346,45 N (S.D.=108,36. SHEAR: (P) n=7; force=1105,77 N (S.D.=226,20): (T) n=6; force=1418,53 N (S.D.=325,36). TORQUE: (P) n=4; force= 0,96 Newton Metres (S.D.=0,37). (T) n=13; force=1,59 Newton Metres (S.D.=1,20).

Some changes will be required in the testing protocol but it appears as though the (T) posts have better retention than the (P) posts.

107 The Pattern and Pathology of Skeletal Osteosarcoma in Pretoria.

W.F.P. VAN HEERDEN & A.J. LIGTHELM. University of Pretoria

The modern intensive surgical and chemotherapeutic approach to the treatment of skeletal osteosarcoma necessitates detailed investigation of the prevalence and pathological features of this tumour. This study was undertaken to determine the age and race incidence, the localization, radiological and pathological appearance as well as the histological classification of osteosarcoma.

One hundred and seven cases of this tumour were diagnosed at departments of Anatomical and Oral Pathology of the University of Pretoria. These cases were all reassessed and revised with regard to histological classification. There were 77 black patients, 28 whites and one coloured and Indian patient respectively. Amongst blacks the sex incidence was M:F=1,5:1 and amongst whites M:F=0,5:1. In both races the peak incidence was in the second decade. Affliction of long-bones was found in 76% of cases with the distal femur the most common anatomical site in both race groups. A high incidence (17%) of jaw tumours was found amongst blacks. The general pattern with regard to histological classification is similar to that reported in other series.

The higher prevalence of osteosarcomas amongst blacks in this series correlates with the higher incidence of sarcomas in general amongst blacks in Pretoria. The pattern of osteosarcoma in this series is largely comparable to other series in the literature, with the exception of an inverted sex-incidence amongst whites. The high incidence of jaw tumours amongst blacks further indicates a distinct difference when compared to other series.

108 Cyst Volume and Cyst Growth Potential – An In vitro Evaluation

A.J. LIGTHELM* & W.J.C. COETZEE
University of Pretoria

The increase in size and growth potential of cysts of the jaws play an important role in their behaviour and prognosis. The parameters used to determine the size of cysts include volume, the greatest area and perimeter as well as the diameter. Longitudinal evaluation of cyst growth is the correct way to evaluate the increase in cyst size. At present there is no reliable method in existence neither in vitro nor in vivo, for the determination of cyst growth. "No contact" three dimensional measuring by use of the reflex microscope offers the possibility of quantifying cyst size and hence growth potential.

Histological sections of implantation cysts in rats were evaluated by three operators with respect to the greatest area and perimeter as well as the greatest and smallest diameter. Sections made at 1,2,4,8 and 12 weeks after implantation were examined.

The reflex microscope has a specific accuracy of 4,5 and 15$\mu$m in respect of X, Y and Z co-ordinates and the differences between the measurements taken by the three operators of the greatest and smallest diameters were significant ($p < 0.05$: Kruskal-Wallis Test). No significant differences could be shown ($p > 0,05$: Kruskal-Wallis Test) in the measurements of the greatest area and diameter made by the three operators.

By the evaluation of the parameters of area and diameter the size of the cysts could be determined with greater precision and could be repeated in respect of the cysts at the above mentioned times. Consequently, longitudinal evaluation of growth potential in such a model is possible and significant.

109 Cleido-cranial Dysplasia (C.C.D.) in the South Western Cape.
L. BARTMANN, P.H. BEIGHTON, E. HORN, M.E. PARKER, M.G. SAMSODIEN, J. STAZ*, C. WALLIS, U.C.T. and U.W.C.

This autosomal dominant genetic disorder is widespread and well documented, most reports however referring usually to individuals or relatively small groups of cases. Jackson (1951) and Beighton (1978) established its prevalence in the South Western Cape. Jackson recorded 356 descendants of a Chinese seaman from Java who arrived at the Cape in 1896, settled in Somerset West, adopted the name of Arnold, embraced the Moslem Faith and seven wives and had an extensive progeny. Of these at least 70 or 19% exhibited the manifestation of this disorder. The present project is designed to pursue further these observations, to trace more family ramifications, to study in detail selected cases and to note trends, if any in the incidence of this dysplasia. To date (June 1987) 828 descendants, some comprising five generations have been noted of whom 68 or 8% are affected. Sixty one were examined in detail, their ages extending from three months (N.A.D.), nine months (with evidence) up to 79 years (marked evidence). There is no sexual differentiation in transmission. Preliminary findings, subject to biostatiscal evaluation, suggest that in many cases the penetration of C.C.D. is decreasing, especially in the clavicles, with an increase in the number of unaffected descendants.

This study is supported by the Medical Research Council of South Africa and the University of the Western Cape.

110 Ameloblastomas of the Jaws at Ga-Rankuwa Hospital : 1982 - 1987.
M.J.P. HARRIS* and E.J. RAUBENHEIMER. Medical University of Southern Africa, P.O. Medunsa.

Modern literature has indicated that there is a variation in the age, sex and site of occurrence of ameloblastomas in the various population groups.

The purpose of this study was to investigate the clinical and histopathological data of 34 patients with ameloblastomas diagnosed over a period of 5 years at Ga-Rankuwa Hospital (a referral hospital for the northern regions of Southern Africa). The age of the patients varied from 7 years to 80 years with an average of 30 years. The ameloblastomas were histologically confirmed and classified accordingly as either unicystic or solid. The gross patterns of the latter subtype were noted as either plexiform or follicular or a mixed appearance. Any differentiation in the stellate reticulum was also noted.

This tumour occurred mainly in females with an average of 32,5 years. The female to male ratio was 1,8:1 and the average age of the males was 25,5 years. Children under 18 years accounted for 26,5% of the total cases and this parallels the findings of Daramola, et al (1975). The preferred site of occurrence was the mandibular body and ramus which contradicts the study of Akinosi and Williams (1969). Six cases of unicystic ameloblastomas were identified and the average age was 18,2 years. It would appear that ameloblastomas with a plexiform growth pattern occur at a younger age than do the follicular type.

111 Quantitative Bone Changes in Rickets. P. DE VILLIERS*, E. RAUBENHEIMER, J. DAUTH and P. POTGIETER. Departments of Oral Pathology, Chemical Pathology and Orthopaedic Surgery, Medical University of Southern Africa, P.O. MEDUNSA

Microscopic diagnostic criteria in rickets are ill defined. This study was undertaken to determine quantitative microscopic bone changes in rickets and correlate these with biochemical findings.

Standardized transcortical iliac bone biopsies of 9 patients admitted at Ga-Rankuwa Hospital with clinical, biochemical and radiographic evidence of rickets were fixed in 70% alcohol and 3 micrometer thick undemineralized sections prepared and stained accordingly with hematoxylin and eosin, von Kossa and picrosirius techniques. All sections were subjected to image analysis using a VIDS II computerized system. The bone parameters assessed were total trabecular bone volume, mean cortical width, trabecular osteoid volume, mean ostecid seam width, osteoblasts per square millimeter biopsy area, trabecular resorptive surface and osteoclastic resorptive surface. Blood levels of alkaline phosphatase, parathyroid hormone, ionized calcium and inorganic phosphorus were correlated with the histomorphometric findings.

This study demonstrated that a reduction of the mean cortical width (< 570 microns), increased trabecular osteoid volume (> 4,68%), increased mean osteoid seam width (> 11,19 microns) and decreased trabecular resorptive surface (< 3,76%) are the most consistent bone changes in rickets. Furthermore, there appears to be a linear function between the high alkaline phosphatase levels and the number of osteoblasts per square millimeter biopsy area.

112 Histologic Monitoring of Mineralization Activity in Rickets.
E.J. RAUBENHEIMER*, P.I.A. DE VILLIERS, J. DAUTH and D. POTGIETER. Departments of Oral Pathology, Chemical Pathology and Orthopaedic Surgery, Medical University of Southern Africa, Pretoria.

Evaluation of the effect of a supplemented diet on the bone formation rate in rickets is based on subjective clinical and radiographic impressions over prolonged periods. This study was undertaken to determine mineralization activity microscopically in rachitic patients receiving a balanced hospital diet.

Standardized transcortical iliac biopsies of nine hospitalized patients suffering rickets were taken after two three day cycles of tetracycline administration twelve days apart. The tissues were fixed in 70 percent alcohol and undemineralized 5 micron thick sections cut. These were stained with hematoxylin and eosin, von Kossa stain for calcium and a further section mounted unstained. The distribution of mineralization fronts were studied on von Kossa stains and unstained sections were subjected to fluorescent microscopy. The percentage trabecular bone surface labelled and the average distance between tetracycline lines were measured and the bone formation rates or BFR (expressed in microns per day) and mineralization lag time or MLT (expressed in days) calculated. Measurements obtained were compared with accepted normal values (Vigorita, 1984).

Evaluation of the mineralization front was found to be subjective. Determination of BFR and MLT proved measurable and significant. 4 cases showed sufficient mineralization activity, 4 cases required additional Vit. D and mineral supplementation and a bone formation rate of zero prompted further examination and the diagnosis of a malformation syndrome in one case.

*Histopathology* 1997, 31, 12–17

# Static and dynamic bone changes in hospitalized patients suffering from rickets — a histomorphometric study

E.J.RAUBENHEIMER, W.F.P.VAN HEERDEN, D.POTGIETER & R.GOLELE
*Departments of Oral Pathology and Orthopaedic Surgery, Medical University of Southern Africa, MEDUNSA, South Africa*

Date of submission 10 October 1996
Accepted for publication 5 February 1997

RAUBENHEIMER E.J., VAN HEERDEN W.F.P., POTGIETER D. & GOLELE R.
(1997) *Histopathology* 31, 12–17

## Static and dynamic bone changes in hospitalized patients suffering from rickets — a histomorphometric study

*Aims*: The aim of this study was to assess static and dynamic bone changes in patients suffering from rickets. *Methods and results*: Transcortical iliac crest biopsies of 15 hospitalized children with rickets were taken after labelling new bone formation with two cycles of tetracycline administration 10 days apart. Undecalcified sections were prepared, appropriately stained and histomorphometric analysis performed. Static and dynamic bone changes were measured including the volume of bone and osteoid, trabecular and cortical bone dimensions and resorptive and mineralization activities. The results were compared with normal values. The nature of the mineralization fronts was noted. Trabecular osteoid volumes of all but one patient was above the normal range of 1.9% (± 0.4%). This patient suffered rickets associated with the Kwashiorkor–Marasmus syndrome. Tetracycline labelling was found to be more sensitive than subjective evaluation of the nature of the mineralization fronts. Despite a balanced hospital diet, a bone formation rate of zero was found in three cases, indicating a need for vitamin D and mineral supplementation. Seven cases had decreased mineralization lag times, indicating response to the balanced diet. *Conclusions*: This study showed that histometric analysis of labelled bone biopsies is a helpful adjunct to the diagnosis but particularly assessment of response to management of deficiency states in children.

Keywords: rickets, histomorphometry, bone metabolism

## Introduction

Rickets is a disease of children characterized by decreased mineralization of osteoid with abnormalities of bone growth. Failure of mineralization occurs when the plasma level of either calcium or phosphate is decreased over a prolonged period. The most common cause of rickets in developing countries is a dietary deficiency of vitamin D or calcium. In developed countries, other causes, notably renal disease, malabsorption states and inherited conditions characterized by increased phosphate loss in the renal tubules or end-organ insensitivity to vitamin D (vitamin D resistant rickets) are more common than nutritional deficiency[1]. The diagnosis of rickets is multidisciplinary. Clinical signs are related to deficient bone mineralization and manifest as skeletal growth retardation with bone loss, enlargement of the metaphysical regions and deformities of weight-bearing bones. Biochemical criteria include decreased plasma concentrations of calcium and phosphate, elevated alkaline phosphatase and chronic acidosis[1].

Bone biopsy is the only reliable technique through which the static bone volume can be established with accuracy. In conjunction with tetracycline labelling, dynamic parameters at cellular level, such as the rate of mineralization, can be expressed and weighted against standardized norms[2]. This study was undertaken to determine the volume of mineralized and unmineralized bone and establish the rate of new bone formation in hospitalized patients with rickets.

Address for correspondence: Professor E.J.Raubenheimer, Medical University of Southern Africa (MEDUNSA), Department of Oral Pathology and Oral Biology, Box D24, P.O. MEDUNSA, 0204, South Africa.



## Materials and methods

Two cycles of tetracycline (250 mg three times a day) for

3 days, respectively, were administered at an interval of 10 days to 15 hospitalized patients suffering rickets (Figure 1). All patients received a normal balanced hospital diet without vitamin D and calcium supplementation 2 weeks prior to the taking of the biopsy. Transcortical iliac crest biopsies were fixed in 80% ethanol and embedded in a plastic polymerizing resin. Undecalcified sections of 5 $\mu$m were cut and stained with haematoxylin and eosin and the von Kossa technique to evaluate mineralization and the Picrosirius technique to highlight osteoid. One unstained section was prepared to determine tetracycline incorporation with ultraviolet illumination. The sections were viewed with a transmission light microscope attached to an image analyser (Flexible Image Processing System, CSIR, Pretoria, South Africa) and microscopic parameters, as proposed by Vigorita in 1984[2], were quantified (Table 1).

## Results

The histomorphometric findings are summarized in Table 2 and the reference values are those for iliac crest bone in children[2]. The trabecular osteoid volume of all cases except case 9 were found to be significantly increased. Microscopic examination of the von Kossa stains of cases[1,2,4,5,9,12–15] showed a sharp interface between mineralized bone and osteoid. A calcification rate (CR) of above 1 $\mu$m per day was generally associated with a mottled and broad mineralization front as seen in cases 3, 6, 7, 8, 10 and 11 (Figure 2). Microscopic examination of unstained sections with ultraviolet illumination showed distinct lines of fluorescence of the tetracycline labels at the interface between osteoid and bone and in varying distance apart in all cases except 1, 12 and 15 (Figure 3).

## Discussion

The taking of a bone biopsy for screening purposes in patients with suspected metabolic bone disease has little justification; less invasive methods such as radiology and blood biochemistry can be employed for this purpose. However, most of the drugs involved in the treatment of rickets are expensive and serious complications are frequently seen from vitamin D intoxication[3]. The taking of a bone biopsy to determine the response to initial therapy is justified as it offers the possibility to quantify the volume of osteoid and establish the rate of new bone formation, thereby providing important information on the prognosis of a specific therapeutic regime. This procedure identifies non-responders during the initial stage of therapy which consisted in our study of a normal balanced hospital diet. The success of

**Figure 1.** Clinical appearance of case 4. Note the bowing of weight-bearing bones.

dynamic bone histomorphometry relies on the labelling of new bone formed over a set period before taking the biopsy. This is done by administering two 3-day cycles of tetracycline at least 10 days apart. The iliac crest is the site most frequently used for biopsy because it is easily accessible, non-weight bearing, and therefore not susceptible to stress-induced skeletal changes[4]. Biopsies are fixed in 80% ethanol to prevent loss of tetracycline which occurs during formalin fixation[2]. The technique requires special image analysis equipment and expertise and clinicians are advised to, before taking a biopsy,

Table 1. Histomorphometric parameters determined

| Term | Abbreviation | Definition |
|---|---|---|
| Trabecular bone volume | TBV | The percentage of the medullary cavity occupied by mineralized and unmineralized bone. |
| Mean trabecular width | MTW | The average width of all trabecular bone spicules. |
| Mean cortical width | MCW | The mean thickness of both cortices. |
| Trabecular osteoid surface | TOS | The percentage of bone surface covered by osteoid. |
| Trabecular osteoid volume | TOV | The osteoid area expressed as a percentage of trabecular bone area. |
| Mean osteoid seam width | MOSW | The osteoid area divided by mm of bone surface covered by osteoid. |
| Trabecular resorptive surface | TRS | The percentage of bone surface showing Howship's lacunae. |
| Osteoclastic resorptive surface | ORS | The percentage of bone surface lined by osteoclasts. |
| Osteoclasts per mm of trabecular perimeter | OTP | The number of osteoclasts per mm of bone perimeter. |
| Calcification (apposition) rate | CR | The distance between the middle of all double tetracycline labels divided by the number of days between the administration of two labels. |
| Mineralization lag time | MLT | The mean osteoid seam width divided by the bone formation rate. |
| Bone formation rate | BFR | The calcification rate times the percentage of trabecular surface labelled. |
| Percentage of trabecular surface labelled | TSL | The percentage of bone surfaces labelled by tetracycline labels. |
| Mineralization front | MF | The nature of the line of mineralization between osteoid and mineralized bone. |

ascertain whether the histopathology laboratory is equipped to perform this investigation.

In contrast to osteoporosis, the bone in rickets and its adult counterpart, osteomalacia, is qualitatively abnormal and characterized by a failure of mineralization. The earliest bone change occurring in rickets is the disappearance of mineralization fronts. The border between osteoid and mineralized bone loses its ill-defined granular nature and is replaced by a distinct line separating unmineralized and mineralized bone. This change is associated with impairment of mineralization of osteoid and impacts on the dynamic measurements as a decreased uptake of the tetracycline label. The percentage of trabecular surface labelled (TSL) subsequently decreases and the calcification rate (CR) falls below 0.54 $\mu$m per day[2,5]. These parameters are also the first to respond to effective treatment. The sharp mineralization fronts (as seen in cases 1, 2, 4, 5, 9, 12–15) are indicative of a lack of sufficient mineralization of osteoid. Tetracycline labelling, however, appears to be more sensitive, as in a number of these cases (2, 4, 5, 9, 13 and 14) the rate of mineralized bone formation (BFR) was found to be adequate despite sharp mineralization fronts. The BFR, which is decreased in untreated rickets, brings the CR into perspective by expressing the dimensional volume of new bone formed more accurately. This parameter prognosticates the potential outcome of a therapeutic regime and may obviate the necessity to introduce vitamin D and mineral supplementation. The three cases in our study with BFRs of zero warrant vitamin D and mineral supplementation. Failing response, further investigations

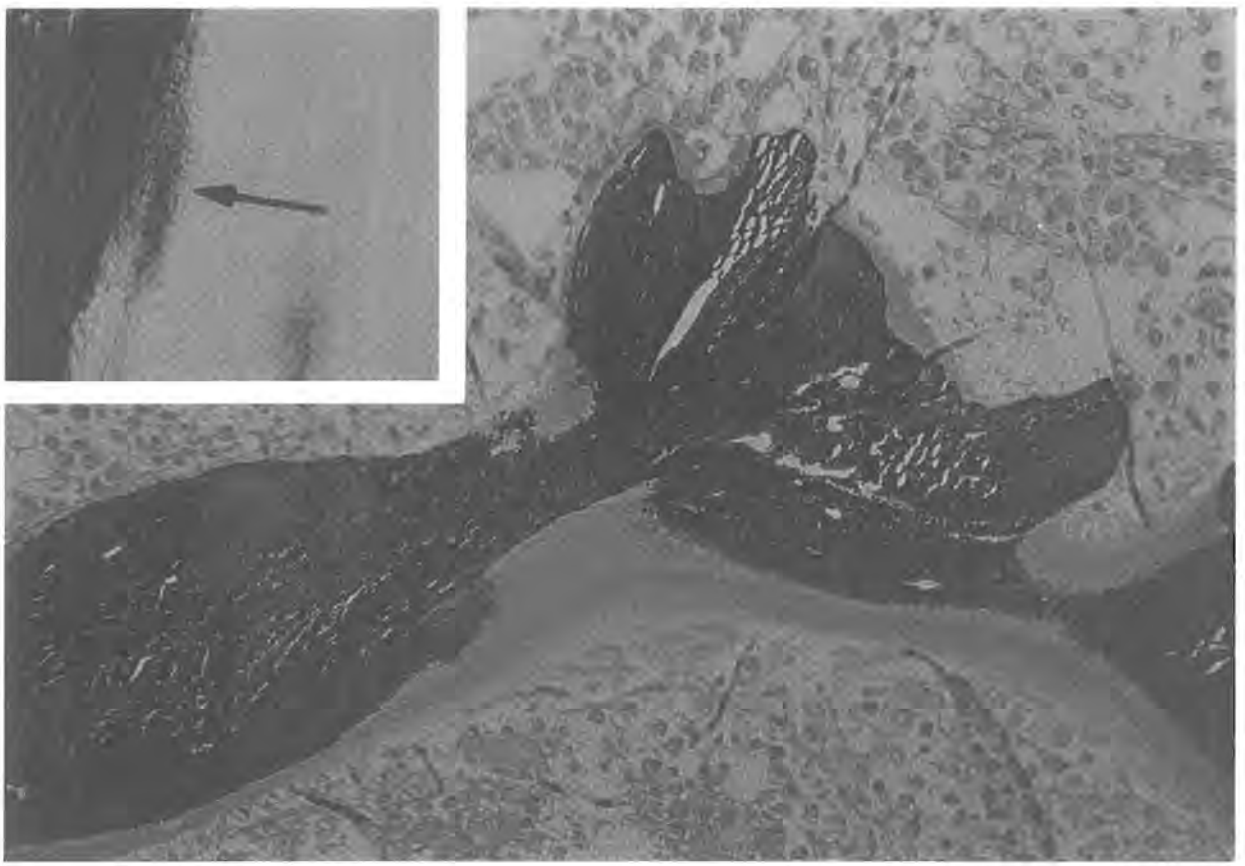

**Figure 2.** Photomicrograph of a mineralized bone trabeculum (black) covered by a wide osteoid seam (von Kossa stain, ×100). The inset shows a higher magnification of a wide and mottled mineralization front (arrow) (von Kossa stain, ×250).

should be employed in order to exclude poor compliance to therapy or establish a non-nutritional cause for their bone deficient state. In the event of not finding any other cause, the status of the osteoid matrix may be so abnormal as to prevent mineralization[6]. The mineralization lag time (MLT), which is generally longer in rickets than in other bone deficiency states, is an indication of the discrepancy between the process of osteoid and mineralized bone formation. This parameter is generally lengthened in rickets and a decrease thereof is an indication of response to therapy, as achieved in seven of our cases.

After mineralization has ceased, the second pathognomonic microscopic feature of rickets is introduced during which the osteoblasts continue to produce osteoid which remains unmineralized, and an increase in the volume of osteoid occurs. This change manifests as a widening of the osteoid seams and reflects as an increased mean osteoid seam width (MOSW). Eventually, the osteoblasts cease to deposit osteoid, dedifferentiate and osteoblasts elsewhere on the bone surface lay down osteoid which also thickens and subsequently becomes inactive. The bone surface covered by osteoid increases and the trabecular osteoid surface (TOS) and volume of osteoid (TOV) subsequently rises. This phase continues until large areas of bone surface are covered by abundant osteoid. The increase in the trabecular bone volume (TBV) in rickets is therefore a result of osteoid formation. Extensive osteoid coverage prevents osteoclast mediated bone resorption and reflects as a decrease in the osteoclast-associated parameters[2,5]. In most of our cases, the osteoclastic resorptive surface (ORS) and osteoclasts per mm of trabecular perimeter (OTP) were found to be elevated despite abundant osteoid. This is probably indicative of the osteoclast activating effect of secondary hyperparathyroidism. In the atrophic (or porotic) form of rickets, osteoid is, however, reduced in volume. This manifestation is seen in the Kwashiorkor–Marasmus syndrome associated with rickets and indicates the coexistence of two deficiency states in the same child[7]. Our case 9, which exhibited narrow osteoid seams and a low trabecular osteoid surface, falls in this category. These changes in

Table 2. Histomorphometric findings in 15 patients treated for rickets

| | Ref. Value (SD)[2] | Case 1 Male 13 years | Case 2 Female 15 years | Case 3 Male 6 years | Case 4 Male 5 years | Case 5 Male 7 years | Case 6 Male 6 years | Case 7 Male 3 years | Case 8 Male 5 years | Case 9 Male 5 years | Case 10 Male 4 years | Case 11 Male 4 years | Case 12 Female 13 years | Case 13 Male 5 years | Case 14 Male 5 years | Case 15 Female 3 years |
|---|---|---|---|---|---|---|---|---|---|---|---|---|---|---|---|---|
| TBV | 22.5% (3.5) | 15.4 | 23.6 | 23.3 | 14.1 | 36.2 | 21.2 | 11.5 | 29.7 | 22.9 | 20.8 | 14.9 | 16.2 | 24.4 | 35.4 | 26.5 |
| MTW | 213 μ (65) | 128.3 | 186.1 | 187.2 | 121.5 | 258.1 | 126.4 | 127.5 | 152.4 | 130 | 155 | 203.8 | 158.5 | 59.4 | 159.8 | 110 |
| MCW | 909 μ (98) | 104.9 | 570.4 | 394 | 416.3 | 1157 | 419 | 120 | 379.4 | 421 | 344 | 748 | 579 | 103.4 | 271.1 | 186 |
| TOS | 18.9% (5) | 29.3 | 8.1 | 68.8 | 34.3 | 55.9 | 20.9 | 24.0 | 21.3 | 14.2 | 31.8 | 10.4 | 15.5 | 95 | 64 | 45.5 |
| TOV | 1.9% (0.4) | 35.3 | 10.3 | 9.4 | 9.9 | 14.8 | 11.0 | 11.3 | 4.7 | 0.6 | 6.1 | 3.9 | 8.5 | 57.8 | 28.9 | 21.8 |
| MOSW | 9.7 μ (0.4) | 44.1 | 27.2 | 29.2 | 23.7 | 31.8 | 29.5 | 13.7 | 18.2 | 5.0 | 10.2 | 10.8 | 16.1 | 33.5 | 40.4 | 16.9 |
| TRS | 5.1% (0.6) | 6.5 | 1.3 | 2.4 | 3.2 | 5.4 | 2.0 | 0.7 | 3.8 | 1.7 | 3.6 | 1.3 | 2.1 | 3.9 | 4.2 | 4.6 |
| ORS | 0.13% (0.6) | 0.8 | 0.3 | 0.5 | 0.8 | 1.4 | 0.1 | 0.2 | 1.4 | 0.2 | 0.6 | 0.3 | 0.1 | 0.2 | 0.6 | 2.5 |
| OTP | 0.03 (0.01) | 0.1 | 0.07 | 0.1 | 0.1 | 0.4 | 0.06 | 0.04 | 0.4 | 0.04 | 0.1 | 0.06 | 0.04 | 0.05 | 0.8 | 5.1 |
| CR | 0.64 μ (0.1) | 0 | 0.9 | 1.6 | 0.6 | 0.8 | 1.3 | 1.4 | 1.9 | 0.9 | 1.6 | 1.6 | 0 | 0.7 | 0.2 | < 0.1 |
| MLT | 29 days (3) | > 100 | 0.8 | 0.5 | 3.3 | 5.6 | 0.5 | 0.2 | 3.6 | 0.4 | 0.4 | 1.5 | > 100 | 0.8 | 33.7 | > 100 |
| BFR | 0.44 μ (0.04) | 0 | 35.8 | 63.2 | 7.1 | 5.7 | 59.0 | 57.7 | 5.1 | 12.8 | 24 | 7 | 0 | 42 | 1.2 | 0 |
| TSL | 12.8% (2.3) | 0 | 39.3 | 39.5 | 11.8 | 7.1 | 45.4 | 41.2 | 13.2 | 14 | 15 | 5 | 0 | 60 | 6 | 0 |

 

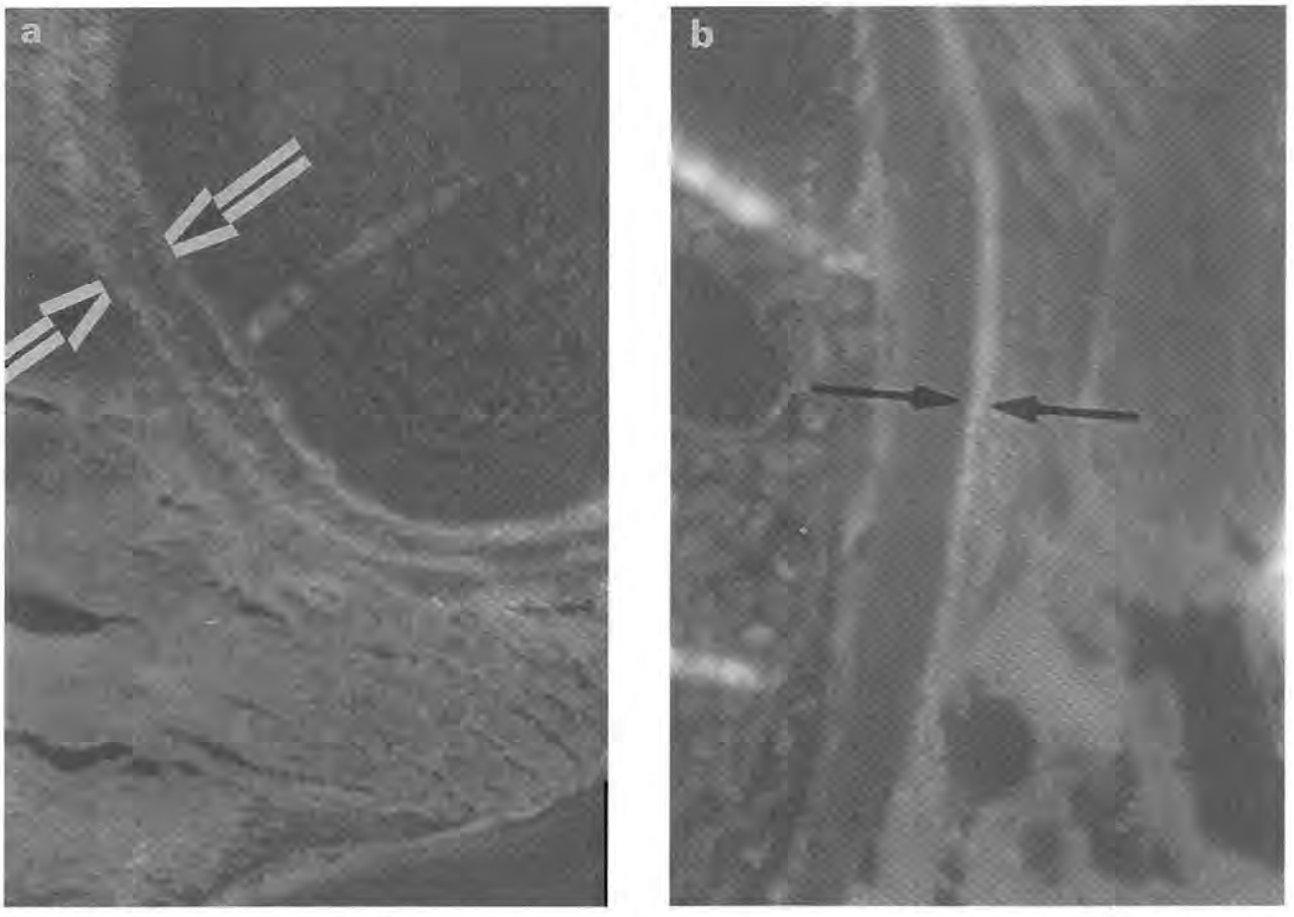


**Figure 3.** Fluorescing tetracycline labels. **a**, The arrows show spacing between the fluorescing lines in a case with a normal CR. **b**, The superimposed lines on the right (arrows) indicate inadequate mineralization activity (unstained sections viewed under ultraviolet light, ×20).

rickets indicate the need for a more extensive therapeutic regime addressing protein and calorific malnutrition.

Histomorphometric analysis of bone is a helpful adjunct to the diagnosis and therapeutic management of bone deficiency states. The refinement which it introduces contributes to accurate diagnosis and limit the usage of broad and non-specific terminology like juvenile osteoporosis. Labelling of dynamic bone changes and the quantification of the response to a normal balanced hospital diet obviates the need for expensive and potential toxic vitamin D supplementation in most patients with rickets. It furthermore contributes significantly to the early identification of those in whom additional investigations are required to diagnose a non-nutritional cause for the bone deficiency state.

## Acknowledgement

Mrs C.S.Begemann is thanked for secretarial assistance.

## References

1. Jaffe HL. Rickets and osteomalacia In Jaffe HL, ed. *Metabolic, Degenerative and Inflammatory Diseases of Bones and Joints.* Philadelphia: Lea & Febiger, 1975; 381–447.
2. Vigorita VJ. The tissue pathologic features of metabolic bone diseases. *Orthop. Clin. N. Am.* 1985; **15** (4); 613–629.
3. Dent CE, Stamp TCB. Vitamin D, rickets and osteomalacia. In Aviol LV, Krane SM, eds. *Metabolic Bone Disease,* Vol. 1. New York: Academic Press, 1977; 237–302.
4. Byers PD. The diagnostic value of bone biopsies. In Avioli LV, Krane SM, eds. *Metabolic Bone Disease,* Vol. 1. New York: Academic Press, 1977; 184–236.
5. Jowsey J. Rickets and osteomalacia (Chapter 21). In Jowsey J, ed. *Metabolic Diseases of Bone.* Philadelphia: WB Saunders Company, 1977; 192–204.
6. Klein GL, Simmons DJ. Nutritional rickets: Thoughts about pathogenesis. *Ann. Med.* 1993; **25**; 379–384.
7. Mekherjee A, Bhattacharyya AK, Sarkar PK, Mondal AK. Kwashiorkor–Marasmus syndrome and nutritional rickets — a bone biopsy study. *Trans. Royal Soc. Trop. Med. Hyg.* 1991; **85**; 688–689.

This presentation will enunciate the following:
1. What is telepathology
2. Classification, description, advantages and disadvantages of different telepathology systems
i Static telepathology
ii Robotic (Dynamic) telepathology
3. Requirements of a telepathology system: The hardware and the software
4. Transmission of images
5. Causes of failure of telepathology systems
6. Results of a study of the use of telepathology in the field of oral pathology

59

## THE ROLE OF HISTOMORPHOMETRY IN THE DIAGNOSIS AND MANAGEMENT OF METABOLIC BONE DISEASES.

E J. Raubenheimer
Department of Oral Pathology, Medical University of Southern Africa, South Africa

*Objectives:* The objective of this study was to determine the role of dynamic microscopic changes in the diagnosis and management of metabolic bone diseases.
*Methods:* Biopsies were taken of tetracycline labeled bone of 30 patients suffering metabolic bone diseases of diverse etiologies. The biopsies were fixed in 80% alcohol, embedded in resin, sectioned and stained with the picrosirius-, von Kossa- and H&E staining techniques. Unstained sections were viewed with ultraviolet illumination. Static and dynamic bone parameters of osteoblastic -, osteoclastic – and mineralization activities were measured with the aid of an image analysis system linked to a light microscope. Histomorphometric findings of each case were matched with reference values, biochemical results, the final diagnosis and therapeutic responses.
*Results:* The study showed that the responses to mineral supplementation of patients suffering rickets and osteomalacia were greatly influenced by the volume of osteoid. Cases in which more than 80% bone surfaces were coved by osteoid were characterized by hypocalcemia. Rickets associated with the kwashiorkor – marasmus syndrome showed low osteoid volumes and a poor clinical response to mineral supplementation. Active tunneling resorption was found to be the benchmark of hyperparathyroidism and diletescence rather than osteoclastic activity the cause of bone loss in disuse osteopenia. In chronic liver failure, hypogonadism and osteogenesis imperfecta all osteoblast – and mineralization activities were found to be reduced. Spindle shaped osteoblasts distinguished the bone changes in osteogenesis imperfecta from those of liver failure and hypogonadism. Renal osteodystrophy could be classified on histomorphometric parameters in hyper- and hypo dynamic subtypes and provided useful information on the need for parathyroidectomy.
*Conclusion:* Histomorphometry plays a central role in the diagnosis and management of metabolic bone diseases.

60

## HUMAN PAPILLOMAVIRUS-ASSOCIATED ORAL LESIONS IN HIV-PATIENTS RECEIVING HIGHLY ACTIVE ANTIRETROVIRAL THERAPY (HAART)

A. M. Schmidt-Westhausen[1], A. Perez-Canto[2], P. A. Reichart[1],
[1]University Hospital Charité, Department of Oral Surgery and Dental Radiology, Berlin, Germany.[2] University Hospital Benjamin Franklin, Institute for Pathology, Berlin, Germany

Oral papillomatous lesions are a manifestation of human papillomavirus infection that have been noted infrequently in HIV-infected persons. In the era of HAART the incidence of oral warts in HIV-seropositive patients appears to be increasing, whereas the prevalence of oral lesions strongly associated with HIV-infection have been noted to be decreasing.
*Objective:* Aim of this study was to characterize oral papillomatous lesions and their relapses in patients with HIV infection treated with HAART on their clinical aspects, to determine the presence of HPV-DNA by PCR and to specify the HPV genotypes by sequencing analysis.
*Material and method:* 25 biopsies of oral papillomatous lesions diagnosed according to accepted features were obtained from six HIV-patients receiving HAART for > 6 months (homosexual males, median age 36.5 year. [29–68 year.], median CD4 ± cells 238/μL [32–460 μL], median viral load < 50/mL [ <50–12000/mL]). 8/25 biopsies were taken from recurrent lesions. Clinically the lesions were diagnosed as verruca vulgaris (7/25), condyloma accuminatum (16/25) and focal epithelial hyperplasia (FEH) 2/25. In two patients the lesions were multiple and spread throughout the entire mucosa. Routine histopathology was performed, additionally, biopsies were tested for the evidence of HPV-DNA by PCR using L1 consensus primers and subjected to sequencing analysis.
*Results:* 22/25 biopsies harboured HPV-DNA. Sequencing analysis revealed HPV-32 in 10/21 specimens, HPV-72 in 6/21, HPV-55 in 1/21 and HPV-7 in 1/21 cases. In one patient an unknown HPV-type was identified. In condylomata accuminata HPV-32 and -72 was detected, in verrucae vulgares HPV-7 and 32, in FEH HPV-55 and one HPV-genotype not yet identified. In one patient the biopsy obtained from recurrent lesion clinically diagnosed as verruca vulgaris revealed two different types of HPV (-7 and -32).
*Discussion:* Studies on HPV-associated oral lesions have suggested a correlation between FEH and HPV-13 and -32, verruca vulgaris with HPV-2 and -4 and condyloma accuminatum with HPV-6 and -11. However, in HIV-patients unusual HPV types such as HPV-7 have been identified from oral warts. In the present study HPV-DNA of a single type could be found in oral papillomatous lesions of different clinical appearances and different HPV-genotypes could be identified in lesions of similar appearance. HPV-55 which was associated with FEH in this study is mainly related to lesions of the genital tract. So far, HPV-72 has only once been identified in an oral wart with atypia in a HIV-positive patient. In our study HPV-72 was evident in two patients with multiple condylomata. This study suggests that (1) HIV-infection seems to predispose individuals to oral infection with uncommon as well as new HPV-types and (2) the increased risk of HPV infection in patients receiving HAART may represent a form of immune reconstitution syndrome occuring in response to improved cell-mediated immune function.

61

## DETECTION OF TP53 MUTATIONS IN ORAL LEUKOPLAKIA BRUSH BIOPSY

C. Scheifele[1], H. Schlechte[2] & P. A. Reichart[1]
[1]Department of Oral Surgery and Dental Radiology, Center for Dental Medicine, [2]Department of Urology (1) and (2): University

# Histopathologic Changes in Metabolic Bone Disease

Erich J. Raubenheimer

*Professor and Consultant for Metabolic Bone Diseases, Medical University of Southern Africa, South Africa.*

Address for correspondence: Prof E J Raubenheimer, Box D24, Medical University of Southern Africa, P.O. Medunsa 0204, South Africa.
Telephone numbers: 12 521 4838 (direct line and fax)
e mail: ejraub@medunsa.ac.za

**Summary:** Metabolic bone disease encompasses a heterogeneous group of disorders that influence skeletal metabolism and structure. They are generally diagnosed at an advanced stage and manifest clinically with stunted skeletal growth in children and pathological fractures in adults. Biochemical markers for bone metabolism are equivocal and microscopic examination of labelled bone remains the gold standard for the diagnosis and accurate monitoring of the response to therapy. This article reviews the role of microscopic bone changes in the diagnosis and management of metabolic bone disease.

Keywords: metabolic bone disease, rate of bone formation, histomorphometry

# INTRODUCTION

Metabolic bone disease encompasses a heterogeneous group of disorders that affect skeletal collagen or mineral deposition. These include malnutrition, malabsorption, ageing, immobilization, endocrine and neoplastic diseases, drugs and toxins, genetic conditions, kidney disease and HIV infection. In developed countries the most common associations are old age, immobility and the use of drugs whereas in the developing world, nutritional factors are more frequently implicated. Metabolic bone disease generally progress sub-clinically and are diagnosed late when clinical manifestations focus attention on end stage skeletal debilitation. During childhood, growth of the skeleton is retarded and although all bones are affected, most changes impact on the growth centres of long bones. Significant mortality, morbidity and societal expense result in adults where pathological fracture is the key manifestation.

# DISCUSSION

## Assessment of bone metabolism

Until recently, the only available biochemical markers for bone turnover were total serum alkaline phosphatase for the monitoring of bone formation and urinary hydroxyproline for bone resorption. Both are not specific to bone metabolism and unable to detect small changes in bone turnover. The lack of sensitive markers for bone metabolism has directed efforts to develop new and more specific biochemical assays. Bone GLA-protein (BGP), also called osteocalcin, is the only protein found to be specific for bone and dentin. It is produced by osteoblasts and might play a role in the recruitment of osteoclasts thereby being one of the mediators that couple the activities of these cells. A fraction of newly synthesized BGP is released into circulation, where it can be measured by radioimmunoassay. Serum BGP measurements should be interpreted with caution as many unresolved questions remain on the volume distribution, metabolic clearance, influence of vitamin D deficiency, circadian rhythm and breakdown thereof by osteoclasts (1). Urinary excretion of pyridinium cross-links is the most tangible improvement in the search for a specific biochemical marker for bone resorption. Hydroxylysylpyrinoline (HP) is widely distributed in type I collagen of bone and the type II collagen of cartilage, but is absent in skin collagen. Lysylpyrinoline (LP) is present

only in type I collagen of bone (2). An increase in urinary HP and LP has limited application and has been associated with hyperparathyroidism (3), menopause (1), rheumatoid arthritis and osteoarthritis (4). Finding a sensitive biochemical marker for bone resorption remains a challenge, the outcome of which may lie in studies on the multitude of peptides released during osteoclast induced bone resorption.

Refinements of histological methods not only established microscopy as the gold standard in the diagnosis of metabolic bone disease (Table 1), but also contributed significantly to the understanding thereof (5,6). In order to assess sub clinical bone changes at cellular level, a transcortical biopsy of a non-weight bearing bone, like the iliac crest, is advised (5). The biopsy is performed 2 days after the last of two 3-day cycles of tetracycline administration, which are at least 10 days apart (7). The presence of both cortical and trabecular bone in the biopsy is important, as significant differences exist in the metabolism of these two bone compartments. Cortical bone, which makes up 85% of the total bone mass of the body, is exposed to the periosteum and is remodelled internally through an extensive network of Haversian and Volkmann canals. Trabecular (or cancellous) bone constitutes the remaining 15% (8), is enveloped in fat and marrow, each spicule is remodelled on its surface and is relatively avascular internally. Fixation of the biopsy in 90% ethanol minimizes loss of tetracycline. Undecalcified sections are stained with the Von Kossa- and Picrosirius techniques which highlight mineral and osteoid content respectively. Unstained sections are examined with ultraviolet illumination in order to assess the extent of tetracycline incorporation. Static and dynamic bone changes are measured with the aid of an image analyzer. The static changes represent the state of the bone at the time at which the biopsy was taken. These include indices reflecting bone mass, volume of osteoid and osteoclastic resorption. The dynamic parameters reflect the rate and extent of incorporation of mineral (tetracycline) into bone between administrations of the labels. Static and dynamic histomorphometric measurements are compared with standardized norms in young healthy adults (Table 2)(5) and correlated with clinical, radiologic and biochemical findings thereby accurately assessing all aspects of bone metabolism. A recommended diagnostic flow chart is reflected in Figure 1.

**Factors influencing bone metabolism**

*Malnutrition*

Failure of mineralization occurs when plasma concentrations of either calcium (Ca) or phosphate (P) are decreased over a prolonged period. The most common causes thereof in developing countries are dietary deficiencies of Vitamin D (Vit D) or Ca whereas in developed countries, other factors like renal disease and malabsorption states are more frequently implicated (9). In growing children these conditions lead to rickets and after skeletal growth has ceased, osteomalacia. Rickets is amongst other clinical features characterized by cranial deformities including frontal bossing and craniotabes (softening of the skull), softening of the metaphysis and bowing of weight bearing bones (Fig. 2). With Vit D and /or Ca deficiencies stimulation of PTH secretion is aimed at maintaining normal serum Ca levels. These biochemical changes are associated with quantifiable microscopic alterations to the morphology of bone. In contrast to osteoporosis, bone in rickets is qualitatively abnormal and characterized by excessive osteoid deposits (reflected as an increase in indices of osteoid) and a lack of mineralization (manifesting as a decrease of indices of mineralization). Secondary hyperparathyroidism, which occurs only in Ca and Vit D deficiency states (10) leads to increased osteoclast induced resorbtive activity. Normal blood Ca concentrations are maintained as long as exposed bone surfaces show resorbtive facets (Fig. 3). When all surfaces are covered by osteoid, further osteoclast-mediated bone resorption is prevented and hypocalcemia develops. The term 'hypertrophic' rickets has been used to describe patients with broad osteoid seams lacking mineralization (9). These patients usually respond favorably to mineral and Vit D supplementation. A broad mineralization front and increased dynamic measurements are therefore indicators of a good response to therapy (Fig. 4). In the 'atrophic' form of rickets osteoid is significantly reduced in volume, dynamic measurements are low and mineralization fronts narrow. This manifestation is often seen as part of the kwashiorrkor-marasmus syndrome (or protein calorie malnutrition) complicated by Ca and P deficiencies. This complex deficiency state is resistant to Vit D and mineral administration alone and requires additional amino acid supplementation in order to provide nutritients for osteoid production (7). The histomorphometric findings in rickets and osteomalacia are diagnostic (Table 3).

Diets high in fibre may adversely affect Ca retention (11) and decrease Ca absorption from the gastrointestinal tract (12). This is the result of the high Ca binding capacity of wheat bran (13). Moreover there is evidence that the Vit D mediated mechanism for active absorption of dietary Ca may be diminished by dietary fibre (14). The diets of vegetarians must be carefully monitored, as they are inadvertently Vit D deficient due to their low fat content (15). Osteomalacia in vegetarians is characterized by a severe reduction of trabecular bone volumes, an increase in the trabecular surfaces covered by osteoid, severely thickened osteoid seams and reduced mineralization activities. Serum markers are of no value as the majority of patients have normal Ca, Vit D and alkaline phosphatase concentrations (16). Magnesium (Mg) deficiency is an important risk factor for osteoporosis in humans. Several studies have reported significant reductions in serum - and bone Mg concentrations in postmenopausal women with osteoporosis. Elderly women who consumed less than 187 mg Mg per day were found to have significantly lower bone mineral densities than women whose average dietary Mg intake exceeded this figure. Western diets have intakes of Mg which are significantly below recommended levels. This leads to reduced bone formation and subsequent reduced bone volume with increased skeletal fragility (17). Vitamin C deficiency results in a decreased bone formation rate with normal resorption, resulting in a decreased bone volume (18). Failure to respond to dietary supplementation should prompt further investigations to exclude vitamin D resistant rickets, malabsorption syndromes, debilitating disease states or poor patient compliance. Causes of malabsorption include gluten sensitive enteropathy, gastrectomy, gastrointestinal tuberculosis, Crohn's disease, sarcoidosis and conditions leading to a deficiency of bile salts in the intestine. Bile salts are an absolute requirement for optimal Vit D and Ca absorption in the gastrointestinal tract (15).

*Ageing*

Although age related bone changes are not classifiable as disease, they are being recognised as a major health and medical economic problem (19). The overall direct cost, including rehabilitation, of osteoporosis (which is defined as quantitively reduced but qualitively normal bone) in both men and women were estimated in 1997 to be 52.5 million US$ per million of the population of the United States annually (20). During puberty bone mass increases about 3-fold over a few years (21). Peak skeletal bone mass is achieved between 25 and 35 years of age (22). It is generally accepted that those who achieve a higher peak bone mass are less at risk of developing osteoporotic fractures in later life. Between 60% and 80% of variance in

bone phenotypic expression at any age is genetically determined and the effect of lifestyle and hormonal factors modifying the remaining. The former include diet, exercise, alcohol consumption and tobacco use amongst a range of others that are less well characterized. Excessive ingestion of common salt, phosphorus or caffeine and the use of tobacco and alcohol have been associated with increased fracture incidence in epidemiological studies. Dietary intake of Ca has been a major focus in age related osteoporosis. Intakes of 1200 – 1500 mg/day have been recommended around puberty and after menopause and 800 – 1000 mg/day suggested for other stages of life (23). The administration of Ca and Vit D reduces the incidence of hip fracture among elderly women in nursing homes (24). Estrogen hormone replacement therapy in estrogen deficient postmenopausal women leads to a gain in alveolar bone density (25) as well as a significantly lower risk for tooth loss than age matched non-estrogen users (26).

Histomorphometric studies are valuable in diagnosing and monitoring the response to therapy of patients suffering osteoporosis (Table 4). Men, like women, loose trabecular bone more rapidly than cortical bone and several studies have shown that the trabecular bone volume of the iliac crest declines with age at approximately equal rates in men and women (27). Data indicate that age related osteoporosis occurs predominantly by a process that removes entire structural elements and is characterized by trabecular bone loss rather than thinning (Fig. 5). The trabeculae that remain are more widely separated and some may even undergo compensatory thickening (28). The concept of two osteoporotic syndromes in women, type I with predominantly trabecular bone loss related to gonadal steroid deficiency and type II with cortical bone loss greater or equal to trabecular bone loss due to ageing (29) has not yet been demonstrated in men. The lower incidence of complications of osteoporosis in men may be due to a higher peak bone mass at skeletal maturity (30), shorter life expectancy and the absence of a distinct menopause equivalent with accelerated bone loss in men (31).

The causes of age related osteoporosis in healthy individuals are certainly multifactorial. A recent study suggests that preserved osteoclast activity and decreased osteoblast function are the cellular events responsible for bone loss during ageing (31). Osteoblasts of both genders appear to deposit inadequate volumes of new bone insufficiently balancing sustained osteoclast resorption. This results in loss of bone trabeculae at foci of resorption. The trabecular bone volume is reported to reduce by 40% between the ages of 20 to 80 years in

healthy individuals and the osteoblast to osteoid interface and osteoid labelling for mineral depositioning each by more than 18% (27). However not all bone is lost through osteoclastic activity. Bone loss from quiescent lamellar bone surfaces, without osteoclastic activity, termed delitescence, could partly be responsible for age related osteoporosis (32). The standardized norms reflected in Table 2 should in practice be adapted to the age of the patient.

*Immobility*

Physical activity is important for the maintenance of skeletal bone mass. In the absence of mechanical stimulation, the surface area of bones decrease significantly when compared to those subjected to mechanical stimulation (33). Disuse osteoporosis may be generalized or confined to immobilized skeletal segments. The loss of skeletal mass could be as high as 25 – 45% over periods as short as 30 – 36 weeks. Orbital space flight, which results in unloading of the skeleton, leads to bone loss approximating 20% of the skeletal mass in some astronauts during short-term weightlessness (34). The resulting bone loss can be arrested by estrogen replacement (35). Disuse osteoporosis results from a combination of a moderate decrease in osteoblastic activity and a marked increase in osteoclastic resorption of trabecular bone. Bone loss is primarily trabecular and subperiosteal scalloping of cortical bone may be evident. Hypocalcemia, hypercalcuria, ectopic calcifications and hydroxyprolinuria frequently occur in disuse osteoporosis. Phosphorus supplementation and corticoids may prove effective in reversing the hypocalcemia and hypercalcuria associated with immobilization and prevent metastatic calcifications from occurring (34).

*Endocrine factors*

Growth hormone (GH) regulate bone resorption and bone formation and has a direct effect on osteoblasts via GH binding sites as well as an indirect effect via insulin–like growth factor (IGF-1). Estrogen facilitates the GH – IGF-1 axis whereas glucocorticoids appear to suppress GH induced action of IGF-1. Although little success has been achieved in the identification of GH receptors on osteoclasts, it has been proven that GH regulates osteoclast formation in bone marrow cultures. This explains the biphasic action of GH. GH secretion initially results in increased bone resorption with a concomitant bone loss followed later by increased bone formation. The point where bone formation balances bone resorption, is usually reached after 6 months. Net bone mass gain after GH therapy may take some time as

the initial decrease in bone mass must first be replaced. Both cortical and trabecular bone parameters are increased by prolonged GH secretion. Conversely, cortical and trabecular bone measurements are reduced in pituitary dwarfism (36).

In normal subjects 0.2 osteclasts should be present per $mm^2$ trabecular bone and 5% of bone surfaces show Howships lacunae (Table 2). Recent onset hyperparathyroidism is characterized microscopically by foci of tunnelling resorption (Fig.3) as well as an elevation of all indices of resorbtive and osteoblastic activities. Subperiosteal osteoclasts are rare, and when present indicative of a high resorbtive state as seen in hyperparathyroidism. The development of brown tumors of hyperparathyroidism is, unlike generally believed, a rare event and occurs only in a small percentage of cases with increased parathyroid activity. Fibrous marrow scars may be indicative of healed or long-standing hyperparathyroidism (7). The rate at which osteoid is deposited in empty Howships lacunae after restoration of normal parathyroid function, is indicative of the efficiency of recruitment of new osteoblasts. Skeletal changes similar to those seen in hyperparathyroidism but associated with normal PTH concentrations are indicative of Jansens disease, a condition characterized by normal PTH secretion with overactive PTH receptors on osteoclast (37).

Sixty seven percent of men with spinal osteoporosis suffer an identifiable cause, which may include ethanol abuse, hypogonadism or hypercortisolism (38). Hypogonadism in males appear to affect mainly the bony cortex (39) whereas gonadal steroid deficiency in females leads predominantly to cancellous bone loss (29). Corticosteroid deficiency manifests as cancellous osteopaenia whereas excess results in decreased bone growth, except in growing males (40). Decreased bone growth is aggravated by corticosteriodal inhibition of gastrointestinal absorption of Ca, which leads to secondary hyperparathyroidism and bone resorption. Excessive thyroid hormone replacement therapy causes accelerated bone loss with subsequent osteoporosis due to thyroid hormone induced osteoclastic activity (41).

*Neoplastic disease*

Malignancy is frequently associated with significant skeletal changes. An excellent summary of the effect of malignant disease on bone was recently published (8). By far the most common causes of hypercalcemia are primary hyperparathyroidism and malignancy, the latter being one of the more common paraneoplastic syndromes. Malignancies most frequently

associated with hypercalcemia are carcinomas of the lungs (35%), breast (25%), hematological system (14%) and the head and neck region (6%). Hypercalcemia associated with malignancies may be due to a combination of humoral factors secreted by the neoplastic cells and that act systemically on target organs, local factors released by neoplastic cells in bone and that directly stimulate bone resorption and coexisting primary hyperparathyroidism. The secretion of an immunologically distinct factor with PTH-like biological activity, better known as PTHrP, has been identified in several neoplasms, including renal carcinoma, squamous cell carcinoma and carcinoma of the breast. PTHrP may also mediate lactation associated bone loss as it is expressed in lactating mammary tissue. Approximately 80% of hypercalcemic patients with solid tumors have detectable plasma PTHrP concentrations. PTHrP may also play a role in hypercalcemia of patients with non-Hodgkin's lymphoma, of these 62% had increased PTHrP concentrations. PTHrP increases renal tubular absorption of Ca, reduces renal phosphorus uptake and increases osteoclastic bone resorption. It differs from the action of PTH by decreasing serum concentrations of $1,25(OH)_2$ Vit D, an important distinction from patients with primary hyperparathyroidism where the opposite applies. Hypercalcemia of malignancy is usually associated with suppressed PTH concentrations and ectopic production of PTH by neoplasms remain a rare event. It differs from hypercalcemia secondary to hyperparathyroidism by the uncoupling of bone formation from bone resorption, two processes that are generally linked. In primary hyperparathyroidism both osteoclastic- and osteoblastic activities increase, whereas in patients with hypercalcemia of malignancy only osteoclastic activities increase (Table 5). Serum osteocalcin concentrations are significantly lower in patients with bone metastases. PTHrP is thought to be responsible for these biochemical changes. Biphosphonates have become the most useful anti-resorbtive agent for the treatment of malignancy-induced hypercalcemia. The action of these drugs is discussed elsewhere in this review.

The mechanism responsible for the hypercalcemia associated with hematological malignancies is multifactorial and includes the secretion of local bone active cytokines, such as IL-6, IL-1 and lymphotoxin or TNBFβ. In the early stages of multiple myeloma both the recruitment of osteoblasts and activity of osteoclasts are enhanced. Stimulated osteoblasts produce IL-6, a potent myeloma cell growth factor and a critical cytokine for the formation of osteoclasts in bone marrow. In overt myeloma, osteoblastic activity becomes significantly reduced resulting in net bone loss (42). Uncoupling of osteoblastic and osteoclastic activities appears to be a

key event in bone loss of myeloma, the latter of which is aggravated by high dose glucocorticoid therapy (43).

*Drugs and toxins*

Drugs and chemical substances may exert profound influences on bone metabolism. Glucocorticoid therapy directly depresses bone formation and inhibits gastrointestinal Ca absorption, leading to hypocalcemia and secondary hyperparathyroidism with increased bone resorption (44). Osteoporosis is a well known complication of ethanol abuse. It results from complex nutritional deficiencies (implicating Ca, Vit D and protein), decreased exposure to sunlight and testosterone deficiency (31). The effect of ethanol on cortisol metabolism (the pseudo Cushing's syndrome) as well as direct inhibition of osteoblastic function by ethanol may contribute to the net bone loss experienced by alcoholics. Cigarette smoking is a risk factor for osteoporosis in both genders (31) and may relate to smoking induced reduction of Ca absorption in the gastrointestinal tract, accelerated estrogen metabolism, decreased testosterone concentrations in men and earlier menopause in women. Diphenylhydantoin and phenobarbital may cause a decrease in Vit D concentrations due to hepatic breakdown of Vit D, secondary hyperparathyroidism and accelerated cortical bone loss (31). Long term intake of slow release sodium fluoride and calcium citrate increases bone mass, improves bone quality and significantly reduces vertebral fracture rate in osteoporotic patients. These improvements are reflected as increases in bone density and mineral apposition rates, reduced trabecular spacing and an increase in the mean number of nodes in cancellous bone (45). People living in communities with high levels of fluoride in their water supply (2.5 mg/l or more) have significantly higher bone mineral densities than their counterparts from communities with low (0.03 mg/l) and moderate (0.7 mg/l) fluoride concentrations. Exposure to fluoride at levels considered to be optimal to prevent dental decay (0.7 - 1.2 mg/l) appears to have no significant impact on bone mineral density (46).

A group of drugs, collectively known as the bisphosphonates and extensively reviewed by Fleisch in 1998 (47), inhibit both ectopic mineralization and bone resorption. The former is due to a direct physicochemical mechanism during which the formation and aggregation of Ca-P crystals from clear solutions are inhibited, transformation of amorphous Ca-P into hydroxyapatite blocked and aggregation of apatite crystals delayed. The inhibiting effect on the formation of calcium salts are valuable in the treatment of diseases with ectopic

mineralization such as atherosclerosis. Prevention of the formation of dental calculus deposits has already been proven as a potential benefit of these drugs. Bisphosphonates are powerful inhibitors of bone resorption. They play an important role in the management of diseases characterized by bone resorption, such as Pagets disease of bone, bone resorption associated with neoplastic disease, hyperparathyroidism and osteoporosis. A decrease in bone loss and increase in bone mineral density have been reported in subjects with postmenopausal osteoporosis and corticosteroid induced bone loss and who were treated with bisphosphonates. When given in high dosage, bisphosphonates impact on the mechanical properties of the skeleton. Strong inhibition of bone resorption can lead to bone fragility as a result of the inability to replace old bone and repair micro cracks (Fig. 6). In humans, bisphosphonates inhibit tumor induced bone resorption, correct hypocalcemia, reduce pain, prevent development of new osteolytic lesions and fractures and improve quality of life. They are now the treatment of choice in hypocalcemia of malignancy. At the cellular level, bisphosphonates inhibit osteoclast recruitment, adhesion and lifespan and decrease their activity. This is reflected histologically as a decrease in osteoclast numbers and shallower than normal resorbtive facets on bone surfaces. As cells of the osteoblastic linage control the recruitment and activity of osteoclasts under physiological and most pathological circumstances, bisphosphonates may act through the modulation of the interaction between osteoclasts and osteoblasts.

Children treated with chemotherapeutic agents experience a decrease in skeletal growth. These agents have a direct effect on the skeleton itself and its effect is not the result of a disturbance in GH secretion. Disruption of the columnar arrangement and a decrease in the number of chondrocytes within the growth plates occur. Some workers reported a permanent deficit whereas others demonstrated a catch-up growth, with only minimal loss in final body height. In addition to chemotherapeutic drugs, glucocorticoids are frequently used in the treatment of certain childhood malignancies. These drugs reduce linear growth, which is variably balanced by GH therapy, as their action is at least in part caused by antagonism of GH's action (48).

Utilizing double tetracycline labelling before biopsy, Compston and co-workers demonstrated reduced bone formation in farm workers exposed to organophosphate pesticides (49) and Gulf war veterans (50). In the latter study a significant reduction in the volume of trabecular

bone was found to be associated with decreased osteoblast activity. Resorbtive facets on bone surfaces were increased, a phenomenon explained on the basis of failure of the suppressed osteoblasts to cover eroded bone surfaces rather than increased osteoclast activity. Nearly all veterans have a history of exposure to organophosphates and pyridostigmine which could explain the suppression of osteoblasts. Another possible cause is that changes in lifestyle of these subjects, including tobacco, excessive alcohol consumption and reduced levels of physical activity may be the key to their bone changes.

*Genetic conditions*

**Racial differences** could account for slight variations in the histomorphometric norms reflected in Table 2. American blacks have a greater bone mass and a lower incidence of osteoporosis and hip fractures than their white counterparts. The rate of bone turnover is lower in blacks than in whites, an observation supported by the significantly lower level of serum GLA in blacks. This provides a mechanism to explain the decrease loss of bone mass in blacks compared to whites during ageing (51).

**Osteogenesis imperfecta** is transmitted as a dominant autosomal trait. The severity of its skeletal manifestations divides affected individuals into a congenita (multiple fractures occur in early life and even in utero) or tarda (fractures generally occur after weight bearing) subtypes. Blue sclera, dental involvement (dentinogenesis imperfecta) and hyper extensile joints are frequent findings, signifying a collagen deficiency as the basis of the disease (52). Microscopy shows a highly variable picture. Many cases show large osteocytic lacunae, an increased proportion of primary lamellar bone and a marked lack of secondary Haversian systems. The osteoblasts are densely staining and resemble fibroblasts (Fig. 7). Sheets of connective tissue lie adjacent to new sites of bone formation.

**Vitamin D resistant rickets** (or hypophosphatasia) is a rare disorder caused by an autosomal recessively inherited defect in P reabsorption in the proximal renal tubules. Cases differ in clinical severity, ranging from fractures in utero to a mild form of rickets. Biochemical abnormalities include hypophosphatasia and hypocalcemia with hypercalcuria (52). The underlying defect appears to correlate with a lack of mineralization activity. The bone has wide osteoid borders, which lack mineralization activity and a diagnosis of hypertrophic rickets is generally proposed on static bone measurements. Analyses of dynamic

measurements however show a lack of mineral deposition despite dietary mineral supplementatioin.

Since it was described by Albers-Schönberg nearly 100 years ago, **osteopetrosis** or marble bone disease has remained one of the most dramatic bone dysplasias affecting humans. It presents in various forms of inheritance and severity, extending from lethal varieties (malignant osteopetrosis) to forms that manifest with mild hematological and neurological symptoms. The clinical manifestations of the mild forms are due to compression of nerves and displacement of marrow by excessive bone. The rate of formation of bone has been reported to be normal or excessive and bone resorption highly suppressed. Osteoclasts are abnormal and exhibit absence of ruffled borders (53,54) (Fig. 8). Cortical width and trabecular volumes are significantly increased resulting in a reduction in the volume of the bone marrow (54). Unresorbed cartilage inclusions and lack of Haversian systems (56,57) are other characteristic microscopic features. Repopulation of the bone marrow with T-cell depleted HLA compatible bone marrow transplants appear to be successful in establishing a normal osteoclast population (54) and reversal of net bone formation.

The mean age of survival of patients with **cystic fibrosis** has increased dramatically to over 30 years during the past decades. The increased life span has resulted in new complications amongst which bone loss and osteoporosis feature. It is well known that patients with cystic fibrosis are growth retarded and young adults have short and narrow bones. Because of a significant decrease in bone volume, these patients may develop osteoporotic fractures prematurely (58).

*Renal disease*

Kidneys play an important role in bone metabolism by producing active Vit D metabolites and through the filtration- and reabsorption of divalent ions. An early and virtually universal feature of chronic renal failure is a rise in serum PTH accompanied by hyperplasia of the parathyroid glands. The stimulus is hypocalcemia and several factors amongst which decreased production of active Vit D, P retention and skeletal resistance to the action of PTH lead to this. The pathological classification of renal bone disease is based on static and dynamic histomorphometric evaluation and divides the bone changes in high turnover - and low turnover uremic bone disease (Table 6). The former is characterized by osteitis fibrosa

and mixed osteopathy. Osteitis fibrosa results from PTH hyper secretion and is characterized by an elevated rate of bone formation, increased number of osteoblasts and osteoclasts, abundant resorbtive facets, increased osteoid production and bone marrow fibrosis (hence the name of the disease) (59). The mixed osteopathy is characterised by increased medullary fibrosis with an increased osteoid volume (60). The major difference from a nutritionally induced osteomalacia is an increased osteoid thickness and not volume for a given rate of bone formation (61). Low turnover uremic bone disease is characterized by a low bone formation rate and a normal or decreased osteoid seam thickness. These changes are also referred to as adynamic bone disease and the mechanism leading to its primary low bone formation rate is complex (59). Accurate assessment of the bone formation rate is essential before a decision is made to perform a parathyroidectomy on a patient in renal failure (62). Once dialysis begins, the bony changes can be complicated by aluminium bone disease, if aluminium is present in the water supply (dialysis patients are exposed to 300 - 400 litres of water across the dialysis membrane per week). Aluminium poisons osteoblasts, as it is readily absorbed and deposited in osteoid and acts in many ways opposite to the action of PTH. Employing the tricarboxilic acid or the solochrome azurine staining method facilitate detection of aluminium in osteoid. An iron stain must be used in conjunction as positive results may be caused by iron deposits (28). Beta 2 microglobulin deposits are furthermore frequently present in the periosteum of patients on prolonged hemodialysis. Of these, the majority develop femoral neck fractures. Periosteal β2 microglobulin may therefore be helpful in predicting a renal dialysis patient's susceptibility to femoral fracture (63).

*HIV infection*

HIV-1 infected patients show a notable decrease in bone turnover. This change appears to correlate with the severity of the disease, according to the CDC classification and the number of CD4+T lymphocytes. All osteoblastic parameters (osteoid volumes, osteoid seam widths and mineralization activity) as well as the number of osteoclasts are reduced. Although the exact mechanism is not yet clear, it has been possible to infect continuous human osteoblast cell lines with different strains of HIV-1, suggesting a direct effect of the virus on bone forming cells (64).

*Ideopathic metabolic bone disease*

A small percentage of patients suffer progressive bone loss with either a speculative or unidentifiable cause (34). **Juvenile idiopathic osteoporosis** is related to reduced bone formation rather than increased resorption and disturbances in GH or IGF-I production have been implicated (65). Although the exact mechanism of osteopenia in patients suffering **ankylosing spondilitis** remains to be determined, both trabecular thinning and loss of structural bony elements are involved (66). The **fragile bone syndrome** is characterised by bone fragility, calvarial and/or gnathial fibro-osseous lesions and metaphesial under modelling of the tubular bones. Bone histomorphometry has shown increased osteoid surfaces and osteoid volumes, making it distinctly different from osteogenesis imperfecta (67). The early phase of **Paget's disease of bone** is characterized by bone resorption (osteoclastic parameters are 10 – 20 times increased). This phase is soon followed by an osteoblastic response with bone depositioning. Both resorption and formation occur in small areas adjacent to each other. Small pieces of bone rather than complete osteones are subsequently formed. The marrow spaces generally show foci of increased spindle shaped cells with mild fibrosis, indicative of increased recruitment of undifferentiated precursor cells. The net result is broadening of the bone with irregular cemental lines referred to as a mosaic pattern (52).

## CONCLUSION

Recent advances in the study of dynamic bone changes provide valuable information on the morphogenesis of metabolic diseases. Early diagnosis and accurate monitoring of these debilitating skeletal states are now within reach of the Pathologist.

## REFERENCES

1. Delmas PD. Biochemical markers of bone turnover for the clinical assessment of metabolic bone disease. *Endocrin Metab Clin North Am* 1990;19(1):1-19.
2. Eyre D. Collagen crosslinking amino-acids. Methods Enzymol 1987;144:115-139.
3. Uebelhart D, Gineyts E, Delmas PD. Uninary excretion of pyridinium crosslinks, a marker for bone turnover. *J Bone Min Res* 1989;4(Suppl 1): S407.
4. Robins S, Stewart P, Astbury C. Measurement of the cross-linking compound, pyridinoline, in urine as an index of collagen degradation in joint disease. *Ann Rheum Dis* 1986;45:969-973.

5. Vigorita VJ. The tissue pathological features of metabolic bone disease. *Orthop Clin North Am* 1984;15(4):613-629.
6. Arnala I. Use of histological methods in studies of osteoporosis. *Calcif Tissue Int* 1991;49(Suppl):531-532.
7. Raubenheimer EJ, Van Heerden WFP, Potgieter D, Golele R. Static and dynamic bone changes in hospitalised patients suffering from rickets – a histomorphometric study. *Histopathology* 1997;31:12-17.
8. Guise TA, Mundy GR. Cancer and bone. *Endocrine Rev* 1998;19(1):18-54.
9. Jaffe HL. Rickets and osteomalacia. In: Jaffe HL, ed. *Metabolic degenerative and inflammatory disease of bones and joints*. Philadelphia: Lea & Febiger, 1975;381-447.
10. Klein GL, Simmons DJ. Nutritional rickets: Thoughts about pathogenesis. *Ann Med* 1993;25:379-384.
11. Spiller G, Story JA, Wong LG, Nunes JD, Alton M, Petro MS, Furumoto EJ, Whittam JH, Scala J. Effect of increasing levels of hard wheat fibre on fecal weight, minerals and steroids and gastrointestinal transit time in healthy young women. *J Nutrition* 1986;116:778-785.
12. Knox TA, Kassarjian Z, Dawson-Hughes B, Golner BP, Dallal GE, Arora S, Russel RM. Calcium absorption in elderly subjects on high- and low fibre diets – effects on gastric acidity. *Am J Clin Nutr* 1991;53:1480-1486.
13. Weaver CM, Heaney RP, Teegarden D, Hinders M. Wheat bran abolishes the inverse relationship between calcium load size and absorption fraction in women. *J Nutrition* 1996;126:303-307.
14. Batchelor AJ, Compston JE. Reduced plasma half life of radio-labelled 25-hydroxyvitamin $D_3$ in subjects receiving a high fibre diet. *Br J Nutr* 1983;49:213-216.
15. Dent CE, Stamp CB. Vitamin D, Rickets and Osteomalacia. In: Avioli LV, Krane SM, eds. *Metabolic Bone Disease* Vol 1. New York: Academic Press, 1977;237-305.
16. Bisballe S, Eriksen EF, Melsen F, Mosekilde L, Sorenson OH, Hessov I. Osteopaenia and osteomalacia after gastrectomy: interrelations between biochemical markers of bone remodelling, vitamin D metabolites and bone histomorphometry. *Gut* 1991;32(11):1303-1307.

17. Creedon A, Flynn A, Cashman K. The effect of moderately and severely restricted dietary magnesium intakes on bone composition and bone metabolism in the rat. *Br J Nutr* 1999;82:63-71.

18. Tsusenari T, Fukase M, Fujita T. Bone histomorphometric analysis for the cause of osteopaenia in vitamin C – deficient rat (ODS-rats). *Calcif Tissue Int* 1991;48(1):18-27.

19. Hannan MR, Felsen DR, Anderson JA. Bone mineral density in elderly men and women: results from the Farmingham osteoporosis study. *J Bone Min Res* 1992;**7**;547-553.

20. Ray NF, Chan JK, Thamer M, Melton LJ. Medical expenditures for the treatment of osteoporotic fractures in the United States in 1995: report from the National Osteoporosis Foundation. *J Bone Min Res* 1997;12:24-35.

21. Lonzer MD, Imrie R, Rogers D, Worley D, Licata A, Secic M. Effects of hereditary, age, weight, puberty, activity and calcium intake on bone and mineral density in children. *Clin Pediatr* 1996;35:185-189.

22. Steiniche T. Bone histomorphometry in the pathophysiological evaluation of primary and secondary osteoporosis and various treatment modalities. *APMIS* Suppl 1995;51:1-44.

23. Eisman JA. Genetics of osteoporosis. Endocrine Rev 1999;20(6):788-804.

24. Cormier C. Epidemiology, diagnosis and treatment of osteoporosis. *Curr Opin Rheumatol* 1994;6(3):329-335.

25. Payne J, Sachs N, Reinhardt R, Numikoski P, Patil K. The association between oestrogen status and alveolar bone density changes in post menopausal women with a history of periodontitis. *J Periodontal* 1997;68(1):24-31.

26. Grodstein F, Colditz G, Stampfer M. Post-menopausal hormone use and tooth loss: A prospective study. *JADA* 1996;127:370-377.

27. Clarke BL, Wynne AG, Wilson DAM, Fitzpatrick LA. Osteomalacia associated with adult Fanconi's syndrome: clinical and diagnostic features. *Clin Endocrinol Oxf* 1995;43(4):479-490.

28. Parfitt AM, Mathews CHE, Villaneauve AR, Kleerekoper M, Frame B, Rao DS. Relationship between surface, volume and thickness of iliac trabecular bone in ageing osteoporosis. *J Clin Invest* 1983;72:1396-1409.

29. Riggs BL, Melton LJ. Evidence for two distinct syndromes of involutional osteopororsis (editorial). *Am J Med* 1983;75:899-901.

30. Mazess RB. On ageing bone loss. Clin Orthop Rel Res 1982;165:239-252.

31. Jackson JA, Kleerekoper M. Osteoporosis in men: Pathophysiology and prevention. *Medicine* 1990;69(3):137-152.

32. Nyssen-Behets C, Dhem A. The fate of Quiescent surfaces of lamellar bone. *Gerontology* 1992;38:153-159.

33. Rubin CT, Gross TS, Mcleod KJ, Bain SD. Morphologic stages in lamellar bone formation stimulated by a potent mechanical stimulus. *J Bone Miner Res* 1995;10(3):488-495.

34. Avioli LV. Osteoporosis: Pathogenesis and Therapy. In: Avioli LV, Krane SM, eds. *Metabolic Bone Disease* Vol. I. New York: Academic Press. 1977;307-370.

35. Cavolina JM, Evans GL, Harris SA, Zhang M, Westerlind KC, Turner RT. The effects of orbital space flight on bone histomorphometry and messenger ribonucleic acid levels for bone matrix proteins and skeletal signalling peptides in overectomized growing rats. *Endocrinol* 1997;138(4):1567-1576.

36. Ohlsson C, Bengtsson BA, Isaksson OGP, Andreassen KT, Slootweg MC. Growth hormone and bone. *Endocrine Rev* 1998;19(1):55-79.

37. Parfitt AM, Schipani E, Rao DS, Kupin W, Han ZH, Juppner H. Hypocalcaemia due to constitutive activity of the parathyroid hormone (PTH)/PTH-related peptide receptor: comparison with primary hyperparathyroidism. *J Clin Endocrinol Metab* 1996;81(10):3584-3588.

38. Delichatsios HK, Lane JM, Rivlin RS. Bone histomorphometry in men with spinal osteoporosis. *Calcif Tissue Int* 1995;56(5):359-363.

39. Turner RT, Wakley GK, Hannon KS. Differential effect of androgens on cortical bone histomorphometry in gonadectomized male and female rats. *J Orthop Res* 1990;8(4):612-617.

40. Li M, Shen Y, Halloran BP, Baumann BD, Miller K, Wronski TJ. Skeletal response to corticosteroid deficiency and access in growing male rats. *Bone* 1996;19(2):81-88.

41. Fallon MD, Perry HM, Bergfeld M, Droke D, Teitelbaum SL, Avioli LV. Exogenous hyperthyroidism with osteoporosis. *Arch Intern Med* 1983; 143: 442 – 444.

42. Bataille R, Chappard D, Marcelli C, Dessau P, Baldet P, Sany J, Alexandre C. Recruitment of new osteoblasts and osteoclasts is the earliest critical event in the pathogenesis of multiple myeloma. *J Clin Invest* 1991; 88: 62-66.

43. Diamond T, Levy S, Day P, Barbagallo S, Manoharan A, Kwan YK. Biochemical, histomorphometric and densitometric changes in patients with multiple myeloma: effects of glucocorticoid therapy and disease activity. *Br J Haematol* 1997;97(3):641-648.

44. Kimberg DV, Baerg RD, Gershon E, Graudusiusus RT. Effect of cortisone treatment on the active transport of calcium by the small intestine. *J Clin Invest* 1971;50:1309-1321.

45. Zerewekh JE, Hagler HK, Sakhaee K, Gottshalk F, Peterson RD, Pak CYC. Effect of slow-release sodium fluoride on cancellous bone histology and connectivity in osteoporosis. *Bone* 1994;15(6):691-699.

46. Phipps KR, Orwoll ES, Bevan L. The association between water-borne fluoride and bone mineral density in older adults. *J Dent Res* 1998;77(9):1739-1748.

47. Fleisch H. Bisphosphonates: Mechanism of action. *Endocrine Rev* 1998;19(1):80-100.

48. Robson H. Bone growth mechanisms and the effects of cytotoxic drugs. *Arch Dis Child* 1999;81:360-364.

49. Compston JE, Vedi S, Stephen AB et al. Reduced bone formation after exposure to organophosphates. *Lancet* 1999; 24: 297-304.

50. Compston JE, Vedi S, Stephan AB, Bord S, Lyons AR, Hodges SJ, Scammell BE. Reduced bone formation in UK Gulf War veterans: a bone histomorphometric study. *J Clin Pathol* 2002; 55:897-899.

51. Weinstein RS, Bell NH. Diminished rates of bone formation in normal Black adults. *New Engl J Med* 1988;319:1698-1701.

52. Jowsey J. *Metabolic diseases of bone.* Philadelphia: W.B. Sounders Company, 1977:172-191.

53. Shapiro F, Gleimcher MJ, Holtrop ME, Tashjian AH, Brickley-Passons D, Kenzora JE. Human osteopetrosis. A histological, ultrastructural and biochemical study. J *Bone and Joint Surg* 1980;62-A:384-399.

54. Helfrich MH, Aronson, Dc, Everts V, Mieremet RHP, Gerritsen EJA, Eckhardt PG, Groot CG, Scherft JP. Morphologic features of bone in human osteoporosis. *Bone* 1991;12:411-419.

55. Bollerslev J, Steiniche T, Melsen F, Mosekilde L. Structural and hisomorphometric studies of iliac crest trabecular and cortical bone in autosomal dominant osteopetrosis: A study of 2 radiological types. *Bone* 1989;10:19-24.

56. Kuo TT, Davis CP. Osteopetrosis: a scanning electron microscopic study. *Human Path* 1981;12(4):376-379.

57. Milgram JW, Jasty M. Osteopetrosis. *J Bone Joint Surg* 1982;64A(6):912-929.

58. Laursen EM, Moldgaard C, Michaaelsen KF, Koch C, Muller J. Bone mineral status in 134 patients with cystic fibrosis. *Arch Dis Child* 1999;81:235-240.

59. Fournier A, Oprisiu R, Said S, Sechet A, Ghazali A, Marie A, El Esper I, Brazier M, Achard JM, Moriniere P. Invasive versus non-invasive diagnosis of renal bone disease. Curr Opin Nephr Hyperten 1997;6:333-348.

60. Wang M, Hercz G, Sherrard DJ, Maloney NA, Segre GV, Pey Y. Relationship between intace 1-84 parathyroid hormone and bone histomorphometric parameters in dialysis patients without aluminium toxicity. *Am J Kidney Dis* 1995;26:836-844.

61. Parfitt AM. The physiologic and pathogenetic significance of bone histomorphometry. In: Coe F, Favus M, eds. *Disorders of bone and mineral metabolism.* New York: Raven Press, 1992:455-474.

62. Dahl E, Nordal KP, Halse J. Chronic renal failure: diagnostic measures before parathyroidectomy. *Scan J Urol Nephrol* 1994;28(3):291-294.

63. Onishi S, Andress DL, Maloney NA, Coburn JW, Sherrard DJ. Beta-2 microglobulin deposition in bone in chronic renal failure. *Kidney Int* 1991;39(5):990-995.

64. Serrano S, Marinoso ML, Soriano JC, Rubies-Prat J, Aubia J, Coll J, Bosch J, Del Rio L, Vila J, Goday A, Nacher M. Bone remodelling in human immunodeficiency Virus-1 infected patients. A histomorphometric study. *Bone* 1995;16:185-191.

65. Johansson AG, Eriksen EF, Lindh E, Langdahl B, Lindahl A, Ljunggren O, Ljunghall M. Reduced serum levels of the growth hormone dependant insulin-like growth factor binding protein and a negative bone balance at the level of individual remodelling units in idiopathic osteoporosis in men. J Clin Endocrinol Metab 1997;82(9):2795-2798.

66. Lee YS, Scholtzhauer T, Ott SM, Van Vollenhoven RF, Hunter J, Shapiro J, Marcus R, Mcguire JL. Skeletal status of men with early and late ankylosing spondylitis. *Am J Med* 1997;103(3):233-241.

67. Nishimura G, Haga N, Ikeuchi S, Yamaguchi T, Aoki Y, Yamato M. Fragile bone syndrome associated with craniognathic fibro-osseous lesions and abnormal moderling of the lobular bones; a report of two cases and a review of the literature. *Skeletal Radiol* 1996;25(8):717-722.

**Legends**:

**FIG. 1.** Outline of a diagnostic flow chart for metabolic bone disease.

**FIG. 2.** Clinical features of rickets.

**FIG. 3.** Trabecular bone in rickets showing extensive coverage of bony surfaces by osteoid. Note the focus of tunnelling resorption, indicative of hyperparathyroidism (arrows) (Picrosirius stain, X150).

**FIG. 4.** Active mineralization of osteoid as depicted by the extent of - and the distance between the two fluorescent lines (arrows) (unstained section viewed with UV light, X250).

**FIG. 5.** Stereo micrograph of trabecular bone in a patient with osteoporosis. Note the loss of structural elements depicted by the blunt ending trabeculae (arrows) (Bar = 0.5 mm).

**FIG. 6.** Stereomicroscopic view of trabecular micro cracks in a patient on high dosage bisphosphonates (Bar = 0.3 mm).

**FIG. 7.** Microscopic features of trabecular bone in osteogenesis imperfecta. Note the large osteocytic lacunae and fibroblast – like osteoblasts (H&E stain, X250).

**FIG. 8.** Osteoclast in a Howships lacuna in osteopetrosis. Note the absence of a ruffled cytoplasmic border (arrows) (Bar = 15 microns).

**Acknowledgement**

The author wishes to thank Mrs. C. S. Begemann for secretarial assistance.

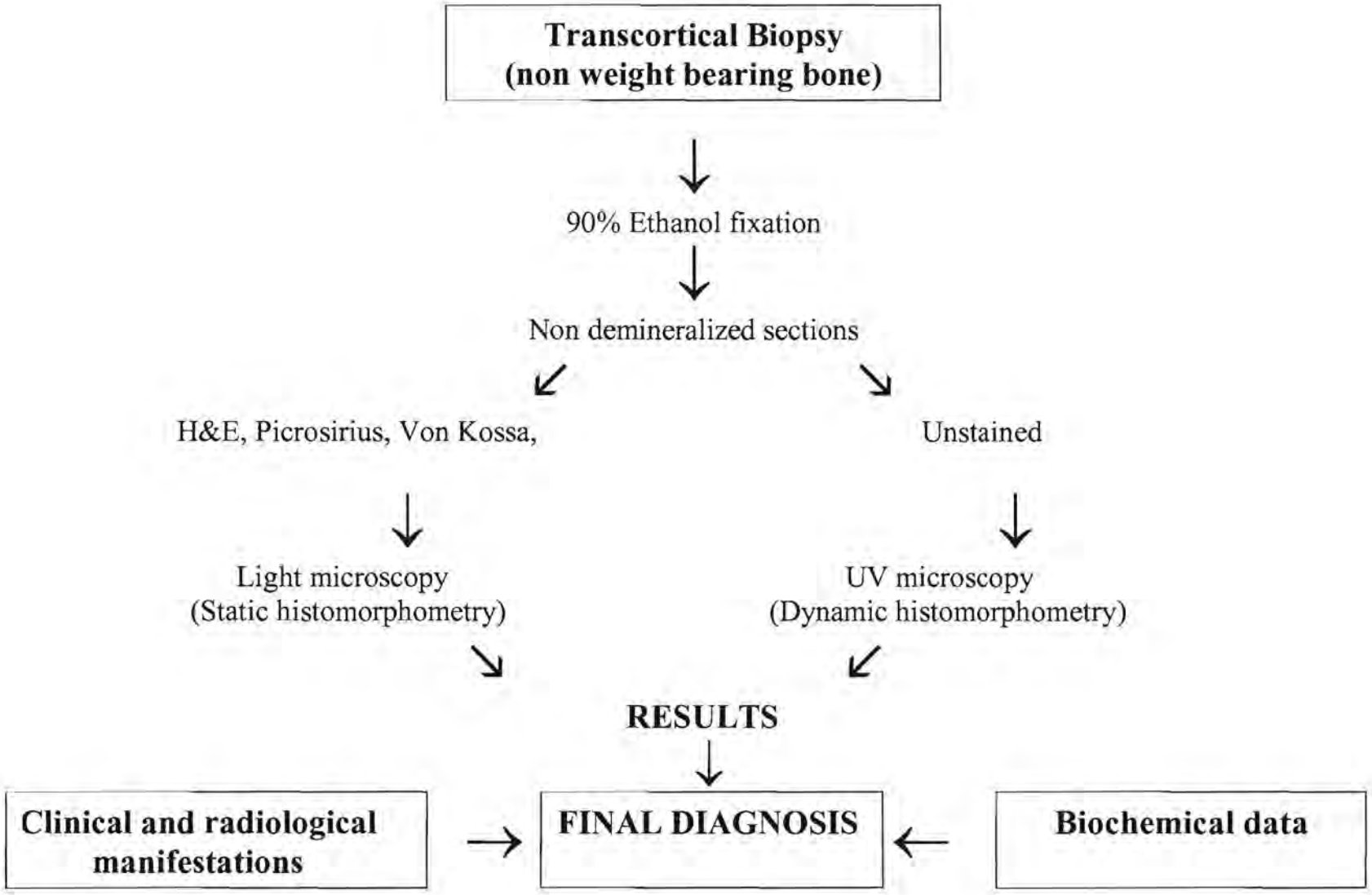
Transcortical Biopsy
(non weight bearing bone)
90% Ethanol fixation
Non demineralized sections
H&E, Picrosirius, Von Kossa,
Unstained
Light microscopy
(Static histomorphometry)
UV microscopy
(Dynamic histomorphometry)
RESULTS
Clinical and radiological manifestations
FINAL DIAGNOSIS
Biochemical data

**TABLE 1:** *Conditions commonly diagnosed and managed through bone histomorphometry*

| | |
|---|---|
| 1. | Rickets/Osteomalacia<br>- acquired type<br>- Vit D resistant type |
| 2. | Osteoporosis<br>- female type<br>- male type<br>- immobility |
| 3. | Hyperparathyroidism |
| 4. | Osteopetrosis |
| 5. | Uremic bone disease |
| 6. | Paget's disease |

**TABLE 2:** *Histomorphometric terms and reference values (5).*

| Term | Definition | Reference Values Mean ± SD |
|---|---|---|
| **Indices of Bone Mass** | | |
| Trabecular bone volume | % of medullary cavity occupied by mineralized and unmineralized bone | 22.5 ± 3.5% |
| Mean trabecular width | Average width of all trabecular bone spicules | 213 ± 65 microns |
| Mean cortical width | Mean thickness of both cortices | 909 ± 98 microns |
| **Indices of Osteoid** | | |
| Trabecular osteoid surface | % of bone surface covered by osteoid | 18.9 ± 5.0% |
| Trabecular osteoid volume | Osteoid area expressed as a % of trabecular bone area | 1.9 ± 0.4% |
| Mean osteoid seam width | Osteoid area divided by the millimetres of bone surface covered by osteoid | 9.7 ± 0.4 microns |
| **Indices of Resorption** | | |
| Trabecular resorptive surface | % of bone surface showing Howship's lacunae | 5.1 ± 0.6% |
| Osteoclastic resorptive surface | % of bone surface lined by osteoclasts | 0.13 ± 0.6% |
| Osteoclasts per mm of trabecular perimeter | Number of osteoclasts per millimetre of bone perimeter | 0.11 ± 0.04% |
| **Indices of Mineralization** | | |
| Calcification (apposition) rate | Distance between double tetracycline labels divided by the number of days between administration of labels | 0.03 ± 0.01% |
| Mineralization lag time | Mean osteoid seam width divided by the bone formation rate | 0.20 ± 0.04% |
| Bone formation rate | Calcification rate times % of trabecular surface labelled | 0.64 ± 0.10 microns/day |
| Percentage of trabecular surface labelled | % of bone surfaces labelled by tetracycline | 12.8 ± 2.3% |
| Mineralization front | Nature of line of mineralization between osteoid and mineralized bone | 73.4 ± 26.5% |

**TABLE 3:** *Characteristic histomorphometric features of rickets/osteomalacia.*

| Feature | Status |
|---|---|
| Mineralized bone mass | decreased |
| Indices of osteoid | increased* or decreased** |
| Indices of resorption | increased |
| Indices of mineralization | decreased |

*hypertrophic rickets/osteomalacia

**atrophic rickets/osteomalacia

**TABLE 4:** *Characteristic histopathologic features of osteoporosis*

| Feature | Status |
|---|---|
| Trabecular bone volume | decreased |
| Mean trabecular width | normal or increased |
| Mean cortical width | normal* or decreased** |

* female type I

** female type II

**TABLE 5:** *Histopathologic differences between bone changes induced by primary hyperparathyroidism (PTH related) and malignancy induced (PTHrP related).*

| | PTH | PTHrP |
|---|---|---|
| Indices of osteoid | increased | normal |
| Indices of resorption | increased | increased |

**TABLE 6:** *Histomorphometric findings in renal bone disease*

| | High turnover renal bone disease | Low turnover renal bone disease |
|---|---|---|
| Indices of osteoid | increased | normal or reduced |
| Indices of resorption | increased | normal |
| Bone marrow fibrosis | prominent | inconspicuous |

*Archs oral Biol.* Vol. 37, No. 2, pp. 157–158, 1992
Printed in Great Britain. 

0003-9969/92 $5.00 + 0.00




## SHORT COMMUNICATION

# AMINO ACID COMPOSITION OF DENTINE IN PERMANENT HUMAN TEETH

F. S. NKHUMELENI,[1] E. J. RAUBENHEIMER,[1] J. DAUTH,[2] W. F. P. VAN HEERDEN,[1] P. D. SMITH[2] and M. J. PITOUT[3]

[1]Departments of Oral Pathology and Biology, [2]Chemical Pathology, Medunsa 0204 and [3]Department of Medical Biochemistry, University of Pretoria, Republic of South Africa

*(Accepted 20 August 1991)*

**Summary**—Dentine of permanent mandibular incisors from nine individuals was hydrolysed and the amino acid composition determined by ion-exchange chromatography against a standard calibrant of 41 amino acids. Nineteen amino acids were detected, including small quantities of 1-methylhistidine and asparagine, two amino acids whose existence had apparently not been recorded before in human dentine. The total content of hydroxylysine plus lysine varied between 2.6 and 3.3 residues per 100 (SD, 0.74) in different teeth, which therefore did not support previous studies that had proposed a constant total value. This and other quantifiable differences between present and previous findings may be the result of the different methods and the influence of dietary and other regional factors on dentinogenesis.

Key words: human dentine, amino acids.

Dentine is the major component of teeth, responsible for most of the weight, volume and overall shape (Butler, Munksgaard and Richardson, 1979). Ninety per cent of the organic matrix of human dentine consists of collagenous proteins (Jones and Leaver, 1974) and the remaining 10% is made up of non-collagenous proteins, proteoglycans, glycoproteins and lipids (Avery, 1987). Various analytical methods, some of which are historic, have been used for determination of amino acids in dentine, namely: microbiological assay (Hess, Lee and Neidig, 1952), quantitative paper chromatography (Battistone and Burnett, 1956) and ion-exchange chromatography (Eastoe, 1963).

Our objective now was to determine the amino acid composition of human dentinal matrix with a modern technique and to compare it with previously published data.

Permanent mandibular incisors were extracted from nine bodies of known age and sex in the Forensic Medicine mortuary of Ga-Rankuwa Hospital, situated 32 km north of Pretoria. Before processing, the crowns and cementum were removed with a dental bur, and the pulp with an endodontic file. Pieces of radicular dentine of approx. 0.20 g were washed, dried and hydrolysed in 6 M hydrochloric acid (HCl) for 24 h at 110°C. The hydrolysates were neutralized with neutralizer (Spitz, 1973) and citrate buffers in the ratio 1:2:2, filtered (Millex-GS 0.22 $\mu$m) and then diluted further 1:1 with the citrate buffer. Calibrants containing 41 amino acids were prepared and diluted as above. The amino acids of dentine and the calibrants were separated in duplicate by ion exchange on a Beckman 6300 amino acid analyser which incorporates a 25-cm lithium column and a four-buffer system. Chromatograms thus obtained were integrated and quantitated with a Hewlett-Packard 3390A integrator and the results expressed as a per cent residues detected. The results were tabled as the average of the total number of residues per 100 and the SD for each amino acid was calculated.

Nineteen amino acids were detected (Table 1). Asparagine and 1-methylhistidine, which have not previously been identified in human dentine, were present in small quantities. Asparagine was present in all our hydrolysates. In a serial study of hydrolysis, asparagine was detected only after 16 h and remained present in all acid hydrolysates for 24 h. In hydrolysates stored at 4°C, asparagine could be detected over as long as 12 months. No explanation for this phenomenon could be found. Acid hydrolysis of a pure mixture of aspartic acid, asparagine, glutamic acid and glutamine showed complete hydrolysis of asparagine and glutamine within 30 min. The concentration of aspartic acid and glutamic acid increased and high levels were detected under these conditions. It is suggested that asparagine in dentine may be 'protected' against complete hydrolysis. Furthermore, our monitoring system may have been more sensitive and with improved resolution as larger quantities of aspartic acid, glutamic acid, arginine, leucine, iso-leucine and valine were found than previously reported (Table 1).

Linde (1984) reported that the total content of hydroxylysine plus lysine in dentine is constant at 3.5 residues per 100. In our study, we found a variation between 2.6 and 3.3 residues per 100 (SD, 0.74), supporting Eastoe's (1963) finding of a variation in the total content of hydroxylysine and lysine over a

Table 1. Comparison of our findings (average of nine cases, with SD) with those of previous investigations (expressed as residues per 100)

| Human dentine amino acids | Hess *et al.* (1952) | Battistone and Burnett (1956) | Eastoe (1963) | Linde (1984) | Present study (1992) | |
|---|---|---|---|---|---|---|
| | | | | | $\bar{X}$ | SD |
| Aspartic acid | 4.4 | 5.4 | 5.5 | 4.5 | 5.9 | 0.06 |
| Hydroxyproline | 10.3 | 11.6 | 10.1 | 9.6 | 10.4 | 0.24 |
| Threonine | 2.7 | 2.0 | 1.9 | 1.8 | 2.1 | 0.11 |
| Serine | 3.4 | 3.0 | 3.8 | 4.1 | 4.0 | 0.28 |
| Asparagine | — | — | — | — | 0.3 | 0.08 |
| Glutamic acid | 7.4 | 7.6 | 7.3 | 7.2 | 8.8 | 0.15 |
| Proline | 14.5 | 9.7 | 11.5 | 11.9 | 11.8 | 0.28 |
| Glycine | 30.9 | 31.3 | 31.9 | 33.4 | 30.1 | 0.30 |
| Alanine | 9.8 | 11.2 | 11.2 | 10.2 | 8.6 | 0.31 |
| Valine | 2.6 | 2.5 | 2.5 | 2.3 | 3.0 | 0.15 |
| Methionine | 0.35 | 0.46 | 0.52 | 0.7 | 0.5 | 0.05 |
| Iso-leucine | 1.0 | * | 1.0 | 1.0 | 1.3 | 0.00 |
| Leucine | 2.8 | * | 2.6 | 2.4 | 3.0 | 0.04 |
| Phenylalanine | 1.2 | * | 1.4 | 1.4 | 1.5 | 0.05 |
| Hydroxylysine | 0.64 | 0.71 | 0.84 | 1.5 | 1.1 | 0.11 |
| Lysine | 2.4 | 2.2 | 2.3 | 2.0 | 2.1 | 0.17 |
| 1-Methylhistidine | — | — | — | — | 0.3 | 0.07 |
| Histidine | 0.54 | 0.43 | 0.53 | 0.4 | 0.3 | 0.19 |
| Arginine | 4.4 | 5.0 | 4.7 | 5.2 | 5.6 | 0.17 |

*Total of leucine, iso-leucine and phenylalanine is 6.4.

comparatively narrow range (2.91–3.35 residues per 100). The presence of two amino acids that have not hitherto been reported in dentine as well as other differences between our study and earlier ones may, amongst other factors, be the result of different methods. The more efficient buffer system and the modern lithium columns that we used facilitate the separation of isomers and increase the resolution of the various amino acids. The reported differences in the amino acid content of human dentine may also reflect dietary and other regional factors that may influence the formation of dental hard tissues.

## REFERENCES

Avery J. K. (1987) *Oral Development and Histology*, Chap. 12, pp. 152–162. Williams and Wilkins, Baltimore, MD.

Battistone G. C. and Burnett G. W. (1956) Studies on composition of teeth III. The amino acid composition of human dentinal protein. *J. dent. Res.* **35,** 255–259.

Butler W. T., Munksgaard E. C. and Richardson W. S. (1979) Dentine proteins: chemistry, structure and biosynthesis. *J. dent. Res.* **58,** 817–824.

Eastoe J. E. (1963) Amino acid composition of proteins from the oral tissues II. *Archs oral Biol.* **8,** 633–652.

Hess W. C., Lee C. Y. and Neidig B. A. (1952) Dentinal protein: amino acid composition. *J. dent. Res.* **31,** 691–792.

Jones I. L. and Leaver A. G. (1974) Studies on the minor components of the organic matrix of human dentine. *Archs oral Biol.* **19,** 371–380.

Linde A. (1984) Dentine and dentinogenesis (Ed. Butler W. T.), Vol. 2, Chap. 8, pp. 37–51. CRC Press, Boca Raton, FL.

Spitz H. D. (1973) A new approach for sample preparation of protein hydroxylysates for amino acid analysis. *Analyt. Biochem.* **56,** 66–73.

086

**9** The Effect of Modern Dentine Bonding Systems on Human Dentine.
F A DE WET* and M R FERREIRA, Faculty of Dentistry, University of Pretoria, Pretoria, South Africa.

Most modern dentine bonding systems contain primers or cleansers which are used to remove or alter the smear layer or dentine before resin application. The purpose of this study was to assess the effect of four modern dentine bonding systems (DBS), three with primers/cleansers and one without, on the appearance of human dentine.

Denthesive Bond (D, Kulzer), Pertac Universal Bond (P, E.S.P.E.), Prisma Universal Bond 3 (PUB3, Dentsply) and Syntac (S, Vivadent) were included in the study. The crowns of 80 sound, human, molar teeth were imbedded in rings, leaving the occlusal surfaces projecting. These surfaces where ground wet on 220 grit SiC paper to expose superficial dentine. Fifteen dentine surfaces were then treated with each of the four DBS. Cylinders of matching composites were thereafter bonded to these surfaces, using a rubber split mould. After 24 hours storage in water the specimens were stressed to failure using a shear load in an Instron. Fracture sites were evaluated in a SEM. Five abraded dentine surfaces were treated with the respective primer/cleanser of each of 3 DBS. Dentine treated with the D and S cleanser/primer, and debonded specimens of D and S, displayed open dentinal tubules. Subsequent application of an adhesive closed almost all the tubules. Pieces of fractured dentine were attached to some composite stubs, showing resin tags clearly penetrating deep into, and even through the dentine fragments. It can be concluded that only 2 of the 4 DBS tested opened the dentinal tubuli.

**10** Evaluation of the Effectiveness of an Oral Health Preventative Programme. S.Dhansay*, H. Lalloo, A. Bawa, M.H. Moola. University of the Western Cape

This study was designed to measure the effectiveness of an oral health preventative programme based in a school population in t Cape Peninsula. The objective of the study was to measure the difference between schoolchildren who were exposed to the programme and children who were not.

Three experimental (programme) and two control schools were selected for the study. A total of 110 children in the experimental group and 102 in the control group were examined (Total = 212) in the age group 11-12 years. The examiners were calibrated for reproducibility using WHO (1986) criteria for dental caries. The results of the study showed a mean DMF(S) o 7.8 (±3.1) for the experimental schools and 24.5 (±8) for the control schools. 84% of the experimental group and 60% of control group were caries free. 98% of the experimental group and 65% of experimental group had an M component of 0.42% of the control group; 8% of experimental group had at least one 1st molar tooth decayed. These results clearly showed that the programme is successful in a community based school dental service.
This project is supported by an MRC grant.

**11** Film Thickness Evaluation - Implementing the BENCOR MULTI-T System. C.H. DRIESSEN*, F.A. DE WET and W.J.C. COETZEE. Faculty of Dentistry, University of Pretoria, South Africa.

Various techniques have been described for the determination of film thickness of dental cements. The purpose of this study was to assess the effectivity of the BENCOR MULTI-T system, and to explore the effect of load variation on the film thickness data. Four luting cements were included in this study i.e. X-R IONOMER (X), a glass ionomer; Mirage-FLC (M), a dual cure resin; UNITY (U), a self curing resin; and POLY-F Plus (P), a polycarboxylate. The BENCOR MULTI-T device (Driessen, 1990) was used for testing. The system is based upon direct force application derived from any calibratable source through it's active rod onto the specimen material placed between two 22mm0 glass discs. The latter is covered with teflon discs for the purpose of: (1) simulating oral temperature, (2) transfering visible light (if needed) for the curing of a VLC material and (3) protecting the 160$\mu$m glass discs from direct metal impact. Measuring of the specimens was done by electronic digital calipers with control by reflex microscope data and SEM image observation. Ten samples of each product were tested using 10Kg and 15Kg forces in order to assess the effect of different loads on the film thickness. All data were statistically analysed. It was found that the technique enabled operators to measure film thickness of dental cements accurately, easily, fast and with only small variations. Statistical analyses showed a significant difference ($p<0.05$) between application of 10Kg and 15Kg load of (X)[25,76:19,60$\mu$m] and (U)[28,60:14,20$\mu$m] but not for (M)[31,14:30,80$\mu$m] and (P)[38,00:34,00$\mu$m]. It can be concluded that the BENCOR MULTI-T system is able to easily assess the film thickness of dental cements, and that a 15Kg load reduces film thickness compared to the 10Kg load.

**12** Cross-Infection Risks Associated with High-speed Dental Handpieces. C.H. HAUMAN.* Department of Oral Pathology, Faculty of Dentistry, University Stellenbosch, Tygerberg, South Africa

Dental handpieces are particularly prone to contamination with patient material, which can then transmitted to the next patient. The common approach of disinfecting handpieces by external chemic wiping in combination with flushing may pose unacceptably high risks to those individuals treated soc after infected patients.
The aim of this study was to evaluate the efficacy of chemical disinfection of high-speed handpiece Autoclavad high-speed handpieces were contaminated with an overnight culture of *Staphylococc aureus* and dried in a hot air oven for 90 minutes. The outer surfaces of equal numbers of the handpieces were wiped with 70% alcohol, alcohol-in-hibitane and Asepsyx (iodophor). The front, bac and sides of the heads of these handpieces were pressed onto the surface of blood agar plates. addition, contaminated handpieces were attached to the dental unit and water was flushed through th handpiece onto the surface of blood agar plates for 2 seconds. Handpieces used in the Tygerber Dental Hospital were tested in a similar way after routine lubrication and alcohol swabbing. Residu contamination of handpieces after flushing for specific periods of time were also tested. Aft overnight incubation, growth was recorded. Although the numbers were reduced, *S. aureus* could st be cultured from the outer surfaces of artificially contaminated handpieces after wiping with all thre disinfectants. Handpieces used in the clinic yielded virtually no growth from the external surfaces aft routine cleansing. Confluent or 2+ growth was obtained with samples from the interior surfaces both artificially contaminated handpieces and handpieces from the clinic. *S. aureus* was still preser on the internal surfaces of artificially contaminated handpieces after flushing for 5 minutes.
Sterilisation of both the internal and external surfaces of handpieces is necessary to exclude the risk cross-infection in the dental surgery.

**13** Effect of Respiratory Acidosis on Faecal Fluoride Excretion in Rats. S.D. JANSE VAN RENSBURG* and C.A. VAN DER MERWE. University of Pretoria, and Medical Research Council, Pretoria, South Africa.

Respiratory acidosis is characterised by a primarily increased $PCO_2$ with a compensated increased $[HCO_3^-]$ which may effect the pH of blood. As the permeation of fluoride (F) through epithelia is dependent on the pH, as well as F concentration, respiratory acidosis could have an effect on faecal F excretion, and therefore on the F balance of the body. Sixteen young adult female Sprague-Dawley rats were used in this study. They were divided into a control group (Group A; receiving a normal atmospheric gas mixture) and an experimental group (Group B; subjected to an atmospheric $CO_2$ content of 7%). All the rats were fed a low F diet (< 1ppm) and received water with a fluoride content ([F]) of 20ppm *ad lib* for 7 weeks. Water and food consumption were monitored daily. F intake/rat/day via water and food was calculated from the data. After sedation, blood was collected anaerobically in heparinised syringes from the descending aorta. Faeces were collected from the large intestine. The [F] of the faeces was determined potentiometrically after HMDS diffusion. Blood gas analysis were done using the ABL blood gas analyser. The data were subjected to the Mann-Whitney procedure to detect differences between the groups, and to multiple regression analysis to explain the variation in the [F] of the faeces. Although the F intake via the water differed significantly ($p<0,05$) between the groups, there was no significant difference between the F intake via food ($p=0,197$) or the total F intake ($p=0,071$). There was a significant difference ($p<0,05$) in the [F] of the faeces (A:$\bar{x}$= 148,33 ppm; B:$\bar{x}$= 213,20 ppm) between the groups. Taking the [F] of faeces as the dependant variable, 68,89% of the variation in the [F] of faeces in the experimental group could be explained by the combination of the independent variables $H_2CO_3$ or $PCO_2$ and total F intake. A 46,92% association between the variables was found in the control group. Respiratory acidosis enhanced faecal excretion of fluoride in rats. The higher [F] of the faeces in the experimental group could possibly be due to net secretion of fluoride into the gut lumen. This project was partially supported by a grant from Afrox Pty Ltd.

**14** Inorganic Contents of Opaque and Translucent Radicular Dentine. F.S. NKHUMELENI*, E.J. RAUBENHEIMER, W.F.P. VAN HEERDEN, M.L. TURNER and M.J. DREYER. Depts. Oral Pathology and Chemical Pathology, MEDUNSA, P.O Medunsa.

This study was undertaken to compare the calcium, magnesium, phosphorus, zinc and fluoride contents of opaque and translucent radicular dentine. Twelve mandibular incisors were utilized. The crowns and cementum were removed using a dental bur. The specimens were then hydrolysed individually in 1M perchloric acid. Calcium, zinc and magnesium were determined utilising the ammonium phosphomolybdate calorimetric method and fluoride by ion selective electrode method. The mean values (mg/g) of opaque and translucent dentine respectively were :

| | | | | | |
|---|---|---|---|---|---|
| Calcium (Ca) | 244.65 | (SD ± 3.60) | and | 244.17 | (SD ± 4.10); |
| Magnesium (Mg) | 8.25 | (SD ± 0.42) | and | 6.97 | (SD ± 0.69); |
| Fluoride (F) | 0.22 | (SD ± 0.01) | and | 0.27 | (SD ± 0.02); |
| Phosphorus (P) | 127.70 | (SD ± 2.43) | and | 125.00 | (SD ± 2.33); |
| Zinc (Zn) | 0.14 | (SD ± 0.01) | and | 0.20 | (SD ± 0.03). |

The Mann Whitney test showed that there was a significant difference between the Mg, F and Zn contents of opaque and translucent dentine ($p<0.05$). Our findings do not support those of Moore and Leaver (1974) who found that only Calcium values were significantly lower in translucent dentine.

**15** Enamel Surface Roughness after $CO_2$ Laser Radiation, in vitro Assessment. S.H. PAN*, C. BAKER, J. DE VRIES, P.J. BECKER and S.S. MASHELE. Dept. of Operative Dentistry, Faculty of Dentistry, MEDUNSA, S.A.

Recently, a $CO_2$ laser has been used successfully to enhance dental bonding. Knowledge of surface roughness is essential to reduce bond failures. The objectives were to: 1) determine the surface roughness after conventional drilling with/without laser radiation and with/without acid etching using the Bendix Profilometer. 2) examine under Scanning Electron Microscope (SEM) the ultrastructure of the enamel surface after $CO_2$ laser radiation. Thirty-two human maxillary central incisor teeth were selected and stored in 10% buffered formalin. Conventional drilling and combined treatment with laser radiation were randomised on the labial enamel surface in the vertical dimension of 3 x 5mm. Laser radiation was set at a repeat pulse energy intensity of below 3W for a period of 10 seconds. Acid etching was performed on half of the specimens and the surface roughness was measured with the Bendix Profilometer. The SEM assessment was also noted. The experiment was designed as a randomised block but test results showed that roughness caused by laser produced the maximum measurable roughness of 10 micron for each sample point. The analysis then focused on conventional high/low speed drilling and no significant difference was found between acid etching techniques. ($p = 0,4270$) or between drilling speeds ($p = 0,7355$). Compared to laser the roughness after conventional drilling was clinically less.
An improved understanding of roughness caused by $CO_2$ laser radiation on enamel surfaces may lead to possible clinical application in aesthetic restorative dentistry.

**16** Relation Between Blood, Molar, Cortical Bone and Trabecular Bone Lead Levels of Rats. R.J. ROSSOUW* and S.R. GROBLER, Faculty of Dentistry, University of Stellenbosch, Tygerberg, South Africa

Bone is the major reservoir of body lead stores. Loosely and deeply bound lead compartments in bone provide short- and long-lived sources of this toxic element to blood and soft tissues.

Several groups of inbred BD-IX rats were continuously exposed to nebulized aerosols of lead for different time periods. Furthermore, the effect of different post-exposed periods on the lead concentrations were also investigated. The lead concentrations were determined in blood, molars, tail vertebra and iliaca crest of the rat. The graphite furnace atomic absorption spectrophotometer was usad.

The blood, molar, tail and iliaca crest lead levels differed significantly ($p<0,05$) among the exposed groups. However, only the blood and iliaca crest lead concentrations differed significantly ($p<0,05$) in the post-exposure periods.

It is concluded that lead is absorbed in the apatite crystal of different kinds of bone. Furthermore, cortical bone is identified as long term storage reservoirs of lead in the body.

This study was supported by the MRC.

## 33

Composition of Tubular and Intertubular Areas in Translucent Dentine. P.S. NKHUMELENI*, E.J. RAUBENHEIMER and M.L. TURNER, Faculty of Dentistry, Medical University of Southern Africa.

Most researchers seem to agree that the changes which cause root dentine to appear translucent occur in the lumina of dentinal tubules. The purpose of this study was to compare the occluding material and adjacent intertubular dentine. The radicular translucent dentine of mandibular incisors from nine subjects were coated with a 10-12nm gold-film. The specimens were examined in an ISI SX30 SEM equiped with a Link Systems EDAX-analyser. Two areas were investigated, namely material occluding the tubules and areas not more than 5 microns from the edge of the obliterated tubule. The mean values of occluding material and intertubular dentine (%) respectively were as follows:

| | | | | |
|---|---|---|---|---|
| Calcium | (Ca) | 67.4 (SD = 12.4) | and | 60.9 (SD = 7.9) |
| Phosphorus | (P) | 40.7 (SD = 8.7) | and | 33.9 (SD = 8.4) |
| Ca:P ratio | | 1.7 (SD = 0.5) | and | 1.8 (SD = 0.6) |

There was a significant difference between the calcium and phosphorus content of the occluding material and adjacent intertubular dentine ($p < 0.05$). Our findings did not support those of Brinkmann and Hartmann (1980) who found no correlation between dentine translucency and its mineral content.

The material occluding the dentinal tubules is more mineralized than intertubular areas in translucent dentine.

## 34

Comparing the Shear Bond Strength of One, Two and Three Step Dentine Bonding Systems. P.J. VAN DER VYVER, F.A. DE WET, W.R. VORSTER and J. OOSTHUYSEN*, Faculty of Dentistry, University of Pretoria, Pretoria, South Africa.

Some of the most important features when chosing a dentine bonding system is the ease to use, and the time required to apply the system. The purpose of this study was to compare the shear bond strengths of one, two, and three step dentine bonding systems.

One hundred and twenty sound, human, molar teeth were collected and the crowns embedded in rings. The occlusal surfaces were ground wet on 220 grit SiC paper in order to expose superficial dentine. The samples were randomly assigned to 6 test groups consisting of 20 teeth each. One group was used to evaluate each of the following materials: Pertac Bond (PB), Tokuso Light Bond (TLB), Art Bond (AB), Prisma Universal Bond 3 (PUB3), Scotchbond Multi-Purpose (SMP) and Optibond (OB). Of the products, two were one-step systems i.e. PB and TLB, another two were two-step systems i.e. AB and PUB3, and the last two were three-step systems i.e. SMP and OB. SMP etchant was used with OB system to achieve total smear-layer removal, making it a three-step system. Twenty dentine surfaces were treated with each of the 6 bonding systems, and cylinders of matching composites thereafter bonded to the surfaces, using a rubber split mould. All samples were stored in distilled water at 37°C for 24 hours before they were stressed to failure using a shear load in an Instron. Data were analyzed statistically (ANOVA). The bond strengths for the different products (MPa) were as follows: PB: 11,21 ± 1,54; TLB: 6,7 ± 1,7; AB: 15 ± 2,3; PUB3: 14,3; SMP: 23,6 ± 2,5 and OB: 24,1 ± 2,5.

The three-step bonding systems showed higher bond strengths to dentine than the 1 and 2 step systems. The two-step systems also had a higher bond strength than the one-step systems.

Amongst the six systems tested, the three step systems provided the best shear bond strength values.

## 35

Laser Effects on Pulpal Floor Thickness and Intercuspal Tooth Strength. S.H. PAN[*1] and C. BAKER[2] and J De Vries[3]. Faculty of Dentistry[1&3], MEDUNSA & MRC/WITS, DRI[1]; E M Unit, MEDUNSA[2], R.S.A.

Carbon dioxide ($CO_2$) lasers have been successfully used to fuse the apatite of enamel with that of dentine. In order to assess the effectiveness of this fusion, it is essential to ascertain that strength of a premolar tooth. The aim of this study was to determine the optimal pulpal floor thickness after $CO_2$ laser irradiation. Repeat pulsed $CO_2$ laser with energy densities of 10-15 J.cm$^{-2}$ was applied to 10 conventionally prepared M-O-D cavities. The remaining 10 teeth were prepared by conventional drilling only. All of the teeth were fitted with the indirect cast resin inlay restorations (Isosit-N) and luted with resin cement (Vivadent). Teeth were subjected to a stress (± 20-50 MPa) causing them to fracture. Compressive strengths of teeth from the experimental and controlled groups were analysed. Measurements of pulpal floor thickness were carried out by image Analysis and SEM. For the overall observation vector (ANOVA), it was found that treatments differed significantly ($p=0,0084$), thickness (≥ 2mm; < 2mm) differed significantly ($p=0,0028$), while no interaction was found between treatment and thickness ($p=0,1164$).

For optimal intercuspal tooth strength, the pulpal floor thickness must be ≥ 2mm, since modern aesthetic dental treatment may involve a combination of conventional drilling and laser irradiation.

## 36

Evaluation of Optibond when used as a Fissure Sealant. P.J. VAN DER VYVER, F.A. DE WET and J. OOSTHUYSEN*. Faculty of Dentistry, University of Pretoria, Pretoria, South Africa.

The Optibond bonding system has multiple uses, including bonding to enamel, dentine, porcelain, composite and metal. Since the system contains a 48% filled, radiopaque and fluoride-releasing, dual-curing catalyst paste, it might have ideal properties for usage as a fissure sealant. The purpose of this study was to evaluate the shear bond strength (SBS) of Optibond (Dual Cure system) when used as a fissure sealant on human dental enamel.

Fourty freshly extracted, sound, human, molar teeth were collected, the roots and pulps removed and the crowns embedded in rings. The exposed occlusal surfaces were ground wet on 220-grit SiC paper to produce a flat enamel surface. All enamel surfaces were etched for 30 seconds with 37% phosphoric acid, rinsed and dried. The Optibond primer was then applied according to manufacturers' instructions and light-cured for 20 seconds. Optibond dual-cure (consisting of a catalyst with resinous liquid and a filled accellerator paste) was mixed, and cylinder stubs of the material then bonded to the treated enamel surface using a silicone rubber split mould. All samples were cured for 1 minute from the occlusal direction, and an additional 2 minutes after removal of the split mould (1 minute each from 2 different directions). Twenty bonded samples were stressed to failure 15 minutes after bonding, by using a shear load in an Instron and the remainder stored for 24 hours in distilled water at 37°C prior to testing. The mean SBS was calculated for each group, the data analysed using the Student-T test and several fracture sites examined in the SEM.

The SBS after 15 minutes and 24 hours were 15,96 ± 3,59 MPa and 20,32 ± 2,71 MPa respectively ($P<0,01$). SEM investigation demonstrated mixed cohesive/adhesive fractures.

It can be concluded that the SBS of Optibond to enamel after periods of both 15 minutes and 24 hours are adequate for usage in clinical fissure sealing situations, with the highest bond strengths being obtained after 24 hours.

## 37

Determination of Patient Trends, Logistics and Appointment Preferences. P.J. COMBRINK* and W.A. WILTSHIRE. Department of Orthodontics, University of Pretoria, Pretoria.

In a concerted effort to continue to improve the service rendered by the Orthodontic Department of the University of Pretoria, it was the purpose of this study to survey patients attending the orthodontic clinic. An anonymous questionnaire which included a variety of questions was completed by 65 patients or parents. The responses were statistically analysed employing the Fishers exact test and the log linear model on frequency tables. Of the 65 patients only 30 were members of medical aid funds and were prepared to pay ±R160 out of their own pockets for treatment. Patients without medical aids were prepared to pay ±R311 for orthodontic treatment. Thirteen respondents were prepared to pay as much as needed to complete treatment. More patients (69.84%) used private transport than public transport (15.87%) to attend the clinic. No correlation was evident between mode of transport and frequency of cancelled ($p=0,363$) or missed ($p=0,292$) appointments. No significant correlation ($p=0,175$) between geographical abode and missed or cancelled appointments was apparent either. 17% of patients regularly missed appointments, 64% maintained that a 24 hour cancellation would suffice and 42.28% used the appointment card in order to remember their appointments. 77% felt a fine should be imposed for broken appointments. There was a highly significant correlation between patients who regularly kept their appointments and who suggested imposition of a fine ($p=0.000$). 60% of patients preferred the 7h15 appointment time to the 14h00 time slot. Patient complaints included: long waiting lists (28.4%), inconvenient times (18%), long appointments (17.2%) and student turnover (10.3%). Regular managerial audits is necessary in order to access patient requirements and protect the patient service at a dental training hospital.

## 38

Frequency of Preventable Malocclusions in the Mixed Dentition: A Preliminary Report. E.R. De Villiers* and W.A. Wiltshire, Department of Orthodontics, Faculty of Dentistry, University of Pretoria, Pretoria

Specific defined malocclusions, where early recognition and simple interceptive treatment may minimise or eliminate the need for complex appliance therapy, have been identified and certain ages of special vigilance in the developing dentition are recognised. The aim of this longitudinal study is to determine the percentage of malocclusions at the age of 10-11 years that could have been prevented or minimised, if causative factors had been diagnosed and treated from the age of 8-9 years. A total of 961 children, aged 8 and 9 years were examined by 3 investigators at 9 schools in the Pretoria suburbs of Pretoria West and Atteridgeville to collect baseline data on the current status of occlusion in these groups. An average of 67,9% of cases presented with a Class I molar relationship; 10,9% with a Class II; 7,45% with a Class III and 12,1% with a cusp-to-cusp molar relationship. Early loss of second primary molars occured in the maxilla (5,5%) and in the mandible (7,5%). First primary molars were lost in 5,4% of cases in the maxilla and in 11,3% in the mandible. Space was sufficient in 71,9% of cases, but 18,3% showed a shortening of arch length. Ectopic eruptions, ankylosis of primary molars, supernumerary teeth were very rare. Single tooth anterior crossbites were evident in 7,2% of cases and 7,1% had more than one tooth in anterior crossbite. Posterior, single tooth crossbites were found in 2,5% and multiple tooth crossbites in 0,6% per quadrant. 45% of children had a normal overbite, 30,1% had a deep bite, 8,8% had an edge-to-edge bite and 14,7% presented with an anterior openbite. The majority of children had Class I malocclusions with sufficient arch length and a seemingly normal developing occlusion.

## 39

Airborne Lead Exposure and Lead Levels in Rat Tissues. R.J. ROSSOUW* and S.R. GROBLER. Faculty of Dentistry, University of Stellenbosch, Tygerberg.

Lead has no metabolic role in the human body and its presence in teeth is associated with various toxic effects. The purpose of this study was to indicate the importance of the combined effect of airborne lead concentration and length of exposure. Experimental work was done on Rattus rattus norvegicus. Groups of 20 inbred rats were exposed to: (1) "clean air" (0.05 µg Pb/m$^3$) for 70 days; (2) 77 µg Pb/m$^3$ for 70 days; (3) 249 µg Pb/m$^3$ for 28 days; and (4) 1 546 µg Pb/m$^3$ for 30 days. Half the rats in each group were then killed and the other half kept in "clean air" until the blood lead of groups 1-3 had returned to normal. Tail vertebrae, iliaca crest and epiphyses' radius, and blood were analyzed for lead by atomic absorption spectrophotometry. In the rats killed immediately after exposure, the lead levels of blood or iliaca crest or epiphyses or tail vertebrae differed significantly ($p<0.05$) among all 4 groups, except between groups 2 and 3 for the tail vertebrae. For the post-exposure rats, the blood showed no significant differences ($p>0.05$) among groups 1, 2 and 3. However, for tail vertebrae or iliaca crest or epiphyses no significant differences were found between groups 2 and 3.

It can be concluded that lead turnover had the following sequence: blood (soft tissue) > iliaca crest (trabecular bone) > epiphyses (trabecular and compact bone) > tail vertebrae (compact bone). Blood lead became supplemented through the process of bone remobilization and different bone compartments exist.

## 40

Longitudinal Study on the Oral Yeast Carraige in Children. E. BLIGNAUT, R. SENEKAL* and J. KROON. Faculty of Dentistry, University of Pretoria, Pretoria.

Yeasts are amongst the very first microorganisms to colonise the oral cavity of the newborne. Since yeasts occur widely in nature, it is inevitable that humans should come into contact with them and previous studies have shown yeasts to be amongst the normal oral flora of 50%-70% of healthy individuals. It was also thought that the tongue is the most likely place of residence for oral yeasts and statistics from previous studies are based mainly on a once only specimen taken from the tongue or saliva of a particular individual.

In order to establish whether the occurance of yeasts are merely incidental at the time of sampling, 172 children ranging in age between 3 and 8 years were studied over a 2 year period. Specimens were taken from both plaque and saliva and immediately plated onto chalk agar. While yeasts were isolated from an average of 22,6% of children at one time or the other, only 2,9% of the children were yeast positive on both occasions of which one had different species from the one year to the next. During the 1992 study, four children had yeasts in both saliva and plaque of which 3 exhibited different species while only one was positive for both specimens during the 1993 study.

From these results it can be concluded that the presence of yeasts in the oral cavity of an individual at a particular point in time, does not implicate a carrier state.

PERGAMON

Archives of Oral Biology 43 (1998) 641–647

ARCHIVES OF ORAL BIOLOGY

# Geographic variations in the composition of ivory of the african elephant *(Loxodonta africana)*

E.J. Raubenheimer[a,*], J.M.M. Brown[a], D.B.K. Rama[b], M.J. Dreyer[c], P.D. Smith[c], J. Dauth[c]

[a]*Departments of Oral Pathology, Medical University of Southern Africa, P.O. MEDUNSA, 0204, RSA*
[b]*Department of Environmental and Occupational Health, Gauteng Health Department, Johannesburg, RSA*
[c]*Chemical Pathology, Medical University of Southern Africa, P.O. MEDUNSA, 0204, RSA*

Received 14 January 1997; accepted 7 April 1998

**Abstract**

Tracing the source of origin of illegal ivory will contribute to the identification of poorly managed game parks and facilitate steps taken to prevent the African elephant from becoming extinct. This study was aimed at establishing a database on the composition of ivory obtained from elephant sanctuary areas in Southern Africa. Fragments of elephant ivory from seven geographically distinct areas in South Africa, Namibia and Botswana were analysed for inorganic and organic content. A total of 20 elements was detected in the inorganic fraction of ivory, some in concentrations as low as 0.25 $\mu$g/g. The concentrations of calcium, phosphate, magnesium, fluoride, cobalt and zinc showed statistically significant differences ($p < 0.007$) between ivory obtained from different regions. Analyses of the organic fraction identified 17 amino acids. Ivory from arid regions showed significantly lower proline plus hydroxyproline content and under-hydroxylation of lysine residues. This study indicates that chemical analyses of ivory could be beneficial in tracing the source of illegal ivory. 

*Keywords:* Elephant ivory; Composition; Environment; Organic and inorganic analyses

## 1. Introduction

The illegal harvesting of ivory is generally restricted to poorly managed game-sanctuary areas in Africa and, if unabated, will lead to the eradication of elephant from large parts of the continent (Armstrong and Bridgland, 1989; Ottichilo, 1986). The rapid decrease in elephant numbers was met by a listing of the African elephant as a protected species by the Convention on Trade in Endangered Species (CITES). Despite doubt about the future of the African elephant, their numbers in protected areas in certain African countries are indisputably growing (Armstrong and Bridgland, 1989; Hall-Martin, 1992).

Dentine (or ivory) forms the bulk of the substance of most teeth of mammals and is composed of organic and inorganic fractions. The inorganic composition of the ivory of the elephant has not yet been investigated in detail except for work done on its isotope composition. The carbon isotope ratios ($^{13}C$:$^{12}C$) of ivory distinguish between elephant roaming the woodland and those in dense forests (Van der Merwe, et al., 1988). Similarly, nitrogen isotope ratios ($^{15}N$:$^{14}N$) in the ivory of the African elephant are related to water stress or rainfall. Overlap in the distribution of carbon and nitrogen isotopes can be expected when dealing with ivory of elephant from similar environments. In such cases, strontium isotopes may be helpful in making a distinction, as $^{87}Sr$:$^{86}Sr$ ratios in tusks reflect the local

* To whom all correspondence should be addressed. Fax: (012) 521 4838; E-mail: ejraub@mcd4330.medunsa.ac.za

0003-9969/98/$19.00 
PII: S0003-9969(98)00051-X

geology of a particular region (Van der Merwe et al., 1990). No scientific information is available on the organic composition of elephant ivory.

Science can contribute to the exposure of those areas in which illegal ivory harvesting is taking place by establishing a databank on geographical variations in the chemical composition of ivory. This would contribute significantly to the identification of the source of origin of illegal ivory, making more specific intervention in poorly controlled elephant sanctuaries possible.

Our purpose now was to determine variations in the inorganic and organic composition of ivory obtained from seven distinct elephant-sanctuary areas in Southern Africa.

## 2. Materials and methods

Sixty-four fragments of ivory were obtained through the National Parks Board of South Africa from the following areas: north-western Namibia (Kaokoveld), northern Namibia (Etosha National Park), north-eastern Namibia (Caprivi), northern Botswana (Kavango), north-eastern South Africa (Kruger National Park), northern Natal (Tembe Elephant Park) and eastern Cape (Addo Elephant Park) (Fig. 1). The habitats vary between arid (Kaokoveld), African woody savannah (Kruger National Park and Caprivi), savannah with salt pans (Etosha), subtropical forests (Kavango), dense Karoo shrub (Addo Elephant Park) and coastal dune forest (Tembe Elephant Park). All ivory was obtained within 7 days of death from animals that had died of natural causes or as part of the population-control programmes employed in the respective areas.

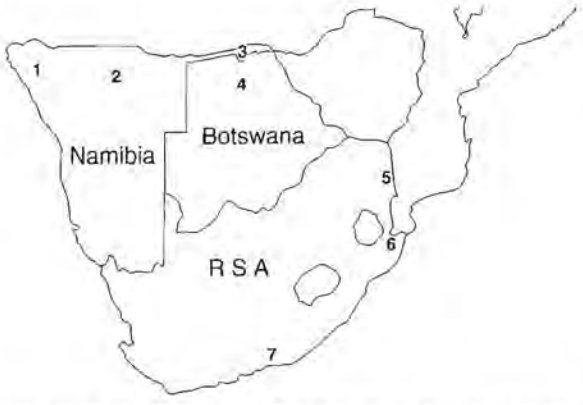


Fig. 1. Origin of ivory (1, Kaokoveld; 2, Etosha National Park; 3, Caprivi; 4, Kavango; 5, Kruger National Park; 6, Tembe Elephant Park; 7, Addo Elephant Park, RSA, Republic of South Africa).

### 2.1. Inorganic analyses

The dry weights of all fragments were determined accurately after carefully removing the ensheathing layer of cementum with a rotating diamond disc. The specimens were agitated in a weak acid (0.1 M HCl) for 10 min to remove traces of metal that may have contaminated the ivory during sample preparation. The fragments were washed for 15 min in distilled water and demineralized in 1 M perchloric acid at room temperature for 3 weeks. Complete demineralization was confirmed microscopically by embedding, sectioning and staining of the organic residue with von Kossa. The inorganic composition was determined by atomic absorption spectrophotometry (Perkin Elmer 500; Norwalk, CT, U.S.A.), Astra 8 analyser (Beckman Instruments Inc., Brea, CA, U.S.A.) and ion-selective electrodes (Radiometer, Copenhagen, Denmark). The mean values obtained per site of origin as well as the SD were expressed in mg/g dry weight and tabulated. The level of significance between the findings for each element and at each site was determined with the aid of the student's $t$-test for unequal variances after standard distribution curves had been established between paired values.

The trace-elemental composition of 27 fragments was determined with an ARL 34000 inductively coupled plasma optical emission spectroscope (ARL, Boston, MA, U.S.A.) consisting of inductively coupled argon plasma operating at 27 MHz with direct reading on a 29-channel spectrometer. Perchloric acid (1 M) was used as control in order to monitor the possibility of contamination of the demineralizing solution. The mean concentrations and SD were expressed in $\mu$g/g ivory and tabulated. The level of significance between the concentrations of each element at different geographical sites was determined by the student $t$-test for unequal variances.

### 2.2. Organic analyses

Fragments of peripulpal ivory devoid of cementum and weighing between 1 and 3 grams were prepared from five tusks of the Kruger National Park, six of Kaokoveld elephant, fifteen from Etosha, four from Tembe and two from Addo Elephant Park. The solid particles were hydrolysed in sealed tubes containing 5 ml 6 M HCl at 110°C for 24 h. The hydrolysates were neutralized, filtered (Millex-GS, 0.22 $\mu$m) and diluted 1:1 with citrate buffer (pH 2.2). Calibrants of a standard of 43 amino acids were prepared, and the amino acids of the hydrolysates and calibrants were separated in a Beckman 6300 amino acid analyser (Beckman Instruments Inc., Palo Alto, CA, U.S.A.), which incorporated a 25-cm lithium column and a four-buffer system. The chromatograms were inte-

grated and quantitated with a Hewlett-Packard 3390A integrator (Hewlett-Packard Co., Palo Alto, CA, U.S.A.). The analyses were done in duplicate in order to eliminate methodological errors. The results were tabulated as the average of the total number of residues per 100 and the SD for each amino acid calculated. The differences in the amino acid compositions between the regions with a sample size of five or more were analysed with the student *t*-test assuming unequal variances.

## 3. Results

### 3.1. Inorganic composition

The fragments of ivory weighed between 1.101 and 3.570 g after drying and Von Kossa staining of all specimens demineralized for 14 days showed complete loss of calcium. The concentrations of calcium, phosphate, magnesium and fluoride are expressed per region and a sample mean is given for each element in Table 1. Statistical analyses showed that the differences between the respective elements in the following geographical locations were highly significant ($p < 0.002$):

*For calcium*: Addo vs all other locations, Etosha vs Caprivi, Etosha vs Kavango, Caprivi vs Tembe.

*For phosphate*: Kruger National Park vs Kaokoveld, Addo vs Kaokoveld.

*For magnesium*: Addo vs Kruger National Park, Caprivi and Tembe vs Addo and Kaokoveld vs Caprivi.

*For fluoride*: Kaokoveld vs all other locations except Etosha and Etosha vs all other locations except Kaokoveld.

The respective concentrations of the trace elements are shown in Table 2. Due to the size of the samples, statistical analyses could be made only on the Addo, Etosha and Kruger National Park groups of specimen. Differences in the concentrations of the following elements between the respective groups were found to be significant:

*For cobalt*: Addo vs Kruger National Park ($p < 0.007$).

*For zinc*: Addo vs Kruger National Park ($p < 0.002$).

Twice the sample mean or higher concentrations were analysed in ivory from a single tusk in the following locations (sample mean in parentheses):

Olifantsbad (Etosha)—*copper* = 7.5 (2.2) μg/g;
Tembe—*manganese* = 11 (0.6) μg/g;
Ombika (Etosha)—*manganese* = 1.5 (0.6) μg/g;
Kavango—*iron* = 8.8 (4.4) μg/g;
Ombika (Etosha)—*iron* = 13 (4.4) μg/g;
Olifantsbad (Etosha)—*zinc* = 40 (20) μg/g;
Ombika (Etosha)—*zinc* = 54 (20) μg/g;
Koinseb (Etosha)—*aluminium* = 23 (6.2) μg/g.

### 3.2. Organic composition

Ivory obtained from the Kaokoveld was more brittle than that from other regions. Complete hydrolysis of Kaokoveld and Etosha ivory was obtained in less than half the time than that required for ivory from other regions. The amino acid composition of hydrolysed ivory is expressed per site of origin in Table 3. Due to the small number of samples, statistical analyses were made on ivory obtained from the Kruger National Park ($n = 5$), Kaokoveld ($n = 6$) and Etosha ($n = 15$) only. Highly significant differences ($p < 0.001$) were found in the respective amino-acid compositions of ivory from the following regions:

*Hydroxyproline* Kruger ivory (10.2 parts/$10^6$, SD 2.6) significantly higher than Etosha ivory (9.2 parts/$10^6$, SD 0.7);

*Proline* Kruger ivory (13.1 parts/$10^6$, SD 0.5) significantly higher than Etosha ivory (11.6 parts/$10^6$, SD 0.8);

Table 1
Inorganic composition of ivory per site of origin (average mg/g dry wt, SD in parentheses)

| Origin | Number of specimens | Ca | $PO_4$ | Mg | F |
|---|---|---|---|---|---|
| KNP[1] | 13 | 195.8(17) | 115.5(5) | 14.6(3.2) | 0.08(0.01) |
| Kaoko[2] | 9 | 193.7 (15.9) | 118 (2.6) | 18.2 (4.2) | 0.11 (0.02) |
| Etosha | 26 | 192 (16) | 116 (3.5) | 15.3 (4.2) | 0.12 (0.03) |
| Caprivi | 6 | 208.9 (6.4) | 114.7 (4) | 13.1 (0.9) | 0.07 (0.01) |
| Kavango | 4 | 205.9 (1.8) | 115.3 (3) | 12.2 (2.7) | 0.06 (0.01) |
| Tembe | 3 | 191.1 (8.9) | 113.1 (5) | 14.7 (1.2) | 0.05 (0.01) |
| Addo | 3 | 170.8 (2.5) | 113 (1.4) | 17.3 (0.4) | 0.03 (0.02) |
| Sample mean | 64 | 195.6 (15.7) | 115.5 (4) | 16.4 (4.4) | 0.09 (0.04) |

[1] Kruger National Park; [2] Koakoveld.

Table 2
Trace elemental composition of ivory per site of origin (mean (μg/g dry wt, SD in parentheses)

| Origin | No. Spec. | As | Cd | Cr | Co | Cu | Pb | Mn | Hg | Ni | Fe | Zn | Mo | Al |
|---|---|---|---|---|---|---|---|---|---|---|---|---|---|---|
| KNP | 5 | 8.5(0.7) | 0.44(0.03) | 4.1(0.2) | 0.8(0.07) | 2.06(0.3) | 8.9(1.0) | 0.3(0.09) | 1.5(0.2) | 0.9(0.08) | 2.3(0.3) | 20.4(3.0) | 0.6(0.02) | 3.8(0.4) |
| Kaoko | 3 | 7.2(0.6) | 0.4(0.02) | 3.4(1.0) | 0.77(0.05) | 1.9(0.2) | 9.7(0.4) | 0.44(0.3) | 1.5(0.2) | 1.0(0.08) | 4.0(1.1) | 17.0(8.4) | 0.56(0.08) | 6.5(0.2) |
| Etosha | 6 | 8(1.4) | 0.4(0.03) | 3.8(0.4) | 0.7(0.09) | 2.8(2.4) | 8.6(1.2) | 0.61(0.4) | 1.4(0.2) | 0.9(0.1) | 6.6(4.5) | 27.8(17) | 0.55(0.06) | 8.8(6.6) |
| Caprivi | 1 | 6.0 | 0.37 | 2.6 | 0.75 | 2.0 | 11.0 | 0.25 | 1.2 | 0.79 | 1.6 | 13.0 | 0.47 | 3.6 |
| Kavango | 3 | 8.2(1.3) | 0.44(0.03) | 4.0(2.0) | 0.68(0.09) | 2.3(0.4) | 9.1(2.7) | 2.43(2.9) | 1.5(0.1) | 0.9(0.13) | 5.8(4.2) | 24(12.7) | 0.58(0.0) | 8.5(5.0) |
| Tembe | 3 | 9.3(2.4) | 0.4(0.2) | 3.9(0.3) | 0.7(0.02) | 2.2(0.6) | 8.4(0.3) | 2.2(4.3) | 1.6(0.1) | 0.9(0.05) | 5.2(2.3) | 22.0(7.0) | 0.6(0.03) | 6.2(1.1) |
| Addo | 4 | 7.8(2.0) | 0.36(0.04) | 3.1(0.5) | 0.64(0.06) | 1.9(0.5) | 8.0(1.4) | 0.39(0.1) | 1.3(0.2) | 0.8(0.1) | 3.3(1.5) | 16.6(5.8) | 0.5(0.07) | 4.6(1.6) |
| Sample mean | 25 | 8.0(1.4) | 0.4(0.04) | 3.7(0.6) | 0.72(0.1) | 2.2(1.2) | 8.7(1.2) | 0.6(0.9) | 1.4(0.2) | 0.89(0.1) | 4.4(3.2) | 20(10.8) | 0.56(0.06) | 6.2(4.3) |

Origin abbreviations as in Table 1.

Table 3
Total amino-acid composition of hydrolysed ivory (expressed as the average of the total number of residues per 100 above, SDs below)

| Origin Specimens | Sample size | Asp | Hypro | Thr | Ser | Glu | Pro | Gly | Ala | Val | Met | Ileu | Leu | Phe | Hylys | Lys | His | Arg |
|---|---|---|---|---|---|---|---|---|---|---|---|---|---|---|---|---|---|---|
| KNP | 5 | 5.3 | 10.2 | 2.2 | 4.2 | 8.3 | 13.1 | 30.6 | 9.8 | 2.6 | 0.3 | 1.1 | 3.0 | 1.5 | 0.7 | 1.4 | 0.8 | 4.2 |
| | | 0.2 | 2.6 | 0.4 | 0.3 | 0.2 | 0.5 | 0.5 | 0.3 | 0.3 | 0.1 | 0.1 | 0.3 | 0.2 | 0.1 | 0.3 | 0.4 | 0.5 |
| Kaoko | 6 | 5.0 | 9.8 | 2.1 | 4.0 | 8.2 | 12.5 | 30.7 | 10 | 2.5 | 0.2 | 1.2 | 3.0 | 1.5 | 0.4 | 2.9 | 0.6 | 4.5 |
| | | 0.3 | 0.8 | 0.2 | 0.1 | 0.2 | 1.0 | 0.7 | 1.1 | 0.3 | 0.1 | 0.1 | 0.2 | 0.2 | 0.2 | 0.6 | 0.1 | 0.5 |
| Etosha | 15 | 5.0 | 9.2 | 1.9 | 4.0 | 8.3 | 11.6 | 31.3 | 10.8 | 2.3 | 0.5 | 1.2 | 2.9 | 1.5 | 0.4 | 3.0 | 0.7 | 4.6 |
| | | 0.3 | 0.7 | 0.2 | 0.2 | 0.2 | 0.8 | 1.2 | 1.2 | 0.3 | 0.1 | 0.1 | 0.1 | 0.1 | 0.1 | 0.2 | 0.2 | 0.3 |
| Tembe | 4 | 5.0 | 11.3 | 2.0 | 4.0 | 8.1 | 12.5 | 30.1 | 9.3 | 1.9 | 0.4 | 1.1 | 3.0 | 1.5 | 0.6 | 1.6 | 0.8 | 4.3 |
| | | 0.2 | 0.2 | 0.1 | 0.2 | 0.1 | 0.1 | 0.4 | 0.1 | 0.1 | 0.1 | 0.1 | 0.2 | 0.1 | 0.1 | 0.2 | 0.1 | 0.4 |
| Addo | 2 | 5.0 | 11.4 | 2.0 | 3.9 | 8.2 | 12.4 | 30.0 | 9.2 | 1.9 | 0.5 | 1.1 | 3.0 | 1.6 | 0.3 | 3.3 | 0.6 | 4.9 |
| | | 0 | 0.1 | 0.1 | 0.1 | 0.0 | 0.0 | 0.1 | 0.1 | 0 | 0 | 0 | 0.1 | 0 | 0 | 0 | 0 | 0 |
| Sample mean | 32 | 5.1 | 9.9 | 2.0 | 4.0 | 8.0 | 12.2 | 30.8 | 10 | 2.3 | 0.4 | 1.2 | 3.0 | 1.5 | 0.4 | 2.7 | 0.7 | 4.6 |
| | | 0.3 | 1.0 | 0.2 | 0.2 | 1.3 | 1.2 | 1.0 | 1.2 | 0.3 | 0.4 | 0.1 | 0.1 | 0.1 | 0.2 | 0.7 | 0.2 | 0.4 |

Asp, aspartic acid; Hypro, hydroxyproline; Thr, threonine; Ser, serine; Glu, glutamic acid; Pro, proline; Gly, glycine; Ala, alanine; Val, valine; Met, methionine; Ile, isoleucine; Le, leucine; Phe, phenylalanine; Hylys, hydroxylysine; Lys, lysine; His, histidine; Arg, arginine.

| | |
|---|---|
| *Lysine* | Etosha (3 parts/$10^6$, SD 0.2) and Kaokoveld (2.9 parts/$10^6$, SD 0.6) significantly higher than Kruger ivory (1.4 parts/$10^6$, SD 0.3); |
| *Hydroxylysine* | Kruger ivory (0.7 parts/$10^6$, SD 0.1) significantly higher than Etosha (0.4 parts/$10^6$, SD 0.1) and Kaokoveld ivory (0.4 parts/$10^6$, SD 0.2). |

The difference in the hydroxylysine content between Kruger and Kaokoveld ivory was significant ($p < 0.01$). Although the number of tusks analysed from Addo and Tembe was too small for statistical analyses, the concentrations of the mentioned amino acids in these regions tended to follow the pattern observed in Kruger ivory and appeared to differ from those of ivory obtained from Etosha and the Kaokoveld in the mentioned respects.

## 4. Discussion

During the formation of dentine (or ivory), which is essentially a biological apatite deposited on an organic matrix, over 45 elements compete for incorporation (Wetherell and Robinson, 1973). It is, however, not clear whether all these elements are structural substitutes in the hydroxyapatite crystal or whether they are absorbed onto the crystal surface. The inorganic composition of ivory reflects greatly the composition of an animal's diet (Posner and Tannenbaum, 1984). Unlike bone or any other tissue, the composition of ivory remains stable after its formation as it is not subject to turnover and remodelling throughout life. This phenomenon can be exploited to monitor environmental pollution and identify the site of origin of a tusk.

An extensive databank on the composition of ivory from the different conservation areas in Africa could assist in tracing the origin of ivory and might play a key role in identifying regions in which illegal tusk harvesting is taking place. This study, as well as others (Van der Merwe et al., 1988; Van der Merwe et al., 1990; Vogel et al., 1990), clearly indicates the realistic possibility of tracing the source of ivory on its chemical composition. The techniques used in the trivariate isotope analyses reported by those groups are expensive and the equipment is not readily available. Our study indicates that the concentrations of elements such as calcium, phosphate, magnesium, fluoride, cobalt and zinc are of potential value in identifying the site of origin of Southern African ivory. Addo, Kaokoveld and Etosha ivory in particular have unique compositions: Addo ivory is distinguished by its low calcium content and Kaokoveld and Etosha ivory by a high fluoride content. Cobalt, zinc and magnesium content hold great potential in facilitating a distinction between ivory from the Kruger National Park and Addo Elephant Park, phosphate to distinguish between Kaokoveld and Kruger ivory, and calcium and magnesium between Caprivi and Tembe ivory. The high concentrations of copper, manganese, iron, zinc and aluminium in selected tusks obtained from different regions in Etosha are interesting and warrant further investigation. The area is characterized by many salt pans. Rain is sporadic and, owing to evaporation, the salinity of water in most of the pans is high. High iron concentrations in ivory should, however, be interpreted with caution as haemolysis or pulpal haemorrhage during death could theoretically lead to an increase in iron. The overlap in composition of ivory obtained from the Kaokoveld and Etosha supports the fact that the geochemistry of the regions is similar in many respects and that elephant migrate between these regions.

The geochemical composition of a particular region is subject to change. Following the rapid economic growth experienced in urban areas after the Second World War, diseases associated with environmental pollution increased due to delayed implementation of countermeasures preventing spillage of heavy metals and other elements in the environment (Kagawa, 1994). The determination of the elemental load in the tissues of man and animals will play an increasing part in future preventive environmental medicine. For reasons already mentioned, the study of the composition of ivory (or dentine) is ideal for this purpose. The concentrations of the 17 elements identified in elephant ivory in this study reflect the chemical nature of the environments in which these animals roam. Most of these elements occur in higher concentrations in heavy industrialized and polluted areas (Hirano and Suzuki, 1996; Andersen et al., 1996; Kusaka et al., 1996) and our findings could serve as baseline values to monitor future pollution of natural resources in Africa.

The presence of minute quantities of mercury and lead in ivory is proof that these elements, which are generally regarded as pollutants, are present in natural ecological systems. In 5000-year-old premolars from Nubia and in 500-year-old teeth from Greenland the lead concentrations were between 0.39 and 3.4 $\mu$g/g or less than 25% of the sample mean of ivory in our study. Modern teeth from the same regions contain 10–100 times more lead (Grandjean and Jorgenson, 1990). Many elements occur in the foliage of plants and seasonal fluctuations in the concentrations of cadmium, lead, copper, zinc, manganese and selenium in the liver and kidneys of reindeer in Svalbard in Norway have been reported (Borch-Ionson et al., 1996). Lead is present in plants and soils, and its metabolism follows closely that of calcium, particularly

its deposition in mineralized tissue (Browning, 1969a), and over 90% of the body's burden of lead is located in the skeleton (McDonald et al., 1951). Mercury occurs in minute quantities in nearly all foods and is widely distributed as free metal in soils, dust and water (Browning, 1969b). Arsenic is present in all soils in amounts varying from less than 10 to 500 parts/$10^6$ and is stored in all tissues, particularly the hair and nails (Browning, 1969c). Most mammals, including man but excluding chimpanzees, methylate arsenic to methylarsonic acid, which is rapidly excreted in the urine (Vahter et al., 1995). The presence of arsenic in all the ivory samples studied is indicative of the elephant's inability to methylate and detoxify arsenic. Cadmium is present in the order of 1 part/$10^6$ in many plant and animal tissues and occurs in abdominal organs and in smaller quantities in bone and teeth (Browning, 1969d). All our ivory samples had a cadmium content of below 1 part/$10^6$. A concentration of 0.2 $\mu$g/l was found in the drinking water in Germany (Muller et al., 1996) and certain plants accumulate all available cadmium from the medium in which they grow (Devi et al., 1996). The vegetation of a particular region could therefore concentrate the available cadmium and contribute to dietary overload. The cadmium content of rice samples from various areas in the world varied between 0.88 and 133.2 ng/g (Watanabe et al., 1996).

Chromium occurs in nature as chrome iron ore and is found in small quantities in soils and plants (Browning, 1969e). Cobalt is present in complex chemical compounds in ore as well as plants growing in cobalt-containing soil. Cobalt is essential to animal nutrition as anaemia develops in its absence (Browning, 1969f). Copper is widely distributed in animal tissues and human ingestion is estimated to be in the region of 2 mg/day. It occurs free as native copper or in ores, and is found in trace amounts in plants (Browning, 1969g). Manganese is essential for the nutrition of plants and animals, and is widely distributed in nature as an oxide, a sulphide, a carbonate, a silicate or in other ores (Browning, 1969h). Nickel constitutes approx. 0.016% of the earth's crust and is widely distributed in plants, especially green leafy vegetables (Browning, 1969i). The chief storage depots are the spinal cord, brain, lungs and heart (Ware et al., 1954). Zinc is estimated to represent 0.004% of the earth's substance and is 25th in order of occurrence, approaching that of iron and greater than copper or manganese (Lutz, 1926). Zinc is required for enzymatic function and the highest amounts have been found in the liver, voluntary muscle and bone, with a total body zinc content of 1.36–2.32 g in man (Browning, 1969j). Molybdenum is essential for all nitrogen-fixing higher plants, and legumes, cereal grains and green leafy vegetables are good sources. Its metabolism in animals is closely linked to that of copper, with which it appears to have reciprocal antagonism. The concentration of molybdenum is similar to that of manganese, where it is highest in the liver (1–3 parts/$10^6$) (Browning, 1969k). Aluminium is present in a natural diet in amounts that are very low in animal products but high in plants. A significant proportion of aluminium is inhaled, and the amount of aluminium in the organs, blood and urine is small (Browning, 1969l).

The increased brittleness and rapid rate of hydrolysation of ivory from the Kaokoveld and Etosha compared to the other regions are of interest. The annual rainfall in the Kaokoveld and parts of Etosha is below 200 mm/year. The aridness of the region, characterized by dry savannah and shrub, has led to the term 'desert elephant' for those elephant that were driven into the region by human inhabitation of the more arable land (Viljoen, 1987; Pauw, 1990). There is good reason to believe that the diet of these elephant differ significantly from those in the other regions studied. Analyses of ivory from the Kaokoveld and Etosha show the highest fluoride concentrations, lowest total proline plus hydroxyproline content and under-hydroxylation of lysine as unique characteristics. The high fluoride content is probably the result of the water that collects in the closed systems of the salt pans and becomes concentrated by evaporation. Although the substitution of the hydroxyl group with fluoride in the hydroxyapatite crystal increases its resistance to dental caries, it softens the mineral phase of the ivory significantly (Lavelle, 1975), thereby weakening the crystal. The low proline plus hydroxyproline content, as well as the under-hydroxylation of lysine, are likely to be the result of malnutrition and may also have a profound effect on the strength of the collagen scaffold of mineralized tissue (Chatterjee, 1978). Vitamin C, iron and oxygen are cofactors required for the enzymatic hydrolysation of lysine during biosynthesis of the tropocollagen molecule (Anderson, 1992). Insufficient dietary vitamin C is likely to be the main cause of synthesis of the under-hydroxylated lysine-containing collagen in Kaokoveld and Etosha ivory. This is supported by the craving of the Kaokoveld elephant for fresh fruit, especially citrus, to the dismay of many travellers through the region.

## Acknowledgements

This study was supported by a grant from the foundation for Research Development.

## References

Anderson, J.C., 1992. Biochemical basis of connective tissue disease. In: L. Gardner (Ed.). Pathological basis of the con-

nective tissue diseases, Ch.4. Lea & Febiger, Philadelphia, pp. 174–226.

Anderson, V., Maage, A., Johannsen, P.J., 1996. Heavy metals in blue muscles (*Mytilus edulis*) in the Bergen harbour area, West Norway. Bull Environ Contam Toxicol 75 (4), 589–596.

Armstrong, S., Bridgland, F., 1989. Elephants and the ivory tower. New Sci. 124 (1679), 37–41.

Borch-Ionsen, B., Nilssen, K.J., Norheim, G., 1996. The influence of season and diet on liver and kidney content of essential elements and heavy metals in Svalbard reindeer. Biol Trace Elemen Res 51 (3), 235–247.

Browning, E., 1969a. Lead. Toxicity of industrial metals, 2nd Edition. Butterworth and Company, London, pp. Ch. 20, pp. 172–199.

Browning, E., 1969b. Mercury. Toxicity of industrial metals, 2nd Edition. Butterworth and Company, London, pp. Ch. 24, pp. 226–242.

Browning, E., 1969c. Arsenic. Toxicity of industrial metals, 2nd Edition, Ch. 4. Butterworth and Company, London, pp. 39–60.

Browning, E., 1969d. Cadmium. Toxicity of industrial metals, 2nd Edition, Ch. 9. Butterworth and Company, London, pp. 98–108.

Browning, E., 1969e. Chromium. Toxicity of industrial metals, 2nd Edition. Butterworth and Company, London, pp. Ch. 12, pp. 119–131.

Browning, E., 1969f. Cobalt. Toxicity of industrial metals, 2nd Edition. Butterworth and Company, London, pp. Ch. 13, pp. 132–142.

Browning, E., 1969g. Copper. Toxicity of industrial metals, 2nd Edition. Butterworth and Company, London, pp. Ch. 15, pp. 145–152.

Browning, E., 1969h. Manganese. Toxicity of industrial metals, 2nd Edition, Ch. 23. Butterworth and Company, London, pp. 213–252.

Browning, E., 1969i. Nickel. In Toxicity of industrial metals. 2nd edn. Ch. 26. Butterworth and Company, London. pp. 249–260.

Browning, E., 1969j. Zinc. In Toxicity of industrial metals. 2nd edn. Ch. 44. Butterworth and Company, London. pp. 348–355.

Browning, E., 1969k. Molybdenum. In Toxicity of industrial metals. 2nd edn. Ch. 25. Butterworth and Company, London. pp. 243–248.

Browning, E. 1969l. Aluminium. In Toxicity of industrial metals. 2nd edn. Ch. 2. Butterworth and Company, London. pp. 3–22.

Chatterjee, G.C., 1978. Nutritional deficiencies in animals: Vitamin C. In: M. Rechcigl (Ed.). CRC Handbook series in nutrition and food, Section E: Nutritional disorders, Vol. II. CRC Press, Florida, pp. 149–176.

Devi, M., Thomas, D.A., Barber, J.T., Fingerman, M., 1996. Accumulation and physiological and biochemical effects of cadmium in a simple aquatic food chain. Ecotoxicol Environ Saf 33 (1), 38–43.

Grandjean, P., Jorgenson, P.J., 1990. Review. Retention of lead and cadmium in prehistoric and modern human teeth. Environ Res 53, 6–15.

Hall-Martin, A., 1992. Distribution and status of the African elephant *Loxodonta africana* in South Africa, 1652–1992, 65, 88. Koedoe.

Hirano, S., Suzuki, K.T., 1996. Exposure, metabolism and toxicity of rare earths and related compounds. Environ Health Perspect 104 (suppl 1), 85–95.

Kagawa, J., 1994. Atmospheric pollution due to mobile sources and effects on human health in Japan. Environ Health Perspect 102 (suppl. 4), 93–99.

Kusaka, Y., Kumagai, S., Goto, S., 1996. Decreased ventilatory function in hard metal workers. Occup Environ Med 53 (3), 194–199.

Lavelle, C.L.B., 1975. Applied physiology of the mouth. John Wright and Sons Ltd., Bristol, pp. 56–60.

Lutz, R.E., 1926. The normal occurrence of zinc in biological materials. J Industr Hyg 8, 177–183.

McDonald, N.S., Ezmirlian, F., Spain, P., McArthus, C., 1951. The ultimate site of skeletal depositioning of strontium and lead. J Biol Chem 187, 387–399.

Muller, M., Anke, M., Hartmann, E., Illing-Gunther, H., 1996. Oral cadmium exposure of adults in Germany. I: Cadmium contents of foodstuffs and beverages. Food Addit Contam 13 (3), 359–378.

Ottichilo, W.K., 1986. Age structure of elephants in Tsavo-National Park, Kenya. Afr J Ecol. 24 (2), 629–675.

Pauw, C., 1990. Desert elephants collared. Afr Wildl. 44 (1), 5.

Posner, A.S., Tannenbaum, P.J., 1984. The mineral phase of dentine. In: A. Linde (Ed.). Dentine and Dentinogenesis, Vol. II. CRC Press, Boca Raton, Florida, pp. 17–36.

Vahter, M., Couch, R., Nermell, B., Nilsson, R., 1995. Lack of methylation of inorganic arsenic in the chimpanzee. Toxicol Appl Pharmacol 133 (2), 262–268.

Van der Merwe, N.J., LeeThorpe, J.A., Bell, R.H.V., 1988. Carbon isotopes as indicators of elephant diets and African environments. Afr J Ecol. 26, 163–172.

Van der Merwe, N.J., LeeThorpe, J.A., Thackeray, J.F., Hall-Martin, A., Kruger, F.J., Coetzee, H., Bell, R.H.V., Lindeque, M., 1990. Source-area determination of elephant ivory by isotope analysis. Nature 346 (6286), 744–746.

Viljoen, P.J., 1987. Status and past and present distribution of elephants in the Kaokoveld, South-West Africa Namibia. S A J of Zool. 22, 247–257.

Vogel, J.C., Eglington, B., Auret, J.M., 1990. Isotope fingerprints in elephant bone and ivory. Nature (Lond) 346 (6286), 747–749.

Ware, A.W., Goss, D.M., Boyd, M.J., 1954. The metabolism of nickel. Arch Biochem 51, 1–14.

Watanabe, T., Shimbo, S., Moon, C.S., Zhang, Z.W., Ikeda, M., 1996. Cadmium contents in rice samples from various areas in the world. Sc. Total Environ 184 (3), 191–196.

Wetherell, J.A., Robinson, C., 1973. The inorganic composition of teeth. In Biological Mineralization. Ed. Zipkin I. Chap. 1, 43.

PERGAMON

Archives of Oral Biology 43 (1998) 969–977

ARCHIVES OF ORAL BIOLOGY

# Histogenesis of the chequered pattern of ivory of the African elephant (*Loxodonta Africana*)

E.J. Raubenheimer[a,*], M.C. Bosman[b], R. Vorster[a], C.E. Noffke[a]

[a]*Department of Oral Pathology, Faculty of Dentistry, Medical University of Southern Africa, P.O. MEDUNSA, 0204, Republic of South Africa*

[b]*Department of Anatomy, Medical University of Southern Africa, P.O. MEDUNSA, 0204, Republic of South Africa*

Accepted 16 June 1998

**Abstract**

This study aimed to propose a hypothesis on the events which lead to the development of the characteristic chequered pattern of elephant ivory. Twenty fragments of ivory and six elephant tusks were obtained through the National Parks Board of South Africa. Polished surfaces were prepared in sagittal and longitudinal planes and the characteristics of the distinctive chequered pattern described. Light- and electron-microscopical techniques and image analyses were employed to determine the morphological basis of the pattern and to describe the spatial distribution, density and morphology of the dentinal tubules. These investigations showed that the distinctive pattern was the result of the sinusoidal, centripetal course followed by dentinal tubules. The apical, slanted part of the sinusoidal curve is the result of the centripetally moving odontoblast, which, during formation of ivory, progresses towards the centre of the tusk on a decreasing circumference. It is suggested that this leads to cell crowding, increased pressure between odontoblasts and subsequent apical movement of their cell bodies, cell degeneration and fusion. Odontoblastic degeneration and fusion probably relieve the pressure between the crowded odontoblasts by reducing their numbers and the remaining odontoblasts now orientate their centripetal course towards the tip of the tusk, thereby forming the anterior-directed part of the sinusoidal path of the tubule. As odontoblasts progress centripetally the diameter of the pulpal cavity decreases further and the processes of apical movement, fusion and degeneration of odontoblasts are repeated. This occurs until the pulpal cavity is obliterated.


*Keywords:* Elephant ivory; Dentinal tubules; Dentine; Odontoblastic movement

## 1. Introduction

Elephants are characterized by a highly pneumatic skull with a premaxilla that descends vertically, bearing the roots of the paired tusks, which represent enormously enlarged maxillary incisors. The growth of the tusk is continuous throughout life and its size at any age is dependent on the sex of the animal, the rate of attrition and breakage of the tooth, as well as genetic and environmental factors (Hall-Martin, 1982). The record length of a single tusk is 3.51 m and record weight 117 kg. The bulk of the tusk consists of ivory (or dentine), ensheathed by a layer of cementum (Sikes, 1971).

The unique chequered pattern of polished ivory, which has not been described in great detail in the literature (Sognnaes, 1960; Miles and Boyde, 1961; Sikes, 1971; Raubenheimer et al., 1990), has made it a sought-after product in the manufacturing of jewellery and other works of art. Our purpose now was to pro-

* Corresponding author. Department of Oral Pathology, Medical University of Southern Africa, Box D24, P.O. MEDUNSA, 0204. Fax: (012) 521 4838; Email: ejraub@mcd4330.medunsa.ac.za.

0003-9969/98/$ - see front matter 
PII: S0003-9969(98)00077-6

pose a hypothesis on the histogenesis of the unique chequered pattern of elephant ivory.

## 2. Materials and methods

Twenty fragments of ivory and five tusks of African elephant (*Loxodonta Africana*) and a developing tusk of a 22-month fetus were obtained through the National Parks Board of South Africa. The ivory was harvested from animals that had died as a result of natural causes or as part of the population-control programme of the National Parks Board. The fetal tissue was obtained within 20 min of death. The biopsies were taken with a sharp scalpel from the peripulpal ivory of the proximal part of the tusk, cut in thin slices and then fixed in 10% phosphate-buffered formalin at 21°C.

The five tusks, with masses between 0.7 and 9.3 kg, were sectioned and polished in sagittal and coronal planes. The morphological characteristics of the chequered pattern were described on polished surfaces prepared in both planes. Irregularities affecting the pattern were noted.

Ground sections were prepared parallel and perpendicular to the long axis of 12 different fragments of ivory by cutting 300-$\mu$m thick slices of ivory from the respective planes with a rotating diamond saw. The thick slices were fixed to glass slides with methylmethacrylate cement and ground to a thickness of approx. 40 $\mu$m on a rotating disc utilizing different grades of diamond pastes. The ground sections were covered with glass cover-slips after debridement with a weak acid solution (0.1 M HCl) and a soft brush, and examined by transmission light microscopy under standard illumination.

Standardized techniques for the preparation of scanning electron micrographs of hard tissues were employed to visualize the morphology and distribution of dentinal tubules of six different tusks when viewed from the pulpal surface of the ivory. The presence of light or dark bands was noted during the preparation of an additional 10 sections at different levels perpendicular to the long axis of the tubules. The levels were selected so that five sections passed through light bands and five through dark bands. All surfaces were cleaned before scanning with a 0.1 M HCl solution and a soft brush, and flushed with deionized water to

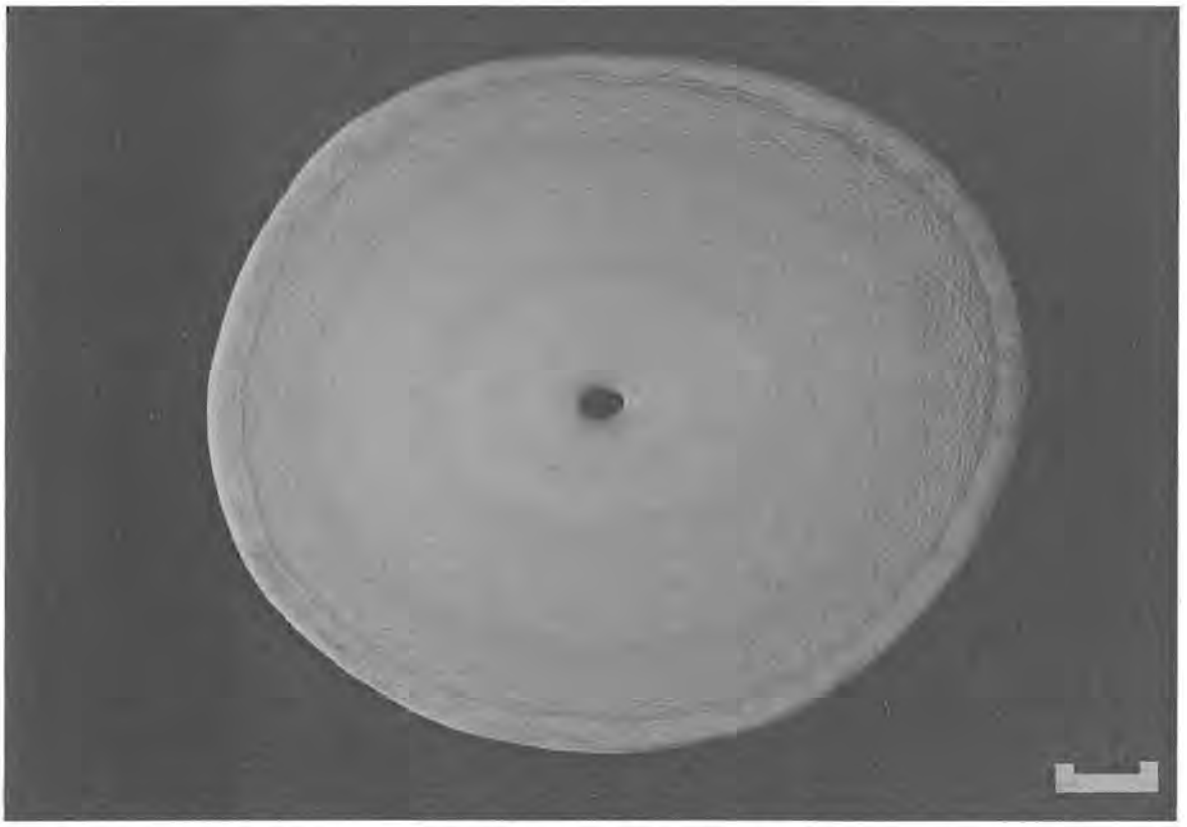

Fig. 1. Cross-section through the solid part of a tusk. Note the undulating course the cementum–ivory junction follows and the geometric chequered pattern (bar = 4 cm).

remove debris. The distance between tubules was expressed as the smallest linear measurement between two adjacent tubules and the tubule density as the number of tubules per $mm^2$. At least $10^3$ tubules were counted for each measurement. An image analyser was used (Flexible Image Processing System, CSIR, Pretoria) and findings were subjected to the Student's *t*-test for unequal variances.

## 3. Results

The entire outer surfaces of the tusks were covered by a layer of cellular cementum. Ivory was exposed on the working surfaces of erupted tusks through cemental abrasion. The cementum–ivory junction was visible as a dark, concentric ring demarcating the peripheral border of the ivory. In cross-sections through the tusk, the cementum–ivory junction followed an undulating circular course, forming irregular excrescences alternating with shallow convexities or concavities (Fig. 1). The excrescences were more pronounced in tusks with smaller diameters. Occasional invaginations of cementum, which were 2–3 mm deep, were present in the outer layer of the ivory. The external contour of the cementum followed the morphology of the cementum–ivory junction, resulting in longitudinal and parallel ridges and troughs had been visible upon external examination of the tusks. These ridges and troughs had been abraded away on the anterior and more exposed surface of the tusk. The pulpal surface of the ivory was smooth and the pulpal cavity conical in shape, with the tip of the tusk composed of solid ivory and the apical foramen wide open (Fig. 2).

The unique chequered pattern was evident on polished surfaces of cross-sections through the tusk (Fig. 1). The pattern consisted of two systems of alternating light and dark lines which started adjacent to the cementum. One system swept clockwise and the other anticlockwise towards the centre of the tusk, intersecting at regular intervals. The chequered pattern corresponded to parallel alternating light and dark lines evident on polished surfaces prepared in the sagittal plane (Fig. 3). The cementum–ivory junction was straight when viewed in this plane. Planes of fracture through ivory tended to follow the contours of the dark bands.

The outermost layer of ivory (mantle ivory) was between 40 and 80 $\mu$m thick and consisted of irregularly spaced dentinal tubules which were slanted api-

Fig. 2. Tusk of an elephant bull (top) and cow (bottom). Note the parallel ridges and troughs on the posterior surface of the bull's tusk (arrows). The broken line in the lower tusk represents the wall of the conical pulpal cavity (bar = 10 cm).

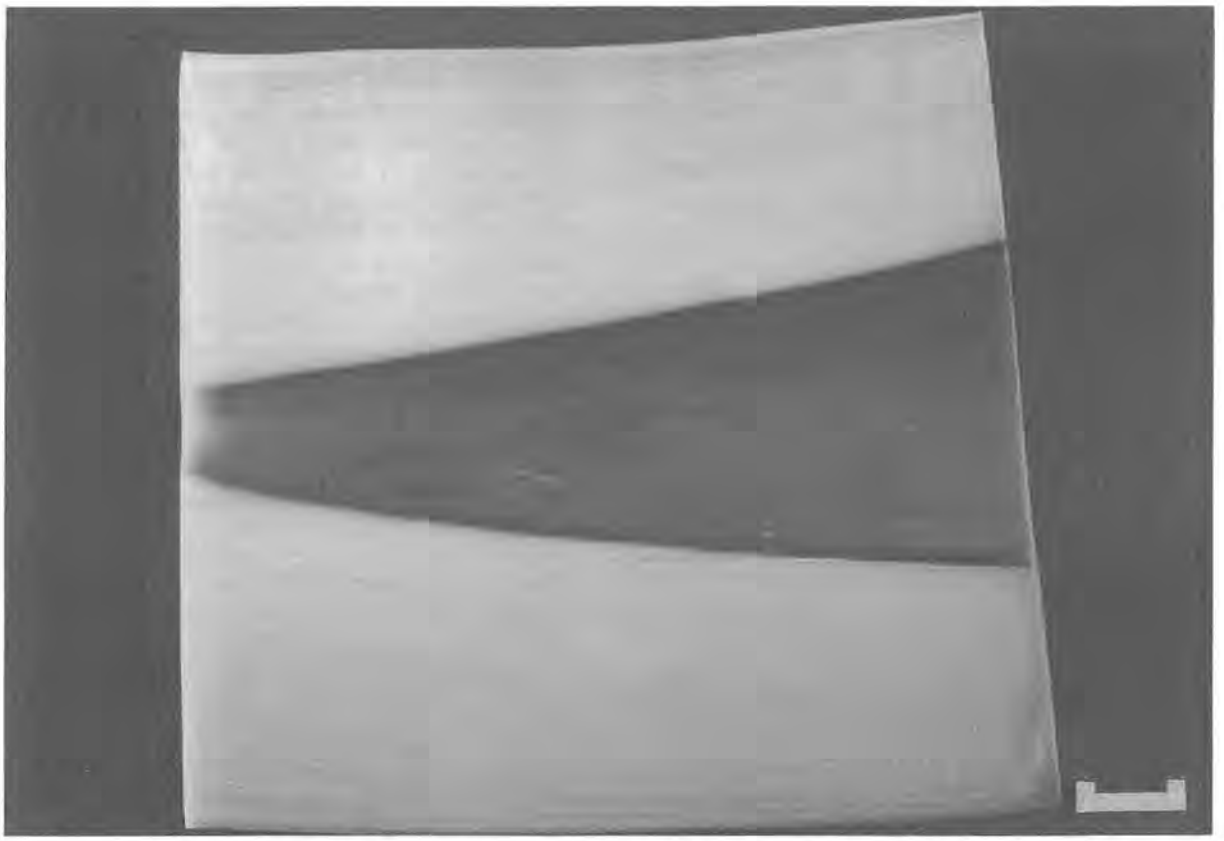

Fig. 3. Sagittal section through a tusk. Note the conical pulpal cavity and parallel light and dark bands in the ivory, the latter of which are evident in the outer third (bar = 4 cm).

cally at a sharp angle to the cementum–ivory junction (Fig. 4). These tubules appeared to branch extensively, a feature which was best observed when focusing at different planes in the section. Morphologically, the mantle ivory resembled the granular layer of human radicular dentine. After passing through the mantle ivory, the tubules became more regularly spaced and gradually changed their course by curving towards the tip of the tusk. This curvature was the beginning of the regular, sinusoidal course followed by the dentinal tubules in a pulpal direction and was evident only in sections prepared in the sagittal plane. The convexities and concavities of this sinusoidal pattern corresponded to the alternating light and dark bands seen macroscopically on surfaces prepared in the sagittal plane (Fig. 5). The dark bands correlated with that part of the dentinal tubules that curved apically. On high-power magnification, many dentinal tubules appeared to end blind and scattered tubules appeared to fuse forming one tubule (Fig. 6). The blind-ending tubules were more frequent in the dark bands in ivory (16 blind-ending tubules per 100 tubules, SD 7 tubules) than in the light bands (6 blind-ending tubules, SD 3 tubules) as measured over 2500 tubules in each of the dark and light bands, respectively ($p < 0.001$). The process of apparent fusion involved the main dentinal tubule and was distinct from the fine lateral branches that seemed to anastomose with those of adjacent tubules. Demineralized sections of newly formed ivory in the fetal tissue showed crowding of distally slanted odontoblasts and scattered pyknotic cells, highly suggestive of individual cell death (Fig. 7).

Scanning electron microscopy showed that the pulpal openings of the dentinal tubules were oval with the greatest dimension parallel to the long axis of the tusk. The indentations of scattered cell bodies, which appeared larger than those of adjacent cells and in which two distinct tubules terminated, were focally evident (Fig. 8). Dentinal tubules were closer packed in areas where they curve apically (i.e., the dark bands) (mean distance $4.6 \pm 1.7\ \mu m$ SD) than in the part of the tubule that curves towards the tip of the tusk (i.e., the light bands) (mean distance $7.2 \pm 2.8\ \mu m$ SD). This difference was significant ($p < 0.001$).

Fig. 4. Microscopic appearance of mantle ivory. Note the sharp, apical-directed slant of the first part of the dentinal tubules (arrows) (bar = 50 $\mu$m; magnification ×200).

## 4. Discussion

The cell responsible for the formation of ivory (or dentine) is the odontoblast. Odontoblasts are derived from the mesenchyme of the adjacent dental papilla, and, after differentiation and cytoplasmic maturation, they move in a centripetal direction and deposit ivory along their pathway. The tip of the conical pulp soon becomes solid and lengthening of the apical edge coincides with forward displacement of the tusk.

The morphological characteristics of ivory can be explained by events which result from the differentiation and centripetal movement of the odontoblast. When the first ivory is formed, cuboidal odontoblasts lie tightly packed around the periphery of the pulp. The circumference of the circular plane along which they lie is $2 \times \pi \times R$. As the odontoblast moves centripetally, a reduction in the radius (or $R$) by one unit would result in a decrease of the circumference by 6.28 units. Because of this significant reduction in the circumference during centripetal movement of odontoblasts, they probably soon become more tightly packed along their course and the lateral pressure between them increases. Differentiation of odontoblasts, which is characterized by an increase in the volume of cytoplasmic organelles (Sasaki and Garant, 1996) and resultant cell enlargement, may also contribute to odontoblastic crowding during the early stages of dentinogenesis. During the first phase of formation of the early (most peripheral) ivory and before mineralization takes place, the pressure caused by cell crowding and cytoplasmic enlargement probably results in the undulating course followed by the ivory–cementum junction. That course accommodates more odontoblasts per unit length than would a regular curve, thereby relieving this pressure. The reduction of the circumference per unit movement of the odontoblast on the radial axis is greater in tusks with a smaller diameter and the undulating course of the ivory–cementum junction is therefore more pronounced in smaller tusks. After mineralization of the first ivory has taken place, further folding of the ivory–cementum junction fails to occur, owing to the rigidity which the deposition of mineral salts introduces to the newly formed ivory. This initiates a new set of events which accommodates odontoblastic crowding during their centripetal movement. These events result in the sinusoidal pathway followed by the odontoblasts when viewed in a sagittal plane along their course toward the centre of the tusk.

The pulpal cavity of the tusk is conical when viewed in a sagittal plane and confined on all aspects by mineralized ivory except for the large apical opening through which the vascular and nerve supplies pass. The only means by which the growing pressure between centripetally moving odontoblasts on an ever-decreasing pulpal perimeter can be accommodated is through apical movement of the odontoblastic cell mass or a reduction in the number of odontoblasts. A reduction in the number of odontoblasts could be achieved through odontoblastic cell death or fusion. There is morphological evidence that all these processes occur during the formation of elephant ivory. The following features favour this hypothesis:

1. Acute slanting of the first part of the odontoblastic processes towards the apical aspect of the tusk is indicative of a force which displaces the odontoblasts bodily and in an apical direction during early centripetal movement from the ivory–cementum junction.

Fig. 5. Microscopic appearance of the regular sinusoidal course followed by the odontoblastic tubules when viewed in the sagittal plane. Note the alternating dark and light bands, the former corresponding with the apically orientated slant of the tubules (bar = 120 $\mu$m; magnification ×80).

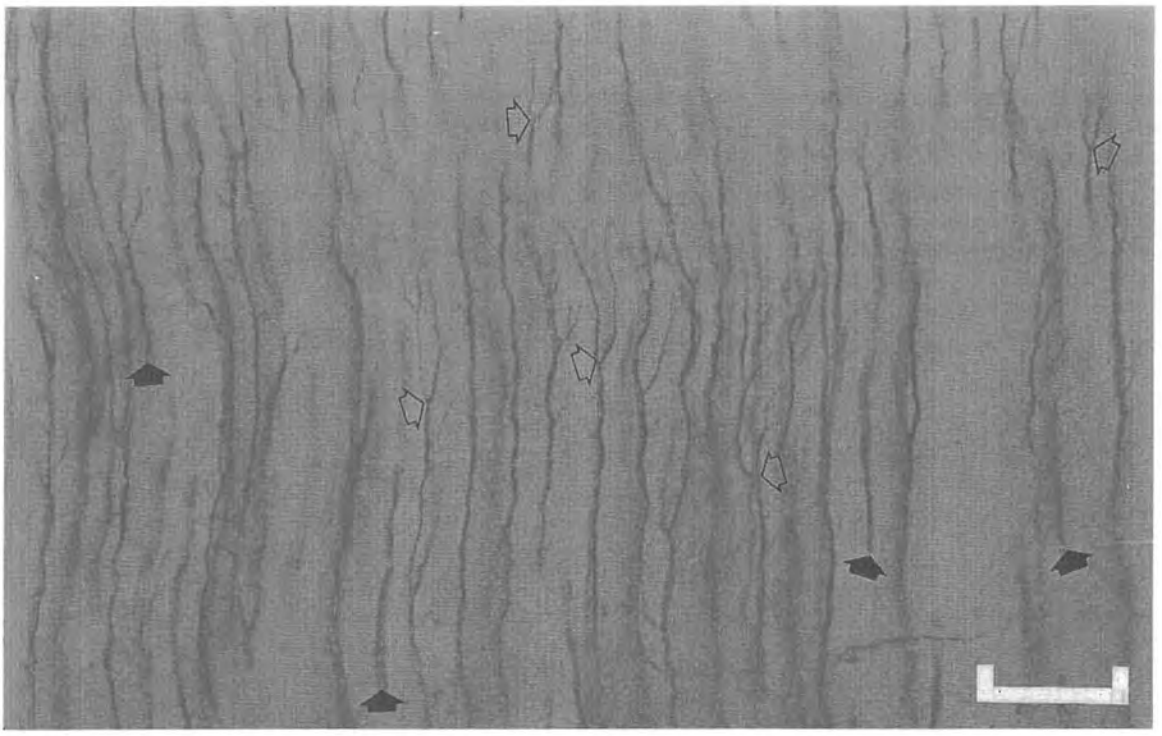

Fig. 6. Blind-ending tubules (dark arrows) and fusing tubules (open arrows) in the dark bands of ivory (bar = 20 μm; magnification ×600). The pulpal cavity is orientated towards the lower margin of the figure.

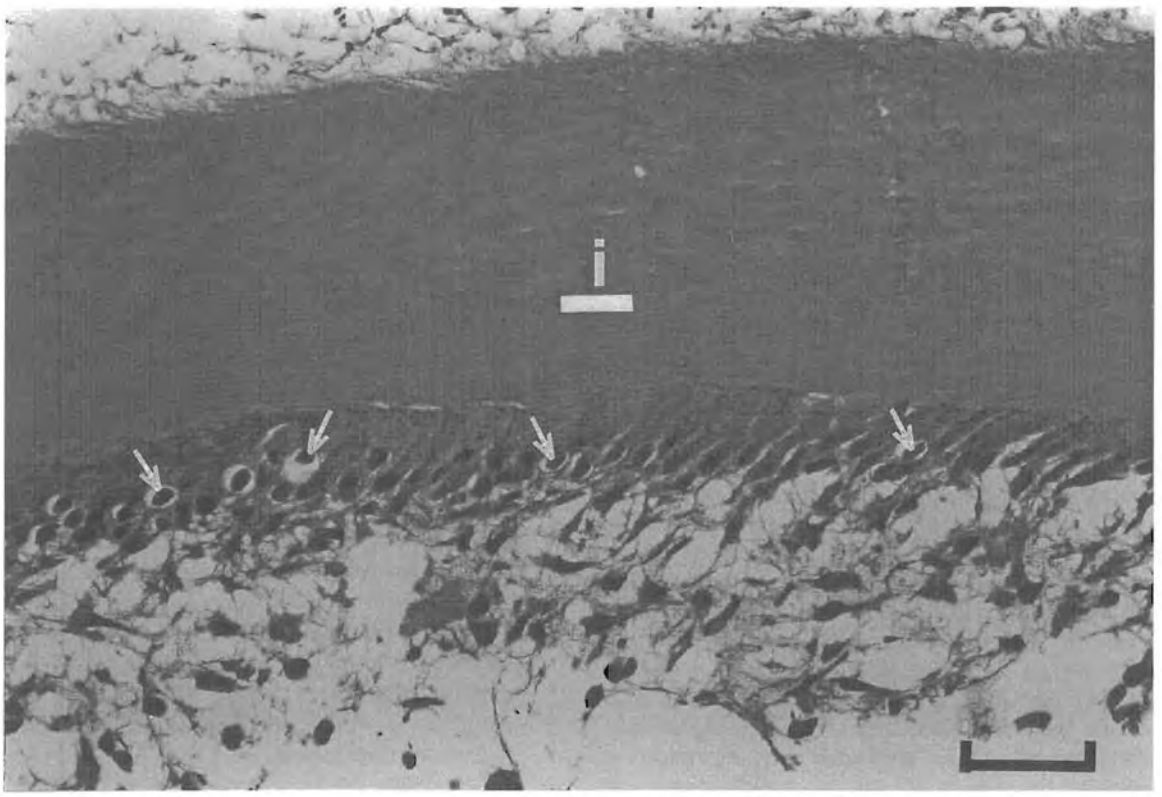


Fig. 7. Apically slanted odontoblasts lining the pulpal surface of newly formed ivory (i). Note scattered pyknotic odontoblasts (arrows) (H&E stain; bar = 40 μm; magnification ×300).

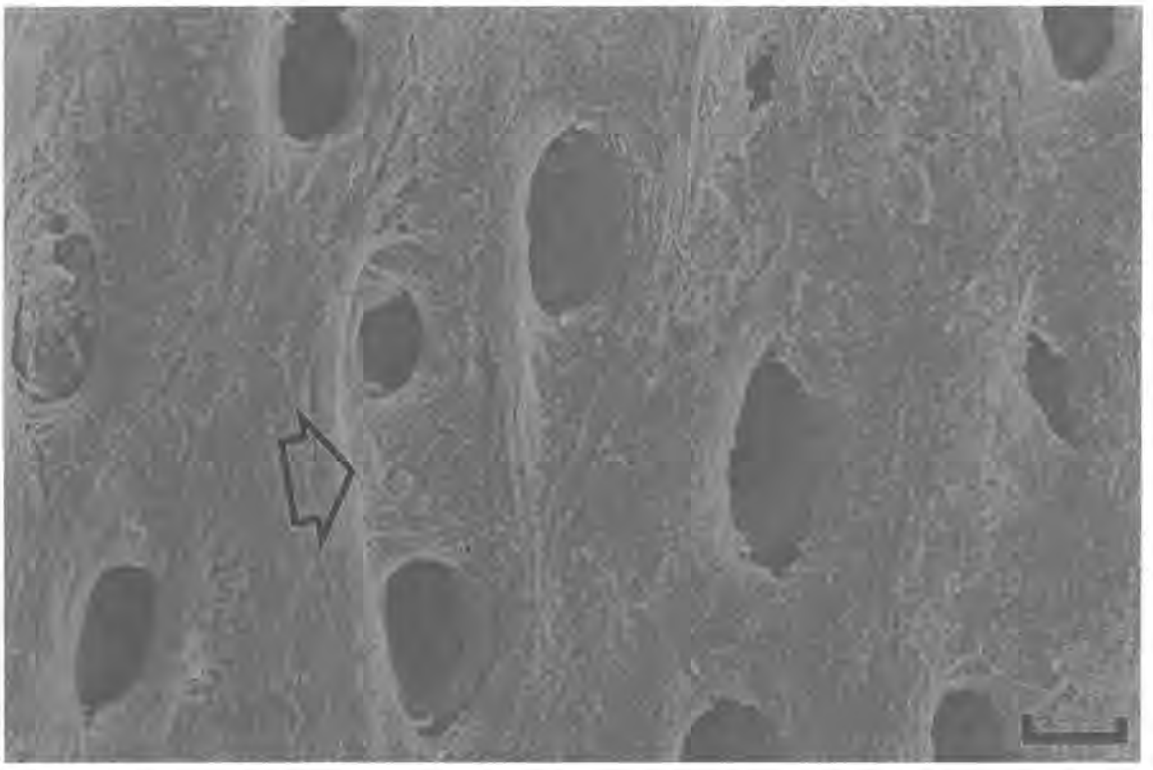

Fig. 8. Scanning electron micrograph of the pulpal surface of ivory. Dentinal tubules are oval with their long axis parallel to the axis of the tusk. Note the large, unilocular indentation (arrow) into which two tubules open (bar = 3 μm).

This displacement is probably due to cell crowding, which is likely to be the result of enlargement of differentiating cells as well as a progressive reduction of the pulpal circumference.

In human dentine major, fine and microbranches have been described along the course of dentinal tubules. The major branches are characteristically Y-shaped, dichotomous or trichotomous, with their general direction being generally parallel, whereas the other forms of branching extend from the main tubules at about 45° (Mjör and Nordahl, 1996).

2. The morphological phenomenon of fusion of dentinal tubules probably represents fusion of odontoblastic cell bodies. Fusing tubules feature in regions represented macroscopically by dark bands and coincide with the point at which the sinusoidal curve begins to turn towards the tip of the tusk. In the subsequent portion of the centripetal course of the odontoblasts (i.e., the light bands), fusion has been shown to be less extensive. This indicates that distinct phases of odontoblastic fusion are triggered through pressure which builds up between the cells during their centripetal course. It is proposed that odontoblastic fusion alleviates cell crowding by reducing the number of cells on a rapidly decreasing pulpal circumference.
3. Microscopic examination of thin sections through ivory indicates that more tubules appear to end blindly when entering the posteriorly slanted portion of their centripetal course. This, together with the scattered pyknotic odontoblasts seen in sections of rapidly fixed fresh specimens of developing tusks, indicates that crowding with resulting intercellular pressure may in fact induce degeneration of individual odontoblasts. The effect of this would be to reduce the number of odontoblastic cell bodies on a progressively decreasing pulpal circumference, thereby making more space available for the remaining odontoblasts.
4. In planes where the odontoblast cell bodies slant posteriorly, and where crowding of cells with fusion and cell death take place, the dentinal tubules are more closely packed. This is supported by the histomorphometric findings, which clearly indicate that dentinal tubules are closer packed in zones where they curve towards the tip of the tusk (i.e., the darks bands) than in those areas where the tubules curve anteriorly (i.e., the light bands). The reduced volume of mineralized ivory and increased density of tubules in the dark bands probably result in inherent planes of weakness. This could be one of the

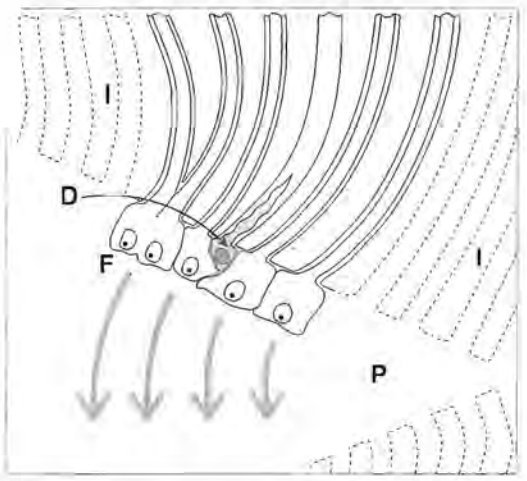


Fig. 9. Schematic representation of part of the sinusoidal pathway followed by the dentinal tubule in its centripetal course. Note the crowding of odontoblasts, odontoblastic fusion (F) and degeneration (D) (I, ivory; P, pulpal cavity).

reasons why planes of cleavage in fractured ivory tend to follow the contours of the dark bands.

A scanning electron-microscopic investigation of human dentinal tubules (Garberoglio and Brännström, 1976) showed that tubule density increases towards the pulp. Their counts ranged from a mean of 19,000 tubules per $mm^2$ 3.1–3.5 mm from the pulp to 45,000 tubules per $mm^2$ in dentine 0.1–0.5 mm from the pulp. This increase in tubule density as the odontoblast progresses towards the human dental pulp is indicative that the human odontoblasts are subjected to the same forces as proposed in the elephant.

5. Scanning electron microscopy of the pulpal surface of ivory shows large, unilocular indentations (possibly representing one large, fused cell body) with two distinctly separate tubules (perhaps representing the cytoplasmic processes of two separate cells) permeating the ivory. These features support our hypothesis that odontoblastic fusion occurs during their centripetal movement.
6. The oval shape of the dentinal tubule when viewed perpendicular to its course, is morphological evidence of circumferential pressure which builds up between centripetally moving odontoblasts.

The processes of odontoblastic crowding, followed by a bodily apical movement of odontoblasts and a relief of the intercellular pressure through cell fusion and death, with a subsequent change in the direction of movement of the cell body of the remaining odontoblasts, are probably responsible for the regular sinusoidal course followed by the odontoblast in its centripetal course during the formation of ivory (Fig. 9). The sinusoidal course of the dentinal tubule is reflected as parallel and alternating light and dark bands which are seen on polished surfaces prepared along the long axis of the tusk. The light and dark bands were found to be the result of the varying compactness of dentinal tubules between the sectors of the sinusoidal curve of the tubules that slant towards the tip of the tusk or its apex, respectively. The scattering of light, which was proposed by Miles and Boyde (1961) as an explanation for the bands, probably has less of a role in the morphogenesis of the pattern. On cross-sections, the chequered pattern is a reflection of the alternating light and dark bands seen on surfaces prepared in length. This implies that when the layer of odontoblasts is viewed from a radial perspective, apical movement of the odontoblasts with curving of the dentinal tubules does not occur at the same time but rather as a wave that spreads circumferentially along the layer of odontoblasts.

## Acknowledgements

Appreciation is expressed to Mrs C. Begemann for editing the manuscript.

## References

Garberoglio, R., Brännström, M., 1976. Scanning electron microscopic investigation of human dentinal tubules. Arch Oral Biol 21, 355–362.

Hall-Martin, A., 1982. Kruger's tuskers. Afr Wildl. 35 (1), 65–88.

Miles, A.E.W., Boyde, A., 1961. Observations on the structure of elephant ivory. J Anat (Lond) 95, 450 (Abstract).

Mjör, I.A., Nordahl, I., 1996. The density and branching of dentinal tubules in human teeth. Arch Oral Biol 41, 401–412.

Raubenheimer, E.J., Dauth, J., Dreyer, M.J., Smith, P.D., Turner, M.L., 1990. Structure and composition of ivory of the African elephant (*Loxodonta africana*). S A J Science 86, 192–193.

Sasaki, T., Garant, P.R., 1996. Structure and organisation of odontoblasts. Anat Rec 245, 235–249.

Sikes, S.K., 1971. The natural history of the African elephant. Part I. Weidenfeld and Nicholson, London, pp. 1–184.

Sognnaes, R.F., 1960. The ivory core of tusks and teeth. J Clin Orthopaedics 17, 43–61.

PERGAMON

Archives of Oral Biology 45 (2000) 983–986

Archives of Oral Biology

www.elsevier.com/locate/archoralbio

# Early development of the tush and the tusk of the African elephant (*Loxodonta africana*)

E.J. Raubenheimer *

*Medical University of Southern Africa, Department of Oral Pathology, P.O. Box D24, Medunsa 0204, South Africa*

Accepted 16 May 2000

**Abstract**

This early development was studied from a serial histological sections of eight elephant embryos with masses varying between 1 and 240 g. The tush and the tusk develop from one tooth germ in a deciduous to permanent tooth relation. In order to study the mineralization of the dental organ of the tush and cap and bell stage of the tusk, embryos older than 3-months' gestation (weighing more than 250 g) would be required. © 2000 Elsevier Science Ltd. All rights reserved.

*Keywords:* Tusk; Tush; Elephant; Embryology

## 1. Introduction

The tusk of the African elephant, *Loxodonta africana*, is a maxillary incisor tooth, which grows continuously throughout life. In contrast to the Asian elephant, *Elephas maximus*, tusks of the African elephant are well developed in both the sexes, with those of males being longer, more conical and thicker for their length than those of females (Pilgram and Western, 1986). Elephant calves exhibit a tooth adjacent to the tusk, which is commonly referred to as the 'tush' (Sikes, 1971). The tush does not erupt, but is pushed aside by the growing tusk and is eventually resorbed in the surrounding tissue (Raubenheimer et al., 1994). Gestation lasts an average of 22 months and the tusk erupts approximately 1 year after birth (Sikes, 1971; Ricuitti, 1980). Although it has been accepted by most that the tusk is the permanent successor to the 'deciduous' tush (Sikes, 1971; Raubenheimer et al., 1994), Anthony, 1933 regarded the tush as a rudimentary incisor belonging to a neighbouring position to the tusk. Furthermore, palaeontological data indicate that these two teeth are not homologous and both pairs of incisors of Proboscideans are teeth of the primary (or deciduous) dentition with no dental replacement by a permanent tooth (Tassy, 1987). No study has been executed on the early embryological development of the tush and tusk of the elephant.

The purpose of this study was to establish whether the tush and the tusk of the African elephant represent separate teeth or develop from one tooth germ in a deciduous to permanent tooth relation.

## 2. Materials and methods

Eight elephant embryos were harvested during the population control programme of the Kruger National Park (de Vos, 1983). All embryos were obtained from cows with tusks, except for the 48.4-g embryo, which had a tuskless mother. The masses (sex and gestational age; Sikes, 1971) of the embryos were 1 g (unknown, less than 1 month), 6.5 g (unknown, 1 month), 48.4 g

* Corresponding author. Tel.: +27-12-5214838; fax: +27-12-5214838.

*E-mail address:* ejraub@medunsa.ac.za (E.J. Raubenheimer).



PII: S0003-9969(00)00068-6

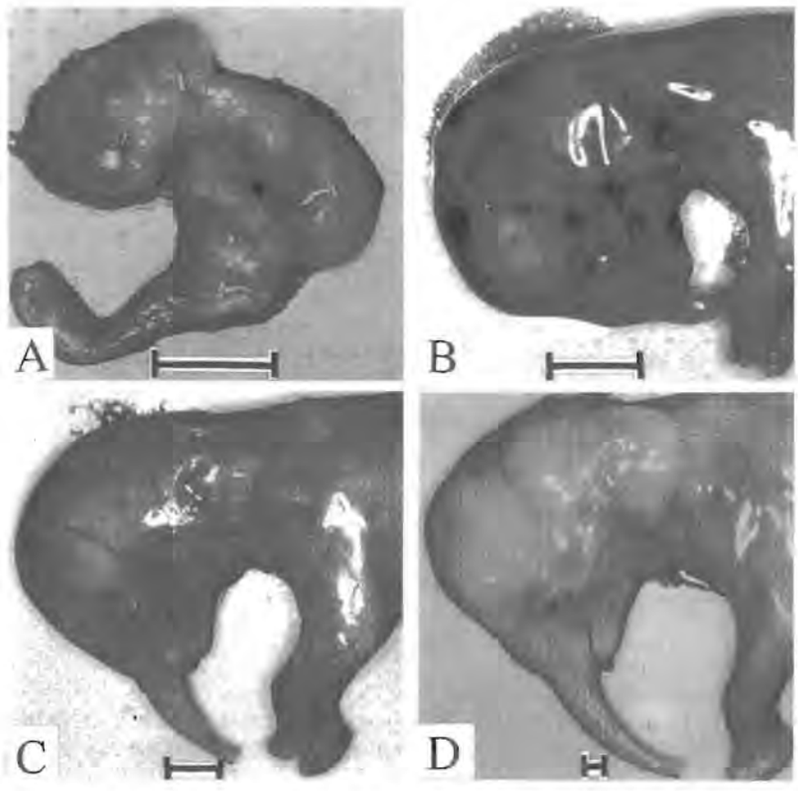


Fig. 1. External features of four of the elephant embryos, (a) 1 g; (b) 6.5 g; (c) 48.4 g and (d) 94.4 g. Bar = 1 cm.

(unknown, 2 months), 93 g (male, 2–3 months), 94.4 g (male, 2–3 months), 107 g (female, 2–3 months), 136 g (male, 2–3 months) and 240 g (male, 3 months). The heads of all but the smallest were hemisected, radiographed, fixed in buffered formalin and processed for routine light microscopy. The head of the 1-g embryo was not hemisected. Serial sections were cut of each in the sagittal plane and stained with haematoxylin and eosin. The developmental chronologies of the lamina dentalis and the primordia of the tush and tusk were recorded through microscopic examination.

## 3. Results

On external examination, the eye placodes and stomodeal openings were macroscopically evident in all embryos and only the 1-g specimen did not show evidence of a developing trunk (Fig. 1). Radiological examination failed to identify mineralized tissues in the nasomaxillary complexes of the 1 and 6.5-g embryos. The earliest stage at which it was possible to identify the os incisivum (the part of the nasomaxillary complex in which the tush and tusk develop) radiologically was in the 48.4-g embryo. The os incisivum in the 136-g embryo showed a central radiolucent area where early development of the tush was taking place.

Microscopic examination of the 1-g embryo showed the stomodeum lined by primitive epithelium. No dental lamina could be identified by serial sectioning. The early development of the dental lamina of the tush was present in the 6.5-g (1 month) embryo. Ectomesenchyme aggregated densely around the tip of the dental lamina at this stage (Fig. 2). Formation of the cap stage of the dental organ of the tush was evident in

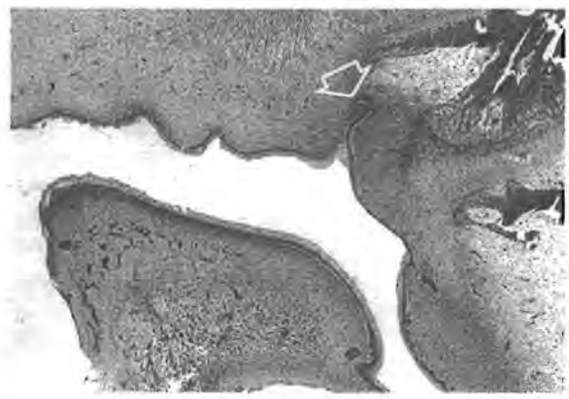

Fig. 2. Low-power microscopic view of the stomodeum of the 6.5-g embryo; note the dental lamina (arrow) growing towards the os incisivum (*). Haematoxylin and eosin, 80 × .

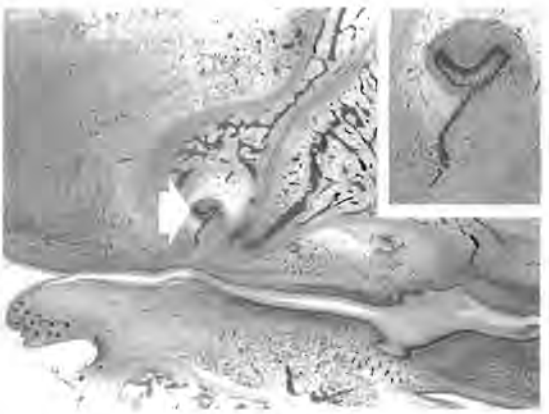

Fig. 3. Cap stage of the tush of the 48.4-g embryo (arrow); note the formation of bone around the dental organ. Haematoxylin and eosin, 30 ×. Inset: Higher magnification of the dental organ 80 ×.

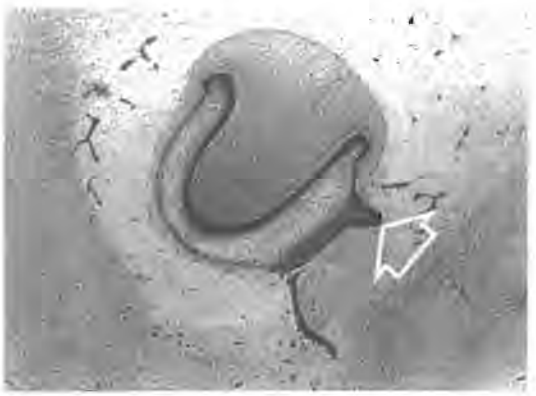

Fig. 4. Bell stage of the dental organ of the tush of the 136-g embryo; note the formation of the bud for the development of the of the tusk which originates from the external epithelial layer of the dental organ of the tush (arrow) 200 ×.

sections of the 48.4-g embryo. The dental lamina of the tush was partially intact and ectomesenchymal aggregates formed the dental follicle and dental papilla. Formation of the bone of the os incisivum was present around the dental organ (Fig. 3). The 94.4-g embryo showed loss of continuity of the dental lamina; development of the bell stage of the dental organ of the tush was evident in sections of the 136-g embryo. At this stage, further epithelial proliferation of the external enamel epithelium of the bell stage of the tush formed the bud stage of the successional tooth germ, the tusk (Fig. 4). Ameloblastic and odontoblastic differentiation with early depositioning of enamel and dentine in the dental organ of the tush were evident in the 240-g specimen.

## 4. Discussion

The bud stage of the tusk of the African elephant has its origin from the cap stage of the developing tush. The tush and the tusk of the African elephant develop in succession and have a deciduous to permanent tooth relation. These findings are contrary to those of Anthony (1933) and Tassy (1987), who proposed the tush and tusk to represent separate teeth of the same series of incisors. My observation is supported by a previous publication (Raubenheimer et al., 1994) on the later embryologic development of the tush, which, in a dissected specimen, had shown the fully developed tush to be located anterior to the follicle of the developing tusk. After completion of development, the tush frequently fails to erupt, is pushed aside by the growing tusk and is eventually resorbed. The displacement of the tush by the enlarging tusk, which is clearly evident in dissected specimens of newly born elephant calves, may have prompted Anthony (1933)in his observation that the tush develops adjacent to and separately from the tusk.

Although the tush could be viewed as a non-functional vestigial dental remnant, it plays an important part in the development of the tusk. The primordium of the tush not only provides the anlage for the development of the tusk, but also orientates the dental organ of the tusk in the os incisivum and creates a pathway for the eruption thereof. It furthermore delays the onset of development of the tusk by several months during the first trimester of pregnancy. This delay may be important in retarding the eruption of the tusk until well after birth, thereby facilitating breast feeding during the first year of life.

## Acknowledgements

The author wishes to acknowledge C.S. Begemann for secretarial assistance and the National Research Foundation for financial support.

## References

Anthony, R., 1933. Recherche sur les incisives superieures des elephantidea actueles et fossils. Arch. Mus. Natn. Hist. Nat. Paris 10, 61–124.

de Vos, V., 1983. Management of large animals in African conservation areas. In: Owen-Smith, M.A. (Ed.), Proceedings of a Symposium held in Pretoria, 29–30 April 1982. Haum, Pretoria, pp. 213–232.

Pilgram, T., Western, D., 1986. Inferring the sex and age of African elephants from tusk measurements. Biol. Conserv. 36, 39–52.

Raubenheimer, E.J., Van Heerden, W.F.P., Van Niekerk, P.J., de Vos, V., Turner, M.J., 1994. Morphology of the deciduous tusk (tush) of the African elephant (*Loxodonta africana*). Arch. Oral Biol. 40 (6), 571–576.

Ricuitti, E.R., 1980. The ivory wars. Anim. Kingd. 83 (1), 6–58.

Sikes, S.K., 1971. The Natural History of the African Elephant. Weidenfeld and Nicholson, London, pp. 8–111.

Tassy, P., 1987. A hypothesis on the homology of proboscidean tusks based on paleontological data. Am. Mus. Novit. 2895, 1–18.

# Development of the tush and tusk and tusklessness in African elephant (*Loxodonta africana*)

E. J. RAUBENHEIMER

Raubenheimer, E.J. 2000. Development of the tush and tusk and tusklessness in the African elephant (*Loxodonta africana*). *Koedoe* 43(2): 57–64. Pretoria. ISSN 0075–6458.

The embryologic development of the tush and tusk of the African elephant was studied by means of serial histologic sections prepared from elephant embryos with masses varying between 1g and 240 g. Statistics on tusklessness obtained during a four year population control programme in the Kruger National Park were analysed and compared with those reported in other elephant reserves in Southern Africa. Maxillae of eight elephant embryos, the maternal histories of which were available in six cases, were radiographed, dissected and examined microscopically. This study has shown that the tush and tusk develop from one tooth germ in a deciduous to permanent tooth relationship. Tusklessness was found to be unilateral or bilateral and associated with either the absence or presence of a tush. The possible causes of the differences in the frequency of bilateral tusklessness in different elephant populations are discussed.

Key words: African elephant, embryology of tusk and tush, tusklessness.

*E. J. Raubenheimer, Department of Oral Pathology, Medical University of Southern Africa, P.O. Medunsa, 0204, South Africa. (ejraub@medunsa.ac.za)*

## Introduction

The tusk of the African elephant (*Loxodonta africana*) is a pre-maxillary lateral incisor tooth which erupts at an age of approximately one year (Grzimek 1972). It is preceded by a deciduous incisor which is commonly referred to as the 'tush' (Sikes 1971). Although it has been accepted by most that the tusk is a permanent successor to the "deciduous" tush (Sikes 1971; Raubenheimer *et al.* 1995), Anthony (1933) regarded the tush as a rudimentary incisor belonging to a neighbouring position to the tusk. Paleontological data indicate that these two teeth are not homologous and incisors of Proboscideans are teeth of the primary (or deciduous) dentition with no dental replacement by a permanent tooth (Tassy 1987). The tush does not appear to erupt frequently and is pushed aside by growing tusk where it is resorbed in the adjacent tissue (Raubenheimer *et al.* 1995).

The tusk grows continuously throughout life, the size of which is important in determining the hierarchical position of a particular elephant in a herd. The most powerful cow, usually the largest tusker fulfils the role of the matriarch and determines the breeding pattern within her herd (Sikes 1971). Although large tusk-bearing elephant receive considerable attention in the literature (Hall-Martin 1981; Pilgram & Western 1986), little is known of those failing to develop tusks other than their low hierarchal status within the herd. In a study performed on foot in the Mana Pools Game Reserve in the Zambezi valley, 10 percent of 150 adult elephant were found to be tuskless. The tuskless elephant were divided in eight different groups, with one herd consisting of six tuskless elephant and only two with tusks. Amongst immature animals, 23 percent were found to be tuskless. This may indicate an increase in tusklessness in immature elephant in the area (Owen-Smith 1966). Although detailed data could not be obtained from the South African National Parks, the majority of elephant cows in the Addo Elephant Park are tuskless (Hall-Martin 1998). The incidence of tusk-

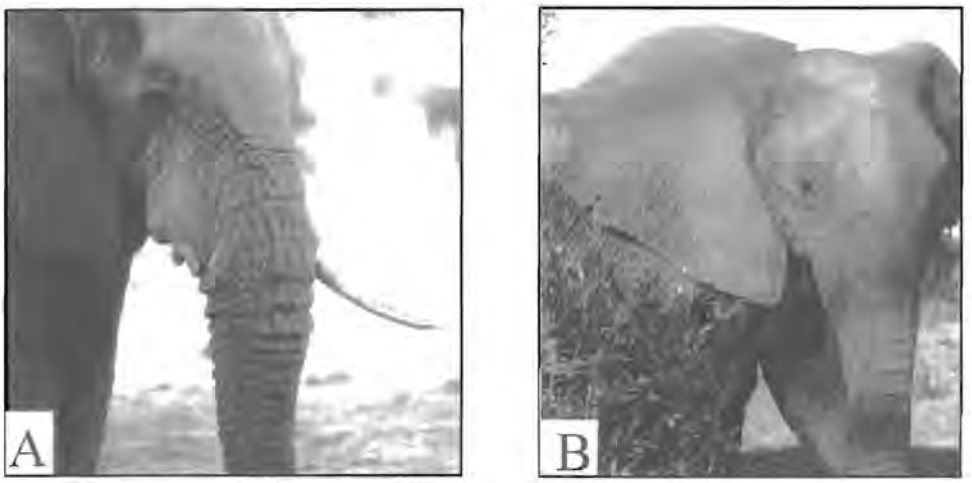


Fig. 1. The external appearances of tuskless elephant. Unilateral tusklessness (A) and bilateral tusklessness (B).

lessness amongst Asian elephant (*Elephas maximus*) is significantly higher than its African counterpart with by far the most animals being born without the capacity to grow tusks (Sikes 1971; Grzimek 1972).

This paper reports on the early development of the tush and tusk and the occurrence and anatomical considerations of tusklessness of elephant in the Kruger National Park. It furthermore proposes a theory on the role human interaction may play in selection for tusklessness in elephant breeding patterns.

## Methods

Eight elephant embryos, varying in mass between 1g (less than one month gestation) and 240g (3 months gestational age) were harvested during the population control programme of the Kruger National Park (De Vos 1983). The heads of all but the smallest were hemisected, radiographed, fixed in buffered formalin and processed for routine light microscopy. The heads of all except the smallest embryo (1 g) was hemisected. Serial sections were prepared of each in the sagittal plane and stained with haematoxylin and eosin. The developmental chronology of the lamina dentalis and the primordial of the tush and tusk were recorded through microscopic examination.

Statistics were obtained during the 1990-1993 elephant population control programme of the Kruger National Park (De Vos 1983). The culling programme was carried out on a random basis and across the whole territory of the park. Results were analysed with particular reference to the occurrence of bilateral- and unilateral absence of tusks in adult

Table 1
*Distribution of bilateral- and unilateral tusklessness amongst elephant bulls and cows*

| | Bilateral | Unilateral | |
|---|---|---|---|
| | | Left | Right |
| Bull ($n$ = 229) | 2(0.87%) | 2(0.87%) | 4(1.75%) |
| Cow ($n$ = 409) | 17(4.16%) | 6(1.46%) | 15(3.67%) |

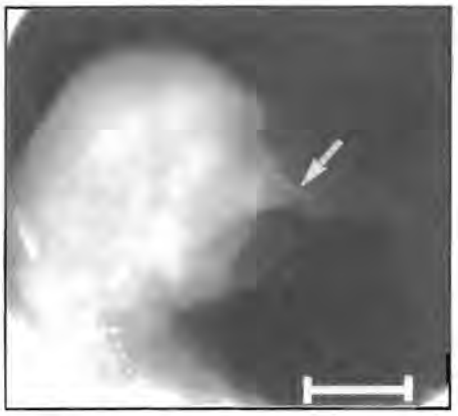

Fig. 2. Os incisivum of a 136-g embryo (arrow) showing a central radiolucent area where the development of the tush and tusk takes place (Bar = 2 cm).

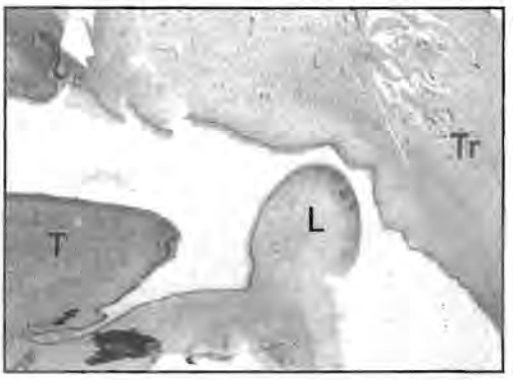


Fig. 3. The early development of the dental lamina (white arrow) in the stomodeum of the 6.5-g embryo. Note the developing tongue (T), lip (L) and trunk (Tr) (H&E stain, magnification x80).

elephant (Figs. 1A & B). The maxillae of four embryos and four foetuses varying in gestational ages from 2-22 months were obtained for radiographic examination, dissection and microscopical examination. The tusked status of the maternal animals of four embryos and two foetuses were known.

## Results

The earliest stage at which it was possible to identify the os incisivum (the part of the nasomaxillary complex in which the tush and tusk develop) radiologically was in a 48.8 g (2 months gestational age) embryo. The os incisivum in a 136 g (2-3 month gestational age) showed a central radiolucent area where early development of the tush and tusk was taking place (Fig. 2).

Microscopic examination of the 1g embryo showed a stomodeum lined by primitive squamous epithelium. No dental development could be identified with serial sectioning. Early development of a dental lamina was evident in the 6.5 g (1 month) embryo (Fig. 3) and the formation of the cap stage of the dental organ of the tush was evident in sections of the 48-g embryo. The dental lamina was partially intact at this stage and ectomesenchymal aggregates formed the dental follicle and dental papilla. Formation of bone was present around the dental organ (Fig. 4). A 94-g embryo showed loss of continuity of the dental lamina and maturation towards the bell stage of the dental organ of the tush was evident in sections of the 136-g embryo. At this

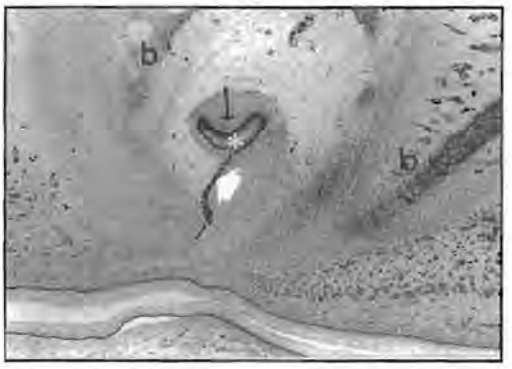


Fig. 4. The dental follicle (asterisk) and dental papilla (black arrow) of the cap stage of the dental organ of the 48-g embryo. Note the partially intact dental lamina (white arrow). Formation of bone around the dental follicle is evident (b) (H&E stain, magnification x180).

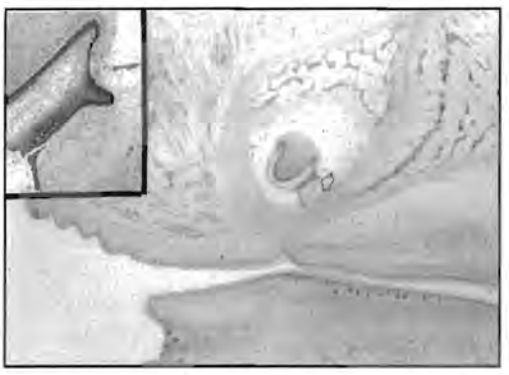

Fig. 5. Formation of the bud stage of the tusk (arrow) from the external epithelial layer of the dental organ of the tush (H&E stain, magnification x100). Inset: High magnification of the bud of the tusk (H&E stain, magnification x250).

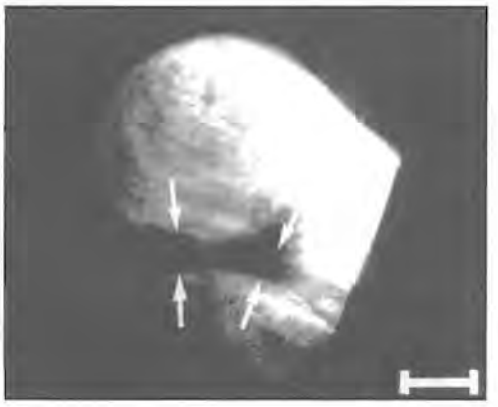

Fig. 7. Lateral radiographic view showing complete absence of tush and tusk (arrows) in the premaxilla of a 59 kg foetus. (Bar = 5 cm).

stage, epithelial proliferation of the external enamel epithelium of the bell stage of the tush formed the bud stage of the succesional tooth germ, the tusk (Fig. 5).

Of the 638 elephant (409 cows and 229 bulls) culled between 1990 and 1993, 46 (38 females and eight males) showed either unilateral or bilateral absence of tusks (Table 1). Bilateral absence of tusks affected 19 elephant (or 3 % of the total) and the frequency thereof was higher in cows than bulls (17:2). This difference was statistically significant when evaluated with the Chi-square test with Yates correction ($P = 0.03$). Although development of the tush and tusk was recorded in the majority of embryos and foetuses either microscopically or radiographically (Fig. 6),

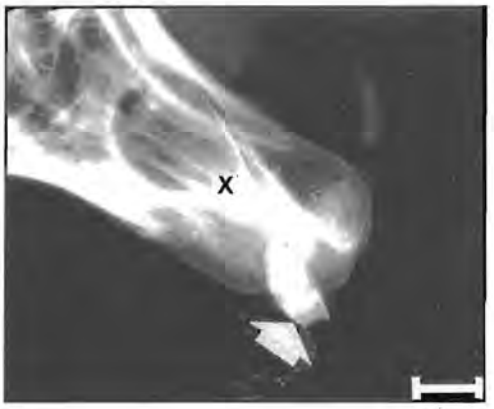


Fig. 6. Radiograph showing normal development of the tush (arrow) and tusk (X) in the premaxilla of the 53 kg foetus. (Bar = 5 cm).

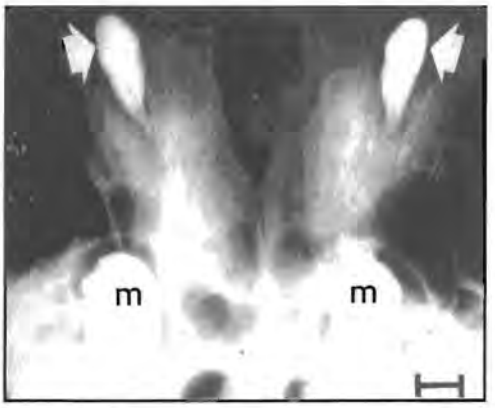


Fig. 8. Occlusal radiograph of the premaxilla of the 90 kg foetus showing the presence of both tushes only (arrows). Note the absence of tusk development between the developing molars ('m') and the tushes. (Bar = 5 cm).

one foetus showed complete absence of both the tush and tusk (Fig. 7) and another the presence of a tush only (Fig. 8). Unilateral absence of a tush or tusk was not seen in any of the embryos or foetuses examined (Table 2).

## Discussion

This study has shown that the tush and tusk of the African elephant develop in succession and have a deciduous to permanent relationship. These findings are contrary to those of Anthony(1933) and Tassy (1987) who proposed the tush and tusk to represent separate teeth of the same series of incisors. This observation is supported by the radiograph in which the tush is demonstrated to lie anterior to the developing tusk. After completion of development the tush frequently fails to erupt, is pushed aside by the growing tusk and eventually resorbed in the connective tissue surrounding the os incisivum. The displacement of the tush by the growing tusk, which is clearly evident in dissected specimen of newly born elephant calves (Raubenheimer *et al.* 1994), may have prompted Anthony's observation that the tush develops adjacent to and separate from the tusk. Although the tush seems to be a non-functional vestigial dental structure, it plays an important role in the development of the tusk. The primordium of the tush not only provides the epithelial anlage for the development of the tusk, but also orientates the enamel organ of the tusk in the os incisivum and creates a pathway for the eruption thereof. Furthermore it delays the onset of the development of the tusk by several months during the first trimester of pregnancy. This delay may be important in retarding the eruption of the tusk until well after birth, thereby facilitating breast-feeding during the first year of life.

Absence of both tusks is generally congenital and may follow an inherited pattern. The occurrence of bilateral tusklessness is significantly higher in females (4.16 %) than males (0.89 %) in the Kruger National Park. Tusklessness in this sanctuary, where no selection through hunting has taken place and breeding herds remain intact, probably represents a natural mutation, which appears to be sex linked. Random culling in the Kruger National Park has contributed to this reserve becoming known for its large ivory bearing elephant (Hall-Martin 1981; Hall-Martin 1982), a sight which has disappeared from most of the African continent (Ottichilo 1986; Pilgram & Western 1986). The approach towards hunting within the ecological boundaries of the Kruger National Park

Table 2
*Status of tush and tusk development in elephant embryos and foetuses*

| Mass | Gestational age (mnths) | Tush | Tusk | Maternal status |
|---|---|---|---|---|
| 1 g | < 1 | unknown[a] | unknown[a] | tusks L&R |
| 6.5 g | 1 | L&R | unknown[a] | tusks L&R |
| 48.4 g | 2 | L&R | unknown[a] | tuskless L&R |
| 107 g | 2-3 | L&R | unknown[a] | tusks L&R |
| 53 kg | 17 | L&R | L&R | unknown |
| 59 kg | 18 | absent L&R | absent L&R | tusk L only |
| 90 kg | 21 | L&R | absent L&R | unknown |
| 94 kg | 21 | L&R | L&R | L&R |

[a] The stage of embryonal development is to early to determine the presence of tush and/ or tusk.

seems to be changing. A hunting concession was recently granted to a neighbouring community in exchange for an agreement not to settle in an ecologically sensitive part of the park that was handed back after a successful land claim (Steyn 2000). Although limited in extent, this concession may hold consequences for future negotiations on the right to hunt in the Kruger National Park.

Individual animals in a tusked herd may become tuskless in later life as a result of injury or disease (Sikes 1971). This occurrence could be designated as acquired tusklessness and is usually unilateral with normal tusk development on the unaffected side. Unilateral tusklessness could however also be congenital resulting from failure of embryological development of the tusk on one side only. Radiographic examination, dissection and a thorough family history are essential in distinguishing unilateral acquired- from unilateral congenital tusklessness. The right-sided absence of a tusk in a cow in our study is probably genetically linked as her foetus failed to develop tushes and tusks on both sides. The 27 elephant with unilateral tusklessness were not examined thoroughly enough to distinguish the congenital from the acquired type. The higher frequency of right sided tusklessness may be indicative of tusk breakage being the most important cause for the absence of a tusk, as elephant are generally right tusked (Sikes 1971).

The involvement of the tush in tuskless elephant has not yet been recorded. Congenital absence of both the tush and the tusk imply failure to develop a lamina dentalis during the first month gestation. The presence of a tush only indicate arrest of development of the primordium of the tusk wich takes place during the second month of gestation. Tusklessness with or without tushlessness will be indistinguishable with external examination only as the tush of elephant does not appear to erupt and is pushed aside into the surrounding tissue by the growing tusk (Raubenheimer *et al.* 1994).

In order to compare the occurrence of tusklessness in the Kruger National Park with those in other elephant sanctuaries, the unilateral absence of tusks in our study was not be taken into account as in most reports only bilateral tusklessness is recorded. This study has shown that the incidence of bilateral tusklessness varies significantly between different regions. Three percent of our total sample suffered bilateral tusklessness compared to 10 % in Mana Pools. The reasons for the more frequent occurrence of tusklessness in Mana Pools when compared with the Kruger National Park are speculative. An explanation for this can possibly be found in the different population control measures employed in the two regions. In the Kruger National Park, culling has been performed randomly (De Vos 1983) and there is no chance of selection of any kind. The Kruger National Park is fenced and illegal hunting is generally under control. The elephant population in Mana Pools is managed through hunting concessions. The area is not fenced and the elephant population is exposed illegal ivory harvesting. Elephant in the Eastern Cape Province of South Africa reached virtual extinction by 1931 when only 11 survived the onslaught of ivory hunters in the dense Addo bush. Most of these elephant were tuskless. The selection for the tuskless gene is presently, 60 years after hunting was prohibited and the region declared a national park still evident, as most of the cows in the present population of 272 elephant are tuskless (Hall-Martin 1998). The shift towards tusklessness is significantly more pronounced in the elephant populations of Asia (Elder 1970; Pilgram & Western 1986) that has been exposed to modern man – hunter for much longer than its African counterpart. Most Asian elephant cows fail to develop tusks (Sikes 1971) whereas the incidence of tusklessness amongst Asian elephant bulls is much higher than on the African continent. Only 10 % of elephant bulls in Sri Lanka are reported to have tusks (Grzimek 1972). Three thousand years of exposure to man who hunted for ivory and domesticated elephant to perform work, thereby disrupting hierarchal order and breeding patterns,

selected for a phenotype, which generally lacks the genetic capacity to develop ivory tusks.

The modern high velocity rifle no longer respects and in fact selects the large tusk bearing elephant as its contribution to the population control programmes of areas managed through hunting concessions. The undisputed illegal ivory harvesting by those who frequently use armour piercing weaponry in immobilising a large tusker, contribute significantly to the heavy demand placed on the already compromised genetic pool of large tusk carriers. This is in contrast to the methods of hunting employed before the arrival of technology to the African continent. During most of the 19th century and even in the early 20th century elephant hunting and trapping methods like the falling spear, the wheel trap, trunk snare, hamstring and tendon slashing as well as group hunting with heavy short shafted spears (Sikes 1971) were more successful in killing smaller and weaker animals and in fact probably contributed positively towards the selection for a larger tusked phenotype. The arrival of the modern weapons in Africa coincided with the rapid disappearance of large tusk bearing elephant (Sikes 1971; Ottichilo 1986). Although elephant with tusks weighing in access of 80 kg was a common sight in the past century, elephant herds in most areas now consist of small-tusked animals only. Over a long period, this selection will not only lead to a decrease in the large tusked population, but also a relative increase in tuskless animals due to the hunters' lack of interest in elephant without tusks. The trend towards bilateral tusklessness is even higher in the sub adult elephant population in Mana Pools (Owen-Smith 1966), implying that a genetic shift towards tusklessness may have taken place amongst younger animals in certain regions. These changes can possibly be explained by the dominant role the matriarch (usually the cow with the largest tusks - Sikes 1971) play in selecting cows for breeding within her breeding herd. If she is shot (her large tusks usually make her the animal of choice during both trophy hunting and illegal ivory harvesting) a breakdown of the hierarchy within her breeding herd could result in cows of lesser status (i.e., those without tusks) entering the reproductive cycle. Once the genetic balance has swung in favour of tusklessness, a return to normal hierarchical order may not be sufficient to re-establish the ivory bearing genome. This is clearly witnessed in the present day Asian elephant population.

Monitoring of the size of tusks as well as the incidence of bilateral tusklessness are important indicators for genetic selection in nature conservation areas. Randomised population control programmes should be introduced where a reduction of elephant numbers are necessary. Authorities issuing hunting concessions in Africa should take note of the trends reported in this manuscript and introduce a tariff structure, which would encourage hunting of a broader spectrum of elephant in a herd. Restoration of the matriarchal dominance in a breeding herd seems imperative to the long-term survival of the ivory bearing gene. The granting of permits for international trade in ivory should, in the long term, be based on whether a region is successful in maintaining the ivory bearing phenotype during their population control programme.

## Acknowledgements

The Research Division, South African National Parks (Dr V. de Vos in particular) is thanked for supplying the data and material and Mrs C.S. Begemann for secretarial assistance. This study was supported by a grant from the National Research Foundation of South Africa.

## References

ANTHONY, R. 1933. Recherche sur les incisives superieures des Elephantidea actueles et fossils. *Archives du Museé national d'Histoire naturelle. Paris* 10: 61 – 124.

DE VOS, V. 1983. Management of large animals in African conservation areas. Pp. 213-32. *In*: OWEN-SMITH, M.A. (ed.). *Proceedings of a Symposium held in Pretoria, 29 – 30 April 1982.* Pretoria: Haum.

ELDER, W. H. 1970. Morphometry of elephant tusks. *Zoologica Africana:* 143 – 59.

GRZIMEK, B. 1972. *Grzimek's Animal Life Encyclopaedia.* (Edited by GRZIMEK B.), Vol. 12. New York: Van Nostrand Reinhold.

HALL-MARTIN, A. 1981. Kruger's big tuskers. *African Wildlife* 35(1): 6–9.

HALL-MARTIN, A. 1982. Kruger's tuskers. *African Wildlife* 36(2): 69.

HALL-MARTIN, A. 1998. Addo. *Africa Environonment and Wildlife* 6(6): 66–77.

OTTICHILO, W.K. 1986. Age structure of elephants in the Tsavo National Park, Kenya. *African Journal of Ecology* 24(2): 629–75.

OWEN-SMITH, N. 1966. The incidence of tuskless elephant in Mana Pools Game Reserve. *African Wildlife* 20: 69–73.

PILGRAM, T. & D. WESTERN. 1986. Inferring the sex and age of African elephants from tusk measurements. *Biological Conservation* 36: 39–52.

RAUBENHEIMER, E.J., W.F.P. VAN HEERDEN, P.J. VAN NIEKERK, V. DE VOS & M.J. TURNER. 1994. Morphology of the deciduous tusk (tush) of the African elephant (*Loxodonta africana*). *Archives of Oral Biology* 40(6): 571–76.

SIKES, S.K. 1971. The Natural History of the African Elephant. London: Weidenfeld and Nicholson.

STEYN, T. 2000. To hunt or not to hunt in a national park. News 24.co.za, 27 January.

TASSY, P. 1987. A hypothesis on the homology of Proboscidean tusks based on paleontological data. *American Museum Novitates* 2895: 1–18.

Pergamon

0003-9969(95)00008-9

*Archs oral Biol.* Vol. 40, No. 6, pp. 571–576, 1995

0003-9969/95 $9.50 + 0.00

## SHORT COMMUNICATION

# MORPHOLOGY OF THE DECIDUOUS TUSK (TUSH) OF THE AFRICAN ELEPHANT (*LOXODONTA AFRICANA*)

E. J. RAUBENHEIMER,[1] W. F. P. VAN HEERDEN,[1] P. J. VAN NIEKERK,[1] V. DE VOS[2] and M. J. TURNER[1]

Department of [1]Oral Pathology and Oral Biology, P.O. Medunsa, 0204 and [2]Research Division, Skukuza, Kruger National Park, Republic of South Africa

*(Accepted 10 January 1995)*

**Summary**—The tusk of the African elephant is preceded by a deciduous tooth generally known as the tush. Tushes from nine elephant fetuses and six calves younger than 1 year were exposed by dissection and described morphologically. All tushes consisted of a crown, root and pulpal cavity, the formation of which is completed soon after birth. They reached a maximum length of 5 cm, appeared not to erupt through the skin and were pushed aside and resorbed during enlargement of the distally located primordium of the tusk. Dental enamel, which covered the crown, could easily be removed and consisted of rods with an interwoven arrangement; the dentine–enamel junction was flat. Cellular cementum extended for variable distances over the crown and the dentine was tubular in nature. Although the tush apparently has no function, it provides the anlage and orientation for the development of its permanent successor.

Key words: tush, African elephant, *Loxodonta africana*, deciduous tusk.

The tusk of the African elephant (*Loxodonta africana*) is a modified premaxillary lateral incisor tooth which erupts at an age of approx. 1 year (Grzimek, 1972). It is preceded by a deciduous tooth commonly referred to as the 'tush'. The tush is reported to develop in the same alveolar cavity as the tusk and may reach a length of 5 cm (Sikes, 1971). Although it is generally accepted that the tush is the deciduous precursor to the tusk, palaeontological data provide some evidence that the two teeth develop independently and that they could represent deciduous central and deciduous lateral incisors, respectively (Tassy, 1987). Our purpose now was to determine the morphology of the tush of the African elephant, *Loxodonta africana*.

The maxillae of the nine elephant fetuses and six calves younger than 1 year were obtained during the elephant population control programme of the Kruger National Park (de Vos, 1983) and fixed in buffered formalin. The specimens were examined radiographically and the tushes exposed by dissection. The relation to the developing tusk was noted and all the tushes removed. Each tush was measured and divided along its length in two halves. One half was processed for light microscopy and the other for scanning electron microscopy. Half of the samples for light microscopy were mineralized, routinely sectioned and stained with a haematoxylin and eosin; ground sections were prepared from the remainder.

All tushes were embedded in the premaxillae and located anteriorly to the primordium of the developing tusk (Fig. 1). The tush and the primordium of the tusk were in the same bony cavity. The crowns of the tushes in the older calves were visible outside the alveolar bone. None of the specimens showed a tush which had erupted through the overlying skin. A radiograph, which was taken of the tusk of a 5-year-old elephant, demonstrated the crown of a tush embedded in the soft tissue around the girth of the tusk (Fig. 2). All tushes could, by external examination, be subdivided into a crown covered by enamel and a slender root. A cervical constriction was absent and the incisal margin rounded (Fig. 3). The formation of enamel was incomplete in the incisor region of five tushes, of which two were from the same animal (Fig. 4). The longest tush measured 5 cm in length and formation of the crown appeared to be completed after 16 months of gestation. Root formation was found to be completed during the first 3 months post partum, whereafter root resorption, mediated by osteoclast-like giant cells, coincided with progressive enlargement of the distally located primordium of the tusk (Figs 5 and 6). External resorption was not only restricted to the root, but also involved the crown of the tushes.

The enamel, which covered the crown, could be removed with a sharp instrument without difficulty from the underlying dentine. It consisted of rods of 4–6 $\mu$ dia. Bundles of enamel rods followed an interwoven course to the surface of the tooth (Fig. 7). This arrangement was consistent throughout the entire enamel. The enamel–dentinal junction was flat, enamel tufts were infrequent and the dentine was of

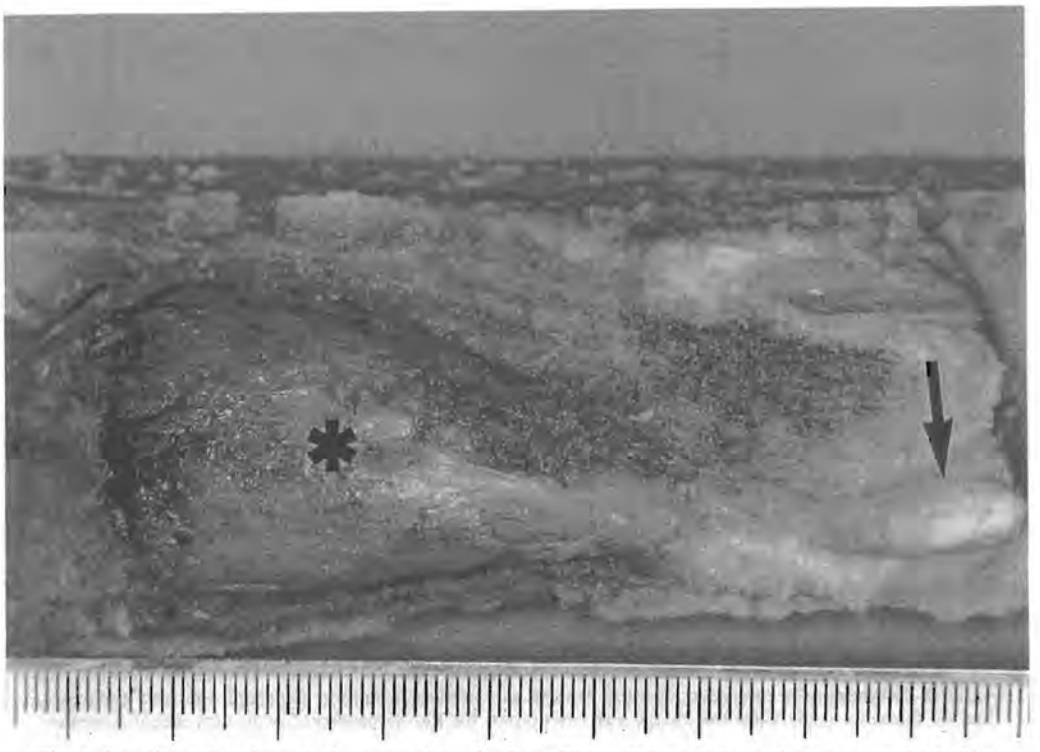

Fig. 1. Length section through the premaxilla of a fetus. The tush (→) is located anterior to the follicle of the developing tusk (*). Scale in mm.

a tubular nature. Cellular cementum covered the roots and in fully formed teeth extended over the external surface of the crown (Fig. 8).

Fig. 2. Radiographic view of the girth of the tusk of a 5-year-old elephant. Note the crown of the tush, its rounded tip pointing anteriorly, which was pushed aside and found to be located in the subcutaneous soft tissue (→). Bar = 1 cm.

The question whether the tush represents a deciduous precursor to the tusk (Sikes, 1971) or whether it is an incisor which develops independently from the tusk (Tassy, 1987) cannot be resolved in a study of this nature. Dissection of embryos at an earlier stage of development will throw more light on the initial relation between the follicles of the two teeth. In the specimens we examined the possibility of independent tush development seems unlikely as both the tush and tusk were located in one alveolar cavity, with the tush anterior to the developing tusk.

Although superficial reference has been made to the tush of the African elephant (Sikes, 1971; Grzimek, 1972), its morphology, structure and functions have never, to the best of our knowledge, been recorded. The function of this deciduous incisor is unclear because, unlike the tusk, it does not appear to make its presence visible by erupting through the skin. The pressure exerted by the growing tusk leads to resorption of the root of the tush by osteoclast-like giant cells soon after birth and it appears as if its crown is pushed aside and into the soft tissue surrounding the girth of the growing tusk. The fate of the displaced crown is speculative, although it seems likely that it is eventually completely resorbed. It may be argued that the tush represents an evolutionary remnant of a tooth that may have had a function in the earlier extinct Proboscideans, where incisor teeth had a more pronounced masticatory function (Grzimek, 1972). When viewed in an embryological context, the primordia of primary teeth provide the anlage and orientation for the development of their permanent successors (Bhaskar, 1980). This may

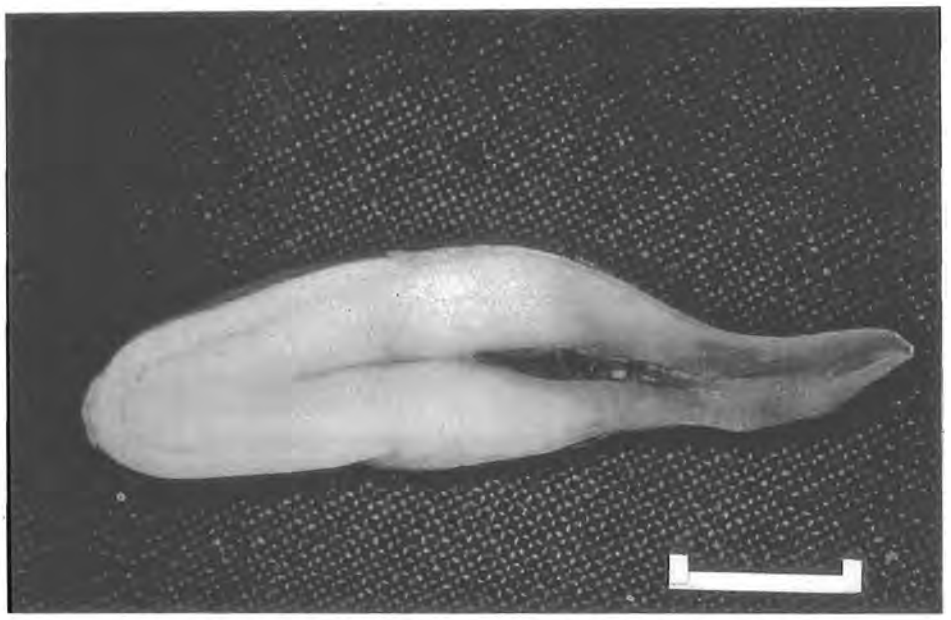

Fig. 3. Section cut in length through a fully formed tush. Bar = 1 cm.

represent the only distinct function of the tush of the African elephant.

Despite its apparent regression in the course of evolution, the tush is composed of an orderly arrangement of all tissue types found in mammalian incisors. The ease with which the enamel could be removed from the underlying dentine is explained by the flat enamel–dentinal junction. Incomplete enamel formation, involving particularly the incisal margin, appears to be a frequent occurrence. Formation of cementum on the external surface of the crown is not uncommon in the animal kingdom. In many animals, the reduced enamel epithelium breaks down long before the tooth erupts, allowing the ectomesenchyme of the tooth follicle to come into contact with the enamel. This is followed by the differentiation of cementoblasts and the deposition of coronal cementum.

The stage of dental development reflects the age of fetuses and infants. Although a limited number of

Fig. 4. A dissected specimen in which the skin and soft tissue of the premaxilla had been removed, thereby partially exposing the crown of a tush, which is viewed from the anterior. Note the area of deficient enamel formation (→). Bar = 2 cm.

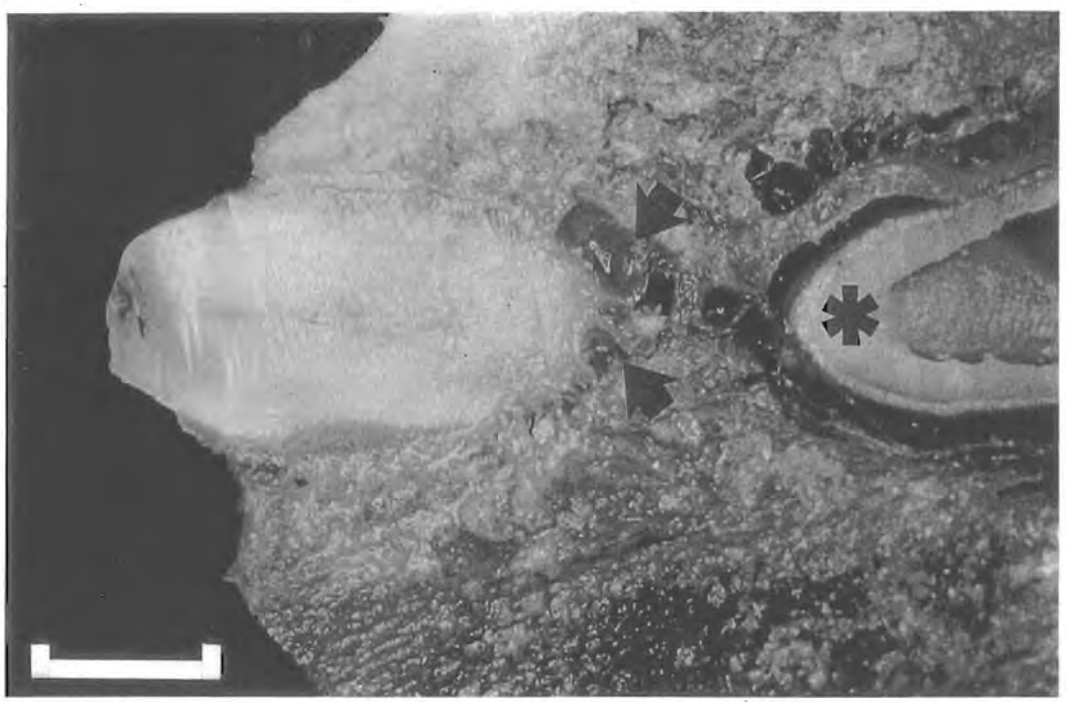

Fig. 5. Longitudinal section through tush of a newborn calf, which has erupted through the cortical plate of the alveolar bone. Note the proximity of the tip of the enlarging tusk (*) and its association with resorption of the root of the tush (→). Bar = 1.6 cm.

elephants have been examined, it appears as if the crown of the tush is completed by the 16th month of intrauterine life and root development ceases 3 months after birth, which follows after 22 months' gestation (Sikes, 1971). After formation of the tush has been completed, the enlarging primordium of the tusk displaces it and resorption commences before the postnatal age of 1 year.

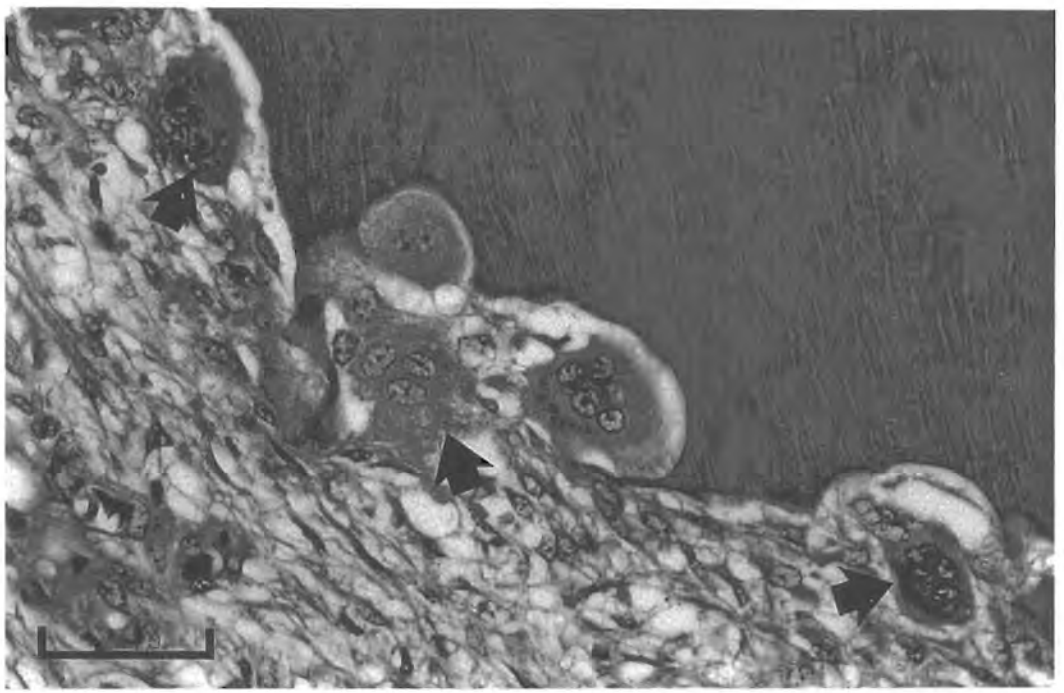

Fig. 6. Photomicrograph showing active resorption of the dentine of the root of a tush by multinucleated giant cells (→). H & E, ×400; bar = 50 μm.

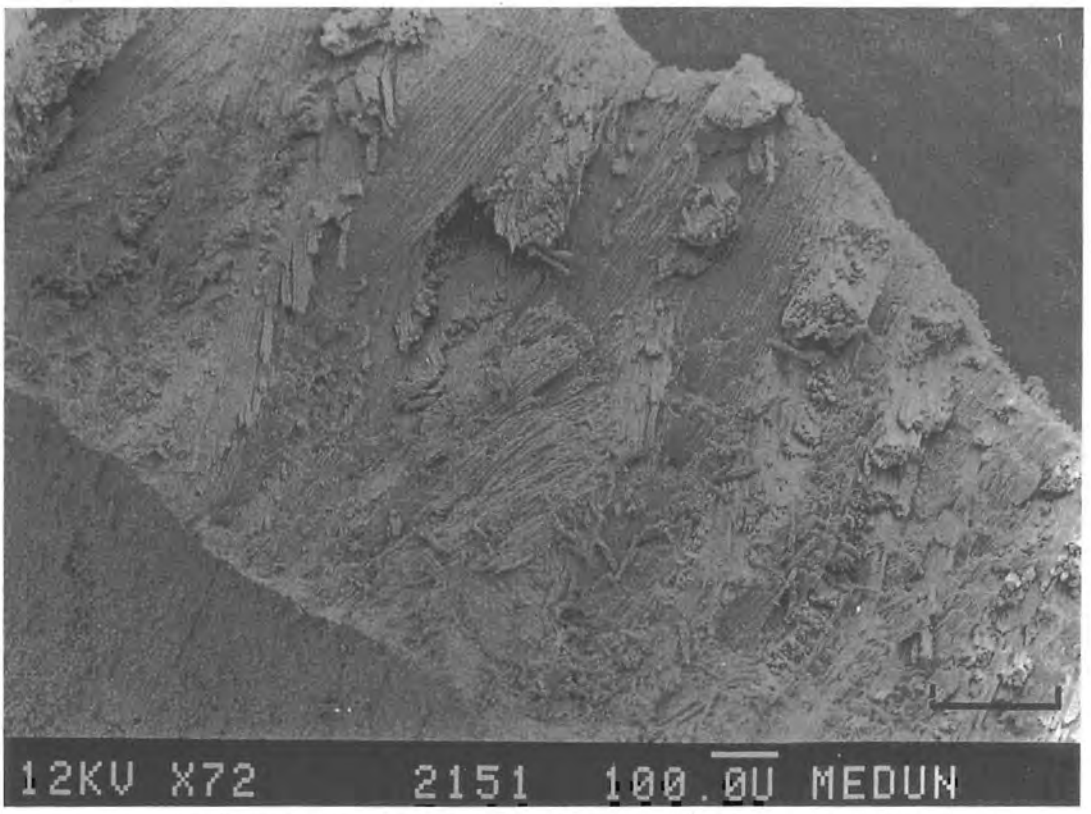


Fig. 7. Scanning electron micrograph of a fracture surface of enamel (bottom left—dentinal junction, top right—outer surface). ×72; bar = 200 μm.

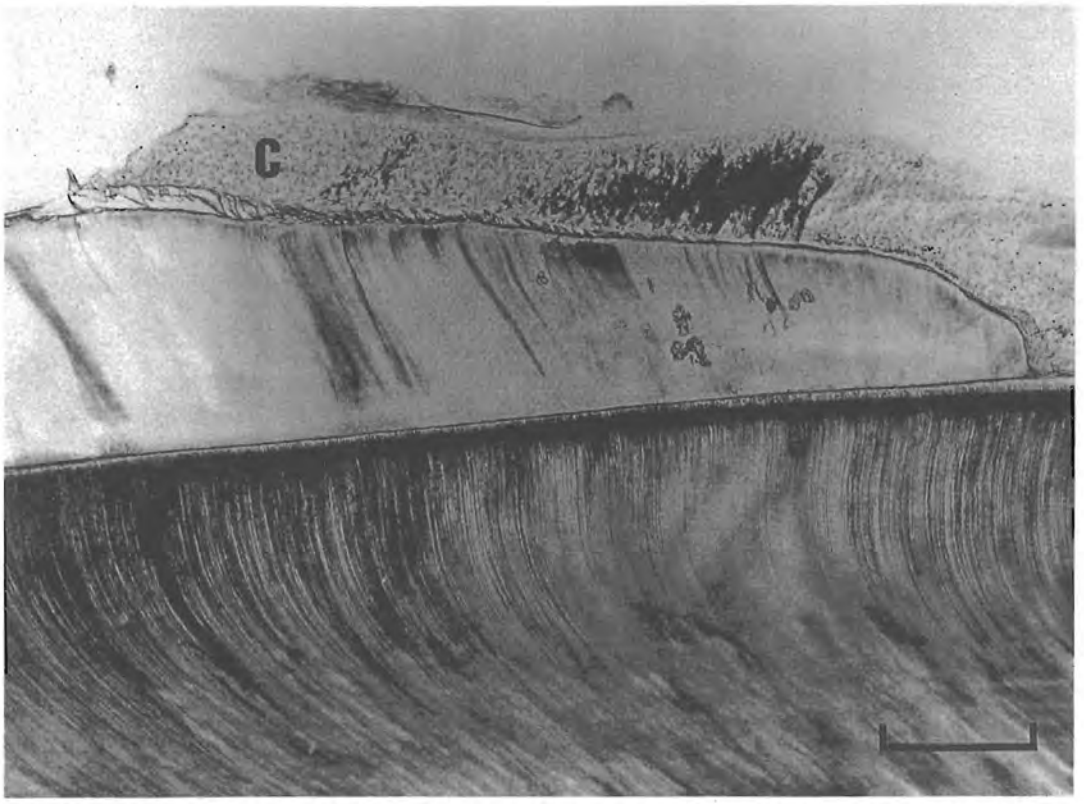


Fig. 8. Cellular cementum (C) extending on to the external surface of the crown. Note the flat dentine–enamel junction. Ground section, ×20; bar = 1 mm.

## REFERENCES

Bhaskar S. N. (1980) *Orban's Oral Histology and Embryology*, Chap. 2, pp. 24–45. The C. V. Mosby Company, St Louis.

Grzimek B. (1972) *Grzimek's Animal Life Encyclopedia*, Vol. 12, p. 479. Van Nostrand Reinhold, New York.

Sikes S. K. (1971) *The Natural History of the African Elephant*, Part 1, pp. 81–82. Weidenfeld and Nicholson, London.

Tassy P. (1987) A hypothesis on the homology of Proboscidean tusks based on paleontological data. American Museum Novitates 2895, 4th November, 1–18.

de Vos V. (1983) Management of large animals in African conservation areas. *In Proceedings of a Symposium held in Pretoria 29–30 April 1982.* (Ed. Owen-Smith M. A.), pp. 213–232. Haum, Pretoria.

# Morphological aspects and composition of African elephant (*Loxodonta africana*) ivory

E.J. RAUBENHEIMER

Raubenheimer, E.J. 1999. Morphological aspect and composition of African elephant (*Loxodonta africana*) ivory. *Koedoe* 42(2): 57–64. Pretoria. ISSN 0075-6458.

This study was aimed at determining the origin of the diamond shaped pattern and composition of ivory of the African elephant. Fragments of ivory and tusks were obtained through the National Parks Board from the Kruger Park, Addo Elephant Park, Kaokoveld, Caprivi, Etosha, Kavango and Tembe Elephant Park. Polished surfaces were prepared in different planes and examined with light and electron microscopical techniques. Analyses of the inorganic composition were performed using atomic absorption spectrophotometry, ion selective electrodes and inductively coupled optical emission spectroscopy. The total amino acid composition was determined with the aid of an amino acid analyser. Morphological investigations showed the distinctive diamond shaped pattern of ivory to be caused by the sinusoidal surface to pulpal course followed by odontoblastic tubules. This course is the result of pressure which builds up between tightly packed odontoblasts on their centripetal course along an ever decreasing pulpal circumference during formation of ivory. A total of 17 elements were detected in the inorganic fraction of ivory, some in concentrations as low as 0.25 µg/g. The concentrations of calcium, magnesium, fluoride, cobalt and zinc showed statistically significant differences ($P < 0.007$) between selected regions and may prove valuable in distinguishing chemically between ivory from different geographical locations. The organic content of ivory showed 17 amino acids in varying concentrations. The possible causes of these variations are discussed.

Key words: elephant ivory, morphology, composition

*E.J. Raubenheimer, Department of Oral Pathology, MEDUNSA, P.O. Medunsa, 0204 Republic of South Africa (ejraub@mcd4330.medunsa.ac.za).*

## Introduction

The paired tusks of the African elephant are incisors which develop in the os incisivum of the nasomaxillary complex of bones and which grow continuously throughout life. The unique diamond shaped pattern of elephant ivory, which has not been researched in great detail (Sognnaes 1960; Miles & Boyde 1961; Sikes 1971; Raubenheimer *et al.* 1990) has made it a sought-after product in the manufacturing of works of art. The flourishing illegal trade in ivory has contributed to a significant decrease in elephant numbers on the African continent over the past decades (Armstrong & Bridgland 1989). The Convention on International Trade in Endangered Species (CITES) at its biennial meeting in Lausanne, Switzerland in October 1989 responded by placing a ban on the trade in elephant products. The effect of this ban on well managed elephant populations in Southern African states remains controversial.

Dentine (or ivory) forms the bulk of most teeth and is composed of organic and inorganic fractions. The inorganic composition of elephant ivory has not yet been investigated in detail except for distinguished work done on its carbon and nitrogen isotope ratios. The carbon isotope ratios ($^{13}C:^{12}C$) of ivory distinguishes between elephant roaming woodland and those in dense forests (Van der Merwe *et al.* 1990). The aims of this study were to determine the origin of the chequered (diamond shaped) pattern of elephant ivory and establish a databank on the inorganic and organic composition of ivory from the Southern African region.

## Material and methods

Twenty fragments of ivory and five tusks, with masses between 0.7 and 9.3 kg were sectioned and polished in cross sections and sagittal planes and the characteristic diamond shaped pattern studied. One developing tusk was harvested from a full-time fetus 20 minutes after death. Biopsies were taken from the pulpal ivory and soft tissue, cut in thin slices and fixed in 10 % phosphate buffered formalin. Ground sections, 40 µ thick were prepared parallel and perpendicular to the long axis of 12 different fragments of ivory and subjected to light microscopic examination. Routine techniques for the preparation of scanning electron micrographs of hard tissue were employed to visualise the morphology and distribution of dentinal tubules of six different tusks. An image analyser (FIPS, CSIR, Pretoria) was used to measure the distances between the tubules in the light and dark bands respectively.

Sixty four fragments of ivory were obtained through the South African National Parks from Kaokoveld, Etosha National Park, Caprivi, Kavango, Kruger National Park, Tembe Elephant Park and Addo Elephant Park. Specimens weighing between 0.5 g and 1.0 g were prepared by removing the ensheathing layer of cementum with a rotating diamond disc. The specimens were agitated in a weak acid (0.1M HCl) for 10 minutes to remove all traces of metal that may have contaminated the ivory during sample preparation. The fragments were washed for 15 minutes in distilled water and the dry weights of each fragment determined accurately. Each specimen was completely demineralised in 1M perchloric acid. The inorganic composition was determined by atomic absorption spectrophotometry (Perkin Elmer 500; Norwalk, CT, U.S.A.), Astra 8 analyser (Beckman Instruments Inc., Brea, CA, U.S.A.) and ion selective electrodes (Radiometer, Copenhagen, Denmark). The mean values obtained per site of origin as well as the standard deviations (SDs) were expressed in mg/g dry weight and tabulated. The level of significance between the concentrations of each element at different geographical sites was determined with the Student *t*-test for unequal variances. The trace elemental composition of 25 fragments was determined with an inductively coupled plasma optical emission spectroscope (ARL 3400, Boston, MA, U.S.A.). Perchloric acid (1M) was used as a control. The mean concentrations and SDs were expressed in µg/g ivory.

Samples of ivory, weighing between one and three grams, were prepared from 32 fragments of ivory obtained from Kruger National Park (5), Kaokoveld (6), Etosha (15), Tembe (4), and Addo Elephant National Park (2). The samples were hydrolysed in sealed tubes containing 5 ml 6M HCl at 110 °C for 24 hours. The hydrolysates were neutralised, filtered (Millex-GS, 0.22 µ) and diluted 1:1 with citrate buffer (pH 2.2). Calibrants of 43 amino acids were prepared and the amino acid composition of the hydrolysate and calibrants determined using a Beckman 6300 Amino Acid Analyser. The chromatograms were integrated and quantified using a Hewlett-Packard 3390A integrator. The results were tabled as the average of the residues per 100 and the standard deviation for each amino acid calculated.

## Results

The pulpal cavity of the tusks were conical in shape, had a smooth surface and a large pulpal opening. The bulk of a large tusk consisted of ivory (Fig. 1a). The entire outer

Fig. 1a. Partially dissected tusk exposing the conical pulpal cavity, diamond-shaped pattern (exposed on a polished surface prepared on a cross section) and parallel and alternating light and dark lines (on polished surface prepared in the sagittal plane). Note the large apical opening of the pulp on the left and the solid ivory forming the bulk of the tip of the tusk.

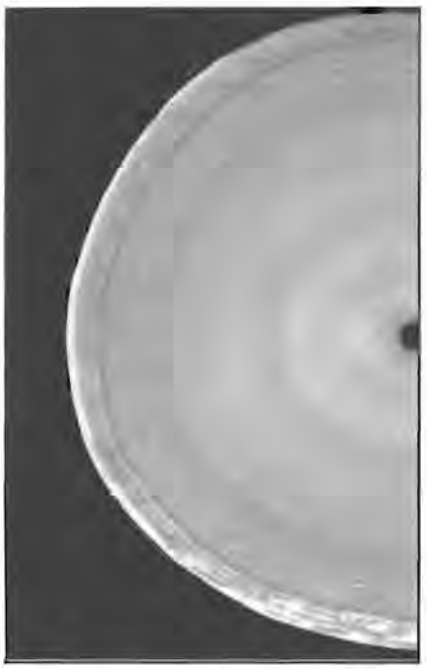

Fig. 1b. Closer view of the diamond-shaped pattern on cross section through the tusk. Note the ensheathing layer of cementum and scalloped ivory to cementum junction.

Fig. 1c. Closer view of the sagittal surface showing the alternating dark and light lines.

surfaces of the tusks were found to be covered by a layer of cellular cementum. The cementum to ivory junction was visible as a dark concentric ring. In cross sections, the ivory to cementum junction followed an undulating circular course, forming irregular excrescences alternating with shallow convexities or concavities (Fig. 1b). In this plane, the unique diamond-shaped pattern of the ivory consisted of two systems of alternating light and dark lines which radiate clockwise and anticlockwise, respectively, from the axis of the tusk. The diamond-shaped pattern corresponded to parallel light and dark lines evident on polished surfaces prepared in the sagittal plane (Fig. 1c). The external surface of the tusk followed the contour of the cementum to ivory junction, resulting in parallel longitudinal ridges and troughs which were visible upon external examination of a tusk.

The outermost layer of ivory (mantle layer) consisted of irregularly-spaced odontoblastic tubules which slanted apically and branched extensively. When followed towards the axis of the tusk, the tubules became more evenly spaced and gradually changed their course by curving towards the tip of the tusk. This curvature was found to be the beginning of the regular, sinusoidal course followed by the odontoblastic tubules in a pulpal direction and was present only in sections prepared in the sagittal plane. The convexities and concavities of the sinusoidal pattern corresponded to the alternating light and dark bands seen macroscopically on surfaces prepared in the sagittal plane. The dark bands corresponded with that part of the tubule that curved towards the pulpal opening (Fig. 2a). On high power maginification many dentinal tubules appeared to end blind and others fused, forming one tubule (Fig. 2b). The process of fusion was distinct from the fine lateral branches that seemed to anastomose with those of adjacent tubules. Blind ending tubuli occured more frequently in the dark bands (16 blind ending tubules per 100 tubules, SD 7) than in the light bands (6 blind ending tubules per 100 tubules, SD 3) as counted over 2 500 tubules in each of the bands respectively. Microscopic sections of biopsies of the foetal tusk confirmed the distal slant of the odontoblasts and scattered pyknotic cells, highly suggestive of individual cell death (Fig. 3).

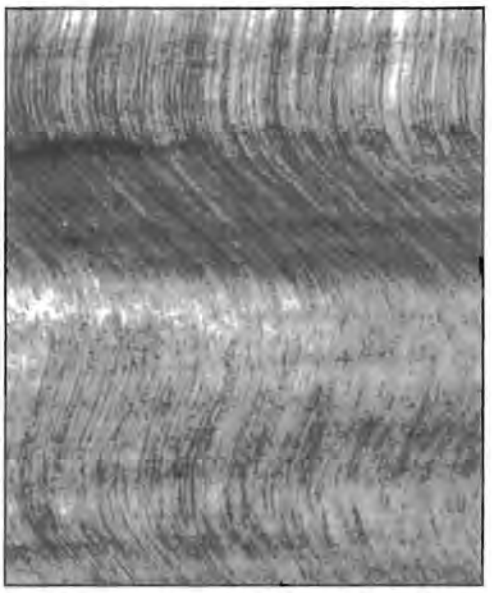

Fig. 2a. The regular sinusoidal curve followed by the odontoblastic tubules. The curve to the right coincides with a dark band (top of figure), an optical phenomenon caused by the increased density of tubules in this region. The tip of the tusk is towards the left. (Unstained section, magnification x180).

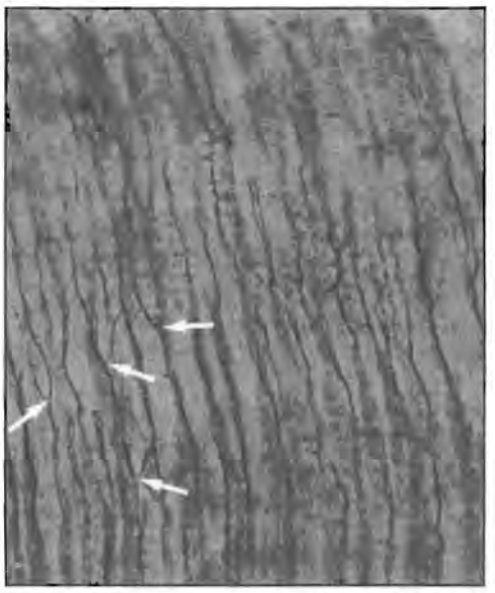

Fig. 2b. Higher power magnification in a dark band, showing fusion of tubles (arrows) (Unstained section, magnification x400).

Scanning electron microscopy showed the pulpal openings of tubules to be oval, with the greatest dimension parallel to the long axis of the tusk (Figs. 4a & 4b). Dentinal tubules were closer packed in areas where they curve towards the pupal opening (i.e. dark bands) (mean distance 4.6 ± 1.7 µm SD) than in the part of the tubule that curves towards the tip of the tusk (i.e. light bands) (mean distance 7.2 ± 2.8 µm SD) (Fig. 2a). This difference was significant ($P < 0.001$). The number of tubules/mm² varied between 31.6 x 103 and 54.3 x 103.

The inorganic composition of ivory is reflected in Table 1. Statistical analyses showed the differences between the respec-

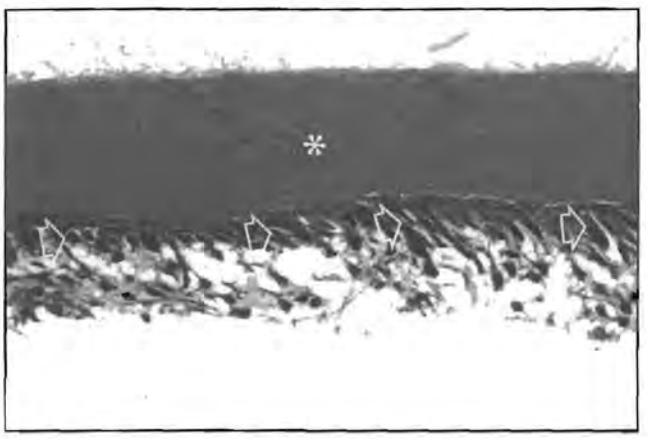

Fig. 3. Microscopic appearance of the foetal tusk. Note the newly formed ivory (asterisk) slanting of the odontoblasts and occasional cells exhibiting cell death (arrows) (H&E stain, magnification x250).

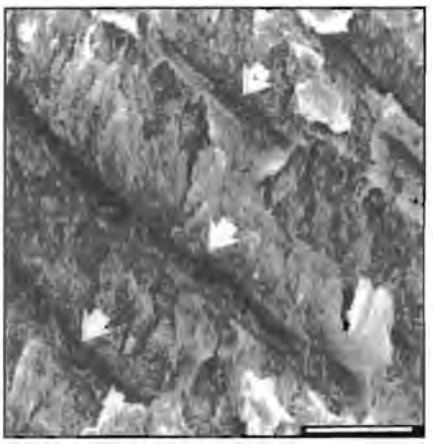

Fig. 4a. Electron micrograph of a fractured surface of ivory. Note the exposed odontogenic tubuli (arrows) (bar = 10 µm).

Fig. 4b. High power magnification of the pulpal opening of an odontoblastic tubule (bar = 1 µm).

tive elements in the following geographical locations were highly significant ($P < 0.002$):

*Calcium*: Addo vs. all other locations, Etosha vs. Caprivi, Etosha vs. Kavango and Caprivi vs. Tembe.

*Phosphate*: Kruger Park vs. Kaokoveld, Addo vs. Kaokoveld.

*Magnesium*: Addo vs. Kruger Park, Caprivi and Tembe vs. Addo and Kaokoveld vs. Caprivi.

Fluoride: Kaokoveld vs. all locations except Etosha and Etosha vs. all locations except Kaokoveld.

The following trace elements were detected in ivory (average content expressed in µg/g dry weight, SD in brackets: As:8.0 (1.4), Cd:0.4 (0.04), Cr:3.7 (0.6), Co:0.72 (0.09), Cu:2.2 (1.2), Pb:8.7 (1.2), Mn:0.9 (0.6), Hg:1.4 (0.2), Ni:0.89 (0.1), Zn:20 (10.8), Mo:0.56 (0.06) and Al:6.2 (4.3).

Table 1
*Main inorganic elements in ivory, expressed per site of origin (average mg/g dry weight, SD in brackets)*

| | KNP[1] | Kaoko[2] | Etosha | Caprivi | Kavango | Tembe | Addo |
|---|---|---|---|---|---|---|---|
| No. of Specimens | 13 | 9 | 26 | 6 | 4 | 3 | 3 |
| Ca | 195.8 (17) | 193.7 (15.9) | 192 (16) | 208.9 (6.4) | 205.9 (1.8) | 191.1 (8.9) | 170.8 (2.5) |
| $PO_4$ | 115.5 (5) | 118 (2.6) | 116 (3.5) | 114.7 (4) | 115.3 (3) | 113.1 (5) | 113 (1.4) |
| Mg | 14.6 (3.2) | 18.2 (4.2) | 15.3 (4.2) | 13.1 (0.9) | 12.2 (2.7) | 14.7 (1.2) | 17.3 (0.4) |
| F | 0.076 (0.014) | 0.106 (0.017) | 0.124 (0.029) | 0.069 (0.012) | 0.058 (0.01) | 0.054 (0.009) | 0.035 (0.019) |

[1] Kruger National Park
[2] Kaokoveld

Ivory obtained from the Kaokoveld was more brittle and hydrolysed more rapidly than those from other regions. The amino acid composition of hydrolysed ivory is expressed in Table 2. The difference in the hydroxylysine content between Kruger and Northern Namibian ivory (Kaokoveld and Etosha) was significant ($P < 0.01$) (Kruger ivory 0.7 ppm, SD 0.1; Etosha 0.4 ppm, SD 0.1; Kaokoveld 0.4 ppm, SD 0.2).

## Discussion

The cell responsible for the formation of ivory (or dentine) is the odontoblast. Odontoblasts are derived from the mesenchyme of the dental pulp and after differentiation they move centripetally (i.e. towards the axis of the tusk) and deposit ivory along their pathway. Each odontoblast is responsible for the formation of a cytoplasmic extension. Mineralisation of ivory around this extension forms tubules which traverse the diameter of the ivory. The microporosity of ivory, which is well beyond the resolution of the human eye, is responsible for the absorbent and tactile characteristics thereof, which has made it an unequalled product for the manufacturing of piano keys.

Table 2
*Total aminoacid composition of 32 samples of hydrolysed ivory*

| Aminoacid | Residues/100 | (SD) |
|---|---|---|
| Aspartic acid | 5.1 | (0.3) |
| Hydroxyproline | 9.9 | (1.0) |
| Threonine | 2.0 | (0.2) |
| Serine | 4.0 | (0.2) |
| Glutamine | 8.0 | (1.3) |
| Proline | 12.2 | (1.2) |
| Glycine | 30.8 | (1.0) |
| Alanine | 10 | (1.2) |
| Valine | 2.3 | (0.3) |
| Methionine | 0.4 | (0.4) |
| Isoleucine | 1.2 | (0.1) |
| Leucine | 3.0 | (0.1) |
| Phenylalanine | 1.5 | (0.1) |
| Hydroxylysine | 0.4 | (0.2) |
| Lysine | 2.7 | (0.7) |
| Histamine | 0.7 | (0.2) |
| Arginine | 4.6 | (0.4) |

The tip of the concial pulp becomes solid as ivory depositioning progresses and lengthening of the proximal edge coincides with forward movement and elongation of the tusk.

The centripetal movement of odontoblasts during the formation of ivory leads to a rapid decline in the pulpal circumference. As a result, odontoblasts become progressively more tightly packed and intercellular pressure increases as the pulpal circumference becomes smaller. Morphological manifestations of the increased pressure between odontoblasts are reflected as a significant reduction in the distance between odontoblastic tubules in the dark bands, the oval shape of the tubules as well as the slanting of odontoblastic cell bodies towards the pulpal opening. The only means by which the growing pressure between the centripetally moving odontoblasts on a rapidly decreasing perimeter can be accommodated, is through two processes namely, movement of the odontoblastic cell mass towards the pulpal opening or a reduction in the number of odontoblasts. There is morphologic evidence that both these phenomena occur during the formation of ivory. Movement of the odontoblastic cell bodies towards the pulpal opening coincide with the dark bands (i.e. slanting of the sinusoidal curve of the odontoblastic tubuli towards the pulpal opening). As pressure increases, the number of odontoblasts are reduced through fusion of cells (represented by fusing tubules) and cell death (represented by blind-ending tubules). The occurance of the latter phenomenon is supported by the presence of pyknotic odontoblasts seen in microscopic sections of the rapidly fixed biopsies of the foetal tusk. The relief of intercellular pressure through these mechanisms results in a change in the direction of odontoblastic movement towards the tip of the tusk. This coincides with the anteriorly directed part of the sinusoidal curve. The process of odontoblastic crowding, followed by a bodily movement of odontoblasts towards the pulpal opening and a relief of intercellular pressure through cell fusion and death, with subsequent change in the direction of movement of the cell bodies are probably responsible for the regular sinusoidal

course followed by odontoblasts. This hypothesis is reflected graphically in Fig. 5. The sinusoidal course of the tubules in ivory is reflected as parallel and alternating light and dark bands which are seen on polished surfaces prepared along the axis of the tusk. The light and dark bands were found to be the result of the varying compactness of dentinal tubules between the sectors of the sinusoidal curve of the tubules that slant towards the tip of the tusk or towards the pulpal opening respectively. On cross sections, the diamond-shaped pattern is a reflection of the alternating light and dark bands seen on surfaces prepared in length. This implies that when the layer of odontoblasts are viewed in a radial perspective, movement of odontoblasts towards the pulpal opening with curving of odontoblastic tubules does not occur at the same time but rather as a wave that spreads circumferentially along the peripulpal layer of odontoblasts. On microscopic examination, it was observed that fractures through ivory generally follow the dark bands. The higher number of tubules per unit area probably makes the dark bands weaker than the light bands.

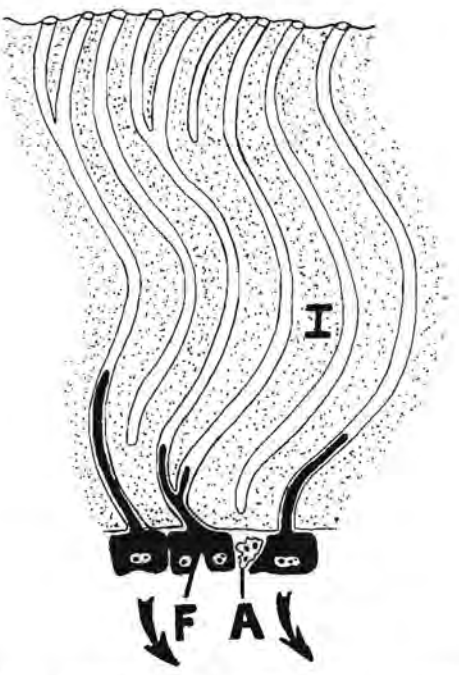


Fig. 5. Schematic representation of the sinusoidal course followed by the odontoblastic tubules (sagittal plane, the tip of the tusk is towards the right, surface towards the top and pulpal cavity towards the bottom of the figure). Note odontoblastic fusion (F) which results in odontoblastic tubules uniting and apoptosis (A) which gives rise to blind ending tubules, thereby effectively reducing the number of odontoblasts during their centripetal movement (arrows indicate the centripetal course followed by the odontoblasts, I - ivory).

Extreme care should be taken when harvesting ivory for chemical analyses. The proximal feather edge of the tusk as well as the layer of mineralised tissue ensheathing the tusk consists of cellular dental cementum and not ivory. Studies which provide no clarity on the exact part of the tusk that was harvested for chemical analyses, should be viewed with caution. During the formation of dentine (or ivory), which is essentially a hydroxyapatite deposited on an organic matrix, over 45 elements could potentially compete for incorporation (Wetherell & Robinson 1973). The inorganic composition of ivory reflects the composition of an animal's diet. Unlike bone, the composition of ivory remains stable and is not subjected to turnover and remodelling after formation thereof (Posner & Tannenbaum 1984). An extensive databank on the composition of ivory from different areas in Africa could assist in tracing the origin of ivory and might play a key role in identifying regions in which illegal ivory harvesting is taking place. This study as well as others (Van der Merwe *et al.* 1988, Van der Merwe *et al.* 1990, Vogel *et al.* 1990), clearly indicate the tracing of the source of ivory on its chemical composition to be a realistic possibility. The techniques used by these groups are expensive and the equipment used is not readily available. Our study indicated that the concentrations of calcium, phosphate, magnesium and fluoride are of potential value in identifying the site of origin of Southern African ivory. Addo, Etosha and Kaokoveld ivory in particular have unique compositions. Addo ivory was distinguished by its low calcium content and Kaokoveld and Etosha ivory by its high fluoride content.

The rapid rate of hydrolisation of ivory from the Kaokoveld and Etosha compared to other regions was of interest. The annual rainfall in these regions are low. The arid environment, characterised by dry savannah and shrub, has led to the term 'desert elephant' to those animals that were driven into the region by human inhabitation of the more arable land (Viljoen, 1987). There is good reason to accept that the diet of these elephant differ significantly from those in the other regions studied. Analyses of ivory from Kaokoveld and Etosha show the highest fluoride concentration, lowest total proline plus hydroxyproline content and under hydroxylation of lysine as unique characteristics. The high fluoride content is likely the result of the water that collects in the closed systems of salt pans and which becomes concentrated due to evaporation. Although excessive fluoride could influence the strength of the hydroxyapatite crystal (Lavelle 1975), the under-hydroxylation of lysine would affect the strength of the organic scaffold of collagen fibres (Chatterjee 1978). Vitamin C, iron and oxygen are cofactors required for the enzymatic hydroxylation of lysine during the biosynthesis of the tropocollagen molecule (Anderson 1992). Insufficient dietary Vitamin C intake, linked to the arid vegetation, is likely to be the main cause of reduced hydroxylation of lysine in the collagen of Kaokoveld and Etosha ivory.

## Acknowledgements

The author wishes to thank Mrs C.S. Begemann for typographical support, the National Parks Board and in particular Dr V. De Vos for making the tusks and fragments of ivory available and the Department of Chemical Pathology and Electronmicroscope Unit at Medunsa for technical support. This study was supported by a grant from the Foundation for Research Development.

## References

ANDERSON, J.C. 1992. Biochemical basis of connective tissue disease. Pp. 174 – 226. *In:* GARDNER, L. (ed.). *Pathological Basis of Connective tissue diseases.* Philadelphia: Lea & Febiger.

ARMSTRONG, S. & F. BRIDGLAND. 1989. Elephants and the ivory tower. *New Scientist* 124(1679):37–41.

CHATTERJEE, G.C. 1978. Nutritional deficiencies in animals: Vitamin C. Pp. 149–176. *In:* RECHCIGL, M. (ed.). *CRC Handbook series in nutrition and food, Section E: Nutritional Disorders.* Vol. 2. Florida: CRC Press.

LAVELLE, C.L.B. 1975. *Applied Physiology of the Mouth.* Bristol: John Wright.

MILES, A.E.W. & A. BOYDE. 1961. Observations on the structure of elephant ivory. *Journal of Anatomy (London)* 95:450.

POSNER, A.S. & P.J. TANNENBAUM. 1984. The mineral phase of dentine. Pp. 17–36. *In:* LINDE, A. (ed.). *Dentine and Dentinogenesis. Vol.2.* Florida: C.R.C. Press.

RAUBENHEIMER, E.J., J. DAUTH, M.J. DREYER, P.D. SMITH & M.L. TURNER. 1990. Structure and composition of ivory of the African elephant (*Loxodonta africana*). *South African Journal of Science* 86:192–193.

SIKES, S.K. 1971. *The natural history of the African elephant.* London: Weidenfeld and Nicholson.

SOGGNAES, R.F. 1960. The ivory core of tusks and teeth. *Journal of Clinical Orthopaedics* 17:43–61.

VAN DER MERWE, N.J., J.A. LEE THORPE & R.H.V. BELL. 1988. Carbon isotopes as indicators of elephant diets and African environments. *African Journal of Ecology* 26:163–172.

VAN DER MERWE, N.J., J.A. LEE THORPE, J.F. THACKERAY, A. HALL-MARTIN, F.J. KRUGER, H. COETZEE, R.H.V. BELL & M. LINDEQUE. 1990. Source area determination of elephant ivory by isotope analysis. *Nature* 346(6286): 744–746.

VILJOEN, P.J. 1987. Status and past and present distribution of elephants in the Kaokoveld, South West Africa Namibia. *South African Journal of Zoology* 22:247–257.

VOGEL, J.C., B. EGLINGTON & I.M. AURET. 1990. Isotope fingerprints in elephant bone and ivory. *Nature (London)* 346(6286): 747–749.

WETHERELL, J.A. & C. ROBINSON. 1973. The inorganic composition of teeth. P. 43. *In:* ZIPKIN, I. (ed.). *Biological Mineralization.* New York: Wiley.

Nuclear Instruments and Methods in Physics Research B 104 (1995) 638–644

NIM B
Beam Interactions with Materials & Atoms

ELSEVIER

# Trace element concentration and distribution in ivory

V.M. Prozesky[a,*], E.J. Raubenheimer[b], W.F.P. Van Heerden[b], W.P. Grotepass[b], W.J. Przybylowicz[a,1], C.A. Pineda[c], R. Swart[d]

[a] *Van de Graaff Group, National Accelerator Centre, P.O. Box 72, 7131 Faure, South Africa*
[b] *Department of Oral Pathology and Oral Biology, Faculty of Dentistry, Medical University of South Africa, Garankua, South Africa*
[c] *Groote Schuur Hospital, P.O. Box 7925, Observatory, Cape Town, South Africa*
[d] *Department of Geology, Stellenbosch University, Stellenbosch, South Africa*

**Abstract**

The trace element content and distribution in ivory from elephants and hippopotami were measured for both natural elements and elements present due to pollution. The National Accelerator Centre Nuclear Microprobe was used to investigate trace elements heavier than Ca, and distributions of these trace elements were measured over small areas (ca. 1 $mm^2$), using the Dynamic Analysis imaging method in the GeoPIXE software package. Quantitativity of elemental maps was checked by complementary point analyses in the same area as where the elemental maps were taken from and found to be accurate to within around 10%. The possibility of locating ivory on the basis of the trace element concentrations, determined by the environment in which these animals live, was demonstrated by using correspondence analysis.

## 1. Introduction

Mineralised tissue from living organisms has been the subject of many studies with analytical techniques during the last few decades [1–7], as the composition and trace elements concentration and distribution is maintained over time. Other reasons are the relatively little sample preparation necessary for analysis, and the fact that thick samples can be analysed with relative ease, due to the fairly constant composition of the matrix. Teeth, in contrast with bone, can generally be considered to be representative of the in vivo matrix for a long time after extraction. Teeth with a matrix consisting of calcium hydroxy-apatite, and ivory in particular, offer excellent opportunities to study a part of the history of an animal over a period of time, and include elements which were part of the environment, whether present naturally or as pollutants added by man. As examples, this allowed the study of trace elements in human teeth with the aim of establishing causes and catalysts for diseases [4, 5] and the effects of pollutants such as Pb on mental health [2, 3, 6]. Teeth in animals have also been analysed, yielding information on the biological process of formation [7]. The environmental history of the subject may also be traced by using the trace elemental composition of the teeth.

Mammalian ivory is a very good example of such material, and this study was aimed at establishing the effect of the environment, such as vegetation, climate and geology, on the trace element composition of ivory, especially elephant, from bearers around Southern Africa and Siberia. These elements absorbed in the plant life and water, become incorporated in the diet of the animals, and are finally reflected in the tissue of the animal, including the ivory.

One of the difficulties in controlling the sales of elephant ivory is the problem of poaching, which has led both the elephant and rhinocerous to become endangered species. For this reason there is a total ban on the sales of ivory, even for countries with legal ivory stocks obtained from culling and natural death of elephants. The development of techniques for tracing the origin of ivory is therefore extremely important to allow authorities to establish the legality of ivory in the market. The determination of trace element concentrations could contribute to solve some of the above problems and this study was partly aimed to determine the possibility of localising ivory on the basis of trace element concentrations, as measured by the PIXE technique.

* Corresponding author.

[1] On leave from the Faculty of Physics and Nuclear Techniques, Academy of Mining and Metallurgy, Cracow, Poland.


*SSDI* 0168-583X(95)00471-8

A further advantage of determination of trace element concentrations in ivory, is the fact that environmental pollution might be detected in the ivory of bearers from different areas. The Eastern Transvaal in South Africa, which includes the Kruger National Park, is partly industrialised with most of these industries based on the extraction of minerals. The detection of heavy elements, which invariably end up in the rivers of these areas, also led to the study of pollution as a function of time and geographical area in ivory bearers. For example it has been shown before that the Olifants river has a F content 5 times higher than normally found in similar areas [8].

Although the PIXE technique has been applied successfully in many studies of teeth, the study of ivory has not received a lot of attention. Elephant and rhino ivory have previously been studied with NAA [9, 10], with the aim of localising ivory from different areas, based on different isotopic ratios (e.g. C, N and Sr) and concentrations of different trace elements. The technique uses the fact that the isotopic ratios and concentrations of elements vary from region to region, due to differences in the environmental conditions. In this pilot study nine trace elements were detected in samples of ashed and raw ivory samples. Samples from different regions could be separated with the aid of statistical packages, such as correspondence analysis, although the number of samples analysed was small, with insufficient statistical information.

## 2. Ivory and sample preparation

The ivory matrix consists of calcium-hydroxy-apatite (CHA), offering an excellent matrix for PIXE analysis of heavy elements. The CHA is partly formed as an amorphous and crystalline structure. A schematic of elephant ivory, with an indication of the growth direction, is indicated in Fig.1. The growth of the ivory is initiated in the pulpal cavity, and the tissue is transported in helical tubili to the growth sites, on the outside of the dentine. The site from where the samples were taken from, is indicated by a polygon.

The ivory samples were cut with a saw, and these surfaces were polished with diamond paste. Paste with grain sizes of 6 and 1 μm were used consecutively, with the resulting surface polished to a high quality. The diamond paste and polishing cloth were separately analysed to establish the possibility of contamination of the samples during polishing. The highest contribution to contamination was found for the diamond paste, with a Cu concentration of around 20 ppm. Considering the concentration of paste left on the surface after polishing, this was considered negligible. The samples were nevertheless then washed in distilled and demineralised water, and wiped dry with the same polishing cloth. Although the ivory samples did not produce significant charge-up problems during analysis, the samples were coated with a thin layer of carbon to ensure that conduction of beam charge was adequate.

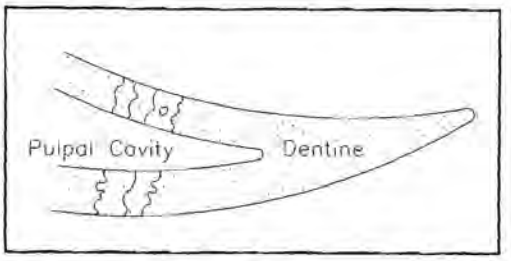


Fig. 1. A schematic of elephant ivory, with the growth direction indicated. The tissue for deposition is transported in the helical tubili for deposition on the outside of the dentine. The location where the samples analysed were taken from is also indicated.

## 3. Experimental

The Nuclear Microprobe (NMP) [11, 12] of the National Accelerator Centre (NAC) was used for the analysis. The beam energy selected was 3.0 MeV protons, and the X-rays were detected in an 80 $mm^2$ Si(Li) detector situated at 135°, with an energy resolution of 175 eV at 5.9 keV. The facility has been described before [11, 13], and details can be obtained from these references. Secondary electrons were maintained on the target using an electron suppression ring with a negative bias of 1500 V. The bulk of the X-rays from Ca were filtered out from the spectra using an 80 μm Al filter. All single point analyses were made with a total collected charge of 2.5 μC. These spectra were analysed using the GeoPIXE software package [14], with full thick target corrections applied. Elemental maps were also collected to study the variation of trace element concentrations as a function of position. The Dynamic Analysis (DA) method of mapping incorporated in this software package, in conjunction with the XSYS [12] data accumulation system, allowed the aquisition of true elemental maps during on-line analysis. The beam size used was around 10 × 10 μm, both for the line scans and the elemental mapping.

## 4. Results

### *4.1. Line scans and elemental maps*

Care was exercised after it was found that some elements, such as Zn, were fairly mobile during beam bombardment. This was studied as a function of ion current and total dose, with the total dose alone showing no contribution to changes in any of the studied trace elements. The beam current was then optimised so as to

ensure no change in elemental concentrations, still ensuring that adequate detection limits could be obtained in a relatively short time. The beam current used was always around 5 nA.

A typical set of results for a few ivory samples are indicated in Table 1, with ivory from different geographical areas yielding different sets of concentrations. The table indicates the elements of interest, with the highest yield for trace elements obtained from Sr, which is biologically competing with Ca. A high yield for Fe was obtained for the Siberian ivory, values which were more than an order of magnitude larger than for all the other samples from other areas in Southern Africa. The lower limits of detection (LLD) were calculated using a 99% confidence interval, and the error values include a 3% filter error.

After establishing that the trace element concentrations were deviating on a relatively small scale in single ivory samples, line scans were made for different areas on the ivory. The results showed large deviations from most of the elements, with some of the results for a Siberian ivory specimen indicated in Fig. 2(a)–(c). In these figures the trace element concentration is indicated as a function of position, with the distance scale corresponding to 1.8 mm.

To eliminate the possibility of beam induced effects, the scan was made in both directions, the backward steps filling the gaps of the forward scan. Elements such as Mn, Zn and Sr showed the largest deviations, with maximum variations of up to 40% for Mn and Zn, and 12% for Sr.

These variations prompted the use of the elemental mapping facility of the GeoPIXE software package, and elemental maps were accumulated for a sample from the Kruger National Park. The scan size used was $1.3 \times 1.3$ mm. The resulting maps of Ca and Sr are indicated in Fig. 3 (a) and (b), showing marked variation in content as a function of position. The scales shown on the right-hand side of the maps are in ppm, and are the result of the quantitative mapping facility of GeoPIXE. Data presentation was made by the Interactive Data Language (IDL) package [15] and the maps are contours linking pixels with similar values.

The variations in these elements complement the line scan results, with large deviations in concentrations over a relatively small area. Although the samples analysed were too small to confirm ( $< 3 \times 3$ mm), the results may show a 'tree ring' effect, of variations based on seasonal variations due to rain and plant differences. This is strengthened by comparing the growth rate of 2 mm per year for elephant ivory. There is also a positive correspondence with the Sr content of the light and dark bands optically seen in ivory, with dark areas containing significantly less Sr than the lighter areas. It is also clear that the concentrations of Sr and Ca are positively correlated.

Quantitativity of elemental maps was checked by complementary point analyses in the same area where

Table 1
A typical set of results of trace element concentrations for ivory samples from different geographical areas

| Location | Fe | FeLLD | Zn | ZnLLD | Br | BrLLD | Sr | SrLLD | Ag | AgLLD | Pb | PbLLD |
|---|---|---|---|---|---|---|---|---|---|---|---|---|
| Siberia | 2338 ± 147 | 3.8 | 49.0 ± 1.5 | 1.8 | < LLD | 1.5 | 710 ± 11.4 | 2.1 | 26.3 ± 3.0 | 4.4 | 12.9 ± 2.2 | 3.2 |
| Kruger Park | 6.7 ± 1.5 | 3.4 | 183 ± 5.6 | 2.4 | 2.1 ± 0.5 | 1.7 | 268 ± 4.5 | 2.0 | 21.3 ± 3.6 | 6.8 | < LLD | 3.9 |
| Addo Park | 48.1 ± 3.6 | 3.8 | 34.8 ± 1.6 | 2.0 | 3.8 ± 0.5 | 1.5 | 372 ± 6.7 | 2.2 | 19.1 ± 3.0 | 5.8 | 7.2 ± 1.5 | 3.4 |
| Botswana | 2.9 ± 1.4 | 4.2 | 39.3 ± 1.4 | 2.2 | < LLD | 1.7 | 143 ± 4.0 | 2.1 | 19.2 ± 3.2 | 7.0 | < LLD | 3.8 |
| Namibia | 9.1 ± 1.5 | 3.6 | 44.2 ± 1.7 | 2.4 | 3.5 ± 0.7 | 1.8 | 883 ± 16.7 | 2.2 | 35.6 ± 3.9 | 7.2 | < LLD | 4.2 |
| North Natal | 15.4 ± 1.9 | 3.6 | 37.5 ± 1.4 | 2.3 | < LLD | 1.8 | 350 ± 5.5 | 1.8 | 23.4 ± 4.4 | 6.8 | < LLD | 4.1 |
| Hippo | 7.9 ± 1.6 | 3.9 | 55.6 ± 1.9 | 2.7 | 3.1 ± 0.5 | 1.8 | 329 ± 6.0 | 2.1 | 23.3 ± 3.5 | 7.7 | < LLD | 4.5 |

Results are given in ppm.

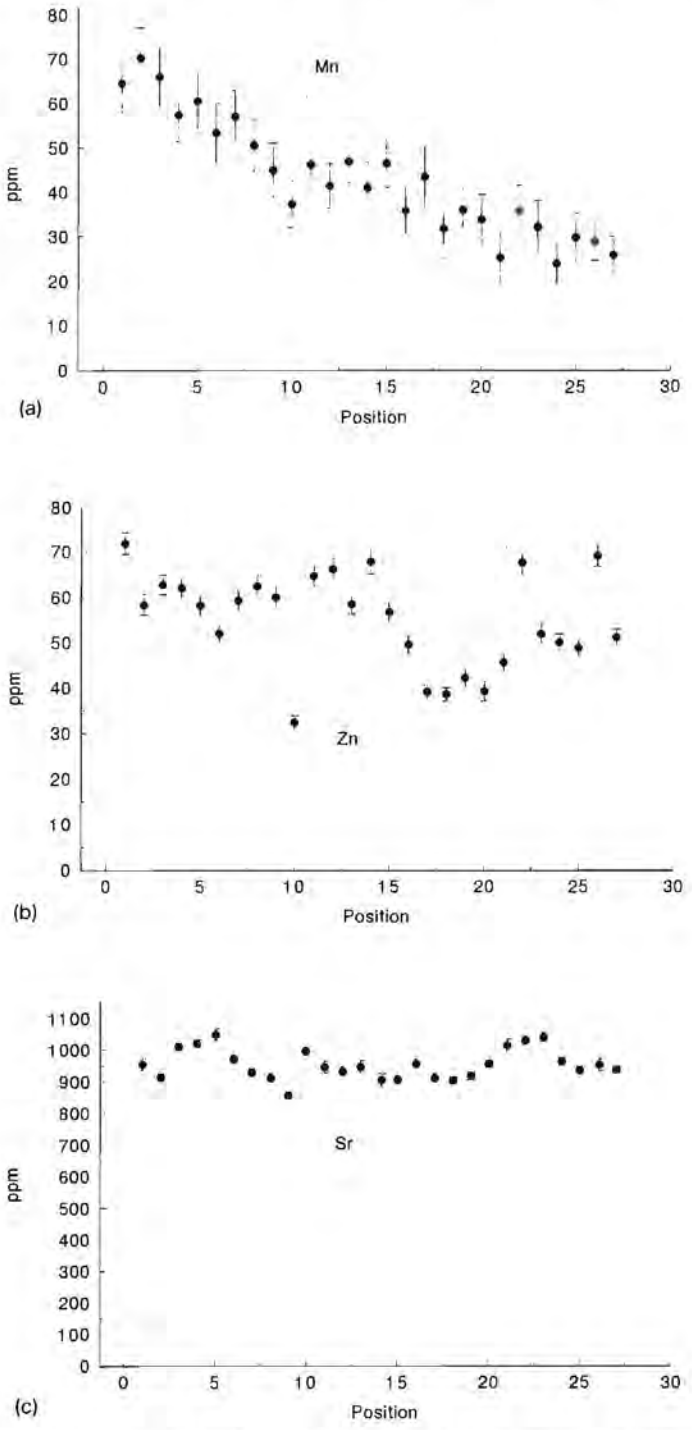


Fig. 2. Results of line scans across an ivory sample, indicating the changes in trace element concentrations for (a) Mn, (b) Zn and (c) Sr. The full scale of the $X$-axis is 1.8 mm. The points were analysed in both the forward and backward direction.

Results are given in ppm.

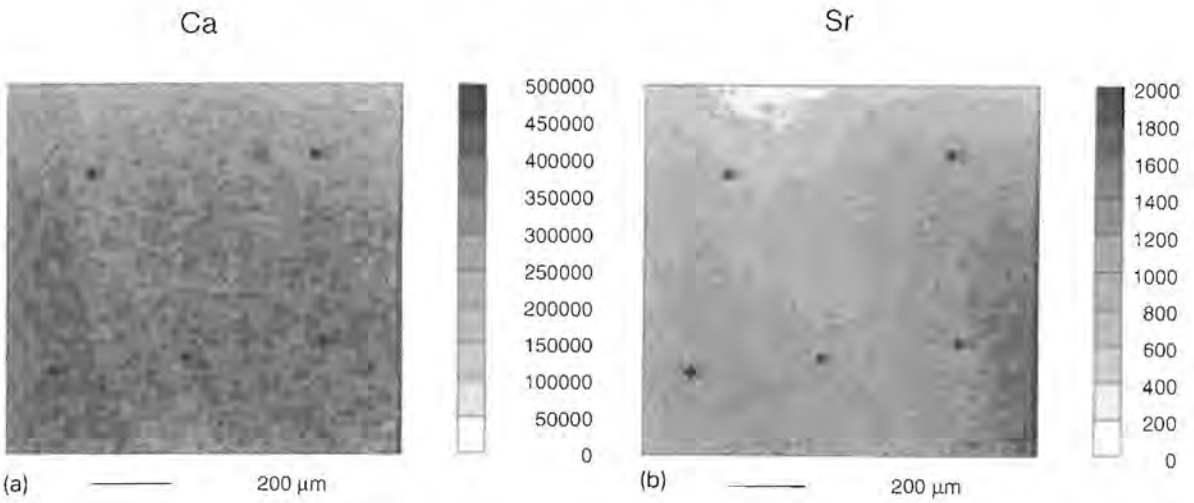


Fig. 3. Elemental maps (1.3 × 1.3 mm) for a sample from the Kruger National Park for (a) Ca and (b) Sr concentration. The intensity scale on the right-hand side of the maps are in ppm. The numbered dots on the maps are the spots analysed to compare with the mapping results. The comparisons are given in Table 2.

Table 2
Comparison of the results of the point analyses and mapping. The points are indicated as small numbered dots on the maps. The results of the mapping are given as the range of the pixel value at that specific spot in the map, compared to the accurate results of the point analyses. The numbers of the points are indicated in Fig. 3(a) and (b)

| Position | Ca concentration (point) (%) | Ca concentration (map) (%) | Sr concentration (point) (ppm) | Sr concentration (map) (ppm) |
|---|---|---|---|---|
| 1 | 34.9 ± 10.5 | 34.4 – 37.5 | 592 ± 9.0 | 625 – 750 |
| 2 | 40.7 ± 12.3 | 37.5 – 40.6 | 615 ± 11.4 | 625 – 750 |
| 3 | 33.7 ± 10.2 | 28.1 – 31.3 | 503 ± 9.5 | 500 – 625 |
| 4 | 39.0 ± 11.8 | 37.5 – 40.6 | 896 ± 16.3 | 1000 – 1125 |
| 5 | 26.5 ± 11.4 | 25.0 – 28.1 | 812 ± 13.3 | 875 – 1000 |

elemental maps were taken from. These points are indicated in Fig. 3(a) and (b) as small numbered dots. The comparison of results of point analyses and mapping results is shown in Table 2. The results of the mapping are given as the range of the pixel value at that specific spot in the map, compared to the results of the point analyses. The results compare favourably, and the mapping results typically agree within 10% of the accurate point analyses. The relatively large error bars of the Ca results are due to the 80 μm Al filter used to reduce the yield of Ca X-rays in the spectrum.

The results of Table 1 also showed no correlated enhancement of elements associated with pollution, such as Pb, Br and Ag. This might be due to the relatively low density of industries in areas with game parks, and might indicate that the rivers are not significantly polluted with heavy metals.

### 4.2. Point analyses

With the large variations obtained it is clear that the analysis of single points with a small beam size would yield erroneous results in attempting to determine the trace element concentrations in ivory. For this reason the beam was defocused to around 80 × 80 μm to allow the analysis of a more representative area of the ivory. In addition to this, three spots were analysed per sample, and the results averaged for final analysis. For this analysis a group of hippopotamus ivory was included. These animals were all from one area, and were considered to be a separate grouping, in addition to the elephant groupings.

From the results in Table 1, it is clear that the localisation of the ivory bearers could not be made by using one or two elements, and that more complex multivariate

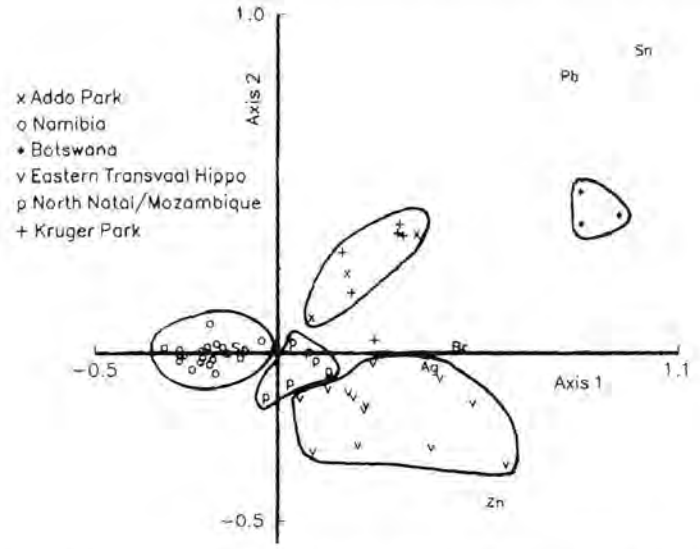


Fig. 4. Plot of the first two axes of the correspondence analysis data showing groupings of ivory from different geographical areas.

techniques should be used to include information on a variety of trace elements studied. The correspondence analysis package SIMCA [16] was used to group the results according to trace element concentration. The elements used were Zn, Br, Sr, Sn, Pb and Ag. The results of the statistical analysis are shown in Fig. 4. The grouping of the ivory is shown in two dimensions which contain almost 90% of the inertia, with the dimensions calculated on the basis of the trace element concentrations. Results from three pieces of ivory from Siberia are not included in the statistical analysis, as they are so far separated from the other results that they distort the scale. In Fig. 4 these results would be about −2.0 on Axis 1 and 0 on Axis 2. There is a strong correlation between the samples from the Kruger National Park and the Addo Park. It is not impossible, however, that elephants from the Kruger Park were relocated in the Addo Park, as such actions are executed from time to time. There is also one outlier in the Kruger Park results, that did not conform to the tight grouping of the rest of the Kruger Park samples. This sample, however, did not lead to overlap with other groups.

## 5. Conclusions

We have shown that trace element concentrations in ivory offer exciting results in terms of differences on a microscale, with environmental effects, such as season, water and plants, playing a role. It was also possible to localise ivory from different geographical areas with the aid of statistical correspondence analysis, showing trace element variation on the macroscale. These results offer new possibilities for localising ivory in trade, and might lead to the detection of poached ivory.

## Acknowledgements

The authors gratefully acknowledge the cooperation of the South African Parks Board, and we thank them for the ivory supplied.

## References

[1] M. Ahlberg and R. Akselsson, Int. J. Appl. Rad. Iso. 27 (1976) 279.
[2] B. Möller, L.E. Carlsson, G. Johansson, K.G. Malmqvist, L. Hammarström and M. Berlin, Scand. J. Work. Envir. Health 8 (1982) 267.
[3] K. Haavikko, A. Antilla, H. Helleland and E. Vuori, Arch. Envir. Health 37 (1984) 78.
[4] H.J. Annegarn, A. Jodaikin, P.E. Cleaton-Jones, J.P.F. Sellschop, C.C.P. Madiba and D. Bibby, Nucl. Instr. and Meth. 181 (1981) 323.
[5] I.D. Svalbe, M.A. Chaudri, K. Traxel, C. Ender and A. Mandel, Nucl. Instr. and Meth. B 3 (1984) 651.
[6] M.A. Chaudri and T. Ainsworth, Nucl. Instr. and Meth. 181 (1981) 333.
[7] G.W. Grime, F. Watt, S. Mann, C.C Perry, J. Webb and R.J.P. Williams, Trend. Biochem. Sci. 10 (1985) 6.
[8] E.J. Raubenheimer et al., South African J. Wildlife Res. 20 (4) (1990) 127.

[9] R.J. Hart, Annual Report of the Schonland Research Centre for Nuclear Sciences (1992) p. 30.
[10] R.J. Hart and M. Tredoux, Abstract in Nucl. Anal. Meth. Life Sci., Prague, Czech Republic, 13–17 September 1993.
[11] U.A.S. Tapper, W.R. McMurray, G.F. Ackermann, C. Churms, G. de Villiers, D. Fourie, P.J. Groenewald, J. Kritzinger, C.A. Pineda, J. Pilcher, H. Schmitt, K. Springhorn and T. Swart, Nucl. Instr. and Meth. B 77 (1993) 17.
[12] C.L. Churms, J.V. Pilcher, K.A. Springhorn and U.A.S. Tapper, Nucl. Instr. and Meth. B 77 (1993) 56.
[13] V.M. Prozesky et al., these Proceedings (ICNMTA '94), Nucl. Instr. and Meth. B 104 (1995) 36.
[14] C.G. Ryan and D.N. Jamieson, Nucl. Instr. and Meth. B 77 (1993) 203.
[15] Interactive Data Language, User's Manual, Version 3.1, RSI Inc., Boulder, USA.
[16] M.J. Greenacre, SIMCA – Version 2, PC Software for Correspondence Analysis (1990).

# THE MYOEPITHELIAL CELL: EMBRYOLOGY, FUNCTION, AND PROLIFERATIVE ASPECTS

Author: Erich J. Raubenheimer
Department of Oral Pathology and Oral Biology
Medical University of Southern Africa
Medunsa, Republic of South Africa; and
South African Medical and Dental Council
Republic of South Africa; and
South African Immunochemistry Society
Republic of South Africa

Referee: John G. Batsakis
Department of Pathology
University of Texas System Cancer Center
M. D. Anderson Hospital
Houston, Texas

## I. INTRODUCTION

Myoepithelial cells (or basket cells) were accurately described and illustrated in salivary, lacrimal, mammary, and sweat glands by histologists of the previous century. They lie within the epithelial basement membrane of the secretory and terminal ductular portion of most exocrine glands and display a cytoplasmic organization quite similar to smooth muscle cells. Although the structure of myoepithelial cells is agreed upon, divergent views are held on many functional and developmental facets and their participation in proliferative glandular disorders. These differences of opinion are the result of nonspecific criteria which had been employed during myoepithelial identification and serve to underscore the subjectivity of conventional light and electron microscopic studies. The rapidly developing fields of immunocytochemistry and immunoelectron microscopy invalidated some long-held concepts and facilitated a surge of advanced information on myoepithelial proliferations, especially in the neoplastic state when definition of participating cells becomes difficult. This paper will revise the current status of myoepithelial research, concentrating on pertinent aspects of their development, functions, microscopic identification, and participation in pathologic conditions of exocrine glands. For more detailed information on the structure of myoepithelial cells in salivary, mammary, and sweat glands, readers are referred to other sources.[1-4]

## II. EMBRYOLOGY AND FUNCTIONS

### A. Salivary Gland Myoepithelium

#### *1. Embryology*

It is generally accepted that the major and a significant number of minor salivary glands are of ectodermal origin; the remainder is derived from entoderm. From their respective germ layers, buds of proliferating progenitor cells extend into the adjacent mesenchyme to form a proximal and a distal epithelial cell mass. The proximal cell mass (excretory duct reserve cell) ultimately gives rise to the main excretory duct and the inter and proximal intralobular ducts.

Reprinted from the CRC Critical Reviews in Clinical Laboratory Sciences, Vol. 25, Issue 2, pages 161–193, © 1987 by CRC Press, Inc.

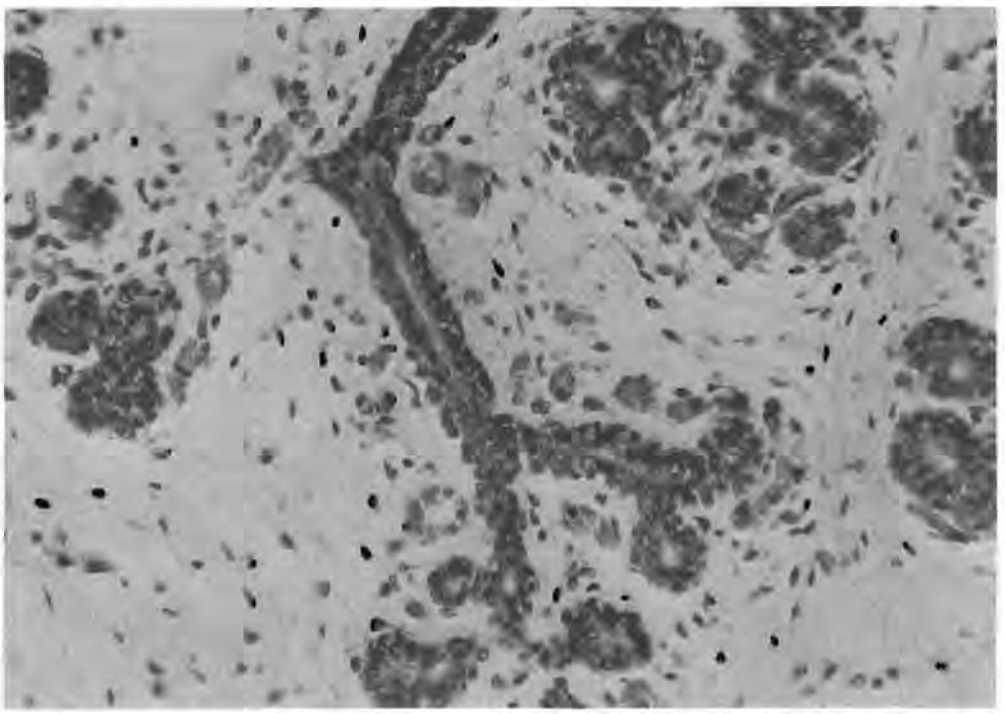

FIGURE 1. A 22-week-old fetal parotid. Formation of terminal tubules. (Hematoxylin-eosin; magnification × 200.)

In the distal cell mass, an elegant process of microfilament contraction narrows the basal portion of discrete groups of cells so that they appear to sink inwards forming clefts.[5,6] Several well-formed epithelial branches extend into the mesenchyme and each terminates in one or more cellular bulbs. Lumen formation gives rise to terminal tubules (Figure 1) lined by progenitor cells which eventually differentiate into intercalated duct cells and other specialized cells of the secretory unit.[7] Myoepithelial and secretory epithelial differentiation, which takes place mainly during postnatal life,[8] appears to be synchronized.[9] Most workers believe that both of these cell types lose their mitotic capacity when fully differentiated.[7,10,11]

In mature human salivary glands, the pluripotential intercalated duct cell or IDC (also referred to as the intercalated duct reserve cell) gives rise to other IDCs, acinar cells, striated duct cells, and myoepithelial cells.[1,7,10,12] The excretory duct reserve cell (or EDRC) acts as stem cell compartment for the remainder of the ductular system (Figure 2). Clear cells which are present in the secretory unit of the submandibular gland transform directly into myoepithelium[13] and should be regarded as an intermediate stage in their development.

Interaction between epithelial cells of the developing salivary gland and mesenchymal elements, basement membrane proteins, and nerve axons appears to be of fundamental importance during the process of morphogenesis and cytodifferentiation; epithelial mesenchymal contacts through the basement membrane of the developing rat submandibular gland have been identified[14] and it has also been proven that collagen is involved in initiating new branching points and stabilizes epithelium participating in this process.[15,16] Furthermore, branching morphogenesis is dependent on the presence of extracellular basement membrane proteoglycan[17] (an acid mucopolisaccaride) and epithelial nerve contacts have been postulated to play a role in salivary gland epithelial differentiation.[7]

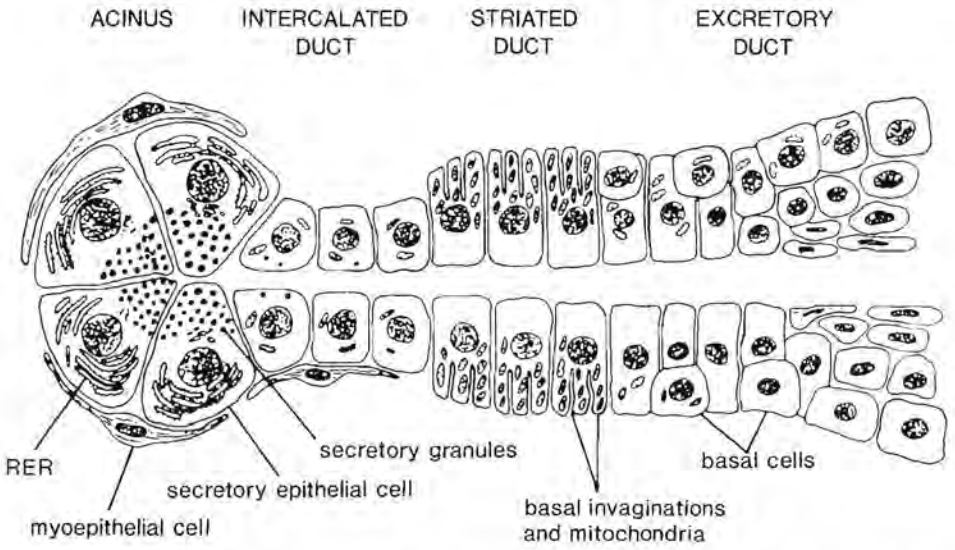


FIGURE 2. Schematic representation of the components of a human salivary gland unit. (Redrawn from Batsakis, J. G., *Tumors of the Head and Neck, Clinical and Pathological Considerations*, Williams & Wilkins, Baltimore, 1979, chap. 1. With permission.)

*2. Functions*

Evidence from structural and functional studies supports the belief that salivary gland myoepithelium has a contractile function.[18-21] Although species differences do exist, these cells have a dual innervation by parasympathetic as well as sympathetic nerves and impulses from both types cause contraction.[22-24] Synchronization of contraction is made possible by gap junctions and overlaps between myoepithelial cell processes.[25,26]

Contraction of the stellate-shaped acinar myoepithelial cells facilitates expulsion of secrete by rupturing "ripe" mucus cells,[21] reducing lumenal volume[22] and preventing distention of acini.[25,27] The acini of the rat,[28-30] rabbit,[31] and African elephant *(Loxodonta africana)*[237] parotid glands which excrete a watery product are devoid of myoepithelial cells. This phenomenon is the most likely explanation for the lower intraductal pressure developed by the rat parotid in comparison with that of the submandibular gland during autonomic stimulation.[32] The sublingual gland of the monotreme echnida, *Tachyglossus aculeatus*, which secretes an extremely viscous saliva, shows well-developed acinar myoepithelial cells, almost forming a complete muscular coat around the endpieces.[11] A similar arrangement has been demonstrated in the submandibular salivary gland of the African elephant (Figure 3). The saliva produced by this gland is, however, of a watery (serous) nature and factors other than the viscosity of the secrete also appear to have a bearing on the prominence of acinar myoepithelial cells.

Acinar myoepithelial contraction may modify the concentration of saliva by decreasing the surface area of the secretory apparatus exposed to interstitial fluid.[21] Such an effect would diminish loss of fluid into the tissues and is probably important when viscid saliva has to be forced through narrow ductules in a gland.[22] Myoepithelial cilia, projecting into invaginations in adjacent secretory cells,[11,21,22] may act as chemoreceptors in this regard as they have been postulated a sensory function.[21]

Contraction of elongated myoepithelial cells surrounding the intercalated ducts shortens and widens these structures,[28,33,34] thereby overcoming peripheral resistance. Extension of their processes onto the proximal regions of allied acini facilitates rigidity and patency in glands which may become distorted by masticatory movements.[28]


FIGURE 3. Scanning electron micrograph of acinar myoepithelium in the submandibular salivary gland of the African elephant after removal of the basement membrane. Note the interdigitating myoepithelial cell processes.

The role of the myoepithelial cell in transportation of metabolites to and from secretory cells is a controversial issue.[22,35] Basal infoldings of human submandibular salivary gland myoepithelium[36] and finger-like extensions on the surface of rat lacrimal myoepithelium[37] could serve to increase the surface area[36] and pinocytotic vesicles;[21,38] positive staining for the iron binding protein ferritin[39] and high levels of alkaline phosphatase and magnesium-dependent adenosine triphosphatase (ATPase) activity[40,41] are all features supporting active myoepithelial involvement in the transportation of metabolites involved in the secretory process. It has been pointed out, however, that ATPase and adenylate cyclase activity in myoepithelial cells of the palatine glands of rats are rather implicated in cell contraction and that the vesicle-like structures are in fact invaginations of the plasma membrane and continuous with the extracellular space.[42]

Finally, myoepithelial cells are important in the formation and maintenance of the basement membrane. Fibronectin, laminin, and elastin are major components of basement membranes and are found to be produced by myoepithelial cells.[39,43] Any epithelial cell in a basal location, however, could be expected to synthesize basement membrane components.[44]

## B. Mammary Gland Myoepithelium

### *1. Embryology*

A thickening of the ectoderm, the ectodermal ridge (or milk line), appears on the anterior body wall during the sixth week of intrauterine development. Normally the thickening regresses except in the pectoral region, where, during the 5th month of intrauterine life, a group of 15 to 20 solid chords grow deeper into the subcutaneous

(s.c.) tissue.[46] After a process of branching and lumen formation which extends throughout juvenile life, the distal portions (or terminal buds) differentiate into two cell types. Radioactive thymidine studies[46] have indicated that these cells represent two distinct lineages; the outer layer ultimately develops into myoepithelium and the inner lumenal epithelium. The early stage of differentiation of myoepithelial cells is characterized mainly by slight condensation of chromatin, numerous polyribosomes, and sparse myofilaments.[47] These cells are probably identical to type I promyoepithelial cells described on immunohistochemical grounds.[48] In a later stage of development, myoepithelial precursors are characterized by rather well-developed ergastoplasmic cisternae and Golgi apparatus, association of myofilaments to form bundles, and the appearance of dense bodies and small attachment areas. These cells are closely associated with basement membrane deposits[47] and correspond to the type II promyoepithelial cell.[48] Although a simple stem cell origin for myoepithelial and lumenal epithelial cell types is not supported by all workers,[49] in vitro tissue culture[50] and ultrastructural studies[47,51] favor this concept. A recent immunohistochemical investigation[48] failed to identify cells with markers for both lineages, an indication that the long-held view of transition between myoepithelial and lumenal epithelial cell types is incorrect.

Multiplication of stem cells, two cell-type differentiation, and cellular maturation in the terminal buds are controlled by both hormones and environmental factors. Estrogen, progesterone, insulin, relaxin, and pituitary polypeptide growth hormones stimulate mitotic activity and facilitate extension of the ductular system.[47,52-54] In males, testosterone, that begins to be secreted in midgestation, inhibits growth and development of the ductules.[55] Hormonal factors may also play a role in selecting morphologic cell types during stem cell differentiation.[56] Attachment of breast epithelial cells to type IV (basement membrane) collagen is a specific environmental requirement for multiplication and differentiation.[57-59] This process is enhanced by the presence of laminin, a glycoprotein found in the lamina lucida of basement membranes, which binds to type IV collagen forming a laminin-type IV collagen complex.[56,58,60] Breast epithelial cells do not grow on type I collagen[57] and collagenase-digested epithelial explants proliferate less markedly than nonenzyme-treated duct explants.[61]

Hormones released during pregnancy result in slight hyperplasia of myoepithelial cells,[62,63] followed by epithelial cell proliferation and formation of the first true lobuloalveolar structures.[49] Before parturition lumenal cells of the acinus enlarge due to their accumulation of secrete and myoepithelial cell processes are stretched and become thin and tenuous.[62] Portions of the secretory epithelial cells bulge outwards and appear to embed myoepithelial cell processes (Figure 4). The number of myoepithelial cells and primary cytoplasmic processes per cell remains unchanged, but that of secondary and tertiary processes increases moderately.[64,65] Myoepithelial hypertrophy ceases by the end of pregnancy.[66]

Electron microscopic investigation of the normal female breast identified, in addition to myoepithelial cells, basally located clear cells.[67] These cells were initially regarded as variants of myoepithelium.[68] A more recent ultrastructural study,[69] however, has proved the clear cells to be unrelated to epithelium and to have phagocytic capacity with an important role in the uptake of cellular debris after lactation. This phenomenon has led Hamperl[70] to incorrectly hypothesize a phagocytic function for myoepithelium.

*2. Functions*

Myoepithelial contraction in the lactating female breast facilitates ejection of milk and is triggered by oxytocin, a pituitary hormone released after mechanical stimulation of the nipple. Specific oxytocin binding sites are present in the cytoplasmic membranes


FIGURE 4. Scanning electron micrograph of acinar myoepithelial cells in the lactating mammary gland of the African elephant after removal of the basement membrane. Note acinar enlargement, stretching of myoepithelial processes, and outward bulging of portions of secretory cells.

of isolated myoepithelial cells,[71] and due to close intercellular contact, stimulation leads to contraction of a functional syncitium of cells.[72] Oxytocin receptor affinity and availability appear to be modified by the presence of certain metal ions.[71] Myoepithelial sensitivity increases with pregnancy and is the greatest post partum. This is the result of an increase in the number of receptor sites on hypertrophied and elongated myoepithelial cells of the lactating breast. Elevation of myoepithelial oxytocin receptor concentration appears to persist after postlactation involution, a phenomenon which facilitates removal of dead secretory epithelial cells by myoepithelial contraction.[71] Furthermore, during postlactation involution, myoepithelial cells are more resistant to degeneration than secretory epithelium and apparently play an important role in maintaining structural integrity of the acinus.[73] The terminal ductules, around which myoepithelial cells are arranged longitudinally, have been shown to widen and shorten in response to oxytocin at a state of involution when degenerating alveoli no longer secrete milk.[33] This dilatation reduces the chance of ductular obstruction during passage of cellular debris.

The myoepithelial cell membrane forms part of the hypothetic epithelial stromal junction (ESJ) of the mammary gland which consists of the plasma membranes of epithelial and myoepithelial cells, intercellular substance, basement membrane, adjacent fibrillar connective tissue, and a layer of delimiting fibroblasts.[74] Transport of metabolites to and from secretory cells is mediated by the ESJ. The concentration of alkaline phosphatase, an enzyme implicated in the transport of substances over cell membranes, was demonstrated to be ten times greater in myoepithelial cells than in purified lumenal epithelium.[71] In addition, the presence of transferrin[75] and frequent pinocytotic vesicles[69] appears to be more than adequate for myoepithelial cell metabolism especially if their relatively low anabolic requirement (proven by the scanty cyto-

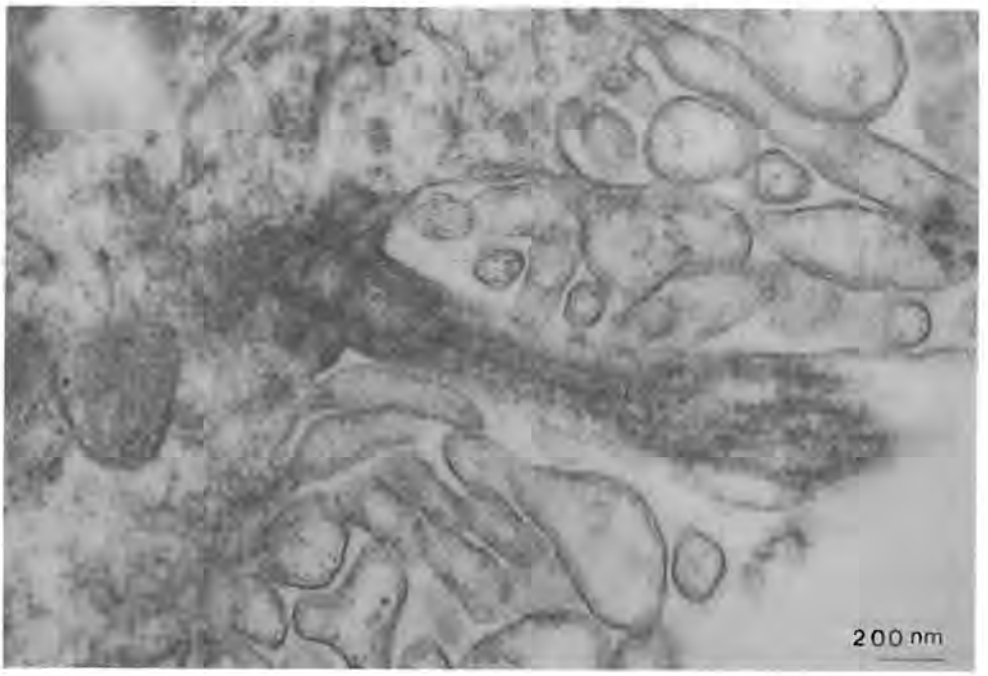


FIGURE 5. Transmission electron micrograph of a cultured rat mammary myoepithelial cell cilium.

plasmic organelles) is taken into account. Morphologic evidence therefore indicates that myoepithelial cells may in fact participate in the transportation of metabolites to and from secretory cells. Plasmalemmal interdigitations and microvilli on surfaces in contact with adjacent secretory cells[69] may serve to enlarge the cell-to-cell contact area, a feature which could increase the effectiveness of a proposed transport mechanism.

Myoepithelial cells synthesize fibronectin, laminin, and collagen type IV[59,76] and are probably responsible for the production of most of the epithelial basement membrane of the breast.[59,76-79] As indicated earlier, basement membrane components are necessary not only for growth and differentiation, but also mammary cell survival.[80] Accumulation of basement membrane deposits seen in the lactating mammary gland is evidence of increased myoepithelial metabolic activity. On the other hand, degeneration of the basement membrane in the involuting gland is a sign of decreased myoepithelial anabolism[77] and leads to a loss of secretory epithelial cell viability.[59]

The function of myoepithelial cilia (Figure 5), which are in close contact with secretory epithelial cells, is speculative. They may act as mechano- or even chemoreceptors and initiate contraction upon stimulation.[81]

## C. Sweat Gland Myoepithelium

### *1. Embryology*

The stratum germinativum of the embryonal skin differentiates into three distinct progenitor cell populations. The basal cells give rise to the keratinizing epidermis, primary epithelial germs to hair follicles, sebaceous glands and apocrine glands and eccrine gland germs to eccrine glands.[82] Of all these structures, only the secretory portions of apocrine[4,83] and eccrine glands[84] contain myoepithelial cells.

Both primary epithelial and eccrine gland germs initially consist of crowding of deeply basophylic cells in the basal layer of the epidermis. Proliferation of these cells gives rise to solid epithelial buds which protrude into the dermis.[82]

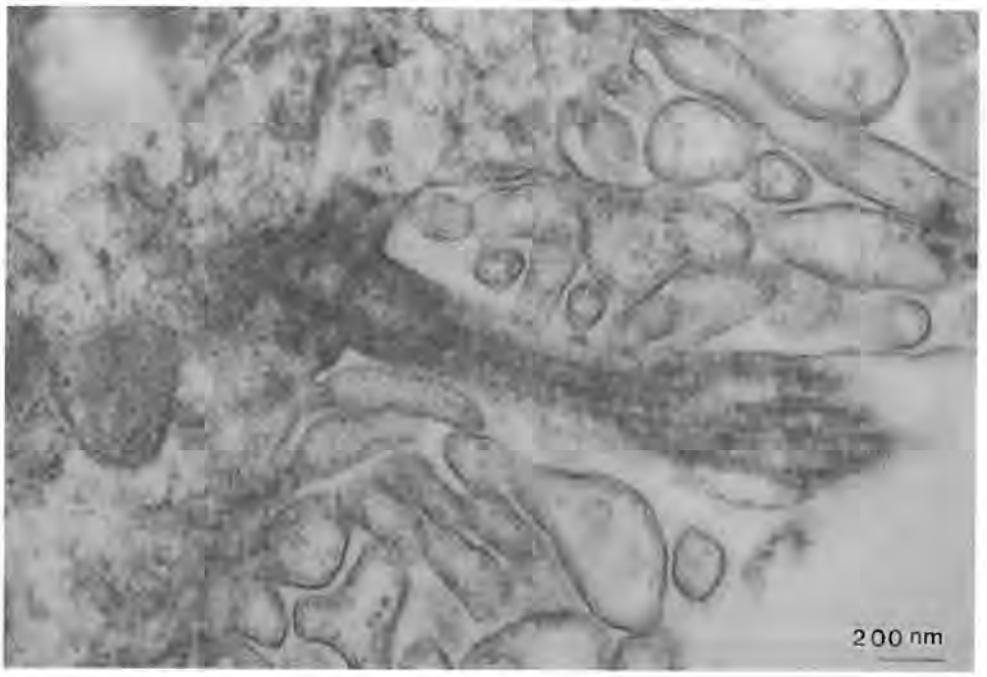


FIGURE 5. Transmission electron micrograph of a cultured rat mammary myoepithelial cell cilium.

plasmic organelles) is taken into account. Morphologic evidence therefore indicates that myoepithelial cells may in fact participate in the transportation of metabolites to and from secretory cells. Plasmalemmal interdigitations and microvilli on surfaces in contact with adjacent secretory cells[69] may serve to enlarge the cell-to-cell contact area, a feature which could increase the effectiveness of a proposed transport mechanism.

Myoepithelial cells synthesize fibronectin, laminin, and collagen type IV[59,76] and are probably responsible for the production of most of the epithelial basement membrane of the breast.[59,76-79] As indicated earlier, basement membrane components are necessary not only for growth and differentiation, but also mammary cell survival.[80] Accumulation of basement membrane deposits seen in the lactating mammary gland is evidence of increased myoepithelial metabolic activity. On the other hand, degeneration of the basement membrane in the involuting gland is a sign of decreased myoepithelial anabolism[77] and leads to a loss of secretory epithelial cell viability.[59]

The function of myoepithelial cilia (Figure 5), which are in close contact with secretory epithelial cells, is speculative. They may act as mechano- or even chemoreceptors and initiate contraction upon stimulation.[81]

## C. Sweat Gland Myoepithelium

### *1. Embryology*

The stratum germinativum of the embryonal skin differentiates into three distinct progenitor cell populations. The basal cells give rise to the keratinizing epidermis, primary epithelial germs to hair follicles, sebaceous glands and apocrine glands and eccrine gland germs to eccrine glands.[82] Of all these structures, only the secretory portions of apocrine[4,83] and eccrine glands[84] contain myoepithelial cells.

Both primary epithelial and eccrine gland germs initially consist of crowding of deeply basophylic cells in the basal layer of the epidermis. Proliferation of these cells gives rise to solid epithelial buds which protrude into the dermis.[82]

At 16 weeks of gestation, the distal tip of the solid eccrine gland anlagen begins to form a coil in the dermis and lumen formation takes place by separation of desmosomal attachments.[85] The primitive tubular structure is lined at this stage by an inner (lumenal) and outer (basal) cell layer. The outer cells of the distal coiled portion give rise to secretory epithelium and small pyramidal-shaped cells wedged in between the basal portions of secretory epithelial cells.[86] These cells develop myoepithelial characteristics at 22 weeks of embryonal age.[85] At birth, most eccrine glands seem to have completed development and resemble that of the adult.[82] Regenerative capacity of eccrine secretory and myoepithelial cells resides in scattered germinal cells in the secretory segment of the gland.[87]

In apocrine glands, which only become fully developed at puberty, myoepithelial cells appear to originate from basal cells of the terminal portion of the intradermal duct. Myoepithelial cell numbers increase gradually towards the secretory portion of the gland where all mitotic activity ceases.[83]

*2. Functions*

Myoepithelial cells are exclusive to the secretory portion of eccrine and apocrine glands and it therefore does not seem unreasonable to postulate their participation in the formation or propulsion of sweat. Furthermore, the smooth muscle-like features of myoepithelium and firm attachment to secretory epithelium[84] support a contractile function. Myoepithelial contraction appears to be responsible for the pulsatile nature of low-grade sweating[88] and peristaltic contractile waves have been identified in apocrine myoepithelial cells after mechanical, neural, and hormonal stimulation.[89] Myoepithelial contraction also influences the composition of the secrete by altering the pore size of the membranes of secretory cells.[88] Moreover, myoepithelial cell processes decrease in diameter during contraction, a phenomenon which may open wide gaps allowing interstitial fluid to come in direct contact with secretory cells.[3] Alkaline phosphatase in apocrine myoepithelium[83] and eccrine myoepithelium[3,87,90] and ATPase[3,90] and micropinocytotic vesicles[90] in eccrine myoepithelium are probably associated with active transport of metabolites to secretory cells (these enzymes are also present in capillary endothelium[87] which are known to have a transport function). Complex foldings of the plasma membrane of myoepithelial cells[83] increase their surface area and could play a role in improving the efficiency of a hypothetic transport mechanism. Most electron microscopic studies failed to identify secretory activity in cells with myoepithelial features,[3,83,85] invalidating a previously held concept of transition between myoepithelial and secretory epithelial cell types.[84]

## III. MYOEPITHELIAL IDENTIFICATION

Although myoepithelial cells are recognized with difficulty in routine paraffin sections, their location in the terminal portion of most exocrine glands (Figure 6) makes reliable identification possible. The value of reports postulating myoepithelial differentiation in pathologic conditions where all landmarks are lost depends to a great extent on the criteria applied during their characterization. Publications dealing with myoepithelial differentiation in pathologic conditions require careful scrutiny in this respect.

The three principle light microscopic presentations of myoepithelial cells in pathologic conditions of salivary glands are reported to be hyaline or plasmacytoid (Figure 7), fibroblastic or myoid (Figure 8), and epithelial-like.[91] The latter often appears as mucin-negative glycogen-rich clear cells (Figure 9). It should be noted that clear cells unrelated to myoepithelium are often found in a number of definable salivary gland

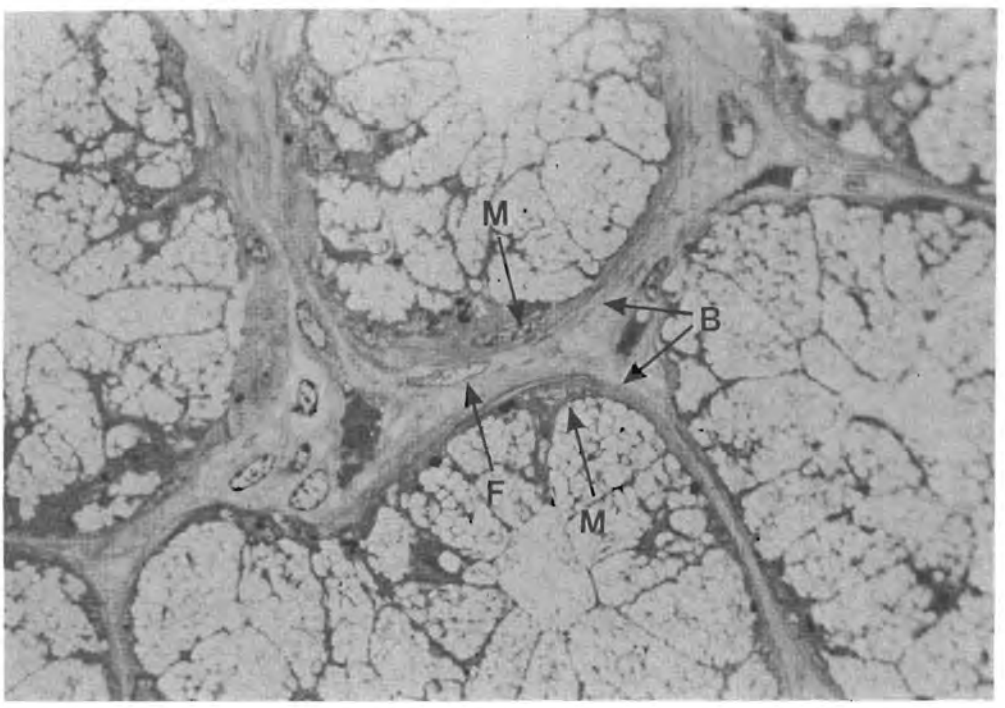


FIGURE 6. Myoepithelial cell (M) located beneath the epithelial basement membrane (B) of the parotid gland of the African buffalo *(Syncerus caffir)*. Note the fibroblast (F) located on the mesenchymal aspect of the basement membrane. (Hematoxylin-eosin; magnification × 1250.)

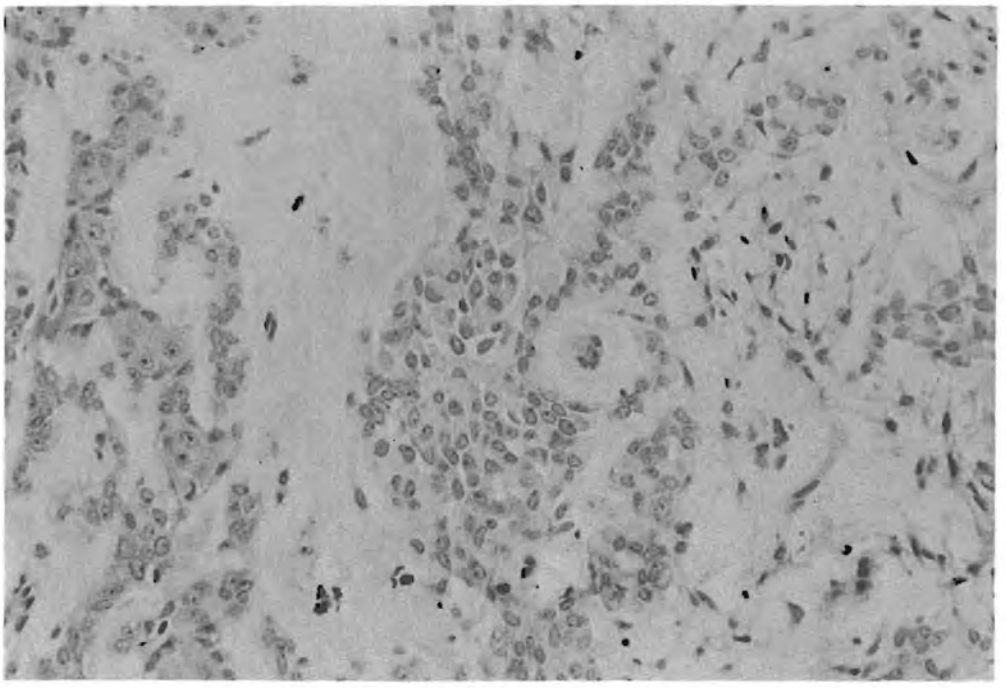

FIGURE 7. Plasmacytoid-type myoepithelial differentation, pleomorphic adenoma of the palate. (Hematoxylin-eosin; magnification × 300.)

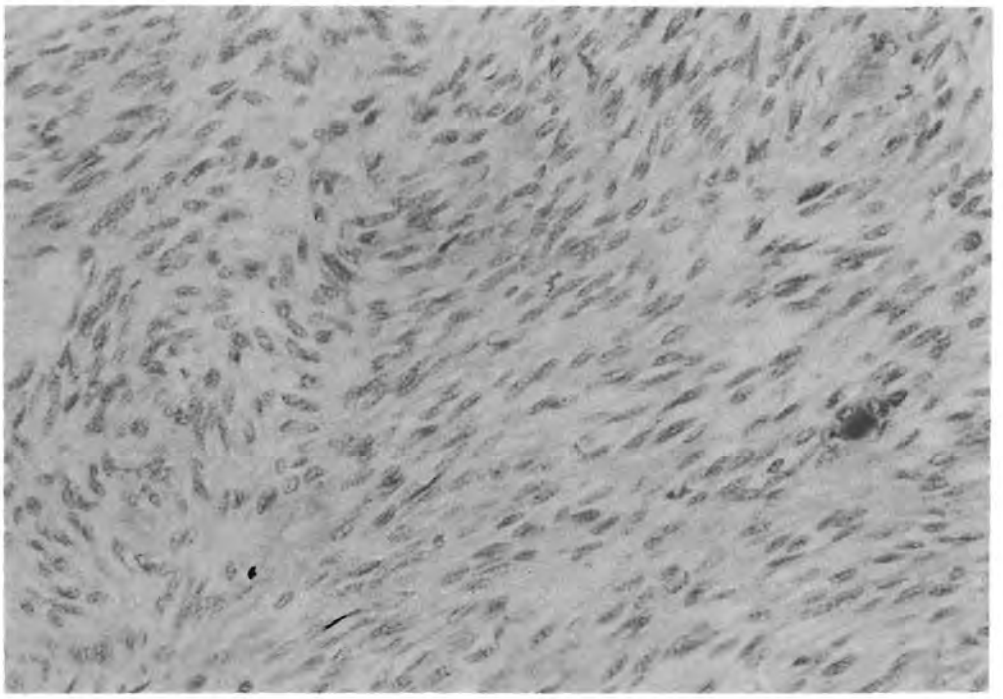

FIGURE 8. Fibroblastic (myoid)-type myoepithelial differentiation, pleomorphic adenoma of the parotid. Note ductular differentiation. (Hematoxylin-eosin; magnification × 300.)

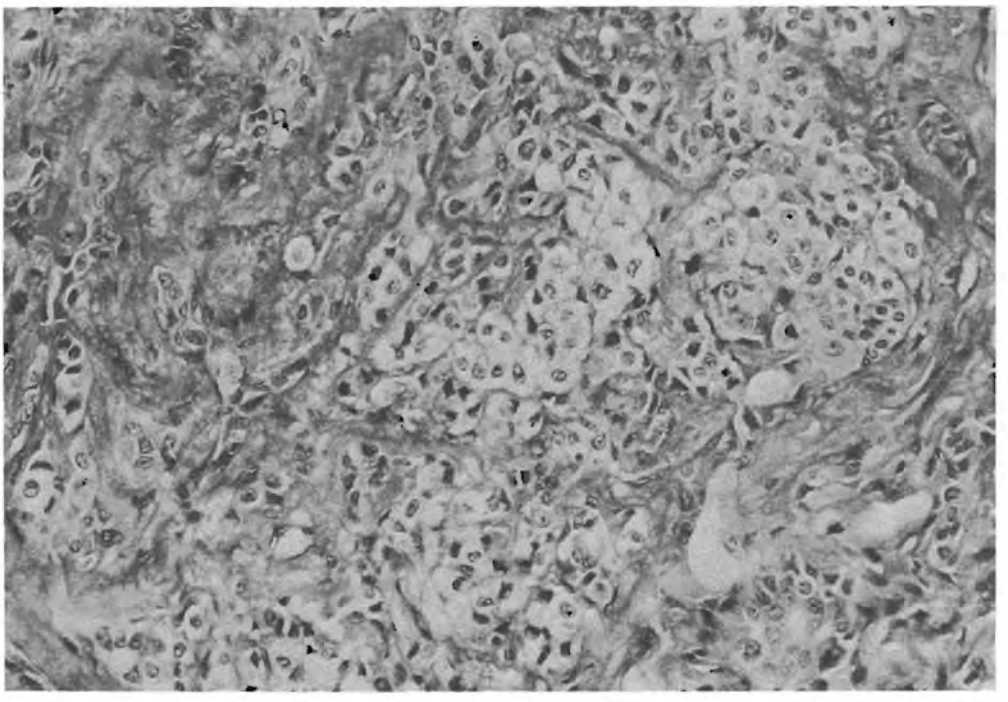

FIGURE 9. Epithelial-like or clear cell-type myoepithelial differentiation, pleomorphic adenoma of the parotid. (Hematoxylin-eosin; magnification × 300.)

tumors of which mucous clear cells in mucoepidermoid tumors and sebaceous clear cells in sebaceous lymphadenomas are only two examples.[92] Furthermore, plasmacytoid (or hyaline cell) differentiation is not uncommon in tumors unrelated to myoepithelium[93] and various mesenchymal proliferations may give rise to cells with fibroblastic or myoid features.

Ultrastructurally, cytoplasmic myofilaments are present in myoepithelial cells, smooth muscle cells, and myofibroblasts. Frequent participation of the latter cell type in pathologic conditions of the breast[94] has led to erroneous reports postulating myoepithelial involvement. In contrast to myoepithelium, myofibroblasts stain positive for collagen type III[95] and vimentin, a marker protein for cells of mesenchymal origin.[96] All eukaryotic cells contain contractile proteins[97] and neoplastic change is usually associated with a sharp increase in their concentration.[98] Furthermore, myofilaments in myoepithelial cells have been reported to exhibit features similar to tonofilaments in epithelial cells,[51,99] an additional source of confusion on the ultrastructural level.[2]

Positive enzyme histochemical reactions for alkaline phosphatase, acid phosphatase, and ATPase were regarded by many as characteristic of myoepithelium. Their presence is of limited value and should not be accepted as exclusive to myoepithelial cells. Alkaline phosphatase activity is also localized in the plasma membranes of endothelium engaged in active transport,[100,101] acid phosphatase has been demonstrated in myoepithelial cells, secretory epithelium of involuting rat mammary glands, and capillary endothelium,[102] and magnesium-dependent ATPase activity is found in both secretory epithelial and myoepithelial cells of rat mammary glands. A second type of ATPase activity, which is not magnesium but sodium and potassium dependent, appears to be an exclusive feature of rat mammary myoepithelial cells.[103] Species differences in the distribution of enzymes in salivary gland myoepithelium appear to make animal studies meaningless; the alkaline phosphatase reaction is useful in salivary gland myoepithelial identification in the cat and rat, but not in man, dog, or opossum, while the ATPase reaction is useful in man, but not in the cat or dog.[24,28,104]

Immunochemical typing of cytoplasmic filaments has aided myoepithelial identification. Archer and Kao,[105] Archer et al.,[45] and others[44,106] demonstrated the presence of myosin and actomyosin related proteins in myoepithelial cells of human salivary, sweat, and mammary glands. The use of antiactin antibodies in salivary myoepithelial identification has been questioned as it appears that although the antibody stains myoepithelial cells, it is not sufficient to differentiate clearly between myoepithelial and duct epithelial cells of normal salivary glands.[44] Identification of myosin appears to be more specific. The presence of this microfilament, however, is by no means exclusive to salivary myoepithelium, as it is found in a wide range of cells, including nonmuscle cells of epithelial origin and their tumors.[107,108] In the human female breast, myoepithelial cells are distinguished from mature lumenal epithelium by staining positive with antibodies to myosin and actin[77,105,109,110] and by staining negative with antimilk protein antibodies.[48] Intermediate-sized cytoplasmic filaments of the cytokeratin type in salivary[111,112] and mammary[77,109,110] myoepithelia and the demonstration of basement membrane proteins, the production of which has already been referred to, are useful immunocytochemical aids in improving the reliability of myoepithelial identification. In addition, S100 protein has been reported to be a marker for myoepithelial cells in normal and neoplastic salivary glands[113] (Figure 10), sweat glands, and mammary glands.[114] Immunoelectron microscopy[113] showed that S100b protein is distributed on the membrane of the endoplasmic reticulum and the outer nuclear membrane of salivary gland myoepithelial cells. This seems to indicate that the protein is produced by myoepithelial cells themselves.

The foregoing discussion emphasizes that myoepithelial cells share features in com-

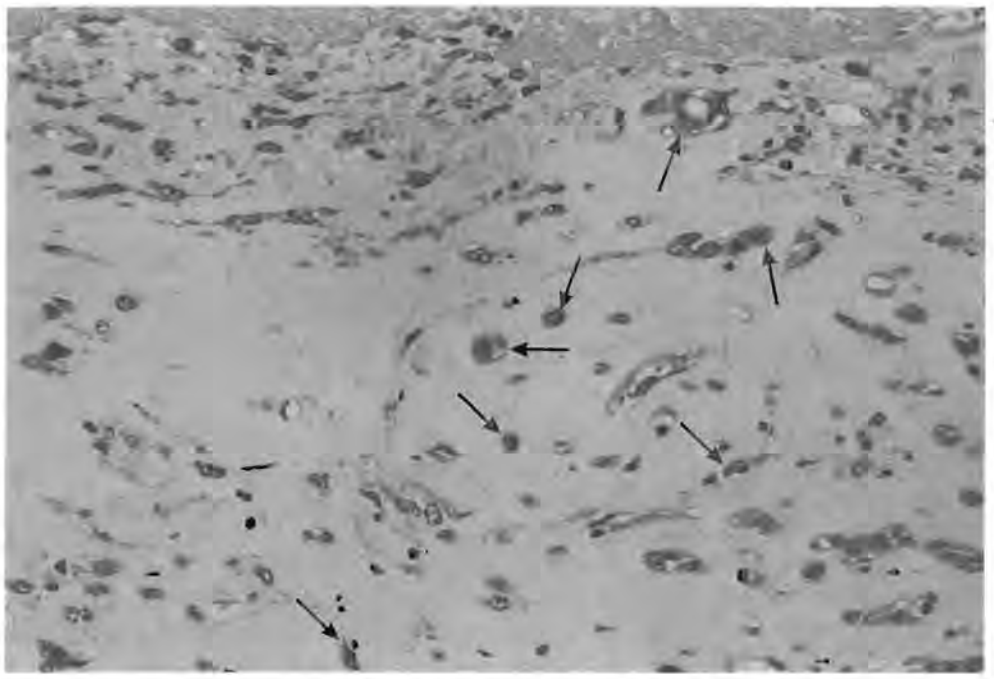

FIGURE 10. S100b positive cells (arrows) embedded in cartilagenous deposits in a pleomorphic adenoma. (Peroxidase antiperoxidase technique; magnification × 400.)

mon with other cell types. Reliable proof of their presence in pathologic conditions is therefore best achieved by a combination of structural, histochemical, and immunocytochemical techniques.

## IV. MYOEPITHELIAL PROLIFERATIONS

### A. Salivary Glands

#### *1. Nonneoplastic Conditions*

The bulk of research on salivary gland myoepithelial proliferations is focused on neoplasms and very little is subsequently known of myoepithelial participation in nonneoplastic conditions.

Emmelin et al.[115] found architectural changes affecting myoepithelial cells of the parotid and submandibular glands of cats after ductal ligation. Processes of myoepithelial cells protruded into the interstitial spaces, giving rise to bizarre appearances. In addition, folds of basal lamina tended to be aggregated, especially around protruberant parts of myoepithelial cells thereby increasing the space between their cell membranes and nerve endings. This probably reduces neuroeffector efficiency and together with the mechanical disadvantage of the altered arrangement of myoepithelial cells helps to explain the modified intraductal pressure responses that occurred after stimulation. Ensuing increase in the intraductal pressure when inducing secretion often caused ballooning disruption of the first parts of the striated ducts which lack support by myoepithelial cells.[22] It is not yet known whether a similar mechanism has any bearing on human sialectasis. Alkaline phosphatase, when present, tends to be lost from myoepithelial cells by the time that extensive parenchymal atrophy has occurred after ductal obstruction.

The diagnostic terms, lymphoepithelial lesion, chronic recurrent (punctate) sialad-

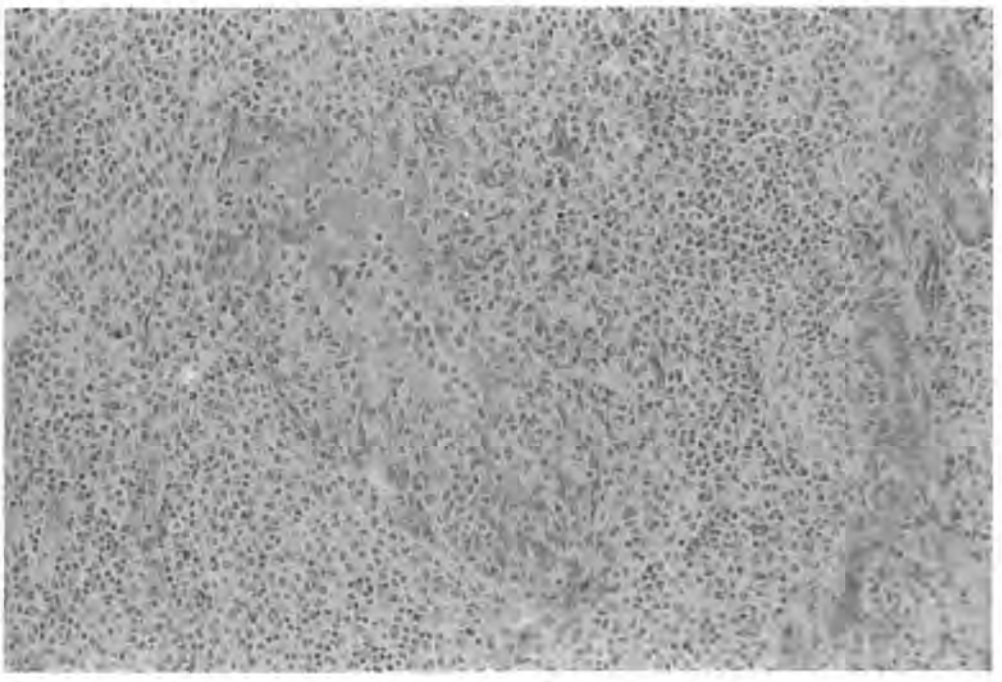

FIGURE 11. Epimyoepithelial island in a benign lymphoepithelial lesion of the parotid. (Hematoxylin-eosin; magnification × 200.)

enitis, sicca syndrome, and Sjogren's syndrome, share nearly common histopathologic changes characterized by a lymphoreticular cell proliferation associated with atrophy of the parenchyma and ductal changes ending in so-called "epimyoepithelial islands" (Figure 11). These islands are formed by metaplastic proliferation of ductal epithelium accompanied by myoepithelial cells. Controversy exists on the prominence of the latter cell type. Some workers believe myoepithelial cells to be few in number and located around the periphery of the islands.[117] The majority, however, agrees that myoepithelial cells are prominent and form an integral part of the epimyoepithelial islands.[118,119] This controversy emphasizes the difficulty in identifying myoepithelial cells in a state other than normal.

*2. Neoplastic Conditions*

It is generally accepted that the basal cells of the excretory duct (or EDRC) and the intercalated duct cells (or IDC) act as stem cell compartments for the more differentiated portions of salivary-type glands both during the later stages of development and in the mature gland. The EDRC gives rise to columnar and squamous cells of the excretory duct and the IDC gives rise to acinar cells, other intercalated duct cells, striated duct cells, and myoepithelial cells.[1,120,121] It is important to note that of the two stem cells, only the IDC has the potential to differentiate into myoepithelial and acinar cells (Figure 12).

The bicellular theory on the histogenesis of salivary gland neoplasms, initially proposed by Eversole[122] and recently modified by Regezi and Batsakis[120] and Batsakis,[121] divides these lesions into two groups, based on the stem cell population of origin. Depending on where on the curve of differentiation an oncogenic stimulus acts, the IDC population is the epithelial source for adenoid cystic carcinomas, acinous cell carcinomas, monomorphic adenomas, mixed tumors, and some of the ductal carcino-

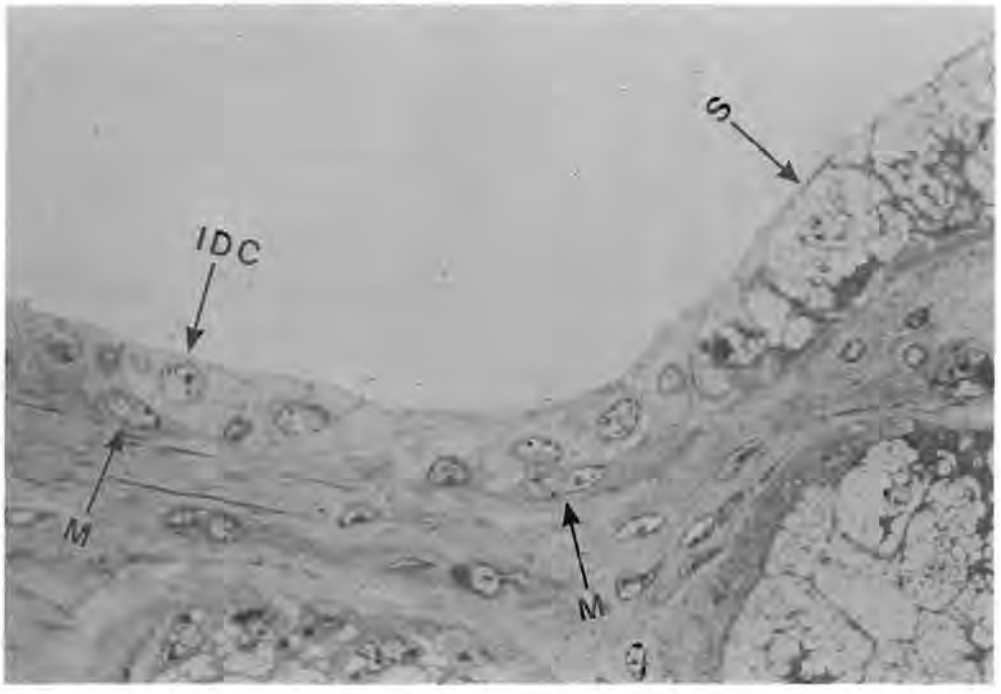


FIGURE 12. Epithelium of the intercalated duct (IDC) indicating its relationship to myoepithelial cells (M) and secretory epithelial cells (S) in the parotid gland of the African buffalo. (Toluidine blue stain; magnification × 1000.)

mas.[121,123-125] Theoretically, most of these tumors and even some monomorphic adenomas may, to a greater or lesser extent, contain myoepithelial cells.[126] The possibility of myoepithelial differentiation on the other hand should, according to this theory, not be considered in tumors that arise from the EDRC (mucoepidermoid carcinomas, papillary mucinous adenocarcinomas, and primary salivary squamous carcinomas).[91]

If the reserve epithelial cell populations of salivary glands are accepted as the progenitor for salivary gland neoplasms, what is the significance of myoepithelial differentiation? Although this question remains greatly unanswered, it should be noted that in the sister exocrine gland, the pancreas, which lacks myoepithelial cells, the variety and diversity of salivary gland neoplasms are absent.[123] Implication, however, is not proof and the deficient evidence on myoepithelial differentiation in neoplasms is in part the result of the difficulty in recognizing myoepithelial cells with certainty.

### *a. Mixed Tumor*

In the past, a variety of cellular differentiation pathways have been proposed to account for the derivation of mixed tumors. Throughout recent years, the mixed epithelial mesenchymal theory of origin[127] has lost ground and differentiation of neoplastic myoepithelial cells in these tumors has been proven beyond doubt.[128,129] Although duct cells are the major component of mixed tumors,[44,130,131] a variety of epithelial cell types participate, ranging from secretory epithelial cells at one end of the spectrum to myoepithelium at the other with less-differentiated cells in between.[39,41,132] This spectrum corresponds to the differentiation potential of the IDC.[1,120,121] In addition, a histogenetic link has been proposed between the IDC and epithelial component of pleomorphic adenomas after detecting lysozyme and lactoferrin in both cell types.[133] Mixed tumors therefore probably represent neoplastic transformation of the IDC[120,134] and

form a central and major component of a class of epithelial neoplasms with monomorphic adenomas (constituted entirely of ductal or excretory cells) at one pole of the spectrum and myoepitheliomas (constituted entirely of myoepithelial cells) at the other.[120,135]

The phenotypic expression of myoepithelial differentiation in mixed tumors may be hyaline (or plasmacytoid)[136] (Figure 7), fibroblastic (or myoid)[91] (Figure 8), or that of mucin-negative glycogen-rich clear cells[92] (Figure 9). Some cellular mixed tumors, sparse in myoepithelial cells, resemble monomorphic adenomas in appearance. In other examples, the bulk of the lesion is largely composed of myoepithelial cells and stroma, i.e., a mixed tumor with myoepithelial dominance. These lesions are often misinterpreted as mesenchymal neoplasms.[137]

Much of the debate on the histogenesis of mixed tumors has centered around the identity of characteristic myxoid, chondroid, osteoid, elastic, and fibrous interstitial deposits. It has been investigated chemically, histochemically, and ultrastructurally and in tissue cultures. The mesenchymal nature of these deposits has been proven beyond doubt[138,139] and evidence on myoepithelial participation in their production has accumulated.[39,43,120,128,138-141] Some of the spindle-shaped cells, often associated with stromal deposits, were found to react positively with immunochemical stains for S100 protein[113,129,142] (Figure 10), microfilaments of the myosin and actin type[129,143] and intermediate-sized filaments of the prekeratin type,[112,144] characteristics not short from proving myoepithelial differentiation. In addition, these cells display a positive vimentin stain[39,132,144,145] which can be regarded as immunochemical evidence of mesenchymal conversation, a phenomenon proved in other epithelial-derived cell lines.[146] This finding introduces new concepts with regard to the mixed nature of these tumors, among which an origin from cells which is characterized by prekeratin filaments, but which after neoplastic transformation acquires the ability to produce vimentin filaments, were suggested,[144] a proposal not far separated from an earlier theory postulating mesenchymal metaplasia of neoplastic myoepithelium.[70,120,141] Since myoepithelial cells already exhibit features of smooth muscle, neoplastic change may expose other mesenchymal characteristics.[120]

Myoepithelial participation in malignant mixed tumors has not yet been determined. Metastatic deposits of these rare lesions contain tissues of epithelial and mesenchymal nature (either as a homologue of a benign appearing mixed tumor or a carcinosarcoma). This could lead one to hypothesize that although the neoplastic cells undergo malignant transformation (i.e., develop metastatic potential), a relatively high level of cytodifferentiation is responsible for the "mixed" features of the malignancy. Metastatic deposits should therefore contain epithelial and myoepithelial cells and mesenchymal interstitial deposits related to the latter cell type. However, whether a direct parallel could be drawn between benign and malignant mixed tumors remains to be proven.

*b. Myoepithelioma*

Myoepitheliomas are histogenetically related to mixed tumors as both lesions originate from IDCs.[120,147] It is extremely rare for these tumors to occur in a pure (monomorphic) form[148] and a diagnosis of myoepithelioma should only be made in the absence of chondroid interstitial deposits and/or conspicuous epithelial differentiation usually in the form of ducts. Pure myoepitheliomas are composed primarily of spindle-shaped cells, plasmacytoid (hyaline) cells (Figure 13), or a combination of the two cell types; stellate and clear cell variants are less common.[147] The neoplastic cells in these tumors have been shown to possess synthetic and secretory activity[149] and are capable of producing connective tissue mucins.[150] A total of 39 of the 41 myoepitheliomas of the head and neck reported in the English literature are benign with a behavior and postoperative recurrence rate similar to that of mixed tumors.[147]

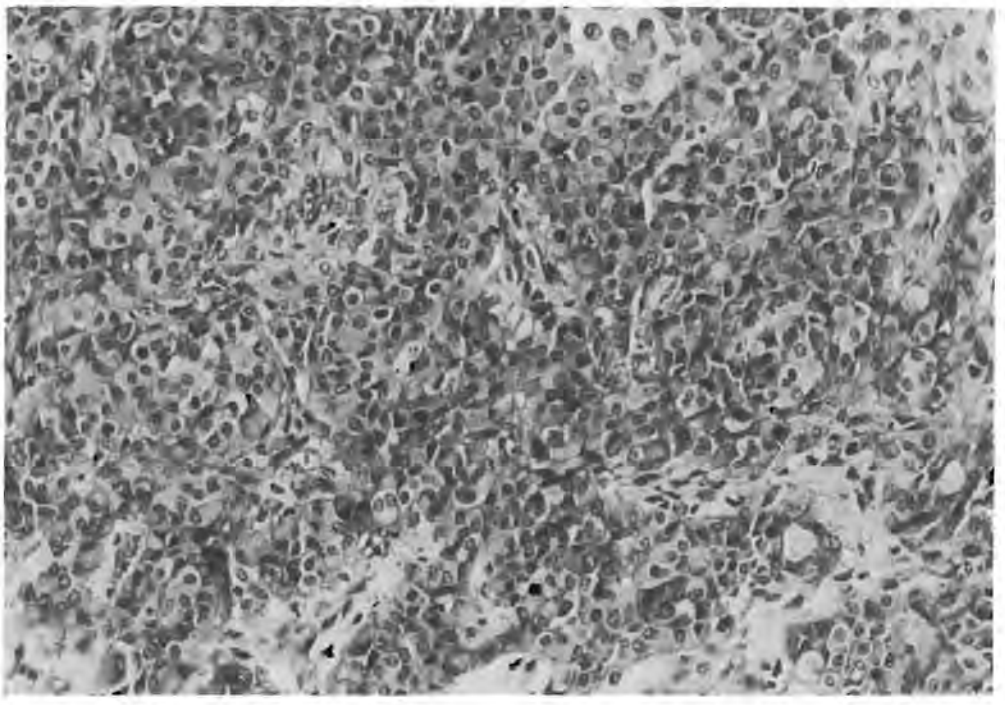

FIGURE 13. Plasmacytoid myoepithelioma of the palate. Note the extensive plasmacytoid differentiation of neoplastic myoepithelial cells. (Hematoxylin-eosin; magnification × 200.)

*c. Adenoid Cystic Carcinoma*

Although adenoid cystic carcinomas occur more commonly in salivary glands, tumors with this growth pattern have been recognized in other organs including the tracheobronchial tree, nasal cavity, paranasal sinuses and larynx, breast, uterine, cervix, Bartholins gland, lacrimal gland, skin, and prostate. Participation of myoepithelial cells in adenoid cystic carcinomas was initially emphasized by Bauer and Fox,[151] who introduced the term "adenomyoepithelioma". Although this concept was initially supported,[152] a few ultrastructural reports failed to identify myoepithelial differentiation in these tumors.[153,154] This failure could be related to embedding artifacts or poorly differentiated features of the tumors studied as recent ultrastructural,[155-157] histochemical,[155,157] and immunofluorescent[158] investigations support myoepithelial differentiation in adenoid cystic carcinoma. Hoshino and Yamamoto[155] go further and consider the myoepithelial cell to be responsible for the high recurrence rate after radiation. The characteristic pseudocysts (Figure 14) are extracellular spaces containing connective tissue mucins, multilayered basement membrane material,[138,156,159] and elastic tissue.[160] These spaces are lined by cells exhibiting cytoplasmic filaments of the actin and keratin types and produce basement membrane collagen type IV,[158] features sufficient for positive myoepithelial identification. Similar deposits surround nests of tumor cells and account for the so-called cylindromatous appearance of one of the forms of adenoid cystic carcinoma.[161] The second cell type in adenoid cystic carcinoma forms true acinar structures and is of a secretory epithelial nature.[155,156,158] Myoepithelial and secretory epithelial differentiation producing epithelial and connective tissue mucins, respectively,[159] are hallmarks of these tumors. These cells correspond to the differentiation potential of the IDC, from which the origin of salivary gland adenoid cystic carcinomas has been postulated.[155]

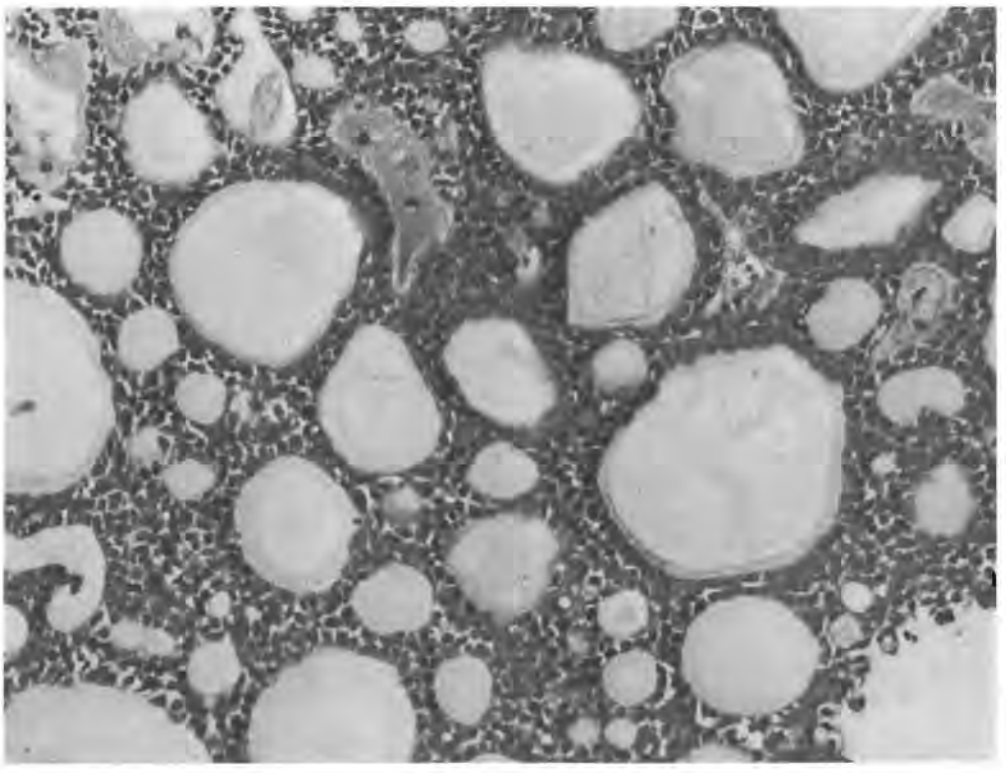

FIGURE 14. Pseudocysts containing basement membrane-like material. (Adenoid cystic carcinoma, PAS stain; magnification × 200.)

*d. Epithelial-Myoepithelial Carcinoma*

Primary malignant tumors of IDC origin not only include adenoid cystic carcinomas and malignant mixed tumors, but also a recently described entity, epithelial-myoepithelial[162] or tubular[92] carcinoma. These lesions have a bicellular histologic composition, with variable proportions of the two cell types evident from case to case as well as within the same lesion.[92,163] Characteristically, dark cells with few cytoplasmic organelles (resembling IDCs) from the inner layer of ductular structures and clear cells rich in glycogen (myoepithelial differentiation) form the outer layer[92,162] (Figure 15). A distinctive interepithelial hyaline-like ground substance separates the double-layered ducts.[92] The appearance of a dual population of cells is expressive of a dichotomatous differentiation pattern of a common precursor, the IDC.[163] The complex growth pattern and stromal complexity of the mixed tumor, however, are not seen in the epithelial-myoepithelial carcinoma.[163] Analogous cases have been described in the literature under a variety of names, including tubular solid adenoma,[164] cystic adenoma,[165] adenomyoepithelioma,[70,166] clear cell adenoma,[167] and glycogen-rich adenoma.[168] Recent publications[162,169,170] clearly point to the strong probability that the majority, if not all of the nonmucinous clear cell tumors of the major and minor salivary glands, are at least low-grade carcinomas. Although epithelial-myoepithelial carcinoma exhibits a high degree of cellular differentiation, it is considered to be malignant because of its infiltrative and destructive growth pattern, multifocal growth tendency, perineural involvement with remote metastasis, frequent recurrences, and foci of necrosis.[92,162]

*e. Lobular Carcinoma of Minor Salivary Glands*

Although this tumor has been referred to in the past as "polymorphous low-grade

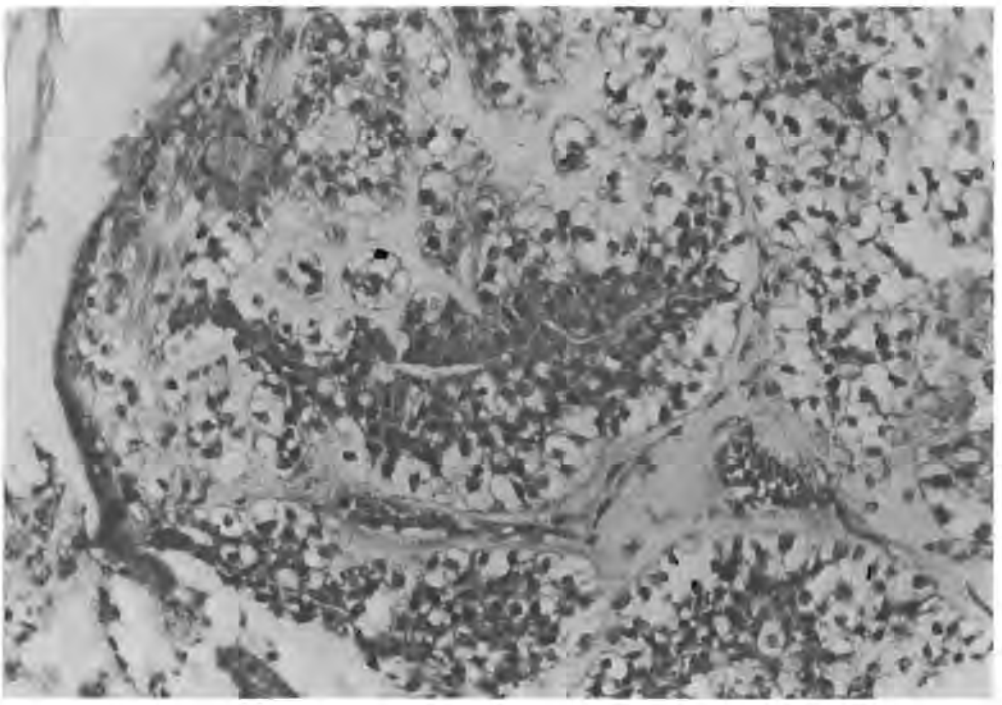

FIGURE 15. Epithelial-myoepithelial carcinoma, parotid. Tubular structures exhibiting two cell-type differentiation. Note the hyaline-like basement membrane interfacing with the clear cell component of the tumor. (Hematoxylin-eosin; magnification × 250.)

adenocarcinoma of minor salivary gland origin"[171] or "terminal duct carcinoma",[125] lobular carcinoma[172,173] appears to be the most appropriate designation as the microscopic appearance of the lesion calls to mind that of mammary lobular carcinoma. Salivary gland lobular carcinomas occur most frequently on the palate[173] and are likely related to the clear cell class of salivary gland neoplasia,[92] specifically the epithelial-myoepithelial carcinoma of intercalated duct cell origin.[125] The peripheral clear cell, often glycogen-rich, mantle distinguishes the latter neoplasm from lobular carcinoma which consists of duct-like structures often surrounded by spindle-shaped cells arranged in a characteristic lobular configuration. Only a small number of these neoplasms have been reported[173] and their clinical course appears to be akin to that of adenoid cystic carcinomas, with neural invasion as a prominent feature.[125] Whether they represent histopathologic variants of adenoid cystic carcinomas, however, cannot be confirmed yet. Although a mucohyaline stromal element, faintly reminiscent of the myxoid change in pleomorphic adenomas, is seen in many lobular carcinomas, myoepithelial differentiation has not yet been proven beyond doubt. The elongated appearance of some cells appears to be the result of stromal compression of a single cell type rather than an expression of biphasic cellularity.[173]

B. Mammary Glands

*1. Nonneoplastic Conditions*

Proliferation of myoepithelial cells has been identified in breast tissue of elderly females, especially in cases of senile involution where glandular atrophy and hyalinization of the fibrous stroma is evident.[174] Groups or "rosettes" of myoepithelial cells with a clear vacuolated cytoplasm are initially seen on the periphery of the ductules.[175]

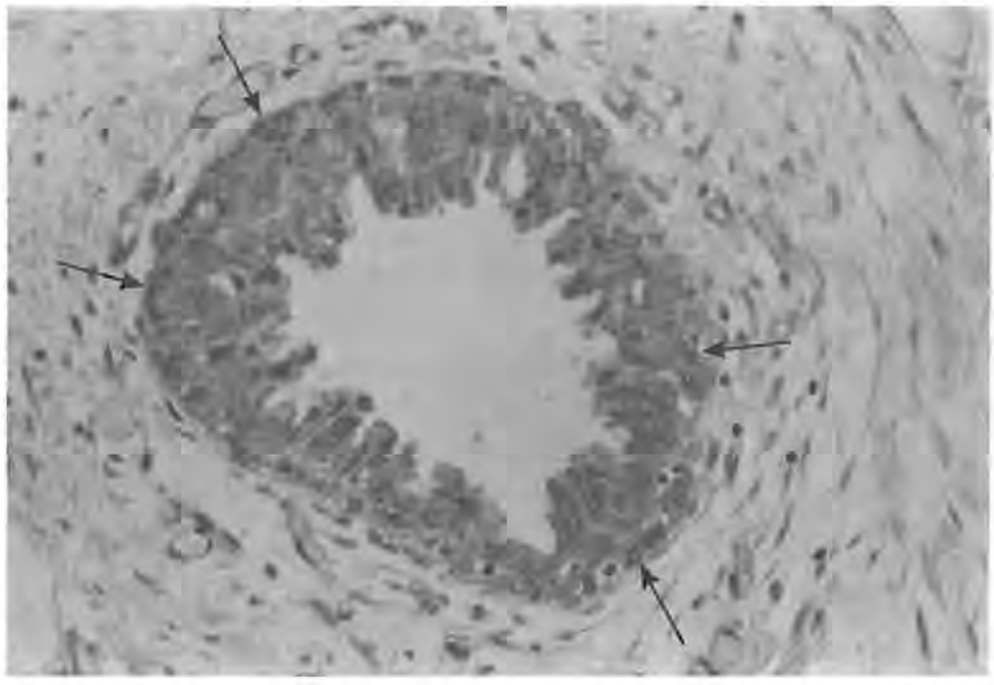

FIGURE 16. Ductular hyperplasia in the early stage of gynecomastia. Note the prominent peripheral flattened myoepithelial cell layer, the cytoplasm of which stains granular with antimyosin serum (arrows). (Indirect immunofluorescence; magnification × 400.)

It has been reported that in some cases glandular structures disappear, resulting in the formation of nests of hyperchromatic densely packed spindle cells, interpreted as myoepithelium, in a dense fibrous stroma.[174] Experimentally, changes similar to senile involution have been induced by blocking basement membrane collagen (type IV) formation by myoepithelial cells.[80] In the quiescent stage of gynecomastia, when ductular atrophy and fibrosis occurs, myoepithelial cells appear to persist longer than lumenal epithelium,[176] supporting the concept of pure myoepithelial islands in breast conditions characterized by fibrosis and atrophy. In the early (florid) stage of gynecomastia, hyperesterinism probably induces ductular hyperplasia (Figure 16).[177] Myoepithelial cells may either proliferate alone, forming projections into the periductule connective tissue, or together, with lumenal epithelium leading to intraductal epithelial growth.[176]

Focal hyperplasia of myoepithelial cells has been demonstrated in cystic disease of the breast[174,175] and it has been postulated that these cells play an important role in initiating the condition.[178] Ultrastructural examination and alkaline and acid phosphatase stains identified stretched myoepithelial cells mainly in the walls of small and medium-sized cysts.[179,180] In areas of apocrine (oncocytic) metaplasia, basally located myoepithelial cells were reported to be quite conspicuous, with well-developed myofilaments[2] and increased numbers of mitochondria,[181] the significance of which appears to be speculative.

Various morphologic types of periductal myoepithelial proliferations have been reviewed by Hamperl.[70] Circumscribed hyperplasia of myoepithelial cells in the lining of a duct may either protrude outwards (centrifugal) or inwards (cetripetal) and both forms occur in gynecomastia. Diffuse hyperplasia of myoepithelial cells is occasionally associated with partial or circumferential basement membrane deposits, the latter leading to so-called "cylindromatous transformation". The occurrence of diffuse myoe-

pithelial proliferations in chronic mastopathies is an indication that the extent of hyperplasia is not an indication of the type, but rather the stage of a proliferative breast disease.

*2. Neoplastic Conditions*

Although a myoepithelial histogenesis has been suggested for certain fibrosarcomas, osteosarcomas, and carcinosarcomas of the breast,[70] all cases studied lack convincing evidence of myoepithelial participation. Only neoplasms in which myoepithelial differentiation has been proved beyond doubt will subsequently be discussed.

*a. Intraductal Epithelial Proliferations*

Epitheliosis (benign intraductal epithelial proliferation) is often difficult to distinguish microscopically from ductal carcinoma *in situ*. This indecision is reflected by the designation "atypical hyperplasia". Ahmed[179] found that ductal epitheliosis is comprised principally of myoepithelial cells and regarded it as an important distinguishing feature from carcinoma. It should be pointed out that the positive enzyme histochemical reactions which he utilized as confirmatory evidence of the principal myoepithelial nature of epitheliosis lack specificity. Only an occasional myoepithelial cell could be demonstrated ultrastructurally in typical epitheliosis by Fischer,[2] substantiating the inaccuracy in Ahmed's description. A recent study, utilizing immunological markers, identified an intact basement membrane and normal peripherally located myoepithelial cells in epitheliosis.[109] In addition, the intralumenal proliferation was found to consist of a major epithelial and minor myoepithelial component. Distinction between epitheliosis and intraduct carcinoma on the myoepithelial cell component appears to be more pragmatic than real and pathologists should rather utilize other cardinal criteria which have proved to be diagnostic.[182] However, loss of definition of the basement membrane, discontinuities in the myoepithelial cell layer, and an epithelial rather than myoepithelial cell type seem to favor a diagnosis of carcinoma *in situ*.[78,99,109,183,184]

Another pitfall in diagnostic histopathology is the interpretation of papillary lesions of the breast. Two cell-type differentiation is for practical purposes a feature of papillomas[110] and statements by various authors that myoepithelial differentiation is present in papillary carcinomas should be rejected as these studies utilized nonspecific techniques and applied doubtful criteria during myoepithelial identification. Immunocytochemical methods for epithelial and myoepithelial cell markers employed on fixed and paraffin-embedded tissue[109] offer the best potential in distinguishing benign from malignant papillary lesions of the breast.[110]

*b. Ductal Carcinoma*

Cellular differentiation in infiltrating ductal carcinomas is predominantly towards cells with epithelial as opposed to myoepithelial characteristics.[109,185] Analogies can perhaps be drawn with rat mammary tumors where neoplastic cells with a common ancestry are capable of differentiating into more than one morphologic cell type.[56] The selection of differentiating patterns appears to be related to clonal, environmental, and/or hormonal factors influencing variation in gene expression.[56,109] Myoepithelial cell differentiation in some infiltrating breast carcinomas is supported by immunohistochemical identification of scattered laminin positive cells[186] and cells staining with antimyosin antibodies.[187] Experimental studies have indicated that laminin may promote the attachment of neoplastic cells to subendothelial basement membrane proteins during the process of metastatic spread[188] and identification of lymph nodal micrometastasis is facilited by staining for laminin.[186] The degree of myoepithelial differentiation and presence of extracellular basement membrane deposits appear to be related to

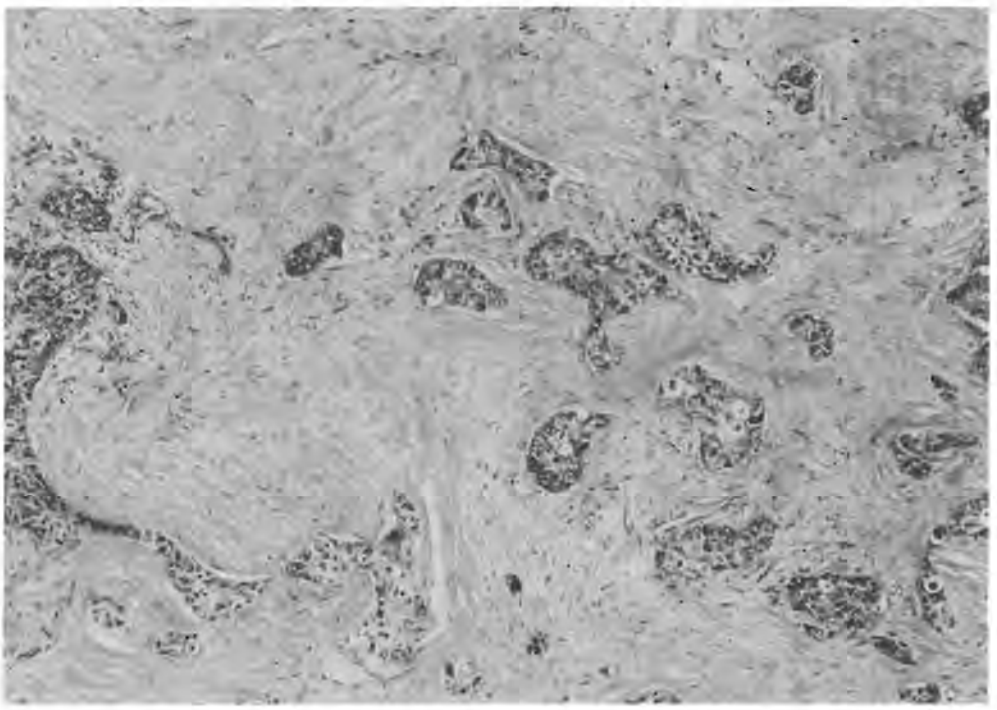

FIGURE 17. Scirrhous carcinoma, female breast. (Hematoxylin-eosin; magnification × 150.)

the differentiation of the neoplasm: in better differentiated lesions, positive staining for basement membrane proteins is present[186] and the number of cells with myoepithelial features appears increased.[189,190] Loss of basement membrane in poorly differentiated tumors could be related to the production of plasminogen activators resulting in proteolytic degradation.[191] As already pointed out, care should be taken not to interpret stromal myofibroblasts, a prominent component in scirrhous carcinomas (Figure 17), as myoepithelial in origin.

*c. Lobular Carcinoma*

In an immunochemical and ultrastructural study of five cases of lobular carcinoma *in situ,*[192] the orientation of myoepithelial cells appeared to identify three distinct phases of the disease: in an early stage, myoepithelial cells exhibited the classic peripheral arrangement. In other cases, they appeared perpendicular to the basement membrane and showed several cytoplasmic projections extending between the neoplastic cells. One advanced case, associated with infiltrative carcinoma, exhibited myoepithelial cells diffusely dispersed among neoplastic cells that filled the ductules. This change in myoepithelial orientation and distribution indicates a process of myoepithelial hyperplasia and migration (tumoral colonization) analogous to that of nonneoplastic melanocytes colonizing infiltrative breast carcinoma[193] or basal cell carcinomas of the skin[194] and could identify a preinvasive stage of lobular carcinoma *in situ.*[192] Furthermore, in light of the supportive nutritional function of myoepithelial cells, hyperplasia may be related to the increased nutritional requirement of the fast-proliferating neoplastic epithelial cells.[99,195] Secretory epithelial differentiation was proven both ultrastructurally[99,196] and immunochemically[196,197] in infiltrating lobular carcinoma, invalidating the long-held view that this neoplasm was primarily of myoepithelial origin.

*d. Fibroadenoma, Sclerosing Adenosis, and Phylloides Tumor*

In fibroadenoma, sclerosing adenosis, and phylloides tumor, myoepithelial cells are generally arranged in a single layer, though multilayering is not infrequent.[78,178,198] The basal portion of myoepithelial cells often appears markedly undulated with long finger-like projections referred to as "budding". In sclerosing adenosis, the number of acini initially increases and then develops through a series of phases in which myoepithelial cells play an ever increasing role, until the epithelial elements become compressed and myoepithelial cells take on a spindle morphology.[109] Apparent bridging of myoepithelial cells from one ductule to the other may also be observed.[78]

Multiple layering of myoepithelial cells appears rather characteristic of well-differentiated proliferative disease processes.[183] It is not surprising to find reduplication of the basement membrane in such areas, as myoepithelial cells are, as already pointed out, responsible for production of basement membrane proteins. Peripherally located myoepithelial cells resting on a delimiting basement membrane are, however, not a feature of all benign epithelial breast lesions. Microglandular adenosis, a tumor often misinterpreted as tubular carcinoma, can be distinguished from other forms of adenosis by the absence of myoepithelial cells and basement membrane deposits.[199]

*e. Mixed Tumor*

Mixed adenomas (salivary type) of the human female breast are very rare and only a few undisputed cases have been reported. The histogenesis is apparently similar to that of its rival in salivary glands.[200,201] In animals, especially dogs, these tumors are more common and electron microscopic,[202,203] histochemical,[204] and immunohistochemical[203] studies support the myoepithelial nature of stromal cells. Demonstration of desosomes between undifferentiated cells, however, is not enough evidence for myoepithelial derivation as they may also be present between a variety of mesenchymal cell types.

*f. Adenoid Cystic Carcinoma*

Adenoid cystic carcinomas of the female breast originate from stem cells in the terminal ducts which have the capacity to produce all the epithelial elements of the gland and so recapitulate the ductal acinar unit.[205] Immunofluorescent,[206] light, and electron microscopic studies[78,207,208] identified myoepithelial cells at the periphery of the ductal epithelial islands in adenoid cystic carcinomas. The biphasic histologic growth pattern[206] and the production of basement membrane proteins by the myoepithelial component[78,207] are well differentiated histologic features compatible with an excellent prognosis.

*g. Myoepithelioma*

Although hyperplasia of myoepithelial cells is encountered in many benign neoplasms of the breast, it is rarely the main component of a tumor. A few undisputed myoepitheliomas of the human female breast have recently been reported.[209-212] These cases probably represent one pole of a spectrum of tumors ranging from uniform spindle-cell proliferations such as the mammary myoepithelioma reported by Erlandson and Rosen[211] and the leiomyoma-like myoepithelioma reported by Toth[210] to proliferations of basiloid ductal cells without a myoepithelial component such as seen in tubular carcinomas.[78,208] In cases where both myoepithelial and epithelial components are active participants in the neoplastic process, the lesions are referred to as adenomyoepitheliomas.[209,212] These observations support a hypothetic stem cell origin with multidirectional differentiating potential.[211] Furthermore, neoplastic transformation of mature myoepithelial cells is not possible as they are highly differentiated and not

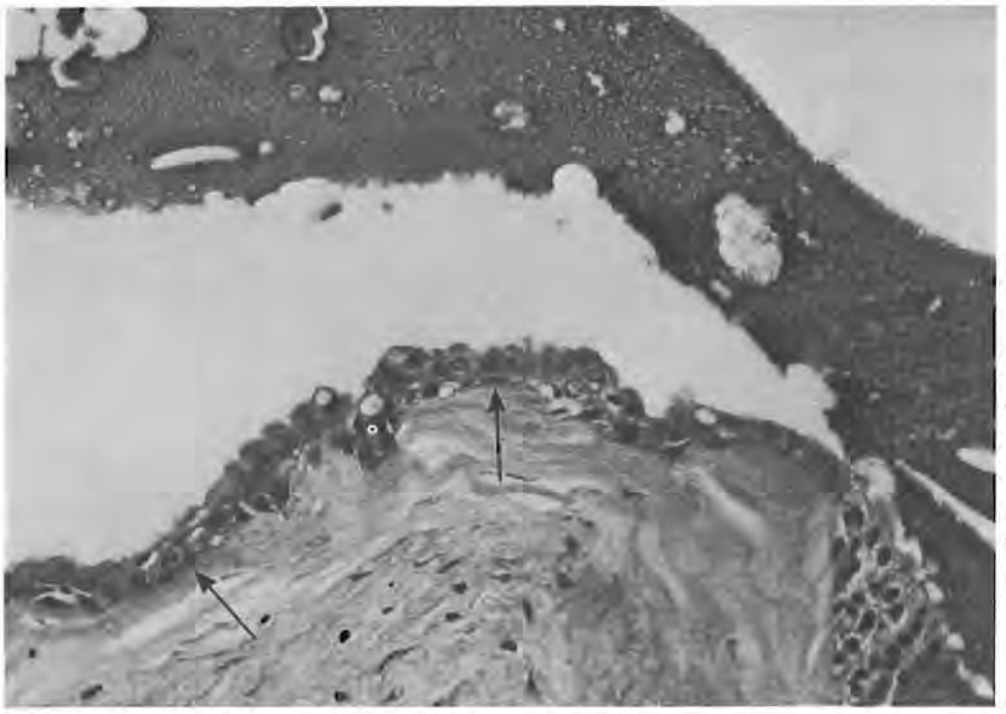

FIGURE 18. Apocrine hydrocystoma. Note myoepithelial differentiation (arrows). (Hematoxylin-eosin; magnification × 400.)

capable of proliferation.[210] Although Schlotke[213] produced a well-documented report of metastasizing malignant myoepitheliomas found in bitch mammary glands, the clinical behavior of a lesion of this nature in humans is unknown and, until larger series are available, therapy should be directed to complete excision of the tumor. The one case reported in the literature as a low-grade malignant myoepithelioma[212] does not warrant this diagnoses as a recurrent growth is not necessarily an indication of malignancy. Furthermore, suggestions that some spindle-cell carcinomas of the breast[214] and even leiomyosarcomas[215] originate from myoepithelial cells should not be accepted without immunocytochemical evidence.

C. Sweat Glands

Neoplastic conditions of skin appendages do not arise from mature cells or dormant embryonal epithelial rests as believed earlier, but from pluripotential precursor cells that form continuously during life.[216] Only tumors originating from the precursor cells of secretory coils of eccrine and apocrine glands have the capacity to differentiate towards myoepithelium.[217]

Apocrine and eccrine nevi, which represent hyperplastic proliferations of apocrine and eccrine glands, respectively, resemble their mature counterparts[216] and contain a normal myoepithelial component.

Apocrine hydrocystoma, a tumor characterized by large cystic spaces lined by cells showing "decapitation secretion",[216] contains a peripheral layer of elongated myoepithelial cells[218] (Figure 18). This feature is in contrast with eccrine hydrocystomas, where a fully differentiated myoepithelial cell layer is reported to be absent.[216] An outer layer of cuboidal cells, staining positive with alkaline phosphatase and containing numerous myofilaments ultrastructurally,[219,220] represents myoepithelial differentiation in hidradenoma papilliferum.

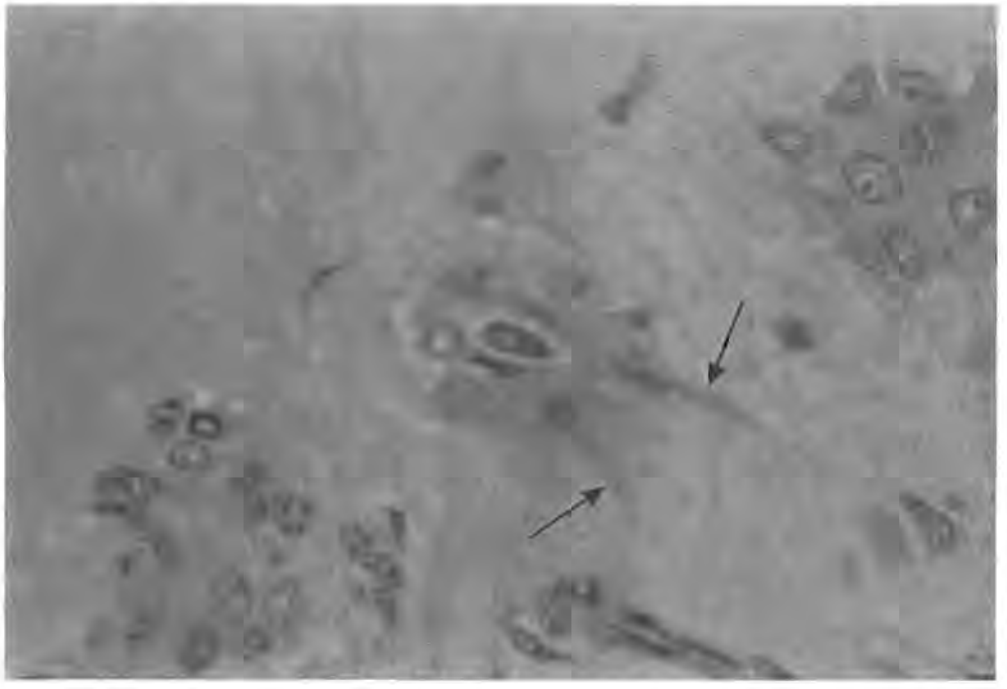

FIGURE 19. Chondroid syringoma. Myoepithelial cells (arrows) proliferating from a ductal structure into the interstitial tissue. (Hematoxylin-eosin; magnification × 1250.)

A few myoepithelial cells have been identified around the periphery of the tubular structures in eccrine spiradenoma.[221,222] Clear cell hidradenoma, referred to in the past as clear cell myoepithelioma,[223,224] shows differentiation towards intraepidermal as well as intradermal eccrine structures, ranging from poral epithelium to cells of the secretory segment.[225] A multipotential reserve cell theory of origin[226] serves as an explanation for the diverse cellular differentiation seen in this tumor. Although myoepithelial differentiation appears to be a hypothetical possibility, the clear cells, which were originally accepted as representing myoepithelial cells,[86,223,224] do not contain alkaline phosphatase or myofilaments and should rather be regarded as immature poral epithelial cells[216] or cells of the outer sheath of hair follicles.[227]

Chondroid syringomas (mixed tumors of the skin) originate from a multipotential stem cell differentiating towards eccrine ductal epithelial and myoepithelial cells[216,228] and are histologically identical to mixed tumors of salivary glands.[229] Myoepithelial cells proliferate into the stroma (Figure 19) and produce the characteristic chondroid deposits.[216,228] This is supported by positive staining of cells incorporated in the chondroid deposits for S100 protein.[114] The cartilage-forming myoepithelial cells differ from chondrocytes by being enveloped in a basement membrane and contain large numbers of intracytoplasmic fibrils and no glycogen.[228] The stroma is, although produced by myoepithelial cells, histochemically similar to normal cartilage.[230]

Tumors dominated by myoepithelial cells are relatively rare in the skin. Efskind and Eker[224] studied 21 tumors which allegedly consisted mainly of myoepithelial cells in two forms: a polygonal cell with a clear glycogen-rich cytoplasm and a spindle-shaped cell arranged in chords and strands. Most examples contained variable numbers of glands lined by epithelium with apocrine features. Their study is unfortunately based on conventional light microscopic techniques only.

Cylindromas (occasionally referred to as turban tumors) are innocuous lesions con-

stituted of tubular structures and epithelial nests, comprised of cells with small dark-staining nuclei arranged in a palissade at the periphery and cells with large light-staining nuclei in the center.[216] Analogous and nearly homologous relationship has been found between dermal cylindromas and certain monomorphic adenomas of salivary gland origin.[231] Although the absence of myoepithelial differentiation in cylindromas has been reported in ultrastructural studies,[232] these tumors warrant further immunohistochemical investigation as their morphology appears to be consistent with variable cytodifferentiation of a basic stem cell of apocrine ductal origin.[216,232]

Primary adenoid cystic carcinoma of the skin has been a very rarely reported neoplasm and due to the absence of ultrastructural and immunohistochemical investigations, it is not possible to delineate myoepithelial participation. Light microscopic evidence appears to indicate that these lesions have a histogenesis and biologic behavior similar to that of adenoid cystic carcinomas of salivary gland origin.[233]

Basal cell epitheliomas are derived not from basal cells, but rather primary epithelial[234] and eccrine gland germs and they represent the least differentiated of the appendage tumors.[216] All studies so far have failed to identify significant myoepithelial differentiation.

D. Other

Myoepithelial cells have not been described in the human uterine cervix. Their differentiation in cervical adenoid cystic carcinomas probably takes place after neoplastic transformation of the subcolumnar reserve cells which are thought to be the progenitors of most other cervical carcinomas.[156,158] A similar histogenesis can be propogated for prostatic adenoid cystic carcinomas as ultrastructural[235] and recent immunofluorescent[45] studies have failed to identify contractile cells in the basal region of human prostatic glands.

The absence of myoepithelial cells in the pancreas should not rule out the possibility of their occurrence in pancreatic tumors. The concept of dedifferentiation, metaplastic neoplasia, or regression could explain their occurrence in a pancreatic microcystic adenoma reported recently.[236] Myoepithelial differentiation in pancreatic tumors should, until further evidence becomes available, be regarded as exceptional.

## ACKNOWLEDGMENTS

The author wishes to thank Dr. V. de Vos (Research Division, Kruger National Park) for making the material reflected in Figures 3, 4, 6, and 12 available and Dr. J. P. van Niekerk (Electron Microscope Unit, Medunsa) for performing all ultrastructural examinations. Valuable assistance was given by D. P. du Plessis and P. Mokonoto of the Research Division of Anatomical Pathology and I am indebted to Mrs. C. S. Begemann for secretarial assistance.

## REFERENCES

1. Batsakis, J. G., *Tumors of the Head and Neck, Clinical and Pathological Considerations*, Williams & Wilkins, Baltimore, 1979, chap. 1.
2. Fischer, E. L., Ultrastructure of human breast and its disorders, *Am. J. Clin. Pathol.*, 66, 291, 1976.
3. Ellis, R. A., Fine structure of myoepithelium of the eccrine sweat gland in man, *J. Cell Biol.*, 27, 551, 1965.
4. Hibbs, R. G., Electron microscopy of the human apocrine sweat gland, *J. Invest. Dermatol.*, 38, 77, 1962.

5. Wessels, N. K., Spooner, B. S., Ash, J. F., Bradley, M. O., Luduena, M. A., Taylor, E. L., Wrenn, J. T., and Yamada, K. M., Microfilaments in cellular and developmental processes, *Science*, 171, 135, 1971.
6. Spooner, B. S. and Wessels, N. K., Effects of Cytochalasin B upon microfilaments involved in morphogenesis of salivary epithelium, *Proc. Natl. Acad. Sci. U.S.A.*, 66, 360, 1970.
7. Cutler, L. S. and Chaudry, A. P., Differentiation of the myoepithelial cells of the rat submandibular gland in vivo and in vitro: an ultrastructural study, *J. Morphol.*, 140, 343, 1973.
8. Line, S. E. and Archer, F. L., The postnatal development of myoepithelial cells in the rat submandibular gland, *Virchows Arch. B*, 10, 253, 1972.
9. Redman, R. S., Sweney, L. R., and McLaughlin, S. T., Differentiation of myoepithelial cells in the developing rat parotid gland, *Am. J. Anat.*, 158, 299, 1980.
10. Chaudry, A. P., Schmutz, J. A., Cutler, L. S., and Sunderraj, M., Prenatal and postnatal histogenesis of myoepithelium in hamster submandibular gland. An ultrastructural study, *J. Submicrosc. Cytol.*, 15, 787, 1983.
11. Young, J. A. and Van Lennep, E. W., *The Morphology of Salivary Glands*, Academic Press, London, 1978, 93.
12. Riva, A., Testa-Riva, F., Del Fiacco, M., and Lantini, M. S., Fine structure and cytochemistry of the intralobular ducts of the human parotid gland, *J. Anat.*, 122, 627, 1976.
13. Tandler, B., Ultrastructure of the human submaxillary gland. III. Myoepithelium, *Z. Zellforsch.*, 68, 852, 1965.
14. Cutler, L. S. and Chaudry, A. P., Intercellular contacts at the epithelial-mesenchymal interface during the prenatal development of the rat submandibular gland, *Dev. Biol.*, 33, 229, 1973.
15. Spooner, B. S. and Faubion, J. M., Collagen involvement in branching morphogenesis of embryonic lung and salivary gland, *Dev. Biol.*, 77, 84, 1980.
16. Grobstein, C. and Cohen, J., Collagenase effect on the morphogenesis of embryonic salivary epithelium in vitro, *Science*, 150, 626, 1965.
17. Bernfield, M. R., Banerjee, S. D., and Cohn, R. H., Dependence of salivary epithelial morphology and branching morphogenesis upon acid mucopolisaccharide (proteoglycan) at the epithelial surface, *J. Cell Biol.*, 52, 674, 1972.
18. Shear, M., The structure and function of myoepithelial cells in salivary glands, *Arch. Oral Biol.*, 11, 769, 1966.
19. Emmelin, N. and Gjorstrup, P., On the function of myoepithelial cells in salivary glands, *J. Physiol. (London)*, 230, 185, 1973.
20. Travill, A. A. and Hill, M. F., Histochemical demonstration of myoepithelial cell activity, *Q. J. Exp. Physiol.*, 48, 423, 1963.
21. Tandler, B., Denning, C. R., Mandel, I. D., and Kutscher, A. H., Ultrastructure of human labial salivary glands. III. Myoepithelium and ducts, *J. Morphol.*, 130, 227, 1970.
22. Garrett, J. R. and Emmelin, N., Activities of salivary myoepithelial cells. A review, *Med. Biol.*, 57, 1, 1979.
23. Emmelin, N. and Thulin, A., Action of drugs on denervated myoepithelial cells of salivary glands, *Br. J. Pharmacol.*, 48, 73, 1973.
24. Pinkstaff, C. A., The cytology of salivary glands, *Int. Rev. Cytol.*, 63, 141, 1980.
25. Taugner, R. and Schiller, A., Gap junctions on myoepithelial cells, *Cell Tissue Res.*, 206, 65, 1980.
26. Brocco, S. L. and Tamarin, A., The topography of the rat submandibular gland parenchyma as observed with S.E.M., *Anat. Rec.*, 194, 445, 1979.
27. Emmelin, N., Garrett, J. R., and Ohlin, P., Neural control of salivary myoepithelial cells, *J. Physiol. (London)*, 19, 381, 1968.
28. Garrett, J. R. and Parsons, P. A., Alkaline phosphatase and myoepithelial cells in the parotid gland of the rat, *Histochem. J.*, 5, 463, 1973.
29. Nagato, T., Yoshida, A., and Uehara, Y., A scanning electron microscopic study of myoepithelial cells in exocrine glands, *Cell Tissue Res.*, 209, 1, 1980.
30. Scott, B. L. and Pease, D. C., Electron microscopy of the salivary and lacrimal glands of the rat, *Am. J. Anat.*, 104, 115, 1959.
31. Cope, G. H., Pratten, M. K., and Williams, M. A., Correlative morphological and biochemical study of the effects of isoprenaline on the organelle and membrane content of the rabbit parotid gland, *Histochem. J.*, 8, 403, 1976.
32. Thulin, A., Motor and secretory effects of nerves on the parotid gland of the rat, *Acta Phys. Scand.*, 96, 506, 1976.
33. Linzell, J. L., Some observations on the contractile tissue of the mammary glands, *J. Physiol. (London)*, 130, 257, 1955.
34. Young, J. A. and Van Lennep, E. W., Morphology and physiology of salivary myoepithelial cells, *Int. Rev. Physiol.*, 12, 105, 1977.

35. Tamarin, A., Myoepithelium of the rat submaxillary gland, *J. Ultrastruct. Res.*, 16, 320, 1966.
36. Nagai, T. and Nagai, M., Scanning electron microscopy of the human submandibular gland, *Arch. Otorhinolaryngol.*, 241, 265, 1985.
37. Leeson, C. R., The electron microscopy of the myoepithelium in the rat extraorbital lacrimal gland, *Anat. Rec.*, 137, 45, 1960.
38. Ruby, J. R., Ultrastructure of the parotid gland of the nine-banded armadillo, *Anat. Rec.*, 192, 389, 1978.
39. Toto, P. D. and Hsu, D. J., Product definition of pleomorphic adenoma of minor salivary glands, *J. Oral Pathol.*, 14, 818, 1985.
40. Bogart, B. I., The fine structural localization of alkaline and acid phosphatase activity in the rat submandibular gland, *J. Histochem. Cytochem.*, 16, 572, 1968.
41. Yoshihara, T., Kanda, T., and Kanedo, T., A cytochemical study on the salivary gland pleomorphic adenoma (mixed tumor) and the fetal and adult salivary gland, *Arch. Otorhinolaryngol.*, 240, 231, 1984.
42. Han, S. S., Kim, S. K., and Cho, M. I., Cytochemical characterization of the myoepithelial cells in palatine glands, *J. Anat.*, 122, 559, 1976.
43. David, R. and Buchner, A., Elastosis in benign and malignant salivary gland tumors, a histochemical and ultrastructural study, *Cancer*, 45, 2301, 1980.
44. Palmer, R. M., Lucas, R. B., Knight, J., and Gusterson, B., Immunocytochemical identification of cell types in pleomorphic adenoma, with particular reference to myoepithelial cells, *J. Pathol.*, 146, 213, 1985.
45. Archer, F. L., Beck, J. S., and Melvin, J. M. O., Localization of smooth muscle protein in myoepithelium by immunofluorescence, *Am. J. Pathol.*, 63, 109, 1971.
46. Dulbecco, R., Henehan, M., and Armstrong, B., Cell types and morphogenesis in the mammary gland, *Proc. Natl. Acad. Sci. U.S.A.*, 79, 7346, 1982.
47. Bani, G., Bigazzi, M., and Bani, D., Effects of relaxin on the mouse mammary gland. I. The myoepithelial cells, *J. Endocrinol. Invest.*, 8, 207, 1985.
48. Dulbecco, R., Unger, M., Armstrong, B., Bowman, M., and Syka, P., Epithelial cell types and their evolution in the rat mammary gland determined by immunological markers, *Proc. Natl. Acad. Sci. U.S.A.*, 80, 1033, 1983.
49. Knight, C. H. and Peaker, M., Development of the mammary gland, *J. Reprod. Fertil.*, 65, 521, 1982.
50. Dulbecco, R., Bologna, M., and Unger, M., Differentiation of rat mammary cell line in vitro, *Proc. Natl. Acad. Sci. U.S.A.*, 76, 1256, 1979.
51. Radnor, C. J. P., Myoepithelial cell differentiation in rat mammary gland, *J. Anat.*, 111, 381, 1972.
52. Chatterton, R. T., Mammary gland: development and secretion, *Obstet. Gynecol. Annu.*, 7, 303, 1978.
53. Rudland, P. S., Hallowes, R. C., Durbin, H., and Lewis, D., Mitogenic activity of pituitary hormones on cell cultures of normal and carcinogen induced tumor epithelium from rat mammary glands, *J. Cell Biol.*, 73, 561, 1977.
54. Stamfer, M., Hallowes, R. C., and Hackett, A. J. Growth of normal human mammary cells in culture, *In Vitro (Rockville)*, 16, 415, 1980.
55. Raynaud, A., Morphogenesis of the mammary gland, in *Milk: The Mammary Gland and Its Secretion*, Kon, S. K. and Coie, A. T., Eds., Academic Press, New York, 1961, 3.
56. Percy, D. H., Morris, V. L., and MacInnes, J. I., Comparison of biologic behaviour and histology of transplanted mammary tumors in GR mice, *J. Natl. Cancer Inst.*, 69, 933, 1982.
57. Wicha, M. L., Liotta, A., Garbisa, S., and Kidwell, W. R., Basement membrane collagen requirements for attachment and growth of mammary epithelium, *Exp. Cell Res.*, 124, 181, 1979.
58. Kleinman, H. K., Klebe, R. J., and Martin, G. R., Role of collagenous matrices in the adhesion and growth of cells, *J. Cell Biol.*, 88, 473, 1981.
59. Warburton, M. J., Ormerod, E. J., Monaghan, P., Ferns, S., and Rudland, P. S., Characterization of a myoepithelial cell line derived from neonatal rat mammary gland, *J. Cell Biol.*, 91, 827, 1981.
60. Terranova, V. P., Rohrbach, D. H., and Martin, G. R., Role of laminin in the attachment of PAM212 (epithelial) cells to basement membrane collagen, *Cell*, 22, 719, 1980.
61. Easty, G. C., Easty, D. M., Monaghan, P., Omerod, M. G., and Neville, A. M., Preparation and identification of human breast epithelial cells in culture, *Int. J. Cancer*, 26, 577, 1980.
62. Radnor, C. J. P., Myoepithelium in the prelactating and lactating mammary glands of the rat, *J. Anat.*, 112, 337, 1972.
63. Waugh, D. and Van Der Hoeven, E., Fine structure of the human adult female breast, *Lab. Invest.*, 11, 199, 1962.
64. Abe, J., Atsuji, K., Tsunakwaki, A., Nishida, T., Inoue, T., Yamasaki, F., Tasaki, K., Iwanaga, S., and Sato, K., Scanning electron microscopic observations of the myoepithelial cells in the prelactating and lactating mammary glands of the rat, *Karume Med. J.*, 28, 233, 1981.

65. Ferguson, D. J. and Anderson, T. J., A morphological study of the changes which occur during pregnancy in the human breast, *Virchows Arch. A*, 401, 163, 1983.
66. Sala, N. L. and Freire, F., Relationship between ultrastructure and response to oxytocin of the mammary myoepithelium throughout pregnancy and lactation: effect of estrogen and progesterone, *Biol. Reprod.*, 11, 7, 1974.
67. Toker, C. and Goldberg, J. D., The small cell lesion of mammary ducts and lobules, *Pathol. Annu.*, 12, 217, 1977.
68. Tannenbaum, M., Weiss, M., and Marx, A. J., Ultrastructure of the human mammary ductule, *Cancer*, 23, 958, 1969.
69. Stirling, J. W. and Chandler, J. A., The fine structure of the normal resting terminal ductal-lobar unit of the female breast, *Virchows Arch. A*, 372, 205, 1976.
70. Hamperl, H., The myothelia (myoepithelial cells), *Curr. Top. Pathol.*, 53, 161, 1970.
71. Soloff, M. S., Oxygocin receptors and mammary myoepithelial cells, *J. Dairy Sci.*, 65, 326, 1982.
72. Caruolo, E. V., Scanning electron microscope visualization of the mammary gland secretory unit and of myoepithelial cells, *J. Dairy Sci.*, 63, 1987, 1980.
73. Hollman, N. H. and Verley, J. M., La regression de la glande mammaire a l'arret de la lactation. II. Etude au microscope electronique, *Z. Zellforsch.*, 82, 222, 1967.
74. Ozello, L., The epithelial-stromal junction of normal and dysplastic mammary glands, *Cancer*, 25, 586, 1970.
75. Mason, D. Y. and Taylor, C. R., Distribution of transferrin, ferritin and lactoferrin in human tissue, *J. Clin. Pathol.*, 31, 316, 1978.
76. Warburton, M. J., Head, L. P., and Rudland, P. S., Redistribution of fibronectin and cytoskeletin proteins during the differentiation of rat mammary tumor cells in vitro, *Exp. Cell Res.*, 132, 57, 1981.
77. Warburton, M. J., Mitchell, D., Ormerod, E. J., and Rudland, P. S., Distribution of myoepithelial cells and basement membrane proteins in the resting, pregnant, lactating and involuting rat mammary gland, *J. Histochem. Cytochem.*, 30, 667, 1982.
78. Gould, V. E., Jao, W., and Battifora, H., Ultrastructural analysis in the differential diagnosis of breast tumours. The significance of myoepithelial cells, basal lamina, intracytoplasmic lumina and secretory granules, *Pathol. Res. Pract.*, 167, 45, 1980.
79. Liotta, L. A., Wicha, M. S., Foidart, J. M., Rennard, S. I., Garbisa, S., and Kidwell, W. R., Hormonal requirements for basement membrane collagen deposition by cultured rat mammary epithelium, *Lab. Invest.*, 41, 511, 1979.
80. Wicha, M. S., Liotta, L. A., Vonderhaar, B. K., and Kidwell, W. R., Effects of inhibition of basement membrane collagen deposition in rat mammary gland development, *Dev. Biol.*, 80, 253, 1980.
81. Stirling, J. W. and Chandler, J. A., Ultrastructural studies of the female breast. I. 9 + 0 Cilia in myoepithelial cells, *Anat. Rec.*, 186, 413, 1976.
82. Lever, W. F. and Schaumburg-Lever, G., *Histopathology of the Skin*, J. B. Lippincott, Philadelphia, 1983, 1.
83. Goldstein, D. J., On the origin and morphology of myoepithelial cells of apocrine sweat glands, *J. Invest. Dermat.*, 37, 301, 1961.
84. Hibbs, R. G., The fine structure of human eccrine sweat glands, *Am. J. Anat.*, 103, 201, 1958.
85. Hashimoto, K., Gross, B. G., and Lever, W. F., The ultrastructure of human embryo skin. II. The formation of intradermal portion of the eccrine sweat duct and of the secretory segment during the first half of embryonic life, *J. Invest. Dermatol.*, 46, 513, 1966.
86. Tulman, L. S. and Jack, M. K., Porosyringoma. Report of a case, *Am. J. Ophthalmol.*, 60, 1116, 1965.
87. Bunting, H., Wislocki, G. B., and Dempsey, E. W., The chemical histology of human eccrine and apocrine sweat glands, *Anat. Rec.*, 100, 61, 1948.
88. Hurley, H. J. and Witkowski, J. A., The dynamics of eccrine sweating in man, *J. Invest. Dermatol.*, 39, 329, 1962.
89. Hurley, H. J. and Shelley, W. B., The role of the human apocrine sweat gland, *J. Invest. Dermatol.*, 22, 143, 1954.
90. Matsuzawa, T. and Kurosumi, K., The ultrastructure, morphogenesis and histochemistry of the sweat gland in the rat foot pads as revealed by electron microscopy, *J. Electron Microsc. (Tokyo)*, 12, 175, 1963.
91. Batsakis, J. G., Kraemer, B., and Scuibba, J. J., The pathology of head and neck tumors: the myoepithelial cell and its participation in salivary gland neoplasia. XVII, *Head Neck Surg.*, 5, 222, 1983.
92. Batsakis, J. G., Clear cell tumors of salivary glands, *Ann. Otol, Rhinol. Laryngol.*, 89, 196, 1980.
93. Warner, T. F. C. S. and Seo, I. S., Hyaline tumor cells: an appearance due to aggregates of cytofilaments, *Ultrastruct. Pathol.*, 1, 395, 1980.
94. Seemayer, T. A., Schurch, W., and Lagace, R., Myofibroblasts in human pathology, *Hum. Pathol.*, 12, 491, 1981.

95. Gabbiani, G., Le Lous, M., Bailey, A. J., Bazin, S., and Delaunay, A., Collagen and myofibroblasts of granulation tissue. A chemical, ultrastructural and immunological study, *Virchows Arch. B*, 21, 133, 1976.
96. Gabbiani, G., Kapanci, Y., Barazzone, P., and Francke, W. W., Immunochemical identification of intermediate-sized filaments in human neoplastic cells. A diagnostic aid for the surgical pathologist, *Am. J. Pathol.*, 104, 206, 1981.
97. Macartney, J. C., Roxburgh, J., and Curran, R. C., Intracellular filaments in human cancer cells. A histological study, *J. Pathol.*, 129, 13, 1979.
98. Gabbiani, G., Csank-Brassert, J., Schneedberger, J. C., Kpanci, Y., Trenchev, P., and Holborow, E. J., Contractile proteins in human cancer cells, *Am. J. Pathol.*, 83, 456, 1976.
99. Tobon, H. and Price, H. M., Lobular carcinoma *in situ*. Some ultrastructural observations, *Cancer*, 30, 1082, 1972.
100. Silver, I. A., Myoepithelial cells in the mammary and parotid glands, *J. Physiol. (London)*, 125, 8, 1954.
101. Dempsey, E. W., Bunting, H., and Wislocki, G. B., Observations on the chemical cytology of the mammary gland, *Am. J. Anat.*, 81, 309, 1947.
102. Bassler, R., Schafer, A., and Paek, S., Elektronmikroskopische und histochemische untersuchung zur morphologie und funktion myoepithelialer zellen, *Verh. Dtsch. Ges. Pathol.*, 51, 301, 1976.
103. Russo, J. and Wells, P., Ultrastructural localization of adenosine triphosphatase activity in resting mammary gland, *J. Histochem. Cytochem.*, 25, 135, 1977.
104. Garrett, J. R. and Harrison, J. D., Alkaline-phosphatase and adenosine triphosphatase histochemical reactions in the salivary glands of cat, dog and man, with particular reference to myoepithelial cells, *Histochemie*, 24, 214, 1970.
105. Archer, F. L. and Kao, V. C. Y., Immunochemical identification of actomyosin in myoepithelium of human tissues, *Lab. Invest.*, 18, 669, 1968.
106. Bussolati, G., Bonfanti, S., Weber, K., and Osborn, M., Staining of myoepithelial cells in fixed and embedded tissues by immunochemical techniques using antibodies to actin, *Riv. Istochim. Norm. Pat.*, 22, 387, 1978.
107. Toh, B. H., Yildiz, A., Sotelo, J., Osung, O., Holborrow, E. J., and Fairfax, A., Distribution of actin and myosin in muscle and nonmuscle cells, *Cell Tissue Res.*, 199, 117, 1979.
108. Macartney, J. C., Trevithick, M. A., Kricka, L., and Curran, R. C., Identification of myosin in human epithelial cancers with iummunofluorescence, *Lab. Invest.*, 41, 437, 1979.
109. Gusterson, B. A., Warburton, M. J., Mitchell, D., Ellison, M., Neville, A. M., and Phillip, S., Distribution of myoepithelial cells and basement membrane proteins in the normal breast and in benign and malignant breast diseases, *Cancer Res.*, 42, 4763, 1982.
110. Papotti, M., Gugliotta, P., Eusebi, V., and Bussolati, G., Immunohistochemical analysis of benign and malignant papillary lesions of the breast, *Am. J. Surg. Pathol.*, 7, 451, 1981.
111. Palmer, R. M., A Study of Myoepithelial Cells in Normal and Pathological Human Salivary Glands, Ph.D. thesis, University of London, 1984.
112. Caselitz, J., Löning, T., Staquet, M. J., Seifert, G., and Thivolet, J., Immunocytochemical demonstration of filamentous structures in the parotid gland. Occurrence of keratin and actin in normal and tumoral parotid gland with special respect to the myoepithelial cells, *J. Cancer Res. Clin. Oncol.*, 100, 59, 1981.
113. Hara, K., Ito, M., Takeuchi, J., Ijima, S., Endo, T., and Hidaka, H., Distribution of S100b protein in normal salivary glands and salivary gland tumors, *Virchows Arch. A*, 401, 237, 1983.
114. Kahn, H. J., Marks, A., Thom, H., and Baumal, R., Role of antibody to S100 protein in diagnostic pathology, *Am. J. Pathol.*, 79, 341, 1983.
115. Emmelin, N., Garrett, J. R., and Ohlin, P., Secretory activity and the myoepithelial cells of salivary glands after duct ligation of cats, *Arch. Oral Biol.*, 19, 275, 1974.
116. Harrison, J. D. and Garrett, J. R., The effects of ductal ligation on the parenchyma of salivary glands of cat studied by enzyme histochemical methods, *Histochem. J.*, 8, 35, 1974.
117. Takeda, Y., Histopathological studies of the labial salivary glands in patients with Sjogrens syndrome. II. Electron microscopic study, *Bull. Tokyo Med. Dent. Univ.*, 27, 27, 1980.
118. Batsakis, J. G., *Tumors of the Head and Neck, Clinical and Pathological Considerations*, Williams & Wilkins, Baltimore, 1979, chap. 3.
119. Seifert, G. and Donath, K., Die morphologie der speicheldrusenerkrankungen, *Arch. Otorhinolaryngol.*, 213, 111, 1976.
120. Regezi, J. A. and Batsakis, J. G., Histogenesis of salivary gland neoplasms, *Otolaryngol. Clin. North Am.*, 10, 297, 1977.
121. Batsakis, J. G., Salivary gland neoplasia: an outcome of modified morphogenesis and cytodifferentiation, *Oral Surg.*, 49, 229, 1980.
122. Eversole, L. R., Histogenic classification of salivary tumors, *Arch. Pathol.*, 92, 433, 1971.

123. Batsakis, J. G. and Regezi, J. A., The pathology of head and neck tumors: salivary glands. I. *Head Neck Surg.*, 1, 59, 1978.
124. Batsakis, J. G., Chinn, E., Regezi, J. A., and Repola, D. A., The pathology of head and neck tumors: salivary glands. II, *Head Neck Surg.*, 1, 167, 1978.
125. Batsakis, J. G., Pinkston, G. R., Luna, M. A., Byers, R. M., Scuibba, J. J., and Tillery, G. W., Adenocarcinomas of the oral cavity: a clinico pathologic study of terminal duct carcinomas, *J. Laryngol. Otol.*, 97, 825, 1983.
126. Batsakis, J. G., Brannon, R. B., and Scuibba, J. J., Monomorphic adenomas of major salivary glands: a histologic study of 96 tumours, *Clin. Otolaryngol.*, 6, 129, 1981.
127. Welsh, R. A. and Meyer, A. T., Mixed tumors of human salivary gland, *Arch. Pathol.*, 85, 433, 1968.
128. Shirasuna, K., Sato, M., and Miyazaki, T., A myoepithelial cell line established from a human pleomorphic adenoma arising in a minor salivary gland, *Cancer*, 45, 297, 1980.
129. Hayashi, Y., Yanagawa, T., Yoshida, H., Yura, Y., Nitta, T., and Sato, M., Induction of other differentiation stages in neoplastic epithelial duct and myoepithelial cells from the human salivary gland grown in athymic nude mice, *Cancer*, 55, 2575, 1985.
130. Chisholm, D. M., Waterhouse, J. P., Kraucunas, J. P., and Scuibba, J. J., A quantiative ultrastructural study of the pleomorphic adenoma (mixed tumor) of human minor salivary glands, *Cancer*, 34, 1631, 1974.
131. Palmer, R. M., Lucas, R. B., and Langdon, J. D., Ultrastructural analysis of salivary gland pleomorphic adenoma, with particular reference to myoepithelial cells, *Histopathology*, 9, 1061, 1985.
132. Krepler, R., Denk, H., Artlieb, U., and Moll, R., Immunocytochemistry of intermediate filament proteins present in pleomorphic adenomas of the human parotid gland: characterization of different cell types in the same tumour, *Differentiation*, 21, 191, 1982.
133. Sehested, M., Barfoed, C., Krogdal, A., and Betlau, P., Immunochemical investigation of lysozyme, lactoferrin, alpha 1-antitrypsin, alpha 1-antichymotrypsin and ferritin in parotid tumors, *J. Oral Pathol.*, 14, 459, 1985.
134. Vigliani, R. and Stramignomi, A., Cytologic localization of antigens from human saliva in pleomorphic adenomas of salivary glands, *Cancer*, 48, 293, 1981.
135. Dardick, I., Van Nostrand, A. W. P., and Phillips, M. J., Histogenesis of salivary gland pleomorphic adenoma (mixed tumor) with an evaluation of the role of the myoepithelial cell, *Hum. Pathol.*, 13, 62, 1982.
136. Buchner, A., David, R., and Hansen, L. S., "Hyaline cells" in pleomorphic adenoma of salivary gland origin, *Oral Surg.*, 52, 506, 1981.
137. Merino, M. J. and LiVolsi, V. A., Pleomorphic adenomas of the parotid gland resembling mesenchymal tumors, *Oral Surg.*, 44, 405, 1977.
138. Azzopardi, J. G. and Smith, O. D., Salivary gland tumours and their mucins, *J. Pathol. Bacteriol.*, 77, 131, 1959.
139. Quintarelli, G. and Robinson, L., The glycosaminoglycans of salivary gland tumors, *Am. J. Pathol.*, 51, 19, 1967.
140. Dardick, I., von Nostrand, A. W. P., Jeans, M. T. D., Rippstein, P., and Edwards, V., Pleomorphic adenoma. II. Ultrastructural organization of "stromal" regions, *Hum. Pathol.*, 14, 798, 1983.
141. Doyle, L. E., Lynn, J. A., Panopio, I. T., and Crass, G., Ultrastructure of chondroid regions — benign mixed tumor of salivary gland, *Cancer*, 22, 225, 1968.
142. Nakazato, Y., Ishizeki, J., Takahashi, O. K., Yamaguchi, H., Kamei, T., and Mori, T., Localization of S100 protein and glial fibrillary acidic protein-related antigen in pleomorphic adenoma of the salivary gland, *Lab. Invest.*, 46, 621, 1982.
143. Caselitz, J. and Loning, T., Specific demonstration of actin and keratin filaments in pleomorphic adenomas by means of immunoelectron microscopy, *Virchows Arch. A*, 393, 153, 1981.
144. Caselitz, J., Osborn, M., Seifert, G., and Weber, K., Intermediate sized filament proteins (prekeratin, vimentin, desmin) in the normal parotid gland and parotid gland tumors. Immunofluorescence study, *Virchows Arch. A*, 393, 273, 1981.
145. Seifert, G., Der einsatz von tumor markern bei der diagnostik von speicheldrusen-tumoren, *Wien. Klin. Wochenschr.*, 84, 372, 1982.
146. Osborn, M., Franke, W. W., and Weber, K., Direct demonstration of the presence of two immunologically distinct intermediate sized filament system in the same cell by double immunofluorescence microscopy, *Exp. Cell Res.*, 125, 37, 1980.
147. Barnes, L., Appel, B. N., Perez, H., and El-Attar, A. M., Myoepithelioma of the head and neck: case report and a review, *J. Surg. Oncol.*, 28, 21, 1985.
148. Scuibba, J. J. and Brannon, R. B., Myoepithelioma of salivary glands: report of 23 cases, *Cancer*, 49, 562, 1982.
149. Delaney, W. E., Transplantable murine salivary gland carcinoma (myoepithelioma). I. Biologic behavior and ultrastructural features, *J. Natl. Cancer Inst.*, 58, 61, 1977.

150. Kahn, L. B. and Schoub, L., Myoepithelioma of the palate. Histochemical and ultrastructural observations, *Arch. Pathol.*, 95, 209, 1973.
151. Bauer, W. H. and Fox, R. A., Adenomyoepithelioma (cylindroma) of palatal mucus glands, *Arch. Pathol.*, 40, 96, 1945.
152. Bock, J. and Feyrter, F., Uber die benignen epithelialen geschwulste der menschlichen orbita, *Arch. Ophthalmol.*, 163, 25, 1961.
153. Markert, J., Zur ultrastruktur des cylindroma, *Arch. Ohr. Nas. Kehlkopfheilk.*, 184, 496, 1965.
154. Fukushima, M., An electron microscopic study of human salivary gland tumors — pleomorphic adenoma and adenoid cystic carcinoma, *Bull. Tokyo Med. Dent. Univ.*, 15, 387, 1968.
155. Hoshino, M. and Yamamoto, I., Ultrastructure of adenoid cystic carcinoma, *Cancer*, 25, 186, 1970.
156. Lawrence, J. B. and Mazur, M. T., Adenoid cystic carcinoma, a comparative study of tumors in salivary gland, breast, lung and cervix, *Hum. Pathol.*, 13, 916, 1982.
157. Osborn, D. A., Morphology and the natural history of cribriform adenocarcinoma (adenoid cystic carcinoma), *J. Clin. Pathol.*, 30, 195, 1977.
158. Mazur, M. I. and Battifora, H. D., Adenoid cystic carcinoma of the uterine cervix, ultrastructure, immunofluorescence and criteria for diagnosis, *Am. J. Clin. Pathol.*, 77, 494, 1982.
159. Bloom, G. D., Carlsoo, B., Gustafsson, H., and Hendriksson, R., Distribution of mucosubstances in adenoid cystic carcinoma. A light and electron microscopic study, *Virchows Arch. A*, 375, 1, 1977.
160. Adkins, K. F. and Daley, T. J., Elastic tissues in adenoid cystic carcinomas, *Oral Surg.*, 38, 562, 1974.
161. Batsakis, J. G. and Regezi, J. A., The pathology of head and neck tumors: salivary glands. IV, *Head Neck Surg.*, 1, 340, 1979.
162. Donath, K., Seifert, G., and Schmitz, R., Zur diagnose und ultrastruktur des tubularen speichelgangcarcinoms: epithelial-myoepitheliales schaltstuckcarcinoma, *Virchows Arch. A*, 356, 16, 1972.
163. Corio, R. L., Scuibba, J. J., Brannon, R. B., and Batsakis, J. G., Epithelial myoepithelial carcinoma of intercalated duct origin. A clinicopathologic and ultrastructural assessment of 16 cases, *Oral Surg.*, 53, 280, 1982.
164. Feyrter, F., Cher das solide (tubular-solide) adenom de schlerm und speicheldrusen, *Frankfurt Z. Pathol.*, 71, 300, 1964.
165. Snellman, A., Ein fall von adenoma cysticum, *Arb. Pathol. Inst. Helsingsfors.*, 7, 42, 1933.
166. Bauer, W. H. and Fox, R. A., Adenomyoepithelioma (cylindroma) of palatal mucus glands, *Arch. Pathol.*, 39, 96, 1945.
167. Saksela, E., Tarkkanen, J., and Wartiovarra, J., Parotid clear-cell adenoma of possible myoepithelial origin, *Cancer*, 30, 742, 1972.
168. Goldman, R. L. and Klein, H. Z., Glycogen-rich adenoma of the parotid gland. An uncommon benign clear-cell tumor resembling certain clear-cell carcinomas of salivary origin, *Cancer*, 30, 749, 1972.
169. Batsakis, J. G. and Regezi, J. A., Selected controversial lesions of salivary tissues, *Otolaryngol. Clin. North Am.*, 10, 309, 1977.
170. Mohamed, A. H. and Cherrick, H. M., Glycogen-rich adenocarcinoma of minor salivary glands. A light and electron microscopic study, *Cancer*, 36, 1057, 1975.
171. Evans, H. L. and Batsakis, J. G., Polymorphous low-grade adenocarcinomas of minor salivary glands: a study of fourteen cases of a distinctive neoplasm, *Cancer*, 53, 935, 1984.
172. Freedman, P. D. and Lumerman, H., Lobular carcinoma of intraoral minor salivary gland origin: report of twelve cases, *Oral Surg.*, 56, 157, 1983.
173. Aberle, A. M., Abrams, A. M., Bowe, R., Melrose, R. J., and Handlers, J. P., Lobular (polymorphous low-grade) carcinoma of minor salivary glands, *Oral Surg.*, 60, 387, 1985.
174. Kuzma, J. E., Myoepithelial proliferation in the human breast, *Am. J. Pathol.*, 19, 473, 1943.
175. Hamperl, H., Uber die myothelien (epithelialen elemente) der brustdruse, *Virchows Arch. A*, 305, 171, 1939.
176. Karnauchow, P. N., Myo-epithelium in gynecomastia, *Am. J. Pathol.*, 30, 1169, 1954.
177. Nicolis, G. L., Modlinger, R. S., and Gabrilove, J. L., A study of the histopathology of human gynecomastia, *J. Clin. Endocrinol.*, 32, 173, 1971.
178. Murad, T. M. and Von Haam, E., Ultrastructure of myoepithelial cells in human mammary gland tumors, *Cancer*, 21, 1137, 1968.
179. Ahmed, A., The myoepithelium in cystic hyperplastic mastopathy, *J. Pathol.*, 113, 209, 1974.
180. Fanger, H. and Barker, B. E., Histochemistry of breast diseases. I. Phosphatases, *Arch. Pathol.*, 67, 293, 1959.
181. Archer, F. and Omar, M., Pink cell (oncocytic) metaplasia in a fibro-adenoma of the human breast: electron-microscope observations, *J. Pathol.*, 99, 119, 1969.
182. Azzopardi, J. G., *Problems in Breast Pathology*, W. B. Saunders, London, 1979, 114.
183. Jao, W., Vazques, L. T., Keh, P. C., and Gould, V. E., Myoepithelial differentiation and basal lamina deposition in fibroadenoma and adenosis of the breast, *J. Pathol.*, 126, 107, 1978.

184. Bussolati, G., Botta, G., and Gugliotta, P., Actin-rich (myoepithelial) cells in ductal carcinoma *in situ* of the breast, *Virchows Arch. B*, 34, 251, 1980.
185. Rudland, P. S., Hallowes, R. C., Cox, S. A., Omerod, E. J., and Warburton, M. J., Loss of production of myoepithelial cell and basement membrane proteins but retention of response to certain growth factors and hormones by a new malignant human breast cancer cell strain, *Cancer Res.*, 45, 3864, 1985.
186. Nielsen, M., Christensen, L., and Albrechtsen, R., The basement membrane component laminin in breast carcinomas and axillary lymphnode metastases, *Acta Pathol. Microbiol. Immunol. Scand. Sect. A*, 91, 257, 1981.
187. Sugano, I., Nagao, K., Matsuzaki, O., Ide, G., and Toyota, N., Immunohistochemical studies on myoepithelial changes in breast tumours, *Acta Pathol. Jpn.*, 31, 35, 1981.
188. Terranova, V. P., Liotta, L. A., Russo, R. G., and Martin, G. R., Role of laminin in the attachment and metastases of murine tumor cells, *Cancer Res.*, 42, 2265, 1982.
189. Toth, J., The role of myoepithelial cells in the morphogenesis of induced mammary tumours, *Virchows Arch. A*, 385, 41, 1979.
190. Machinami, R., Histological grading, histochemistry and electronmicroscopy scirrhous carcinoma of the breast, *Gann*, 67, 11, 1976.
191. Liotta, L. A., Goldfarb, R. H., and Terranova, V. P., Cleavage of laminin by thrombin and plasmin: alpha thrombin selectivity cleaves the beta chain of laminin, *Thromb. Res.*, 21, 663, 1981.
192. Russolati, G., Micca, F. B., Eusebi, V., and Betts, C. M., Myoepithelial cells in lobular carcinoma *in situ* of the breast: a parallel immunocytochemical and ultrastructural study, *Ultrastruct. Pathol.*, 2, 219, 1981.
193. Azzopardi, J. G. and Eusebi, V., Melanocyte colonization and pigmentation of breast carcinoma, *Histopathology*, 1, 21, 1977.
194. Eusebi, V., Mambelli, V., Tison, V., De Lellis, R., and Betts, C. M., Endocrine differentiation in basal cell carcinoma, *Tumori*, 65, 191, 1979.
195. Hackett, A. J., Smith, H. S., Springer, E. J., Owens, R. B., Nelson-Rees, W. A., Riggs, J. L., and Gardner, M. B., Two syngeneic cell lines from human breast tissue: the aneuploid mammary epithelial (Hs578T) and the diploid myoepithelial (Hs578Bst) cell lines, *J. Natl. Cancer Inst.*, 58, 1795, 1977.
196. Eusebi, V., Pich, A., Macchiorlatti, E., and Bussolati, G., Morpho-functional differentiation in lobular carcinoma of the breast, *Histopathology*, 1, 301, 1977.
197. Gad, A. and Azzopardi, J. G., Lobular carcinoma of the breast: a special variant of mucin-secreting carcinoma, *J. Clin. Pathol.*, 28, 711, 1975.
198. Jao, W., Recant, W., and Swerlow, M. A., Comparative ultrastructure of tubular carcinoma and sclerosing adenosis of the breast, *Cancer*, 38, 180, 1976.
199. Clement, P. B. and Azzopardi, J. G., Microglandular adenosis of the breast — a lesion simulating tubular carcinoma, *Histopathology*, 7, 169, 1983.
200. Azzopardi, J. G., *Problems in Breast Pathology*, W. B. Saunders, London, 1979, chap. 13.
201. Makek, M. and von Hochstetter, A. R., Pleomorphic adenoma of the human breast, *J. Surg. Oncol.*, 14, 281, 1980.
202. Bomhard, D. and von Sandersleben, J., Uber die feinstruktur von Mammamischtumoren der Hundin. IV. Das Vorkommen von Myoepithelzellen in Spindelzellverbandin, *Virchows Arch. A*, 371, 219, 1976.
203. Von Sandersleben, J., Die myoepithelzelle und ihre bedeutung fur die histogenese der mammatumoren der hunden, *Berl. Munch. Tierarztl. Wochenschr.*, 89, 67, 1976.
204. Schlotke, B., Histochemical studies on the role of myoepithelial cells in the morphogenesis of mammary tumors in the bitch. II. Enzyme histochemical findings in mammary tumors, *Zentralbl. Veterinarmed. A*, 8, 670, 1976.
205. Zaloudek, C., Oertel, Y. C., and Orenstein, J. M., Adenoid cystic carcinoma of the breast, *Am. J. Pathol.*, 81, 297, 1984.
206. Anthony, P. P. and James, P. D., Adenoid cystic carcinoma of the breast. Prevalance, diagnostic criteria and histogenesis, *J. Clin. Pathol.*, 28, 647, 1975.
207. Peters, G. N. and Wolff, M., Adenoid cystic carcinoma of the breast. Report of 11 new cases: review of the literature and discussion of biologic behaviour, *Cancer Res.*, 52, 680, 1982.
208. Gould, V. E., Miller, J., and Jao, W., Ultrastructure of medullary, intraductal, tubular and adenoid cystic breast carcinomas. Comparative patterns of myoepithelial differentiation and basal lamina deposition, *Am. J. Pathol.*, 78, 401, 1975.
209. Zarbo, R. J. and Oberman, H. A., Cellular adenomyoepithelioma of the breast, *Am. J. Surg. Pathol.*, 7, 863, 1983.
210. Toth, J., Benign human mammary myoepithelioma, *Virchows Arch. A*, 374, 263, 1977.
211. Erlandson, R. A. and Rosen, P. P., Infiltrating myoepithelioma of the breast, *Am. J. Surg. Pathol.*, 6, 785, 1982.

Journal of the Dental Association of South Africa, **42**, 631-637

# Salivary myoepithelium: distribution, structure, functions and pathologic proliferations

E.J., Raubenheimer., J.P. van Niekerk and C.H.J. Hauman

*Professor and Head: Oral Pathology and Oral Biology, Medunsa **Director, Electron Microscope Unit, Medunsa ***Senior Lecturer, Oral Pathology and Oral Biology, Medunsa

*Keywords: myoepithelium; salivary glands*

**SUMMARY**

*Myoepithelial cells are difficult to identify on routine microscopic preparations and before the advent of modern scanning electron microscopic and immunochemical techniques, little was known of their distribution and functions in salivary glands. Acinar myoepithelial cells have been proven to play an important role in the formation and propulsion of saliva, and contraction of intercalated duct associated myoepithelium reduces peripheral resistance by dilating and shortening the ductular portion of the secretory unit. Myoepithelial cells are furthermore responsible for the production of basement membrane proteins and their cilia, which project into invaginations in adjacent secretory cells, may act as salivary chemoreceptors.*

*The study of myoepithelial participation in pathologic conditions gained momentum by the identification of stem cell populations in mature salivary glands. Myoepithelial differentiation has been proven in neoplasms of intercalated duct origin and although epithelial in nature, they play a central role in the production of mesenchymal stromal deposits in mixed salivary gland tumors.*

**OPSOMMING**

*Mioepiteelselle is moeilik aantoonbaar met roetine mikroskopiese tegnieke en voor die era van moderne skandeer elektronmikroskopie en immunositochemiese tegnieke, was baie min bekend oor hulle verspreiding en funksies in speekselkliere. Asinêre mioepiteel speel 'n belangrike rol in die formasie en voortdrywing van speeksel en sametrekking van mioepiteelselle geassosieer met die interkalêre buis, verminder perifere weerstand deur dilatasie en verkorting van die tubulêre gedeelte van die sekretoriese eenheid. Mioepiteelselle is verder verantwoordelik vir die produksie van basaalmembraan proteiene en hulle silia, wat in invaginasies van sekretoriese epiteel projekteer, funksioneer waarskynlik as speeksel chemoreseptore.*

*Die studie van mioepiteel deelname in patologiese toestande is bevorder deur die identifikasie van stamsel populasies in volwasse speekselkliere. Mioepiteel differensiasie is aangetoon in neoplasms van interkalêre buise oorsprong en alhoewel epiteel van aard, speel hulle 'n sentrale rol in die neerlegging van mesenkiemale stromale weefsel in gemengde speekselklier tumore.*

## INTRODUCTION

Myoepithelial cells are located beneath the basement membrane of the terminal portion of most exocrine glands. Those surrounding acini of salivary glands are stellate- or star shaped whereas intercalated duct associated myoepithelial cells are spindle shaped and their cytoplasmic processes usually run parallel to the direction of the duct. In view of the presence of prominent cytoplasmic myofilaments, they have long been accepted as contractile in nature and probably play an important role in propulsion of the secretion (Shear, 1966).

Positive identification of salivary gland myoepithelial cells on routine microscopic preparations is unreliable and until recently very little was known of their distribution and functions in salivary glands. Fortunately, modern sophisticated microscopic techniques have resulted in a surge of new information on this cell. Exposure of myoepithelial cells by chemical removal of periacinar connective tissue and basement membrane deposits, a technique which was partially developed in our laboratory (van Niekerk and Raubenheimer, 1986) has made three dimensional scanning electron microscopic examinations possible (Fig. 1).

The difficulty with which myoepithelial cells are identified in salivary glands is compounded by disease processes which disturb glandular architecture. Myoepithelial identification reaches virtually speculative proportions in neoplastic states where all microscopic landmarks are lost and participating cells exhibit various degrees of cytodifferentiation. Fortunately, immunocytochemical identification of myoepithelial cytoplasmic filaments such as cytokeratin, actin (Caselitz *et al*, 1981), myosin (Palmer *et al*, 1985) and S100 protein (Hara *et al*, 1983) have facilitated the study of their participation in pathologic salivary gland conditions. These proteins are unfortunately shared by many other cell types and reliable myoepithelial identifications in diseased salivary

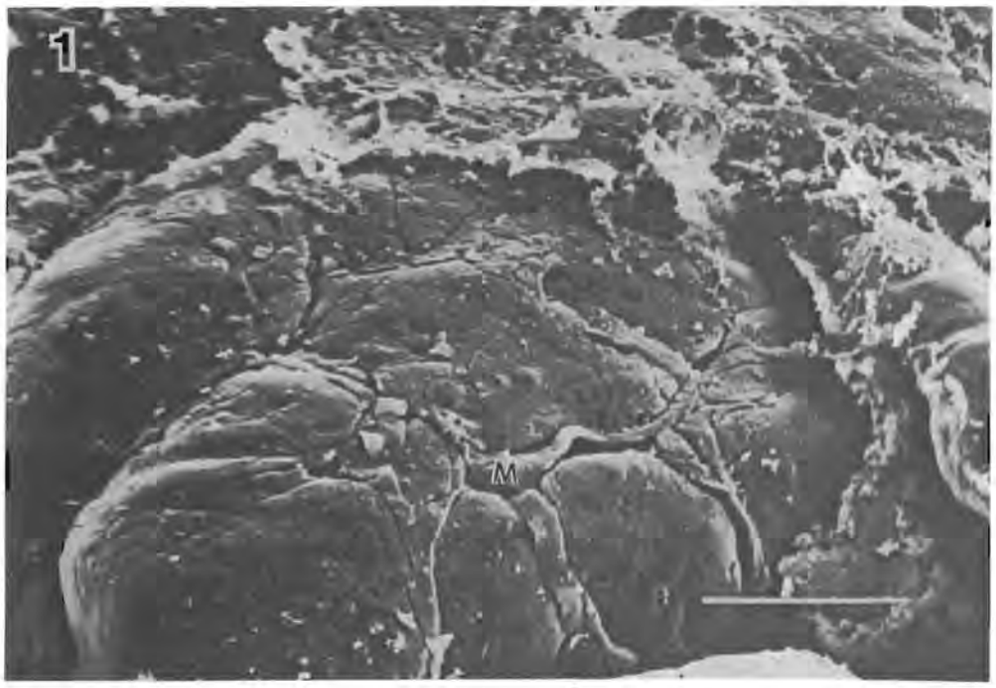


*Fig. 1:* **Scanning electron micrograph of a periacinar myoepithelial cell (M) of the sublingual salivary gland of a vervet monkey after chemical removal of periacinar connective tissue and basement membrane deposits. (Bar = 10 $\mu$m.)**

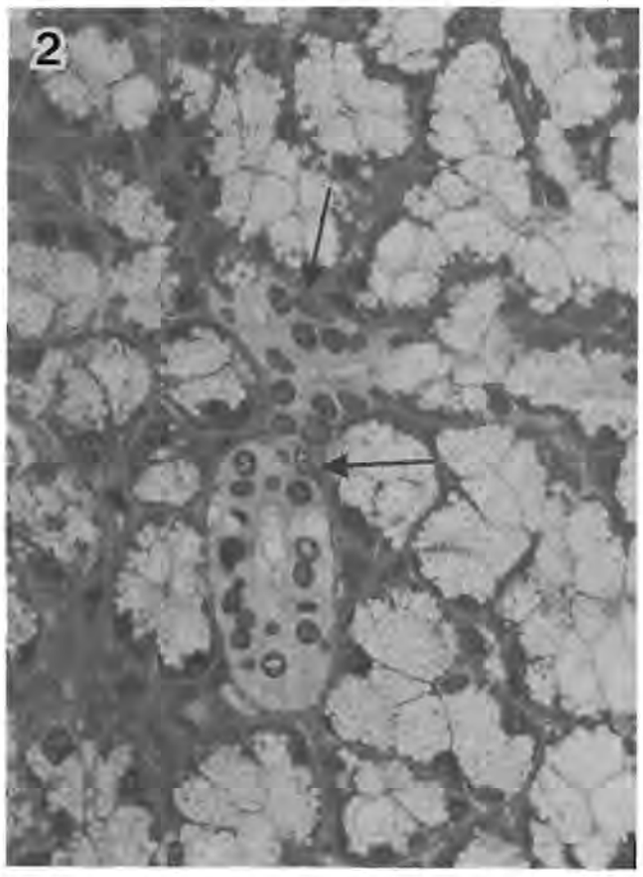


*Fig. 2:* **High power photomicrograph demonstrating intercalated duct associated myoepithelial cells (arrows) in the parotid salivary gland of the African elephant. Note the absence of myoepithelium on allied acini.**

glands is best achieved by a combination of structural, ultrastructural and immunochemical techniques (Raubenheimer, 1986).

## DISTRIBUTION OF SALIVARY GLAND MYOEPITHELIAL CELLS

Species differences and also differences in the distribution of myoepithelial cells in salivary glands of the same animal exist. The acini of the rat (Redman, Sweney and McLaughlin, 1980), rabbit (Cope, Pratten and Williams, 1976) and African elephant, which secrete a serous (watery) saliva, are devoid of myoepithelial cells and only cytoplasmic processes of intercalated duct associated myoepithelium extend onto the adjacent surfaces of allied acini (Fig. 2). Acinar myoepithelial cells have been identified in the human submandibular gland (Nagai and Nagai, 1985 and Tandler, 1965) and labial salivary gland (Tandler *et al*, 1970) where they cover only a portion of the acinar surface. Myoepithelial cells appear to be more prominent around the acini of palatal mucous glands of humans (Han, Kim and Cho, 1976). The acini of the sublingual glands of the monotreme echnida, *Tachyglossus ucleatus,* which secretes a viscous saliva, are ensheathed by interdigitating myoepithelial processes, almost forming a continuous periacinar muscular coat (Young and van Lennep, 1978). These observations have led to the belief that acinar myoepithelial development is amongst other factors, related to the viscosity of the secretory product. Myoepithelial cells of the retrolingual salivary gland of the hedgehog have an unusual three dimensional configuration, the significance of which is unknown. Many of their cytoplasmic processes are not closely apposed to secretory epithelial cells but pursue a seemingly independant course in the connective tissue (Tandler, 1986).

The processes of intercalated duct associated myoepithelial cells often extend onto the striated duct (Riva *et al*, 1976). Although they are usually fusiform (or spindle shaped) and run parallel to the length of the duct, myoepithelial cells in the parotid of the nine banded armadillo (Ruby, 1978) and retrolingual salivary gland of the European hedgehog (Tandler, 1986) encircle the intercalated duct. In the rat submandibular salivary gland, the intercalated ducts are devoid of myo-

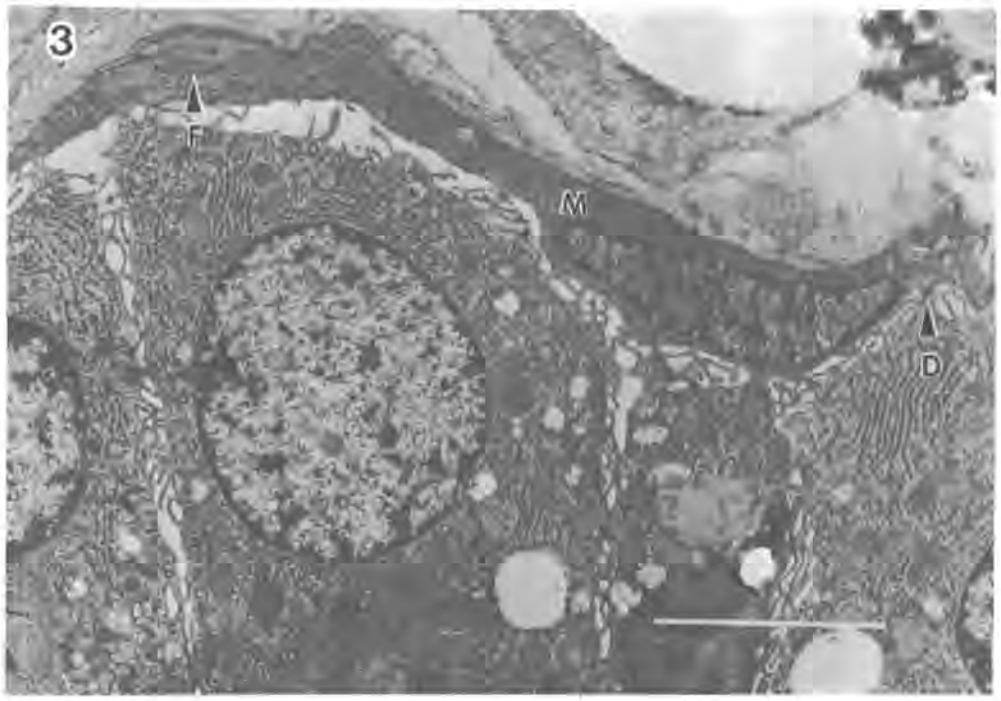


*Fig. 3:* **Transmission electron micrograph of a myoepithelial cell (M) of an elephant submandibular salivary gland. Desmosomal attachments (D) and cytoplasmic myofilaments (F) feature prominent. (Bar = 5 $\mu$m.)**

epithelial cells and those identified adjacent to these ducts on transmission electron micrographs are probably an expression of a myoepithelial network extending between adjacent acini (Brocco and Tamarin, 1979).

## STRUCTURE OF MYOEPITHELIAL CELLS

Myoepithelial cells appear to be similar in structure, irrespective of the organ or species in which they are studied. Those on secretory endpieces (or acini) have 4-8 primary cytoplasmic branches each with two or more secondary branches. The cytoplasmic extensions of myoepithelial cells located on intercalated ducts usually lie longitudinal and seldom divide.

The stromal (or outer) surface of myoepithelial cells contain caveolar invaginations which are abundant in areas where nerve fibres abut (Young and van Lennep, 1978). The visceral cell surface is smooth, attached by desmosomes to secretory cells (Tandler, 1965) (Fig. 3) and contain isolated cilia which invaginate the basal cytoplasmic membrane and protrude deep into the cytoplasm of the secretory epithelial cell (Tandler *et al*, 1970). Micropinocytotic vesicles are often present on the surface facing secretory cells (Ruby, 1978).

Myoepithelial nuclei are ellipsoidal, surrounded by a few ribosomes and mitochondria are scattered throughout the cytoplasm of the cell body. Other cytoplasmic organelles are in the juxtanuclear position (Tamarin, 1966). Cytoplasmic myofilaments are uniform in diameter, their density varying because of the distance between individual filaments. They run in bundles which often fuse with other bundles, are compact in areas resembling dense elongated bodies characteristic of smooth muscle cells and terminate in attachment devices on the stromal cell membrane (Young and van Lennep, 1978). Intermediate sized cytoplasmic filaments of the cytokeratin type (Caselitz *et al*, 1981) are demonstrable in salivary gland myoepithelium .

Myoepithelial cells are often adjacent to cells which have a similar shape, but possess an extremely electron-lucent cytoplasm that contains almost no organelles. Electron microscopic observations indicate that these cells, termed clear cells, are transformed directly into myoepithelium, since all morphological intergrades between the two cell types have been recognised. These clear cell appear to develop from intercalated duct cells (Tandler, 1965). Myoepithelium therefore probably shares a common ancestry with secreting epithelial cells, which are also of intercalated duct cell origin (Riva *et al*, 1976).

## FUNCTIONS OF SALIVARY MYOEPITHELIAL CELLS

Although species differences do exist, it is generally accepted that salivary myoepithelial cells have a dual innervation of parasympathetic as well as sympathetic nerves and impulses from both types cause contraction (Garrett and Emmelin, 1979). The association between nerve axons and salivary gland myoepithelial cells suggests that activation occurs by diffusion of a transmitter substance comparable to that suggested for smooth muscle cells (Tamarin, 1966). Synchronisation of contraction is made possible by gap junctions and overlaps between myoepithelial cell processes (Brocco and Tamarin, 1979).

Acinar myoepithelial contraction (as demonstrated in Fig. 4) facilitates rapid expulsion of the secretion by rupturing 'ripe' mucous cells (Tandler *et al*, 1970), preventing distension of secretory endpieces (Emmelin, Garret and Ohlin, 1968) and reducing lumenal volume (Garrett and Emmelin, 1979). All salivary glands lacking acinar myoepithelial cells (which were referred to previously), notably secrete a watery (serous) saliva. It has recently been shown that the intraductal pressure developed by the rat parotid gland during autonomic nerve stimulation is always lower than that of the rat mandibular gland (Tandler, 1976). The paucity of acinar myoepithelial cells in the rat parotid gland would lead

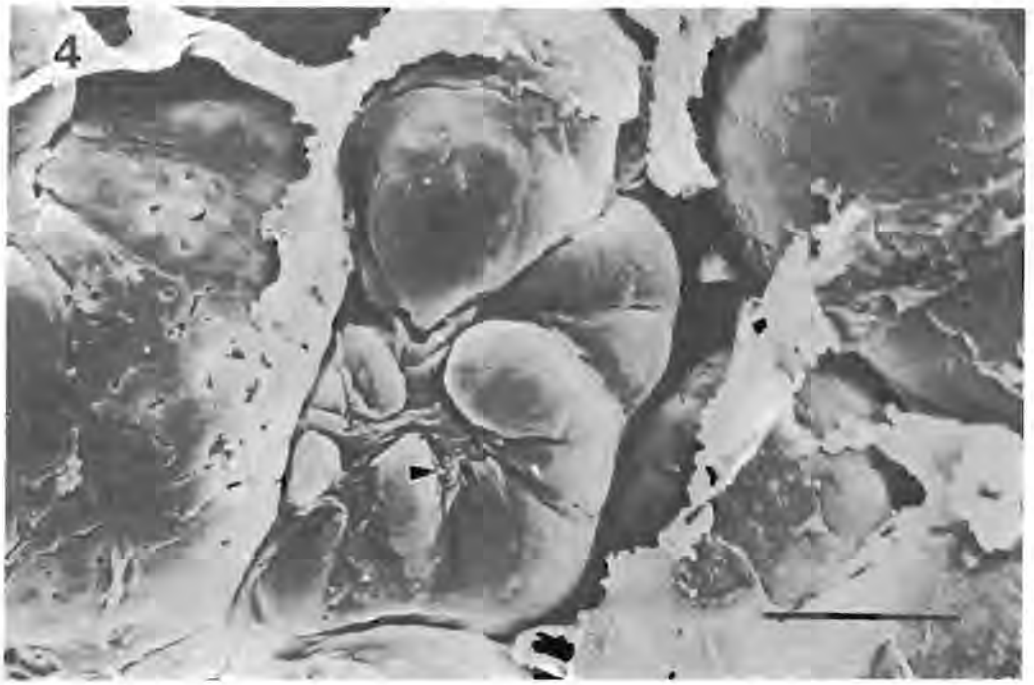


*Fig. 4:* **Scanning electron micrograph of a contracted myoepithelial cell surrounding the acinus of the submandibular salivary gland of a vervet monkey. Note the contracted appearance of the cytoplasmic processes (arrow). (Bar = 10 μm.)**

one to expect such a result. Furthermore, the pancreas which lacks myoepithelial cells, secretes a watery product and is more prone to irreparable acinar or duct rupture from degrees of obstruction slight enough to produce no ill effects in salivary glands. In contrast, the sublingual salivary gland of the monotreme echnida, *Tachyglossus ucleatus,* which has been referred to, shows extraordinary development of acinar myoepithelial cells. The supporting and contractile functions of acinar myoepithelial cells is therefore likely to be particularly valuable when the viscosity of the saliva is high (Garrett and Emmelin, 1979). However, other factors such as the anatomical location of the gland may also be important. Salivary glands in the floor of the mouth continuously excrete against a vertical pressure gradient and will theoretically require more acinar myoepithelial support than glands located above the orifice of their main excretory duct.

Acinar myoepithelial contraction may also modify the concentration of saliva by decreasing the surface area of the secretory apparatus exposed to interstitial fluid (Tandler *et al*, 1970). Such an effect would diminish the loss of fluid from the secretion and is probably important when viscid saliva has to be forced through narrow channels in a gland (Garrett and Emmelin, 1979). Myoepithelial cilia, which have already been referred to, may act as chemoreceptors in this regard as they have been postulated to have a sensory function (Tandler *et al*, 1970).

Contraction of myoepithelial cells surrounding intercalated ducts reduces lumenal volume and shortens and widens these structures thereby decreasing peripheral resistance (Young and van Lennep, 1977). Extension of their processes onto proximal surfaces of allied acini may serve to align the acinar lumen with that of the duct during contraction, a function which may be particularly important in glands which are continuously distorted during mastication.

The role of the myoepithelial cell in transportation of metabolites to and from secretory cells is a controversial issue. Basal infoldings of human submandibular salivary gland myoepithelium (Nagai and Nagai, 1985) could serve to increase the surface area exposed to tissue fluid. Pinocytotic vesicles (Tandler *et al*, 1970), positive staining for the iron binding protein ferritin (Toto, 1985) and an increased alkaline phosphatase and magnesium dependant adenosine triphosphatase (ATPase) activity (Yoskihara, Kanda and Kaneko, 1984) are all features supporting this view. It has been pointed out however, that ATPase activity in myoepithelial cells of the palatine glands of rats are rather implicated in cell contraction and, that the vesicle-like structures are in fact invaginations of the plasma membranes and are continuous with the extracellular space (Han *et al*, 1976).

Finally, myoepithelial cells are important in the formation and maintenance of the enveloping basement membrane. Fibronectin, laminin and elastin are major components of basement membranes and are found to be produced by myoepithelial cells (Toto, 1985). Basement membrane proteins are not only an essential scaffold for epithelial multiplication and differentiation (Kleinman, Klebe and Martin, 1981) but also form part of the hypothetic epithelial mesenchymal junction through which all metabolites involved in the synthesis of saliva, pass.

## NON-NEOPLASTIC MYOEPITHELIAL PROLIFERATIONS

The bulk of research is focused on the role of myoepithelium in salivary gland neoplasms and very little is known of their participation in non-neoplastic conditions.

After ductal ligation of the parotid and submandibular salivary glands of cats, processes of myoepithelial cells extend into the interstitial spaces and folds of basal lamina aggregate around protruberant parts of the cell thereby increasing the distance between the cell membrane and nerve endings (Emmelin, Garrett and Ohlin, 1974). These alterations may reduce the neuro-effector

efficiency and together with the mechanical disadvantage of rearranged myoepithelial processes, help to explain the altered intraductal pressure responses that occurred after stimulation. Induction of secretion leading to a rise in the intraductal pressure of ligated glands, often causes distention and even disruption of the first part of the striated duct, which lacks myoepithelial support (Garrett and Emmelin, 1979).

Lymphoreticular cell proliferation associated with atrophy of the glandular parenchyma and ductal changes ending in so-called 'epimyoepithelial islands' are characteristics of chronic recurrent (punctate) sialadenitis, sicca syndrome, Sjögrens syndrome and benign lymphoepithelial lesion. The epimyoepithelial islands are formed by metaplastic transformation of ductal epithelial and myoepithelial cells. Some believe myoepithelial cells are few in number and located only around the periphery of the islands (Takeda, 1980) whereas the majority of workers agree that myoepithelium forms an integral part of epimyoepithelial islands (Seifert and Donath, 1976). This controversy underlines the difficulty by which myoepithelial cells are identified microscopically in a state other than normal.

## NEOPLASTIC MYOEPITHELIAL PROLIFERATIONS

It is generally known that the exocrine pancreas, which is phylogenetically and structurally related to salivary glands except for the absence of myoepithelial cells, lacks the variety and diversity of salivary gland neoplasms. The wide spectrum of morphologic presentation of salivary gland neoplasms, exceeded only by neoplasms of gonadal origin, is to a great extent a result of the two sided expression of myoepithelium: although epithelial in origin, their cytoplasmic organization is quite similar to mesenchymal smooth muscle. It is therefore not surprising that neoplastic myoepithelial cells have three principal morphologic presentations namely, fibroblastic (or myoid) (Fig. 5a), epithelial-like (or glycogen rich clear cell) (Fig. 5b) and hyaline (or plasmacytoid) (Fig. 5c). Care should be taken not to interpret clear cell formation arising from fixation artefact as myoepithelial differentiation.

As neoplasms develop after oncogenic transformation of mitotically active undifferentiated cells, a study of the reserve (or stem cell) compartments of salivary glands are necessary before attempting to master salivary gland oncogenesis. The basal cells of the excretory duct (the excretory duct reserve cell or EDRC) and the intercalated duct cell (or IDC) act respectively as stem cells for the differentiated ductal and secretory portions of mature salivary glands (Fig. 6). The EDRC has a genetic potential to give rise to columnar and squamous cells (and metaplastic mucus producing cells) lining the excretory duct and the IDC to acinar cells, intercalated duct cells, striated duct cells and myoepithelial cells (Batsakis, 1979).

According to the "bicellular theory" on salivary gland oncogenesis the IDC population is postulated to be the epithelial source for myoepitheliomas, mixed tumours (pleomorphic adenomas), adenoid cystic carcinomas, epithelial myoepithelial carcinomas (or tubular carcino-

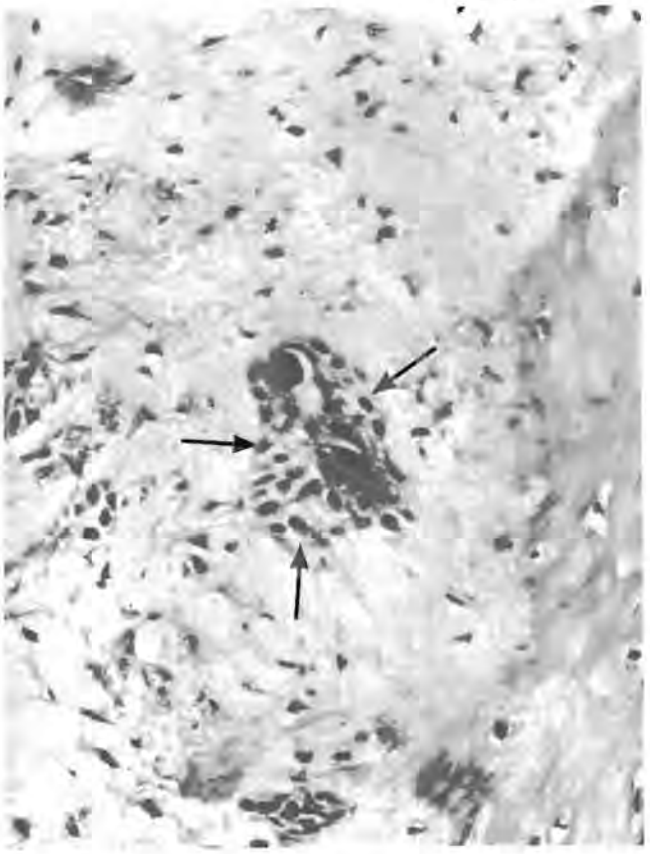

*Fig. 5(a):* **Fibroblastic (or myoid) myoepithelial differentiation in a myoepithelioma of the palate. Arrows indicate intercalated duct differentiaiton (H & E, X200).**

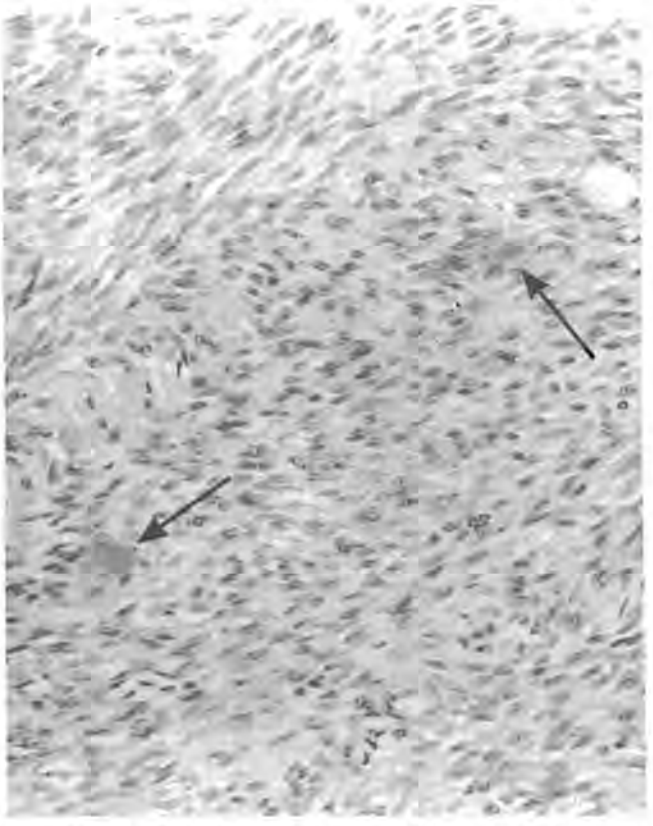

*Fig. 5(b):* **Epithelial (or clear cell) differentiation (arrows) surrounding an intercalated duct-like structure in a mixed salivary gland tumour of the parotid (H & E, X200).**

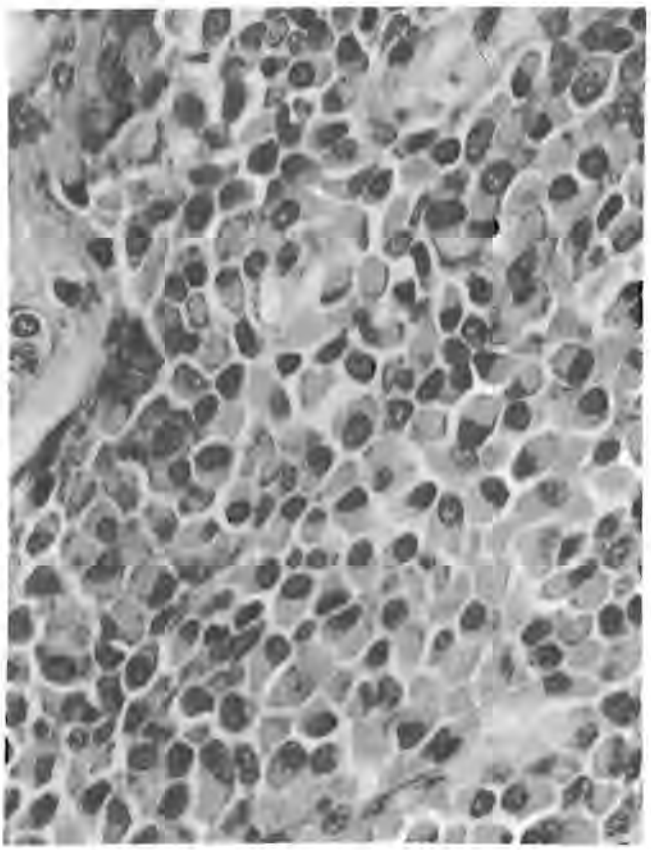

*Fig. 5(c):* **Hyaline (or plasmacytoid) myoepithelial differentiation in the myoepithelioma of the palate (H & E X300).**

mas) lobular carcinoma (or terminal duct adenocarcinoma) monomorphic adenoma and acinous cell carcinoma (Batsakis, 1980). Theoretically most of these neoplasms and even monomorphic adenomas may, to a greater or lesser extent, exhibit myoepithelial differentiation (Batsakis, Brannon and Scuibba, 1981). The possibility of myoepithelial differentiation, on the other hand should, according to the bicellular theory, be excluded from neoplasms that are postulated to arise from the EDRC (muco-epidermoid carcinoma, papillary mucinous adenocarcinoma and primary salivary squamous carcinoma) (Batsakis, Kraemer and Scuibba, 1983).

Much of the debate on the significance of myoepithelial differentiation in salivary gland neoplasms, have focused around the identity of the characteristic myxoid, chondroid, osteoid, elastic and fibrous interstitial deposits in mixed tumours. After tissue culturing and chemical and ultrastructural investigations, the mesenchymal nature of these deposits has been proven beyond doubt (Azzopardi and Smith, 1959) and evidence of myoepithelial participation in their production has accumulated (Toto and Hsu, 1985; Regezi and Batsakis, 1977; Doyle *et al*, 1968 and Caselitz and Loning, 1981). Some of the spindle shaped cells, often associated with stromal deposits, were found to react positively with immunochemical stains for S100 protein (Nakazato *et al*, 1982) (Fig. 7) and cytoplasmic filaments of the myosin, actin (Caselitz and Loning, 1981) and prekeratin types, (Caselitz *et al*, 1981) characteristics which strongly suggest myoepithelial differentiation. Since myoepithelial cells already exhibit features of smooth muscle, neoplas-

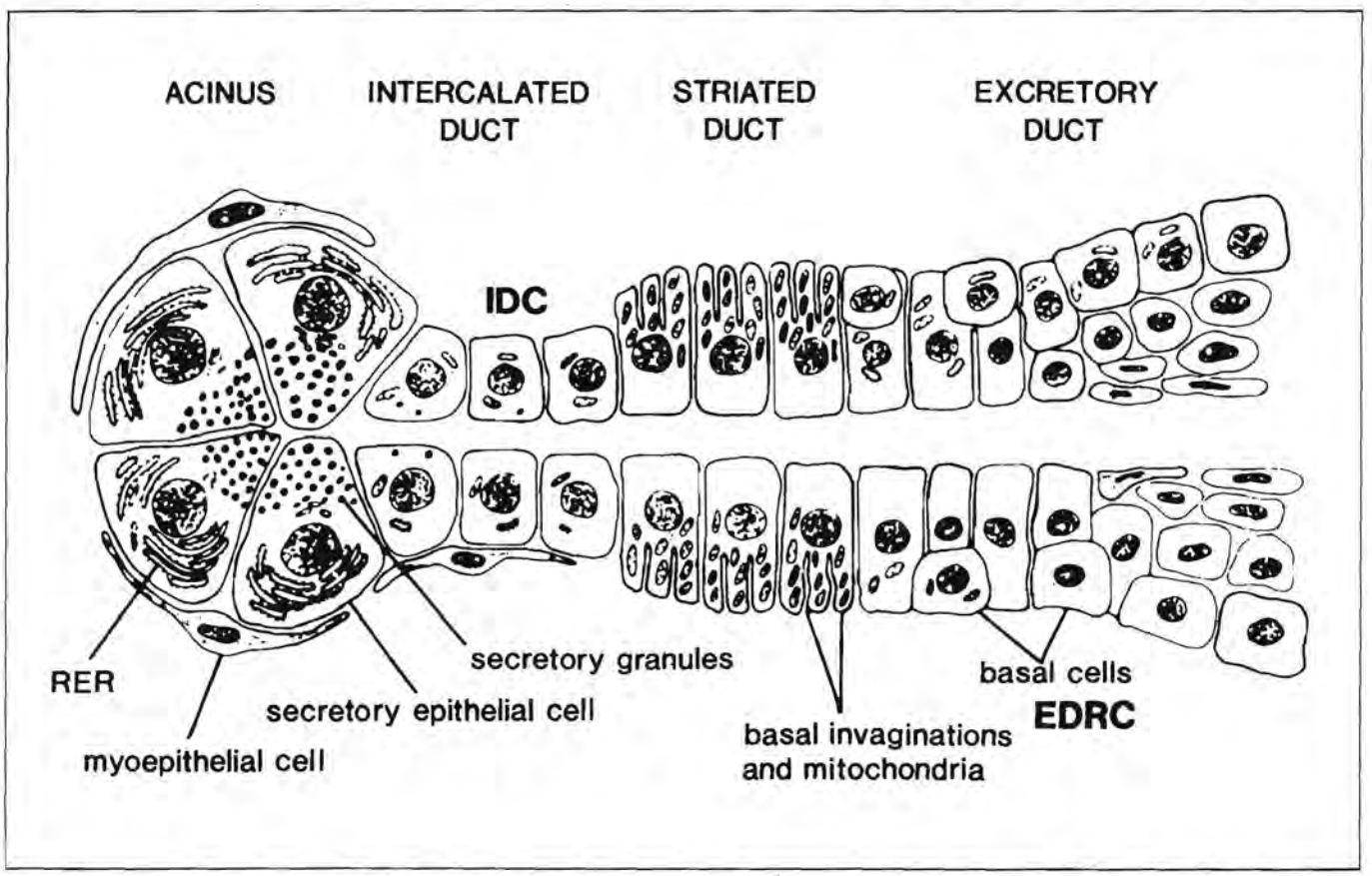


*Fig. 6:* **Diagrammatic representation of the stem cell compartments of mature salivary glands (IDC = intercalated duct cell and EDRC = excretory duct reserve cell). (Reproduced with permission from Batsakis, 1979, pp.4).**

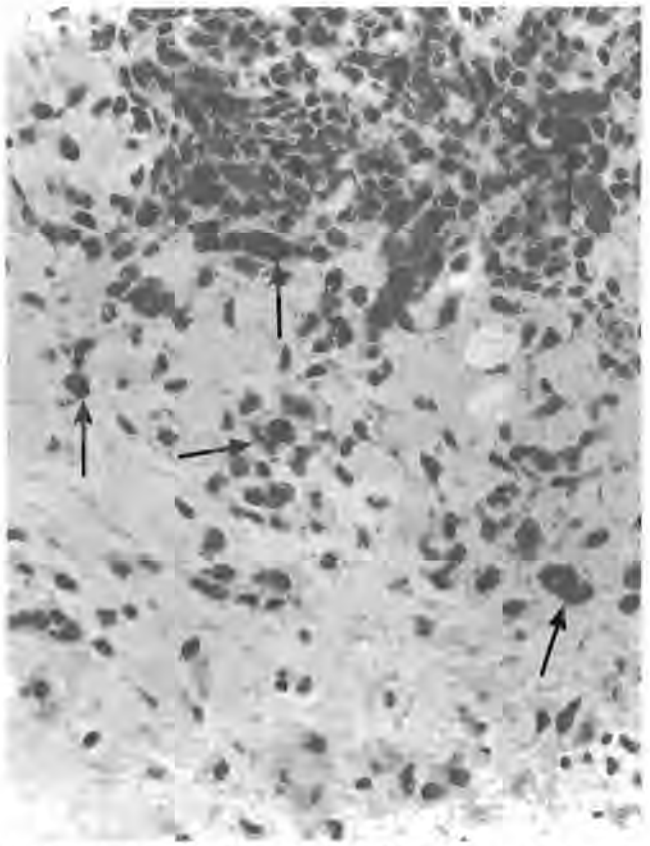

*Fig. 7:* **Cytoplasmic S100 protein positivity (arrows) indicating myoepithelial differentiation in a myxoid area of a mixed tumour of the parotid salivary gland (Immunoperoxidase stain for S100 protein, X200).**

tic change may expose other mesenchymal characteristics which could lead to the deposition of myxoid, chondroid, fibrous, elastic and even osteoid tissues. These findings not only introduce a new pathologic concept of mesenchymal metaplasia of neoplastic epithelium, but also lessens the rigid classical distinction, based on product definition, made between tissues of ectodermal and mesodermal origin.

## ACKNOWLEDGEMENT

We are indebted to Dr V de Vos (National Parks Board) for making some of the material available and Mrs C.S. Begemann for secretarial services rendered during preparation of the manuscript.

## REFERENCES

Azzopardi, J.G. & Smith, O.D. (1959) Salivary gland tumors and their mucins. *Journal of Pathology and Bacteriology*, 77, 131-140.

Batsakis, J.G. (1979) *Tumors of the Head and Neck*. Clinical and Pathological Considerations, 2nd ed., Chap. 1, pp.1-75.

Batsakis, J.G. (1980) Salivary gland neoplasia: An outcome of modified morphogenesis and cytodifferentiation. *Oral Surgery, Oral Medicine and Oral Pathology*, **49**, 229-232.

Batsakis, J.G., Brannon, R.B. & Scuibba, J.J. (1981) Monomorphic adenomas of major salivary glands: a histologic study of 96 tumours. *Clinical Otolaryngology*, **6**, 129-143.

Batsakis, J.G. Kraemer, B. & Scuibba, J.J. (1983) The myoepithelial cell and its participation in salivary gland neoplasia. *Head and Neck Surgery*, **5**, 222-233.

Brocco, S.L. & Tamarin, A. (1979) The topography of the rat submandibular gland parenchyma as observed with S.E.M. *Anatomical Record (New York)*, **194**, 445-459.

Caselitz, J. & Löning, T. (1981) Specific demonstration of actin and keratin filaments in pleomorphic adenomas by means of immunoelectron microscopy. *Virchows Archives (A)*, **393**, 153-158.

Caselitz, J., Löning, T., Staquet, M.J., Seifert, G. & Thivolet, J. (1981) Immunocytochemical demonstration of filamentous structures in the parotid gland. Occurence of keratin and actin in normal and tumoral parotid gland with special respect to the myoepithelial cells. *Journal of Cancer Research and Clinical Oncology*, **100**, 59-68.

Cope, G.H., Pratten, M.K. & Williams, M.A. (1976) Correlative morphological and biochemical study of the effects of isoprenaline on the organelle and membrane content of the rabbit parotid gland. *Histochemical Journal (London)*, **8**, 403-418.

Doyle, L.E., Lynn, J.A., Panopio, I.T. & Cross, G. (1968) Ultrastructure of chondroid regions — benign mixed tumor of salivary gland. *Cancer*, **22**, 225-233.

Emmelin, N., Garrett, J.R. & Ohlin, P. (1968) Neural control of salivary myoepithelial cells. *Journal of Physiology (London)*, **196**, 381-396.

Emmelin, N., Garrett, J.R. & Ohlin, P. (1974) Secretory activity and the myoepithelial cells of salivary glands after duct ligation in cats. *Archives of Oral Biology*, **19**, 275-283.

Garrett, J.R. & Emmelin, N. (1979) Activities of salivary myoepithelial cells. A review. *Medical Biology (Helsinki)*, **57**, 1-28.

Han, S.S., Kim, S.K. & Cho, M.I. (1976) Cytochemical characterization of the myoepithelial cells in palatine glands. *Journal of Anatomy*, **122**, 559-570.

Hara, K., Ito, M., Takeuchi, J., Tjima, S., Endo, T. & Hidaka, H. (1983) Distribution of S100b protein in normal salivary glands and salivary gland tumors. *Virchows Archives (A)*, **401**, 237-249.

Kleinman, H.K., Klebe, R.J. & Martin, G.R. (1981) The role of collagenous matrices in the adhesion and growth of cells. *Journal of Cellular Biology*, **88**, 473-485.

Nagai, T. & Nagai, M. (1985) Scanning electron microscopy of the human submandibular gland. *Archives of Otolaryngology*, **241**, 265-266.

Nakazato, Y., Ishizeki, J., Takahashi, O.K., Yamaguchi, H., Kamei, T. & Mori, T. (1982) Localization of S100 protein and glial fibrillary acidic protein-related antigen in pleomorphic adenoma of the salivary gland. *Laboratory Investigation*, **46**, 621-626.

Palmer, R.M., Lucas, R.B., Knight, J. & Gusterson, B. (1985) Immunocytochemical identification of cell types in pleomorphic adenoma, with particular reference to myoepithelial cells. *Journal of Pathology*, **146**, 213-220.

Raubenheimer, E.J. (1987) The myoepithelial cell: Embryology, Function and Proliferative Aspects. *Critical Reviews in Clinical Laboratory Sciences*, **25**, 161-193.

Redman, R.S., Sweney, L.R. & McLaughlin, S.T. (1980) Differentiation of myoepithelial cells in the developing rat parotid gland. *American Journal of Anatomy*, **158**, 299-320.

Regezi, J.A. & Batsakis, J.G. (1977) Histogenesis of salivary gland neoplasms. *Otolaryngologic Clinics North America*, **10**, 297-307.

Riva, A., Testa-Riva, F., Del Fiacco, M. & Lantini, M.S. (1976) Fine structure and cytochemistry of the intralobular ducts of the human parotid gland, *Journal of Anatomy*, **122**, 627-640.

Ruby, J.R. (1978) Ultrastructure of the parotid gland of the nine banded armadillo. *Anatomical Record (New York)*, **192**, 389-405.

Seifert, G. & Donath, K. (1976) Die morphologie der speicheldrusenerkrangkungen. *Archives of Otorhinolaryngology*, **213**, 11-124.

Shear, M. (1966) The structure and function of myoepithelial cells in salivary glands. *Archives of Oral Biology*, **11**, 769-781.

Takeda, Y. (1980) Histopathological studies of the labial salivary glands in patients with Sjögrens syndrome. Part II: electron microscopic study. *Bulletin of the Tokyo Medical and Dental University*, **27**, 27-42.

Tamarin, A. (1966) Myoepithelial of the rat submaxillary gland. *Journal of Ultrastructural Research*, **16**, 320-338.

Tandler, B. (1965) Ultrastructure of the human submaxillary gland. III. Myoepithelium. *Zeitung fur Zellforschung*, **68**, 852-863.

Tandler, B. (1986) Unusual myoepithelium in the retrolingual salivary gland of the European hedgehog. *Journal of Submicroscopic Cytology*, **18**, 261-270.

Tandler, B., Denning, C.R., Mandel, I.D. & Kutscher, A.H. (1970) Ultrastructure of human labial salivary glands, III. Myoepithelium and ducts. *Journal of Morphology*, **130**, 227-245.

Toto, P.D. & Hsu, D.J. (1985) Product definition of pleomorphic adenoma of minor salivary glands. *Journal of Oral Pathology*, **14**, 818-832.

Van Niekerk, J. & Raubenheimer, E.J. (1986) Ultrastructure of myoepithelium in salivary glands of African elephant (Loxodonto africana). *Proceedings of the IXth Internation Congress on Electron Microscopy*, 2 869-2 870.

Yoshihara, T., Kanda, T. & Kaneko, T. (1984) A cytochemical study on the salivary gland pleomorphic adenoma (mixed tumor) and the fetal and adult salivary gland. *Archives of Otorhinolaryngology*, **240**, 231-238.

Young, J.A. & van Lennep, E.W. (1977) Morphology and physiology of salivary myoepithelial cells. *International Review of Physiology*, **12**, 105-125.

Young, J.A. and van Lennep, E.W. (1978) *The Morphology of Salivary Glands*, 1st ed. Ch. 5, pp.93-99. London: Academic Press.

# PAROTID SALIVARY GLAND OF THE AFRICAN ELEPHANT (LOXODONTA AFRICANA): STRUCTURE AND COMPOSITION OF SALIVA

E J RAUBENHEIMER*, J DAUTH**, M J DREYER** and V DE VOS***

**ABSTRACT**

Specimens from parotid salivary glands of full-grown elephant *Loxodonta africana* (n=6) and saliva aspirated from their main excretory ducts were examined macroscopically and microscopically and analysed biochemically. The composition of the saliva was compared to that of the blood. The parotids (n=12; $\bar{x}$ = 7,4 kg) are homocrine and of a seromucous nature. Myoepithelial cells are well-developed along intercalated ducts and their processes extend to proximal portions of allied acini. The saliva is hypotonic and contains relatively low concentrations of sodium and glucose and high concentrations of potassium, urea, calcium and phosphorus. Absence of detectable levels of $\alpha$-amylase negates a digestive role and the voluminous secrete evidently aids swallowing by moisturising and lubricating the large mass of ingested leaves, grass and bark.

Key words: Parotid salivary gland, African elephant, *Loxodonta africana*, saliva

Raubenheimer E.J.; Dauth J.; Dreyer M.J.; De Vos V. Parotid salivary gland of the African elephant (*Loxodonta africana*): structure and composition of saliva. *Journal of the South African Veterinary Association* (1988) 59 No. 4, 184-187 (En). Department of Oral Pathology, Medical University of Southern Africa, 0204 Medunsa, Republic of South Africa.

## INTRODUCTION

The bulk of research on salivary glands and most studies on the composition of saliva have been performed in man and laboratory animals. Little is known of the structure of the salivary glands of large mammals and the compositon of their saliva. Investigations which correlate the feeding habits of animals with the structure of their salivary glands and the composition of saliva, could throw more light on many findings which are apparently of a speculative nature.

The functional development of salivary glands is generally adapted to the feeding habits of an animal. Among aquatic mammals, where lubrication of food is not necessary, the glands may be absent, as in most Cetacea (dolphins and whales)[8]. At the opposite extreme are ruminants that habitually ingest dry food; their salivary glands are often exceptionally large and well-developed and the volume of saliva secreted is so great that major changes in plasma pH and electrolyte concentrations occur in a tidal fashion with each feeding period[15].

In general terms, salivary glands of mammals can be considered as subservient to various different functions. First, and perhaps most important, they evidently provide lubrication to aid the swallowing of food. The lubricant may take the form of slimy mucus as is usual in lower vertebrates. More serous secretions, as are formed by the parotid glands of most mammals, clearly achieve the same purpose when the ingested food is very dry. Secondly, by secreting enzymes, salivary glands are able to play a role in digestion. Most mammals have relatively high concentrations of amylase in parotid saliva. Nevertheless, the parotid saliva of animals of the order Carnivora (which includes the dog and cat) and the family Bovidae (which include sheep) contains no amylase. Other possible functions of salivary glands include the secretion of hormones, regulation of body temperature by wetting of the fur and the excretion of toxic substances which play an important role in defence, paralysing and killing of prey[21].

The functional unit of all compound tubulo-acinar salivary glands is composed of a secretory endpiece which may be spheroid (acinar) or tubular in shape, an intercalated duct and a striated duct which leads to the larger interlobular and eventually the main excretory duct[21]. Greatly modified striated ducts, referred to as granular ducts, are found in the salivary glands of certain animals and are probably implicated in the production and secretion of digestive enzymes[14]. Traditionally, homocrine glands are classified according to the acinar secretory cell type as either serous, mucinous or seromucous (mucoid). The term "heterocrine" (or mixed) is used to describe glands with both serous (or seromucous) and mucinous cells in acini. Both acini and intercalated ducts are generally accepted to be surrounded by myoepithelial cells which lie on the inside of the epithelial basement membrane. Their distribution appears to depend, amongst other factors, on the viscosity of the secretion[10]. Saliva is secreted into the acinar lumen and propelled along the duct system by pressures which develop during the process of secretion and myoepithelial cell contraction. Resorption of water and exchange of electrolytes take place in the striated duct[19].

The African elephant, *(Loxodonta africana)*, belongs to the order Proboscidea and is the largest land animal: an adult animal can weigh close to 7000 kg[1]. It occurs only in Africa south of the Sahara Desert and occupies large areas of semi-arid wooded savannah. According to their feeding habits, elephants are classified as grazers and browsers[5]. Each animal ingests up to 170 kg of forage a day[9] consisting of leaves, dry grass and bark.

As no scientific information is available on the salivary gland system of the African elephant, we undertook this study to determine the structure of the parotid gland and the composition of its saliva.

## MATERIAL AND METHODS

The parotid salivary glands of fully grown African elephant (n=6) immobilised during a population control programme[6], were removed and the mass determined. Fresh tissue specimens, representing all areas of the glands, were selected, excised and fixed in buffered formalin and 2,5% gluteraldehyde. Specimens were embedded in Epon, serially sectioned (1 micrometer thick) and alternate haematoxylin/eosin and periodic acid Schiff stains performed.

Saliva was aspirated from the main excretory ducts of 2 animals and stored at 4°C before biochemical analyses.

Whole venous blood samples were collected from 20 animals, centrifuged and subjected to biochemical analyses in a batch. The viscosity of the serum and saliva was measured with a Coulter Harkness Viscometer and expressed in centipoise or cp (one hundredth of dyne per second per square centimetre).

## RESULTS

The parotid salivary glands of the African elephant are paired organs located caudal to the mandibular ramus and condylar process, rostral to the external auditory meatus and deep to the cervical musculature. Each gland measures 29 x 22 x 19 cm and has an average mass of 7,4 kg (range 6,4 - 8,2 kg). The main excretory duct has a diameter of 9 - 13 mm and leaves the gland at the rostro-ventral pole, follows a rostral and ventral course and opens up on the buccal mucosa in the oral vestibule in relation to the upper caudal teeth. On cut surface, the parotid is seen to have a well-developed fibrous capsule with fibrous septae dividing the gland into many lobes (Fig. 1).

Microscopically the parotid gland is of a complex tubulo-acinar type with slightly elongated homocrine acini, the latter containing secretory cells of the seromucous type (Fig. 2). These cells are intermediate between serous and mucinous cells, contain secretory granules

* Department of Oral Pathology, Medical University of Southern Africa, 0204 Medunsa, Republic of South Africa
** Department of Chemical Pathology, Medical University of Southern Africa
*** Research Division, Kruger National Park

which are larger than those of serous cells and no stainable epithelial mucin. The intercalated ducts vary in length (4 - 12 cells) and are lined with flattened, glycogen-rich cells. The transition between intercalated ducts and striated ducts is abrupt (Fig. 2). Striated ducts show extensive branching and extend into the interlobular fibrous septae and are surrounded by a rich capillary network (Fig. 3). The striated ducts are lined by cuboidal to columnar cells with centrally placed nuclei and foldings of the basal cytoplasmic membrane. The larger interlobular ducts are lined by pseudostratified cylindrical epithelium with scattered goblet cells. Stratified squamous epithelium is evident close to the orifice of the main excretory duct.

The composition and viscosity of the parotid saliva in comparison to blood values are reflected in Table 1.

## DISCUSSION

The parotid of the African elephant is probably the largest salivary gland in the animal kingdom. It has been shown[19] that stimulated salivary gland tissue produces between 60 and 200 microlitres of saliva $min^{-1}$ gram wet $tissue^{-1}$. Both parotids of elephant theoretically therefore could secrete in excess of 50ℓ saliva $h^{-1}$. During a normal feeding cycle, which extends over the greatest part of 24h[18], this voluminous secretion evidently aids swallowing by moisturising and lubricating the large mass of ingested leaves, bark and grass. The seromucous nature and hypotonicity of the saliva, which, although watery, contains more glycoproteins than serous saliva[17], are best adapted to fulfil these functions.

Structurally, the parotid is less varied among different species than are the other major salivary glands. Although tubular secretory endpieces are occasionally encountered, they usually have an acinar configuration as in the

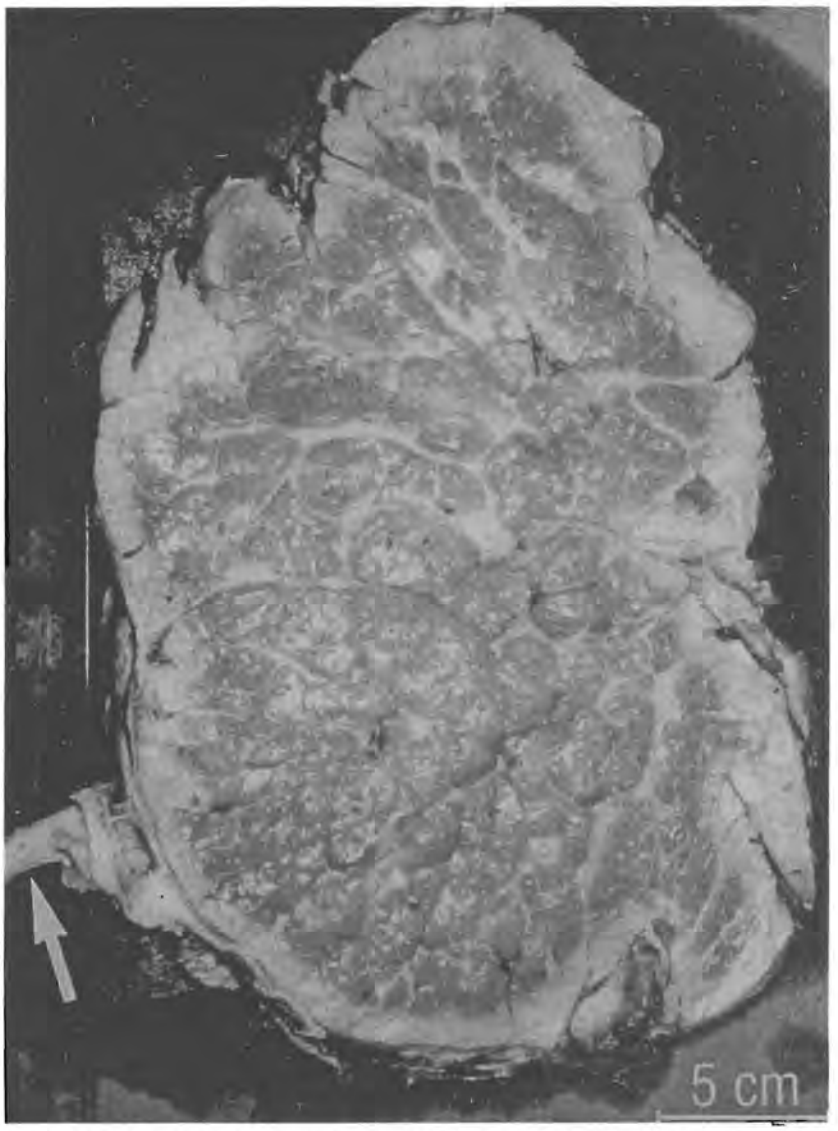


**Fig. 1:** Cut surface of the parotid of the African elephant. Note the main excretory duct (arrow) leaving the rostro-ventral surface of the gland

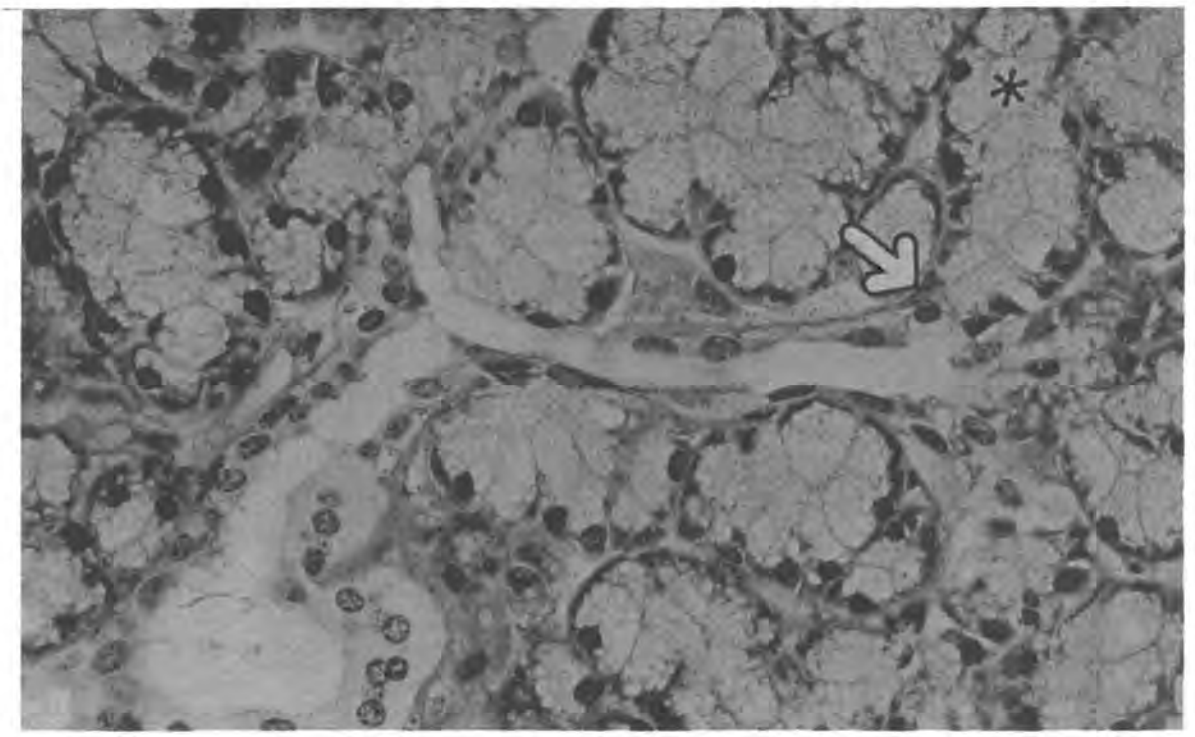

**Fig. 2:** Homocrine seromucous acinus (asterisk) opening up in an intercalated duct, lined by flattened epithelium and which leads into a striated duct (right upper corner). Note myoepithelial cell body located on interface between acinus and duct (arrow). (H.E. stain, magnification x500)

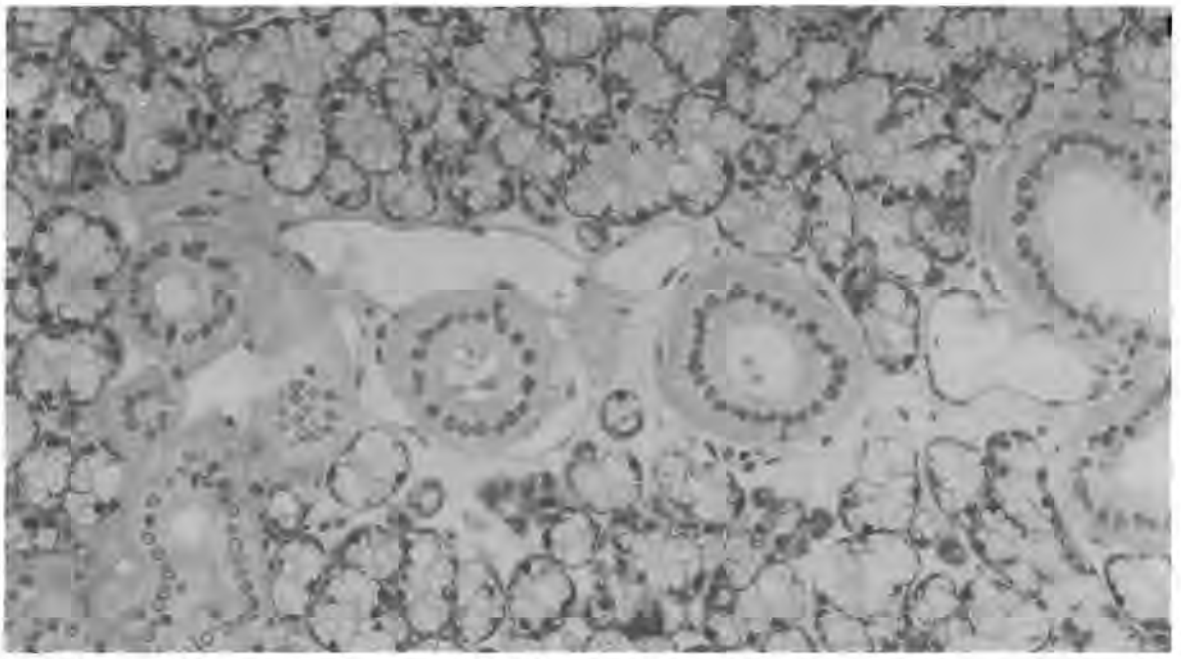

**Fig. 3:** Striated ducts in a vascular-rich environment. (H E stain magnification x200)

Table 1: **Biochemical findings in serum and saliva of the African elephant**

| | Serum (±SD) | Saliva (Mean values) |
|---|---|---|
| Sodium (mmol $\ell^{-1}$) | 127 (2) | Negative |
| Potassium (mmol $\ell^{-1}$) | 6,6 (0,9) | 63 |
| Chloride (mmol $\ell^{-1}$) | 85 (2) | 26 |
| Urea (mmol $\ell^{-1}$) | 2,7 (0,5) | 6,3 |
| Creatinine ($\mu$mol $\ell^{-1}$) | 123 (25) | 130 |
| Total protein (g $\ell^{-1}$) | 89 (5) | 41 |
| Albumin (g $\ell^{-1}$) | 33 (2) | Negative |
| Phosphorus (mmol $\ell^{-1}$) | 1,92 (0,26) | 15,7 |
| Total calcium (mmol $\ell^{-1}$) | 2,92 (0,13) | 5,74 |
| Magnesium (mmol $\ell^{-1}$) | 1,57 (0,23) | 4,25 |
| Actual $Ca^{++}$ (mmol $\ell^{-1}$) | 1,48 (0,07) | 2,05 |
| pH | 7,01 (0,13) | 6,53 |
| $Ca^{++}$ at pH 7,4 (mmol $\ell^{-1}$) | 1,17 (0,9) | 1,10 |
| Glucose (mmol $\ell^{-1}$) | 7,11 (1,26) | 0,4 |
| Viscosity (cp) | 1,81 (plasma) | 2.01 |
| Amylase (IU $\ell^{-1}$) | 923 (321) | Negative |

elephant, but the secretory cells are mostly homocrine and of a serous nature[21]. Seromucous parotid glands, similar to those of the African elephant, were also reported in the domestic cat and dog[13 21], in the brush-tail possum and Trichosurus[21], Djungarian hamster[16] and in man[11 21]. In most animals, the junction of the endpiece and intercalated duct, is usually sharply defined and the intercalated ducts are fairly uniform. The striated ducts, on the other hand, are more varied among species. They are conspicuous in the African elephant and dog and completely absent in some marine carnivora[21]. Myoepithelial development in the gland reflects the relatively low viscosity of the secretion. Unlike the case of mucinous glands which secrete saliva with a high viscosity[21], myoepithelial cells are absent from the peripheral portion of the acini. Intercalated duct-associated myoepithelial cell processes which extend to acini, probably align the latter with allied ducts and ensure patency, especially when the gland is distorted during masticatory movements of the mandible. The bulk of the parotid lies above or on the same level as the orifice of the main duct and the main forces propelling the saliva probably include gravitation, pressures which develop during the process of secretion and contraction of intercalated duct-associated myoepithelial cells. The latter probably not only facilitate propulsion by reducing luminal volume, but also regulate the salivary flow rate by dilating the intercalated ducts, thereby decreasing peripheral resistance.

The absence of $\alpha$-amylase in the saliva of the elephant probably negates a digestive role. This is in contrast to human parotid saliva which is considerably richer in $\alpha$-amylase than saliva from the other major human salivary glands. The concentrations of sodium, chloride, total protein, albumin and glucose are significantly less in saliva when compared to serum, whereas the concentrations of potassium, urea, phosphorus, calcium and magnesium are higher. Although the functional significance of many of these alterations are unknown, it supports the proposed active role played by the striated ducts and their vascular environment in rendering the saliva sodium-free and hypotonic[12 20]. Furthermore, it has been proven that the ducts of the rat a rabbit mandibular gland reabsor sodium and chloride and secrete potassium and bicarbonate[19].

The total calcium, ionised calcium ($Ca^{++}$) and magnesium concentrations of the elephant saliva appear to be higher than serum concentrations, contrary to what is generally found[19]. The high concentration of salivary calcium may, however, be the result of sympathetic nerve activity, as Burgen & Emmelin[2] reported an increase in salivary calcium in the dog mandibular gland after sympathetic stimulation. The phosphorus concentrations are comparable to those of human[4] and sheep[3] parotid saliva. It should be emphasised however, that the electrolyte composition of saliva may vary with the age, hydration state and hormonal status of the animal and the salivary secretory rate[19]. Elephant parotid saliva is low in glucose and hypotonic owing to the absence of sodium. These findings are comparable to those reported in human parotid saliva[7 12]. In contrast to humans however where the salivary urea concentration is approximately 75 - 90% of the content in blood[7], elephant saliva contains a much higher urea concentration, which is probably indicative of a recycling mechanism similar to that found in cattle where digestive protozoa and bacteria utilise urea for metabolic processes. Future investigations of this nature on other animals may clarify the function of the other components of saliva.

**ACKNOWLEDGEMENTS**

We are indebted to officials of the National Parks Board for their support and Mrs C S Begemann for secretarial services.

**REFERENCES**

1. Boolootian R A, Stiles K A 1981 College Zoology 10th edn Macmillan Publishing Company, New York
2. Burgen A S V, Emmelin N G 1961 Physiology of the salivary glands. Arnold, London
3. Compton J S, Nelson J, Wright R, Young J A 1980 A micropuncture investigation of electrolyte transport in the parotid glands of

sodium-replete and sodium-depleted sheep. Journal of Physiology, London 309: 429-446
4. Dawes C 1969 The effects of flow rate and duration of stimulation on the concentrations of protein and the main electrolytes in human submandibular saliva. Archives of Oral Biology 14: 277-294
5. Delaney M J, Happold D C D 1979 Ecology of African mammals Longman, London: 118
6. De Vos V 1983 Management of large animals in African conservation areas. In: Owen-Smith R N (ed.) Proceedings of a symposium held in Pretoria 29-30 April 1982 Haum, Pretoria: 213-232
7. Diem K 1982 Documenta Geigy Scientific Tables 6th edn J R Geigy S A, Basle: 517-519
8. Fahrenholz C 1967 Drüsen der mundhöhle. In: Bolk L, Göppert E, Kallius E, Lubosch N (ed.) Handbuch der vergleichenden Anatomie der Wirbeltiere Vol 3 Asher, Amsterdam: 115-210
9. Guy P R 1975 The daily food intake of the African elephant *Loxodonta africana* Blumenbach, in Rhodesia. Arnoldia Rhodesia 7 (26): 1-8
10. Raubenheimer E J 1987 The myoepithelial cell: embryology, function and proliferative aspects. Critical Reviews in Clinical Laboratory Sciences 25: 161-193
11. Riva A, Riva-Testa F 1973 Fine structure of acinar cells of human parotid gland. Anatomical Record, New York 176: 149-165
12. Schneyer L H, Young J A, Schneyer C A 1972 Salivary secretion of electrolytes. Physiological Review, Bethesda M.D. 52: 720-777
13. Shackleford J M, Klapper C E 1962 Structure and carbohydrate histochemistry of mammalian salivary glands. American Journal of Anatomy 111: 25-47
14. Smith R J, Frommer J 1972 Effects of prepubertal castration on development of granular tubules and amylase activity in the male mouse submandibular gland. Archives of Oral Biology 17: 1561-1571
15. Stacy B D 1969 Augmented renal excretion of calcium and magnesium in sheep after feeding. Quarterly Journal of Experimental Physiology 54: 1-10
16. Suzuki S, Ago A, Mohri S, Nishinakagawa H, Otsuka J 1983 Fine structure of the parotid gland of the Djungarian hamster *(Phodopus sungarus)*. Jikken Dobutsu 32: 175-184
17. Vinning R F, McGinley R A 1985 Hormones in saliva. Critical Reviews in Clinical Laboratory Sciences 23: 95-146
18. Wyatt J R, Eltringham S K 1974 The daily activity of the elephant in the Rwenzori National Park, Uganda. East African Wildlife Journal 12: 273-290
19. Young J A, Schneyer C A 1981 Composition of saliva in mammalia. Australian Journal of Experimental Biology and Medical Science 59: 1-53
20. Young, J A, Van Lennep E W 1978 Transport in salivary and salt glands. In: Giebisch G, Tosteson D C, Ussing H H (ed.) Membrane Transport in Biology Vol 4 Springer, New York
21. Young J A, Van Lennep E W 1978 The morphology of salivary glands Academic Press, London: 1-48, 99

Proc. XIth Int. Cong. on Electron Microscopy, Kyoto, 1986

# ULTRASTRUCTURE OF MYOEPITHELIUM IN SALIVARY GLANDS OF AFRICAN ELEPHANT (LOXODONTA AFRICANA)

J P VAN NIEKERK and E J RAUBENHEIMER

Electron Microscope Unit and Department of Oral Pathology
Medical University of Southern Africa, Republic of South Africa

The great potential of scanning electron microscopy (SEM) in salivary gland research has not yet been realized. This technique has however, been utilized in describing the three dimensional features of acinar myoepithelial cells of the submandibular gland of the male mouse (1) and rat (2), sublingual gland of the rat (2,3) and human submandibular gland (4). The acinus of the rat parotid gland appears to be devoid of myoepithelium (2,5), with only the processes of the intercalated duct myoepithelial cells extending onto the basal region of the acinus (6). A similar distribution has also been observed in the parotid of the rabbit (7).

The purpose of this study was to establish the surface morphology of myoepithelial cells of the parotid and submandibular salivary glands of the largest terestrial animal, the African elephant (Loxodonta africana). Fresh surgical specimens of the parotid and mandibular salivary glands of three full grown elephant bulls were fixed in 2,5% glutaraldehyde and buffered in 0,1M sodium cacodylate. After fixation the samples were treated in 8N HCl and ultrasonically cleaned.

With stromal tissue and basement membranes removed, myoepithelial cell bodies or processes could not be identified on the parenchymal aspect of the acini of the parotid glands (Fig. 1). The absence of acinar myoepithelial cells was confirmed with transmission electron microscopy (Fig. 2). The submandibular glands on the other hand, showed prominent interdigitating myoepithelial processes forming an uninterrupted layer around the acini (Fig. 3). The cell bodies appeared to be situated eccentrically towards the junction of the acinus and intercalated duct.

The prominence of myoepithelial cells in the submandibular glands of the animals under study, is reminiscent of myoepithelial development in the sublingual gland of the monotreme echnida, Tachyglossus aculeatus, which is reported to secrete an extremely viscous saliva (8). This phenomenon lead some investigators to postulate that the supporting function of salivary myoepithelial cells is likely to be particularly valuable when the content of mucin in the secretory product is high (9). This observation is also supported by other independent studies (2). Although we agree that the viscosity of saliva could parallel acinar myoepithelial development, other factors probably have an equal bearing on the prominence of these cells as both the submandibular and parotid salivary glands in elephants secrete a serous (watery) saliva. Much of the parotid gland of the elephant is located on the level of or above the orifice of the main excretory duct. Propulsive forces created by the secretory process and contraction of myoepithelial cells surrounding

intercalated ducts should therefore be sufficient for flow of saliva in this gland. The submandibular gland, however, which is situated much lower than its orifice, excretes against a higher pressure gradient. Acinar myoepithelial cells therefore not only play an important supportive role against acinar distention potentiated by this increased luminal pressure, but also add a supplementary propulsive force through their well established contractile function.

REFERENCES


1. Taugner, B., Schiller, A. Cell Tissue Res. 206:65-72 (1980).
2. Nagato, T., Yoshida, A. and Uehara,Y. Cell Tissue Res. 209:1-10 (1980).
3. Nagato, T. J. Electron Microsc. (Tokyo) 27(3):235-236 (1978).
4. Nagai, T. and Nagai, M. Arch. Otolaryngol. 241:265-266 (1985).
5. Mark, M.R., Sharawy, M., Pennington, C. Scan. Elec. Micro. III:137-145 (1981).
6. Garrett, J.R. and Parsons, P.A. Histochem. J. 5:463-471 (1973).
7. Cope, G.H., Prattern, M.K. and Williams, M.A. Histochem. J. 8:403-418 (1976).
8. Young, J.A. and van Lennep, E.W. The morphology of salivary glands. Academic Press Inc. (London) (1978).
9. Garrett, J.R., Emmelin, N. Med. Biol. 57:1-28 (1979).



Fig 1: SEM of acini of parotid gland

Fig 2: TEM of parotid gland

Fig 3: SEM of acinus of submandibular gland illustrating interdigitating myoepithelial processes

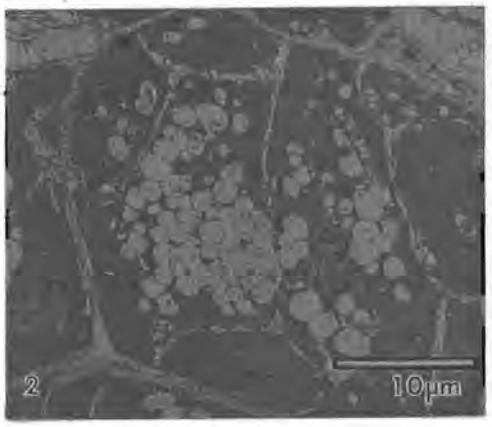


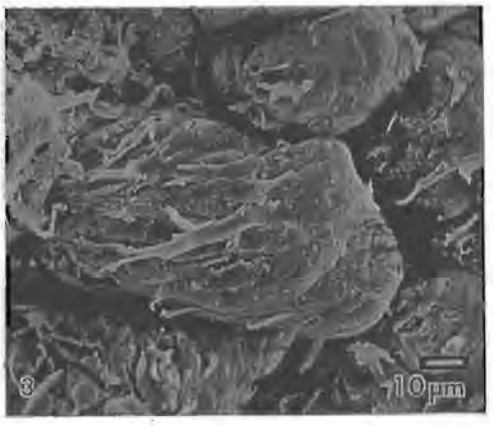

# Tyrosine-rich crystalloids in a polymorphous low-grade adenocarcinoma

*Erich J. Raubenheimer, MChD,[a] Willem F. P. van Heerden, MChD,[b] and Thomas Thein,[c]*
*Medunsa, Republic of South Africa*

MEDICAL UNIVERSITY OF SOUTHERN AFRICA

A polymorphous low-grade adenocarcinoma with tyrosine-rich crystalloid deposits is reported. The literature is reviewed, and diagnostic and histogenetic implications of this finding are discussed.
(ORAL SURG ORAL MED ORAL PATHOL. 1990;70:480-2)

Tyrosine-rich crystalloids occur mainly in salivary gland mixed tumors where they are reported in between 1.5% and 21% of cases.[1-4] The incidence of these deposits appears higher in mixed tumors involving black patients than white patients.[2, 5] Salivary gland carcinomas that have been reported to contain tyrosine-rich crystalloids include one terminal duct adenocarcinoma,[6] an adenoid cystic carcinoma,[7] and a malignant mixed tumor.[8]

The origin of tyrosine-rich crystalloids in salivary gland neoplasms is speculative. The principal tumor cell associated with these deposits is the modified neoplastic myoepithelial cell,[6] which is also believed to be the source of the stromal matrix deposits in mixed tumors.[9]

## CASE REPORT

A 36-year-old black female patient had a 3 × 2 cm, firm midline swelling at the junction of the hard and soft palate. No ulceration was present. A clinical diagnosis of benign mixed tumor was made and an incisional biopsy taken. Although tyrosine crystals were observed, perineural invasion prompted a provisional diagnosis of a polymorphous low-grade adenocarcinoma and wide excision was recommended. Microscopic examination of the surgical specimen showed an infiltrative neoplastic growth with a lobular architecture. Solid masses of epithelial cells, areas exhibiting ductlike differentiation, and cells arranged in long, single-layered strands were observed. The neoplasm was further characterized by a low mitotic activity, histologic diversity with cylindric, clear cell, and mucus cell differentiation, and a lack of pleomorphism. Evidence of perineural invasion was present (Fig. 1). Extensive crystalloid deposits were present in the connective tissue stroma and between the cells in the solid epithelial masses (Fig. 2). These crystals showed distinct brown staining with the Millon reaction and were nonbirefringent under polarized light. A diagnosis of polymorphous low-grade adenocarcinoma of minor salivary gland origin with tyrosine-rich crystalloid deposits was made.

## DISCUSSION

Polymorphous low-grade adenocarcinoma, also referred to as *terminal duct adenocarcinoma* or *lobular carcinoma of minor salivary gland origin*,[9, 10] is a recently described entity occurring most commonly in the palate and is characterized by a favorable prognosis. Histologically, the lesion is distinguished from other malignant tumors of salivary gland origin by its frequent lobular growth pattern, low mitotic rate, and cytologic uniformity. Although extensive nerve invasion and a cribriform growth pattern may resemble adenoid cystic carcinoma, polymorphous low-grade adenocarcinomas are characterized by histologic diversity, with cells exhibiting cuboidal to low columnar differentiation and an eosinophilic cytoplasm. The stroma, furthermore, often exhibits mucohyaline change in contrast to the bland basement membrane–like deposits of adenoid cystic carcinoma.[10-12] If these criteria are to be applied, it appears as if the adenoid cystic carcinoma containing tyrosine-rich crystalloids reported by Gould and coworkers[7] might possibly have been a polymorphous low-grade adenocarcinoma. If this case were to be accepted as a polymorphous low-grade adenocarcinoma, it would bring the total

[a]Professor.
[b]Senior Lecturer.
[c]Guest Lecturer, Department of Oral Pathology and Oral Biology.
7/14/20170

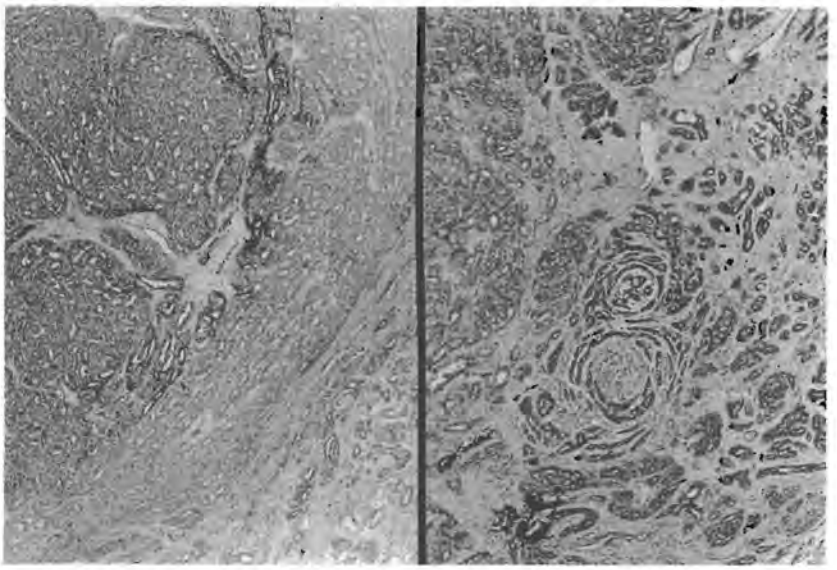

**Fig. 1.** Distinctly lobular arrangement and infiltrative growth of tumor *(left)* with perineural infiltration *(right)*. (Hematoxylin-eosin stain; original magnification, ×40.)

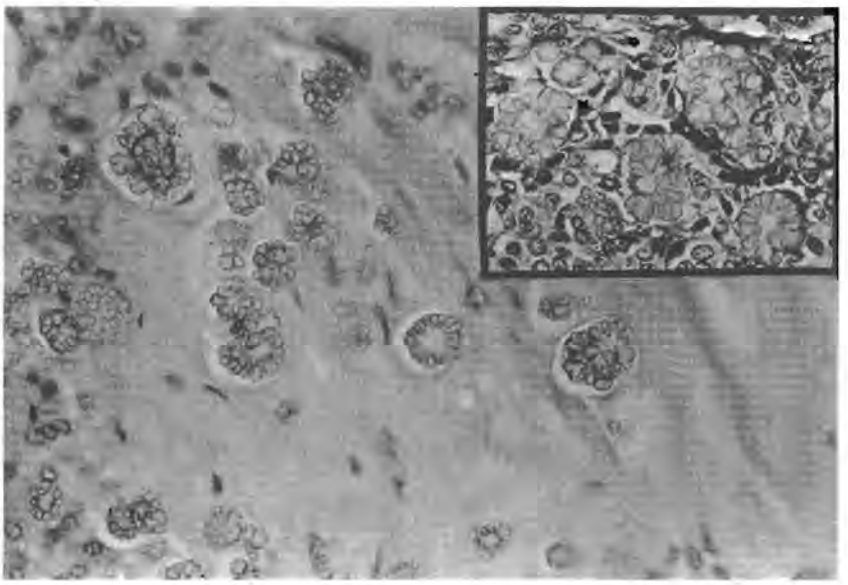

**Fig. 2.** Stromal and interepithelial *(inset)* deposits of tyrosine-rich crystalloids. (Hematoxylin-eosin stain; original magnification, ×200.)

number with tyrosine-rich crystalloids to three, including the case described by Harris and Shipkey[6] as a "terminal duct adenocarcinoma."

The identification of tyrosine-rich crystalloids in a neoplasm other than benign mixed tumor has important diagnostic implications, as many recent publications regard these crystalloids as a unique microscopic feature of salivary gland mixed tumors.[13-15] It is speculated that the formation of tyrosine-rich crystalloids in polymorphous low-grade adenocarcinomas may place these lesions on a level of cytodifferentiation closer to that of benign mixed tumors than to the other more malignant tumors of salivary gland origin.

We thank Mrs. C. S. Begemann for secretarial assistance in preparing the manuscript.

## REFERENCES

1. Humphrey PA, Ingram P, Tucker A, Shelburne JD. Crystalloids in salivary gland pleomorphic adenomas. Arch Pathol Lab Med 1989;113:390-3.
2. Thomas K, Hutt MSR. Tyrosine crystals in salivary gland tumours. J Clin Pathol 1981;34:1003-5.
3. Campbell WG, Priest RE, Weathers DR. Characterization of two types of crystalloids in pleomorphic adenomas of minor salivary glands. A light microscopic, electron-microscopic, and histochemical study. Am J Pathol 1985;118:194-202.
4. Chaplin AJ, Darke P, Patel S. Tyrosine-rich crystals in pleomorphic adenomas of parotid glands. J Oral Pathol 1983; 12:342-6.
5. Thackray AC, Lucas RB, eds. Tumors of the major salivary glands. Washington, D.C.: Armed Forces Institute of Pathology, 1974:32.
6. Harris BR, Shipkey F. Tyrosine-rich crystalloids in neoplasms and tissues of the head and neck. Arch Pathol Lab Med 1986;110:709-12.
7. Gould AR, Van Arsdall LR, Hinkle SJ, Harris WR. Tyrosine-rich crystalloids in adenoid cystic carcinoma: histochemical and ultrastructural observations. J Oral Pathol 1983;12:478-90.
8. Gerughty RM, Scofield HH, Brown FM, Hennigar GR. Malignant mixed tumors of salivary gland origin. Cancer 1969; 24:471-86.
9. Raubenheimer EJ. The myoepithelial cell: embryology, function, and proliferative aspects. CRC Crit Rev Clin Lab Sci 1987;25:161-93.
10. Aberle AM, Abrams AM, Bowe R, Melrose RJ, Handlers JP. Lobular (polymorphous low-grade) carcinoma of minor salivary glands. A clinicopathologic study of twenty cases. ORAL SURG ORAL MED ORAL PATHOL 1985;60:387-95.
11. Evans HL, Batsakis JG. Polymorphous low-grade adenocarcinoma of minor salivary glands. A study of 14 cases of a distinctive neoplasm. Cancer 1984;53:935-42.
12. Freedman PD, Lumerman H. Lobular carcinoma of intraoral minor salivary gland origin. ORAL SURG ORAL MED ORAL PATHOL 1983;56:157-65.
13. Nochomovitz LE, Kahn LB. Tyrosine crystals in pleomorphic adenomas of the salivary gland. Arch Pathol 1974;97:141-5.
14. Thomas KM, Hutt MSR, Borgstein J. Salivary gland tumors in Malawi. Cancer 1980;46:2328-34.
15. Bottles K, Ferrell LD, Miller TR. Tyrosine crystals in fine needle aspirates of a pleomorphic adenoma of the parotid gland. Acta Cytol 1984;28:490-2.

*Reprint requests to:*
Prof. E. J. Raubenheimer
Department of Oral Pathology and Oral Biology
MEDUNSA
P.O. Medunsa, 0204
Republic of South Africa

# Evaluation of the nucleolar organizer region associated proteins in minor salivary gland tumors

**Willie F. P. van Heerden and Erich J Raubenheimer**

*Department of Oral Pathology and Oral Biology, Medical University of Southern Africa, Medunsa, Republic of South Africa*

Van Heerden WFP, Raubenheimer EJ: Evaluation of the nucleolar organizer region associated proteins in minor salivary gland tumors. J Oral Pathol Med 1991; 20: 291–5.

Forty-three intraoral salivary gland tumors were studied to determine the value of the AgNOR technique in the assessment of these neoplasms. Well defined black dots were visible in the nucleii of all the specimens studied. The mean AgNOR count per nucleus for each tumor was calculated as follows: pleomorphic adenoma ($n=15$) 1.52; Polymorphous low-grade adenocarcinoma ($n=12$) 1.90; adenoid cystic carcinoma ($n=6$) 2.92; mucoepidermoid carcinoma ($n=4$) 1.93; carcinoma ex mixed tumor ($n=4$) 2.05; undifferentiated carcinoma ($n=1$) 3.13 and epithelial-myoepithelial carcinoma ($n=1$) 2.23. The difference between the means of benign and malignant tumors ($P<0.01$) and polymorphous low-grade adenocarcinoma and adenoid cystic carcinoma ($P<0.01$) were highly significant. The overlapping of the AgNOR count betwen various tumors prohibited the use of this technique as an absolute criterion in establishing a final diagnosis. It could however be used as a diagnostic aid in differentiating between salivary gland neoplasms.

Key words: nucleolar organizer regions; salivary gland tumor.

Willie F. P. van Heerden, Department of Oral Pathology and Oral Biology, Medical University of Southern Africa, P.O. Medunsa, 0204, Republic of South Africa.

Accepted for publication January 18, 1991.

Nucleolar organizer regions (NORs) are loops of ribosomal DNA that transcribe to ribosomal RNA and thus ultimately to protein (1). NORs have been utilized by cytogeneticists for the evaluation of certain genetic disorders, notably trisomies and are located on the short arms of the five acrosentric chromosomes 13, 14, 15, 21, and 22 (2). The NORs can be demonstrated by means of a silver staining technique (AgNORs) that is performed at room temperature on paraffin embedded tissues (3). This technique is based on the argyrophylia of the NOR-associated proteins. The known NOR associated proteins are RNA polymerase I, C23 (nucleolin), B23, 100K and 80K protein (1). Their function is uncertain although a role in rDNA transcription is postulated (1).

AgNOR counts appear to relate to cell ploidy (4) as well as the rate of cellular proliferation of individual cells (5). Quantification of NORs by means of the AgNOR technique has been used to distinguish between high and low grade lymphomas (5) and between benign and malignant counterparts of various origins (6–9).

Small biopsy specimens from salivary gland tumors is often difficult to interpret and additional microscopic criteria can only benefit the diagnostic process. MORGAN *et al.* (10) and MATSUMURA *et al.* (11) have found a statistically significant difference between the numbers of AgNORs in the nuclei of benign versus malignant salivary gland neoplasms. For this technique to have an application in diagnostic histopathology, it's ease of interpretation and reproducibility between laboratories is important. This study was undertaken to evaluate the AgNOR staining technique as a diagnostic aid for salivary gland neoplasms.

## Material and methods

Forty-three intraoral salivary gland tumors were retrieved from the files of the Department of Oral Pathology, Medical University of Southern Africa. Fifteen were diagnosed as pleomorphic adenomas (PA) twelve as polymorphous low-grade adenocarcinomas (PLA), six as adenoid cystic carcinomas (ACC), four carcinomas ex pleomorphic adenoma, four as mucoepidermoid carcinomas (MEC), one as an undifferentiated carcinoma and one as an epithelial-myoepithelial carcinoma. The tissue samples had all been fixed in 10% formalin and processed to paraffin wax. Two 3 μm paraffin sections of each specimen were cut. One was stained with hematoxylin-eosin and the other with the AgNOR method as described by PLOTON *et al.* (3). The H&E sections were all reassessed and revised with regards to histologic classification. The AgNOR stained sections were examined under a 100X oil immersion lens by the two authors and intranuclear dots were counted in 200 randomly selected nuclei using an eyepiece graticule to prevent recounting. Nuclei of overlapping tumor cells were not included. Nucleolar clusters were counted as a single AgNOR and no attempt was made to resolve the clusters into their discernible number of discrete dots. The mean number of AgNOR dots per nucleus was determined for each specimen. The resulting data were analyzed by means of student's t-test for uncorrelated data.

## Results

The NOR associated proteins were visible as well defined black dots inside and

Table 1. Mean number of AgNORs in the nuclei of salivary gland neoplasms

| Specimen | PA (Type) | PLA | ACC (Growth Pattern) | MEC (Grade) | (Ca ex PA) | Undiff ca | EPI |
|---|---|---|---|---|---|---|---|
| 1 | 1.11 (I) | 1.30 | 3.06 (T) | 1.19 (IG) | 2.37 | 3.13 | 2.23 |
| 2 | 1.37 (I) | 1.96 | 2.00 (T) | 1.80 (IG) | 1.40 | | |
| 3 | 1.23 (III) | 1.53 | 3.01 (T) | 2.34 (HG) | 2.63 | | |
| 4 | 1.75 (I) | 1.84 | 4.29 (C) | 2.36 (HG) | 1.79 | | |
| 5 | 1.73 (I) | 1.86 | 2.84 (C) | | | | |
| 6 | 1.71 (I) | 1.88 | 1.78 (C) | | | | |
| 7 | 0.98 (I) | 2.02 | | | | | |
| 8 | 1.52 (II) | 1.93 | | | | | |
| 9 | 1.93 (I) | 2.47 | | | | | |
| 10 | 1.41 (I) | 2.09 | | | | | |
| 11 | 1.60 (I) | 2.24 | | | | | |
| 12 | 1.48 (I) | 1.64 | | | | | |
| 13 | 1.30 (I) | | | | | | |
| 14 | 2.25 (I) | | | | | | |
| 15 | 1.37 (III) | | | | | | |
| Mean | 1.52 | 1.90 | 2.83 | 1.93 | 2.05 | 3.13 | 2.23 |
| SD | 0.32 | 0.31 | 0.89 | 0.55 | 0.55 | | |

PA = pleomorphic ademona; PLA = polymorphous low-grade adenocarcinoma; ACC = adenoid cystic carcinoma; MEC = mucoepidermoid carcinoma; CA ex PA = carcinoma ex pleomorphic adenoma; Undiff Ca = Undifferentiated carcinoma; EPI = epithelial-myoepithelial carcinoma; T = tubular/trabecular; S = solid; C = cribriform; IG = intermediate grade; HG = high grade

outside of the nucleolus of the tumor cells studied. Careful focussing was essential to clearly identify all the dots. The results were summarized in Table 1. The lowest mean of AgNOR dots per nucleus was found in PA (Fig. 1) and the highest in an ACC (Fig. 2). The dots in the malignant neoplasms had a greater variability in size and shape compared to those in the PA. The difference in the mean number of dots per nucleus between PA and PLA (Fig. 3) and between PLA and ACC were statistically highly significant ($P < 0.01$). The correlation coefficient between the two observers was 0.97.

## Discussion

The reason for the varying quantities of AgNORs in nuclei of different tumors is uncertain. The NORs are located on the 5 acrocentric chromosomes resulting in 10 NOR bearing chromosomes during metaphase. These individual NORs are usually not discernible because they are tightly aggregated in the one or two nucleoli normally present in a cell (12). Active cell proliferation may be accompanied by nucleolar dissociation, resulting in dispersed AgNORs throughout the nucleus. This as well as an increase in transcriptional activity

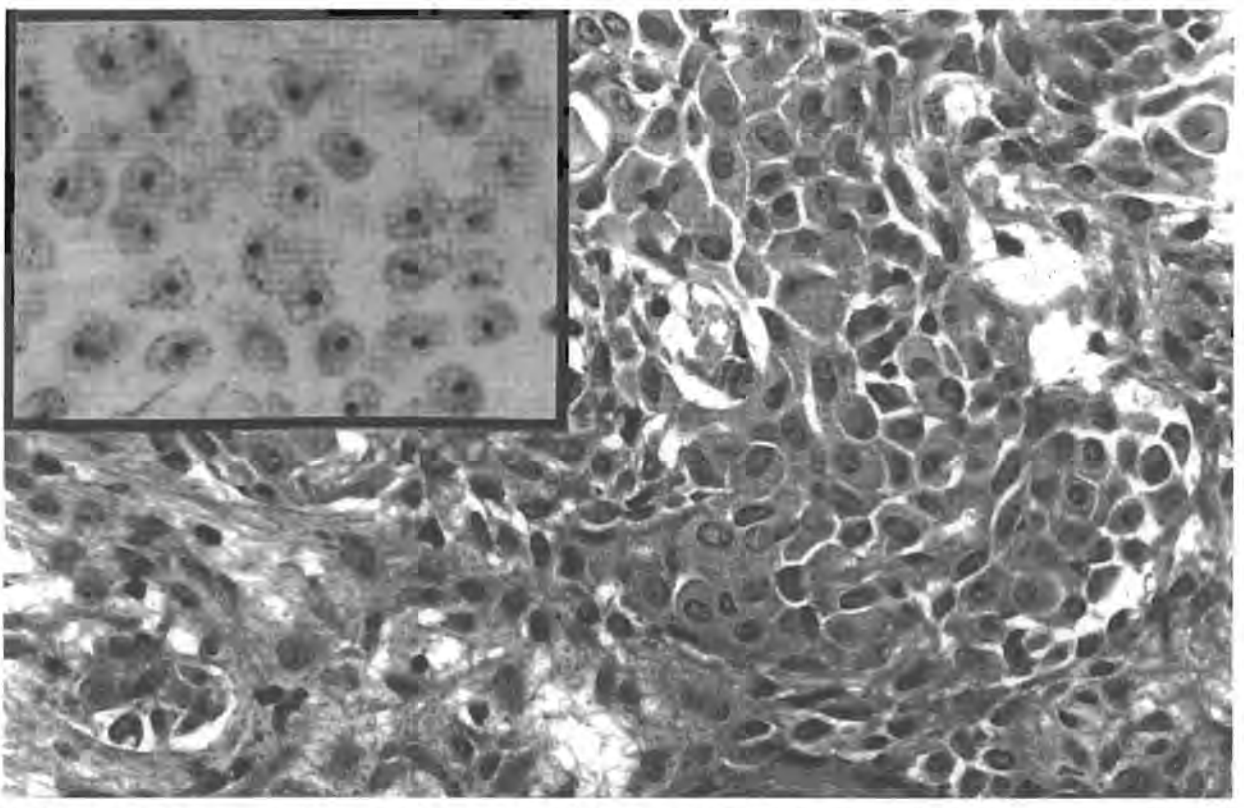

*Fig. 1.* Pleomorphic adenoma with plasmacytoid tumor cells. × 200. Inset: most cells contained one AgNOR dot per nucleus. × 400.

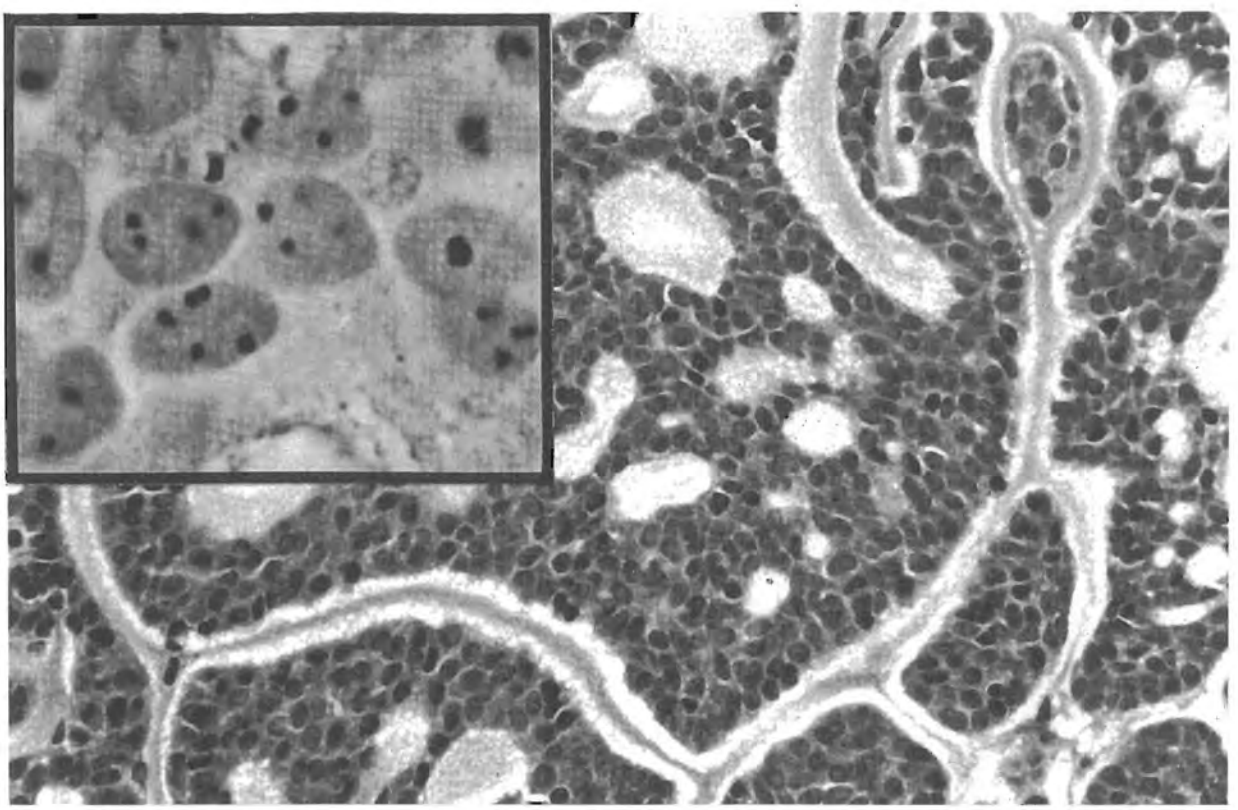

*Fig. 2.* Adenoid cystic carcinoma with cribriform growth pattern. × 200. Inset: multiple small AgNOR dots were present in nuclei. × 1000.

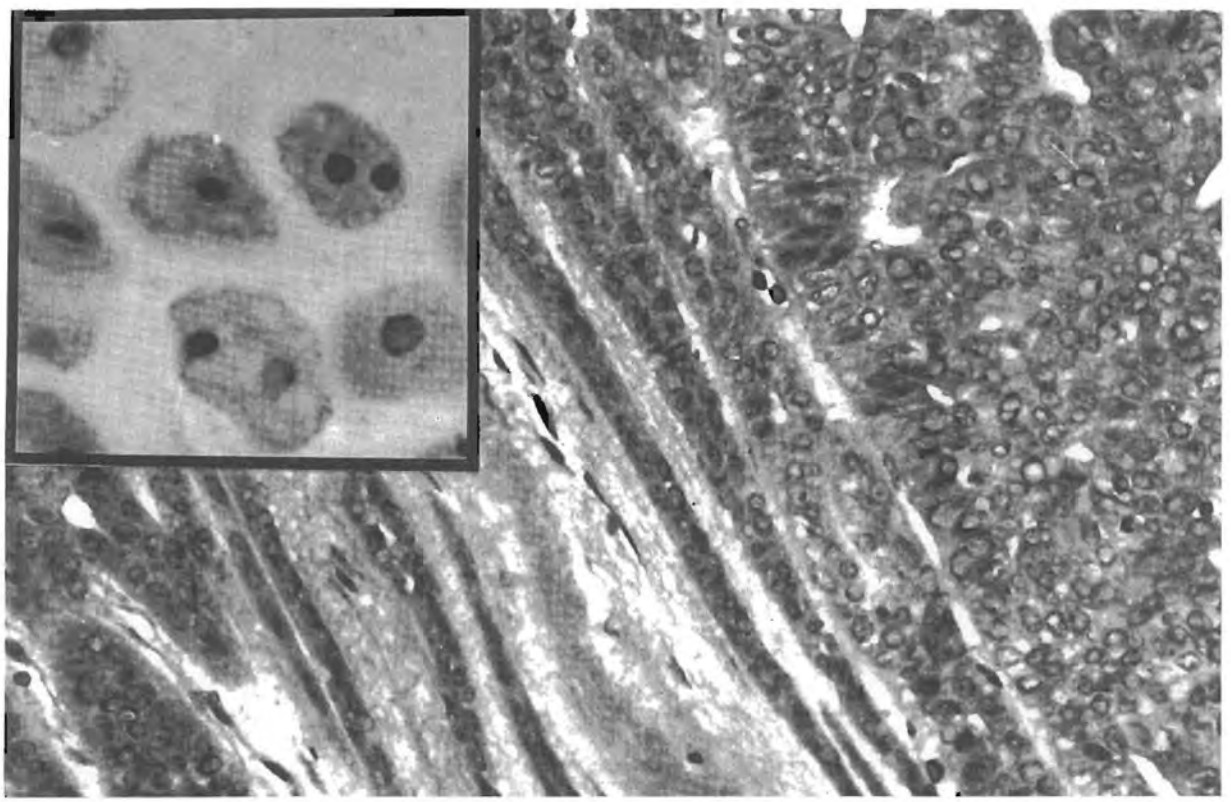

*Fig. 3.* Polymorphous low-grade adenocarcinoma. × 200. Inset: nuclei contained one or two large AgNOR dots. × 1000.

Table 2. Reported mean AgNOR counts in salivary gland neoplasms

| Neoplasm | Present study | MORGAN *et al.*(10) | MATSUMURA *et al.* (11) |
|---|---|---|---|
| PA | 1.52 | 1.47 | 1.62–1.68* |
| ACC | 2.83 | 3.92 | 2.78 |
| MEC | 1.93 | 4.25 | 2.59 |

PA = pleomorphic adenoma; ACC = adenoid cystic carcinoma; MEC = mucoepidermoid carcinoma; * = different cell types in the same tumor were separately counted

will result in an increase in the mean AgNOR count of a cell population. In malignancy, the AgNORs tend to become more dispersed through the nucleus and thus more readibly discernable (12). HALL *et al.* (13) have shown that there is a significant correlation between the AgNOR count and presence of positive Ki-67 immunostaining in cells. Ki-67 is a monoclonal antibody that recognizes a nuclear antigen present only in proliferating cells (14). The possibility that the AgNOR count is related to cellular activity is also suggested by PLOTON *et al.* (3). SURESH *et al.* (4) have shown that AgNOR counts in non neoplastic trophoblastic tissue are a reflection of ploidy rather than cell proliferation. They suggested that the relationship between cell ploidy and AgNOR counts can be obscured in neoplastic lesions because of excessive proliferative activity of tumor cells.

Both ACC and PLA have an infiltrative growth pattern with an affinity for perineural spread. Cribriform, tubular and solid tumor cell arrangements can be found in ACC and PLA (15). Histologically, ACC differs from PLA in that the tumor cells have very little cytoplasm and contains hyperchromatic nucleii. Mitotic activity can be found in both tumors, although none of the PLA in our collection had a mitotic index of more than 5 mitotic figures per 10 high power fields (×400). Pleomorphism is absent in PLA whereas polymorphism is seldom seen in ACC. Despite these differences, it can be very difficult to distinguish between PLA and ACC, especially when only a small tissue fragment is submitted for histologic examination. ACC and PLA are thought to develop from the same precursor cell line (16) with the result that special staining techniques used as diagnostic procedures must be able to distinguish between cellular differentiation or activity of the two lesions. Various immunohistochemical techniques have shown potential with regards to the pathogenesis and differentiation of salivary gland tumors, although their reliability and diagnostic value is often unclear (10). A statistically significant difference between the mean AgNOR count in PLA and ACC was found in the present study. The higher count in ACC could probably be related to the more aggressive behaviour of this neoplasm when compared to PLA. The mean count in ACC did not correlate with the histologic growth pattern, a prognostic factor for tumor behavior in ACC. The highest count was present in a tumor with a predominantly cribriform growth pattern. In a study to evaluate the prognostic factors for ACC, HAMPER *et al.* (17) inter alia assessed DNA contents of the tumor cells using single cell scanning cytophotometry. They concluded that the shortest survival time was found in patients with tumors showing atypical histograms of nuclear contents of which 42% had a cribriform growth pattern. Previous studies (10, 11) evaluating the AgNOR technique in salivary gland neoplasms did not identify PLA as a separate entity, making comparison with the present study regarding PLA impossible. The overlapping of the AgNOR count between PLA and ACC prohibited the use of this technique as an absolute criterion to establish a final diagnosis but it could be used as a diagnostic aid to differentiate between these two neoplasms.

The mean value for MEC in the present study was lower than the value determined by MORGAN *et al.* (10) and MATSUMURA *et al.* (11) (Table 2). They do not specity the histologic grade of MEC included in their study. Although only four MEC's were examined in the present study, a substantial higher AgNOR count was found in the two high grade MEC. No significant difference in the AgNOR counts was found between the different types of BMT as classified using the criteria of SEIFERT *et al.* (18). This is supported by the findings of CHAU & RADDEN, (19) that there is no difference in the recurrence rate and frequency of capsular infiltration between the different subtypes of BMT.

The overlap between the AgNOR ranges in different tumors can be expected, since the absolute numbers of AgNORs in nucleii are not counted in 3 µm sections. Some AgNORs may have been missed in the 3 µm sections, especially in the malignant and high grade tumors where the nuclei were large and multiple small AgNORs were present.

The argyrophilic staining of AgNOR is not a method for demonstrating the nucleolus, but rather a technique to demonstrate its substructures in such a way as to allow study of their shape and number. Although the evaluation of AgNOR stains are time consuming, it appears to be of value in differentiating between salivary gland neoplasms.

*Acknowledgments* – The authors wish to thank Mrs. C. S. BEGEMANN for secretarial services, Mrs. R. VORSTER for technical assistance and Miss L. I. HOPE, Audio Visual Department of the Medical Univeristy of Southern Africa for photographic services.

## References

1. CROCKER J. Nucleolar organiser regions. In: UNDERWOOD J C E, ed. *Current topics in pathology*. New York: Springer-Verlag, 1990: 92–143.
2. ANONYMOUS. NORs – a new method for the pathologist. *Lancet* 1987; 1: 1413–4.
3. PLOTON D, MENAGER M, JEANNESSON P, HIMBERG G, PIGEON F, ADNET J J. Improvement in the staining and in the visualization of the argyrophilic proteins of the nucleolar organizer region at the optical level. *Histochem J* 1986; **18**: 5–14.
4. SURESH U R, CHAWNER J, BUCKLEY C H, FOX H. Do Agnor counts reflect cellular ploidy or cellular proliferation? A Study of trophoblastic tissue. *J Pathol* 1990; **160**: 213–5.
5. CROCKER J, NAR P. Nucleolar organizer regions in lymphomas. *J Pathol* 1987; **151**: 111–8.
6. MACKIE R M, WHITE S I, SEYWRIGHT M M, YOUNG H. An assessment of the value of AgNOR staining in the identification of dysplastic and other borderline melanocytic naevi. *Br J Dermatol* 1989; **120**: 511–6.
7. SMITH R, CROCKER J. Evaluation of nucleolar organizer region-associated proteins in breast malignancy. *Histopathology* 1988; **12**: 221–3.
8. ROSA J, MEHTA A, FILIPE M I. Nucleolar organizer regions in gastric carcinoma and its precursor stages. *Histopathology* 1990; **16**: 265–9.
9. CROCKER J, SKILBECK N. Nucleolar organizer region associated proteins in cutaneous melanotic lesions: a quantitive study. *J Clin Pathol* 1987; **40**: 885–9.
10. MORGAN D W, CROCKER J, WATTS A, SHENOI P M. Salivary gland tumours studied by means of the AgNOR technique. *Histopathology* 1988; **13**: 553–9.

11. Matsumura K, Sasaki K, Tsuji T, Shinozaki F. The nucleolar organizer regions associated protein (AgNORs) in salivary gland tumors. *Int J Oral Maxillofac Surg* 1989; **18**: 76–8.
12. Underwood J C R, Giri D D. Nucleolar organizer regions as diagnostic discriminants for malignancy. *J Pathol* 1988; **155**: 95–6.
13. Hall P A, Crocker J, Watts A, Stansfield A G. A comparison of nucleolar organizer region staining and Ki-67 immunostaining in non-Hodgkin's lymphoma. *Histopathology* 1988; **12**: 373–81.
14. Gerdes J, Schwab U, Lemke H, Stein H. Production of a mouse monoclonal antibody reactive with a human nuclear antigen associated with cell proliferation. *Int J Cancer* 1983; **31**: 13–20.
15. Evans H L, Batsakis J G. Polymorphous low-grade adenocarcinoma of minor salivary glands. *Cancer* 1984; **53**: 935–42.
16. Aberle A M, Abrams A M, Bowe R, Melrose R J, Handlers J P. Lobular (polymorphous low-grade) carcinoma of minor salivary glands. *Oral Surg Oral Med Oral Pathol* 1985; **60**: 387–94.
17. Hamper K, Lazarf, Dietelm *et al*. Prognostic factors for adenoid cystic carcinoma of the head and neck: a retrospective evaluation of 96 cases. *J Oral Pathol Med* 1990; **19**: 101–7.
18. Seifert G, Miehlke A, Haubrich J, Chilla R, eds. *Diseases of the salivary glands*. Stuttgart: Georg Thieme Verlag, 1986: 182–94.
19. Chau M N Y, Radden B G. A clinicopathological study of 53 intra-oral pleomorphic adenomas. *Int J Oral Maxillofac Surg* 1989; **18**: 158–62.

# Intraoral salivary gland neoplasms: A retrospective study of seventy cases in an African population

*Willem F. P. van Heerden, MChD,[a] and Erich J. Raubenheimer, MChD,[b]*
*Medunsa, Republic of South Africa*

MEDICAL UNIVERSITY OF SOUTHERN AFRICA

Intraoral salivary gland neoplasms diagnosed in the Department of Oral Pathology, Medical University of Southern Africa, Medunsa, were reassessed and revised with regard to histologic diagnosis. New entities and subclassifications that have been described in recent years were taken into account. Seventy cases were diagnosed during an 8-year period, and the sample consisted of black patients only. Benign mixed tumor was the most common entity and accounted for 48% of all tumors. Polymorphous low-grade adenocarcinoma comprised 15.7% of the sample and was the most frequent malignant tumor. The mean age of patients with benign and malignant tumors were 36.5 and 49.8 years, respectively ($p < 0.05$), and the palate was the most common site involved. Geographic differences do exist in the pattern and pathology of intraoral salivary gland neoplasms when compared with findings in other studies.
(ORAL SURG ORAL MED ORAL PATHOL 1991;71:579-82)

The distribution and frequency of intraoral salivary gland neoplasms has been discussed in several published series,[1-5] in the majority of which the World Health Organization (WHO) classification[6] was used. However, various new entities and subclassifications that are not included in these articles have been described in recent years.[7,8] This study was undertaken to determine the relative frequency and distribution of intraoral salivary gland neoplasms in a predominantly rural black African population and to provide data for comparison with findings in other geographic locations.

## MATERIAL AND METHODS

All the intraoral salivary gland neoplasms diagnosed during the last 8 years were retrieved from the files of the Department of Oral Pathology, Medical University of Southern Africa, Medunsa. Most patients seen at the hospitals served by the department are black and of rural southern African origin. Representative slides stained with hematoxylin and eosin were available for review, and, where necessary, appropriate special stains were used to establish a diagnosis. All cases were reassessed and revised with regard to histologic classification. Diagnosis was made with the WHO classification[6] as the basis. New entities such as polymorphous low-grade adenocarcinoma, and subclassifications that have been described in recent years, were taken into account. This includes the subclassification of mixed salivary gland tumors into types I to IV according to the proportion of the stroma in the tumor mass.[8] The polymorphous low-grade adenocarcinomas were divided into the terminal duct type and the papillary type according to the criteria of Slootweg and Müller.[9] The working classification used in this study is shown in Table I. Age, sex, and site were noted from the clinical records.

[a]Senior Lecturer, Department of Oral Pathology and Oral Biology.
[b]Professor, Department of Oral Pathology and Oral Biology.
7/14/25498

**Table I.** Working classification

- Benign
  - Mixed tumor
    - Type I (stroma 30%-50%)
    - Type II (stroma >80%)
    - Type III (stroma <20%)
    - Type IV (myoepithelioma)
  - Monomorphic adenoma
- Malignant
  - Mucoepidermoid carcinoma
    - Low grade
    - Intermediate grade
    - High grade
  - Adenoid cystic carcinoma
    - Cribriform
    - Tubular/trabecular
    - Solid
  - Polymorphous low-grade adenocarcinoma
    - Terminal duct
    - Papillary
  - Acinic cell carcinoma
  - Carcinoma ex mixed tumor
  - Epidermoid carcinoma
  - Adenocarcinoma
  - Epithelial-myoepithelial carcinoma
  - Undifferentiated carcinoma

## RESULTS

The sample consisted of a total of 70 cases of intraoral salivary gland neoplasms. Forty-three (62%) of the patients were female and 27 (38%) were male, yielding a female/male ratio of 1.6:1. The patients ranged in age from 10 to 85 years. Thirty-four cases (48%) were classified as benign; all these were mixed tumors in patients ranging in age from 10 to 64 years, with a mean age (±SD) of 36.5 ± 14.7 years. The female/male ratio was 2.4:1, with the mean age for females 34.9 ± 14.9 years and 40.3 ± 13.1 years for males. The palate was most commonly affected, accounting for 31 tumors (91%). The remaining mixed tumors were found on the upper lip. The location and subclassification of mixed tumors according to the criteria of Seifert et al.[8] are shown in Table II.

Thirty-six cases (52%) were classified as malignant. The patients ranged in age from 22 to 85 years, with a mean age of 49.8 ± 16.3 years. The difference in the mean age of patients with benign tumors and that of those with malignant tumors was statistically significant ($p < 0.05$). The female/male ratio was 1.1:1 for patients with malignant neoplasms. The distribution and location of the malignant tumors are shown in Table III.

Eleven tumors were diagnosed as polymorphous low-grade adenocarcinoma, accounting for 30% of the malignant neoplasms and 15.7% of all neoplasms. The patients' ages were between 32 and 70 years, with a mean age of 53 ± 12.6 years, and the female/male ratio was 1.2:1. Nine lesions (82%) occurred on the palate, and one each in the buccal mucosa and upper lip, respectively. Two tumors had a papillary-type growth pattern, and nine were either lobular or tubular in appearance. Nerve infiltration was present in one papillary-type and in two terminal duct–type tumors.

**Table II.** Location and subclassification of 34 mixed tumors

| *Type* | *Palate* | *Upper lip* | *Total (%)* |
|---|---|---|---|
| I | 25 | 1 | 26 (76) |
| II | 2 | 1 | 2 (6) |
| III | 5 | 1 | 6 (18) |
| IV | | | 0 |
| Total (%) | 31 (91) | 3 (9) | 34 (100) |

Nine cases of adenoid cystic carcinoma accounted for 12.8% of all tumors and 25% of the malignant tumors. The patients had a age range of 33 to 85 years with a mean of 54 ± 15.5 years, and the male/female ratio was 1.2:1. Seven patients had lesions on the palate, and one lesion each was located in the floor of the mouth and on the upper lip. Five tumors had a predominantly cribriform growth pattern, and two each had solid and tubular or trabecular growth, respectively.

Six patients with mucoepidermoid carcinoma accounted for 8.6% of all tumors and 16.7% of malignant tumors. The youngest patient was 22 years and the oldest 52 years of age, and the mean age at time of consultation was 39.8 ± 10.1 years. Sex distribution was equal, and the most common site of occurrence was the palate, with four tumors. One tumor was located on the buccal mucosa and mandibular gingiva, respectively. One mucoepidermoid carcinoma was classified microscopically as low grade, three as intermediate grade, and two as high grade.

Five carcinomas ex mixed tumor were diagnosed. Three of the patients were women and two were men; they ranged in age from 31 to 70 years, with a mean age of 48.2 ± 19.3 years. Four tumors occurred on the palate, and one in the retromolar area. The carcinomatous component in all five was classified as undifferentiated.

Three cases were diagnosed as adenocarcinomas, not otherwise specified. Two tumors were located in the buccal mucosa and one on the palate. Two cases occurred in females, and the mean age of this group was 57.3 ± 13.2 years. One tumor that occurred on the palate of a 49-year-old woman was diagnosed as an undifferentiated carcinoma.

One patient, a 65-year-old woman, had a epithelial-myoepithelial carcinoma of the palate. No case of monomorphic adenoma, acinic cell carcinoma, or

**Table III.** Distribution and location of malignant tumors

| *Tumor* | *Palate* | *Upper lip* | *Buccal mucosa* | *Mouth floor* | *Retromolar* | *Mandibular gingiva* | *Total* | *% of total* | *% of malignant* |
|---|---|---|---|---|---|---|---|---|---|
| PLA | 9 | 1 | 1 | | | | 11 | 15.7 | 30 |
| ACC | 7 | 1 | | 1 | | | 9 | 12.8 | 25 |
| Mucoepidermoid CA | 4 | | 1 | | | 1 | 6 | 8.6 | 16.7 |
| CA ex mixed tumor | 4 | | | | 1 | | 5 | 7.1 | 14 |
| Adenocarcinoma | 1 | | 2 | | | | 3 | 4.3 | 8.3 |
| Undifferentiated CA | 1 | | | | | | 1 | 1.4 | 2.8 |
| E-M CA | 1 | | | | | | 1 | 1.4 | 2.8 |
| Total (%) | 27 (75) | 2 (5.5) | 4 (11) | 1 (2.8) | 1 (2.8) | 1 (2.8) | 36 | | |

*ACC*, Adenoid cystic adenocarcinoma; *CA*, carcinoma; *E-M*, Epithelial-myoepithelial; *PLA*, polymorphous low-grade adenocarcinoma.

epidermoid carcinoma of the minor salivary glands occurred in this series.

## DISCUSSION

In most studies benign mixed tumors constitute the jority of minor salivary gland neoplasms.[1-5] The frequency of benign mixed tumors is reported as 43% in the study of Eveson and Cawson,[4] 41% by Waldron et al.,[1] and 54% by Chau and Radden.[5] In Isacsson and Shear's series[2] 70% of the tumors were classified as benign mixed tumors. They postulated that the high frequency in their series was the result of the relative higher number of black than white patients, although 60% of their white patients had mixed tumors diagnosed. Schulenburg[10] reported that intraoral benign mixed tumors in his South African sample were 3.5 times more common in black than in white patients. In the present series, where the sample consisted of black patients only, 34 (48%) of the tumors were classified as benign mixed tumors, a frequency comparable to that reported in population samples in the United States and Europe.[1,4]

The majority of tumors (52%) in the present study were malignant, a finding that does not support the of benign to malignant tumors in recent reports. The proportion of benign tumors varied from 53%[11] to 72%[2] in recent studies. However, 80% of the cases reported by Spiro et al.[12] were classified as malignant. This high percentage of malignant tumors can be explained by the fact that their institution is a major cancer referring center.

The palate was the most common site of involvement of both malignant and benign tumors. The proportion of benign tumors occurring on the palate was larger than in the malignant group, although the difference is not statistically significant. Eighty-one percent of benign mixed tumors reported by Isacsson and Shear[2] occurred on the palate. This high frequency of palatal involvement might be due to the presence of black patients in both samples. The distribution of palatal tumors from several large series compared with our findings is reflected in Table IV.

**Table IV.** Reported frequency of intraoral salivary gland tumors of palate

| *Author* | *Frequency (%)* | |
|---|---|---|
| | *Mixed tumor* | *Malignant tumor* |
| Present study | 91 | 75 |
| Thomas et al.[14] | 65 | 63 |
| Isacsson and Shear[2] | 81 | 60 |
| Eveson and Cawson[4] | 60 | 55 |
| Waldron et al.[1] | 54 | 42 |
| Regezi et al.[3] | 55 | 49 |
| Chau and Radden[5] | 70 | 54 |
| Chaudhry et al.[11] | 65 | 35 |

The benign mixed tumors occurred at a significantly younger age than did the malignant tumors ($p < 0.05$), and a high percentage of the benign tumors affected female patients. These observations support the proposal by Isacsson and Shear[2] that in an African population a salivary gland tumor of the palate occurring in a relatively young patient is more likely to be benign than malignant. This appears to be especially true in women.

Seifert et al.[8] divided benign mixed tumors into four types according to the volume and properties of the stroma and the differentiation of the epithelial cells. Although types III and IV constituted 35% of minor salivary gland mixed tumors in their series, almost 50% of the carcinomas ex mixed tumor arose from tumors with these growth patterns.[8] We are unable to comment on the rate of malignant transformation of types III and IV because only small fragments of benign mixed tumor were present in the carcinomas ex mixed tumor in our series. The finding of Seifert et al.[8] could be related to the more common occurrence of mitotic activity in the solid areas. The majority of benign mixed tumors in the present series were classified as type I. Although mitotic activity, when present, was usually restricted to the solid parts of the tumor, the subclassification depended on the

amount of sections taken, because the growth pattern varied through the tumor.

The absence of monomorphic adenomas in the present study may be due to the fact that our sample consisted of black patients only. Isacsson and Shear[2] found three monomorphic adenomas (2.2%) in their sample of 136 black patients. Davies et al.,[13] in a study of salivary gland tumors in Uganda, found no monomorphic adenomas in 33 intraoral tumors. Thomas et al.,[14] who analyzed salivary gland tumors in Malawi, found one monomorphic adenoma (2%) in their total of 57 minor tumors. These frequencies are in contrast with the 10.7% reported by Waldron et al.,[1] 11% by Evenson and Cawson,[4] and 10% by Regezi et al.[3]

Polymorphous low-grade adenocarcinoma was the most common malignant tumor in the present series. Comparison of the frequency of polymorphous low-grade adenocarcinoma with that reported in other studies is difficult because the majority employed the WHO classification,[6] which does not recognize polymorphous low-grade adenocarcinomas as a separate entity. Polymorphous low-grade adenocarcinoma constituted 30% of the malignant tumors in the present study. Freedman and Lumerman[15] found polymorphous low-grade adenocarcinoma to constitute 7% of the 150 malignant intraoral tumors they examined. Aberle et al.[16] reviewed 109 cases of adenocarcinoma not otherwise specified, malignant mixed tumor, and adenoid cystic carcinoma, and found that 17% of their cases met the criteria of polymorphous low-grade adenocarcinoma. In the study of Waldron et al.[1] 26% of the malignant tumors were diagnosed as polymorphous low-grade adenocarcinoma. The differences among these findings are probably related to the criteria used for diagnosis of polymorphous low-grade adenocarcinoma, because overlapping histologic features with adenoid cystic carcinoma do exist.

The frequency of adenoid cystic carcinoma (12.8%) in our series is similar to that reported in the literature, for example, 13.1% by Eveson and Cawson,[4] 10.9% by Regezi et al.,[3] and 10.4% by Isacsson and Shear.[2] Adenoid cystic carcinoma accounted for 25% of the malignant tumors in our series, a figure lower than the 38% reported by Isacsson and Shear[2] and the 31% of Regezi et al.[3] Polymorphous low-grade adenocarcinoma was not classified as a separate entity in the previously mentioned series, and the reported frequencies of adenoid cystic carcinoma are probably too high.

In the majority of studies mucoepidermoid carcinoma was the most frequent type of malignant tumor, accounting for 15%[1] to 34%[11] of all intraoral salivary gland tumors. Mucoepidermoid carcinoma accounted for 8.6% of all tumors in the present series. This figure compares with the 6.5% reported by Isacsson and Shear,[2] also in a South African population. This corroborates the suggestion by Everson and Cawson[17] that a geographic variation in the frequency of mucoepidermoid carcinoma exists.

We thank Mrs. C. S. Begemann for secretarial assistance in preparing the manuscript.

## REFERENCES

1. Waldron CA, El-Mofty SK, Gnepp DR. Tumors of the intraoral minor salivary glands: a demographic and histologic study of 426 cases. ORAL SURG ORAL MED ORAL PATHOL 1988;66:323-33.
2. Isacsson G, Shear M. Intraoral salivary gland tumors: a retrospective study of 201 cases. J Oral Pathol 1983;12:57-62.
3. Regezi JA, Lloyd RV, Zarbo RJ, McClatchey KD. Minor salivary gland tumors: a histologic and immunohistochemical study. Cancer 1985;55:108-15.
4. Eveson JW, Cawson RA. Tumours of the minor (oropharyngeal) salivary glands: a demographic study of 336 cases. J Oral Pathol 1985;14:500-9.
5. Chau MNY, Radden BG. Intra-oral salivary gland neoplasms: a retrospective study of 98 cases. J Oral Pathol 1986;15:339-42.
6. Thackray AC, Sobin LH. Histological typing of salivary gland tumours. Geneva: World Health Organization, 1972.
7. Evans HL, Batsakis JG. Polymorphous low-grade adenocarcinoma of minor salivary glands. Cancer 1984;53:935-42.
8. Seifert G, Michlke A, Haubrich J, Chilla R. Diseases of the salivary glands. New York: Georg Thieme, 1986:184-7.
9. Slootweg PJ, Müller H. Low-grade adenocarcinoma of the oral cavity: a comparison between the terminal duct and the papillary type. J Craniomaxillofac Surg 1987;15:359-64.
10. Schulenburg CAR. Salivary gland tumors: a report on 105 cases. S Afr Med J 1954;23:910-4.
11. Chaudhry AP, Labay GR, Yamane GM, Jacobs MS, Cutler LS, Watkins KV. Clinico-pathologic and histogenetic study of 189 intraoral minor salivary gland tumors. J Oral Med 1984;39:58-78.
12. Spiro RH, Koss LG, Hajdu SI, Strong EW. Tumors of minor salivary origin: a clinicopathologic study of 492 cases. Cancer 1973;31:117-29.
13. Davies JNP, Dodge OG, Burkitt DP. Salivary gland tumors in Uganda. Cancer 1964;17:1310-22.
14. Thomas KM, Hutt MSR, Borgstein J. Salivary gland tumors in Malawi. Cancer 1980;46:2328-34.
15. Freedman PD, Lumerman H. Lobular carcinoma of intraoral minor salivary gland origin. ORAL SURG ORAL MED ORAL PATHOL 1983;56:157-65.
16. Aberle AM, Abrams AM, Bowe R, Melrose RJ, Handlers JP. Lobular (polymorphous low-grade) carcinoma of minor salivary glands: a clinicopathologic study of twenty cases. ORAL SURG ORAL MED ORAL PATHOL 1985;60:387-95.
17. Eveson JW, Cawson RA. Salivary gland tumours: a review of 2410 cases with particular reference to histologic types, site, age and sex distribution. J Pathol 1985;146:51-8.

*Reprint requests to:*
W. F. P. van Heerden, MChD
Department of Oral Pathology and Oral Biology
Medical University of Southern Africa
P.O. Medunsa 0204
Republic of South Africa

# The relationship between Nucleolar Organiser Regions and DNA content in Salivary Gland Neoplasms

W.F.P. VAN HEERDEN[1], E.J. RAUBENHEIMER[1], R. LE ROUX[2]
[1]Departments of Oral Pathology and Oral Biology, and [2]Anatomical Pathology, Medunsa

Abstract
Thirty-three intraoral salivary gland neoplasms were evaluated to determine the proliferative index (+ G2M fraction) and ploidy status and to correlate these findings with the nucleolar organiser regions (NOR) counts. Formalin fixed, paraffin-embedded tissue was used in all the cases. The mean proliferative index for each tumour was calculated as follows: pleomorphic adenoma (n = 11) 4.1; polymorphous low grade adenocarcinoma (n = 8) 6.8; adenoid cystic carcinoma (n = 3) 6.7; mucoepidermoid carcinoma (n = 4) 7.3; carcinoma ex pleomorphic adenoma (n = 3) 5.1; undifferentiated carcinoma (n = 1) 4.5 and epithelial-myoepithelial carcinoma (n = 1) 8.2. Three tumours, two adenoid cystic carcinomas and one carcinoma ex pleomorphic adenoma showed aneuploid stemlines.

Although a positive correlation between the AgNOR count and proliferative index of the salivary gland neoplasms was found, it was statistically not significant.

## Introduction

Nucleolar organiser regions (NORs) are collections of nucleolar proteins associated with ribosomal genes that can be demonstrated in histologic sections using a silver staining technique (AgNOR)[1]. This technique is based on the argyrophylia of the NOR-associated proteins[2]. NORs are located on the short arms of the five acrocentric chromosomes 13, 14, 15, 21 and 22. The known NORs are RNA polymerase I, nucleolin, B23, 100K and 80K protein[1]. Their function is uncertain but a role in rDNA transcription is postulated. The quantification of AgNORs in histologic sections has been used as a diagnostic aid in distinguishing between benign and malignant tumours of various origins[3-6].

DNA content can be determined by flow cytometry by sing fluorescent dyes that bind stoichiometrically to DNA[7]. The fluorescence intensity emitted by each nucleus through laser excitation is directly proportional to the DNA content of the cell[7]. The cell cycle is divided according to the amount of DNA in the nucleus at a particular time. Nuclei of cycling cells in the pre synthesis or G1 phase has a diploid or 2N amount of DNA. When the cells start to duplicate their DNA they have an intermediate amount of DNA between 2N and 4N. This phase is referred to as the synthesis phase (S-phase) and is of variable duration. After completion of the S-phase the cells enter the post synthesis phase (G2 phase) in which they have a 4N amount of DNA. The cells finally enter the mitotic phase (M-phase) and divide, whereafter they return to the G1 phase or enter a resting (G0 phase). In flow cytometry, cells in the G0 and G1 phases cannot be distinguished from each other, as they all have 2N DNA content. The same implies to cells in the G2 and M phases with a 4N DNA content (**Figure 1**).

The association between aneuploidy and aggressive tumour behaviour has been established for neoplasms from various sites[8-10]. The proliferation rate as defined by the S-phase fraction has also been used as a prognostic factor in adenoid cystic carcinomas of the head and neck[11].

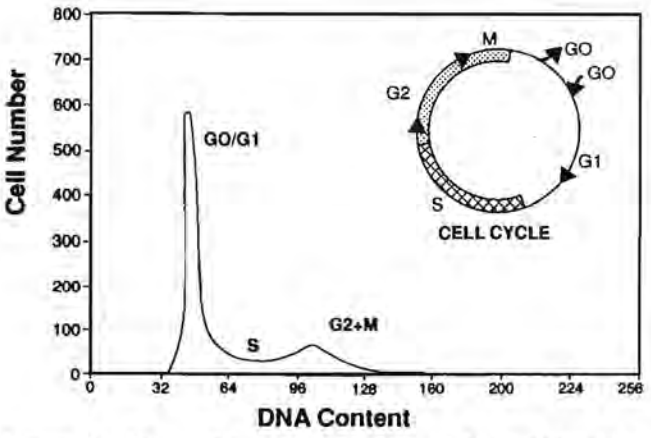


**Figure 1:** *Schematic representation of the relationship between DNA changes during the cell cycle and DNA histogram by flow cytometry. G0 represents the resting cells not taking part in the cell cycle.*

The reason for different quantities of AgNORs in nuclei is uncertain. The relationship between the AgNOR count and cellular activity has been demonstrated by Crocker and Nar[3]. Suresh *et al* however, have shown that AgNOR counts in non-neoplastic trophoblastic tissue are a reflection of ploidy rather than cell proliferation[12]. The purpose of this study was to determine the proliferative index and the ploidy status of minor salivary gland neoplasms and to correlate these findings with the AgNOR counts previously evaluated in the same tumours.

## Materials and Method

Formalin fixed, paraffin embedded tissue from thirty-three intraoral salivary gland neoplasms, all included in a previous study where the AgNOR counts were evaluated[13] were retrieved. The tissue samples had all been fixed in 10% formalin and processed to paraffin wax. Sections were cut at 3cm thickness and dewaxed. The AgNOR solution comprised 2% gelatin in 1% formic acid that was mixed in a proportion of 1:2 volumes with 50% aqueous silver nitrate. This was immediately poured over the tissue sections and left for 30 min at room temperature. Counter staining was not performed. The AgNOR stained sections were examined under a 100x oil immersion lens and intranucleur dots were counted in 200 randomly selected nuclei using an eyepiece graticule to prevent recounting. Nuclei of overlapping tumour cells were not included. Nucleolar clusters were counted as a single AgNOR and no attempt was made to resolve the clusters into their discernible number of descrete dots. The mean number of AgNOR dots per nucleus was determined for each specimen. Eleven were diagnosed as pleomorphic adenomas (PA), eight as polymorphous low grade adenocarcinomas (PLA), five as adenoid cystic carcinomas (ACC), four as mucoepidermoid carcinomas (MEC), three as carcinoma ex pleomorphic adenoma, one as an undifferentiated carcinoma and one as an epithelial-myoepithelial carcinoma. Four 50μm sections from each

paraffin embedded block were cut and prepared for flow cytometry according to the Hedley method using a 0,5% pepsin solution[14]. The final cell suspension was passed through a 35mm mesh and the cell concentration established by means of a Coulter counter (Model FZ, Coulter Electronics, Hialeah, F1). The cell concentration was adjusted to $\pm 2.0 \times 10^6$ cells/ml. The nuclei were stained with Propidium Iodide using a Coulter DNA Prep system, according to the manufacturers instructions. The cells were then analysed on an Epics Elite flow cytometer (Coulter Electronics, Hialeah, F1) which had been calibrated with chicken red blood cells and DNA check beads. The Elite was operated at 15 mW and emitted an Argon ion laser at 488nm. The date rate varied between 20 – 200 events/second and 10 000 – 20 000 events were collected on a single parameter histogram. All data was collected in listmode fashion and the DNA histograms were analysed using Multicycle DNA analysis software program (Phoenix Flow Systems, San Diego, CA).

By convention, when using paraffin embedded tissue, the first peak was considered to be the normal DNA diploid peak representing the G0G1 phase of the cycle. DNA aneuploidy was reported when at least 2 separate G0/G1 peaks could be demonstrated. The coefficient of variation (CV) was calculated using the width of the peak (number of channels) at 61% of the maximum peak height divided by the peak height channel number, multiplied by a factor of 2.

The proliferative index (PI) was defined as the percentage of cells in the S + G2M phases combined. The correlation between the AgNOR count and PI were analysed using the Pearson's method while the Mann-Whitney Test was used to compare the PI between benign and malignant salivary gland neoplasms.

## Results

Three tumours had aneuploid stemlines. Two were adenoid cystic carcinomas and the other was a carcinoma ex pleomorphic adenoma (**Figure 2**). The predominant growth pattern in the ACC were cribriform and tubular/trabecular respectively. Their AgNOR counts were 4.29 and 3.01 (**Figure 3**). The AgNOR count for the carcinoma ex PA was 2.37. Diploid stemlines were present in the remaining 30 neoplasms (**Figure 4**). The mean CV of the flow cytometry results were 3.96 ± 3.1 (SD). The proliferative index and AgNOR counts of the diploid tumours are summarised in **Table 1.**

A positive correlation between the mean PI and mean AgNOR counts in the various neoplasms were found. This

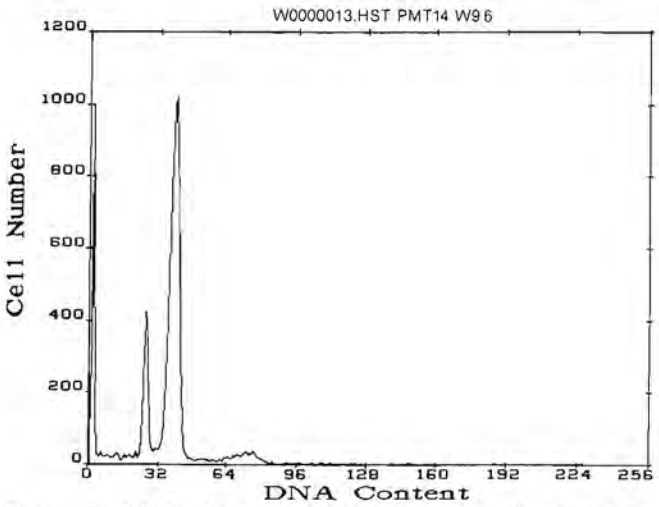


**Figure 2:** *DNA histogram of an adenoid cystic carcinoma showing aneuploidy.*

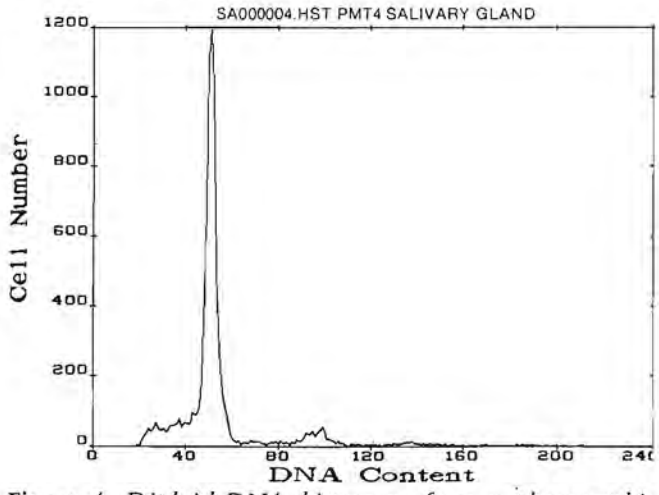


**Figure 4:** *Diploid DNA histogram from a pleomorphic adenoma.*

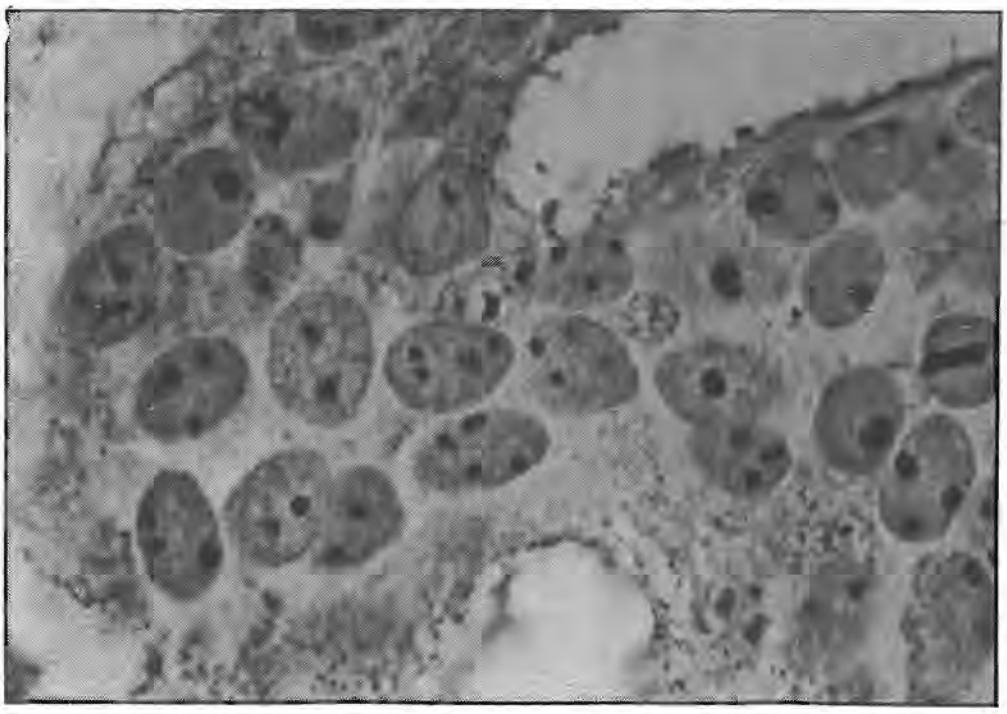

**Figure 3:** *AgNOR stain of a cribriform adenoid cystic carcinoma with an aneuploid DNA content. Original magnification, × 400.*

TABLE 1:
The PI and AgNOR count of the diploid salivary gland neoplasms

| | PA | PLA | ACC | MEC | Ca ex PA | Undiff Ca | EPI |
|---|---|---|---|---|---|---|---|
| PI | 4.1 ± 1.5 | 6.8 ± 5.3 | 6.7 ± 5.55 | 7.3 ± 2.3 | 5.1 ± 5.6 | 4.5 | 8.2 |
| AgNOR | 1.48 ± 0.3 | 1.85 ± 0.3 | 2.28 ± 0.7 | 1.93 ± 0.5 | 1.60 ± 0.3 | 3.13 | 2.23 |
| n | 11 | 8 | 3 | 4 | 2 | 1 | 1 |

PA = pleomorphic adenoma; PLA = polymorphous low grade adenocarcinoma;
ACC = adenoids cystic carcinoma; MEC = mucoepidermoid carcinoma;
Ca ex PA = carcinoma ex pleomorphic adenoma; Undiff Ca = undifferentiated carcinoma;
EPI = epithelial-myoepithelial carcinoma; PI = proliferative index

correlation however, was statistically not significant ($P = 0.45$). The difference between the mean PI of the benign salivary gland neoplasms and the diploid malignant salivary gland neoplasms was also not significant.

## Discussion

The cell cycle distribution as determined by flow cytometry is usually calculated using commercially available mathematical software programs. Corrections are made to subtract background debri which intervene with the various phases of the cell cycle. Creation of debri by means of tissue preparation is a problem especially when using paraffin-embedded tissue for flow cytometric analysis. Although these corrections have shown to enhance the prognostic value of particularly the S-phase[15], it must always be borne in mind that neoplastic cells might be eliminated as debri. Expression of exact percentages of cells in the various stages of cell is therefore proliferation, a questionable practice. It is much more reliable to use the PI as a rough indicator of proliferative activity, especially when evaluating paraffin embedded tissues.

The number of aneuploid tumours (n = 3) in the present study was too small to make definite comments regarding its correlation with the AgNOR counts. It is interesting to note however, that the two AgNOR counts of the aneuploid ACC were the first and third highest count among the salivary gland neoplasms. In a study to evaluate the prognostic factors for ACC, Hamper *et al* concluded that the shortest survival time was found in patients with tumours showing aneuploid DNA contents[16]. Forty-two percent of these tumours had a predominant cribriform growth pattern. This fact correlates with our finding that the mean AgNOR count in ACC did not correspond with the histologic growth pattern, a prognostic factor for tumour behaviour in ACC. The highest count was present in a tumour with a predominant cribriform growth pattern. The same applied for the flow cytometric analysis. The two aneuploid ACC had more favourable cribriform and tubular growth patterns respectively. Luna *et al* however, found that aneuploidy is more frequently present in the solid pattern[17]. This is an indication that the growth pattern in ACC alone is not solely responsible for tumour behaviour.

The fact that only 3 tumours of the sample that included 22 malignant neoplasms were aneuploid is probably related to the phenomenon that malignant salivary gland neoplasms generally have a less aggressive behaviour compared to other malignancies.

A high AgNOR count in neoplasms may be related to an increase in cell ploidy due to a real increase in the number of chromosomes. Since the NORs are present only on the 5 acrocentric chromosomes, it may be possible that these chromosomes are not affected in a neoplastic transformation that is accompanied with hyperploidy. The NORs are usually tightly aggregated in one or two nucleoli in a cell[18]. Proliferative activity may be associated with nucleolar dissocation resulting in spreading of AgNORs through the nucleus. This, together with the transcriptional activity may result in an increase in the mean AgNOR count[18].

A variety of techniques are available to determine cellular proliferation in histological material. Visualisation of the NORs by means of a silver staining technique is frequently used. The percentage of cells in the S + G2M phases of the cell cycle can be determined with flow cytometry and immunohistochemical techniques using antibodies against proliferating cell nuclear antigen (PCNA) as well as Ki-67, a monoclonal antibody that recognises a nuclear antigen present only in proliferating cells, are some of the more advanced methods used.

This study failed to show a significant relationship between the mean PI and mean AgNOR count of the various neoplasms although they were positively correlated. Crocker *et al* found a significant linear correlation between the mean AgNOR count and S-phase fraction of high and low grade non Hodgkin's lymphomas, but not between the AgNOR count and ploidy status[19]. The difference between the mean PI of the benign and malignant tumours was not significant. This is in contrast to the highly significant difference between the same tumours when evaluating the mean AgNOR counts[13]. From this study it would appear that the AgNOR technique, which is fast and inexpensive, may be more suitable to accurately determine the proliferative activity when using paraffin embedded tissues

References


1. Crocker J., *Nucleolar organiser regions.* In: Underwood JCE, ed. *Current topics in pathology* New York: Springer-verlag, 1990: 92 – 143.
2. Ploton D., Menager M., Jeannesson P., Himberg G., Pigeon F., Adnet J.J., *Improvement in the staining and in the visualisation of the agyrophilic proteins of the nucleolar organiser region at the optical level* Histochem J 1986 **18**: 5 – 14.
3. Crocker J., Nar P., *Nucleolar organiser regions in lymphomas* J Pathol 1987 **151**: 111 – 118.
4. Mackie R.M., White S.I., Seywright M.M., Young H., *An assessment of the value of AgNOR staining in the identification of dysplastic and other borderline melanocytic naevi* Br J Mermatol 1989 **120**: 511 – 516.
5. Smith R., Crocker J., *Evaluation of nucleolar organiser region-associated proteins in breast malignancy* Histopathology 1988 **12**: 221 – 223.
6. Rosa J., Mehta A., Filipe M.I., *Nucleolar organiser regions in gastric carcinoma and its precursor stages* Histopathology 1990 **16**: 265 – 269.
7. Shapiro H.M., *Flow cytometry of DNA content and other indicators of proliferative activity* Arch Pathol Lad Med 1989 **113**: 591 – 597.
8. Visakorpi T., *Proliferative activity determined by DNA flow cytometry and proliferating cell nuclear antigen (PCNA) immunohistochemistry as a prognostic factor in prostatic carcinoma* J Pathol 1992 **168**: 7 – 13.
9. Sigurdson H., Baldetorp B., Borg A., et al., *Indicators of prognosis in node-negative breast cancer* N Engl J Med 1990 **322**: 1045 – 1053.
10. Merkel D.E., McGuire W.L., *Ploidy, proliferative activity and prognosis. DNA flow cytometry of solid tumors* Cancer 1990 **65**: 1194 – 1205.
11. Greiner T.C., Robinson R.A., Maves M.D., *Adenoid cystic carcinoma. A clinicopathologic study with flow cytometric analysis* Am J Clin Pathol 1989 **92**: 711 – 720.
12. Suresh U.R., Chawner J., Buckley C.H., Fox H., *Do Agnor counts reflect cellular ploidy or cellular proliferation? A study of trophoblastic tissue* J. Pathol 1990 **160**: 213 – 215.
13. Van Heerden W.F.P., Raubenheimer E.J., *Evaluation of the nucleolar organiser region associated proteins in minor salivary gland tumours* J. Oral Pathol Med 1991 **20**: 291 – 295.
14. Hedley D.W., Friedlander M.L., Taylor I.W., Rugg C.A., Musgrave E.A., *Method for analysis of cellular DNA content of paraffin-embedded pathological material using flow cytometry* J Histochem Cytochem 1983 **31**: 1333 – 1335.
15. Kallioniemi O.P., Visakorpi T., Holli K. Heikkinen A., Isola J., Koivula T., *Improved prognostic impact of S-phase values from paraffin-embedded breast and prostate carcinomas after correcting for nuclear slicing* Cytometry 1991 **12**: 413 – 421.
16. Hamper K., Lazar F., Dietel M., et al., *Prognostic factors for adenoid cystic carcinoma of the head and neck: a retrospective evaluation of 96 cases* J Oral Pathol Med 1990 **19**: 101 – 107.
17. Luna M.A., El-Nagger A., Batsakis J.G., Weber R.S., Gernser L.A., Geopfert H., *Flow cytometric DNA content of adenoid cystic carcinoma of submandibular gland. Correlation of histologic features and prognosis* Arch Otolaryngol Head Neck Surg 1990 **116**: 1291 – 1296.
18. Underwood J.C.R., Giri D.D., *Nucleolar organiser regions as diagnostic discriminants for malignancy* J. Pathol 1988 **155**: 95 – 96.
19. Crocker J., McCartney J.C., Smith P.J., *Correlation between DNA flow cytometric and nucleolar organiser region data in non-Hodgkin's lymphoma* J. Pathol 1988 **154**: 151 – 156.


Received for publication 30.03.93
Accepted for publication 24.05.93

*33rd FSASP Congress*

# A review of recent developments in the diagnosis of epithelial neoplasms of salivary gland origin

E. J. RAUBENHEIMER[a], W.F.P. VAN HEERDEN[a]

**Abstract** The adoption by the World Health Organization of a revised classification for salivary gland neoplasms has introduced a new chapter in the diagnosis of these diverse growths. Universal acceptance of this proposal will contribute significantly to diagnostic uniformity. The introduction of an outline for the grading of malignant salivary gland neoplasms benefit preoperative prognostication and rationalize therapeutic regimes. The utilization of fine needle aspiration and frozen section for the establishment of a diagnosis are discouraged. Despite recent developments in histochemistry, immunohistochemistry and DNA content analyses of salivary gland neoplasms, the diagnosis still relies mainly on the growth pattern and cytologic features of a tumor. *(Eur J Lab Med 1995;1:107-112).*

## Introduction

Although salivary glands share similar cellular phenotypes with sweat glands, mammary glands and the exocrine pancreas, neoplastic proliferations in the former are infinitely more complex and, from a cellular viewpoint, represent the most heterogenous group of proliferations in the human body. Despite recent developments in the understanding of the histogenesis of salivary gland neoplasms, the diagnostic process still relies mainly upon growth characteristics and cellular morphology. Special laboratory investigations like electron microscopy and cellular markers form a minor part of the diagnostic process and often only subtle microscopic differences distinguish neoplasms with diverse clinical outcomes. The subjectivity involved in the diagnosis of salivary gland neoplasms is highlighted in a recent study where 101 salivary gland neoplasms were reevaluated by a panel of senior pathologists. In a third there were minor disagreements, mostly related to subclassification, whereas major diagreements relating to benign versus malignant occurred in 7.9% of cases[1].

The purpose of this paper is to give an overview of recent developments in the diagnosis of salivary gland neoplasms.

## Classification

For universal acceptance, a classification of pathologic proliferations should be based on patterns of differentiation that reflect the cell types of the parental tissue and simultaneously group neoplasms in prognostic categories. The most likable classification of salivary gland neoplasms is the morphologic working classification initially proposed by the Armed Forces Institute of Pathology[2] (Table I) and later adopted by the World Health Organization's Committee on salivary gland tumors. Although the patterns of differentiation of salivary gland neoplasms is not addressed systematically in this classification, malignant growths are now for the first time prognostically grouped. The diagnostic refinement introduced by this new approach is clearly evident in a study which revised salivary gland neoplasms originally diagnosed according to the 1972 World Health Organizations classification[3]. In 29 cases the original diagnosis was changed and in 7 it resulted in a change from benign to malignant or vice versa[4]. Although the new approach to the classification has valuable clinical implications, it is by no means complete. Entities like the salivary gland anlage tumor[5], sialoblastoma[6,7] and hyalizing clear cell carcinoma[8] lack suffi-

[a] Department of Oral Pathology and Oral Biology, Medical University of Southern Africa.

*Correspondence to*: Prof. E.J. Raubenheimer, Department of Oral Pathology & Oral Biology, Box D24, P.O. Medunsa, 0204, Republic of South Africa

*Paper received 01-03-1995*

Table I. AFIP classification of primary epithelial neoplasms of salivary gland origin

**Benign**

- Mixed tumor (pleomorphic adenoma)
- Papillary cystadenoma lymphomatosum (Warthin's tumor)
- Oncocytoma
- Cystadenoma
- Basal cell adenoma
- Ductal papillomas
  - Sialadenoma papilliferum
  - Inverted ductal papilloma
  - Intraductal papilloma
- Myoepithelioma
- Sebaceous adenomas
  - sebaceous adenoma
  - sebaceous lymphadenoma
- Adenoma NOS

**Malignant**

*Low-Grade*

- Mucoepidermoid carcinoma (low grade)
- Acinic cell adenocarcinoma
- Polymorphous low grade adenocarcinoma
- Basal cell adenocarcinoma
- Adenocarcinoma (NOS) low grade
- Metastasizing mixed tumor

*Intermediate-Grade*

- Mucoepidermoid carcinoma (intermediate grade)
- Adenoid cystic carcinoma (cribriform-tubular types)
- Epithelial-myoepithelial carcinoma
- Adenocarcinoma NOS (intermediate grade)
- Clear cell carcinoma
- Cystadenocarcinoma
  - papillary
  - non papillary
- Sebaceous carcinomas
  - sebaceous carcinoma
  - sebaceous lymphadenocarcinoma
- Mucinous adenocarcinoma

*High-Grade*

- Mucoepidermoid carcinoma (high grade)
- Adenoid cystic carcinoma (solid)
- Malignant mixed tumor
  - carcinoma ex mixed tumor
  - carcinosarcoma
- Adenocarcinoma NOS (high grade)
- Squamous cell carcinoma
- Undifferentiated carcinoma
- Oncocytic carcinoma
- Adenosquamous carcinoma
- Salivary duct carcinoma
- Myoepithelial carcinoma

cient numbers for the establishment of behavioral patterns and may only find their way into future reappraisals of this classification.

## Terminology

Arguments on the preferentiability of the designation "mixed tumor" or the term "pleomorphic adenoma" are unproductive and both are now accepted. "Adenolymphoma" as a synonym for papillary cystadenoma lymphomatosum should fall in disuse because any implication that this benign tumor is linked to lymphoma is misleading. Oxyphil cell adenoma and oncocytoma are used interchangebly. The ambiguous term "monomorphic adenoma" has fallen into disuse and all unclassifiable adenomas are now proposed to be designated as "adenoma, not otherwise specified". Although myoepithelioma is classified as a separate entity, no counter argument exists that this neoplasm is in fact an extreme differentiation on the diverse spectrum of pleomorphic adenoma. Separate categorization of myoepithelioma may however, prevent confusion with benign mesenchymal neoplasms, many of which resemble myoepitheliomas microscopically.

The term malignant mixed tumor (or malignant pleomorphic adenoma) should not be used as a specific diagnosis as it includes three different entities: carcinoma ex mixed tumor (or a carcinoma arising in a mixed tumor), carcinosarcoma (true malignant mixed tumor) and metastasizing mixed tumor. The suffix-tumor is now replaced by "carcinoma" in two neoplasms which are now known to be malignant: acinic cell carcinoma and mucoepidermoid carcinoma. As refinements in classifications proceed, the utilization of terms like "adenocarcinoma not otherwise specified" decrease. Although new clinico-pathological entities such as salivary duct carcinoma, terminal duct carcinoma and epithelial-myoepithelial carcinoma reduce the frequency by which this category is used, there still remain those adenocarcinomas which cannot be accommodated in other categories.

## Frozen sections and fine needle aspirations

Frozen sections (FS) and fine needle aspirations (FNA) are increasingly accepted as cost effective and time saving techniques for the diagnosis of abnormal body masses. The cellular diversity which may be experienced within a salivary gland neoplasm decreases the potential accuracy of all techniques which suffer the disadvantage of not representing all cell types in a neoplastic proliferation. The status of invasion is one of the most important parameters in predicting the biologic behavior of salivary gland neoplasms[2]. The small sample obtained through FNA precludes the disclosure of this important parameter. Studies investigating the sensitivity and specificity of FNA frequently compare its diagnostic accuracy with histological diagnoses

based on dated classification systems, most of which do not recognize modern refinements in the diagnosis of salivary gland neoplasms. FNA appears to have a high success rate in distinguishing between benign and malignant salivary gland neoplasms[9-11]. The distinction between benign and malignant in a diagnosis on which the therapeutic approach is decided, is probably equally important to the grading of a specific malignant growth. In this respect, the limited sample obtained through FNA is often inadequate and its results cannot be compared with those obtained through incision biopsy. The cytological atypia frequently present in benign salivary gland neoplasms[9,12,13] and potential confusion with non-epithelial stromal neoplasms[14] are further pitfalls in the interpretation of FNA. Although there are unquestionable clinical indications for FNA, none merit its inclusion as part of the systematic evaluation on which the therapeutic approach is based[15].

In a series of 310 patients subjected to FS, the correct type of malignancy was diagnosed in only 51% of cases and in four patients, a false positive diagnosis of malignancy was made. The authors of this study conclude that FS is no more accurate in the evaluation of salivary gland tumors than FNA[16]. Although there are no indications against the utilization of FS for determining clear margins during excision, a primary diagnosis should not be established on FS alone.

## Grading of salivary gland malignancies

This aspect of the diagnosis of malignant neoplasms is important particularly in the case of mucoepidermoid carcinomas, adenoid cystic carcinoma and adenocarcinoma which may be classified in more than one grade of malignant behavior. The microscopic criteria applied for grading are controversial and often highly subjective. Auclair, Goode and Ellis[17] proposed a point scoring system for the objective grading of muco-epidermoid carcinomas. The histopathologic features that indicate high grade behavior are an intracystic component of less than 20%, four or more mitoses per 10 high-power fields, neural invasion, necrosis and cellular anaplasia. Most differences of opinion involve the distinction between low and intermediate grades and their proposed point system may provide a basis for an objective solution. Factors that indicate a poor prognosis in adenoid cystic carcinomas encompass failure of local disease control at the initial surgical procedure, a solid pattern histologically, recurrent disease and distant metastases[2]. Despite the description of new clinicopathological entities like the salivary duct carcinoma and epithelial myoepithelial carcinoma which were formerly grouped in the adenocarcinoma "not otherwise specified" category, there still remain a group of adenocarcinomas that cannot be accommodated in conventional classifications. These malignancies are divided into low-, intermediate- and high grade categories on growth patterns and cytologic features[2]. Although histopathologic grading of acinic cell adenocarcinomas is possible, the influence of the different grades on the prognosis is debateable[18,19]. The limited malignant potential and excellent survival of patients with polymorphous low-grade adenocarcinoma is little affected by patterns of differentiation[20].

## Histochemistry and immunohistochemistry

Although histochemical and immunohistochemical techniques have played an important role in investigations of the histogenesis of salivary gland neoplasms, their diagnostic applications are limited. This is mainly due to the wide spectrum of differentiation which may occur within a single salivary gland neoplasm, with each growth pattern exhibiting its own immunohistochemical characteristics[21-23]. Salivary gland neoplasms furthermore often share immunohistochemical staining characteristics with other neoplasms. Positive staining for prostate-specific antigen and prostate-specific acid phosphatase are frequently found in benign and malignant salivary neoplasms[24], a pitfall in the microscopic distinction between salivary gland carcinomas and metastatic deposits of prostatic carcinoma. Alpha 1-antitrypsin is a useful marker of basement membrane-like material[25] and can be helpful in distinguishing this product from myxoid interstitial deposits. A potential distraction to the diagnosis of myoepithelial tumors of salivary glands (i.e. myoepithelioma and myoepithelial carcinoma) is confusion with spindle cell mesenchymal proliferations. Demonstration of myoepithelial differentiation requires careful evaluation of immunohistochemical stains. The identification of S100 protein, actin and keratin either focally or diffusely, is helpful in confirming myoepithelial differentiation[26].

Microscopically, myoepitheliomas differentiate into three distinct cellular patterns: a spindle cell-, plasmacytoid- or a combination of plasmacytoid and spindle shaped cellular patterns[2]. If immunohistochemical criteria had to be applied rigorously, it is debateable whether the plasmacytoid variety, which is reported to stain negative for muscle specific actin, does represent true myoepithelial differentiation[27].

Confusion between the microscopic appearances of polymorphous low grade adenocarcinoma and benign pleomorphic adenoma may be avoided by employing stains for glial fibrillary acidic protein (GFAP). The former does not stain for this antigen

whereas its positivity is common in pleomorphic adenomas[28]. A greater diagnostic dilemma is the distinction between polymorphous low grade adenocarcinoma and adenoid cystic carcinoma. The immunochemical reactions of these two tumors are not sufficiently dissimilar to be of any practical value[29] and differences are mainly cytological and to a lesser extent morphological in nature. The presence of both sex steroids and the receptor for progesterone in adenoid cystic carcinomas[30] suggests a good possibility that some tumors in this group may respond to endocrine therapy.

Various reports propose a useful place for the counting of nucleolar organizer regions (NOR's) in order to predict the proliferative activity and prognosis of malignant salivary gland neoplasms[31-33] and distinguish between benign and malignant growths[34]. Our experience with this technique[35] as well as those of other researchers[36] were less rewarding and we believe this technique provides nothing but redundant information.

Research into the use of cellular markers to predict the behavior of salivary gland tumors is in its infancy. An association is reported between the expression of erbb2 oncoprotein and aggressiveness of malignant salivary gland tumours[37,38]. Loss of cellular differentiation appears to be linked with under expression of the c-fos oncogene[39] and evaluation of Ki-67 expression[40], immunoreactivity for PCNA[41] and c-myc, ras p21 and p53 expression[42] may become important determinants for malignant behavior.

## DNA content analysis

The positive correlation between prognosis and ploidy status of malignant neoplasms is well established. Despite the presence of atypical cells in benign pleomorphic adenomas, all benign salivary gland tumours have diploid DNA contents and the malignant ones frequently display an aneuploid pattern[43,44]. A statistically significant correlation was found between DNA content and tumor size, histological grade, lymph node metastasis and lethality of 55 salivary gland carcinomas[45]. Flow cytometry was however, unable to predict the development of metastasis in cases of proven metastasizing mixed tumor[46]. DNA ploidy was shown to correlate with the prognosis of epithelial-myoepithelial carcinoma[47] myoepithelioma[48] and muco-epidermoid carcinoma[49]. The value of this technique in prognosticating adenoid cystic carcinomas is debateable[50,51] whereas no prognostic correlation could be found between DNA ploidy and the course of acinic cell adenocarcinomas[52,53]. Larger series will shed more light on the usefulness of DNA content analysis in the prediction of the behavior of salivary gland tumors.

## Acknowledgment

*The authors wish to thank Mrs. C.S. Begemann for secretarial assistance.*

## References

1. Van der Wal JE, Carter RL, Klijanienko J, Micheau C, Rilke F, Seifert G, et al. Histological reevaluation of 101 intraoral salivary gland tumours by an EORTC-study group. J Oral Pathol Med 1993;22: 21-2.
2. Ellis GL, Auclair PL, Gnepp DR. Surgical Pathology of the Salivary Glands. W.B. Saunders Company, Philadelphia. 1991.
3. Thackray AC, Sobin LH. Histological Typing of Salivary Gland Tumours. Geneva. World Health Organization, 1972.
4. Van der Wal JE, Snow GB, van der Wal I. Histological reclassification of 101 intraoral salivary gland tumour (new WHO classification). J Clin Pathol 1992;45:834-5.
5. Dehner LP, Valbuena L, Perez-Atayde A, Reddick RL, Askin FB, Rosai J. Salivary gland anlage tumor (congenital pleomorphic adenoma). A clinicopathologic, immunohistochemical and ultrastructural study of nine cases. Am J Surg Pathol 1994;18: 25-36.
6. Hsueh C, Gonzalez-Crussi F. Sialoblastoma: a case report and review of the literature on congenital epithelial tumors of salivary gland origin. Pediatr Pathol 1992; 12:205-14.
7. Batsakis JG, Frankenthaler R. Embrioma (sailoblastoma) of salivary glands. Ann Otol Laryngol 1992;101:958-60.
8. Milchgrub S, Gnepp DR, Vuitch F, Delgado R, Albores-Saavedia J. Hyalinizing clear cell carcinoma of salivary gland. Am J Surg Pathol 1994;18:74-82.
9. Chan MKM, McGuire LJ, King W, Li AKC. Cytodiagnosis of 112 salivary gland lesions. Correlation with istologic and frozen section diagnosis. Acta Cytologica 1992;36:353-63.
10. Barnard NA, Paterson AW, Irvine GH, Mackenzie EDF, White H. Fine needle aspiration in maxillofacial surgery - experience in a district general hospital. Br J Oral Maxfac Surg 1993;31:223-6.
11. Pitts DB, Hilsinger RL, Karanday E, Ross JC, Caro JE. Fine-Needle Aspiration in the diagnosis of salivary gland disorders in the community hospital setting. Acta Otolaryngol Head Neck Surg 1992;118 479-82.
12. Laucirica R, Farnum JB; Leopold SK, Kalin GB, Youngberg GA. False positive diagnosis in fine-needle aspiration of an atypical Warthin tumor: histochemical differential stains for cytodiagnosis. Diagn Cytopathol 1989;5:412-5.
13. Thunnissen FB, Peterse LJ, Bucholtz R, van der Beek JM, Bosman FT. Polypoidy in pleomorphic adenomas with cytological atypia. Cytopathology 1992;3:101-9.
14. Mair S, Leiman G. Benign neurilemmoma (Schwan-

noma) masquerading as a pleomorphic adenoma of the submandibular salivary gland. Acta Cytol 1989;33:907-10.
15. Batsakis JG, Sneige N, el-Naggar A. Fine needle aspiration of salivary glands: its utility and tissue effects. Ann Otol Rhinol Laryngol 1992;101:185-8.
16. Heller KS, Attie JN, Dubner S. Accuracy of frozen section in the evaluation of salivary tumors. Am J Surg 1993;166:424-7.
17. Auclair PL, Goode RK, Ellis GL. Mucoepidermoid carcinoma of intraoral salivary glands. Evaluation of application of grading criteria in 143 cases. Cancer 1992;69:2021-30.
18. Batsakis JG, Luna MA, el-Naggar A. Histopathologic grading of salivary gland neoplasms: II. Acinic cell carcinomas. Ann Otol Rhinol Laryngol 1990; 99:929-33.
19. Oliveira P, Fonseca I, Soares J. Acinic cell carcinoma of the salivary glands. A long term follow-up study of 15 cases. Eur J Surg Oncol 1992;18:7-15.
20. Norberg LE, Burford-Mason AP, Dardick I. Cellular differentiation and morphologic heterogeneity in polymorphous low grade adenocarcinoma of minor salivary gland. J Oral Pathol Med 1991;20:373-9.
21. Takahashi H, Tsuda N, Fujita S, Tezuka F, Okabe H. Immunohistochemical investigation of vimentin, neuron-specific enolase, alpha 4 1-antichymotrypsin and alpha 1-antitrypsin in adenoid cystic carcinoma of the salivary gland. Acta Pathol Jpn 1990;40: 655-64.
22. Huang JW, Mori M, Yamada K, Isono K, Ueno K, Shinohara M, et al. Mucoepidermoid carcinoma of the salivary glands: immunohistochemical distribution of intermediate filament proteins, involucrin and secretory proteins. Anticancer Res 1992;12:811-20.
23. Mori M, Kasai T, Yuba R, Chomette G, Auriol M, Vaillant JM. Immunohistochemical studies of S100 protein alpha and beta subunits in adenoid cystic carcinoma of salivary glands. Virchows Arch B Cell Pathol 1990;59:115-23.
24. Van Krieken JH. Prostate marker immunoreactivity in salivary gland neoplasms. A rare pitfall in immunohistochemistry. Am J Surg Pathol 1993;17:410-4.
25. Takahashi H, Fujita S, Okabe H, Tsuda N, Tezuka F. Distribution of tissue markers in acinic cell carcinomas of salivary gland. Pathol Res Pract 1992; 188:692-700.
26. Herrera GA. Light microscopic, ultrastructural and immunochemical spectrum of malignant lacrimal and salivary gland tumors, including malignant mixed tumours. Pathobiology 1990;58:312-22.
27. Franquemont DW, Mills SE. Plasmacytoid monomorphic adenoma of salivary glands. Absence of myogenous differentiation and comparison to spindle cell myoepithelioma. Am J Surg Pathol 1993;17: 146-53.
28. Anderson C, Krutchoff D, Pederson C, Cartun R, Barman M. Polymorphous low grade adenocarcinoma of minor salivary gland: a clinicopathologic and comparative immunohistochemical study. Mod Pathol 1990;3:76-82.
29. Simpson RH, Clarke TJ, Sarsfield PT, Gluckman PG, Babajeus AV. Polymorphous low-grade adenocarcinoma of the salivary glands: a clinicopathological comparison with adenoid cystic carcinoma. Histopathology 1991;19:121-9.
30. Ozoho S, Onozuka M, Sato K, Ito Y. Immunohistochemical localization of estradiol, progesterone and progesterone receptor in human salivary glands and salivary adenoid cystic carcinomas. Cell Struct Funct 1992;17:169-75.
31. Freitas RA, de Araujo VC, Araujo NS. Argyrophilia in nuclear organizer regions (AgNOR) in adenoid cystic carcinoma and polymorphous low grade adenocarcinoma of the salivary glands. Eur Arch Otorhinolaryngol 1993;250:213-7.
32. Chomette G, Auriol M, Wann A, Guilbert F. Acinic cell carcinomas of salivary glands histoprognosis. Value of NOR's stained with AgNOR-technique and examined with semi-automatic image analysis. J Biol Buccale 1991;19:205-10.
33. Landini G. Nuclear organizing regions (NOR's) in pleomorphic adenomas of the salivary glands. J Oral Pathol Med 1990;19:257-60.
34. Cardillo MR. AgNOR technique in fine needle aspiration cytology of salivary gland masses. Acta Cytol 1992;36:147-51.
35. Van Heerden WFP, Raubenheimer EJ. Evaluation of the nuclear organizer region associated proteins in minor salivary gland tumors. J Oral Pathol Med 1991;20:291-5.
36. Cardillo R, el-Naggar A, Luna MA, Roderiques-Peratto JL, Batsakis JG. Nuclear organized (NOR's) and myoepitheliomas: a comparison with DNA content and clinical course. J Laryngol Otol 1992; 106:616-20.
37. Stenman G, Sandros J, Nordkuist A, Mark J, Sahlin P. Expression of the ERBB2 protein in benign and malignant salivary gland tumors. Genes Chromosom Cancer 1991;3:128-35.
38. Sugano S, Mukai K, Tsuda H, Hirohashi S, Furuya S, Shimosato Y, et al. Immunochrotochemical study of c-erB-2 oncoprotein overexpression in human major salivary gland carcinoma: an indicator of aggressiveness. Laryngoscope 1992;102:923-7.
39. Birek C, Lui E, Dardick I. C-Fos oncogene underexpression in salivary gland tumors as measured by in situ hybridization. Am J Pathol 1993;142:917-23.
40. Murakami M, Ohtani I, Hojo H, Wakasa H. Immunohistochemical evaluation with Ki-67: an application to salivary gland tumours. J Laryngol Otol 1992;106:35-8.
41. Yang L, Hashimura K, Quin C, Shrestha P, Sumitomo S, Mori M. Immunoreactivity of proliferating cell nuclear antigen in salivary gland tumours: an assessment of growth potential. Virchows Arch A Pathol Anat Histopathol 1993;422:481-6.
42. Deguchi H, Hamano H, Hayashi Y. c-myc, ras p21 and p53 expression in pleomorphic adenoma and its malignant form of the human salivary glands. Acta Pathol Jpn 1993;43:413-22.
43. Tytor M, Gemryd P, Wingren S, Grenko RT, Lundgren J, Lundquist PG. Heterogeneity of salivary gland tumors studied by flow cytometry. Head Neck 1993;15:514-21.

44. Felix A, Fonseca I, Soares J. Oncocytic tumors of salivary gland type: a study with emphasis on nuclear DNA ploidy. J Surg Oncol 1993;52:217-22.
45. Carillo R, Batsakis JG, Weber R, Luna MA, el-Naggar A. Salivary neoplasms of the palate: a flow cytometric and clinicopathological analysis. J Laryngol Otol 1993;107:858-61.
46. Wenig BM, Hitchcock CL, Ellis GL, Gnepp DR. Metastasizing mixed tumor of salivary glands. A clinicopathologic and flow cytometric analysis. Am J Surg Pathol 1992;16:845-58.
47. Fonseca I, Soares J. Epithelial-myoepithelial carcinoma of the salivary glands. A study of 22 cases. Virchows Arch A Pathol Anat Histopathol 1993; 422:389-96.
48. el-Naggar A, Batsakis JG, Luna MA, Goepfert H, Tortoledo ME. DNA content and proliferative activity of myoepitheliomas. J Laryngol Otol 1989;103: 1192-7.
49. Hamper K, Caselitz J, Arps H, Askensten U, Auer G, Seifert G. The relationship between DNA content in salivary gland tumors and prognosis. Comparison of mucoepidermoid tumors and acinic cell tumors. Arch Otorhinolaryngol 1989;246:328-32.
50. Greiner TC, Robinson RA, Maves MD. Adenoid cystic carcinoma. A clinicopathologic study with flow cytometric analysis. Am J Clin Pathol 1989;92: 711-20.
51. Eibling DE, Johnson JT, McCoy TP, Barnes EL, Syms CA, Wagner RL, et al. Flow cytometric evaluation of adenoid cystic carcinoma: correlation with histologic subtype and survival. Am J Surg 1991;162:307-172.
52. el-Naggar A, Batsakis JG, Luna MA, McLemore D, Byers Rm. DNA flour cytometry of acinic cell carcinomas of major salivary glands. J Laryngol Otol 1990;104:410-6.
53. Hamper K, Mausch HE, Caselitz J, Arps H, Berger J, Askensten U, et al. Acinic cell carcinoma of the salivary glands: the prognostic relevance of DNA cytomorphometry in a retrospective study of long duration (1965-1987). Oral Surg Oral Med Oral Pathol 1990;69:68-75.

J Oral Maxillofac Surg
61:126-131, 2003



# Intraoral Salivary Duct Carcinoma: A Report of 5 Cases

*Willie F.P. van Heerden, BChD, MChD, PhD,**
*Erich J. Raubenheimer, BChD, MChD, PhD,†*
*Theuns J.P. Swart, BChD, MChD, MSc,‡ and*
*Sonja C. Boy, BChD§*

Salivary duct carcinoma (SDC) is a high-grade malignant epithelial tumor of salivary glands first described by Kleinsasser et al.[1] It has also been termed cribriform salivary carcinoma of excretory ducts,[2] infiltrating salivary duct carcinoma,[3] and intraductal carcinoma.[4] SDC has a poor prognosis,[2,5,6] although patients with prolonged disease-free survival have been reported.[2,5] Low-grade variants of SDC have also been described.[7,8]

The peak incidence of SDCs is in the sixth and seventh decades of life, and it has a male predominance.[6,9] This neoplasm has a striking resemblance to ductal breast carcinoma and is characterized by the presence of intraductal, circumscribed tumor islands with a papillary, cribriform, or solid growth pattern associated with an infiltrative component. Comedonecrosis is frequently present.

SDCs occur almost exclusively in the major salivary glands with the parotid gland predominantly affected.[10] Only isolated cases involving minor salivary glands have been reported.[1,8,11-18] In this study, we report the clinicopathologic and immunohistochemical features of 5 cases of intraoral SDC. The DNA ploidy status of these tumors was also studied.

*Professor and Head, Department of Oral Pathology and Oral Biology, Faculty of Dentistry, University of Pretoria, Pretoria, South Africa.

†Professor and Head, Department of Oral Pathology, Medical University of Southern Africa, Pretoria, South Africa.

‡Senior Specialist, Department of Oral Pathology and Oral Biology, Faculty of Dentistry, University of Pretoria, Pretoria, South Africa.

§Senior Registrar, Department of Oral Pathology and Oral Biology, Faculty of Dentistry, University of Pretoria, Pretoria, South Africa.

Address correspondence and reprint requests to Dr van Heerden: Department of Oral Pathology and Oral Biology, University of Pretoria, PO Box 1266, Pretoria, 0001, South Africa; e-mail: wvheerd@medic.up.ac.za



0278-2391/03/6101-0021$35.00/0
doi:10.1053/joms.2003.50021

## Materials and Methods

Malignant intraoral salivary gland tumors diagnosed at the Departments of Oral Pathology at the University of Pretoria and Medical University of Southern Africa were reviewed. Four cases of SDC were included while an additional case was reclassified as an SDC according to the criteria of the World Health Organization.[19] Clinical and follow-up information was obtained from the patients' files and supplemented by communication with the referring practitioners or clinics and immediate family members. All the specimens were fixed in 10% buffered formalin, and the histologic features were evaluated by reviewing all the sections stained with hematoxylin and eosin. Additional slides of paraffin blocks were prepared for immunohistochemical analysis using the standard avidin-biotin peroxidase method. A panel of commercially available antibodies with appropriate controls was used (Table 1). The extent of immunohistochemical staining was evaluated and scored as + (1% to 9% of tumor cells), ++ (10% to 50% of tumor cells), and +++ (>50% of tumor cells). Staining intensity was not evaluated.

Flow cytometry was performed on 50 μm sections of the formalin-fixed paraffin-embedded tumor blocks. Tissue was processed according to the modified method described by Heiden et al.[20] The sections were enfolded with 50-μm nylon mesh and deparaffinized in xylene, hydrated in graded alcohols, and digested with Carlsberg solution. The nuclei were stained with DAPI solution (4′,6-diamidino-phenylindole) containing 0.2 M trisodium citrate dihydrate, and at least 10,000 events from each case were analyzed using a PAS III flow cytometer equipped with a high-pressure 100-W mercury lamp (Partec, Münster, Germany).

## Results

The patients ranged in age from 47 to 71 years (mean age, 58.2 years). Two were female and 3 were male. All of the tumors were located in the palate and ranged in size from 5 to 14 cm. The tumors presented

**Table 1. SPECIFICATIONS OF ANTIBODIES USED**

| Antibody | Source | Dilution | Antigen Retrieval | Detection |
|---|---|---|---|---|
| High-molecular-weight cytokeratin | DAKO (34BE12) | Prediluted | * | DAKO LSAB2 |
| α-Smooth muscle actin | DAKO (1A4) | Prediluted | None | DAKO LSAB2 |
| Vimentin | DAKO (V9) | Prediluted | None | DAKO LSAB2 |
| Anti-S-100A | DAKO | Prediluted | * | DAKO LSAB2 |

*Microwave pressure cooker in citric buffer, pH 6.0.

as painful masses (Figs 1 through 3). No association with the parotid gland could be shown in any case using computed tomography investigation (Fig 4). The possibility of metastasis from an intraductal breast carcinoma was also excluded. Clinical evidence of regional lymph node metastasis was present in 2 cases. Three patients refused any form of treatment and were subsequently lost to follow-up. No information could be obtained from the referring clinics. One patient was treated with radical resection and is currently receiving postoperative radiotherapy. The clinicopathologic findings are summarized in Table 2.

Microscopically, all tumors consisted of an intraductal component with a predominantly cribriform pattern and central comedonecrosis (Fig 5). Infiltrating tumor islands, in a trabecular and cribriform pattern, in a stroma that varied from cellular to regions of hyalinization were also present in all 4 cases (Fig 6). The tumor cells had well-defined cell borders with eosinophilic cytoplasm and vesicular nuclei. Mitotic activity varied from moderate to high (Fig 7). The immunohistochemical results are shown in Table 3.

Flow cytometry analysis showed 4 tumors to be aneuploid (Fig 8) and one diploid (case 2) (Fig 9). The coefficient of variance (CV) of all the measurements was less than 3%.

## Discussion

The possibility of metastases should be eliminated before a final diagnosis of SDC is made. Metastatic ductal carcinoma from the breast could be excluded with careful clinical examination and mammography. The histologic features of these tumors are very similar, although the presence of estrogen receptor protein and absence of carcinoembryonic antigen in breast carcinomas have been used to differentiate between SDC and ductal carcinoma of the breast.[21] Metastatic prostatic carcinoma can in the majority of cases be excluded by the absence of both prostate-specific antigen and prostate-specific acid phosphatase in the tumor cells.

The histologic differential diagnosis of SDC includes high-grade mucoepidermoid carcinoma, undifferentiated carcinoma, adenocarcinoma (not otherwise specified), dedifferentiated acinic cell carcinoma, and adenoid cystic carcinoma. High-grade mucoepidermoid carcinomas have epidermoid and intermediate basaloid cells as well as cells with mucicarmine demonstrable intracellular mucin, whereas only luminal mucin is found in SDC. Cribriform and papillary-cystic growth patterns are not found in mucoepidermoid carcinomas. Undifferentiated carcinoma lacks the eosinophilic cytoplasm of SDC and does not form glandular structures. Adenocarcinoma,

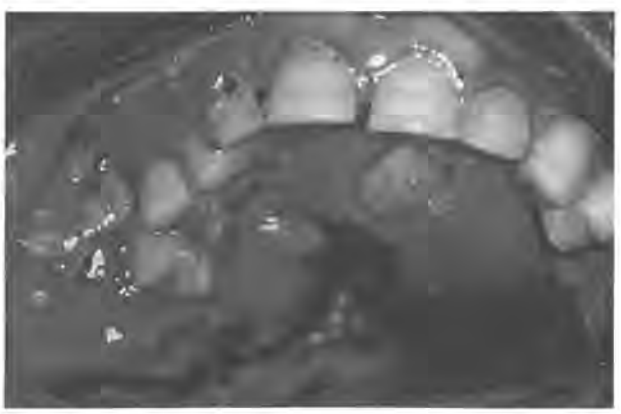

**FIGURE 1.** Intraoral view of case 1 showing a massive tumor destroying the right maxilla, extending across the midline.

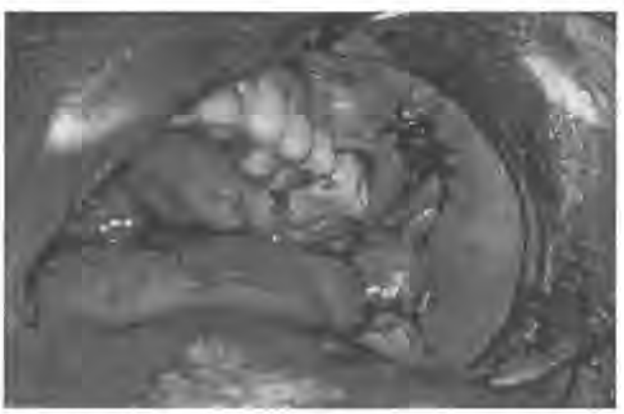

**FIGURE 2.** A tumor located in the left maxilla with buccal and palatal expansion from case 2.

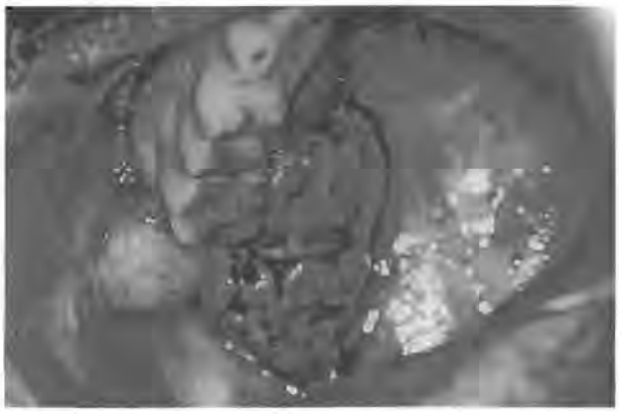

**FIGURE 3.** Case 3 presenting with an ulcerated tumor in the right palate involving the alveolar ridge.

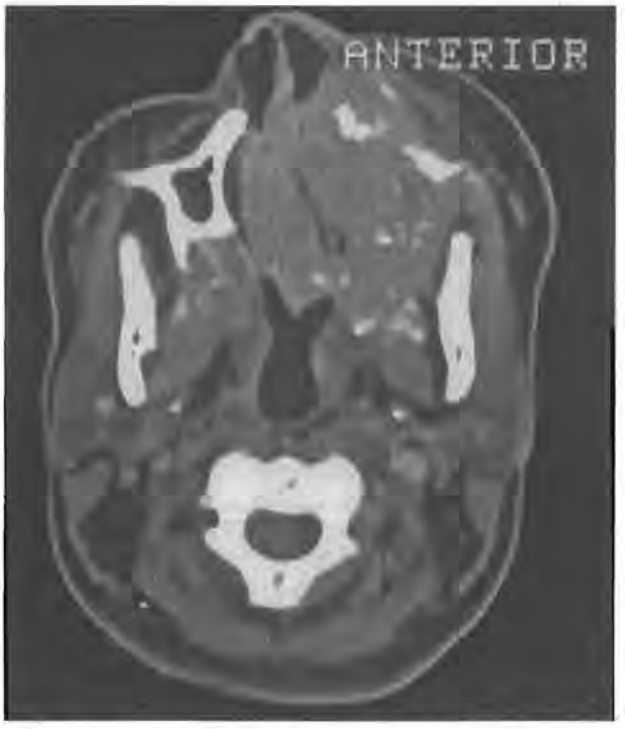


**FIGURE 4.** Computed tomography-scan of patient described in case 2 showing a tumor in the left maxilla and palate with no parotid involvement.

not otherwise specified, shows glandular and ductal differentiation but lacks the distinctive features of SDC and is basically a diagnosis of exclusion.[10] Dedifferentiated acinic cell carcinoma may present as a poorly differentiated adenocarcinoma or undifferentiated adenocarcinoma but always in association with a usual-type low-grade acinic cell carcinoma.[22] Adenoid cystic carcinoma cells usually contain little cytoplasm and have angulated, basophilic nuclei. Comedonecrosis is also not a feature of adenoid cystic carcinoma.

The diagnosis of primary intraoral SDC necessitates exclusion of direct spread from one of the major salivary glands, especially the parotid, where most SDC arise. Computed tomography scans and other imaging techniques should not show any association with the parotid or any other major salivary gland. This is especially true when SDC of the cheek is diagnosed, which is not a common site for minor salivary gland tumors.[23]

**Table 2. CLINICOPATHOGIC FEATURES OF 5 PATIENTS WITH INTRAORAL SDCs**

| Patient | Age (yr) | Gender | Site | Clinical Presentation | Tumor Size (cm) | Treatment | Follow-Up |
|---|---|---|---|---|---|---|---|
| 1 | 53 | F | Right palate and right alveolar ridge | Fungating mass; difficulty in breathing and eating; lymphadenopathy | ±14 | Biopsy | Patient refused treatment, lost to follow-up |
| 2 | 71 | M | Left palate and buccal sulcus | Pain, nerve fallout of II, III, $V_b$, and VII; lymphadenopathy | ±5 | Biopsy | Patient refused treatment, lost to follow-up |
| 3 | 57 | M | Right palate | Ulcerated tumor | ±6 | Biopsy | Patient refused treatment, lost to follow-up |
| 4 | 63 | F | Left palate | Painful, ulcerated tumor | ±7 | Maxillectomy, left neck dissection, postoperative radiotherapy | No recurrences after 10 months |
| 5 | 47 | M | Left palate | Fungating, nonulcerated tumor | ±5 | Biopsy | Patient still considering surgical treatment |

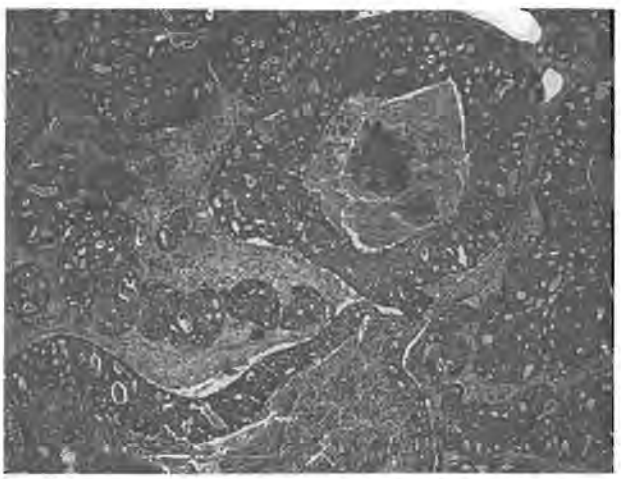

**FIGURE 5.** Photomicrograph of an SDC showing intraductal growth pattern with a cribriform appearance and comedonecrosis in the larger tumor islands (hematoxylin-eosin stain, original magnification × 25).

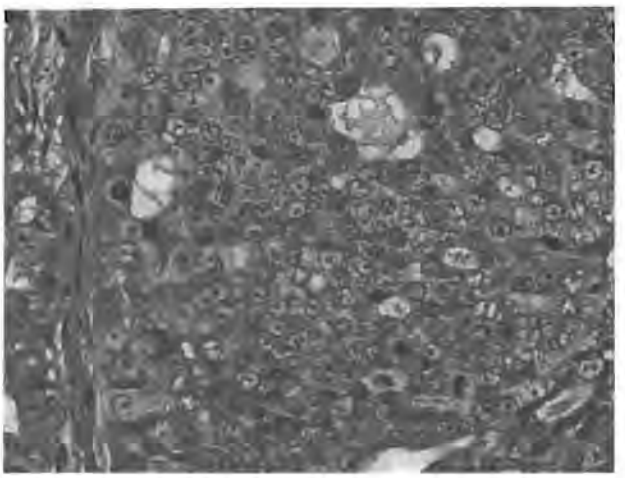

**FIGURE 7.** The tumor cells had vesicular nuclei with prominent nucleoli. Mitotic figures were prominent (hematoxylin-eosin stain, original magnification ×200).

Carcinoma ex pleomorphic adenoma is not uncommon in minor salivary glands[23] and SDC have been reported as the malignant component of these malignancies.[6,15,24] None of our cases had any histologic evidence of a preexisting pleomorphic adenoma, nor did a longstanding history suggest such an association. SDC has also been reported as a hybrid carcinoma of the minor salivary glands combined with an adenoid cystic carcinoma[25] and Warthin's tumor.[13]

SDC of the major salivary glands is an aggressive, high-grade malignancy. Comparison of the behavioral quality of SDC originating from minor salivary glands with that of the major glands is difficult, as only isolated cases of SDC have been reported. The clinical characteristics of our cases are similar to other studies reported for SDC of the major glands in that predominantly older male patients were involved. It was not possible to determine the clinical behavior of our 5 cases due to lack of follow-up information. However, the clinical appearance (large size and ulceration) of these tumors together with detectable peripheral neuropathy (ie, paresthesia, paralysis) and presence of fixed lymph nodes suggesting metastatic spread was supportive of an aggressive clinical behavior. The size of primary SDC was found to correlate with malignant potential. Hui et al[26] reported that tumors smaller than 3 cm correlate with a lower malignant potential, whereas Delgado et al[15] found a similar correlation with tumors smaller than 2 cm.

Immunohistochemical evaluation of some intermediate filaments in the tumor cells indicated that SDC is composed of predominantly ductal cells with little or no myoepithelial cell involvement. The strong expression of cytokeratin in the tumor cells is supported by the majority of studies on SDCs.[2,6,15,27] The tumor cells were negative for vimentin and smooth muscle actin, whereas positive staining with S-100 antibody was found in less than 10% of tumor cells in all 5 cases. Diffuse positive staining of S-100 was found by Brandwein et al[2] in 7 of 9 cases as well as in a single case of SDC reported in the palate.[25] Most studies, however, reported no immunoreactivity with S-100

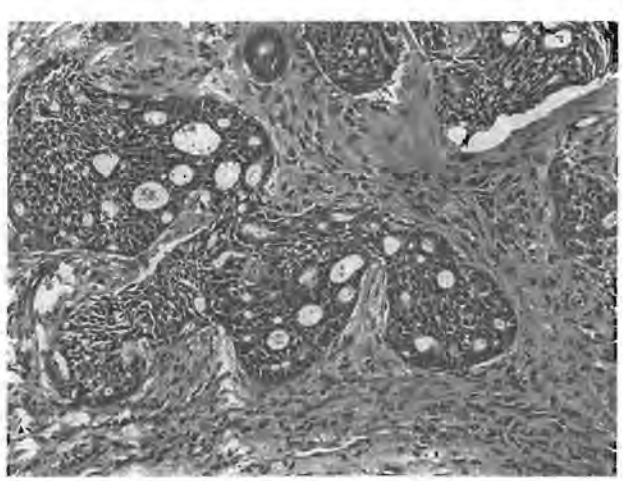

**FIGURE 6.** Infiltrating tumor islands in a cellular strama (hematoxylin-eosin stain, original magnification ×100).

**Table 3. IMMUNOHISTOCHEMICAL FINDINGS IN THE 5 INTRAORAL SDCs**

| Antibody | Patient 1 | 2 | 3 | 4 |
|---|---|---|---|---|
| Keratin | +++ | ++ | +++ | ++ |
| α-Smooth muscle actin | − | − | − | − |
| Vimentin | − | − | − | − |
| S100 | + | + | + | + |

NOTE. −, Negative; +, 1% to 9% of tumor cells; ++, 10% to 50% of tumor cells; +++, more than 50% of tumor cells.

antibody.[15,17,27] The isolated (1% to 10%) positive staining of S-100 in our 4 cases may be due to the presence of Langerhans cells between the tumor cells, although tumor cells with a ductal differentiation may express S-100 protein.[28] Ultrastructurally, SDCs are composed of cuboidal to polygonal cells with interdigitations and cells forming ductlike structures with microvilli and apical vesicles; myoepithelial cells are absent. These findings support the ductal origin of SDC.[29]

Four of the SDCs in the present study displayed DNA aneuploidy. Several studies have measured the DNA content of SDC using flow cytometry with varied results. The majority found no correlation between the ploidy status and prognosis,[6,24,30] whereas Martinez-Barba et al[27] found a positive correlation between aneuploidy and the presence of distant metastases and fatal clinical outcome. Nuclear suspensions for flow cytometry analyses were obtained from paraffin-embedded sections in all of the above-mentioned studies, but none of these studies mentioned the CV obtained for the flow cytometry measurements. The CV of DNA measurements using paraffin-embedded tissue will invariably be higher than when using fresh tissue from the same tumor. It is possible that the reported diploid cases were in fact false diploid as tumor cells with a near diploid peak, implying small deviations of their DNA content from normal diploid cells, could not be distinguished due to the relatively high CV.

SDC is a distinct tumor that can originate from minor salivary glands. The histologic features are similar to those of tumors originating in the major salivary glands. The palate appeared to be the most common intraoral site for SDC. Although clinical features were suggestive of an aggressive behavior, more reported cases are required to determine the behavior in SDCs of minor salivary glands.

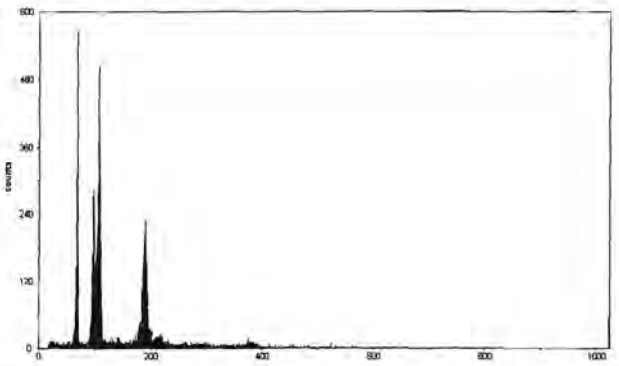

**FIGURE 8.** DNA histogram of case 1 showing the normal diploid peak at channel 100. Hypodiploid and hyperdiploid tumor cells were present.

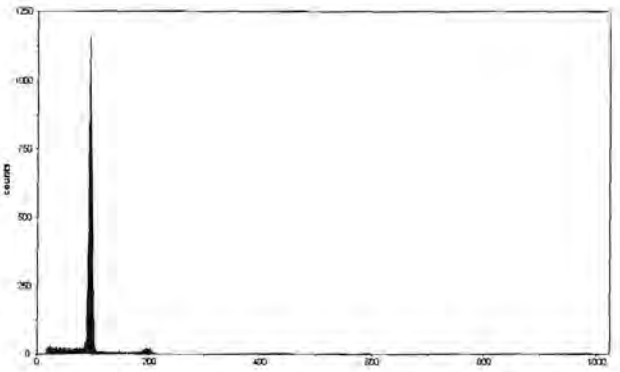

**FIGURE 9.** Diploid DNA histogram with diploid cells at channel 100 and the small peak at channel 200 representing the cells at $G_2M$ phase.

## References


1. Kleinsasser O, Klein HJ, Hubner G: [Salivary duct carcinoma. A group of salivary gland tumors analogous to mammary duct carcinoma]. Arch Klin Exp Ohr Nasen Kehlkopfheilkunde 192: 100, 1968
2. Brandwein MS, Jagirdar J, Patil J, et al: Salivary duct carcinoma (cribriform salivary carcinoma of excretory ducts). A clinicopathologic and immunohistochemical study of 12 cases. Cancer 65:2307, 1990
3. Chen KT, Hafez GR: Infiltrating salivary duct carcinoma. A clinicopathologic study of five cases. Arch Otolaryngol 107:37, 1981
4. Anderson C, Muller R, Piorkowski R, et al: Intraductal carcinoma of major salivary glands. Cancer 69:609, 1992
5. Afzelius LE, Cameron WR, Svensson C: Salivary duct carcinoma: A clinicopathologic study of 12 cases. Head Neck Surg 9:151, 1987
6. Lewis JE, McKinney BC, Weiland LH, et al: Salivary duct carcinoma. Clinicopathologic and immunohistochemical review of 26 cases. Cancer 77:223, 1996
7. Delgado R, Klimstra D, Albores-Saavedra J: Low grade salivary duct carcinoma. A distinctive variant with a low grade histology and a predominant intraductal growth pattern. Cancer 78:958, 1996
8. Tatemoto Y, Ohno A, Osaki T: Low malignant intraductal carcinoma on the hard palate: A variant of salivary duct carcinoma? Eur J Cancer Oral Oncol 32B:275, 1996
9. Barnes L, Rao U, Krause J, et al: Salivary duct carcinoma. Part I. A clinicopathologic evaluation and DNA image analysis of 13 cases with review of the literature. Oral Surg Oral Med Oral Pathol 78:64, 1994
10. Ellis GL, Auclair PL: Tumors of the salivary glands, *in* Ellis GL, Auclair PL (eds): Atlas of Tumor Pathology (3rd Series, Fascicle 17). Washington, DC, Armed Forces Institute of Pathology, 1996, p 324
11. Chen KT: Intraductal carcinoma of the minor salivary gland. J Laryngol Otol 97:189, 1983
12. Watatani K, Shirasuna K, Aikawa T, et al: Intraductal carcinoma of the tongue: Report of a case. Int J Oral Maxillofac Surg 20:175, 1991
13. Yoshimura Y, Tawara K, Yoshigi J, et al: Concomitant salivary duct carcinoma of a minor buccal salivary gland and papillary cystadenoma lymphomatosum of a cervical lymph node: Report of a case and review of the literature. J Oral Maxillofac Surg 53:448, 1995
14. Pesce C, Colacino R, Buffa P: Duct carcinoma of the minor salivary glands: A case report. J Laryngol Otol 100:611, 1986
15. Delgado R, Vuitch F, Albores-Saavedra J: Salivary duct carcinoma. Cancer 72:1503, 1993
16. Guzzo M, Di Palma S, Grandi C, et al: Salivary duct carcinoma: Clinical characteristics and treatment strategies. Head Neck 19:126, 1997

17. Suzuki H, Hashimoto K: Salivary duct carcinoma in the mandible: Report of a case with immunohistochemical studies. Br J Oral Maxillofac Surg 37:67, 1999
18. Kumar RV, Kini L, Bhargava AK, et al: Salivary duct carcinoma. J Surg Oncol 54:193, 1993
19. Seifert G, Sobin LH: Histological typing of salivary gland tumours, *in* Seifert G, Sobin LH (eds): World Health Organization International Histological Classification of Tumours (ed 2). New York, NY, Springer-Verlag, 1991
20. Heiden T, Wang N, Tribukait B: An improved Hedley method for preparation of paraffin-embedded tissues for flow cytometric analysis of ploidy and S-phase. Cytometry 12:614, 1991
21. Wick MR, Ockner DM, Mills SE, et al: Homologous carcinomas of the breasts, skin, and salivary glands. A histologic and immunohistochemical comparison of ductal mammary carcinoma, ductal sweat gland carcinoma, and salivary duct carcinoma. Am J Clin Pathol 109:75, 1998
22. Henley JD, Geary WA, Jackson CL, et al: Dedifferentiated acinic cell carcinoma of the parotid gland: A distinct rarely described entity. Hum Pathol 28:869, 1997
23. van Heerden WF, Raubenheimer EJ: Intraoral salivary gland neoplasms: A retrospective study of seventy cases in an African population. Oral Surg Oral Med Oral Pathol 71:579, 1991
24. Grenko RT, Gemryd P, Tytor M, et al: Salivary duct carcinoma. Histopathology 26:261, 1995
25. Kamio N, Tanaka Y, Mukai M, et al: A hybrid carcinoma: Adenoid cystic carcinoma and salivary duct carcinoma of the salivary gland. An immunohistochemical study. Virchows Arch 430:495, 1997
26. Hui KK, Batsakis JG, Luna MA, et al: Salivary duct adenocarcinoma: A high grade malignancy. J Laryngol Otol 100:105, 1986
27. Martinez-Barba E, Cortes-Guardiola JA, Minguela-Puras A, et al: Salivary duct carcinoma: Clinicopathological and immunohistochemical studies. J Cran Maxillofac Surg 25:328, 1997
28. Chen J-C, Gnepp DR, Bedrossian CWM: Adenoid cystic carcinoma of the salivary glands: An immunohistochemical study. Oral Surg Oral Med Oral Pathol 65:316, 1988
29. de Araujo VC, de Souza SO, Sesso A, et al: Salivary duct carcinoma: Ultrastructural and histogenetic considerations. Oral Surg Oral Med Oral Pathol 63:592, 1987
30. Felix A, El-Naggar AK, Press MF, et al: Prognostic significance of biomarkers (c-erbB-2, p53, proliferating cell nuclear antigen, and DNA content) in salivary duct carcinoma. Hum Pathol 27:561, 1996

# ODONTOMA IN AN AFRICAN ELEPHANT *(Loxodonta africana)*

E J RAUBENHEIMER*, W F P VAN HEERDEN*, M L TURNER* and L K MARÉ**

**ABSTRACT**

**The first known case of an odontoma in an African elephant *(Loxodonta africana)* is described. The tumour was fused with the coronal cementum of the sixth right mandibular molar tooth, thus preventing its eruption.**

Key words: African elephant, *Loxodonta africana*, odontoma

**Raubenheimer E.J.; van Heerden W.F.P., Turner M.L., Maré L.K. Odontoma in an African elephant *(Loxodonta africana)*. *Journal of the South African Veterinary Association* (1989) 60 No. 3, 149-150 (En.) Department of Oral Pathology and Biology, Medical University of Southern Africa, 0204 Medunsa, Republic of South Africa.**

## INTRODUCTION

The term "odontoma" by definition alone, refers to any tumour of the dental tissues[4]. Through usage, however, it has come to be employed in a much more restricted sense and refers to a tumour in which induction has resulted in the development of both enamel and dentine[1].

Odontomas represent a hamartomatous malformation rather than a neoplasm[9]. Thus, they are frequently formed in the place of a missing tooth, or if all the teeth are present, an odontoma may represent a malformation of a supernumerary tooth germ[6]. Odontomas are subdivided according to morphological features into complex and compound odontomas. The complex odontoma consists of a mass of irregularly-arranged enamel, dentine, cementum and connective tissue, bearing no morphologic similarity to teeth. In the compound odontoma the enamel, dentine and cementum are laid down in an orderly fashion so that toothlike structures can be identified. In humans the complex type of odontoma is less common than the compound type, although some lesions are a combination of both types[6].

Odontomas have been reported in various animals, including dogs[11], horses[2 3 8] and nonhuman primates[10 12]. This report describes the first known case of an odontoma occurring in an African elephant *(Loxodonta africana)*.

## CASE REPORT

A dried mandible of an African elephant, containing a 350 x 250 x 200 mm calcified tumour in the right corpus was submitted to the Department of Oral Pathology for examination and diagnosis. The tumour caused buccal and lingual expansion (Fig. 1) and was partially erupted and functional: the abraded occlusal surface showed haphazardly-arranged cementum, enamel and dentine. The tumour had an irregular surface and was not attached to the surrounding bone which showed features of osteomyelitis. A portion of a molar tooth protruded from the anterior (rostral) surface of the lesion which had a total mass of 7,8 kg (Fig. 2). The associated molar tooth was clearly visible on the sectioned surface and the cementum of the tooth was fused to the tumour, the latter of which was composed of cementum-like tissue surrounding well-formed enamel and dentinal structures (Fig. 3).

Radiographic examination of the distal corpus and ramus of the right mandible failed to exhibit additional developing teeth. The 6th molar tooth on the left was fully developed, erupted and partially abraded.

Microscopic examination of the tumour revealed cellular cementum, dental enamel and regular dentine arranged in an orderly fashion (Fig. 4).

## DISCUSSION

Odontomas develop in place of a tooth or, if the normal complement of teeth are present, from a supernumerary tooth germ. They follow the normal growth pattern of a developing tooth and even though quite large dimensions may be attained, the cellular activity of odontomas cease after completion of hard tissue formation.

Unlike humans, elephant have a total of 6 successive developing molar teeth in each quadrant which are abraded and shed throughout the life of the animal. Examination of the left mandible of our specimen showed the 6th molar to be fully developed and erupted and the age of the animal was estimated to be in excess of 35 years. As the chronology of tooth development in the specimen is unknown, the origin of the odontoma suggests two possibilities. The lesion may have originated from the germ of the 5th molar which develops and erupts between the ages of 16 and 43 years[5]. Alternatively, in the presence of a normal complement of teeth, the odontoma could have developed from a supernumerary tooth germ. The occurrence of supernumerary molar teeth in elephant however, has not been described.

The macroscopic and microscopic appearance of the lesion were consistent with a mature compound type odontoma. Enamel, dentine and cementum were arranged in an orderly fashion and the interface between these tissue types resembles that found in a normal tooth. Fusion between the cementum of the odontoma and the associated molar tooth was the result of cementum formation on the enamel surfaces in both structures. The formation of cementum on enamel is a normal phenomenon in many animals[7]. The forces of eruption of the fused molar tooth probably forced the odontoma into occlusion with the opposing maxillary molar tooth, hence the smooth abraded area on the ventral surface thereof. Partial exposure of the odontoma to the oral environment resulted in the development of an osteomyelitis in the bone surrounding the lesion.

## ACKNOWLEDGEMENT

We wish to express our appreciation to Mrs C S Begemann for secretarial services.

## REFERENCES

1. Batsakis J G 1979 Tumours of the Head and Neck 2nd edn Williams & Wilkins, Baltimore
2. Dillehay D L, Schoeb T R 1986 Complex odontoma in a horse. Veterinary Pathology 23: 341-342
3. Dubielzig R R, Beck K A, Levine S, Wilson J W 1986 Complex odontoma in a stallion. Veterinary Pathology 23: 633-635
4. Gabell D P, James W W, Payne J L 1914 The Report on Odontomes 1st edn British Dental Association, London
5. Grzimek B 1975 Grzimek's Animal Life Encyclopedia Volume 12 1st edn Van Nostrand Reinhold Company, New York
6. Lucas R B 1976 Pathology of Tumours of the Oral Tissues 3rd edn Churchill Livingstone, Edinburgh
7. Osborn J W 1981 Dental Anatomy and Embryology Volume 1 Book 2 1st edn Blackwell Scientific Publications
8. Peter C P, Myers V S, Ramsey F K 1968 Ameloblastic odontoma in a pony. American Journal of Veterinary Research 29: 1495-1498
9. Shafer W G, Hine M K, Levy B M 1983 A Textbook of Oral Pathology 4th edn W B Saunders Company, Philadelphia
10. Splitter G A, Pryor W H, Casey H W 1972

* Department of Oral Pathology and Biology, Medical University of Southern Africa, 0204 Medunsa, Republic of South Africa

** P.O. Box 553, 1240 White River

Received: February 1989 Accepted: March 1989

Ameloblastic odontoma in a Rhesus Monkey. Journal of the American Veterinary Medical Association 161: 710-713
11. Valentine B A, Lynch M J, May J C 1985 Compound odontoma in a dog. Journal of the American Veterinary Medical Association 186: 177-79
12. Ziemer E L, Turrel J M, Duhamel G, George L W 1986 Surgery and radiotherapy for management of compound odontoma in a heifer. Journal of the American Veterinary Medical Association 189: 794-796



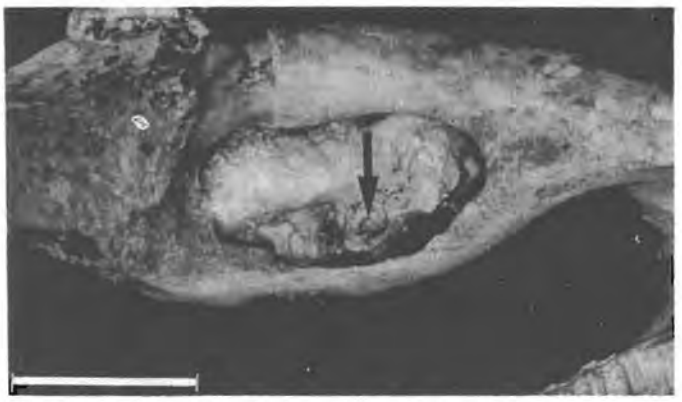

Fig. 1: Right corpus of mandible with partially erupted odontoma. (arrow) and buccal and lingual bone expansion (bar = 10 cm) Note abraded surface

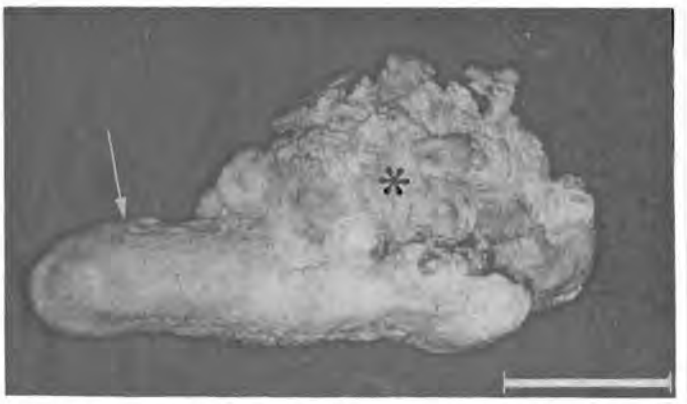

Fig. 2: Molar tooth (arrow) with attached odontoma (asterisk) (bar = 10 cm)


Fig. 3: Length section through odontoma (asterisk) and molar tooth (arrows), showing the enamel (e), dentine (d) and cementum (c) of both structures (bar = 2 cm)

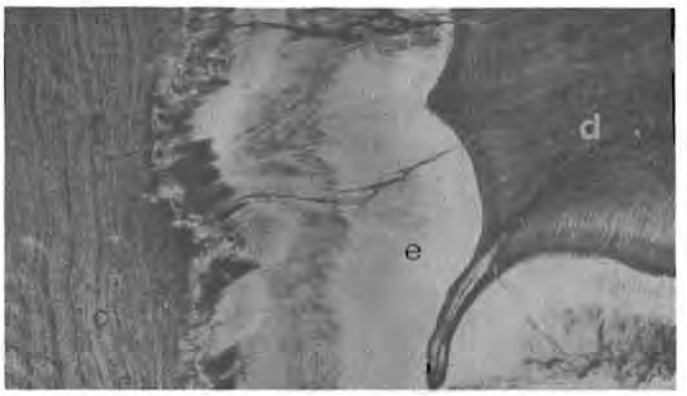


Fig. 4: Micrograph of the orderly-arranged cementum (c), enamel (e) and dentine (d) of the odontoma (Ground section, x 20)

# Giant ossifying fibroma: a clinicopathologic study of 8 tumors

**W. F. P. van Heerden[1], E. J. Raubenheimer[1], R. G. Weir[2] and J. Kreidler[1]**

*Departments of [1]Oral Pathology and Oral Biology, [2]Maxillofacial and Oral Surgery, Medical University of Southern Africa, Medunsa, Republic of South Africa*

van Heerden WFP, Raubenheimer EJ, Weir RG, Kreidler J: Giant ossifying fibroma: a clinicopathologic study of 8 tumors. J. Oral Pathol Med 1989; 18: 506–509.

Clinical, radiographic and microscopic features of 8 ossifying fibromas diagnosed in 7 patients and measuring more than 8 cm in greatest diameter, were reviewed. The tumors occured in both juvenile and middle aged patients and all lesions in women involved the maxilla. The abundance of fibrous connective tissue and resorption of mineralized deposits are indicative of altered cellular differentiation and proliferative activities in large ossifying fibromas. Focal areas of aneurysmal bone cyst formation were identified in the majority of lesions.

Key words: fibro-osseous lesion; giant ossifying fibroma; juvenile aggressive ossifying fibroma.

W. F. P. van Heerden, Department of Oral Pathology, Medical University of Southern Africa, P. O. Medunsa, 0204, Republic of South Africa.

Accepted for publication August 9, 1989.

Ossifying fibromas are generally regarded as slow growing and well circumscribed jaw tumors which contain foci of trabecular and spherical calcifications resembling bone and cementum respectively (1). They are reported to be more common in blacks, occur frequently in women and the majority of lesions involve the mandible (1, 2).

Although no convincing definition of giant ossifying fibromas are to be found in the literature, these neoplasms were reported by various authors as large tumorous fibro-cemento-osseous proliferations (3–7). Unfortunately, many of the reported cases are not documented satisfactorily. HAMNER *et al.* (1968) however, arbitrarly defined giant lesions as those exceeding 2 × 2 cm in size or involving the space occupied by two or more teeth.

There is no published series of giant ossifying fibromas in the literature. Therefore, this study was undertaken to determine the clinical and radiographic appearances and the microscopic features of the large ossifying fibromas diagnosed by the Department of Oral Pathology at the Medical University of Southern Africa (Medunsa) over a 6-yr period.

## Material and methods

All the cases diagnosed as ossifying fibroma over the last 6 yr were retrieved from the files of the Department of Oral Pathology, Medunsa, Most patients seen at the hospitals served by the department are black and of rural origin. The pathology reports were reviewed and all lesions with a longitudinal diameter of 8 cm or more as measured on the excision specimen, were included in this study. Radiographs were available in all the selected cases. Histologic evaluation was done by means of light microscopy. Three specimens (Cases 1, 3, 4) were bivalved in the longitudinal diameter, and a 5 mm slice of the entire cut surface was obtained by means of a band-saw. The slice was then radiographed and blocked into multiple squares, each of which was numbered on a scheme corresponding to the radiograph and processed for routine light microscopy. Representative histologic sections were avialable in the remaining cases.

## Results

Seven patients from a total of 30 cases of ossifying fibroma were found to have tumors larger than 8 cm in greatest diameter (Fig. 1). The age, sex, site and size of the tumors are indicated in Table 1. Case 5 presented with a mandibular and a maxillary tumor, both exceeding 8 cm. Signs and symptoms varied, the most common of which was swelling. At the age of 2 yr, Case 1 presented with a mandibular tumor 4 cm in diameter. Biopsy showed a benign fibro-osseous proliferation and due to parenteral refusal the lesion was followed over a period of 7 yr during which it became less radiopaque and tripled in diameter. The duration of the other lesions could not be determined reliably. Although the post-operative follow-up is in some cases as short as one year, none of the lesions have recurred.

All tumors involved the tooth-bearing areas of the jaws and were well demarcated with scattered foci of radiopacities (Fig. 2). Root resorption were present in three cases.

Case 1 was treated with hemimandibulectomy, Enucleation of the tumor was done in the other cases. No cortical perforation was present, only expansion in all directions. On cut surface, the tumors had a gray-white color with a gritty consistency. Cystic spaces representing aneurysmal bone cyst changes and measuring up to 1 cm in diameter could be seen focally in six tumors.

The histologic features correlated with the radiographic appearance of the corresponding area. The inconspicuous radiodense areas consisted of woven trabecular bone, although a few lamellar bony trabeculae and psammomatous calcifications were also found. Active resorption of the trabeculae with accumulation of osteoclast type giant cells were evident in all tumors (Fig. 3). Vascularity was more prominent in the areas of resorption and the fibrous component adjacent to these areas were cellular.

The radiolucent zones consisted

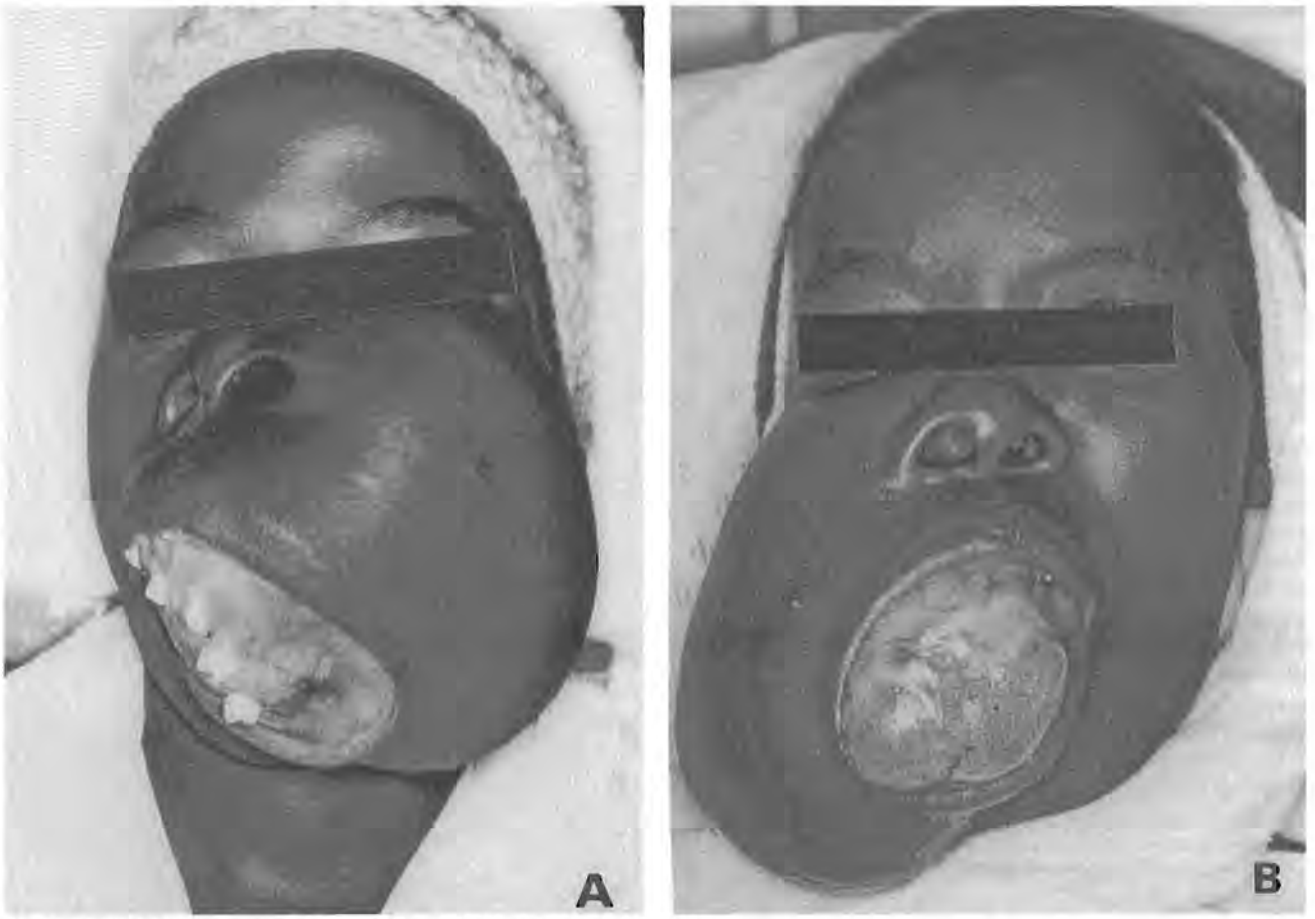


Fig. 1. A, clinical appearance of Case 3. B, clinical appearance of Case 4.

mainly of fibrous tissue. The stroma varied from mature collagen to tissue with a cellular storiform pattern (Fig. 4). Small amounts of mineralized tissue, mainly of a psammomatous cementum-like nature were present in the fibrous tissue. The aneurysmal bone cyst changes were found in areas where the fibrous tissue had a loose, edematous structure.

## Discussion

The sizes of the eight tumors described surpass that of all giant ossifying fibromas reported in the literature. HAMNER *et al.* (3), defining 'giant' lesions as those exceeding 2 × 2 cm in diameter, found 17% of their cases of cementoossifying fibromas to have reached these dimensions. Seven (or 23%) of our collection of ossifying fibromas had a diameter of more than 8 cm. If the criteria of *Hamner et al.* (3) had to be applied to our collection of ossifying fibromas, almost all of the 30 cases diagnosed in our department over the last 6 yr will be regarded as 'giant'. The large dimensions of our tumors is related to the rural character of the populations served where proper diagnosis and treatment is often delayed through tribal customs.

Table 1. Clinical data of the seven patients.

| Case No | Age | Gender | Site | Size |
|---|---|---|---|---|
| 1 | 9 | M | Mandible | 12 cm |
| 2 | 7 | W | Maxilla | 8 cm |
| 3 | 13 | W | Maxilla | 13 cm |
| 4 | 46 | W | Maxilla | 15 cm |
| 5 | 40 | M | Mandible | 8 cm |
| | | | Maxilla | 10 cm |
| 6 | 49 | M | Mandible | 10 cm |
| 7 | 57 | W | Maxilla | 10 cm |

The age range of our patients was 7–57 yr with an age peak in the first and fifth decades, a distribution corresponding to that generally reported for ossifying fibromas (1). The occurrence of large ossifying fibromas in young children is of particular interest as it is believed that these tumors require many years of growth to attain large dimensions (2). One of our cases, diagnosed at 2 yr of age, showed an increase of 8 cm in diameter over a follow-up period of 7 yr. As far as we can ascertain, this represents the youngest age at which an ossifying fibroma had been diagnosed. Five of the eight tumors and all lesions in women involved the maxilla. This is in contrast to the generally held view that ossifying fibromas occur more frequently in the mandible (2).

Radiographically, the large ossifying fibromas in our study contain relatively less mineralized tissue than smaller lesions. This finding is substantiated by the microscopic appearance of the giant lesions where the balance of cellular activity favor fibrous tissue formation and bone resorption at the expense of new bone formation. Although the majority of our lesions showed foci of aneurysmal bone cyst formation, STRUTHERS & SHEAR (8) found this change to occur in only 4% of their ossifying fibromas and *Eversole et al.* (9) noted aneurysmal bone cyst features in three of their 64 cases. The high prevalence of aneurysmal bone cyst formation in our lesions is probably due to the prominent fibrous com-

ponent which contains more loose edematous areas than is found in smaller ossifying fibromas. This feature is not responsible for the giant dimensions, as the foci of aneurysmal bone cyst change are limited and the cystic spaces are of relative small size.

HAMNER *et al.* (3) stated that ossifying fibromas containing cementum are larger and more aggressive than pure ossifying or cementifying lesions. HALL *et al.* (10) consider mixed cementifying and ossifying fibromas as a potentially aggresive variant of ossifying fibroma. WALDRON & GIANSANTI (11) however stated that a separation into cementifying and ossifying types is artificial as they could find no difference in the behaviour of tumors with these histologic designations. Cementum-like as well as osseous deposits were present in all tumors in our series and we believe that if representative tissues of ossifying fibromas are taken for microscopic examination, most tumors will be found to be of a mixed nature.

Our study furthermore suggests that ossifying fibromas with a gigantiform growth potential are characterized by the appearance of large fibrous areas which are represented radiographically by less radiodense areas. This is in contrast to the normal progression of these lesions where the islands of mineralizations are reported to increase in size and coalesce resulting in a more radiopaque lesion (2).

The microscopic appearance of the giant lesions does not resemble that of juvenile aggressive ossifying fibromas. The criteria defined by WALDRON (12) for the diagnosis of juvenile aggressive ossifying fibroma include a cellular vascular stroma with varying amounts of giant cells and little collagen production. Osteoid lined by osteoblasts are usually present. These lesions furthermore appear most often in young patients – predominantly younger than 20 yr and almost always below 40 yr of age (13). None of the lesions in the three young patients in our series can be classified as the aggressive variant because of the prominent fibrous tissue and collagen component and the scarcity of osteoid formation. This however does not exclude the possibility that at some earlier stage our lesions may have had the microscopic features of juvenile aggressive ossifying fibromas.

This study suggests that the shift in cellular activity from osteoblastic in small ossifying fibromas to fibroblastic in the giant lesions represents a phenomenon associated with gigantiform tumor enlargement.

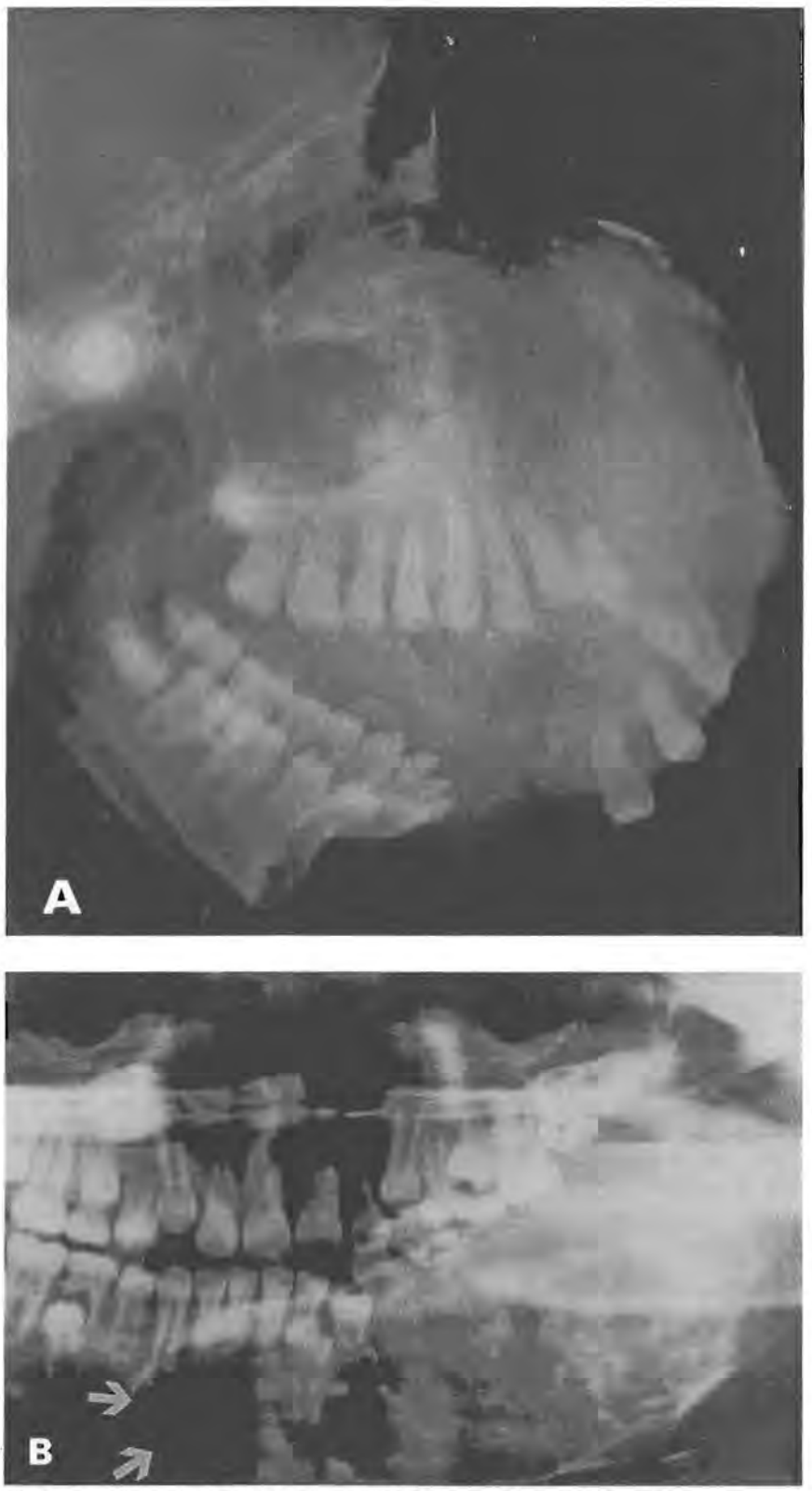


Fig. 2. A, radiograph of Case 3 shows a well demarcated lesion with smokescreen appearance and irregular radiolucent areas. B, Prominent lytic areas are present in Case 1 (arrows).

*Acknowledgments* – We wish to thank Mrs. C. S. BEGEMANN for secretarial services and Miss L. I. HOPE, Audio Visual Department of the Medical University of Southern Africa for photographic services.

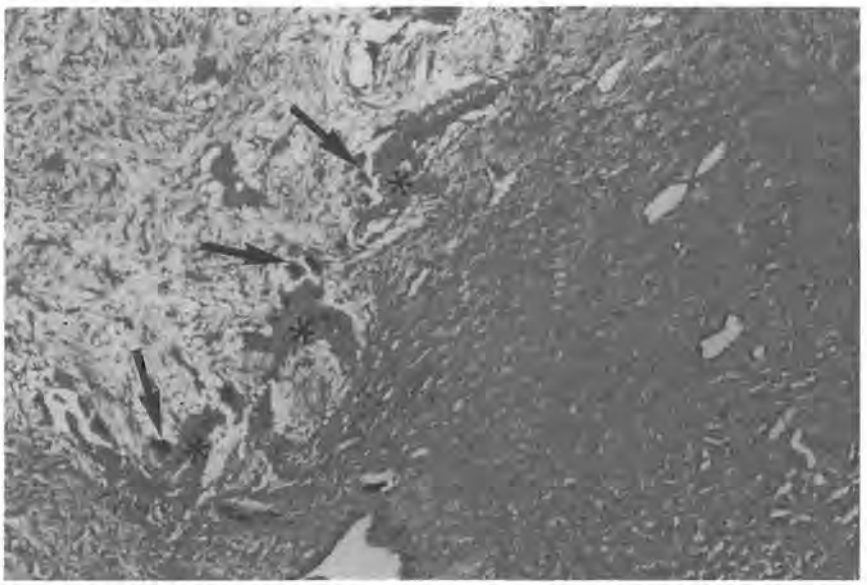

Fig. 3. Interface between dense fibrous zone and area of bone resorption. Note bony trabeculae (asterisks) and osteoclasts (arrows) in loose fibrous tissue. H&E, × 40.

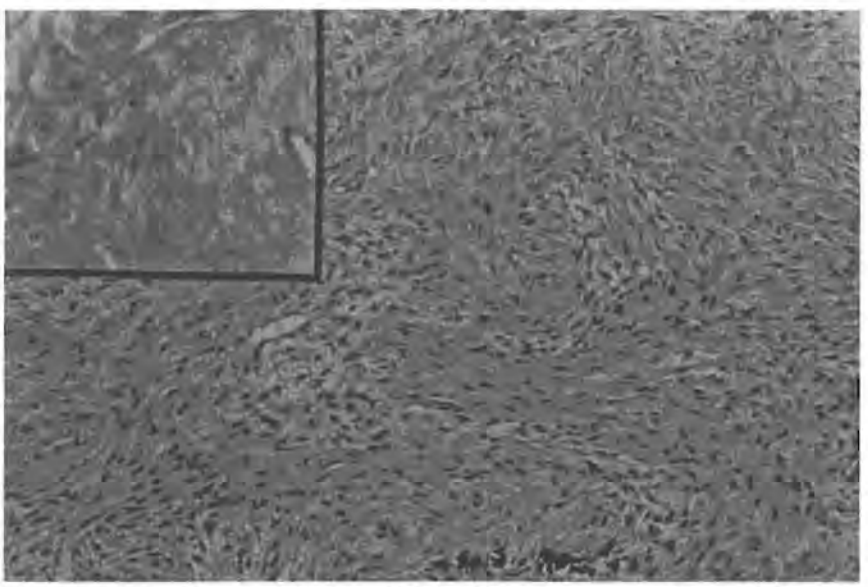

Fig. 4. Cellular storiform growth pattern. H&E, × 100. Inset: mature collagen. H&E, × 150.

## References


1. Lucas RB. *Pathology of tumours of the oral tissues*. 4th ed. Edinburgh: Livingstone, 1984, 402–5.
2. Shafer WG, Hine MK, Levy BM. *A textbook of oral pathology*. 4th ed. Philadelphia: W. B. Saunders Co, 1983; 142–4.
3. Hamner JE, Scofield HH, Cornyn J. Benign fibro-osseous jaw lesions of periodontal membrane origin: an analysis of 249 cases. *Cancer* 1968; **22**: 861–8.
4. Carlisle JE, Hamner WB. Giant central ossifying fibroma of the mandible: report of case. *J Oral Surg* 1979; **37**: 206–11.
5. Vuolo SJ, Berg H, Pierri LK, Jandinski J, Yamane GM, Chaudry AP. Giant ossifying fibroma of the maxillary sinus. *J Oral Med* 1986; **41**: 152–5.
6. Anand SV, Davey WW, Cohen B. Tumours of the jaw in West Africa: a review of 256 patients. *Br J Surg* 1967; **54**: 901–17.
7. Kennet S, Curran JB. Giant cemento-ossifying fibroma: report of a case. *J. Oral Surg* 1972; **30**: 513–6.
8. Struthers PJ, Shear M. Aneurismal bone cyst of the jaws (II). Pathogenesis. *Int J Oral Surg* 1984; **13**: 92–100.
9. Eversole LR, Leider AS, Nelson K. Ossifying fibroma: a clinicopathologic study of sixty-four cases. *Oral Surg* 1985; **60**: 505–11.
10. Hall EH, Naylor GD, Mohr RW, Warnock GR. Early aggressive cemento-ossifying fibroma: a diagnostic and treatment dilemma. *Oral Surg* 1987; **63**: 132–6.
11. Waldron CA, Giansant JS. Benign fibro-osseous lesions of the jaws: a clinical-radiologic-histologic review of sixty-five cases. *Oral Surg* 1973; **35**: 340–50.
12. Waldron CA. Fibro-osseous lesions of the jaws. *J Oral Maxillofac Surg* 1985; **43**: 249–62.
13. Walter JM, Terry BC, Small EW, Matteson SR, Howell RM. Aggressive ossifying fibroma of the maxilla. *J Oral Surg* 1979; **37**: 276–86.

# Adenomatoid odontogenic tumour: a report of two large lesions

**E.J. Raubenheimer, J.E. Seeliger*, W.F.P. van Heerden and A.F. Dreyer***

Medical University of Southern Africa, Faculty of Dentistry, Medunsa and *University of Pretoria, Faculty of Dentistry, Pretoria, Republic of South Africa

Received 30 January 1990 and in final form 30 May 1990

Adenomatoid odontogenic tumours with a diameter of more than 4 cm are uncommon. Two cases, both measuring in excess of 7 cm, are described and the differential diagnosis discussed. The progressive growth and cortical perforation in these two cases support the view that it is a benign neoplasm rather than a hamartoma.

*Keywords: Odontogenic tumours; maxilla*

The adenomatoid odontogenic tumour (AOT) is a rare, benign odontogenic tumour of which approximately 170 verifiable cases have been reported in the English literature. It occurs most often in young females and commonly involves the anterior maxilla. Although many AOTs are detected during routine radiographic examination, patients may present with a gradually enlarging, painless swelling which can lead to facial asymmetry. Radiographs generally show a clearly demarcated, radiolucent lesion surrounding an unerupted tooth, usually a maxillary canine[1,2]. Radiopaque foci frequently occur in the tumour. The size of an AOT varies between 1.5 and 3.0 cm but some as large as 9.0 cm have been reported[3]. It is usually diagnosed radiographically as a follicular, lateral periodontal[1], residual[4] or 'globulo-maxillary' cyst[2,5]. If calcification is present, the differential diagnosis should also include calcifying odontogenic cyst, central ossifying fibroma, calcifying epithelial odontogenic tumour and ameloblastic fibro-odontome. Microscopically, AOTs are characterized by a well-defined fibrous capsule surrounding sheets, strands and nodular masses of epithelial cells which form tube-like structures and rosettes[1]. The purpose of this paper is to report two large AOTs with diameters of more than 7 cm.

## Case reports

### *Case 1*

A 12-year-old black female presented complaining of a maxillary swelling obstructing her nose; the duration of the swelling was unknown. On examination, a maxillary tumour, extending from the lower border of the right eye and crossing the midline of the face, was present. The size of the lesion interfered with lip closure. The nose was deviated, the nasal passage obstructed and on palpation the bony cortex was perforated, resulting in fluctuation. The skin overlying the lesion had three parallel scars (each 4 cm long). Intra-oral examination showed mobile and displaced maxillary permanent incisors and a primary canine, and bulging of the right palatal shelf and buccal plate (Figure 1). Radiographs revealed a well-circumscribed unilocular radiolucency containing the crown of the unerupted permanent canine (Figures 2, 3). A clinical diagnosis of follicular cyst was made and the lesion was enucleated through an intra-oral approach. The specimen submitted for pathological examination consisted of a cystic lesion measuring $12 \times 10 \times 10$ cm which contained a normal maxillary canine. The lining of the cyst contained multiple nodules measuring up to 5 mm in diameter. Microscopic examination showed an epithelial lining containing nodular masses of odontogenic epithelial cells forming rosettes and pseudoglandular spaces. A diagnoses of AOT was made.

### *Case 2*

A 9-year-old black female presented with a complaint of swelling in the right maxilla obstructing her nose. The lesion was painless and had been present for 3 years. On examination, there was a $9 \times 8$ cm swelling in the right maxilla, which had elevated the right ala (Figure 4). The maxillary permanent central incisors,

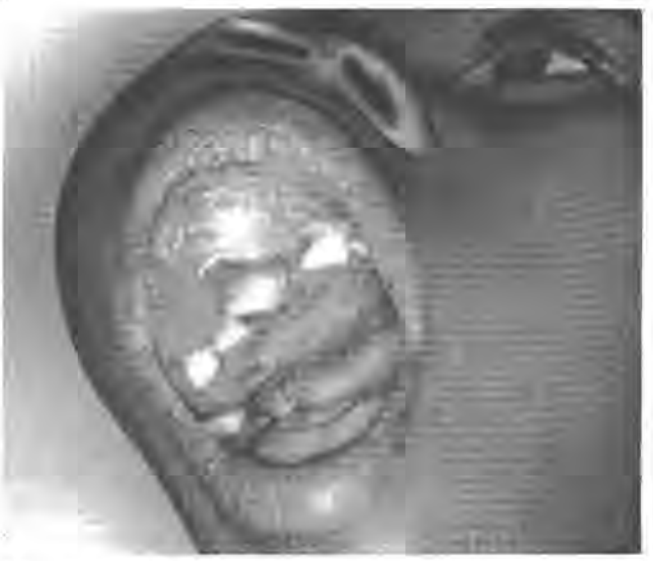

**Figure 1** Case 1. Intraoral view of the tumour


0250–832×91/010043–03

**Figure 2** Case 1. Lateral cephalometric radiograph. Note the displacement of the permanent maxillary canine (arrow)

primary canines and molars were erupted and the palatal shelf and buccal plate were expanded by a firm swelling. Radiographically, there was a well-circumscribed radiolucent lesion, surrounding the crown and neck of an unerupted maxillary canine; the developing maxillary premolars were dilacerated and the second incisor displaced and impacted (Figure 5). In the absence of calcification in the wall of the lesion, a clinical diagnosis of a follicular cyst was made. The lesion was enucleated and an opened cyst, 8 cm in diameter, surrounding the crown and neck of an unerupted maxillary canine and containing mural granules, was submitted for pathological examination. Microscopically, the cyst wall consisted of abundant connective tissue lined by thin and inactive odontogenic epithelium which surrounded nodular masses of epithelial cells exhibiting rosettes and pseudoglandular structures. A diagnosis of AOT was made.

## Discussion

As far as can be ascertained, Case 1 represents the largest AOT reported in the English literature.

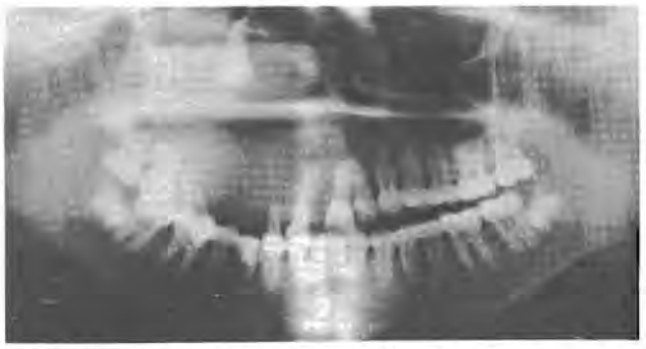

**Figure 3** Case 1. Panoramic radiograph. Note the well circumscribed, expansile lesion in the right maxilla with displacement of the roots of involved teeth as well as the canine

**Figure 4** Case 2. Frontal photograph

Another large tumour had a diameter of 9 cm and formed part of a series of 13 cases occurring in Nigerian patients[3]. The large size of our two cases could be related to their more rapid growth in younger patients, certainly, the average age is higher in previous reports. However, the size may also result from a delay in seeking proper dental treatment. This view is supported by the presence of linear scars on the skin overlying the tumour in Case 1, an indication of regular visits to tribal medicine men before seeking hospital treatment.

The histogenesis of the AOT is unknown but the possibilities range from the dental lamina to reduced enamel epithelium[6–8]. One investigator[9] suggested that the epithelial rests of Malassez at the apex of deciduous teeth is the progenitor tissue. His argument is based, in

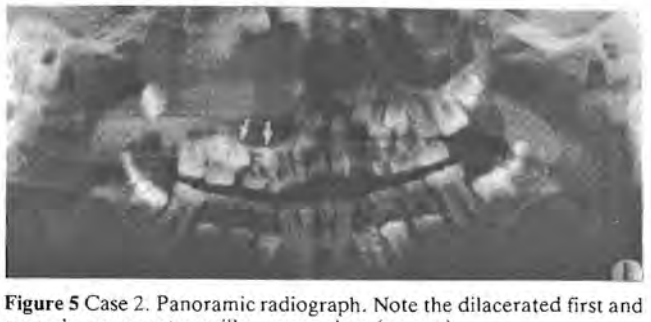

**Figure 5** Case 2. Panoramic radiograph. Note the dilacerated first and second permanent maxillary premolars (arrows)

part, on the fact that AOTs have never occurred in association with impacted deciduous teeth nor in areas not preceded by deciduous teeth. The existence of those lesions not associated with an unerupted tooth and therefore not arising from the reduced enamel epithelium, may be explained on this basis.

Courtney and Kerr[10] from a study of 20 AOTs, as well as others[11–13], believe the lesion to be an hamartoma rather than a benign neoplasm. However, hamartomas have a limited growth potential and progressively differentiate into more mature tissue with ageing[14]. Our cases do not support a limited growth potential as postulated by Saito *et al.*[4] nor did they exhibit maturation into more differentiated dental tissues. We therefore believe the lesion to be a benign neoplasm. The growth potential of AOTs is supported by Ajagbe *et al.* and others[15, 16] and earlier detection is likely to be the reason for the small size of most cases reported in the literature.

Radiographically both of our cases resembled a follicular cyst, the most common lesion to consider in the differential diagnosis of AOT. The well demarcated radiolucency associated with an AOT is reported to extend more apically on the root of the associated unerupted tooth than in the case of a follicular cyst[17]. Another feature that could be helpful in distinguishing between these two lesions is the virtual absence of root resorption in AOTs[18]. The dilaceration of the permanent premolars in Case 2 is most likely the result of pressure exerted by the enlarging tumour on the roots of the developing teeth.

Nasal obstruction is a common complaint in patients with maxillary AOTs measuring 5 cm or more in diameter[3, 19]. Furthermore, erosion of bone has been reported in a large AOT and actual perforation has led to it being described as a 'fluctuant mass'[19]. Our Case 1 also exhibited this feature but we do not agree with Poulson and Greer[20] that its presence warrants the exclusion of an AOT and the consideration of a more aggressive tumour in the differential diagnosis.

## Acknowledgement

We would like to express our gratitude to Mrs C.S. Begemann for typing the manuscript.

## References

1. Lucas RB. *Pathology of Tumours of the Oral Tissues*. 4th edn. London: Churchill Livingstone, 1984: 61–6.
2. Kuntz AA, Reichart PA. Adenomatoid odontogenic tumor mimicking a gobulo-maxillary cyst. *Int J Oral Maxillofac Surg* 1986; **15:** 632–6.
3. Ajagbe HA, Daramola JO, Junaid TA, Ajagbe OA. Adenomatoid odontogenic tumor in a black African population. *J Oral Maxillofac Surg* 1985; **43:** 683–7.
4. Saito I, Ide F, Umemura S. An unusual adenomatoid odontogenic tumor presenting as a residual cyst. *J Oral Maxillofac Surg* 1983; **41:** 534–5.
5. Glickman R, Super S, Sunderaj M, Jain R, Chaudhry A. An adenomatoid odontogenic tumour simulating globulo-maxillary cyst. *J Oral Med* 1983; **38:** 26–9.
6. Shear M. The histogenesis of the 'Tumour of enamel organ epithelium'. *Br Dent J* 1962; **112:** 494–8.
7. Bhaskar SN. Adenoameloblastoma: its histogenesis and a report of 15 new cases. *J Oral Surg* 1964; **22:** 218–26.
8. Spouge JD. The adenoameloblastoma. *Oral Surg Oral Med Oral Pathol* 1967; **23:** 472–82.
9. Chambers KS. The adenoameloblastoma. *Br J Oral Surg* 1973; **10:** 310–20.
10. Courtney RM, Kerr DA. The odontogenic adenomatoid tumor. A comprehensive study of twenty new cases. *Oral Surg Oral Med Oral Pathol* 1975; **39:** 424–35.
11. Abrams AM, Melrose RJ, Howell FV. Adenoameloblastoma. A clinical pathologic study of ten new cases. *Cancer* 1968; **22:** 175–85.
12. Milobsky L, Miller GM. Adenomatoid odontogenic tumor (adenoameloblastoma). Report of a case. *Oral Surg Oral Med Oral Pathol* 1975; **40:** 681–5.
13. Khan MY, Kwee H, Schneider LC, Saber I. Adenomatoid odontogenic tumor resembling a globulo maxillary cyst: light and electron microscopic studies. *J Oral Surg* 1977; **35:** 739–42.
14. Anderson WAD, Scotti TM. *Synopsis of Pathology*, 10th edn. St Louis: CV Mosby, 1980: 241.
15. Hacihanefio-glu U. The adenomatoid odontogenic tumor. *Oral Surg Oral Med Oral Pathol* 1974; **38:** 65–73.
16. Tsaknis PJ, Carpenter WM, Shade NI. Odontogenic adenomatoid tumor. Report of a case and review of the literature. *J Oral Surg* 1977; **35:** 146–9.
17. Giansanti JS, Someren A, Waldron CA. Odontogenic adenomatoid tumor (adenoameloblastoma). Survey of 3 cases. *Oral Surg Oral Med Oral Pathol* 1970; **30:** 69–86.
18. Shear M. *Cysts of the Oral Regions*. Bristol: John Wright and Sons 1976: 63.
19. Webb DJ, Colman MF, Moore L, Correll RW. Expansile radiolucent mass in the maxilla. *J Am Dent Assoc* 1985; **111:** 474–6.
20. Poulson TC, Greer RO. Adenomatoid odontogenic tumor: clinicopathologic and ultrastructural concepts. *J Oral Maxillofac Surg* 1983; **41:** 818–24.

Address: Professor E.J. Raubenheimer, Department of Oral Pathology, Medical University of Southern Africa, PO Medunsa, 0204, Republic of South Africa.

Journal of the Dental Association of South Africa **45**, 467-471

# Amelogenesis imperfecta: multiple impactions associated with odontogenic fibromas (WHO) type

WFP van Heerden*, EJ Raubenheimer*, AF Dreyer† and AML Benn‡

*Department of Oral Pathology and Oral Biology, †Department of Maxillofacial and Oral Surgery, ‡Department of Conservative Dentistry, Medical University of Southern Africa, PO Medunsa, 0204, South Africa.

*Keywords: Amelogenesis imperfecta; fibroma; odontogenic fibroma*

**SUMMARY**

*Three types of amelogenesis imperfecta (AI) are recognised, namely hypoplastic, hypomature and hypocalcified varieties. We report on two cases of hypoplastic AI, the type which occurs most frequently. Both patients presented with multiple impacted permanent teeth. Odontogenic fibromas of the WHO type were found to be associated with the crowns of all the impacted teeth and are considered to have prevented normal eruption. Dentinal dysplasia found only in the furcation area of the multirooted impacted teeth was evident. The macroscopic, microscopic and radiological appearance of the affected teeth, pericoronal lesions and interradicular dentinal dysplasia are described, and the most likely origins of the odontogenic fibromas and calcifications observed, are discussed.*

**OPSOMMING**

*Drie tipes amelogenese imperfekta (AI) word aangetref namlik hipoplasties, hipovolwasse en hipogekalsifiseerde tipes. Hierdie artikel beskryf twee gevalle van hipoplastiese AI, die mees algemene tipe. Altwee pasiënte het veelvuldige geïmpakteerde tande gehad. Odontogene fibrome, WGO tipe, is aangrensend tot die geïmpakteerde tandkrone gevind en het moontlik erupsie vertraag. Dentinale displasie is slegs in die furkasiegebied van die geïmpakteerde molaartande gevind. Die makroskopiese, mikroskopiese en radiologiese beelde van die betrokke tande, perikoronale letsels en dentinale displasie word beskryf en die moontlike oorsprong van die odontogene fibrome en kalsifikasies wat waargeneem is, word bespreek.*

## INTRODUCTION

Amelogenesis imperfecta (AI) is an inherited, congenital defect that primarily affects enamel formation and which is not accompanied by morphologic or metabolic defects in other body systems except abnormal tooth form or eruption (Witkop, 1989). The recent classification of Witkop (1989) describes different types of AI according to the predominant clinical and histological characteristics as well as the mode of Mendelian inheritance. The enamel abnormality can be either hypoplastic, hypomature, hypocalcified or a combination of these with autosomal dominant, autosomal recessive, sex-linked dominant or sex-linked recessive modes of inheritance (Table I). The hypoplastic type is characterised by thin, hard enamel of normal radiographic translucency. This type is the result of insufficient matrix formation with normal mineralisation. Hypomature enamel is a result of a defect in the formation of crystalline apatite in various parts of the enamel rods and sheaths. The enamel is of normal thickness with a mottled appearance, is slightly softer than normal and chips off the dentine. Radiographically it has approximately the same density as dentine. Hypocalcified enamel develops to a normal thickness but is lost soon after eruption. It is the result of defective mineralisation of the formed matrix and radiographically the enamel is less radiodense than dentine (Witkop and Sauk, 1976).

The combined prevalence of all types of AI has been reported to be 1:14 000 in the United States (Witkop and Sauk, 1976); 1:8 000 in Israel (Chosack *et al*, 1979) and 1:4 000 in Sweden (Sundell and Valentin, 1986). The most common type of AI is the hypoplastic variety with a reported prevalence that varies from 1:8 800 (Chosack *et al*, 1979) to 1:6 700 (Sundell and Valentin, 1986). Impacted teeth are often associated with the smooth hypoplastic type and, less frequently, with the rough hypoplastic type (Witkop and Sauk, 1976).

The purpose of this paper is to report two cases of rough hypoplastic amelogenesis imperfecta associated with impacted teeth and pericoronal odontogenic fibromas of the WHO type.

## CASE 1

A 14-year-old girl presented for treatment with the main complaint of delayed eruption of her teeth. The child had no systemic abnormalities. Intraoral examination revealed thin, hard enamel on all the erupted teeth. The enamel surface varied from smooth to rough and had a yellow-white colour. The teeth failed to meet at the interproximal contact points. The patient had 5 sisters of whom 3 had AI with the same enamel appearance. The mother had normal teeth but the father was edentulous. His teeth had been extracted at a young age. This mode of inheritance was suggestive of an autosomal dominant inheritance pattern.

Radiographic examination revealed the normal number of teeth, of which 13 were unerupted, including the 4 developing third molars. Dilated follicles or cyst-like lesions were apparent as well demarcated radiolucencies with sclerotic margins associated with the crowns of the unerupted teeth (Fig 1). No well developed enamel could be seen. The roots of the molar teeth showed gross disfigurement with structures suggestive of pulpal calcifications.

*Table 1:* **Classification of amelogenesis imperfecta according to Witkop (1989)**

| | |
|---|---|
| Type I | – Hypoplastic |
| IA | – hypoplastic, pitted autosomal dominant |
| IB | – hypoplastic, local autosomal dominant |
| IC | – hypoplastic, local autosomal recessive |
| ID | – hypoplastic, smooth autosomal dominant |
| IE | – hypoplastic, smooth X-linked dominant |
| IF | – hypoplastic, rough autosomal dominant |
| IG | – enamel agenesis, autosomal recessive |
| Type II | – Hypomaturation |
| IIA | – hypomaturation, pigmented autosomal recessive |
| IIB | – hypomaturation, X-linked recessive |
| IID | – snow capped teeth, autosomal dominant |
| Type III | – Hypocalcified |
| IIIA | – autosomal dominant |
| IIIB | – autosomal recessive |
| Type IV | – Hypomaturation-hypoplastic with taurodontism |
| IVA | – Hypomaturation-hypoplastic with taurodontism, autosomal dominant |
| IVB | – Hypoplastic-hypomaturation with taurodontism, autosomal dominant |

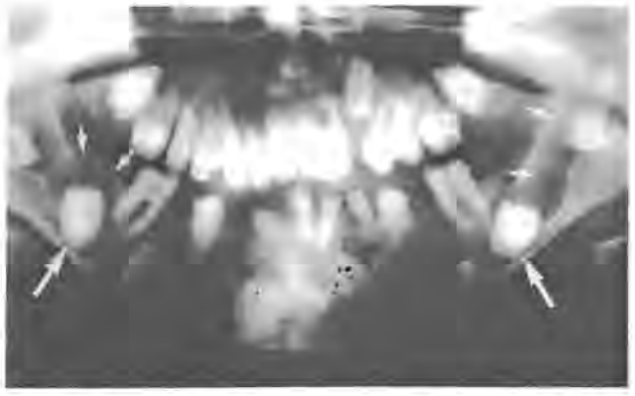

*Fig. 1:* **Case 1. Pantomograph showing unerupted teeth with pericoronal radiolucencies (small arrows). No evidence of enamel is present and the unerupted molar teeth show gross root disfigurement (large arrows).**

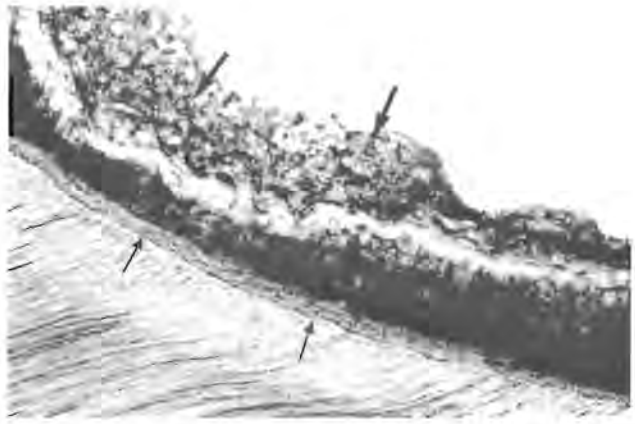

*Fig. 2:* **Ground section of an unerupted molar tooth with irregular enamel and globular calcifications (bold arrows). Note the straight dentinoenamel junction (fine arrows) × 100.**

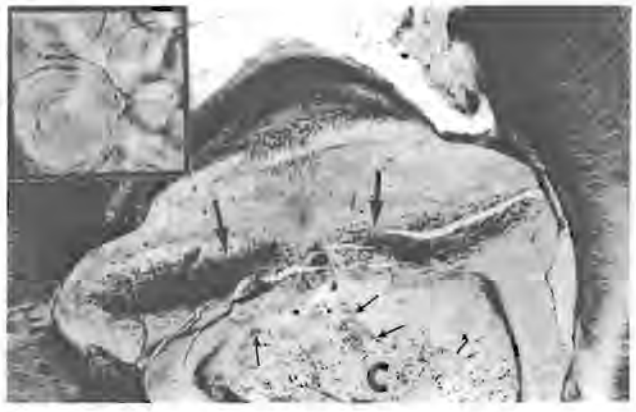

*Fig. 3:* **Interradicular dentine dysplasia (bold arrows) associated with hypercementosis (c) and globular calcifications (fine arrows). Ground section, unstained × 10. Inset: Calcified globules with an onion-like appearance. Ground section, unstained × 200.**

All the unerupted teeth with the associated pericoronal tissue were removed surgically under general anaesthesia. The bone was found to be normal in texture and no excessive haemorrhage was encountered. Post-operative healing was uneventful.

Light microscopy of ground sections of the molar teeth showed irregular hypoplastic enamel with globular calcifications. The dentinoenamel junction lacked the normal scalloping (Fig 2). The dentine of the crowns and roots showed no abnormalities. An irregular mass of dentine was present in the interradicular area at the level of root bifurcation in all the molar teeth. Hypercementosis, consisting of cellular cementum extending into the interradicular space of the roots, was present.

Calcified globules with an onion-like appearance were present in the cementum in close association with the irregular dentine (Fig 3). False pulpal stones, not associated with the dentinal wall, were observed.

Scanning electron microscopy (SEM) of the outer enamel surface showed irregular globular and linear masses in association with depressions (Fig 4). SEM of the fractured surface confirmed the straight dentinoenamel junction and showed normal dentine. The enamel had voids and loss of structure with a resulting honeycomb appearance throughout its full thickness (Fig 5).

The pericoronal tissue consisted of fibrous tissue that varied in cellularity. No evidence of a cystic lining was found. Odontogenic epithelial cell rests were scattered in the connective tissue. These epithelial cells appeared to be inactive with no peripheral pallisading of ameloblast like cells. Some of the epithelial cells had a vacuolated appearance. Two types of calcifications were present in the fibrous tissue. The most common type consisted of psammomatous lamellar bodies with an eosinophilic centre and a more basophilic peripheral zone. The second type consisted of eosinophilic material with a fibrillar matrix and peripheral tufts resembling Sharpey's fibres. Both types were closely associated with the odontogenic epithelial cell rests (Fig 6). The lesions were considered to be odontogenic fibromas, WHO type.

## CASE 2

A 26-year-old black female reported to the hospital, requesting that she be fitted with full upper and lower dentures. The patient was clinically edentulous and had marked vertical enlargement of the entire alveolar ridge in all four quadrants. No abnormalities were found on systemic examination.

Radiological examination confirmed the enlargement of all four quadrants with both maxillary tuberosities markedly overdeveloped. There was evidence of recent tooth extractions in the mandible in the form of healing sockets and 13

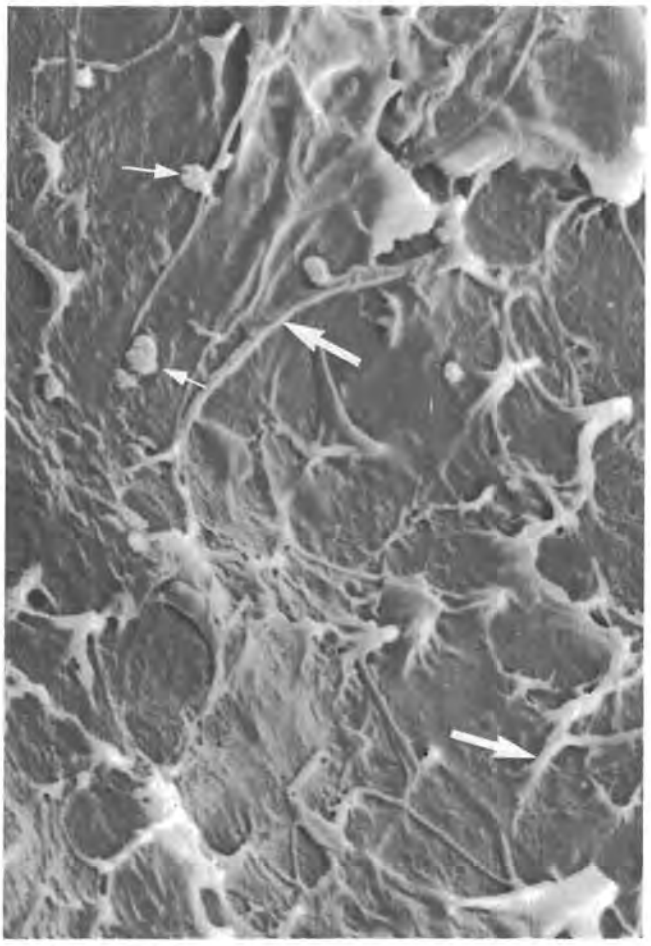

*Fig. 4:* **The outer enamel surface showing globular (fine arrows) and linear (bold arrows) masses associated with depressions × 2 000.**

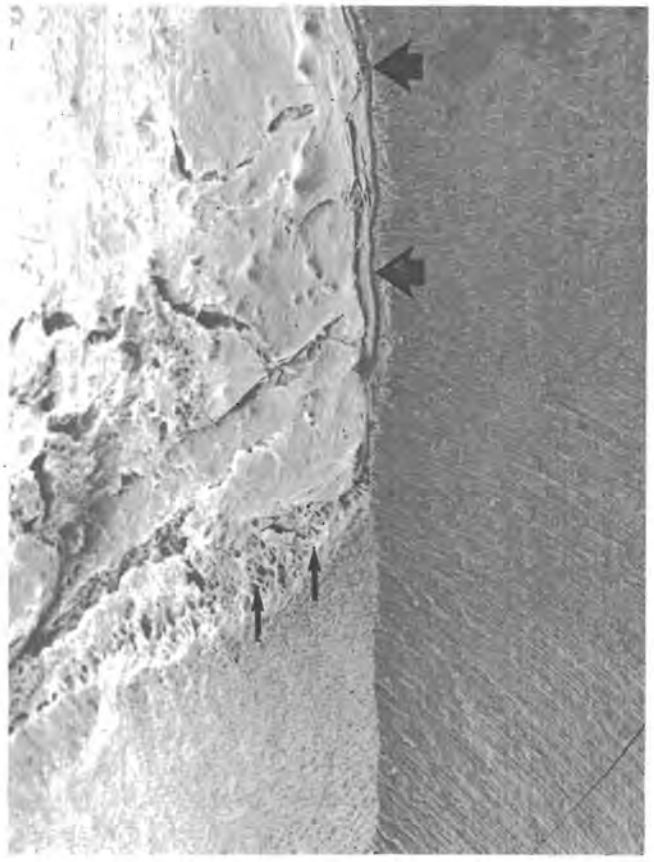

*Fig. 5:* **SEM of the fractured surface confirmed the straight dentinoenamel junction (bold arrows) and a honeycomb appearance in the enamel (fine arrows) × 72.**

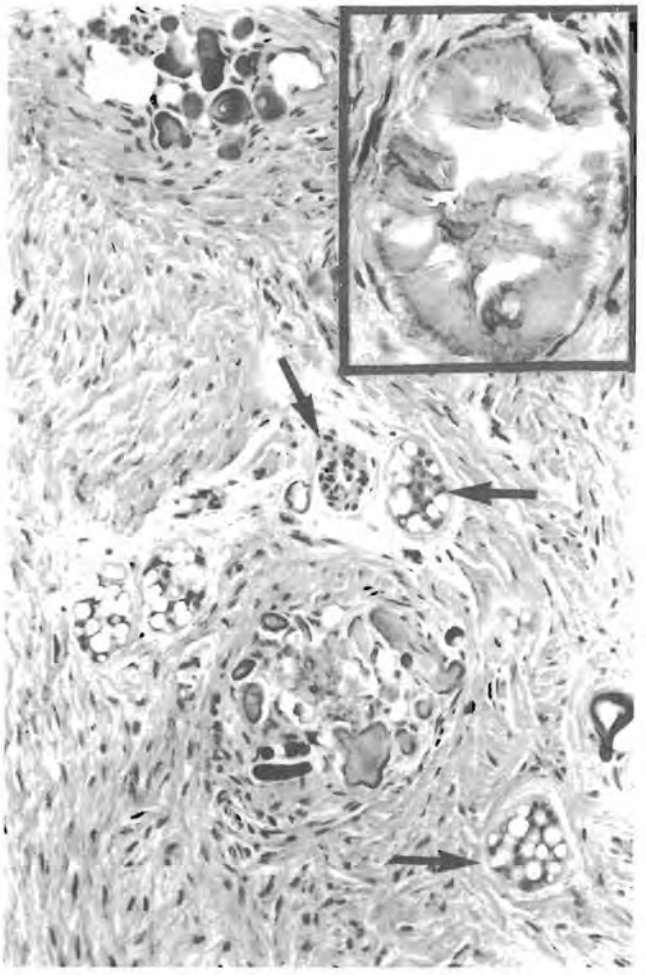

*Fig. 6:* **Odontogenic epithelium (arrows) associated with psammomatous calcifications in a fibrous stroma. H and E × 100. Inset: Fibrillar calcification with peripheral tufts. H and E × 200.**

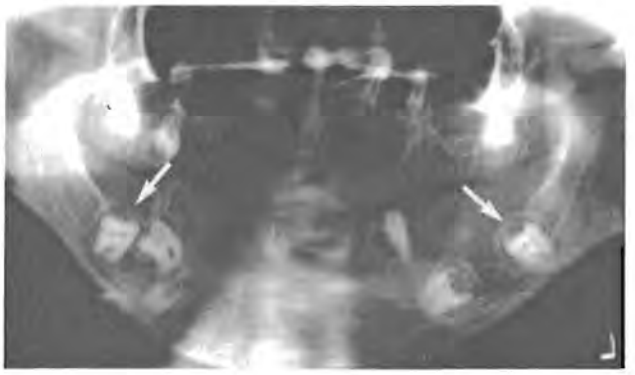

*Fig. 7:* **Case 2. Pantomograph showing impacted teeth with pericoronal radiolucencies (arrows).**

impacted teeth could be observed within the four quadrants. The enamel of the crowns of all teeth appeared markedly hypoplastic, with abnormally shaped pulp chambers which were smaller than normal. The roots of the teeth were malformed, shorter than normal, with occasional dilaceration. The crowns of the impacted teeth were surrounded by what looked like hyperplastic follicles. The follicular spaces were less radiolucent than normal (Fig 7). Radiological examination of the skeleton showed no abnormalities.

Macroscopic examination of an impacted molar tooth revealed thin, hard enamel with a granular appearance. The enamel could easily be chipped off. Microscopic examina-

tion of a 50 $\mu$m ground section showed normal dentine with an almost flat dentinoenamel junction. The enamel was thinner than normal and short curling enamel rods were seen. These were covered by irregular globular calcified masses (Fig 8). These features were consistent with rough hypoplastic amelogenesis imperfecta. The mode of inheritance could not be established. The pericoronal lesions had the same microscopic appearance as in case 1 (Fig 9).

## DISCUSSION

Calcifications associated with odontogenic epithelial remnants have been reported in odontodysplasia, impacted dens in dente, congenitally absent teeth in which there is an attempt at tooth formation and several types of AI (Witkop and Sauk, 1976). Odontogenic epithelium was present in 60 cases and calcifications in 54 cases of the 130 cases of opercula of impacted third molars (Cutright, 1976). Gardner and Sapp (1973) described two types of calcifications designated types A and B associated with the soft tissue and a periapical area of an involved tooth of a patient with regional odontodysplasia. The type A and B calcifications are similar in appearance to the two types that were found in our cases. Calcifications are also frequently found in the excised gingivae covering unerupted teeth in patients with AI (Nakata, Kimura and Bixler, 1985; Bab *et al* 1985, Ooya, Nalbandian and Noikura, 1988).

Our radiological differential diagnosis of pericoronal radiolucent lesions was dilated dental follicles, hyperplastic dental follicles, follicular cysts or odontogenic fibromas. Normally some teeth have dilated follicles in the preeruptive phase but according to Shear (1983) it does not signify a cyst unless the pericoronal width is at least 3-4 mm as measured on a radiograph. The hyperplastic follicle presents macroscopically as a solid rather than cystic lesion and no signs of a cyst can be seen microscopically. The histological appearance of hyperplastic follicles and odontogenic fibromas are similar. According to Gardner (1980) the distinction is based on the size and location of the lesion. The follicles are invariably associated with the crowns of unerupted teeth whereas it is not necessarily true for odontogenic fibromas. Sandler *et al* (1988) reported a case of a 16-year-old boy with 13 unerupted teeth, each one associated with hyperplastic pericoronal tissue that had histological features suggestive of the WHO type of odontogenic fibroma. The erupted as well as removed impacted teeth in their case were macroscopically normal. Gardner (1980) considers the WHO type of odontogenic fibroma to be a fibroblastic neoplasm. The pericoronal location of the tumours in our two patients suggested a follicular origin. The association of this fibroma-like tissue with impacted and unerupted teeth in AI suggested a hamartomatous lesion rather than a neoplasm. It is possible that the WHO type of odontogenic fibromas associated with impacted teeth, as in our cases, have a different histogenesis than the tumours described by Doyle, Lamster and Baden (1985), as none of their 6 cases was in a pericoronal location. Dunlap and Barker (1984) consider the central odontogenic fibroma of the WHO type to be the morphologic and histogenetic counterpart of the peripheral odontogenic fibroma. The authors postulated an ectomesenchymal-epithelial interaction in the histogenesis of this tumour. The close association of calcifications with odontogenic epithelium in both our cases supported their theory.

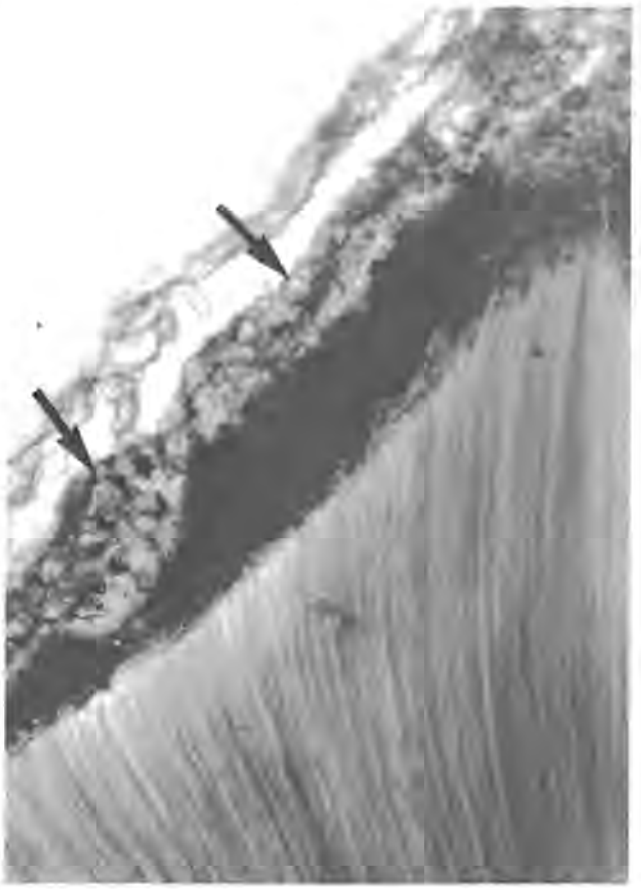

*Fig. 8:* **Thin abnormal enamel covered by irregular globular calcifications (bold arrows). Unstained × 100.**

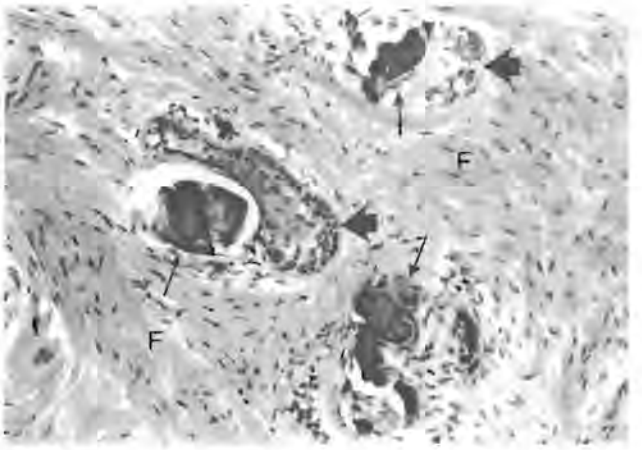


*Fig. 9:* **Odontogenic epithelium (bold arrows) closely associated with psammomatous calcifications (fine arrows) in a cellular fibrous tissue (F). H and E × 150.**

AI associated with interradicular dentinal dysplasia has been reported by Nakata *et al* (1985). They suggested 3 possible mechanisms for the presence of dysplastic dentine: resorption of the interradicular area followed by secondary calcification; gene influence on matrix formation in this area; and secondary calcification for some unknown reason. No sign of resorption of roots or crowns of the impacted teeth in our cases was found. No abnormalities in the roots of single rooted teeth were seen on radiological and microscopic examination. This is an indication that the underlying cause is likely to be associated with the process of root branching. A genetic influence responsible for the abnormal interradicular dentine is unlikely since the abnormal

dentine present in our first patient did not occur in her 3 sisters who had AI. They had no other dental abnormalities or impacted teeth. The erupted molar teeth of the first patient showed no radiological evidence of root abnormalities. The association between the interradicular abnormalities and impactions was unclear. No abnormalities apart from AI could be seen on the impacted single rooted teeth. It is unlikely that a disturbance affecting the eruption occurred first and then caused a secondary abnormality of the interradicular area of the impacted teeth as suggested by Nakata *et al* (1985). It has been shown that eruption proceeds normally in the absence of root formation (Cahill and Marks, 1980). Both erupted and impacted molars in the AI patient reported by Nakata *et al* had interradicular dentinal dysplasia. The odontogenic fibromas WHO type associated with the pericoronal areas were probably the main reason for the impaction of teeth in both our cases. The suggested follicular origin of the odontogenic fibromas as a hamartomatous growth under the influence of the follicular epithelium supported this statement as Cahill and Marks (1980) have shown that a dental follicle is required for the eruption of a tooth.

**ACKNOWLEDGEMENTS**

Our gratitude to Mrs CS Begemann for secretarial services, Mr M Turner for the electron microscopy and Miss L Hope for photographic services.

**REFERENCES**

Bab, I., Lustmann, J., Azaz, B., Gazit, D. & Garfunkel, A. (1985) Calcification of non-collagenous matrix in human gingiva; a light and electron microscopic study. *Journal of Oral Pathology*, **14**, 573-580.

Cahill, DR. & Marks, SC. Jr. (1980) Tooth eruption: evidence for the central role of the dental follicle. *Journal of Oral Pathology*, **9**, 189-200.

Chosack, A., Eidelman, E., Wisotski, I. & Cohen, T. (1979) Amelogenesis imperfecta among Israeli Jews and the description of a new type of local hypoplastic autosomal recessive amelogenesis imperfecta. *Oral Surgery*, **47**, 148-156.

Cutright, DE. (1976) Histopathologic findings in third molar opercula. *Oral Surgery*, **41**, 215-224.

Doyle, JL., Lamster, IB. & Baden, E. (1985) Odontogenic fibroma of the complex (WHO) type: Report of six cases. *Journal of Oral and Maxillo-facial Surgery*, **43**, 666-674.

Dunlap, DL. & Barker, BF. (1984) Central odontogenic fibroma of the WHO type. *Oral Surgery*, **57**, 390-394.

Gardner, DG. (1980) The central odontogenic fibroma: An attempt at clarification. *Oral Surgery*, **50**, 425-432.

Gardner, DG. & Sapp, JP. (1973) Regional odontodysplasia. *Oral Surgery*, **35**, 351-365.

Nakata, M., Kimura, O. & Bixler, D. (1985) Interradicular dentin dysplasia associated with amelogenesis imperfecta. *Oral Surgery, Oral Medicine, Oral Pathology*, **60**, 182-187.

Ooya, K., Nalbandian, J. & Noikura, T. (1988) Autosomal recessive rough hypoplastic amelogenesis imperfecta. *Oral Surgery, Oral Medicine, Oral Pathology*, **65**, 449-458.

Sandler, HJ., Nersasian, RR., Cataldo, E., Pochebit, S. & Dayal, Y. (1988) Multiple dental follicles with odontogenic fibroma-like changes (WHO) type. *Oral Surgery, Oral Medicine, Oral Pathology*, **66**, 78-84.

Shear, M. (1983) *Cysts of the Oral Regions*, 2nd ed. Ch. 5, pp. 62-63. Bristol: Wright.

Sundell, S. & Valentin, J. (1986) Hereditary aspects and classification of hereditary amelogenesis imperfecta. *Community Dentistry and Oral Epidemiology*, **14**, 211-216.

Witkop, CJ. Jr. (1989) Amelogenesis imperfecta, dentinogenesis imperfecta and dentin dysplasia revisited: problems in classification. *Journal of Oral Pathology*, **17**, 547-553.

Witkop, CJ. Jr. & Sauk, JJ. Jr. (1976) Heritable defects of enamel. *In Oral Facial Genetics*, ed. Stewart, RE. & Prescott, GH., Ch. 7. Saint Louis: Mosby.

# Diffuse peripheral odontogenic fibroma: report of 3 cases

**A. Weber[1], W. F. P. van Heerden[2], A. J. Ligthelm[1] and E. J. Raubenheimer[2]**

*Departments of Oral Pathology and Oral Biology, [1]University of Pretoria, [2]Medical University of Southern Africa, South Africa*

Weber A, van Heerden WFP, Ligthelm AJ, Raubenheimer EJ: Diffuse peripheral odontogenic fibroma: report of 3 cases. J Oral Pathol Med 1992; 21: 82–4.

Since peripheral odontogenic fibroma (POF) is characteristically described as a solitary lesion and no diffuse POF had been reported in the literature, our cases should be considered as extremely unusual. Three diffuse cases of POF are described of which one case was seen in association with ocular and skin lesions. The question arises whether POF should be considered as a true odontogenic tumor rather than a diffuse hamartomatous lesion caused by uncontrolled induction of the gingiva. It is also possible that such lesions could be part of a yet undescribed syndrome.

Key words: hamartoma; mouth, neoplasms; odontogenic fibroma; peripheral odontogenic lesions.

A Weber, Department of Oral Pathology and Oral Biology, University of Pretoria, P.O.Box 1266, Pretoria, 0001, South Africa

Accepted for publication July 16, 1991

The odontogenic fibroma is defined by the World Health Organization as a benign odontogenic neoplasm of fibroblastic origin characterized by relatively mature collagenous fibrous tissue and varying amounts of odontogenic epithelium, with the potential to occur in either a central or extraosseous location. The extraosseous counterpart is designated peripheral odontogenic fibroma (POF) (1).

All the POF's described in the literature presented as single, exophytic tumors which frequently prompted a clinical diagnosis of localized gingival hyperplasia. Diffuse involvement of the gingiva has not yet been reported. Three cases with the histologic appearance of POF with diffuse involvement of the gingiva, of which one case was associated with dermatological and ocular abnormalities, are presented.

## Material and methods

### Case 1

An 8-yr-old Black girl presented with diffusely enlarged gingiva in both jaws, causing delayed eruption of the perma-

*Fig. 1.* Clinical photograph of Case 1 showing diffusely enlarged gingivae in both jaws.

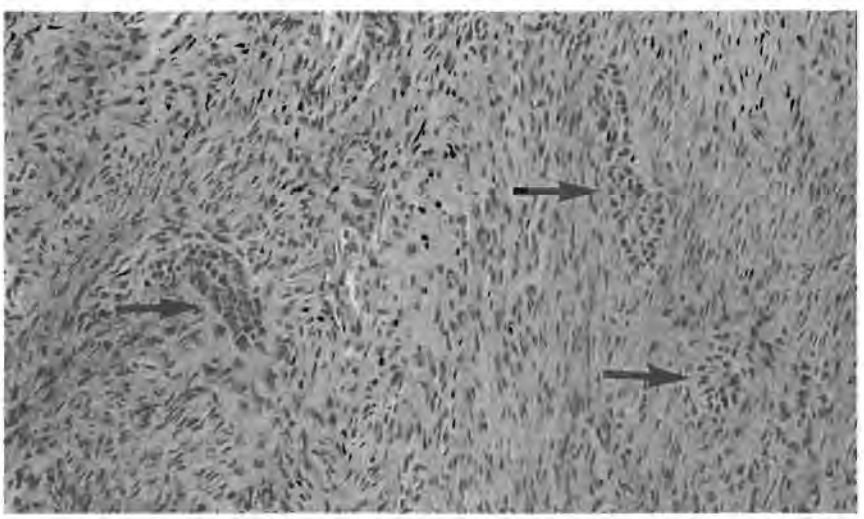

*Fig. 2.* Histologic appearance of lesion in Case 1 showing cellular fibrous tissue with inactive odontogenic epithelium arranged in nests and strands (arrows).100.

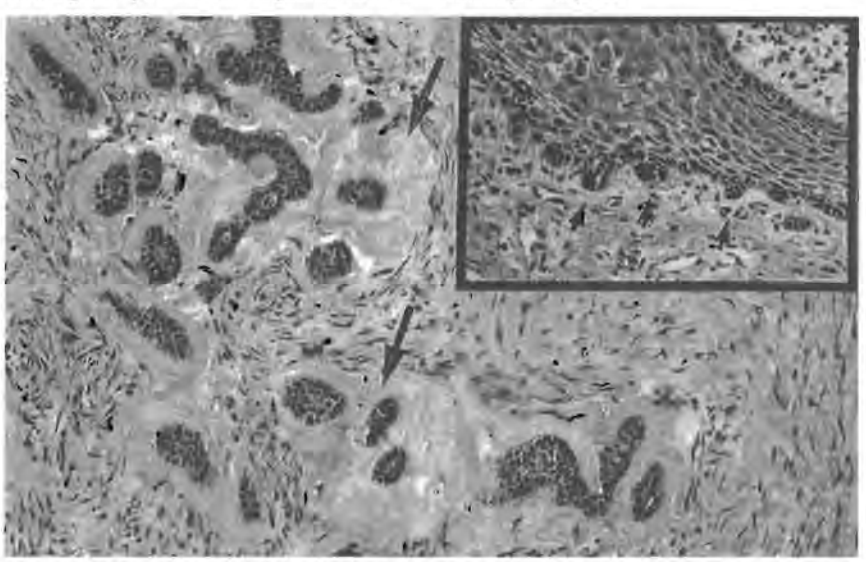

*Fig. 3.* Microscopic examination of lesion in Case 2 showing strands of odontogenic epithelium with prominent hyalinization (arrows).100. Inset: budding of overlying epithelium (arrows).100.

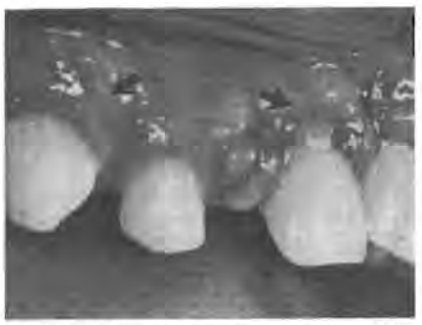

*Fig. 4.* Diffuse nodular gingival hyperplasia (arrows) in Case 3.

nent incisors. Nodules were present in the gingival masses which were firm in consistency (Fig. 1). The duration of the lesions could not be determined and no evidence of a family history was found. Radiographic examination showed no bone involvement or disturbance in tooth development. Gingivectomy of the hyperplastic tissue was done and the tissue sent for histologic examination.

Microscopically, the lesion consisted of cellular fibrous tissue with myxomatous areas. The odontogenic epithelium appeared inactive and was arranged in cell nests and strands (Fig. 2). No hard tissue formation was seen. The overlying epithelium was hyperplastic without evidence of downward proliferation of the rete ridges.

#### Case 2

A 56-yr-old black woman presented with diffuse gingival hyperplasia of both jaws resulting in enlarged alveolar ridges. The duration of the lesions was not known. The mandibular canines were displaced. All teeth were severely afflicted by plaque and calculus deposits. A biopsy of the lesion was performed and oral hygiene procedures implemented.

*Fig. 5.* Clinical photograph of Case 3 showing xanthogranuloma on skin (arrows).

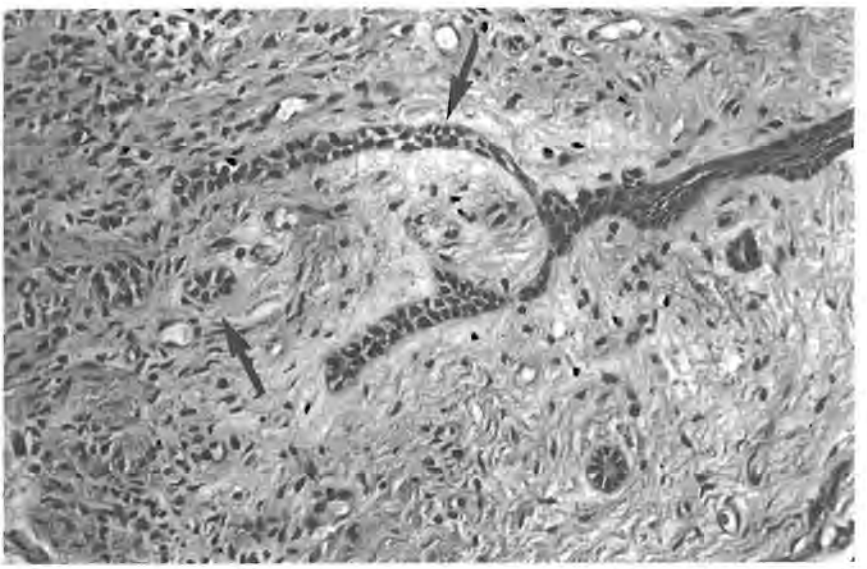

*Fig. 6.* Histologic appearance of tumor in Case 3 showing islands and strands of odontogenic epithelium (arrows) scattered in connective tissue.100.

Microscopically the gingival enlargement resulted from a proliferation of loose cellular connective tissue with scattered islands of inactive odontogenic epithelium. Hyalinization and calcifications were present in relation to the odontogenic epithelial rests. Budding of the overlying oral epithelium (Fig. 3) and focal areas of chronic inflammation were seen.

#### Case 3

A 3-yr-old white boy presented with diffuse nodular maxillary and mandibular gingival hyperplasia which became evident soon after birth (Fig. 4). The normal eruption pattern was disturbed but no other abnormalities were found radiographically. The patient also had small nodular skin lesions diagnosed as xanthogranulomas (Fig. 5), as well as corneal opacities. Corneal transplants were done in the eye lesions which could not be diagnosed as any specific pathological entity as yet. The oral lesions were clinically diagnosed as gingival hyperplasia and a biopsy performed.

Microscopically the lesion was composed of cellular fibrous tissue with islands and strands of odontogenic epithelium scattered in the connective

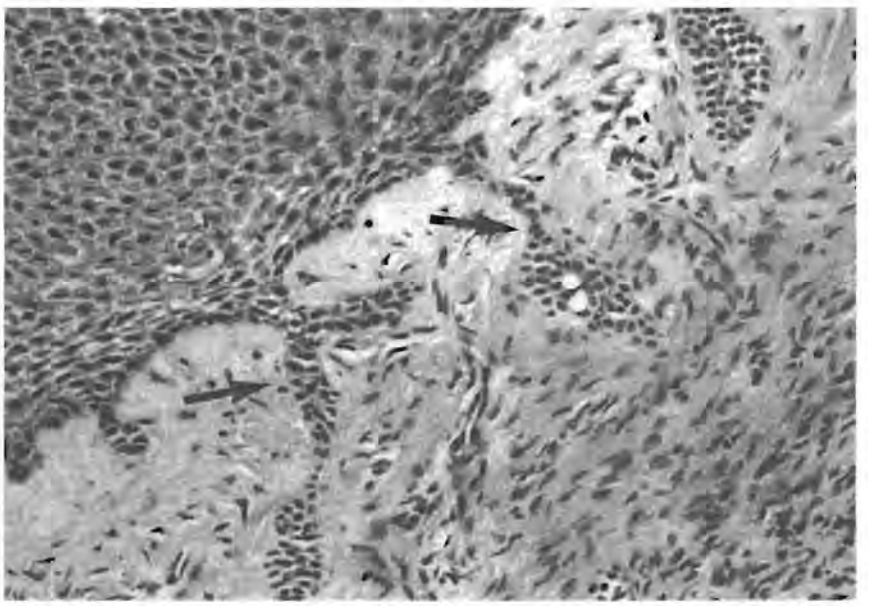

*Fig. 7.* Overlying epithelium in Case 3 showing downward proliferation into the connective tissue (arrows).200.

tissue (Fig. 6). No mineralized matrix formation was evident and the surface epithelium exhibited mild hyperplasia with downward proliferation (Fig. 7). A diagnosis of POF was suggested and gingivectomy of the hyperplastic tissue was performed. All the tissue submitted exhibited similar microscopic features.

## Discussion

Not one of the accepted cases of POF in the literature were described as a diffuse gingival lesion. Furthermore, POF was never before described in relation to any other lesions as was seen in Case 3.

The question arises as to whether POF is a true neoplasm or whether it should be regarded as an hamartomatous developmental anomaly. The diffuse involvement of the gingiva in our three cases supports the possibility that POF does have an hamartomatous origin rather than being a true benign neoplastic lesion. We agree however, that the distinction between an hamartoma and a benign neoplasm is at best difficult and is differently interpreted.

The authors are of the opinion that POF should be considered as solitary or diffuse hamartomatous lesions which are caused by uncontrolled induction in the gingiva in a local or diffuse manner. Furthermore, the possibility that POF is an hamartomatous growth, which could be part of a yet undescribed syndrome, cannot be excluded, and should be investigated.

*Acknowledgments* – The authors thank C. S. BEGEMANN for secretarial services.

## References

1. PINDBORG JJ, KRAMER IRH, TORLONI H. *Histoligical typing of odontogenic tumours, jaw cysts and allied lesions.* International histological classification of tumours No. 5, Geneva, World Health Organization, 1971; 30–1.

# Central odontogenic fibroma-like tumors, hypodontia, and enamel dysplasia: Review of the literature and report of a case

Erich J. Raubenheimer, MChD, PhD,[a] and Claudia E. Noffke, MSc(Odont),[b] Medunsa, South Africa
MEDICAL UNIVERSITY OF SOUTHERN AFRICA

A patient with multiple odontogenic fibroma-like tumors in the mandible and enamel dysplasia is presented, bringing the total number of cases reported in the literature to 3. In addition to these manifestations, this case had hypodontia. The absence of associated teeth, the size of the lesions, the lingual expansion, and the green-yellow polarization of collagen with Picrosirius stains supported the neoplastic nature of the central odontogenic fibroma-like tumors in the case presented. Laminated psammomatous deposits distinguished the tumors from the World Health Organization–type central odontogenic fibroma. **(Oral Surg Oral Med Oral Pathol Oral Radiol Endod 2002;94:74-7)**

Odontogenic fibromas are defined by the World Health Organization (WHO) as benign fibroblastic odontogenic neoplasms containing varying amounts of apparently inactive odontogenic epithelium.[1] These neoplasms occur either within jaw bones (central) or in an extra osseous location (peripheral). Central odontogenic fibromas (COFs) present over a wide age range with a marked predilection for females. Most cases occur in the maxilla anterior to the first permanent molar tooth. In the mandible, half of the cases are located posterior to the first permanent molar tooth. Most COFs present as unilocular radiolucencies with well-defined borders, but they may also show multilocular appearances and in rare instances exhibit mixed radiolucent-radiopaque features with poorly defined borders.[2]

Microscopically, the spectrum of differentiation is diverse. The simple type odontogenic fibroma is composed of stellate fibroblasts, fine collagen fibrils, and considerable ground substance. Small groups of odontogenic epithelium and foci of dystrophic calcifications may be present. The so-called WHO type is more complex, with, in addition to the simple type, long strands of odontogenic epithelium and calcifications composed of cementum-like material and dentinoid.[3] Other histologic variants include the granular cell type and a hybrid odontogenic fibroma giant cell-like tumor.[4-6] COFs have been linked to intracranial aneurysm and tuberous sclerosis.[7] Normal dental follicles associated with unerupted teeth are frequently misinterpreted histologically as COF.[8] Unerupted teeth occur commonly in patients with amelogenesis imperfecta.[9] Two cases with amelogenesis imperfecta and multiple unerupted teeth, the crowns of which were surrounded by large pericoronal radiolucencies that had been described as WHO–type COF–like lesions, were reported from our laboratory more than a decade ago.[10] Hyperplastic dental follicles with COF–like features and associated with amelogenesis imperfecta were reported by Peters, Cohen, and Altini[11] shortly thereafter. The Picrosirius red staining technique has subsequently been shown to be helpful in distinguishing hyperplastic dental follicles from COFs, the latter exhibiting green to greenish-yellow fluorescence of collagen bundles with polarization microscopy.[12] This article documents an association between enamel dysplasia, hypodontia, and multiple large well-demarcated multilocular tumors resembling WHO–type COFs.

## CASE REPORT

A 19-year-old black man was seen with pain during mastication from unerupted molar teeth. Medical history and general physical condition were unremarkable. Intraoral examination revealed hypodontia, with only the mandibular incisors, right mandibular canine, 2 mandibular first premolars, maxillary incisors, left maxillary canine, and 2 maxillary first premolars being fully erupted. Except for the recent removal of maxillary canine, mandibular molar, and mandibular canine teeth, the patient reported that he had had no previous extractions. The crowns of the erupted teeth showed diasthemas and thin enamel coverage of normal hardness. The corpus of the mandible showed bilateral expansion of the lingual cortices. An anterior open bite was evident, and a clinical diagnosis of enamel dysplasia and hypodontia was established. Radiographic examination confirmed a diagnosis of hypodontia, and no unerupted teeth were present. The

[a]Professor and Head, Oral Pathology, Medical University of Southern Africa, Medunsa, South Africa.
[b]Senior Lecturer and Section Head, Oral and Maxillofacial Radiology, Medical University of Southern Africa, Medunsa, South Africa.
Received for publication Dec 11, 2001; returned for revision Dec 31, 2001; accepted for publication Feb 11, 2002.

1079-2104/2002/$35.00 + 0 **7/14/124862**
doi:10.1067/moe.2002.124862

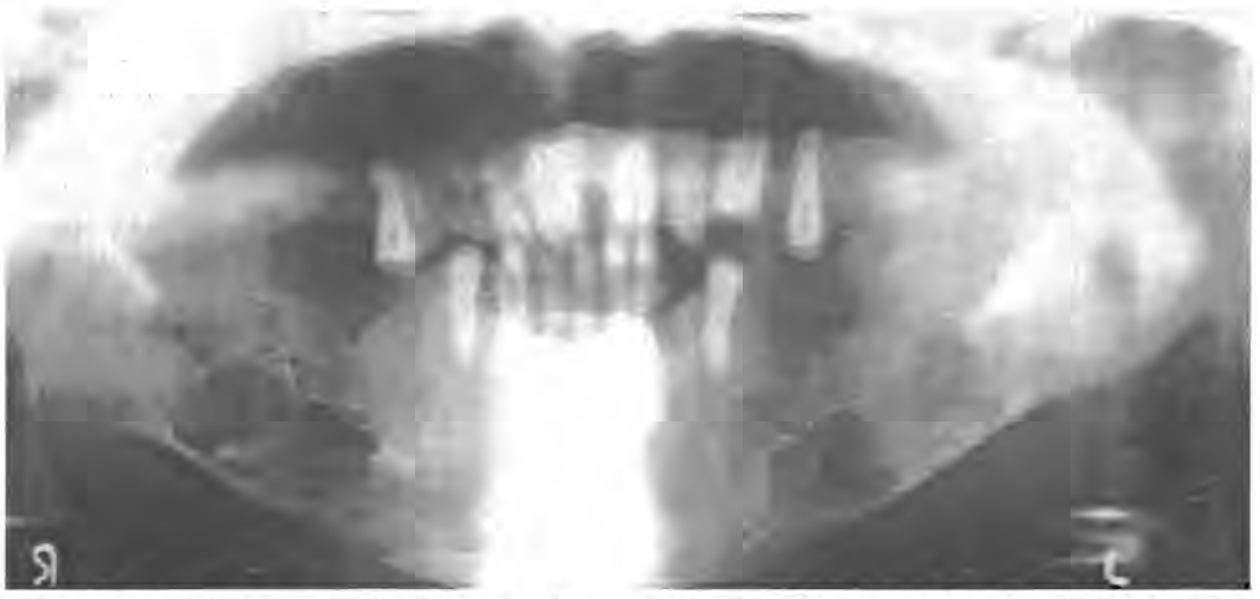

Fig 1. Bilateral multilocular mixed radiolucent-radiopaque lesions in mandible with well-defined corticated borders.

extraction sockets of the maxillary canine, mandibular canine, and mandibular molar teeth were evident, and the enamel of the remaining teeth appeared thin and of normal radiodensity. Multiple mixed radiolucent-radiopaque lesions with partially sclerotic margins were seen in the left and right corpus of the mandible (Fig 1). The patient was referred for biopsy.

An incision biopsy of a lesion in the left corpus of the mandible was performed. On macroscopic examination, the tissue appeared solid and contained calcifications. Microscopic examination showed fibrous connective tissue exhibiting strands of inactive odontogenic epithelium with calcifications resembling dentine and globular laminated psammomatous deposits, some of which were calcified (Figs 2 and 3). Thioflavin T staining of the deposits showed fluorescence. The fibrous connective tissue was mature and dense in areas and exhibited foci of myxomatous change. Examination of Picrosirius red stains showed thick collagen fibers exhibiting green and greenish-yellow change with polarizing microscopy. The other mandibular tumors were removed and showed similar microscopic features. The lesions were diagnosed as WHO-type COF-like tumors.

## DISCUSSION

This case is the third case of multiple COF-like lesions associated with enamel dysplasia reported in the literature. The first 2 cases of COF-like proliferations and enamel dysplasia, the latter diagnosed as amelogenesis imperfecta, were reported from our laboratory.[10] The COF-like tumors in these cases differed from the present case by being smaller and associated with the crowns of unerupted teeth. One of the patients reported initially had a normal number of permanent teeth, whereas the second had hypodontia. The remaining teeth of the latter patient were all unerupted and showed abnormal development with short dilacerated roots. The multiple COF-like tumors in the present case developed in place of teeth and were larger than those previously reported. Calcified psammomatous laminar deposits, frequently associated with inactive odontogenic epithelium, were present in all 3 cases. The morphology and staining characteristics of these deposits were similar to those in calcifying epithelial odontogenic tumors.[1] The deposits exhibited the staining characteristics of amyloid and may have, as in calcifying epithelial odontogenic tumors, represented degradation of lamina densa material produced by the associated epithelium.[3] It is interesting to note that these deposits have not yet been reported in COFs and could be regarded as an important microscopic feature in distinguishing the COF-like tumors in the case reported from true WHO-type COFs.

In addition to the 3 cases, the case reported by Peters, Cohen, Altini[11] in 1992 with amelogenesis imperfecta and hyperplastic dental follicles with COF-like features may have in fact represented lesions, which had the capacity, if untreated, to become as large as the COF-like tumors in our patient. This case also showed laminar psammomatous deposits microscopically.

It is interesting to note that all COF-like proliferations associated with enamel dysplasia reported in the literature occurred in South Africa (2 black females aged 14 and 26 years and a black male aged 26 years). Hamartomatous versus neoplastic nature of the lesions is, however, speculative. Gardner[13] separates hyperplastic dental follicles from odontogenic fibromas but acknowledges the difficulty in distinguishing them.

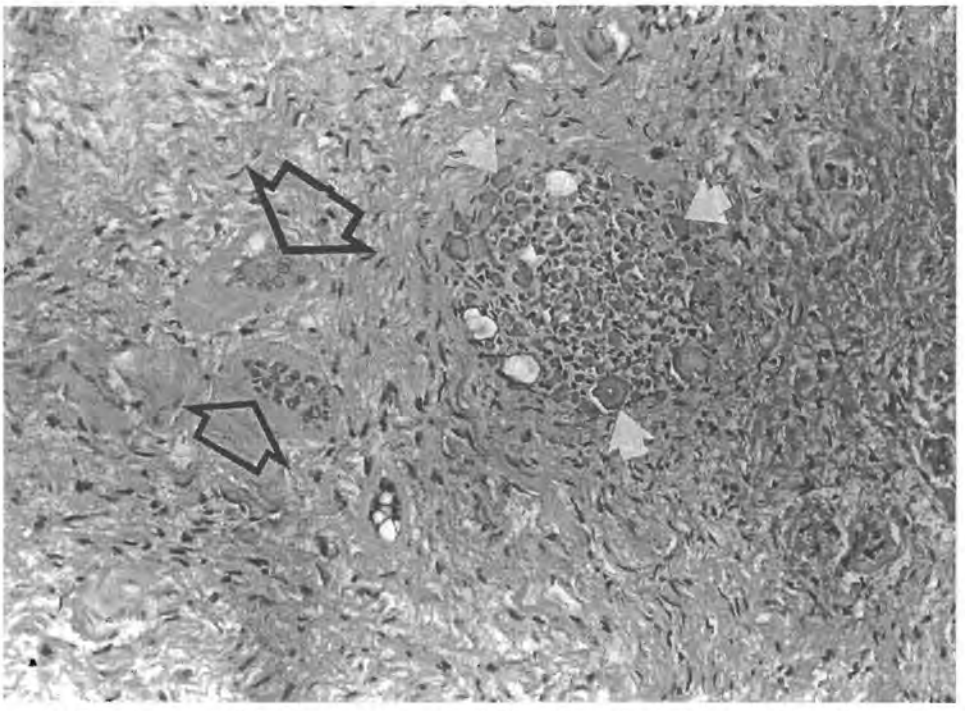

Fig 2. Fibrous connective tissue containing psammomatous calcifications (*white arrows*) and inactive islands of odontogenic epithelium (*black arrows*; hematoxylin-eosin stain; original magnification, ×200).

Fig 3. Inactive odontogenic epithelial islands (*arrows*), one of which is associated with ovoid calcified body with concentric lamination (hematoxylin-eosin stain; original magnification, ×300).

Hirschberg, Buchner, and Dayan[12] used Picrosirius red stains examined with polarized light to differentiate between COF and hyperplastic dental follicles. The greenish to yellow polarizing fibers of COFs suggest that the collagen in COFs is loosely packed and might be composed of procollagens, intermediates, or other

pathologic collagens rather than the tightly packed fibers seen in hyperplastic dental follicles. The COF-like tumors in this case cannot be regarded as hyperplastic follicles as the associated teeth failed to develop. Furthermore, the size of the lesions, lingual expansion, and Picrosirius stains showing green-yellow polarizing collagen support a diagnosis of a neoplastic and yet unclassified variant of COF.

We thank Mrs C. S. Begemann for secretarial assistance.

## REFERENCES

1. Kramer IRH, Pindborg JJ, Shear M, editors. Histological typing of odontogenic tumours. Berlin: Springer-Verlag; 1992. p. 22.
2. Kaffe I, Buchner A. Radiological features of central odontogenic fibroma. Oral Surg Oral Med Oral Pathol 1994;78:811-8.
3. Waldron CA. Odontogenic cysts and tumors. In: Neville BW, Damm DD, Allen CM, Bouquot JE, editors. Oral and maxillofacial pathology. Philadelphia: WB Saunders Company; 1995. p. 522-35.
4. Dunlap CL. Odontogenic fibroma. Semin Diagn Pathol 1999;16:293-6.
5. Allen CM, Hammond HL, Stimson PG. Central odontogenic fibroma, WHO type. A report of three cases with an unusual associated giant cell reaction. Oral Surg Oral Med Oral Pathol 1992;73:62-6.
6. Odell EW, Lombardi T, Barrett AW, Morgan PR, Speight PM. Hybrid giant cell granuloma and central odontogenic fibroma-like lesions of the jaws. Histopathology 1997;30:165-71.
7. Swarnkar A, Jungreis CA, Peel PL. Central odontogenic fibroma and intracranial aneurysm associated with tuberous sclerosis. Am J Otolaryngol 1998;19:66-9.
8. Kim J, Ellis GL. Dental follicular tissue: misinterpretation as odontogenic tumors. J Oral Maxillofac Surg 1993;51:762-7.
9. Neville BW, Damm DD, Allen CM, Bouquot JE, editors. Oral and maxillofacial pathology. Philadelphia: WB Saunders Company; 1995. p. 79-84.
10. Van Heerden WFP, Raubenheimer EJ, Dreyer AF, Benn AML. Amelogenesis imperfecta: multiple impactions associated with odontogenic fibromas (WHO) type. J Dent Assoc S Afr 1990;45:467-71.
11. Peters E, Cohen M, Altini M. Rough hypoplastic amelogenesis imperfecta with follicular hyperplasia. Oral Surg Oral Med Oral Pathol 1992;74:87-92.
12. Hirschberg A, Buchner A, Dayan D. The central odontogenic fibroma and the hyperplastic dental follicle: study with Picrosirius red and polarizing microscopy. J Oral Pathol Med 1996;25:125-7.
13. Gardner DG. The central odontogenic fibroma: an attempt at clarification. Oral Surg Oral Med Oral Pathol 1980;50:425-30.

*Reprint requests:*

Professor Erich J. Raubenheimer
Department of Oral Pathology
Medical University of Southern Africa
Box D24
Medunsa 0204
Republic of South Africa
ejraub@medunsa.ac.za

# Peripheral dentinogenic ghost cell tumor

**E. J. Raubenheimer[1], W. F. P. van Heerden[1], F. Sitzmann[2] and B. Heymer[3]**

*Departments of [1]Oral Pathology and Biology, Medical University of Southern Africa, Medunsa, South Africa, [2]Dental Surgery and Radiology, and [3]Pathology, University of Ulm, Ulm, Germany.*

Raubenheimer EJ, van Heerden WFP, Sitzman F, Heymer B: Peripheral dentinogenic ghost cell tumor. J Oral Pathol Med 1992; 21: 93–5.

A case of dentinogenic ghost cell tumor, that has originated peripherally in the jaw, is presented and the literature reviewed with particular reference to the origin of the tumor. The total number of central and peripheral cases reported in the English literature is 10 and although mucosal infiltration is common, peripheral origin of the neoplasm could be verified in only 3 cases.

Key words: dentinogenic ghost cell tumors; jaws, neoplasms; odontogenic tumors

E. J. Raubenheimer, Department of Oral Pathology, Medical University of Southern Africa, P.O. Medunsa, Republic of South Africa.

Accepted for publication August 4, 1991

The calcifying odontogenic cyst is a unique jaw lesion described as a distinct entity in 1962 by GORLIN *et al.* (1). In a study of 16 cases by PRAETORIUS *et al.* (2), it became evident that this group of lesions contains two entities, a cyst (Type I) and a neoplasm (Type II), and for the latter the term 'dentinogenic ghost cell tumour' was proposed. The neoplasm occurs predominantly in later life and consists microscopically of ameloblastoma-like odontogenic epithelial proliferations infiltrating the bone and connective tissue. Ghost-cells are present as well as varying amounts of dentinoid the latter being closely associated with odontogenic epithelium.

The purpose of this paper is to present an unique case of a dentinogenic ghost cell tumour originating in an extraosseous location.

## Case report

An 82-yr-old man presented in the Department of Dental Surgery and Radiology, University of Ulm, complaining of a slow growing nodule on the mandibular right alveolar ridge. The lesion started 6 yr ago after extraction of the mandibular right canine. On examination the patient was found to be edentulous. A 6 mm broad based polypoid lesion was located on the mandibular right alveolar ridge. Radiographic examination revealed no underlying bone involvement (Fig. 1) and a clinical diagnosis of a peripheral giant cell granuloma was made. During surgical removal, the lesion was found to be located within the alveolar mucosa and the alveolar bone was not involved.

The surgical specimen measured 6 × 6 × 4 mm and had a firm consistency with foci of calcifications. Microscopic examination revealed hyperplasia of overlying epithelium and a solid tumor, composed of odontogenic epithelium associated with calcifications in the subepithelial connective tissue (Fig. 2). The neoplastic epithelium showed a well defined cuboidal to cylindrical basal cell layer closely associated eosinophilic cells with abrupt keratinization, resembling ghost cells (Fig. 3). Although the epithelial cells displayed nuclear pleomorphism, no mitotic figures were present. In focal areas, stellate reticulum-like differentiation as well as the formation of dental lamina-like structures were observed. Masses of acellular calcified material, resembling dentinoid, were evident in close association with the epithelium (Fig. 3). The surrounding connective tissue contained strands of inactive epithelium associated with small globular dentinoid deposits. Slight inflammation with vasodilatation and edema was present and a diagnosis of peripheral dentinogenic ghost cell tumor was made. Six year follow-up after removal failed to reveal a recurrence.

## Discussion

Peripheral occurence of the cystic types of calcifying odontogenic cysts (Type I) is well documented in the English literature (1, 3). This may result from cortical bone perforation by a central lesion or more rarely, true peripheral origin from gingival epithelial remnants (4).

*Fig. 1.* Panoramic radiographic view showing lack of bony involvement of the mandibular right alveolar ridge.

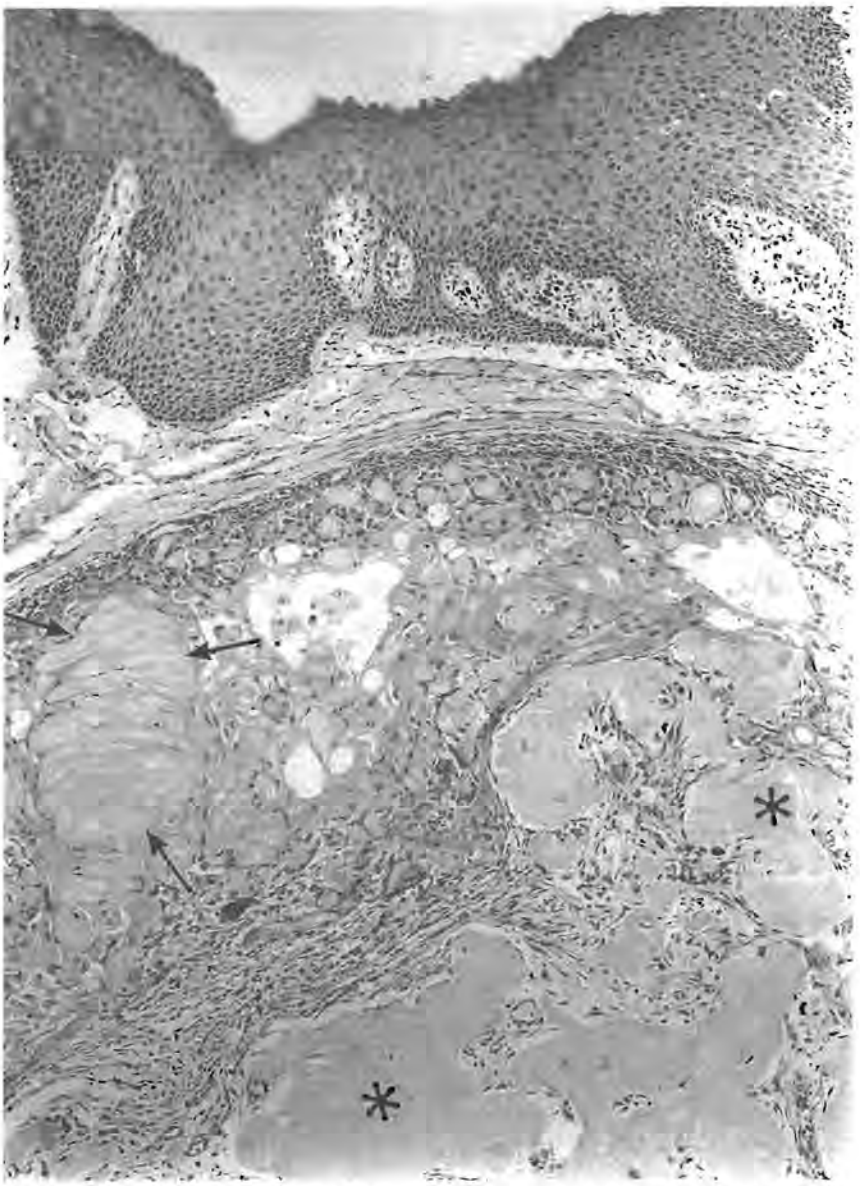

*Fig. 2.* Well encapsulated tumor with ghost cell formation (arrows) and dentinoid deposits (asterisks). H&E stain, ×30.

Conflicting data on the origin of the solid type calcifying odontogenic cyst (Type II) or dentinogenic ghost cell tumor are present in the literature. A recent review article summarizes the clinico-pathological features of 10 cases published in the English literature. In this article gingival swelling is considered to be the most frequent clinical feature. Radiographically all cases presented as lucencies with poorly defined margins (5). An earlier paper, reviewing 5 cases, proposed that dentinogenic ghost cell tumors usually occur peripherally and on the gingiva (6). Analysis of the original publications, mostly case reports, proves the discrepancy to lie in the interpretation of the clinical descriptions. Both cases reported by PRAETORIUS (2) are described as being 'extraosseous', despite radiographic signs of bony and dental involvement. Although peripheral involvement is probably implied by the authors, true peripheral origin of these lesions need to be questioned. The first of two cases reported by FEJERSKOV & KROGH (7) is described as an exophytic palatal mass. Unfortunately roentgenograms were not available and central origin of this case can therefore not be excluded. Central dentinogenic ghost cell tumors were also reported by GÜNHAN & SENGÜN (8) – 1 case, – TAJIMA (9) – 1 case – and COLMENERO *et al.* (5) – 1 case –, bringing the total number of central dentinogenic ghost cell tumors in the literature to 7. The 'peripheral odontogenic tumor with ghost-cell keratinization' reported by VULETIN *et al.* (10) contained no dentinoid deposits and exhibited odontogenic epithelium surrounded by cellular fibroblastic tissue, resembling and primitive dental pulp. On microscopical grounds, this lesion can not be classified as a dentinogenic ghost cell tumor since ghost cells are found in many other odontogenic neoplasms (2).

Peripheral presentation of dentinogenic ghost cell tumors is related to their infiltrative behaviour and although this feature appears to be common, true peripheral origin is not as frequently reported. ABRAHAMS & HOWELL (11) describe a dentinogenic ghost cell tumor located entirely extraosseous and palatal to a maxillary cuspid. Peripheral dentinogenic ghost cell tumors involving only the gingiva or alveolar mucosa, with radiographic support, were also reported in the lingual mandibular left premolar region (6) and the anterior part of the maxilla (12). This brings the number of true peripheral tumors to four, including our case.

The average age reported in the literature is 50, the oldest being 72 and the youngest 17 (5). Our patient, with an age of 82 yr, represents the most advanced age at which a dentinogenic ghost cell tumour has been diagnosed. Although the central tumors have a high rate of recurrence after removal (5), long term follow-up of our case and lack of proof of recurrence of any of the other peripheral dentinogenic ghost cell tumors suggests a favourable course for the peripheral type.

*Acknowledgments* – We are indebted to Ms C. S. BEGEMANN for secretarial assistance.

## References

1. GORLIN RJ, PINDBORG JJ, CLAUSEN FP, VICKERS RA. The calcifying odontogenic cyst - a possible analogue of the cutaneous calcifying epithelioma of Malherbe. *Oral Surg Oral Med Oral Pathol* 1962: **15**: 1235–43.
2. PRAETORIUS F, HJÖRTING-HANSEN E, GORLIN RJ, VICKERS RA. Calcifying odontogenic cyst. Range, variations and neoplastic potential. *Acta Odontol Scand* 1981: **39**: 227–40.
3. ALTINI M, FARMANN AG. The calcifying odontogenic cyst. Eight new cases and a review of the literature. *Oral Surg Oral Med Oral Pathol* 1975: **40**: 751–9.
4. BHASHAR CS. The gingival cyst and the keratinizing ameloblastoma. *Oral Surg Oral Med Oral Pathol* 1965: **19**: 796–8.

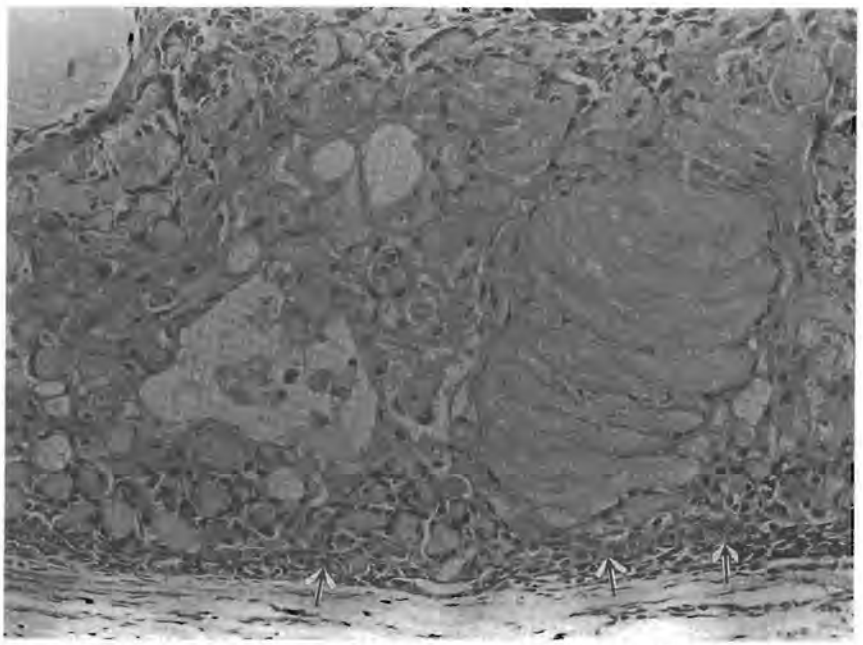

*Fig. 3.* Cuboidal peripheral basal cell layer (arrows) and adjacent cells exhibiting abrupt keratinization with ghost-cell formation. H&E stain, × 150.


5. Colmenero C, Patron M, Colmenero B. Odontogenic ghost cell tumours. The neoplastic form of calcifying odontogenic cyst. *J Cranio-Max Fac Surg* 1990: **18**: 215–8.
6. Hirshberg A, Dayan D, Horowitz I. Dentinogenic ghost cell tumor. *Int J Oral Maxillofac Surg* 1987: **16**: 620–5.
7. Fejerskov O, Krogh J. The calcifying ghost cell odontogenic tumor – or the calcifying odontogenic cyst. *J Oral Pathol* 1972: **1**: 273–7.
8. Günhan O, Sengün O, Celasun B. Epithelial odontogenic ghost cell tumor: report of a case. *J Oral Maxillofac Surg* 1989: **47**: 864–7.
9. Tajima Y, Utsumi N. The dentinogenic ghost cell tumor. *J Oral Pathol* 1986: **15**: 359–62.
10. Vuletin JC, Solomon MP, Pertschuk LP. Peripheral odontogenic tumor with ghost-cell keratinization. *Oral Surg Oral Med Oral Pathol* 1978: **45**: 407–15.
11. Abrams AM, Howell FV. The calcifying odontogenic cyst. *Oral Surg Oral Med Oral Pathol* 1968: **25**: 594–606.
12. Sauk JJ. Calcifying and keratinizing odontogenic cyst. *J Oral Surg* 1972: **30**: 893–7.

# GLANDULAR ODONTOGENIC CYST

**Willem F.P. van Heerden, MChD, Erich J. Raubenheimer, MChD, and Martin L. Turner, DipTech(Med)**

Two cases of glandular odontogenic cysts are reported. The unique histological features, eg, the intraepithelial glandular structure, papillary processes, and eosinophilic cuboidal and larger granular superficial cells are sufficient to warrant glandular odontogenic cyst as a distinct entity. Electron microscopic examination of the superficial eosinophilic cuboidal cells are suggestive of a process similar to apoptosis. Eroded cortical plates suggest an aggressive behavior.
**HEAD & NECK 14:316–320**

The glandular odontogenic cyst (GOC) is a rare cystic lesion that is not incorporated in classifications of jaw cysts. Only a few examples of this lesion have been described in the literature. Gardner et al[1] collected eight cases of GOC. Padayachee and van Wyk[2] reported two cases, which they described as "sialo-odontogenic cysts."

The GOC has an equal sex distribution and occurs in both the mandible and maxilla of adults.[1,2] These lesions, which can attain a large size, appear on radiographs as uni- or multilocular lytic lesions. The histologic features described by Gardner et al[1] include a cyst lining consisting of stratified squamous epithelium of varying thickness that contains pools of mucicarmine-positive material. The superficial layer consists of eosinophilic cubiodal and occasionally mucous- and ciliated cells. Spherical structures produced by swirling epithelium and lack of cell polarization are focally present in the epithelium lining. Irregular-shaped calcifications are occasionally found in the subepithelial connective tissue.

This report describes the clinical, histopathologic, and ultrastructural features of two cysts.

From the Department of Oral Pathology and Oral Biology, Medical University of Southern Africa, Medunsa, South Africa.

Acknowlegment: The authors thank Mrs. Colleen Begemann for secretarial services and Miss Laura Hope for photographic services.

Address reprint requests to Dr. W. F. P. van Heerden at the Department of Oral Pathology and Oral Biology, P.O. Medunsa 0204, Republic of South Africa.

Accepted for publication August 8, 1991

CCC 0148-6403/92/040316-05 $04.00


## CASE 1

A 27-year-old woman reported to the clinic complaining of a painless swelling in the anterior mandible of three years' duration. Intraoral examination revealed a 6 × 3 cm sized swelling extending from the left first mandibular molar to the right second premolar with buccal as well as lingual bone expansion. The mucosa was intact, but the bone was eroded in areas causing the swelling to fluctuate on palpation (Figure 1). No sensory nerve fallout was found. Radiography revealed a well-defined unilocular radiolucent lesion with a scalloped border. Displacement of the anterior teeth was present (Figure 2). During biopsy, a unicystic cavity containing yellow serous fluid was found. Differential diagnoses included a unicystic ameloblastoma and odontogenic keratocyst.

Histologic examination of the incisional biopsy revealed a cyst lining consisting of a nonkeratinized epithelium. The epithelium varied in thickness from double-layer cuboidal to

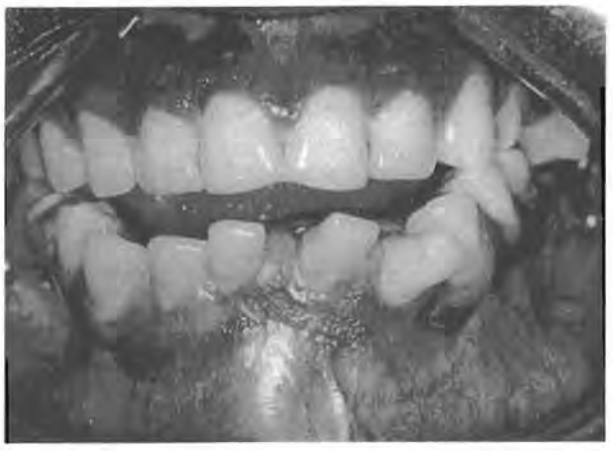

**FIGURE 1.** Mandibular lesion showing buccal and lingual expansion associated with tooth displacement.

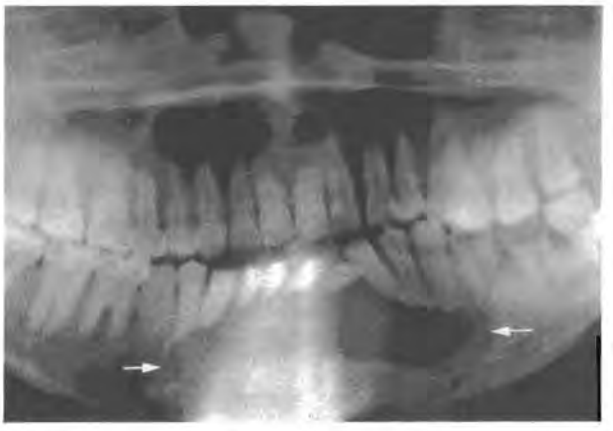

**FIGURE 2.** Pantomograph exhibiting an unilocular radiolucency (arrows) of the anterior mandible.

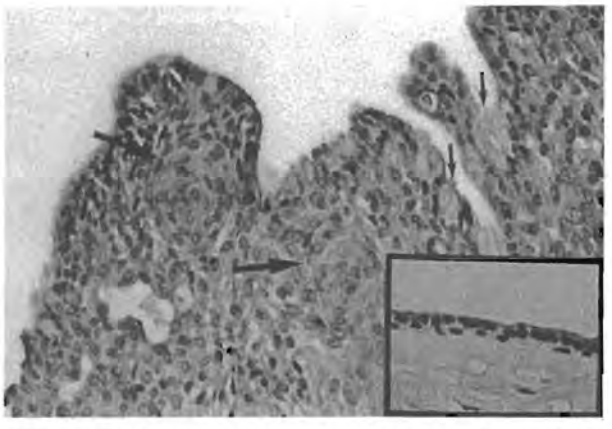

**FIGURE 3.** Papillary processes associated with epithelial spheres (bold arrows) and superficial mucous cells (fine arrows). Hematoxylin & eosin; original magnification, ×200. Inset: The cyst lining is partly composed of a double layer cuboidal epithelium. Hematoxylin & eosin; original magnification ×200.

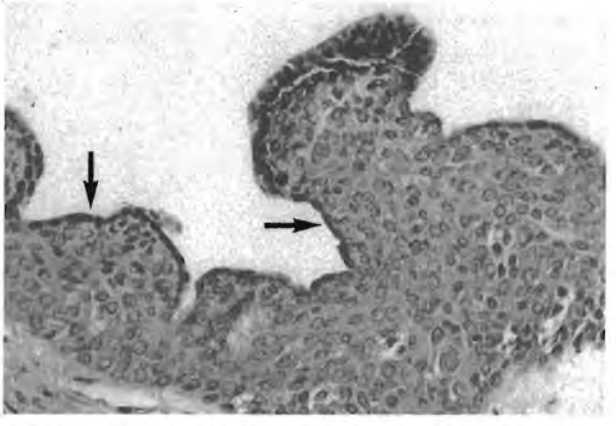

**FIGURE 4.** Superficial cell layer consisting of small cuboidal cells with hyperchromatic nucleii and eosinophilic cytoplasms (arrows). Note the papillary processes. Hematoxylin & eosin; original magnification, ×200.

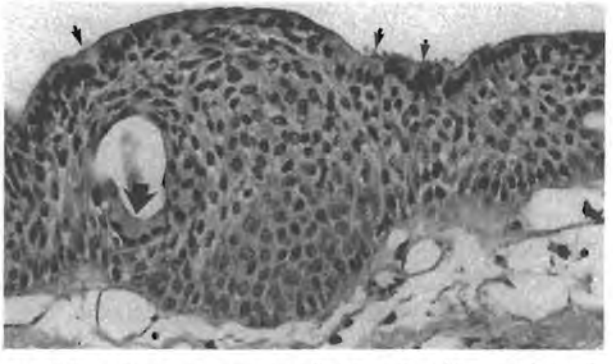

**FIGURE 5.** Glandular structure lined partly with granular cells (bold arrow). Note the granular superficial cells (fine arrows). Hematoxylin & eosin; original magnification, ×200.

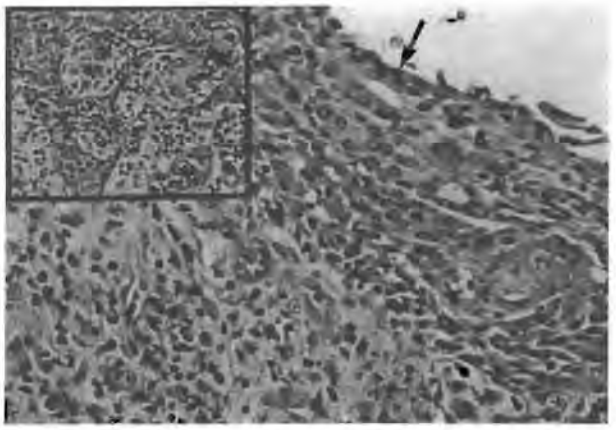

**FIGURE 6.** Inflammatory induced changes in lining of case 1. A glandular structure is visible (arrow). Hematoxylin & eosin; original magnification, ×200. Inset: Epithelial arcading associated with lymphocytes. Hematoxylin & eosin; original magnification ×100.

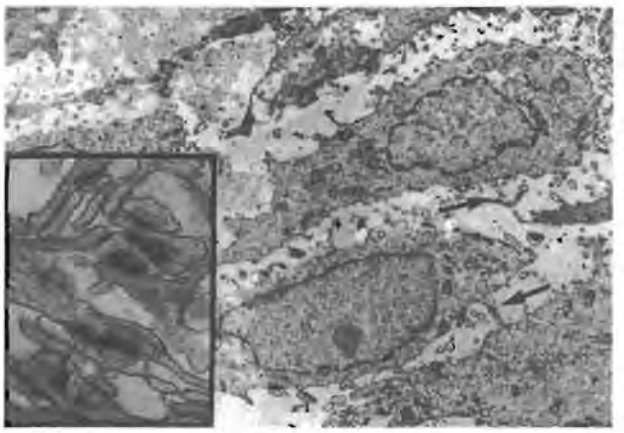

**FIGURE 7.** Transmission electron micrograph of the inflammed lining revealed widened intercellular spaces containing finger-like protrusions (arrows). Original magnification, ×2600. Inset: Well-formed desmosomes were present between the protrusions. Original magnification, ×8300.

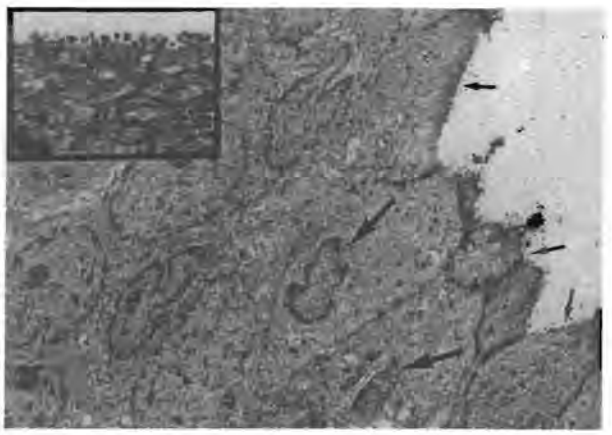

**FIGURE 8.** Electron micrograph of the lining of case 1 representing the superficial eosinophilic cuboidal cells. Note the smaller, denser nucleoli in the more superficial cells (bold arrows) and the absence of nuclear material in the remainder of the superficial cells (fine arrows). Original magnification, ×3300. Inset: Microvilli on the luminal aspect of the superficial cells. Original magnification, ×10,000.

**FIGURE 9.** Occlusal radiograph revealed a well-circumscribed radiolucency causing root divergence of the lateral and incisor teeth.

stratified squamous. Papillary epithelial processes into the lumen were noted, especially where epithelial thickenings were present. Epithelial spheres consisting of swirled epithelial cells were found occasionally (Figure 3). The superficial cell layer consisted mainly of small cuboidal cells with scanty eosinophilic cytoplasm and hyperchromatic nuclei (Figure 4). Larger cells with an eosinophilic granular cytoplasm and a round nucleus, which was oriented away from the surface, as well as scattered mucous cells were also present in the superficial layer. Ciliated cells were focally seen.

Intra-epithelial glandular structures, filled with an eosinophilic, mucicarmine-positive material were present, the majority located in the superficial half of the epithelium (Figure 5). These glandular spaces were lined mainly by granular cells, although mucous cells were focally present. No mitotic figures were noted. Palisading of the basal cells were focally seen, and no maturation changes of the epithelial cells were noted. Cleaving between the epithelium and connective tissue was focally observed. The underlying connective tissue consisted of dense fibrous tissue with a few vascular spaces. No epithelial islands nor calcifications were noted.

A diagnosis of a glandular odontogenic cyst

was made, and the cyst lining was enucleated under general anesthesia. The wound was closed primarily and healing was uneventful. Small fragments of the lining were fixed separately in 3% gluteraldehyde for electron microscopic examination. Light microscopic examination of the enucleated material revealed a dense, chronic inflammatory cell infiltrate consisting mainly of lymphocytes in the subepithelial connective tissue and neutrophils in the epithelium. The epithelial lining had lost most of the features described in the incisional biopsy material. Epithelial hyperplasia and proliferation into the underlying connective tissue with an arcading effect were present. The eosinophilic cuboidal superficial cell layer as well as glandular structures in the epithelium were focally present (Figure 6).

Electron microscopic examination revealed widened intercellular spaces with numerous fingerlike protrusions that attached adjoining epithelial cells by well-formed desmosomes (Figure 7). As the biopsies taken for electron microscopy were not representative of all epithelial types as seen in the sections of the incision biopsy, a small fragment was then removed from the wax block of the noninflammed biopsy specimen and processed for electron microscopy. This epithelial lining consisted of tightly aggregated cells with well-formed desmosomes. Microvillilike projections were present on the luminal aspect of the superficial cells, the majority of which contained no nucleii. Their cell volume seemed to be decreased, resulting in a closer association of the desmosomes (Figure 8). The cells immediately underneath the superficial cells contained a denser nucleus, and signs of nuclear fragmentation were present.

### CASE 2

A 14-year-old boy presented with swelling of the right upper lip. Oral examination revealed a firm buccal and palatal swelling involving the right maxillary canine area. Radiographs showed a well circumscribed, unilocular lytic lesion in the globulo-maxillary area causing root divergence of the lateral and incisor teeth (Figure 9). A biopsy was taken, and microscopic examination showed a cyst lining with similar features as described in case 1 (Figure 10). A diagnosis of a glandular odontogenic cyst was made. The patient did not return for treatment.

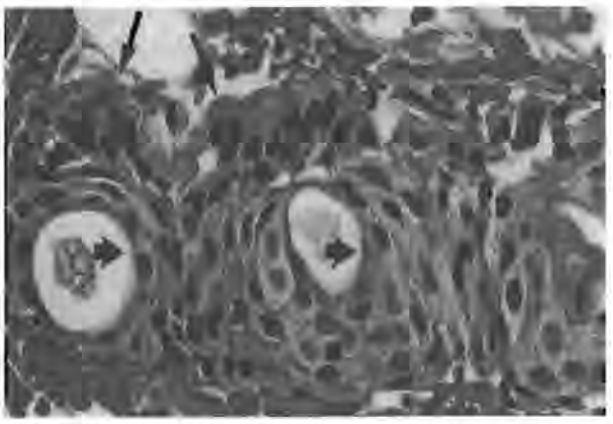

**FIGURE 10.** Glandular structures were present in the lining epithelium (short arrows). The superficial cells had a granular appearance (long arrows). Hematoxylin & eosin; original magnifications, ×400.

### DISCUSSION

There are sufficient criteria to regard GOC as a distinct entity and not a variant of any other cyst. The unique features include the presence of eosinophilic cuboidal and larger granular superficial cells, intraepithelial glandular structures lined by granular and mucous cells, and papillary processes protruding into the lumen. Epithelial spheres are also found in both lateral periodontal cysts and dentigerous cysts.[3] The presence of numerous mucous cells alone does not warrant the diagnosis of GOC. Browne has shown that mucous metaplasia is fairly common in dentigerous cysts, and can be found in the majority of jaw cysts.[4]

The widened interepithelial cell spaces and the finger-like protrusions found in inflammed GOC tissue on electron microscopic examination are also present in inflammed as well as noninflammed radicular and follicular cysts.[5] The spinous cells of odontogenic keratocysts, however, show a close intercellular relationship with desmosomes rarely detected.[5] The tissue fragment removed from the wax block for electron microscopy study contained superficial eosinophilic cuboidal cells. It is tempting to speculate that the superficial cells undergo a process similar to apoptosis. This will explain the eosinophilic light microscopic appearance of the superficial cells with hyperchromatic nucleii, although the microvilli-like projections seen on electron microscopy are too small to represent apoptotic bodies.[6]

The prevalence of GOC is low. The two cases reported in this study are the only GOCs in our

collection of 152 jaw cysts that were diagnosed during an 8-year period. A contributory factor to this low prevalence may be the difficulty in identifying the characteristic features of a GOC in inflammed tissue, especially if only material from an incisional biopsy is available. The changes brought about by an inflammatory process were evident in the excised tissue in case 1.

Glandular odontogenic cysts are considered to be aggressive. One of the cases reported by Padayachee and van Wyk[2] recurred, and recurrences were present in two of the eight cases described by Gardner et al.[1] Although no recurrence was present in case 1, after 2 years, the eroded cortical plates suggested aggressive behavior.

## REFERENCES


1. Gardner DG, Kessler HP, Morency R, Schaffner DL. The glandular odontogenic cyst: an apparent entity. *J Oral Pathol* 1988;17:359–366.
2. Padayachee A, van Wyk CW. Two cystic lesions with features of both the botryoid odontogenic cyst and the central mucoepidermoid tumor: sialo-odontogenic cyst? *J Oral Pathol* 1987;16:499–504.
3. Shear M. Cysts of the oral regions. 2nd ed. Bristol: Wright PSG, 1983:52–72.
4. Brown RM. Metaplasia and degeneration in odontogenic cysts in man. *J Oral Pathol* 1972 11:145–158.
5. Meurman JH, Ylipaavalniemi P. Ultrastructure of odontogenic jaw cysts. *Scand J Dent Res* 1984;92:577–586.
6. Wyllie AH, Morris RG, Smith AL, Dunlop D. Chromatin cleavage in apoptosis: association with condensed chromatin morphology and dependence on macromolecular synthesis. *J Pathol* 1984;142:67–77.

Dentomaxillofacial Radiology (2002) 31, 333–338

www.nature.com/dmfr

REVIEW

# The glandular odontogenic cyst: Clinical and radiological features; review of the literature and report of nine cases

C Noffke*,[1] and EJ Raubenheimer[2]

[1]*Departments of Oral and Maxillofacial Radiology, Faculty of Dentistry, Medical University of Southern Africa, South Africa;*
[2]*Department of Oral Pathology, Faculty of Dentistry, Medical University of Southern Africa, South Africa*

Nine cases with glandular odontogenic cysts (GOC's) are presented bringing the total number reported in the literature to 54. Our study confirmed that most GOC's occur in the mandible, whereas maxillary lesions present only in the globulo-maxillary region. The radiological features were found to be non-distinctive and presented as well-defined radiolucencies with uni- and multilocular appearances. Most of the mandibular GOC's were unilocular, involved the symphysis region and only one extended into the ramus. All GOC's larger than 6 cm in diameter showed perforated margins radiologically. Our two multilocular GOC's demonstrated microscopic features supporting their infiltrative radiological appearance. The invasive clinical and radiological features of GOC support the notion of a possible histo-pathologic overlap between GOC and low-grade central mucoepidermoid carcinoma of the jaw.
*Dentomaxillofacial Radiology* (2002) **31**, 333–338. doi:10.1038/sj.dmfr.4600730

**Keywords:** odontogenic cysts; radiography, dental; jaw cysts; review literature

## Introduction

Two multilocular mandibular cysts were originally described by Padayachee and Van Wyk[1] who speculated on the possibility of salivary gland origin and proposed the term sialo-odontogenic cyst. Histological characteristics, which supported their choice of terminology, were mucinous material within the cystic spaces and epithelial thickening or plaques in the epithelial lining. One of their cysts recurred. The histological characteristics led to the association of the cysts with the central mucoepidermoid tumour. Gardner[2] reported eight cases in 1988 involving both the maxilla and mandible, which occurred over a wide age range in both genders and recurred if not excised adequately. One of their cases was associated with an ameloblastoma. Radiologically the lesions were reported to be either unilocular or multilocular with smooth or scalloped margins. Based on their histopathological features they assumed the cysts to be of odontogenic origin and a histologic variant of the botryoid odontogenic cyst. The term glandular odontogenic cyst (GOC) was suggested. Shear[3] favoured the term muco-epidermoid cyst, which was advocated by Sadeghi and co-workers.[4] However, the latter term had already been used by Hodson[5] to describe simple radicular, residual and dentigerous cysts showing mucous metaplasia of the epithelial linings. In 1992 the World Health Organisation accepted GOC as a distinct pathological entity and classified it as a developmental odontogenic cyst.[3] Patron, Colmeri and Larrauri[6] reported three cases in 1991, which did not recur after surgical removal. One case was associated with a squamous odontogenic tumour-like proliferation in its wall. They included thirteen previously reported cases in their study and found predilections for males (9/13) and the mandible (10/13) and an age range of 19 to 85 years with a mean age of 50 years. Radiologically they described the lesions as well defined, uni- or multilocular without specific diagnostic characteristics. The occurrence during the fifth to seventh decade, location in the mandibular premolar region, multilocularity, tendency to recur and histological similarity of the epithelial lining led them to support the suggestion that GOC's are histologic variants of the botryoid odontogenic cyst. In 1994 Takeda[7] reported a GOC in the mandibular third molar region that presented as a

*Correspondence to: C Noffke, Department of Oral Radiology, Box D16, P.O. Medunsa, 0204, South Africa; E-mail: ejraub@medunsa.ac.za
Received 14 November 2001; revised 13 April 2002; accepted 19 August 2002

lateral periodontal cyst with a unilocular appearance. He supported the unsubstantiated hypothesis that a lateral periodontal cyst may develop in a GOC. Hussain, Edmondson and Browne[8] described four new cases of GOC in the mandible, with a predilection for females and a mean age of 44 years. The clinical and the radiological features were described as non-specific. Semba *et al*[9] added one new case in 1994, reviewed the clinical features of GOC and compared it with botryoid odontogenic cysts. He suggested that the GOC and the latter are histological variants in a separate group of non-keratizing odontogenic cysts, but share the same epithelial origin, namely the dental lamina, its remnants or reduced enamel epithelium. There was no sign of recurrence 2 years after surgical removal of their case.

Agreement has been reached on the aggressive, somewhat neoplastic nature of GOC's and their tendency to recur.[2,6,10,11] Toida and co-workers (1994)[12] in their review of the literature found a predilection for the mandible (14/18), notably the anterior region (13/18) and an equal gender distribution. The age range was reported to be 14 to 85 years (mean age of 49 years) and the majority of patients were older than 40 years. Radiologically the lesion lacked specific features making distinction from ameloblastoma and odontogenic keratocyst difficult. A more aggressive surgical removal rather than simple curettage was suggested and cases should be carefully followed up. Economopoulou and Patrikiou[13] added one case to the literature in 1995 and reviewed 19 cases in total. They found that GOC's occurred over a wide age range, with a predilection for men and the anterior mandible. The cysts may reach large dimensions, are often associated with expansion and radiological findings were reported to be non-specific.[14] The most recent literature research revealed a total of 47 reported cases, a male to female ratio of 19:28 and mean age 46.7 years (range 14–75 years) in males and 50.0 years (range 21–72 years) in females, resulting in a mean age of 48.3 years for both genders.[15]

Our study was aimed at analysing the clinical, radiological and histopathological features of seven new cases of GOC's in a rural African population and to compare our findings with those reported in the literature. The aggressive nature of GOC's makes distinction from other cystic lesions of the jawbones important. Diagnosis prior to surgical intervention is essential in this regard.

## Report of new cases

Nine cases of GOC were diagnosed over the past 10 years in the Department of Oral Pathology at Medunsa, which serves mainly a rural Black population. Two of these were previously published as case reports.[11] None of our cases recurred, however follow-up is poor due to the remoteness of the region. Clinical and radiological data are reflected in Table 1. Radiographic examination was performed with panoramic, occlusal, Waters and peri-apical radiographs and measurements were made in horizontal and vertical dimensions on standardized panoramic films.

All GOC's showed cortical expansion (Figure 1) and those with a diameter of more than 6 cm, perforation. Maxillary GOC's had a well-circumscribed unilocular radiological appearance without exception (Figure 2). Both multilocular GOC's in our sample occurred in the

**Table 1** Clinical and radiological features of eight cases

| *Case no.* | *Gender* | *Age* (years) | *Site* | *Size* (cm) | *Radiological features* | *Clinical* |
|---|---|---|---|---|---|---|
| 1* | M | 14 | R Max 12–13 | 3.2 × 2 | Unilocular, well circumscribed, smooth contour, tooth displacement | Expansion |
| 2* | F | 27 | L & R Mand 36–45 | 6 × 3 | Unilocular, well circumscribed, irregular borders, tooth displacement | Expansion Perforation |
| 3 | M | 50 | L & R Mand 34–43 | 7 × 2.5 | Unilocular, well circumscribed, smooth borders, tooth displacement | Expansion Perforation |
| 4 | M | 15 | R Max 22–23 | 3 × 3 | Unilocular, well circumscribed, smooth borders, tooth displacement | Expansion |
| 5 | M | 17 | L Max 12–17 | 4.5 × 4 | Unilocular, well circumscribed, smooth borders, tooth displacement | Expansion |
| 6 | F | 58 | L & R Mand 37–48 | 16.5 × 4 | Multilocular, variable circumscription, irregular borders, partially sclerotic with perforations, tooth displacement | Expansion Perforation |
| 7 | F | 11 | L & R Mand 33–46 | 5.7 × 3 | Unilocular, well circumscribed, irregular borders, tooth displacement | Expansion |
| 8 | F | 59 | RMand 47-ramus | 4 × 2.7 | Unilocular, well circumscribed, smooth sclerotic borders | Expansion |
| 9 | F | 59 | Lmand 36–42 | 9 × 4.5 | Multilocular, scalloped borders with perforation and tooth displacement | Expansion Perforation |

*Appeared as case reports[11]

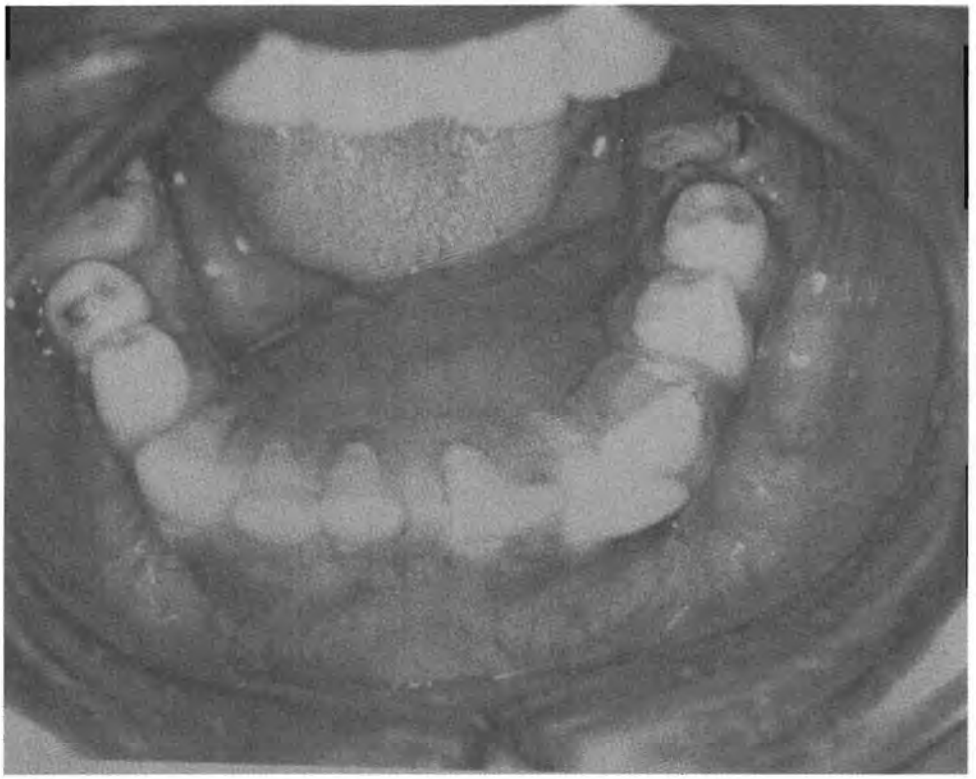

**Figure 1** Case 3: buccal and lingual expansion with tooth displacement

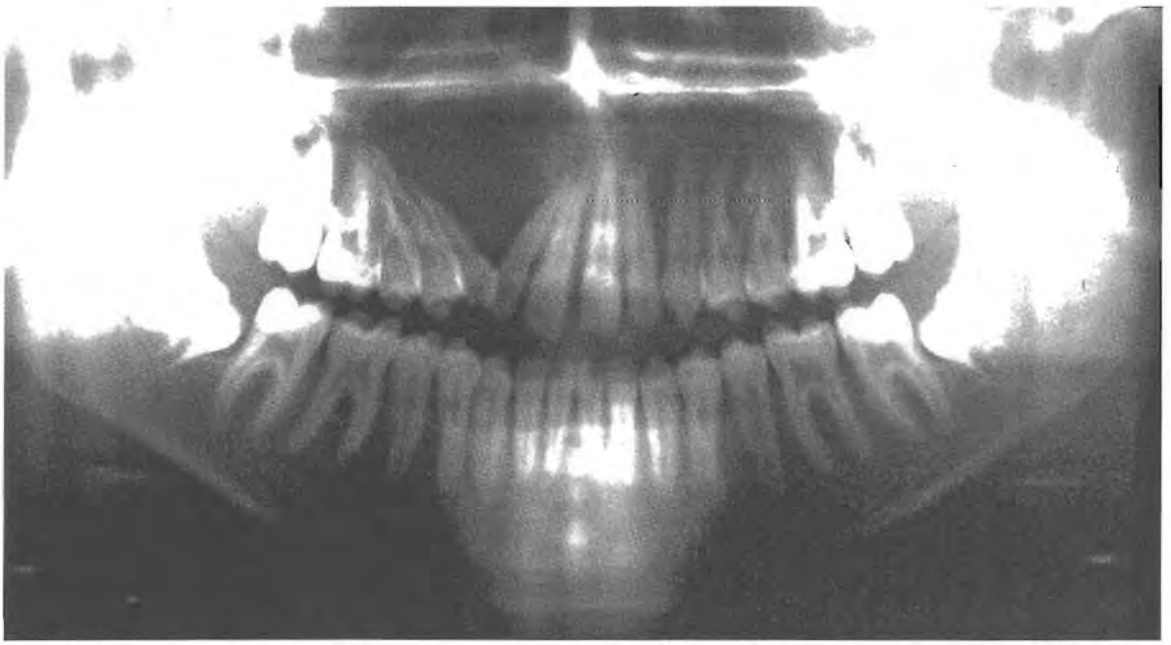

**Figure 2** Case 4: unilocular well-circumscribed cyst in the maxilla between teeth 12 and 13, with smooth borders and tooth displacement

mandible and perforated through the cortex and into the alveolar mucosa (Figures 3 and 4). All mandibular cases were limited to the body and symphysis except one case that extended into the ramus (Figure 5).

All cases fulfilled the histopathological criteria for a diagnosis of GOC advocated by Gardner and co-workers in 1988.[2] The multilocular cases exhibited daughter cyst formation. Early invasion was character-

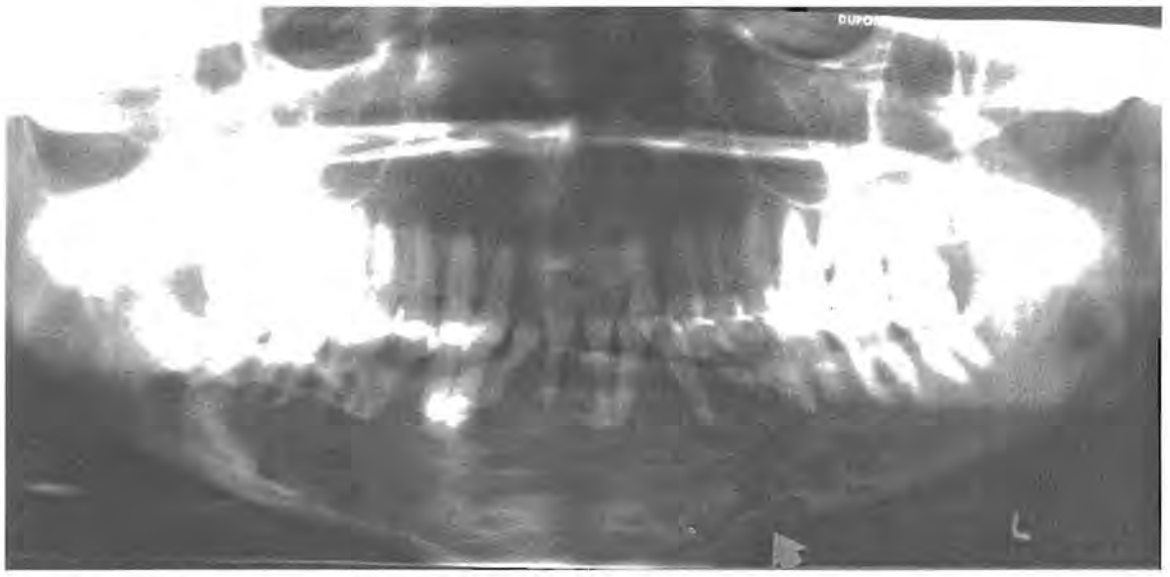

Figure 3 Case 6: multilocular mandibular lesion with partially sclerotic margins showing foci of perforation (arrows)

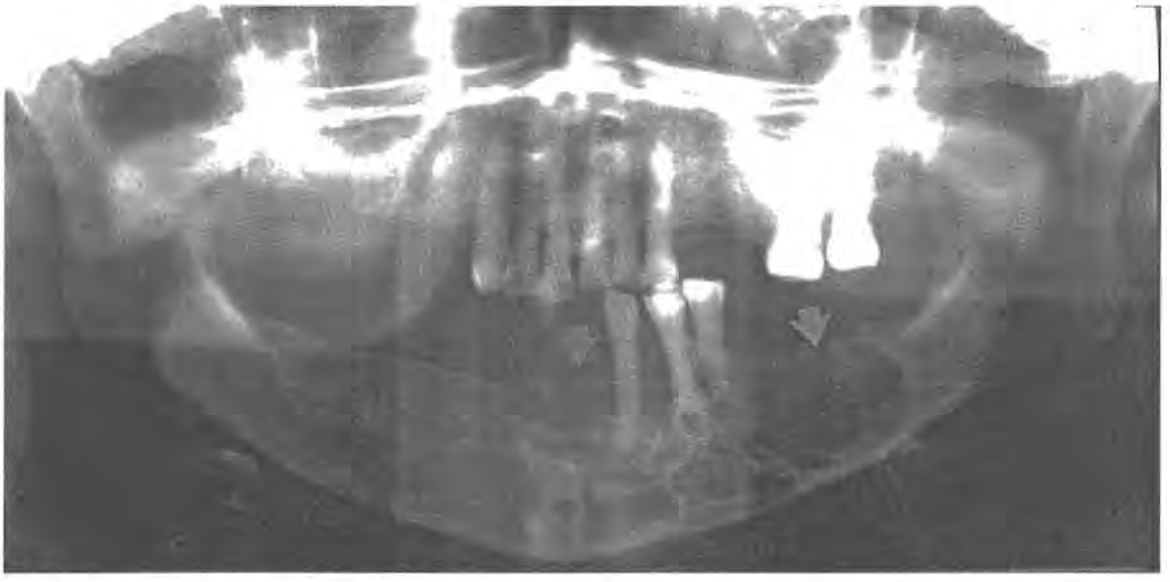

Figure 4 Case 9: multilocular mandibular lesion showing mild tooth displacement and perforation into the alveolar mucosa (arrow)

ized by the formation of adenoid structures which penetrated the connective tissue wall. These features were not seen in the unilocular types.

## Discussion

Our series of nine cases of GOC, of which two had previously been reported[11] was diagnosed over a period of 10 years, confirming its low prevalence. The male to female ratio in our sample was found to be equal. Our mean age (35 years) was a decade younger than generally reported[14,15] mainly due to the significantly younger average age of 24 years at presentation of our male patients. The younger age may represent a racial difference in the manifestation of GOC. This tendency is, however, in agreement with the literature where males are generally reported to be affected at a younger age. Twice as many cases occurred in the mandible than maxilla, corresponding with the findings of other studies.[6,12,14,16] In our sample five of the six mandibular cases involved the symphysis area, the site of prevalence reported in other series. One of our cases occurred in the molar area of the mandible and extended into the ramus. All our maxillary GOC's were present in the globulomaxillary area. Two of these were pear shaped and associated with divergence of the roots of the lateral incisor and canine teeth and one

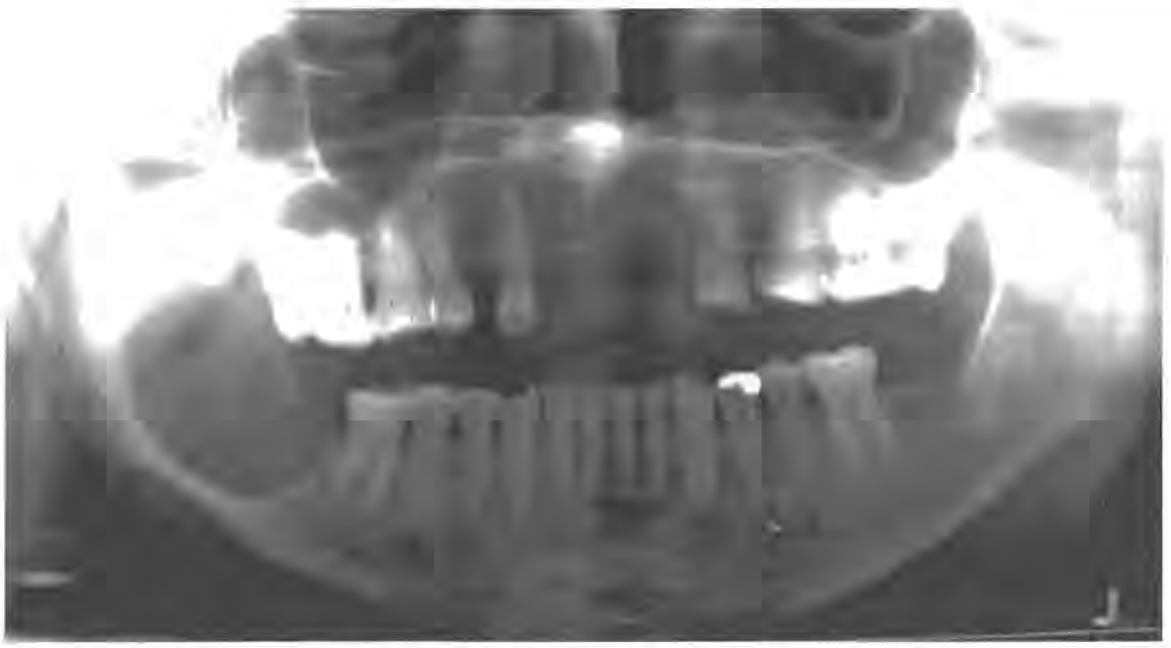

**Figure 5** Case 8: unilocular well-circumscribed lesion with smooth sclerotic borders involving the mandibular ramus

extended distally to the second molar tooth. No maxillary GOC has been reported to occur in another location. The sizes of our lesions ranged between 2 and 16.5 cm in horizontal dimensions, the latter being the largest GOC reported thus far. The two multilocular GOC's were the largest lesions in our series, measuring 16.5 and 9 cm in horizontal dimension respectively. This may indicate that multilocularity is a size dependant phenomenon, developing only in the larger lesions. All our GOC's which measured in excess of 6 cm showed bone expansion with perforation, a feature supporting their aggressive expansile behaviour.[3]

Most authors conclude that there is no radiological feature distinctive for GOC.[14–16] All maxillary GOC's in our series were well circumscribed unilocular with regular borders, findings that correspond with those of a previous paper.[15] In our sample unilocular GOC's with irregular borders were common in the mandible (two out of four lesions). Two of our mandibular lesions showed sclerotic borders and one case scalloped between the roots of mandibular canine and premolar teeth. The two largest GOC were multilocular and resembled ameloblastoma radiologically. Radiological features which may be helpful in distinguishing multilocular GOC's from ameloblastomas include irregular loculations and a partially sclerotic border with foci of perforation. One GOC was, however, reported to be associated with an ameloblastoma[2] and representative histological sampling of large multicystic lesions is required to exclude the possibility of this manifestation. The question whether a GOC in association with an ameloblastoma represents a collision growth of two initially distinct lesions or a metaplastic phenomenon within an ameloblastoma (or GOC) remains speculative. The epithelial lining of a GOC may possess the ability to induce an ameloblastomatous proliferation in the connective tissue wall, similar to the phenomenon described in calcifying odontogenic cysts.[17] The proliferative capacity of the lining of GOC's could explain the histogenesis of the squamous odontogenic tumour-like proliferation reported in the wall of a GOC.[6] The presence of the epithelial plaques in a small number of GOC's is in our opinion not sufficient to confirm an association between this aggressive cyst type and the more innocuous lateral periodontal–and botryoid odontogenic cysts. Both our multilocular GOC's showed proliferations that infiltrated the connective tissue wall. This should not be confused with the plaques in the latter two cyst types, which are in fact localized thickenings consisting of mitotically inactive clear cells.[18] The GOC's in our sample were not associated with impacted teeth but rather tended to displace erupted teeth. This finding is indicative that GOC's generally develop after all permanent teeth have erupted. No significant resorption of the roots of involved teeth were observed in our study.

Taking the above mentioned radiological appearances into account, the provisional diagnoses for GOC on a radiograph would include odontogenic keratocyst, unicystic and multicystic ameloblastoma, lateral periodontal cyst, botryoid odontogenic cyst, simple bone cyst and central mucoepidermoid tumour. Features which may increase a suspicion of GOC include a sclerotic border with fine perforations or a pear shaped unilocular cyst with smooth margins in the globulo-maxillary region of the maxilla. Histologically the central muco-epidermoid carcinoma is considered the most important differential diagnosis.[18] Care should

furthermore be taken not to interpret mucous cell metaplasia, which occurs commonly in a variety of odontogenic cysts and even ameloblastomas[19] as foci of GOC transformation. In order to prevent this from occurring, microscopic criteria for the diagnosis of GOC should stringently be applied. These include a superficial layer of cuboidal or columnar epithelial cells occasionally with cilia and a glandular or pseudoglandular structures and intraepithelial crypts frequently containing mucin. The remaining of the cyst may be lined by thin non keratinised stratified squamous epithelium.[3] Our study showed that the multicystic type exhibits neoplastic features with infiltration of the surrounding tissue and daughter cyst formation. The distinction between low-grade central mucoepidermoid carcinoma and GOC is difficult, if not impossible. Both are reported to be unilocular or multilocular and may infiltrate and destroy bone. Microscopically, the lining of the cystic spaces of both exhibit squamous-, cylindrical- and cuboidal epithelium and mucus producing cells arranged in papillary folds. Within the epithelial lining of both mucus containing crypts (or gland-like structures) are found.[20,21] The only feature which has not been reported in low-grade central mucoepidermoid carcinoma and which may justify the existence of GOC as a separate entity is occasional presence of epithelial plaques, similar to those seen in lateral periodontal cysts.

In conclusion, in view of the histogenetic relationship that had been proposed between GOC and central mucoepidermoid carcinoma of the jaw,[1,10,22] the possibility that both entities represent a spectrum of one disease, should be investigated.

## References

1. Padayachee A, Van Wyk CW. Two cystic lesions with features of both the botryoid odontogenic cyst and the central mucoepidermoid tumor: sialo-odontogenic cyst? *J Oral Pathol* 1987; **16:** 499–504.
2. Gardner DG, Kessler HP, Morency R, Schaffner DL. The glandular odontogenic cyst: an apparent entity. *J Oral Pathol* 1988; **17:** 359–366.
3. Shear M. *Cysts of the oral regions*. 3rd edn, Cambridge: University Press, 1992: pp.72–74.
4. Sadeghi EM, Weldon LL, Kwon PH, Sampson E. Mucoepidermoid odontogenic cyst. *Int J Oral Maxillofac Surg* 1991; **20:** 142–143.
5. Hodson JJ. Muco-epidermoid odontogenic cysts of the jaws with special reference to those in the mandible. *Proc R Soc Med* 1956; **49:** 637–641.
6. Patron M, Colmero C, Larrauri J. Glandular odontogenic cyst: Clinicopathologic analysis of three cases. *Oral Surg Oral Med Oral Pathol* 1991; **72:** 71–74.
7. Takeda Y. Glandular odontogenic cyst mimicking a lateral periodontal cyst: a case report. *Int J Oral Maxillofac Surg* 1994; **23:** 96–97.
8. Hussain K, Edmondson HD, Browne RM. Glandular odontogenic cysts. Diagnosis and treatment. *Oral Surg Oral Med Oral Pathol* 1995; **79:** 593–602.
9. Semba I, Kitano M, Mimura T, Miyawaki A. Case Report. Glandular odontogenic cyst: analysis of cytokeratin expression and clinicopathological features. *J Oral Pathol Med* 1994; **23:** 377–382.
10. Ficarra G, Chou L, Panzoni E. Glandular odontogenic cyst (sialo-odontogenic cyst). *Int J Oral Maxillofac Surg* 1990; **19:** 331–333.
11. Van Heerden WFP, Raubenheimer EJ, Turner MJ. Glandular odontogenic cyst. *Head and Neck* 1992; **14:** 316–320.
12. Toida M, Nakashima E, Okumura Y, Tatematsu N. Glandular odontogenic cyst: A case report and literature review. *J Oral Maxillofac Surg* 1994; **52:** 1312–1316.
13. Economopoulou P, Patrikiou A. Glandular odontogenic cyst of the maxilla: a report of a case. *J Oral Maxillofac Surg* 1995; **53:** 834–837.
14. Magnusson B, Göransson L, Ödesjö B, Gröndahl K, Hirsch JM. Glandular odontogenic cyst. Report of seven cases. *Dentomaxillofac Radiol* 1971; **26:** 26–31.
15. Koppang HS, Johannessen S, Haugen LIC, Haanaes HR, Solheim T, Donath K. Glandular odontogenic cyst (sialo-odontogenic cyst): a report of two cases and literature review of 45 previously reported cases. *J Oral Pathol Med* 1998; **27:** 455–462.
16. Ramer M, Montazem A, Lane SL, Lumerman H. Glandular odontogenic cyst. Report of a case and review of the literature. *Oral Surg Oral Med Oral Pathol* 1997; **84:** 54–57.
17. Praetorius F. Calcifying odontogenic cyst. Range, variations and neoplastic potential. *Acta Odontol Scand* 1981; **39:** 237–240.
18. Waldron CA. Odontogenic cysts and tumors. In: Neville BW, Damm DD, Allen CM, Bouquot JE (eds). *Oral and Maxillofacial Pathology*. Philadelphia: WB Saunders 1995: pp. 493–530.
19. Raubenheimer EJ, van Heerden WFP, Noffke CEE. Infrequent clinicopathological findings in 108 ameloblastomas. *J Oral Pathol Med* 1995; **24:** 227–232.
20. Auclair PL, Ellis GL. Mucoepidermoid carcinoma. In: *Surgical Pathology of the Salivary Glands*. Philadelphia: WB Saunders 1991: pp. 291–295.
21. Kramer IRH, Pindborg JJ, Shear M. *Histological typing of odontogenic tumours*. 2nd edn. Berlin: Springer-Verlag, 1992; p. 28.
22. Waldron CA, Koh ML. Central mucoepidermoid carcinoma of the jaws: a report of four cases with analysis of the literature and discussion of the relationship to mucoepidermoid, sialodontogenic, and glandular odontogenic cysts. *J Oral Maxillofac Surg* 1990; **48:** 871–877.

SPECIAL ARTICLE

# Classification of Odontogenic Cysts of the Jaws

E.J. Raubenheimer, J. Kreidler, W.F.P. van Heerden

*Recent developments in the classification and diagnosis of cysts of the jaws necessitate a revision of the topic. This paper discusses the revised World Health Organisation classification of odontogenic cysts and illustrates short descriptions of cyst types with appropriate examples.*

## INTRODUCTION

Cysts are pathological, fluid filled cavities lined by epithelium. They are more common in the jaws than in any other bone because of the epithelial rests remaining in the tissue after dental development. Cysts of odontogenic origin are the most common cause of chronic swelling of the jaws and have been recognised as diagnostic problems for a long time. During the past few years, numerous articles have appeared regarding the pathogenesis, behaviour, diagnosis and treatment of the different types of jaw cysts and various new concepts have since emerged. In order to standardize the diagnoses of jaw cysts, utilization of uniform diagnostic criteria is essential. The purpose of this article is to present the revised World Health Organisation's classification of odontogenic cysts of the jaws and to illustrate the typical features with appropriate examples obtained from the files of the Department of Oral Pathology, Medical University of Southern Africa.

*Erich J Raubenheimer, MChD (Oral Path); Joachin Kreidler*, PhD; Willie FP van Heerden, MChD (Oral Path), Department of Oral Pathology and Oral Biology, MEDUNSA, and *Department of Maxillofacial and Oral Surgery, Ulm, Germany.*

## CLASSIFICATION

The classification of the odontogenic cysts of the jaws is based on that recommended in the World Health Organization's (WHO) publication *Histological Typing of Odontogenic Tumours*[1] and a recently published textbook on oral cysts[2] (Table 1). The histogenetic division into 'Developmental' and 'Inflammatory' groups remain unchanged.

*Table 1.*

**1. Developmental**
- 1.1 Gingival cyst of infants
- 1.2 Odontogenic keratocysts
- 1.3 Dentigerous (follicular) cyst
- 1.4 Eruption cyst
- 1.5 Lateral periodontal cyst
- 1.6 Gingival cyst of adults
- 1.7 Botryoid odontogenic cyst
- 1.8 Glandular odontogenic cyst

**2. Inflammatory**
- 2.1 Radicular cyst (apical and lateral)
- 2.2 Residual cyst
- 2.3 Paradental cyst
- 2.4 Inflammatory collateral cyst

This classification excludes the calcifying odontogenic cyst (which is now categorized as an odontogenic tumour) as well as other cystic tumours like the unicystic ameloblastoma. It is furthermore noteworthy that the concept of cysts developing in the closure lines of embryologic processes (such as median palatine cyst, median mandibular cyst and globulo-maxillary cyst) which were previously classified as of non odontogenic origin, has been rejected after detailed clinical[3,4] and embryological[5,6] studies.

## DEVELOPMENTAL

### Gingival cysts of infants

Gingival cysts of infants, also referred to as Bohn's nodules, occur commonly on the alveolar processes of newborn infants (Figure 1). They soon disappear through involution and are seldom seen after three months of age. These cysts arise from the dental lamina and although rarely biopsied, are lined by keratinizing squamous epithelium.[2]

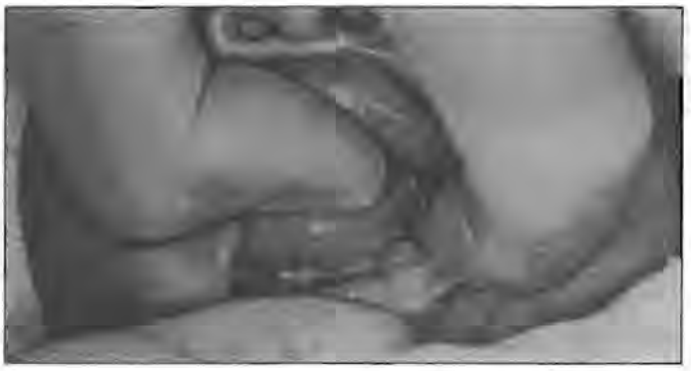

**Figure 1.** *Gingival cyst of the infant on the left mandibular alveolus.*

## Odontogenic keratocysts

The term 'primordial cyst', which was often used synonomously with odontogenic keratocyst, has fallen in disuse because no convincing evidence for development from a tooth primordium has yet been forwarded. There is however, evidence supporting origin from primordial odontogenic epithelium, that is, dental lamina or its remnants[7,8]. Although other odontogenic cysts may exhibit foci of squamous metaplasia, odontogenic keratocysts are primarily recognised by their stretched and keratinized epithelial lining with a well defined, often palisaded basal cell layer. Basal cell budding, as well as daughter cyst formation are found in odontogenic keratocysts and are especially pronounced in patients with the naevoid basal cell carcinoma syndrome in which multiple keratocysts occur. These phenomena as well as the fragility of the cyst wall are the primary causes for incomplete surgical removal and the high recurrance rate. Odontogenic keratocysts may occur in the place of a tooth (replacement variety), around the crown of an impacted tooth (envelopmental variety) in the ramus of the mandible (extraneous variety) or between the roots of adjacent teeth (collateral variety)[9]. Although the majority present as unilocular radiolucencies (Figure 2), scalloped margins may be misinterpreted as multilocularity leading to an erroneous diagnosis of ameloblastoma[2]. The envelopmental variety is often indistinguishable radiologically from a dentigerous cyst and the collateral variety from a lateral periodontal or lateral placed radicular cyst.

## Dentigerous (follicular) cysts

A dentigerous cyst is one which encloses the crown of an unerupted tooth by expansion of its follicle, and is attached to its neck[2] (Figure 3). It probably developes by accumulation of fluid between the reduced enamel epithelium and the enamel after formaton of the crown has been completed. The diagnosis of dentigerous cyst should not be made on radiographic evidence only, otherwise keratocysts of the envelopmental variety and unilocular ameloblastomas involving adjacent unerupted teeth, are liable to be misdiagnosed. The wall of a dentigerous cyst is lined by thin epithelium of two to three layers of undifferentiated cells derived from reduced enamel epithelium.

**Figure 2.** *Odontogenic keratocyst in the anterior mandible. Note the sclerotic margin surrounding the cyst.*

**Figure 3.** *Panoramic view of a dentigerous cyst surrounding the crown of an impacted maxillary central canine. Note the displacement of the permanent lateral incisor and canine.*

## Eruption cyst

An eruption cyst is in effect a dentigerous cyst which occurs in the soft tissues. There is usually no radiographic evidence of bone involvement. The cyst is exposed to masticatory trauma and many eruption cysts burst spontaneously with only few requiring surgical exposure of the involved tooth.

## Lateral periodontal cyst

The designation 'lateral periodontal cyst' is confined to those cysts which occur in the lateral periodontal position and in which an inflammatory aetiology and a diagnosis of collateral keratocyst have been excluded on clinical and histological grounds.[10] Radiographs show a round or oval, well circumscribed, radiolucent area somewhere between the apex and cervical margin of a vital tooth (Figure 4). Various theories on the histogenesis of this cyst type were forwarded, of which the proposal that it arises initially as a dentigerous cyst developing by expansion of the follicle along the lateral surface of the erupting tooth is an attractive one[11]. Most commonly, the lateral periodontal cyst is lined by a thin, non keratinized layer of squamous or cuboidal epithelium with small inconspicuous nucleii and convoluted epithelial plaques, which develop as a result of localized proliferation of cells[2].

The botryoid odontogenic cyst is a multilocular variant of the lateral periodontal cyst. This rare cyst has a

**Figure 4.** *Periapical radiograph showing a lateral periodontal cyst in the alveolus between teeth 35 and 36.*

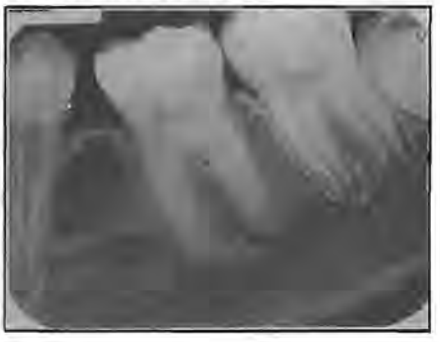

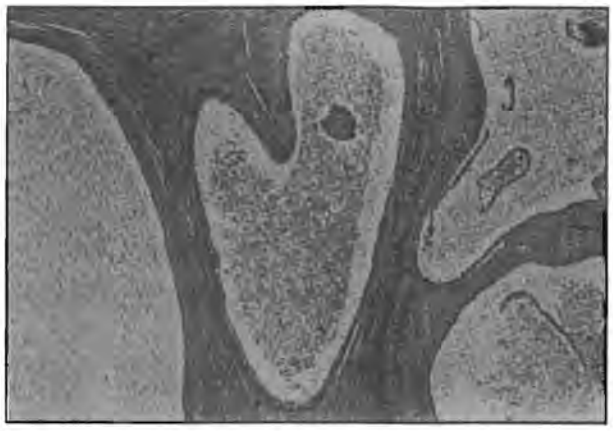

**Figure 5.** *Multicystic appearance of a botryoid odontogenic cyst (H&E stain X40).*

lining similar to the lateral periodontal cyst with thin connective tissue septae separating distinct cystic cavities (Figure 5).

## Gingival cyst of adults

The gingival cysts of adults is located in the gingival soft tissue and presents as a gingival swelling without any radiographic signs of bone destruction. Although many theories have been proposed on its histogenesis, the most favoured is derivation from gingival odontogenic epithelial cell nests[2] or reduced enamel epithelium after the eruption of a tooth.[12,13] If the latter theory is accepted, gingival cysts in adults may represent the soft tissue counterpart of lateral periodontal cysts. This is supported by the numerous similarities both clinically and histologically between these two cyst types.

## Glandular odontogenic cyst

A cyst with fairly typical histological features and which has some characteristics in common with lateral periodontal cyst has recently been reported[14,15]. Radiographically, some cases exhibit a unilocular radiolucency with either smooth or scalloped margins (Figure 6), while others are distinctly multilocular. The cyst may be lined in parts by a non-keratinized stratified squamous epithelium. The superficial layer of the epithelial lining consists of columnar or cubiodal cells with occasional cilia and the epithelium has a glandular or pseudo glandular structure, with intra-epithelial crypts lined by cells similar to those on the surface.

# INFLAMMATORY

## Radicular cyst

A radicular cyst is one which arises from epithelial residues in the periodontal ligament as a result of inflammation[2]. The inflammation usually follows necrosis of the dental pulp and the identification of a non vital tooth associated with the cyst is an important diagnostic parameter. Although these cysts are usually located around the apex of a tooth (Figure 7), they may also be found on the lateral surfaces of a root in association with the opening of an accessory pulpal canal. Radiographically these cysts are characterized by round or ovoid radiolucencies surrounded by a narrow radio-opaque margin which extends from the lamina dura of the involved tooth. The size of the lesion is not reliable in distinguishing it from a periapical granuloma, unless it is larger than 2 cm in diameter in which case the lesion is most likely a radicular cyst.[16] Almost all radicular cysts are lined

**Figure 6.** *Glandular odontogenic cyst presenting as an unilocular cyst in the maxilla. Note the displacement of the adjacent teeth.*

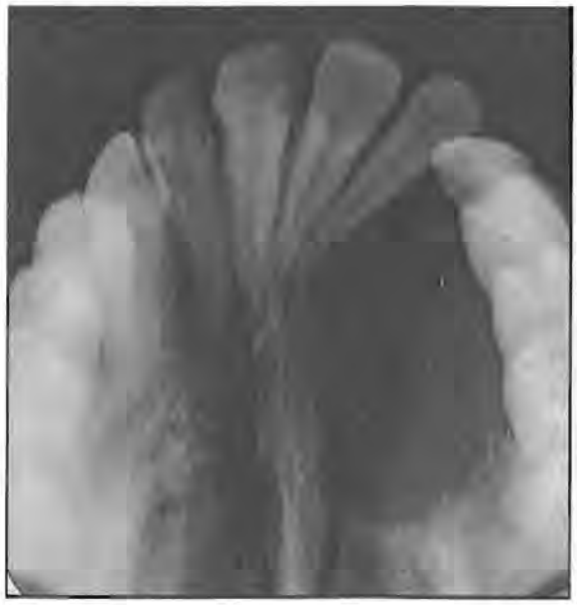

**Figure 7.** *Radiograph of a radicular cyst surrounding the apex of a maxillary incisor.*

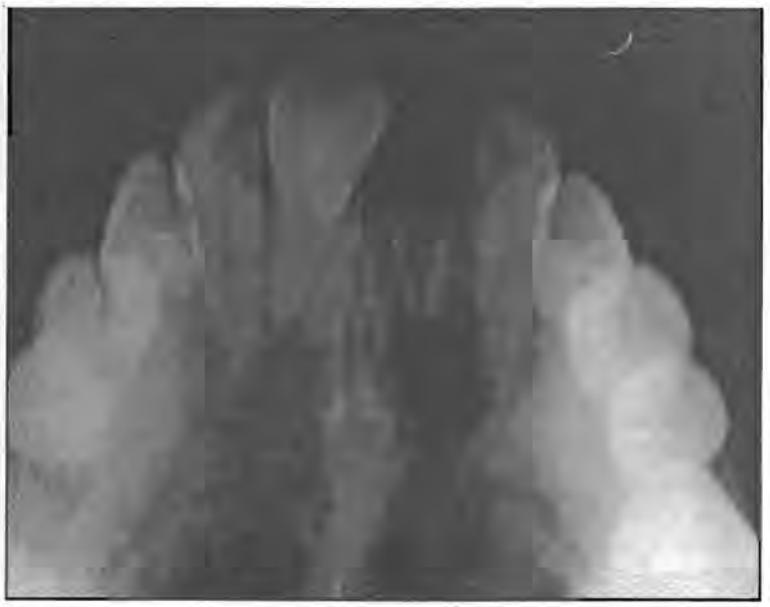

wholly or in part by stratified squamous epithelium. The epithelial lining may proliferate and exhibits arcading and a considerable degree of spongiosis with an intense inflammatory infiltrate.

### Residual cyst

A residual cyst can be described as a radicular cyst of which the associated tooth has been extracted. All the radiographic and histological features of radicular cysts except for the association with a non-vital tooth therefore apply to residual cysts.

### Paradental cyst

Craig (1976) wrote the first detailed account of a cyst of inflammatory origin which occured on the lateral aspect of the roots of partially erupted mandibular third molars where there was an associated history of pericoronitis. In these cases the teeth are vital and radiographic examination shows a well demarcated radiolucency distally to a partially erupted tooth: Ackerman, Cohen and Altini[17] like Craig[18] favour origin from reduced enamel epithelium but suggested that cyst formation occurs as a result of unilateral expansion of the dental follicle secondary to inflammatory destruction of the periodontium and alveolar bone. This is different from the histogenesis of dentigerous cysts where expansion occurs primarily with consequent bone destruction.

Paradental cysts are microscopically indistinguishable from radicular cysts and a proper clinical history and radiograph must accompany the biopsy in order to facilitate a correct diagnosis.

### Inflammatory collateral cyst

This rare cyst type occurs as a result of inflammatory process in the periodontal pocket[2]. The associated tooth is vital and the cyst is microscopically indistinguishable from radicular cysts. Microscopic diagnosis relies heavily on adequate clinical information. This cyst appears to favour developing buccally to the lower first or second molars.

## CONCLUSION

Accurate diagnosis of cysts of odontogenic origin is important as various cyst types like odontogenic keratocysts and glandular odontogenic cysts are aggressive lesions and tend to recurr after incomplete removal. It is important that clinicians are aware of the unreliability of radiographic interpretations. On the other hand, a microscopic diagnosis of biopsies taken from densely inflamed cyst walls is often difficult, if not impossible, to interpret without clinical information and radiographs. A high degree of diagnostic accuracy, when dealing with jaw cysts, can only be achieved through communication between the clinician and resident pathologist.

#### REFERENCES

1. Kramer IRH, Pindborg JJ and Shear M. *Histological Typing of Odontogenic Tumours* 1992. Berlin, Springer Verlag.
2. Shear M. *Cysts of the Oral Regions.* Third Edition. Oxford, Wright 1992.
3. Christ TF, The globulo-maxillary cyst - an embryological misconception. *Oral Surg* 1970; **30**, 515-26.
4. Kitimura H. Origin of non-odontogenic cysts: an embryological consideration of fissural cysts. *Bull Kanagawa Dent Coll* 1976; **4**, 1-18.
5. Sicher H. Anatomy and Oral Pathology. *Oral Surgery, Oral Medicine, Oral Pathology* 1962; **15**, 1264-69.
6. Arey LB. *Developmental Anatomy,* 7th edn. Philadelphia and London, Saunders 1965; p 205.
7. Soskolne WA and Shear M. Observations on the pathogenesis of primordial cysts. *Br Dent J* 1967; **123**, 321-26.
8. Toller PA. Origin and growth of cysts of the jaws. *Ann Royal Coll Surg.* 1967; **40**, 306-336.
9. Main DMG. Epithelial jaw cysts - a clinicopathological reappraisal. *Br J Oral Surg* 1970; **8**, 114-125.
10. Shear M and Pindborg JJ. Microscopic features of the lateral periodontal cyst. *Scan J Dent Res* 1975; **83,** 103-110.
11. Shafer WG, Hine MK and Levy BM. A textbook of Oral Pathology, 4th edn, Philadelphia and London, Saunders 1983.
12. Wysocki GP, Brannon RB, Gardner DG and Sapp P. Histogenesis of the lateral periodontal cyst and the gingival cyst of the adult. *Oral Surg* 1980; **50**, 327-334.
13. Buchner A, Hansen LS. The histomorphologic spectrum of the gingival cyst in the adult. *Oral Surg* 1979; **48**, 532-539.
14. Padayachee A and van Wyk CW. Two cystic lesions with the features of both the botryoid odontogenic cyst and the central mucoepidermoid tumor: sialo-odontogenic cyst. *J Oral Path* 1987; **16**, 449-504.
15. Gardner DG, Kessler HP, Morency R and Schaffner DL. The glandular odontogenic cyst: an apparent entity. J *Oral Path* 1988; **17**, 359-366.
16. Natkin E, Oswald RJ and Carnes LI. The relationship of lesion size to diagnosis, incidence and treatment of periapical cysts and grandulomas. *Oral Surg* 1984; **57**, 82-94.
17. Ackerman G, Cohen M and Altini M. The paradental cyst: a clinicopathological study of 50 cases. *Oral Surg* 1987; **64**, 308-12.
18. Craig GT. The paradental cyst. A specific inflammatory odontogenic cyst. *Br Dent J* 1976; **141**, 9-14.

## COMING IN FUTURE ISSUES

### ARTICLES WRITTEN BY LOCAL AUTHORS

- **Intra-oral porcelain fractures: Repair techniques and materials**
- **The role of orthodontics in restorative dentistry and periodontics**
- **C&B-Metabond: The difference between success and failure**
- **Pulpal obliteration in a case of renal transplantation and anorexia nervosa**
- **Dentine bonding: The indispensible link in modern dentistry**

Journal of the Dental Association of South Africa, **48**, 557-559.

# Differential diagnosis of dentigerous cyst-like lesions: Clinico-pathologic features of 63 cases



KS Hauk, EJ Raubenheimer, WFP van Heerden, *B Buch and **AF Dreyer

Department of Oral Pathology and Oral Biology, *Department of Diagnostics and Radiology, **Department of Maxillo-Facial and Oral Surgery, PO Medunsa, 0204.

*Keywords: odontogenic cyst; dentigerous cyst; unicystic ameloblastoma; keratocyst.*

## SUMMARY

*A series of unilocular pathological conditions resembling dentigerous cysts was analyzed and the clinical and radiographic features correlated with the microscopic diagnosis. The most common lesions were found to be true dentigerous cysts followed by unicystic ameloblastomas and odontogenic keratocysts. Unicystic ameloblastomas with a dentigerous cyst-like appearance occurred most frequently in the mandibular third molar region and commonly caused expansion of the mandible. The adjacent teeth in these cases showed a high occurrence rate of root resorption. Unlike the site distribution of true dentigerous cysts reported in other series, 50 per cent of our cases occurred in the maxillary anterior and premolar regions. Our study emphasizes the importance of microscopic examination of all pericoronal cystic lesions.*

## OPSOMMING

*Die kliniese- en radiologiese beeld van 63 gevalle van unilokulêre patologiese toestande wat tandhoudende siste naboots, is vergelyk met die mikroskopiese diagnose. Die mees algemene toestand wat voorgekom het, was tandhoudende siste, gevolg deur unisistiese ameloblastoom en odontogene keratosiste. Unisistiese ameloblastome met die radiologiese beeld van 'n tandhoudende sist, het mees algemeen in die mandibulêre derde molaar area presenteer en het dikwels beenekspansie veroorsaak. Die aangrensende tande het 'n hoë frekwensie van eksterne wortelresorpsie getoon. Anders as in ander reekse, het 50 persent van tandhoudende siste in die maksillêre anterior en premolaar areas voorgekom. Hierdie studie beklemtoon die belang van mikroskopiese ondersoek van alle perikoronale sisteuse letsels.*

## INTRODUCTION

A dentigerous cyst is defined as a unicystic cavity which encloses the crown of an unerupted tooth by expansion of its follicle and is attached to the neck of the tooth (Shear, 1992). In a radiographic context, a radiolucent area surrounding the crown of an unerupted tooth may be seen with odontogenic keratocysts of the envelopmental or follicular variety as well as unicystic ameloblastomas involving adjacent unerupted teeth, and these may be misinterpreted as dentigerous cysts. This could have prognostic consequences as the recurrence rates of the various pathologic lesions that envelop the crown of a tooth vary significantly. Simple enucleation is an adequate form of treatment for dentigerous cysts but more extensive surgery is required for unicystic ameloblastomas and odontogenic keratocysts. Even with adequate treatment, the recurrence rates of unicystic ameloblastomas and keratocysts are reported to be high (Vedtofte and Praetorius, 1979; Ueno *et al.*, 1986). Accurate diagnosis of jaw cysts is therefore essential for adequate treatment planning.

The purpose of this study was to appraise the clinico-pathologic features of pericoronal radiolucencies resembling dentigerous cysts.

## MATERIAL AND METHODS

Sixty three lesions with a radiologic appearance of a dentigerous cyst were retrieved from the files of the department of Maxillo-Facial and Oral Surgery at the Medical University of Southern Africa. This hospital is a reference centre for the Northern Transvaal region and all patients in the study are Black and mostly of rural origin. The radiologic appearance with special reference to the size (longest axis measured on panoramic radiograph) and location of the lesion, the presence or absence of root resorption of adjacent teeth, expansion of cortical plates and displacement of the associated tooth, was compared with the age, sex and microscopic diagnosis of the lesion.

## RESULTS

Sixty-three unilocular paracoronal cystic lesions resembled dentigerous cysts radiologically. The histological diagnosis of these lesions are listed in

Article received: 18/1/93
approved for publication: 24/3/93

KS Hauk, Dr Med, Dr Med.Dent, was a visting lecturer from Ulm University, Germany, at the time of compiling this article.
EJ Raubenheimer, MChD
WFP van Heerden, MChD
B Buch, BSc Hons., MSc Dent.
AF Dreyer, M Dent

*Fig. 1:* **Unicystic ameloblastoma with root resorption of the associated teeth.**

*Fig. 2:* **Adenomatoid odontogenic tumour causing tooth displacement and root resorption.**

*Fig. 3:* **Unicystic ameloblastoma of the left mandible showing enlargement in all dimensions.**

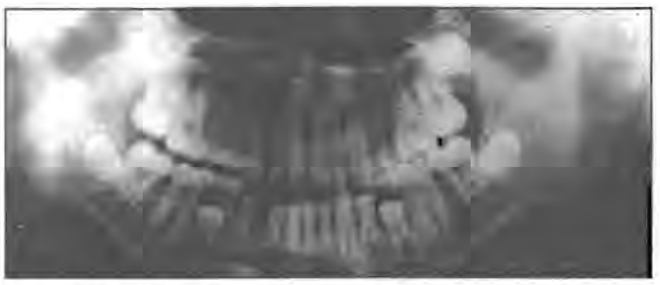

*Fig. 4:* **Dentigerous cyst of the mandible showing enlargement along the medullary space.**

*Fig. 5:* **Calcifying odontogenic cyst of the mandible associated with an impacted canine and exhibiting mural calcifications (arrows).**

Table I. Three of the calcifying odontogenic cysts with a dentigerous cyst-like appearance were subclassified according to Praetorius *et al.*, (1981) as type IA, and one each as type IB and IC respectively. The sex distribution, mean age at presentation, average size of the cyst as measured on a

*Fig. 6:* **Multiple keratocysts involving the left and right mandibular ramus and right globulomaxillary area in a patient with the naevoid basal cell carcinoma syndrome.**

panoramic radiograph and the presence of root resorption and tooth displacement are shown in Table I.

Unicystic ameloblastomas showed an equal sex distribution, while dentigerous cysts, odontogenic keratocysts and calcifying odontogenic cysts were more common in males. Adenomatoid odontogenic tumours were found in females only. The mean age at presentation of the six cyst types were not found to differ significantly. The mean size of the unicystic ameloblastomas were significantly larger than the odontogenic keratocysts and dentigerous cysts ($p<0,005$) while odontogenic keratocysts' mean size were significantly larger than that of dentigerous cysts ($p<0,05$). Root resorption was most frequently observed in unicystic ameloblastomas (64 per cent of cases) (Fig. 1) and calcifying odontogenic cysts (60 per cent of cases). Displacement of non-involved teeth was a constant finding in cystic adenomatoid odontogenic tumours (Fig. 2). The enlargement of unicystic ameloblastomas occurred in all dimensions and frequently caused bony expansion (Fig. 3). Enlargement of follicular and odontogenic keratocysts in the mandible appeared to follow the medullary space initially (Fig.4) with bony expansion seen only in the largest examples.

All paradental cysts were associated with partially erupted third molars. Six cystic adenomatoid odontogenic tumours occurred in the maxilla and one in the mandible. One very large lesion of the latter type extended across the maxillary midline. Three calcifying odontogenic cysts presented in the maxilla and two in the mandible. One cyst in each jaw showed radiographic evidence of calcifications (Fig. 5).

Thirteen dentigerous cysts were located in the maxilla, the majority of which were associated with impacted central incisors (4 cysts), canines (2 cysts) and premolars (4 cysts). In the mandible, only 3 dentigerous cysts involved third molars; one, a second molar, while two involved canines. One dentigerous cyst was associated with a primary maxillary canine. Eight odontogenic keratocysts were located in the mandibular (7 cases) or maxillary (one case) third molar areas and 5 presented in the canine region (3 maxillary and 2 mandibular). Two patients presenting with the basal cell nevus syndrome had multiple cysts

Table I: *Clinical data.*

| | n | Sex | | Mean Age (SD) | Mean Size in mm (SD) | Root Resorption | Tooth Displacement |
|---|---|---|---|---|---|---|---|
| | | Male | Female | | | | |
| Unicystic Ameloblastoma | 14 | 7 | 7 | 15,5 ±6,3 | 80 ±22,7 | 9 | 5 |
| Dentigerous Cyst | 21 | 16 | 5 | 16 ±16,2 | 35 ±11,5 | 4 | 5 |
| Odontogenic Keratocyst | 13 | 10 | 3 | 15 ±12,5 | 45 ±20,1 | 1 | 3 |
| Adenomatoid Odontogenic Tumour | 7 | 0 | 7 | 12 ±3,9 | 45 ±15,7 | 1 | 7 |
| Calcifying Odontogenic Cyst | 5 | 4 | 1 | 23 ±7,0 | 40 ±6,5 | 2 | 3 |
| Paradental Cyst | 3 | 2 | 1 | 21 ±2,0 | 10 ±12,7 | 0 | 0 |

(Fig. 6). The unicystic ameloblastomas showed a predeliction for the mandibular third molar region (11 cysts) followed by the mandibular canine region (3 cysts). No unicystic ameloblastomas with a dentigerous cyst-like appearance occurred in the maxilla.

## DISCUSSION

The importance of an accurate diagnosis of a lesion with a dentigerous cyst-like appearance, especially in a Black population sample in which dentigerous cysts are less common than in Whites (Shear, 1992), cannot be over emphasized. By the same token the presence of unicystic ameloblastomas must not be underestimated, being the second most common cystic lesion found in our patients. Outstanding characteristics of this potentially aggressive neoplasm is its large size when compared to the other cysts, its tendency to expand more symmetrically than other cystic lesion in the mandible as well as its common association with root resorption of adjacent teeth. Adenomatoid odontogenic tumours were found in females only but although the majority seem to affect the anterior maxilla, it also occurred in the mandible in one instance. Tooth displacement was more frequently observed in adenomatoid odontogenic tumours than in any of the other cystic lesions. Dentigerous cysts were more frequently encountered in the anterior maxilla and their most frequent association with impacted mandibular third molars (Shear, 1992) was not found in our study. The lower frequency of impacted third molars in Blacks (Brown *et al.*, 1982) may account for this observation in our exclusively Black sample. The attachment of the cyst wall to the impacted tooth is reported to extend more apically in ameloblastomas than dentigerous cysts (Ikeshima *et al.*, 1990). In large examples of dentigerous cysts the associated tooth is often rotated, making this measurement difficult to interpret on panoramic radiographs.

Our study does not support the report that there is a frequent occurrence of root resorption in association with dentigerous cysts (Struthers and Shear, 1976). The site distribution of odontogenic keratocysts in our study conform to that of another series (Shear, 1992). Forssell (1980) observed a relationship between the cyst and the crown of a tooth in 41 per cent of a series of 135 cases. McIvor (1972) however, demonstrated this relationship exclusively in the mandible. In our study, 4 maxillary odontogenic keratocysts presented in association with impacted teeth. The frequent association of odontogenic keratocysts with impacted teeth have led Altini and Cohen (1980) to introduce the term "follicular primordial cyst" for this group of lesions. They postulated that this association may arise following eruption of a tooth into a pre-existing cystic cavity in the same way as a tooth erupts into the oral cavity. Although we have no microscopic evidence, we believe that this hypothesis may be extended to all cysts in our series, except for the follicular and paradental cysts, in both of which types their association with an impacted tooth have been satisfactorily explained (Shear, 1992).

Although certain specific features seen on radiographs, such as the size of lesion, its location, the presence or absence of root resorption or tooth displacement and other factors such as age and sex of the patient may influence the clinical differential diagnosis, a thorough histological examination is essential in establishing an accurate diagnosis.

## ACKNOWLEDGEMENT

We are indebted to Mrs CS Begemann for typographical assistance.

## REFERENCES

Altini, M & Cohen, M (1982) The follicular primordial cyst (odontogenic keratocyst). *International Journal of Oral Surgery*, **11**, 175-82.

Brown, LH, Beckman, S, Cohen, D, Kaplan, AL & Rosenberg, M (1982) A radiological study of the frequency and distribution of impacted teeth. *Journal of the Dental Association of South Africa*, **37**, 627-30.

Forssell, K (1980) The primordial cyst. A clinical and radiographic study. *Proceedings of the Finnish Dental Society*, **76**, 129-74.

Ikeshima, A, Ozawa, M, Yamamoto, M, Araki, H & Sairenji, E (1990) Differential diagnosis between cyst and tumour. Dentigerous cyst and ameloblastoma containing teeth. *Journal of the Nihon University School of Dentistry*, **32**, 19-26.

McIvor, J (1972) The radiological feature of odontogenic keratocyst. *British Journal of Oral Surgery*, **10**, 116-25.

Praetorius, F, Hjorting-Hansen, E, Gorlin, RJ & Vickers, RA (1981) Calcifying odontogenic cyst. Range, variations and neo-plastic potential. *Acta Odontologica Scandinavia*, **39**, 227-33.

Shear, M (1992) *Cysts of the Oral Regions*. 3rd ed., Oxford: Wright.

Struthers, PJ & Shear, M (1976) Root resorption produced by the enlargement of ameloblastomas and cysts of the jaws. *International Journal of Oral Surgery*, **5**, 128-32.

Ueno, S, Nakamara, S, Mushimoto, K & Shirasu, R (1986) A clinico-pathologic study of ameloblastoma. *Journal of Oral Maxillofacial Surgery*, **44**, 361-65.

Vedtofte, P & Praetorius, F (1979) Recurrence of the odontogenic keratocyst in relation to clinical and histological features. *International Journal of Oral Surgery*, **8**, 412-20.

*Journal of Cranio-Maxillo-Facial Surgery* (1993) 21, 339–341


JOURNAL OF CRANIO-MAXILLO-FACIAL SURGERY

# A retrospective analysis of 367 cystic lesions of the jaw—the Ulm experience

Joachim F. Kreidler[1], Eric J. Raubenheimer[2], Willy F. P. van Heerden[2]

[1] *Department of Oral and Maxillofacial Surgery (Head: J. F. Kreidler, MD, DMD), University of Ulm, Bundeswehrkrankenhaus, Germany,* [2] *Department of Oral Pathology (Head: E. J. Raubenheimer, MChD), Medunsa, 0204, Republic of South Africa*

*SUMMARY.* **Out of 846 cyst-like lesions of the jaws, 367 cases were retrieved from the files of the Department of Oral and Maxillofacial Surgery at the University of Ulm and classified according to the new World Health Organization's classification for odontogenic tumours and cysts. Radicular and residual cysts comprised 56.9%, dentigerous cysts 21.3%, odontogenic keratocysts 10.6%, unicystic ameloblastomas 4.1%, nasopalatine duct cysts 2.7%, glandular odontogenic cysts 1.6% and paradental cysts, traumatic bone cyst, calcifying odontogenic cyst and lateral periodontal cyst each less than 1% of the sample. Nearly one third of the specimens were obtained from military patients; despite an expected bias towards young males, unicystic ameloblastomas presented one and a half decades later than is generally reported.**

## INTRODUCTION

Before the recent adoption of the revised World Health Organization's classification of odonotogenic tumours and cysts (*Kramer* et al., 1992), epidemiological studies on cystic jaw lesions were difficult to interpret due to the omission of recently described entities, which had not been taken up in any classification system. Examples of these are the paradental cyst which arises from odontogenic epithelial residues stimulated into activity by inflammation (*Craig*, 1976) and the aggressive glandular odontogenic cyst, the exact origin of which is less clear (*Shear*, 1992). The calcifying odontogenic cyst, which is now classified as an odontogenic tumour, occurs both in neoplastic and cystic subtypes (*Hong* et al., 1991). Unicystic ameloblastomas are divided into three subtypes, a division which is based on the histological nature of its epithelial lining. Type I unicystic ameloblastomas exhibit a simple ameloblastic epithelial lining whereas Type II shows intraluminal proliferation and Type III mural invasion. The latter type is reported to be associated with a higher recurrence rate (*Ackermann* et al., 1988).

The purpose of this study was to revise and reclassify cystic lesions of the jaws diagnosed and treated in the Department of Oral and Maxillofacial Surgery, University of Ulm, over the last 5 years.

## MATERIAL AND METHODS

The clinical examination forms and radiographs of all cystic lesions affecting the jaws were retrieved from the files of the Department of Oral and Maxillofacial Surgery at the University of Ulm, Germany. 367 out of 846 microscopic sections were supplied for re-examination by the Department of Pathology at the Bundeswehrkrankenhaus Ulm as well as from the University Department. Only cases on which clinical information, a radiograph and representative microscopic sections where available, were included in the study. Each case was re-evaluated and classified independently according to the criteria set in the second edition of the World Health Organisations classification of jaw cysts and tumours (*Kramer* et al., 1992) by two oral pathologists.

## RESULTS

367 cases were included in the study and 22 excluded due to a lack of radiographs and/or unrepresentative microscopic sections. Nearly one third of the cases

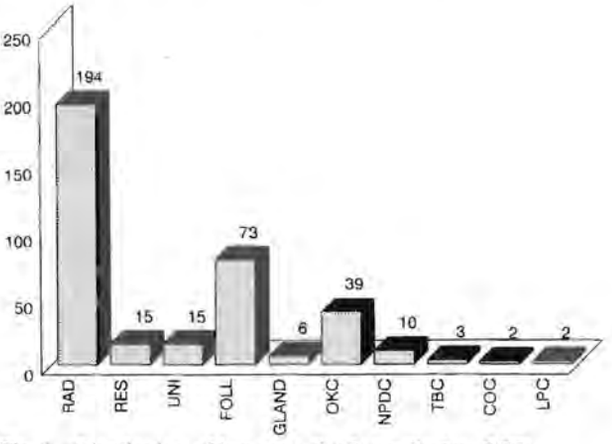


**Fig. 1** – Distribution of jaw cysts. RAD – radicular; RES – residual; UNI – unicystic ameloblastoma; FOLL – follicular; GLAND – glandular odontogenic; OKC – odontogenic keratocyst; NPDC – nasopalatine duct cyst; TBC – traumatic bone cyst; COC – calcifying odontogenic cyst; LPC – lateral periodontal cyst.

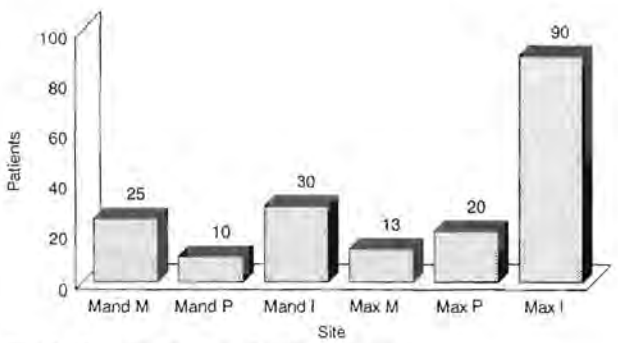


**Fig. 2** – Site distribution of radicular cysts.

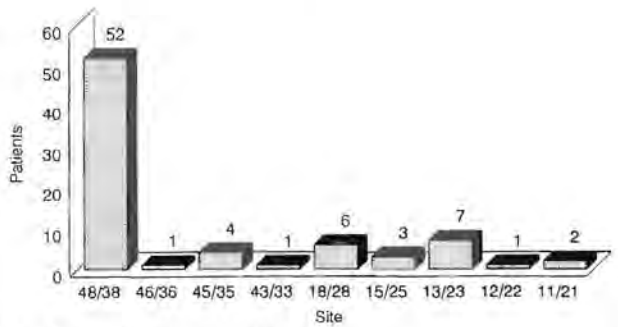


**Fig. 3** – Site distribution of dentigerous cysts.

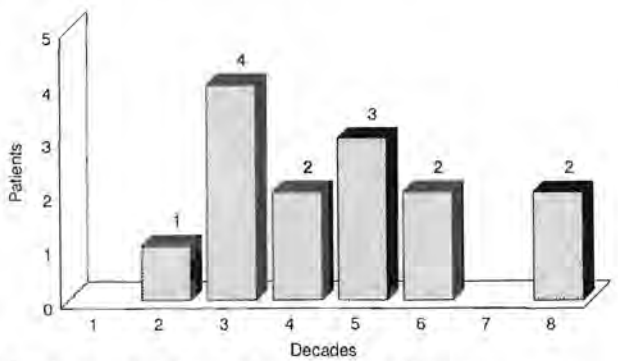


**Fig. 4** – Age distribution of unicystic ameloblastomas.

recorded were military patients treated in the Bundeswehrkrankenhaus. The distribution of cystic jaw lesions in this study is reflected in Figure 1.

Radicular (n = 194) and residual cysts (n = 15) comprised 56.9 % of lesions diagnosed. The mean age at presentation of radicular and residual cysts was 34.4 years (SD = 14.2) and 52.7 years (SD = 13.2) respectively. Radicular cysts occurred most commonly in the maxillary incisor region (Fig. 2).

Dentigerous cysts (n = 78) comprised 21.3 % of the sample and presented at a mean age of 37.1 years (SD = 15.3 years). The mandibular third molars were most frequently involved (Fig. 3).

Three patients out of a total of 39 with odontogenic keratocysts, the latter comprising 10.6 % of the sample, suffered from the basal cell naevus syndrome. The mean age at presentation of odontogenic keratocysts was 40.3 years (SD = 19.5 years) and the majority of cases (n = 21) involved the mandibular molar area. In 10 of those cysts, X-ray examination showed teeth or rudiments inside the cavity which led to a primary misdiagnosis of dentigerous cyst.

Unicystic ameloblastomas (n = 15) comprised 4.1 % of the sample and presented at a mean age of 40.7 years (SD = 18.8 years). The youngest patient was in the second decade of life whereas 2 cases presented in the eighth decade (Fig. 4). 8 unicystic ameloblastomas occurred in the mandibular molar area, 6 of which appeared radiographically as dentigerous-like cysts, and 4 lesions affected the maxilla. 13 unicystic ameloblastomas were lined by non-invasive odontogenic epithelium (Type I) and 2 cases exhibited foci of mural invasion (Type III).

The mean ages at presentation of nasopalatine duct cysts (n = 10, 2.7 % of the sample) and glandular odontogenic cysts (n = 6, 1.6 % of the sample) were 44.9 years (SD = 13.5 years) and 46 years (SD = 14.3 years) respectively. The paradental cyst (n = 3), traumatic bone cyst (n = 3), calcifying odontogenic cyst (n = 2) and lateral periodontal cyst (n = 2) each contributed to less than 1 % of the sample. No examples of gingival cysts of infants and adults, eruption cysts and nasolabial cysts were found in this study.

## DISCUSSION

Accurate diagnosis of cystic lesions of the jaw is crucial as various types are aggressive and may lead to local recurrence if incorrectly diagnosed and inappropriately treated. Many cystic lesions of the jaw share clinical and radiographic features and microscopic examination forms an important part of the diagnostic process. For this purpose, an in-depth knowledge of an internationally accepted classification system, such as that proposed by the World Health Organization (*Kramer* et al., 1992) is essential.

The description of new cyst entities in combination with the new WHO-classification on the one side and improbable lack of diagnosed ameloblastomas on the other prompted this retrospective investigation. It shows the incapability of a general pathologist to make a correct and specific diagnose of jaw cysts and necessitates cooperation with an experienced oral pathologist.

Due to their association with the ghost cell odontogenic tumour, the calcifying odontogenic cyst is no longer grouped amongst cysts in this classification but is classified as a benign tumour originating from the odontogenic apparatus. This cystic tumour, as well as the odontogenic keratocyst (*Brown*, 1970; *Niemeyer* et al., 1985), unicystic ameloblastoma (*Ackermann* et al., 1988) and glandular odontogenic cyst (*Patron* et al., 1991), are notorious for their aggressive behaviour and high recurrence rates (*Machtens* et al., 1972). This implies that in the present study, 17 % of the total sample of cystic jaw lesions, required more than simple enucleation as a curative surgical procedure. Type III unicystic ameloblastomas, of which 2 cases were diagnosed in this study, exhibit infiltrative features and should be treated

similarly to the polycystic types, with wide excision or even resection of the involved jaw segment (*Ackermann* et al., 1988). These results have induced a recall of those patients with diagnosed aggressive cysts or ameloblastomas in order to prove the necessity for further treatment.

A large percentage of patients in this study were military personnel and our data is probably biased towards young males. The high mean age of 40.7 years for unicystic ameloblastomas was therefore surprising as these cystic tumours are reported to occur most frequently in the first half of the third decade (*Robinson* and *Martinez*, 1977; *Gardner*, 1981; *Ackermann* et al., 1988). As no literature is available on unicystic ameloblastomas in the German population, this finding may point towards an older age incidence for unicystic ameloblastomas in Germany. Unicystic ameloblastomas frequently involved the mandibular molar area where impaction of a mandibular third molar in the cyst wall was common. Unless these lesions are examined microscopically, they will be misdiagnosed as dentigerous cysts.

The frequency of the different cyst types encountered in this study, as well as the sites of involvement of radicular, residual, dentigerous and odontogenic keratocysts and unicystic ameloblastomas, are in agreement with the recent literature (*Shear*, 1992). The lack of examples of gingival cysts of infants and adults and eruption cysts, as well as the infrequent occurrence of paradental cysts is the result of exclusion of all cases without a microscopic diagnosis. Most of these lesions either go unnoticed or are not submitted for microscopic examination after removal and are probably more common than is reflected in a study of this nature.

## References

*Ackermann, G. L., M. Altini, M. Shear:* The unicystic ameloblastoma: a clinicopathological study of 57 cases. J. Oral Pathol. 17 (1988) 541–546

*Browne R. M.:* The odontogenic keratocyst—clinical aspects. Br. Dent. J. 128 (1970) 225–231

*Craig, G. T.:* The paradental cyst. A specific inflammatory odontogenic cyst. Br. Dent J. 141 (1976) 9–14

*Gardner, D. G.:* Plexiform unicystic ameloblastoma; a diagnostic problem in dentigerous cysts. Cancer 47 (1981) 1358–1363

*Hong, S. P., G. L. Ellis, K. S. Hartmann:* Calcifying odontogenic cyst. A review of ninety-two cases with reevaluation of their nature as cysts or neoplasms, the nature of ghost cells and subclassification. Oral Surg. 72 (1991) 56–64

*Kramer I. R. H., J. J. Pindborg, M. Shear:* Histological Typing of Odontogenic Tumours. Springer, Berlin, 1992

*Machtens, E., E. Hjorting-Hansen, H.-J. Schmallenbach, L. Werz:* Keratozyste—Ameloblastom, ein klinisch diagnostisches Problem. Dtsch. Zahn Mund Kieferheilk. 58 (1972) 157

*Niemeyer K., H.-P. Schlien, G., Habel, C. Mentler:* Behandlungssergebnisse und Langzeitbeobachtungen bei 62 Patienten mit Keratozysten. Dtsch. Zahnärztl. Z. 40 (1985) 637–640

*Patron, M., C. Colmenero, J. Larrauri:* Glandular odontogenic cyst; clinicopathological analysis of three cases. Oral Surg. 72 (1991) 71–74

*Robinson, L., M. G. Martinez:* Unicystic ameloblastoma. A prognostically distinct entity. Cancer 40 (1977) 2278–2285

*Shear, M.:* Cysts of the oral regions. 3rd ed. Wright, Oxford, 1992

**Prof. Dr Dr J. Kreidler**
Ärztlicher Direktor der Abteilung
Mund-Kiefer-Gesichtschirurgie der Universität Ulm im
Bundeswehrkrankenhaus Postfach 12 20
D-89070 Ulm
Germany

Paper received: 31 March 1993
Accepted: 7 July 1993

Scientific Article

Journal of the Dental Association of South Africa, 49, 559-562.



# Clinico-pathological study of 30 unicystic ameloblastomas

RE Roos, EJ Raubenheimer and WFP van Heerden

Department of Oral Pathology, Medical University of Southern Africa, PO Medunsa, 0204

*Keywords: ameloblastoma; odontogenic tumour.*

## SUMMARY

*The clinico-pathological records of 30 unicystic ameloblastomas collected over a period of 10 years were studied. The mean age at diagnosis was 18,0 years (SD ±8,1), most lesions were located in the mandible and were frequently associated with impacted teeth, root resorption and tooth displacement. The unicystic ameloblastomas in 11 patients (4 females and 7 males) exhibited invasion of the fibrous wall, 4 cases (1 female and 3 males) showed intra-luminal proliferation and the remaining 15 specimens (9 females and 6 males) were lined by non-proliferating ameloblastic epithelium. Two cases recurred 3 and 7 years after initial surgical removal. This study reveals the potential aggressive behaviour of unicystic ameloblastomas and underlines the importance of a thorough microscopic examination for sub-classification.*

## OPSOMMING

*Die klinies-patologiese rekords van 30 unisistiese ameloblastome, wat oor 'n tydperk van 10 jaar versamel is, is bestudeer. Die gemiddelde ouderdom by diagnose was 18,0 jaar (SD ±8,1). Die meeste letsels was in die mandibula en was met geïmpakteerde tande, wortelresorbsie en tandverplasing geassosieer. In 11 pasiënte (4 vroulik, 7 manlik) het die unisistiese ameloblastome die fibreuse wand binnegedring, in 4 gevalle (1 vroulik, 3 manlik) was intraluminale proliferasie teenwoordig en in die oorblywende 15 gevalle (9 vroulik, 6 manlik) was die sist deur 'n nie-prolifererende ameloblastiese epiteel. In twee gevalle het herhaling onderskeidelik 3 en 7 jaar na die aanvanklike chirurgiese verwydering voorgekom. Hierdie studie bevestig die potensiële aggressiewe gedrag van unisistiese ameloblastome en beklemtoon die noodsaaklikheid van deeglike mikroskopiese ondersoek vir subklassifikasie.*

## INTRODUCTION

The unicystic ameloblastoma is a unilocular, cystic epithelial odontogenic tumour initially described by Robinson and Martinez in 1977. Males and females are affected approximately equally. The lesions usually occur in the mandible and especially in the molar-ramus area, while the maxilla is only occasionally affected (Ackerman, Altini and Shear, 1988). They usually occur in the second to fourth decades and the mean age at the time of diagnosis is reported to be 23,8 years. The lesions appear radiologically as a well defined unilocular radiolucency of varying size (Ackermann *et al.*, 1988). When associated with an unerupted tooth, the appearance closely resembles a dentigerous cyst. Involvement of the roots of teeth may give it a radicular cyst-like appearance (Lucas, 1984) and in many cases can only be distinguished from odontogenic keratocysts by microscopic examination. Unicystic ameloblastomas are divided into three groups. Group 1 include the simple cystic lesions lined by an epithelium that does not infiltrate into the fibrous cyst wall. Lesions in Group 2 show intra-luminal epithelial proliferation and the epithelium in Group 3 lesions invade the fibrous cyst wall. Group 1 and 2 lesions may be treated by enucleation, whereas Group 3 lesions should be treated more radically to prevent recurrences (Ackermann *et al.*, 1988).

As a rule unicystic ameloblastomas behave more aggressively than other odontogenic cysts. It is important therefore to recognise the clinical features which may facilitate an accurate diagnosis of the condition. This study was undertaken to determine the clinico-pathological features of unicystic ameloblastomas in a rural black population.

## MATERIALS AND METHODS

Microscopic sections of all unicystic lesions that were biopsied between 1982 and 1992 at Medunsa were retrieved and re-evaluated. The unicystic ameloblastomas were subdivided into three groups using the criteria of Ackermann *et al.*, 1988. Clinical data and radiographs were obtained from patient files. The site of occurrence was designated as molar-ramus, premolar or incisor according to the centre of the radiolucent lesion on a panoramic radiograph.

Article received: 7/6/1993; approved for publication: 16/8/1994
RE Roos, BChD (Pta) is a Lecturer in the Department of Oral Pathology at MEDUNSA.
EJ Raubenheimer, BChD, MChD (Pta)
WFP van Heerden, BChD, MChD (Pta)

## RESULTS

Thirty cases were diagnosed as unicystic ameloblastoma, 16 were males and 14 females. The mean age of the patients was 18,0 years (SD =±8,1) (range 8-43 years) and 63,3 per cent occurred in the second decade (Fig. 1). Twenty seven of the lesions were present in the mandible and only 3 in the maxilla (Fig. 2). The lesions varied in size from 2,5-12 cm mesio-distally and 22 of the lesions were more than 5 cm in diameter on the panoramic radiographs. One mandibular tumour was associated with a pathological fracture.

Radiologically, 11 of the lesions were associated with impacted teeth (Fig. 3), 13 with root resorption, 15 with tooth displacement and 8 with tooth displacement and root resorption. The impacted teeth associated with the lesions were mainly the mandibular third molars (n=7), followed by mandibular second molars (n=3) and mandibular canines (n=2). Two of the 3 maxillary lesions presented in the "globulo-maxillary" area. Of the 14 lesions in females, 9 were classified as Group I (Fig. 4), 1 as Group II (Fig. 5) and 4 as Group III. There were 6 Group I lesions and 7 Group III lesions amongst the 16 males, the remaining 3 were Group II lesions (Fig. 6).

In 7 unicystic ameloblastomas, 50 per cent or more of the lining was a nondescript type of epithelium (Fig. 7). Three out of 4 Group III lesions had a plexiform intra-luminal proliferation, the other had multiple mural nodules projecting into the lumen (Fig. 8). Inflammation in 3 lesions was associated with extensive epithelial arcading and 4 showed sub-epithelial hyalinization. Two cases recurred as polycystic ameloblastomas 3 and 7 years after surgical treatment respectively. The first was originally classified as Group III (Fig. 9), whereas the other case was a Group I unicystic ameloblastoma.

## DISCUSSION

Since the original description of unicystic ameloblastoma (Robinson and Matinez, 1977) various reports on the aggressive behaviour of this cystic lesion have appeared (Ackermann *et al.*, 1988; Gardner, Morton and Worsham, 1987; Kahn, 1989; Keszler and Dominques, 1986; Punnia-Moorthy, 1989). Two patients in our study, which extends over a period of 10 years, presented 3 and 7 years after initial surgery with recurrences. Both recurrences exhibited the growth pattern of a polycystic ameloblastoma. Although Ackermann *et al.*, (1988) propose a more radical form of treatment for Group III lesions, a Group I lesion recurred in our study and this emphasizes the potentially aggressive behaviour of all unicystic ameloblastomas and

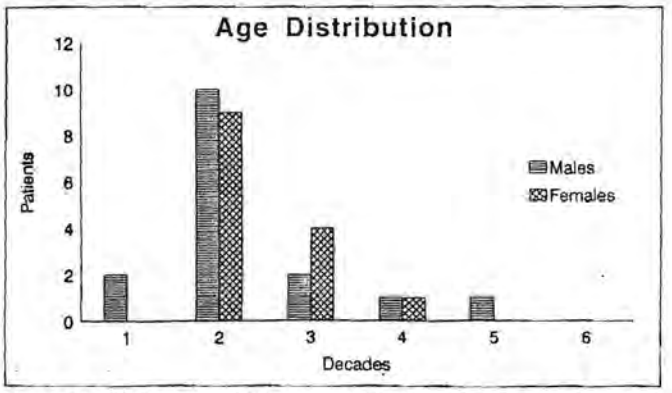


*Fig. 1:* **The histogram of the age distribution of males and females.**

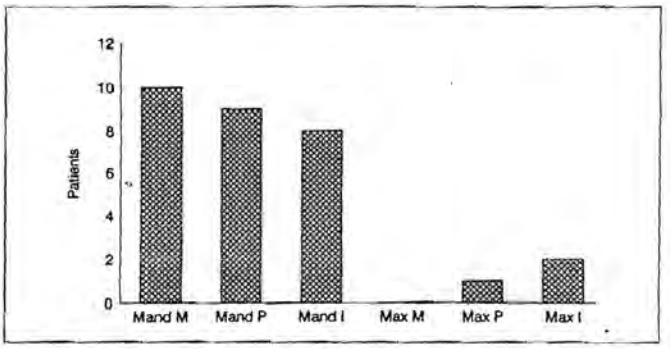


*Fig. 2:* **The site distribution of 30 unicystic ameloblastomas. Mand=mandibular, Max=maxilla, M=molar ramus area, P=premolar area, I=incisor area.**

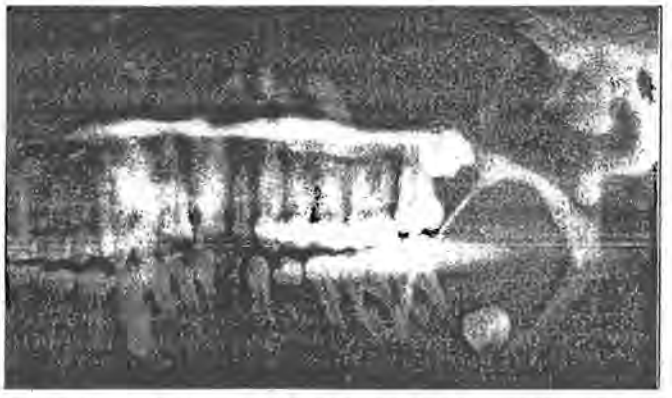

*Fig. 3:* **Panoramic radiograph of an unicystic ameloblastoma associated with an impacted mandibular third molar.**

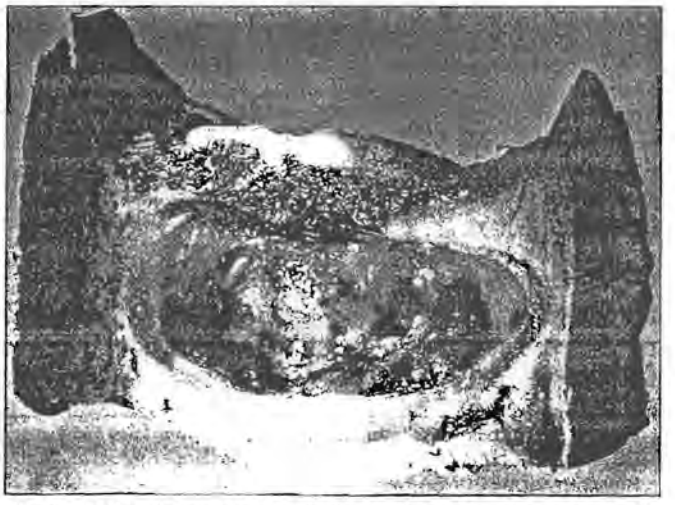

*Fig. 4:* **Section through a resected mandible with a microscopically confirmed Group I lesion. Note the simple unicystic cavity.**

*Fig. 5:* Cross section through a microscopically confirmed mandibular Group II lesion. Note the intra-luminal proliferation (arrow).

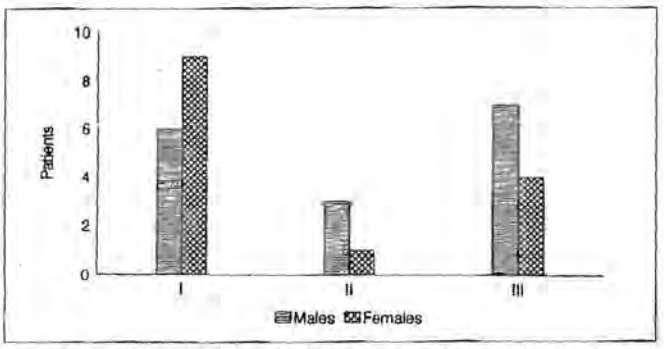


*Fig. 6:* The histogram of the different groups for females and males.

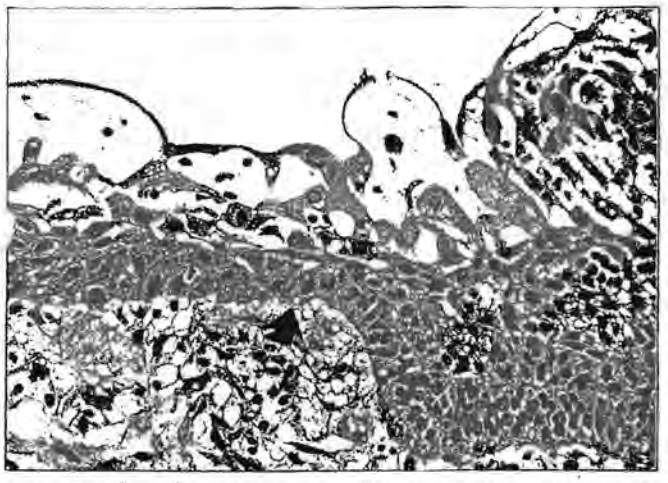

*Fig. 7:* Photomicrograph of a Group I lesion. Note the nondescript epithelium (left) and the sharp transition (arrow) to typical ameloblastic epithelium. (HE, X300).

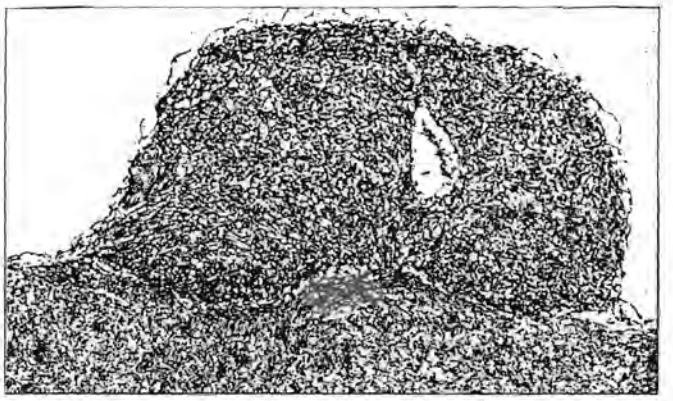

*Fig. 8:* The lining of a Group II lesion showing an intra-luminal nodular proliferation (HE, X100).

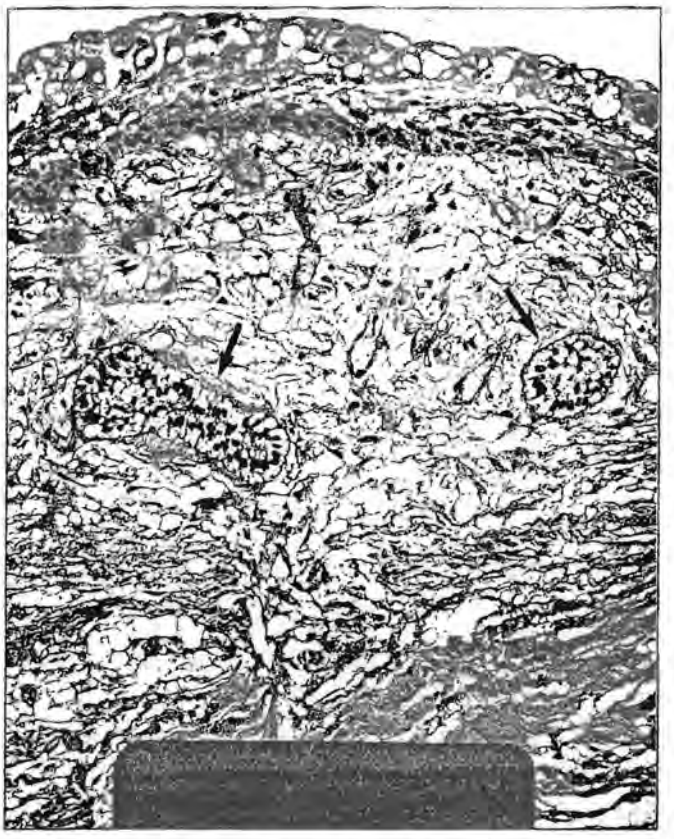

*Fig. 9:* The lining of the Group III lesion that recurred. Note the islands of ameloblastic epithelium in the connective tissue wall (arrows). (HE, X180).

highlights the importance of complete surgical removal. This recurrence may, on the other hand, reflect an inherent weakness in the proposed sub-grouping of unicystic ameloblastomas. If the whole cyst wall is not examined microscopically, an exercise which is highly impractical if not impossible in larger examples, mural invasion cannot be excluded categorically. The diagnosis of an unicystic ameloblastoma on a small biopsy specimen is not recommended. Moreover, the frequent occurrence of nondescript epithelium and inflammation may mask the typical characteristics of the ameloblastic epithelial lining. This microscopic sub-classification of unicystic ameloblastomas should therefore not be attempted on anything less than a thorough microscopic examination of the whole cyst wall. After such an examination the number of lesions placed in Group III would probably increase.

Our study supports the finding that there is an equal sex distribution for the unicystic ameloblastoma as well as a tendency for it to occur in young patients. Our cases however, presented on average 6 years earlier than those of Ackermann *et al.*,

(1989), probably because patients were seeking treatment sooner and had easier access to the hospital in the years 1981-1991. Most tumours occurred in the mandible and maxillary involvement was less common. A large number of mandibular lesions could be easily mistaken for dentigerous cysts, because of their association with impacted molars and canines. This is related further to the frequent occurrence of root resorption, a feature often found in dentigerous cysts (Shear, 1992). In order to establish a correct diagnosis, microscopic examination of all cystic jaw lesions is mandatory.

Group I lesions predominated in our study and then followed Group III and lastly Group II unicystic ameloblastomas. This is in contrast to Ackermann's 1988 study in which Group III lesions were most frequent. The ratio between female and male in Group I lesions was 1,5:1 and in Group III lesions 1,75. The significance of this finding is not known.

It is important to note that all unicystic ameloblastomas, irrespective of grouping, are neoplastic in nature and will recur if incompletely removed.

Although limited evidence is available on recurrences of unicystic ameloblastomas, it appears as if the latter may present either as a regrowth of the original unicystic lesion or as a multicystic ameloblastoma.

## ACKNOWLEDGEMENT

We are grateful to Mrs CS Begemann for the typing of the manuscript.

## REFERENCES

Ackermann, GL, Altini, M & Shear, M (1988) The unicystic ameloblastoma: a clinicopathological study of 57 cases. *Journal of Oral Pathology*, 17, 541-6.

Gardner, DG, Morton, TH & Worsham, JC (1987) Plexiform unicystic ameloblastoma of the maxilla. *Journal of Oral Surgery Oral Medicine Oral Pathology*, **63**, 221-3.

Kahn, MA (1989) Ameloblastoma in young persons: A clinicopathologic analysis and etiologic investigation. *Journal of Oral Surgery Oral Medicine Oral Pathology*, **67**, 706-15.

Keszler, A & Domingues, FV (1986) Ameloblastoma in childhood. *Journal of Oral Maxillofacial Surgery*, **44**, 609-13.

Lucas, RB (1984) *Pathology of tumours of the oral tissues*, 4th ed., pp.371-8. Great Britain: William Clowes Ltd.

Punnia-Moorthy, A (1989) An unusual late recurrence of unicystic ameloblastoma. *British Journal of Oral and Maxillofacial Surgery*, **27**, 254-259.

Robinson, L & Martinez, MG (1977) Unicystic ameloblastoma. A prognostically distinct entity. *Cancer*, **40**, 227-31.

Shear, M (1992) *Cysts of the oral regions*, 3rd ed., pp.75-98. Oxford:Wright.

# Serving Dentistry — ISO TC106

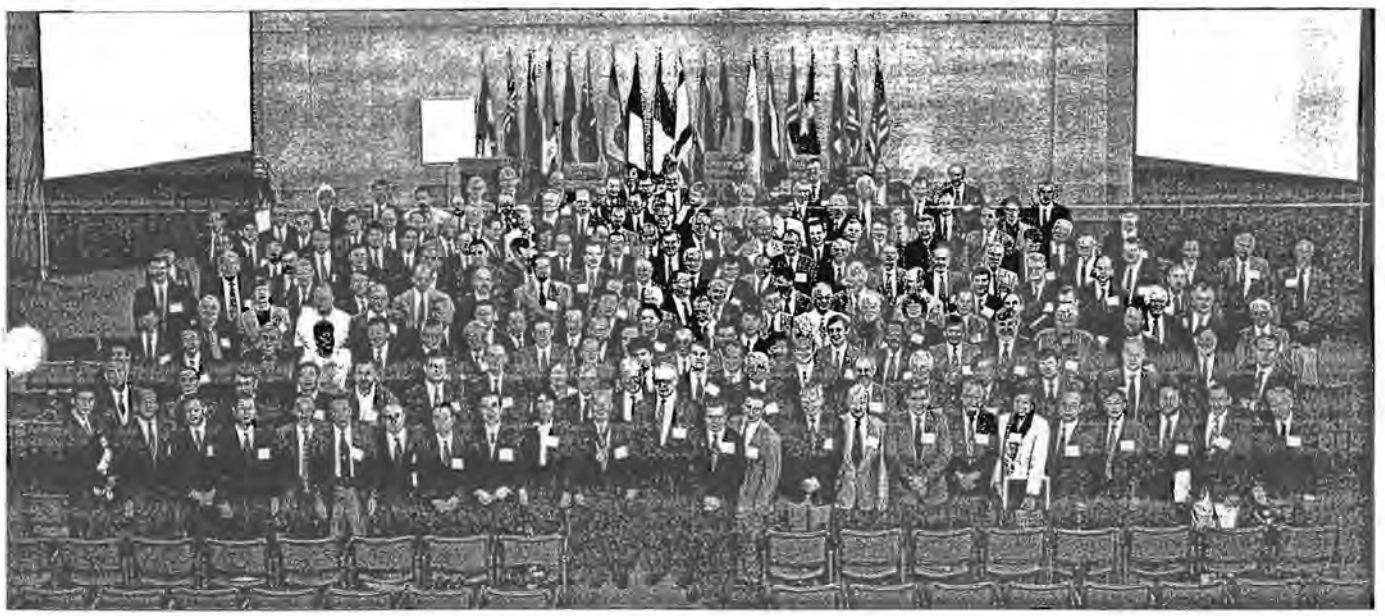

The 30th meeting of the International Standards Organisation's Technical Committee took place in Ottawa, Canada from 10-15 October 1994.

The countries represented were Australia, Brazil, Canada, China, France, Germany, Hong Kong, Italy, Japan, Netherlands, Norway, South Africa, Switzerland, Sweden, Thailand, United Kingdom and USA. The new South African flag was given a place of honour at the centre of the display seen in our photograph, which was taken at the conclusion of the opening ceremony. **Dr John Stanford**, Chairman of the Committee since 1991 is seen in the front of the picture with his predecessor, **Prof Pierre Laplaud** (1982-1990). the South African Bureau of Standards is a Participating Member of the Committee and Dr Heydt was their representative at the meeting. A detailed report on the work of the Committee will appear in a forthcoming issue of the ***JOURNAL***.

J Oral Pathol Med, 1993, 22, 109–12
Printed in Denmark 



JOURNAL OF
Oral Pathology & Medicine
ISSN 0904-2512

# Detection of human papillomavirus DNA in an ameloblastoma using the in situ hybridization technique

**W. F. P. van Heerden[1], E. J. van Rensburg[2], E. J. Raubenheimer[1] and E. H. Venter[3]**

*Departments of [1]Oral Pathology and Oral Biology, Medical University of Southern Africa, [2]Medical Virology, University of Pretoria and [3]Department of Infectious Diseases, Faculty of Veterinary Science, University of Pretoria, South Africa*

Van Heerden WFP, van Rensburg EJ, Raubenheimer EJ, Venter EH: Detection of human papillomavirus DNA in an ameloblastoma using the in situ hybridization technique.

HPV type 18 DNA was identified in an intrabony ameloblastoma using radiolabelled in situ hybridization. The viral DNA was found in a verrucous lesion in a cystic area of the tumor. The absence of HPV DNA in other epithelial areas of the ameloblastoma is suggestive of a secondary infection. HPV is not considered to be an etiological factor in the pathogenesis of this ameloblastoma.

Key words: ameloblastoma; DNA; human papillomavirus type 18; in situ hybridization

WFP van Heerden, Department of Oral Pathology and Oral Biology, Medical University of Southern Africa, P.O. Medunsa, 0204, Republic of South Africa.

Accepted for publication October 1992

Human papillomaviruses (HPVs) are DNA viruses that infect only squamous epithelium at selected locations in the skin and mucosa. The virus usually infects the basal cell layers and viral DNA are observed in low copy numbers in these cells. An increase in copy numbers of replicating viral DNA are found in the more differentiated epithelial cells while production of viral particles is restricted to the fully differentiated superficial epithelial cells (1). Since this state of differentiation has not yet been achieved in culture, it has not been possible to reproduce HPV in the laboratory to study their natural life cycle (2). These viruses induce papillomatous, hyperplastic or verrucous lesions depending on the site of infection and the HPV type implicated. HPV involvement in upper respiratory and digestive tract lesions like focal epithelial hyperplasia, squamous cell papillomas, laryngeal papillomas, leukoplakia and squamous cell carcinoma has been demonstrated by means of immunohistochemical, DNA hybridization and polymerase chain reaction studies (2–6). More than 60 types of HPV have been isolated to date, of which types 1, 2, 4, 6, 7, 11, 13, 16, 18, 32 and 57 were found in the different oral lesions (7).

The association between HPV and odontogenic tumours and cysts has not been studied to a great extent. HPV 16 DNA has been demonstrated in an odontogenic keratocyst using Southern blot hybridization (8), while KHAN found HPV capsid antigen in 3 out of 10 ameloblastomas in young persons (9). The purpose of this study was to investigate an ameloblastoma with typical HPV histologic changes for HPV DNA using the in situ hybridization technique. This is a sensitive technique and has the advantage of localizing viral DNA in tissue sections to the extent of detecting them at the resolution of single cells.

## Material and methods

A 25-yr-old man reported to the Maxillofacial and Oral Surgery clinic complaining of a painless, bony hard swelling in the anterior mandible. Examination showed a tumor extending from the right mandibular angle to the contralateral first molar region. Expansion of the lingual and buccal cortices was evident with thinning and erosion of the buccal cortex in the right premolar area. Radiographs showed a well-circumscribed, multilocular lesion with root resorption of the associated teeth. No signs of mucosal ulceration were present.

After an incisional biopsy, a diagnosis of a follicular aneloblastoma was made and the tumor was resected through an intraoral approach. The specimen was fixed in 10% buffered formalin for pathologic examination.

Macroscopic examination showed a gray-white solid tumor with cystic areas of varying size. A papillomatous lesion presenting as a luminal growth was present in one cyst. Microscopy revealed a follicular ameloblastoma with acanthomatous as well as granular cell differentiation (Fig. 1). The papillomatous lesion showed verrucous hyperplasia with hyperparakeratosis, elongation of the rete-ridges and groups of koilocytes lying in the upper part of the epithelium. These features resembled those of a verruca vulgaris (Fig. 2).

The biopsy material containing the papillomatous lesion, as well as blocks exhibiting the characteristic ameloblastomatous epithelium and including areas of granular cell and acanthomatous differentiation, were examined for the presence of HPV antigen using an ABC immunoperoxidase kit for the HPV group specific antigen (Lipshaw Corporation, Detroit) as well as in situ hybridization.

For HPV typing, the specific DNA probes of HPV 2, 6, 7, 11, 13, 16, 18 and 30 cloned in either pBR322 or pUC19 were used (kindly provided by Dr E-M de Villiers, Human Papillomav-

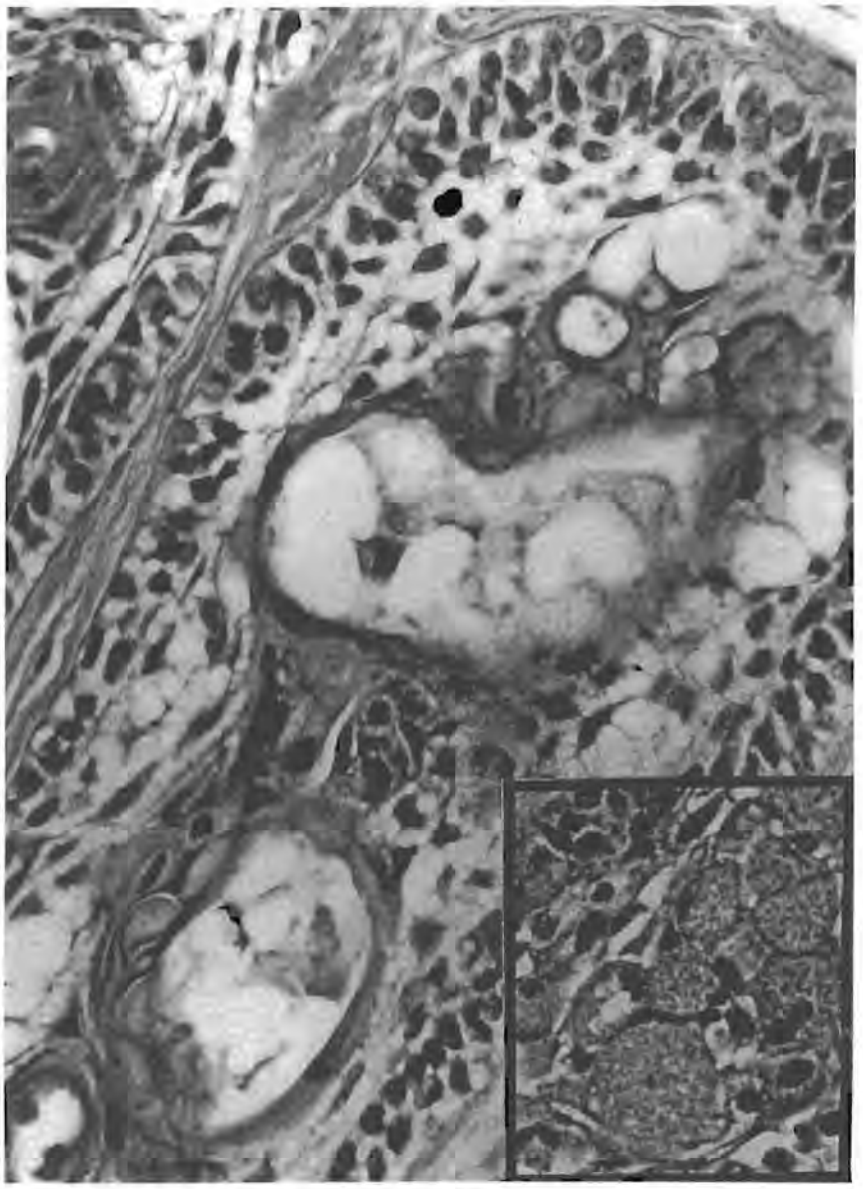

*Fig. 1.* Follicular ameloblastoma with central acanthomatous differentiation. HE × 200. *Inset.* Areas of granular cell differentiation. HE × 200.

irus Reference Centre, DKFZ, Heidelberg, Germany). The probes were labelled with $^{32}$p dCTP using the multiprime DNA labelling system (Amersham, U.K.). The labelled probes had a specific activity of $2–5 \times 10^8$ counts/min/μg of DNA. For in situ hybridization 5–10 ng of each probe was used on individual sections.

pBR322 and pUC19 vectors served as negative control probes. Two paraffin embedded tissue sections (a cervical intraepithelial neoplasia and vulvar carcinoma positive for HPV 6 and 16 respectively) were used as positive control slides.

The tissue sections were incubated at 60°C overnight using 3-aminopropyltriethoxysilane coated slides (10). Slides were deparaffinised and rehydrated by sequential immersion into xylene (3 × 10 min) and ethanol. They were then incubated in 0.2 N HCl for 20 min at room temperature and transferred to 2 × SSC at 70°C for 10 min. The tissue sections were digested with a 2 × SSC, 0.1% SDS buffer solution containing Proteinase K (Boehringer, Mannheim, Germany) at a concentration of 0.01 μg/ml at 37°C for 30 min. Sections were post-fixed for 5 min in 4% paraformaldehyde, 2 × SSC and 5 mM $MgCl_2$; 5 min in 50% formamide, 2 × SSPE and acetylated (2 × 5 min). The slides were prehydridised (50% formamide, 10% dextran sulfate, 2 × SSPE, 100 mM glycin, 0.1% SDS, 2% 50 × Denhardts, 10 mM Tris pH 7.4 and 200 μg/ml salmon sperm DNA) for 30 min at 52°C prior to the application of the probe solution. Heat-denatured probe solution (either HPV 2, 6, 7, 11, 13, 16, 18 or 30) was added to each section and slides were incubated for 16 hours at 52°C in a humidified chamber.

Following hybridisation, the slides were washed twice in a 2 × SSPE/50% formamide solution and once in 50% fomamide, 0.1% SDS, 2 × SSC, each wash for one hour at 37°C. Slides were dehydrated through graded ethanols containing 0.3 M $NH_4$ acetate. Slides were dipped in LM-1 emulsion (Amersham, UK), following instructions of the manufacturer. After exposure, slides were developed, fixed and counterstained with hematoxylin-eosin. The presence of HPV DNA sequences in the lesions was indicated by the condensations of black silver grains superimposed on the nuclei of cells.

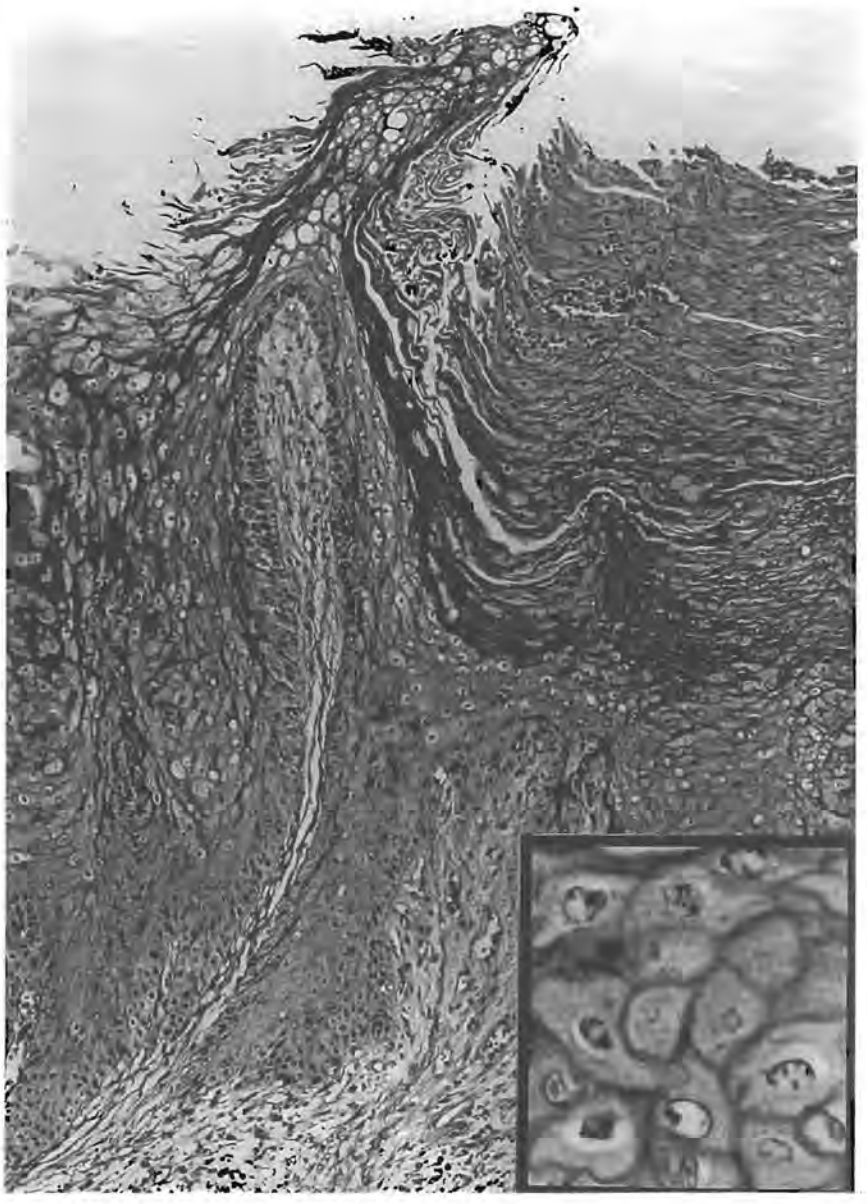

*Fig. 2.* Micrograph of the papillomatous lesion showing parakeratosis, epithelial papillary processes and elongation of rete-ridges. HE × 100. *Inset.* High power detail of koilocytes showing enlarged cells with slightly irregular nuclei surrounded by a halo. HE × 250.

## Results

Immunohistochemical examination of both the papillomatous lesion and typical ameloblastoma areas was negative. The in situ hybridization technique revealed HPV DNA type 18 in the papillomatous lesion (Fig. 3). The blocks containing the typical ameloblastoma features, including foci of granular cell and acanthomatous differentiation, were negative for the HPV DNA types examined.

## Discussion

Radiolabelled HPV DNA in situ hybridization was used instead of the more commonly used biotinylated DNA in situ hybridization because it is a more sensitive method to detect HPV DNA (11). The sensitivity of the radiolabelled HPV DNA probe is 20–100 genome copies per cell compared to the 100–800 genome copies per cell of the biotin-labelled HPV DNA probe (1). The negative immunohistochemical staining in our study may be due to the fact that this technique identifies only the productive phase of the viral infection. Furthermore, as this method is based on an antigen-antibody reaction, the target antigenic determinants may be distorted by heating in paraffin, fixation in formalin or digestion by trypsin (12).

The presence of HPV type 18 DNA in a primary intrabony tumor of odontogenic epithelial origin is difficult to explain. Contact between the tumor epithelium and the oral mucosa may have facilitated cross-infection between oral epithelium and the ameloblastoma. Although no ulceration of the oral mucosa or skin was noted in this patient, expansion of the buccal and lingual cortices with erosion of the buccal cortex in the right premolar area were present. This area corresponded with the location of the papillomatous lesion in the ameloblastoma. The specimen was thoroughly examined for the presence of similar lesions without success, supporting the link between the HPV-associated lesion and the eroded bone cortex. Direct contact between tumor epithelium and surface epithelium could not be demonstrated.

Cox *et al.* demonstrated HPV 16 DNA in an odontogenic keratocyst

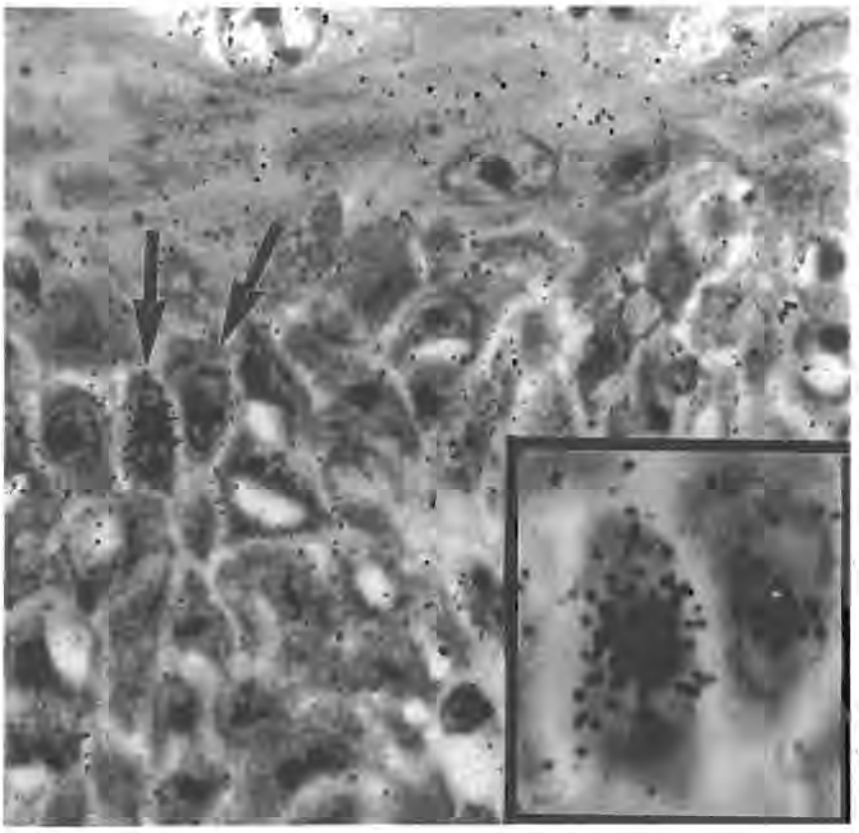

*Fig. 3.* Micrograph of the verrucous lesion subjected to in situ hybridization shows the presence of HPV 18 DNA as condensations of black silver grains superimposed on the nuclei (arrows). ×200. *Inset.* High power detail of positive cells. ×400.

lacking the typical histologic features of an HPV infection (8). This HPV was implicated in the pathogenesis of the odontogenic keratocyst because the keratin-producing lining of the cyst provided squamous epithelium for viral persistence as well as completion of the virus life cycle. HPV 18 has an even higher oncogenic potential than HPV 16 (13), and has also been detected in oral epithelial dysplasias and oral squamous cell carcinomas (14). In our case HPV DNA was detected only in the solitary papillomatous lesion and not in the other epithelial regions permissive for viral infections, i.e. the acanthomatous and granular cell areas. We feel that the restriction of HPV DNA positivity to the verrucous lesion represents a secondary infection and is therefore not an etiological factor in the pathogenesis of this ameloblastoma.

*Acknowledgements* – The authors wish to thank Dr A. F. DREYER, Department of Maxillofacial and Oral Surgery for his contribution, Mrs C. S. BEGEMANN for secretarial services, Mrs. R. VORSTER for technical assistance and Miss. L. HOPE, Audio Visual Department of the Medical University of Southern Africa for photographic services.

## References

1. DE VILLIERS EM. Papilloma viruses in cancers and papillomas of the aerodigestive tract. *Biomed. & Pharmacother* 1989; **43**: 31–6.
2. VOUSDEN KH. Human papillomaviruses and cervical carcinoma. *Cancer Cells* 1989; **1**: 43–50.
3. PADAYACHEE A, VAN WYK CW. Human papillomavirus (HPV) DNA in focal epithelial hyperplasia by in situ hybridization. *J Oral Pathol Med* 1991; **20**: 210–4.
4. YOUNG SK, MIN KW. In situ hybridization analysis of oral papillomas, leukoplakias, and carcinomas for human papillomavirus. *Oral Surg Oral Med Oral Pathol* 1991; **71**: 726–9.
5. CORBITT G, ZAROD AP, ARRAND JR, et al. Human papillomavirus (HPV) associated with laryngeal papilloma. *J Clin Pathol* 1988; **41**: 284–8.
6. SHROYER KR, GREER RO. Detection of human papillomavirus DNA by in situ DNA hybridization and polymerase chain reaction in premalignant and malignant oral lesions. *Oral Surg Oral Med Oral Pathol* 1991; **71**: 708–13.
7. CHANG F, SYRJÄNEN S, KELLOKOSKI J, SYRJÄNEN K. Human papillomavirus (HPV) infections and their associations with oral disease. *J Oral Pathol Med* 1991; **20**: 305–17.
8. COX M, EVESON J, SCULLY C. Human papillomavirus type 16 DNA in an odontogenic keratocyst. *J Oral Pathol Med* 1991; **20**: 143–5.
9. KHAN MA. Ameloblastoma in young persons; A clinicopathologic analysis and etiologic investigation. *Oral Surg Oral Med Oral Pathol* 1989; **67**: 706–15.
10. PRINGLE JH, PRIMROSE L, KIND CN, TALBOT IC, LAUDER I. In situ hybridization demonstration of poly-adenylated RNA sequences in formalin-fixed paraffin sections using a biotinylated oligonucleotide polyd(T) probe. *J Pathol* 1989; **158**: 279–86.
11. FURUTA Y, SHINOHARA T, SANO K, MEGURO M, NAGASHIMA K. In situ hybridisation with digoxigenin-labelled DNA probes for detection of viral genomes. *J Clin Pathol* 1990; **43**: 806–9.
12. GRODY WW, CHENG L, LEWIN KJ. In situ viral DNA hybridisation in diagnostic surgical pathology. *Human Pathology* 1987; **18**: 535–43.
13. KURMAN RJ, SHIFFMAN MH, LANCASTER WD, et al. Analysis of individual human papillomavirus types in cervical neoplasia: A possible role for type 18 in rapid progression. *Am J Obstet Gynecol* 1988; **159**: 293–6.
14. SYRJÄNEN SM, SURJÄNEN KJ, HAPPONEN RP. Human papillomavirus (HPV) DNA sequences in oral precancerous lesions and squamous cell carcinoma demonstrated by in situ hybridization. *J Oral Pathol* 1988; **17**: 273–8.

J Oral Pathol Med 1995; 24: 227–32
Printed in Denmark. All rights reserved



JOURNAL OF
Oral Pathology&Medicine
ISSN 0904-2512

# Infrequent clinicopathological findings in 108 ameloblastomas

**Erich J. Raubenheimer, Willem F. P. van Heerden and Claudia E. E. Noffke**
*Department of Oral Pathology and Oral Biology, Medical University of Southern Africa, Republic of South Africa.*

Raubenheimer EJ, van Heerden WFP, Noffke CEE: Infrequent clinicopathological findings in 108 ameloblastomas. J Oral Pathol Med 1995; 24: 227–32.


One hundred and eight ameloblastomas diagnosed in a rural black Africa population were analysed for clinicopathologic findings other than those classically described. One patient had a polycystic ameloblastoma adjacent to an ameloblastic fibroma. Two other polycystic ameloblastomas showed aneurysmal bone cyst formation and one mandibular tumour was diagnosed as a keratoameloblastoma. Microscopic changes resembling an adenomatoid odontogenic tumour were present in association with two unicystic ameloblastomas and a HPV18-positive verrucous lesion occurred in the lining of a cystic space of a polycystic ameloblastoma. Two ameloblastomas contained eosinophilic granules in all tumor cells and melanocytes were diffusely present in another. One case exhibited a focus of mucous cell metaplasia. Two polycystic ameloblastomas showed diffuse interstitial ossification. One mandibular tumor was diagnosed as a desmoplastic ameloblastoma and another as an odontoameloblastoma. This study demonstrated that although ameloblastomas are regarded as a fairly homogeneous group of neoplasms, detailed investigations prove clinicopathologic diversity in a significant number of lesions.

Key words: ameloblastoma; infrequent findings; jaw tumors; odontogenic tumors.

E.J. Raubenheimer, Department of Oral Pathology and Oral Biology, Medunsa, P.O. Medunsa, 0204, Republic of South Africa.

Accepted for publication October 20, 1994

Ameloblastoma is the most common neoplasm affecting the jaws. It is derived from odontogenic epithelium and although located primarily intraosseously, peripherally occuring ameloblastomas involving soft tissue only have occasionally been reported. Two clinicopathologic variants of intraosseous ameloblastomas are commonly recognised. Polycystic ameloblastomas occur mainly in the body and ascending ramus of the mandible and most patients with this type present in the 4th decade of life (1). Unicystic ameloblastomas present on average a decade earlier (2) and are generally associated with a lower post-operative recurrence rate then the polycystic types. They can be divided microscopically into Groups 1, 2 or 3 depending on either the presence of a non-proliferating lining, intraluminal proliferations or mural invasion respectively (2). Ameloblastomas may occur more frequently in black Africans than in other racial groups (3).

Several recently published large series on ameloblastomas make no mention of coincidental and infrequent clinicopathologic findings (2–5) and most information about these is obtained through individual case reports. The secretion of interleukin-1 and a parathyroid hormone-like substance by an ameloblastoma was alleged to be the cause of hypercalcemia in one patient (6). A multilocular lytic mandibular lesion in a patient with hyperparathyroidism was proven microscopically to represent an ameloblastoma associated with a brown tumor of hyperparathyroidism (7). The occurrence of an ameloblastoma in a patient with the basal cell nevus syndrome (8) appears to be a sporadic rather than a regular feature. Other tumors that have been reported to be associated with ameloblastomas include the calcifying odontogenic cyst (9), acinic cell carcinoma and adenolymphoma of salivary gland origin (10), osteogenic sarcoma (11), traumatic neuroma (12) and aneurysmal bone cyst (13). HPV capsid antigen was proven positive with the immunoperoxidase staining technique in 3 out of 10 ameloblastomas in children (14) and mucormycosis infection was reported to have been superimposed on an ameloblastoma in an elderly diabetic woman (15). Stromal desmoplasia in a significant number of ameloblastomas has led to the use of the term 'desmoplastic ameloblastoma' (16) and extensive interstitial bone formation in ameloblastomas has recently been reported in two Japanese patients (17, 18). A case of papilliferous keratoameloblastoma was reported by ALTINI *et al.* (19) and other microscopic rarities include melanocytes between (20), and granular cell change in all tumor cells (21).

The purpose of this study was to determine the spectrum of uncommon clinical and pathological findings in a large sample of ameloblastomas diagnosed in a rural black African population.

## Material and methods

Clinical records, radiographs and hematoxylin and eosin-stained microscopic slides of biopsies and surgical resections of 108 primary intraosseous ameloblastomas were scrutinized for extraordinary and coincidental pathologic features. At least four wax blocks were available in most cases. The following special staining techniques were employed on selected cases: Mucicarmine for epithelial mucins, Masson-Fontana for melanin, Perl's Prussian blue for hemosiderin pigment and the *in situ* hybridization technique for the presence of HPV antigen. All cases were diagnosed and treated in the Medunsa Dental Hospital which serves a black and mainly rural African community.

## Results

The sample consisted of 108 ameloblastomas of which 75 were polycystic and 33 unicystic. All cases originated intraosseously. The sex and age distributions are shown in Table 1. All polycystic and 29 of the unicystic ameloblastomas occurred in the mandible and four unicystic ameloblastomas presented as maxillary swellings. The left mandible was involved in 65 cases, right mandible in 26 and symphysis area in 13 cases. Twelve polycystic and 4 unicystic ameloblastomas perforated the bony cortex and caused soft tissue ulceration. A mandibular ameloblastic fibroma in a 19-year-old woman was adjacent to and continuous with a polycystic ameloblastoma (Fig. 1). Aneurysmal bone cyst changes were identified in the latter patient as well as in another polycystic ameloblastoma in a 20-year-old woman. A polycystic ameloblastoma which involved the anterior mandible of a 13-year-old girl was associated with a compound odontome (Fig. 2).

Microscopically, 47 polycystic ameloblastomas were follicular, 23 plexiform and 5 were of mixed follicular and plexiform patterns. The stellate reticulum showed no differentiation in 35 cases, 22 cases presented with acanthomatous differentiation, 9 cases with granular cell differentiation, 6 cases with both granular cell and acanthomatous differentiation, and basal cell differentiation was seen in one case. A follicular ameloblastoma showed acanthomatous differentiation and foci of mucous cell metaplasia (Fig. 3). One tumor, which occurred in the mandible of a 57-year-old woman, showed extensive keratinisation and was diagnosed as a keratoameloblastoma. The unicystic ameloblastomas showed mural invasion in 15 cases and intraluminal proliferation in one case. The remaining 17 unicystic ameloblastomas were lined by non-infiltrative epithelium. In 9 of the latter group, less than 3 blocks were available for microscopic examination. Microscopic changes resembling an adenomatoid odontogenic tumor were presention the walls of two unicystic ameloblastomas (Fig. 4). HPV type 18 was identified in a verrucous lesion which occurred in a polycystic ameloblastoma and in one case melanocytes were uniformly present between the neoplastic epithelial cells. In two patients aged 15 and 26 years respectively, ameloblastic epithelium contained eosinophilic granules in all tumor cells (Fig. 5). Hemosiderin pigment was identified in the cytoplasm of neoplastic odontogenic epithelial cells next to an area of hemorrhage. A desmoplastic re-

Table 1. Sex and age distribution

| | N | Sex M | Sex F | Average age (range in years) |
|---|---|---|---|---|
| Total sample | 108 | 50 | 58 | 29.3 (8–84) |
| Polycystic | 75 | 33 | 42 | 35.4 (13–84) |
| Unicystic | 33 | 17 | 16 | 16.5 (8–37) |

*Fig. 1.* A resected specimen showing a polycystic ameloblastoma associated with an ameloblastic fibroma (arrows).

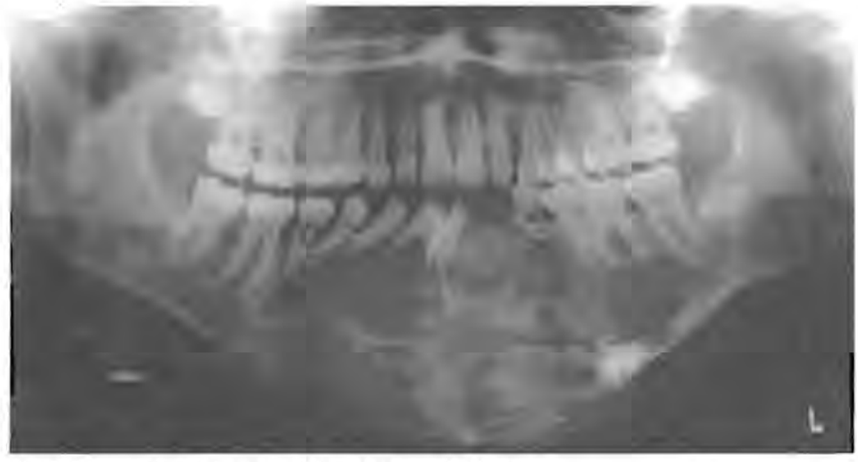

*Fig. 2.* Panoramic radiograph of the odontoameloblastoma.

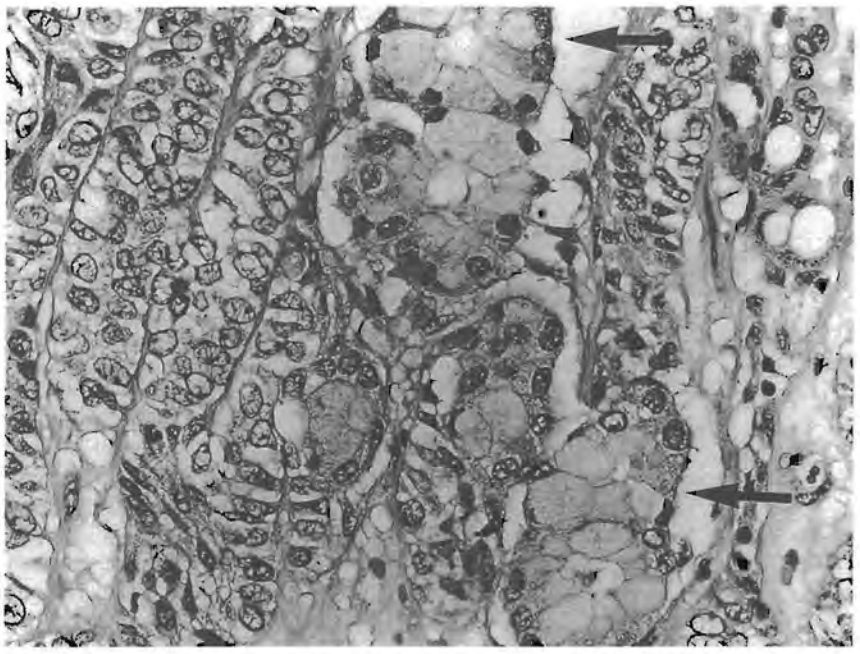

*Fig. 3.* Mucous-cell metaplasia (arrows) in an ameloblastoma (H&E, X240).

action was a common feature in the extraosseous component of ameloblastomas which perforated the bony cortex. Desmoplasia of the intrabony part of ameloblastomas was variable both between tumors and within the same tumor and depended upon the degree of inflammation. Only one case was diagnosed as a desmoplastic ameloblastoma on the basis of a uniform and mature connective tissue proliferation in the absence of inflammation and which impinged upon the neoplastic epithelial component (Fig. 6). Two polycystic ameloblastomas were associated with diffuse interstitial bony deposits which led to radiographic diagnoses of fibro-osseous lesions.

## Discussion

Large series published on ameloblastomas often make no mention of features other than those classically described and most infrequent findings are re-

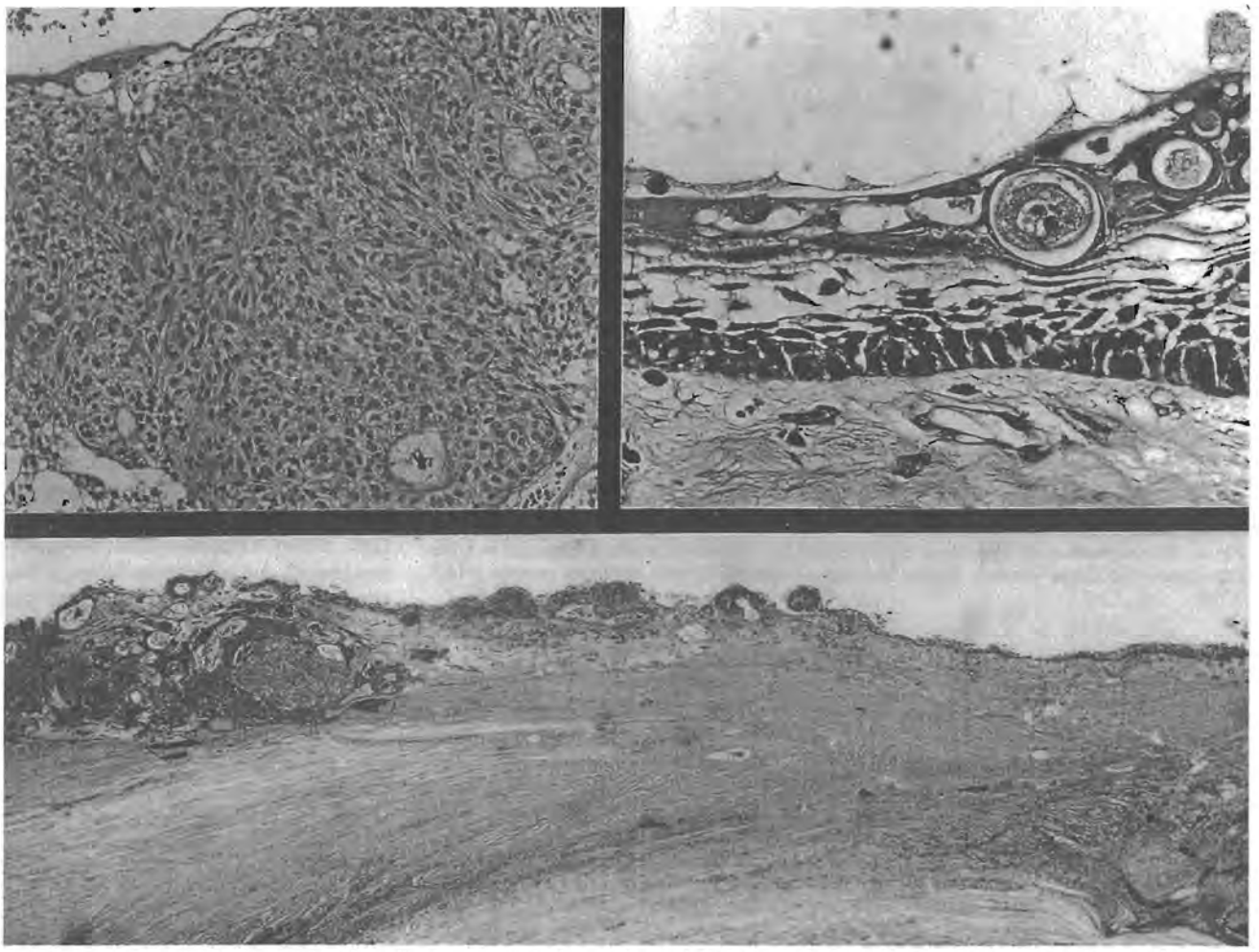

*Fig. 4.* A unicystic ameloblastoma (right side of low power view and top right insert) which exhibited adenomatoid odontogenic tumour differentiation (left side low power view and top left insert). (H&E, ×40, X120, X200).

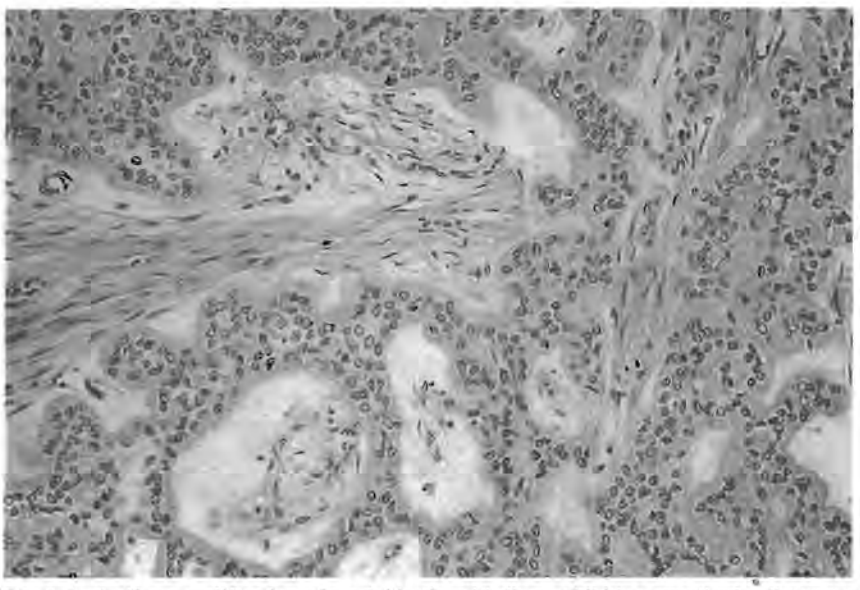

*Fig. 5.* A plexiform proliferation of ameloblastic epithelium exhibiting granules in all tumour cells. Typical features of ameloblastoma were not present (H&E, ×180).

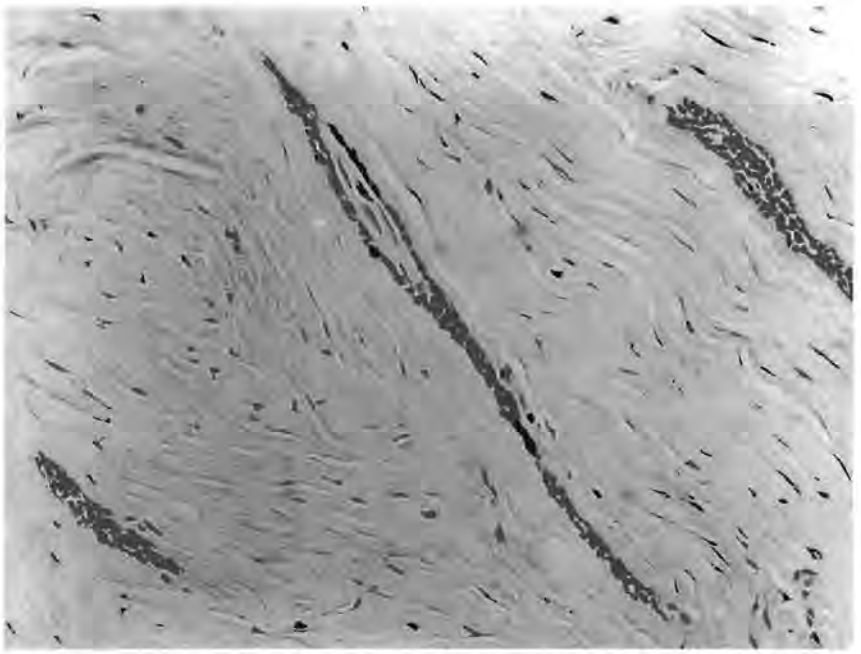

*Fig. 6.* Desmoplastic ameloblastoma characterized by compressed epithelial strands in a mature connective tissue stroma. Typical features of ameloblastoma were not present (H&E, ×180).

ported as case studies. This has led to a generally accepted view that ameloblastomas are fairly homogeneous in their clinical and pathologic presentation. This review was undertaken to establish the spectrum of extraordinary and coincidental clinical and pathologic findings in a large collection of ameloblastomas diagnosed in a rural African population.

In the total sample, the left mandible was affected 2.5 times more commonly than the right. Although there appears to be no apparent explanation for left mandibular predominance in our study, this finding is supported by a large Japanese series in which only 40% occurred on the right hand side (4).

The subclassification of unicystic ameloblastomas according to the microscopic appearance of the lining (2) was found to be impractical. Although areas of intraluminal proliferation or mural invasion positively confirmed unicystic ameloblastomas in Groups 2 and 3 respectively, the subdivision into Group 1 lesions was found to be of limited value unless the whole tumor was processed for microscopic examination. In the case of large unicystic ameloblastomas, this was either impractical or even impossible, making the microscopic identification of foci of mural invasion in larger lesions unlikely. This dilemma is clearly illustrated in our study where fewer than three wax blocks were available for microscopic examination in 9 cases ultimately subclassified as Group 1 unicystic ameloblastomas.

Tumors which occur within bone generally predispose to pathologic fracture and aneurysmal bone cyst formation (22). Both these findings are, however, infrequently reported in association with ameloblastomas. The presenting symptom in only three of our patients was directly associated with pathologic fracture of the mandible. Aneurysmal bone cysts are reported to be rare in the jaws, occur mainly in young patients, and approximately one-third are found in association with other pathologies (23). A microscopic study of 42 ameloblastomas found hallmarks of aneurysmal bone cysts in 7 (13). Although the frequencey of aneurysmal bone cyst change in our study was not as high, both our cases occurred in young patients. The coexistence of aneurysmal bone cyst with ameloblastoma is significant because of the excessive bleeding which may be encoutered during surgery.

The association of an ameloblastic fibroma with ameloblastoma has not previously been reported. The example described here could be regarded as coincidental, as the patient was at an age when ameloblastic fibroma occurs most frequently. Simultaneous occurrence of ameloblastoma and odontoma is rare (24). These tumors, which have been designated as odontoameloblastomas, consists of epithelial proliferations typical of ameloblastomas associated with highly differentiated dental tissues either scattered throughout the tumor or, as in our case, as a single radiopaque mass (1). Squamous metaplasia is a well described and variable feature in ameloblastoma. Extensive squamous change, where follicles consist entirely of squamous epithelium with only traits of the original ameloblastomatous structure, is less frequent (23). One tumor in our series, which occurred in an elderly woman patient, exhibited this change and was diagnosed as a kera-

toameloblastoma. Although adenomatoid odontogenic tumor-like differentiation has been reported in a dentigerous cyst (25), this change in a unicystic ameloblastoma has not yet been described. Both our examples occurred in the anterior mandible and this, together with the hitherto undescribed phenomenon of mucous cell metaplasia, illustrates the differentiation protential of ameloblastic epithelium.

The presence of an HPV-induced verucca in the epithelial lining of a polycystic ameloblastoma adds an interesting parameter to the study of papillomavirus-induced epithelial proliferations. These lesions occur commonly on the skin and lining mucosa, to our knowledge this case, which was published recently (26), represents the first description of a verucca in a cystic epithelial tumor, the lining of which was within bone and not in contact with the oral mucosa. The origin of the melanocytes in odontogenic tumors and cysts is speculative. The cells of the neural crest interact in the development of teeth and it is not surprising that melanocytes can occur in odontogenic tissues. Although it is believed that melanotic odontogenic tumors occur more frequently in black patients (25), the number of cases reported is too low to draw conclusions. Our one melanotic ameloblastoma in the 108 cases studied places the frequency of this phenomenon below 1% in a black African sample and thus can hardly be regarded as common. The presence of hemosiderin in the neoplastic epithelium adjacent to an area of hemorrhage emphasizes the phagocytic capacity of neoplastic odontogenic epithelium. Varying amounts of granular cells are seen in the stellate reticulum of granular cell ameloblastomas. However, the presence of granules in all cells, including the peripheral layer, is rare. We believe this feature, which was present in two of our cases, represents full expression of granular cell differentiation. The plexiform granular cell odontogenic tumor reported by ALTINI *et al.* (1986) (27) is probably an example of this variant.

Quantification of stromal desmoplasia was found to be difficult as it varied between tumors and within the same tumor. Generally, ameloblastomas which infiltrate soft tissue and those which are inflamed exhibit more desmoplasia than others. Terminology such as "desmoplastic ameloblastoma' (16) should be used with great circumspection as the intensity of the desmoplasia is variable and forms part of a continuous spectrum of stromal fibroplastic reaction in ameloblastomas. We suggest that certain criteria must be applied before the diagnosis of a desmoplastic ameloblastoma is made. These should include the absence of inflammatory changes and cortical bone perforation as well as the uniform presence of a mature, diffuse collagenous stromal tissue compressing the neoplastic epithelial component into strands. The two tumors which contained extensive interstitial bony deposits resemble the Japanese cases published recently (17, 18) and their clinical and radiographic differentiation from benign fibro-osseous proliferations is a pitfall to be avoided. The prominent bone formation appeared to be reactive in nature, probably linked to a process of interstitial connective tissue metaplasia rather than a result of induction, as the bony deposits were generally separated from the neoplastic epithelium by a broad band of inactive connective tissue. Unlike a recently published paper (28), we believe the desmoplastic and osteoplastic ameloblastomas are not distinct clinicopathologic entities but rather variants of the microscopic spectrum of stromal reactions in ameloblastomas.

This study demonstrates that although ameloblastomas are generally regarded as a homogeneous group of neoplasms, detailed investigations prove clinicopathologic diversity in a significant number of tumors. Many of these changes emphasize the differentiation potential of neoplastic odontogenic epithelium and add interesting parameters to the study of tissue reactions associated with this common odontogenic tumor.

*Acknowledgement* – The authors thank Mrs. C.S. BEGEMANN for secretarial assistance.

## References


1. SHAFER GS, HINE MK, LEVY BM, eds. *A textbook of oral pathology*. Philadelphia: WB Saunders, 1983: 276–85.
2. ACKERMANN GL, ALTINI M, SEHAR M. The unicystic ameloblastoma: a clinicopathological study of 57 cases. *J Oral Pathol* 1988; **17**: 541–6.
3. AJAGBE HA, DARAMOLA JO. Ameloblastoma; a survey of 199 cases in the University College Hospital, Ibadan, Nigeria. *J Natl Med Assoc* 1987; **79**: 324–7.
4. KAMEYAMA Y, KAKEHANA S, MIZOHATA M, NONOBE M, HARA K, KAWAI M, FUKAYA M. A clinicopathological study of ameloblastomas. *Int J Oral Maxillofac Surg* 1987; **16**: 706–12.
5. UENO S, NAKAMURA S, MUSHIMOTO K, SHIRASU R. A clinicopathologic study of ameloblastoma. *J Oral Maxillofac Surg* 1986; **44**: 361–5.
6. MACPHERSON DW, HOPPER C, MEGHJI S. Hypercalcaemia and the synthesis of interleukin-1 by an ameloblastoma. *Br J Oral Maxillofac Sug* 1991; **29**: 29–33.
7. ZAMUROVIC D, ANDRY G, LEMORT M, DAGNELIE J, PERETZ A, DOUROV N, MAYER R, FAMAEY JP. Concomitant osteitis fibrosa cystica and ameloblastomas of the mandible. *J Rheumatol* 1989; **16**: 397–401.
8. SCHULTZ SM, TWICKLER DM, WHEELER DE, HOGAN TD. Ameloblastoma associated with basal cell nevus (Gorlin) syndrome: C T findings. *J Comput Assist Tomogr* 1987; **11**: 901–4.
9. PRAETORIUS F, HJORTING-HANSEN E, GORLIN RJ, VICKERS RA. Calcifying odontogenic cyst. Range, variations and neoplastic potential. *Acta Odontol Scand* 1981; **39**: 227–40.
10. NAKAMURA N, HIGUCHI Y, TASHIRO H, SHIRATSUCHI Y. Mandibular ameloblastoma associated with salivary gland tumor. *Int J Oral Maxillofac Surg* 1988; **17**: 103–5.
11. FEUN LG, ALBORES-SAAVEDRA J, SAVARAJ N. Osteogenic sarcoma arising adjacent to a longstanding ameloblastoma. A case report. *Oral Surg Oral Med Oral Pathol* 1991; **7**: 77–9.
12. ZAIN R, LING KC. Traumatic neuroma in the wall of a recurrent unicystic ameloblastoma: a case report. *Med J Malaysia* 1985; **40**: 49–51.
13. NADIMI H, TOTO PD, MCREYNOLDS HD. Co-existant aneurysmal bone cysts with ameloblastomas: a histologic survey. *J Oral Med* 1986; **41**: 242–3.
14. KAHN MA. Ameloblastoma in young persons: a clinicopathologic analysis and etiologic investigation. *Oral Surg Oral Med Oral Pathol* 1989; **67**: 706–15.
15. MOLERO X, CANALS J, RILO A, ORTEGA A. Mucormycosis and ameloblastoma of the upper jaw. *Infection* 1985; **13**: 225–7.
16. WALDRON CA, EL-MOFTY SK. A histopathologic study of 116 ameloblastomas with special reference ot the desmoplastic variant. *Oral Surg Oral Med Oral Pathol* 1987; **63**: 441–51.
17. TAKEDA Y, YAMAMOTO H. Ameloblastoma located in the alveolar bone: a case report. *J Nihon Univ Sch Dent* 1990; **32**: 270–4.
18. OKADA Y, SUGIMURA M, ISHIDA T. Ameloblastoma accompanied by prominent bone formation. *J Oral Maxillofac Surg* 1986; **44**: 555–7.
19. ALTINI M, SLABBERT HD, JOHNSTON T. Papilliferous keratoameloblastoma. *J Oral Pathol Med* 1991; **20**: 46–8.
20. LURIE HI. Congenital melanocarcinoma, melanotic adamantinoma, retinal anlage tumor, progonoma and pigmented epulis

of infancy. Summary and review of the literature and report of the first case in an adult. *Cancer* 1961; **14**: 1090–108.

21. YAMAMOTO G, YOSHITAKE K, TADA K, YOSHIDA K, YOKOTA H, FUKUDA Y, ISHIDA T. Granular cell ameloblastoma. A rare variant. *Int J Oral Maxillofac Surg* 1989; **18**: 140–1.
22. STRUTHERS PJ, SHEAR M. Aneurysmal bone cyst of the jaws (II). Pathogenesis. *Int J Oral Surg* 1984; **13**: 92–100.
23. LUCAS RB. *Pathology of tumours of the oral tissues*. 4th ed. Edinburgh: Churchill Livingstone 1984; **31**: 380.
24. FRISSELL CT, SHAFER WG. Ameloblastic odontoma; a report of a case. *Oral Surg Oral Med Oral Pathol* 1953; **6**: 1129–32.
25. WARTER A, GEORGE-DIOLOMBI G, CHAZAL M, ANGO A. Melanin in a dentigerous cyst and associated adenomatoid odontogenic tumor. *Cancer* 1990; **66**: 786–8.
26. VAN HEERDEN WFP, VAN RENSBURG EJ, RAUBENHEIMER EJ, VENTER EH. Detection of human papillomavirus DNA in an ameloblastoma using the in situ hybridization technique. *J Oral Pathol Med* 1993; **22**: 109–12.
27. ALTINI M, HILLE JJ, BUCHNER A. Plexiform granular cell odontogenic tumor. *Oral Surg Oral Med Oral Pathol* 1986; **61**: 163–7.
28. PHILIPSEN HP, ORMISTON IW, REICHART PA. The desmo- and osteoplastic ameloblastoma. Histologic variant or clinicopathologic entity? Case reports. *Int J Oral Maxillofac Surg* 1992; **21**: 352–7.

Vol. 90 No. 5 November 2000

269

ORAL SURGERY,
ORAL MEDICINE,
ORAL PATHOLOGY,

ORAL AND MAXILLOFACIAL RADIOLOGY Editor: Sharon L. Brooks

# Calcifying epithelial odontogenic tumor with intracranial extension: Report of a case and review of the literature

M. M. R. Bouckaert,[a] E. J. Raubenheimer,[b] and F. J. Jacobs,[a] Medunsa, South Africa
MEDICAL UNIVERSITY OF SOUTHERN AFRICA

The calcifying epithelial odontogenic tumor (CEOT) is a rare benign neoplasm, possibly of stratum intermedium origin and occurring predominantly in the mandible of adults. The treatment varies, depending on its size, location, and histology. A case of an advanced CEOT arising in the maxilla with intracranial extension is reported. The report is supplemented by a review of the literature. **(Oral Surg Oral Med Oral Pathol Oral Radiol Endod 2000;90:656-62)**

The calcifying epithelial odontogenic tumor (CEOT) is a rare benign odontogenic neoplasm of the jaws. Many names have been given to this lesion.[1] Pindborg[2] was the first to describe this lesion as a separate clinicopathologic entity, and he named it a calcifying epithelial odontogenic tumor. Today, nearly 200 cases have been reported in the literature. The origin of this neoplasm is controversial, though it is generally accepted to have derived from the oral epithelium, reduced enamel epithelium, or stratum intermedium.[3-7] Pindborg's proposed origin, from reduced enamel epithelium, is plausible because more than half are associated with unerupted or impacted teeth.[2] Chaudry's histochemical studies support the theory that the CEOT arises from the stratum intermedium.[4,8]

Clinically, CEOT manifests as an intraosseous lesion (central type) in the majority of cases (95%). Extraosseous or peripheral lesions account for less than 5% of cases. The latter are usually in the anterior region of the jaws. Most investigators agree that the central type is usually located in the premolar and molar regions, with a mandibular to maxillary ratio of 2 to 1. The majority of CEOTs (52%) are associated with impacted or unerupted teeth.[1,2] There is an almost equal distribution between men and women. The age of the patients affected by this tumor ranges from 8 to 92 years, with a mean age of 40. This neoplasm occurs in different population groups, with a slight predilection for whites.[1,2] However, this may merely reflect a reporting bias. The most common radiographic finding is a well-defined unilocular radiolucency, which resembles a dentigerous cyst. The neoplasm may appear as a multilocular lesion mimicking an ameloblastoma. Classically, areas of scattered flecks of calcifications in the central radiolucency may be seen; however, calcifications may sometimes not be evident on radiographs.[1]

The histologic criteria listed by Franklin and Pindborg [1] and others[6,8-11] for the diagnosis of CEOT are sheets of polyhedral epithelial cells that have well-defined borders and often show prominent intercellular bridges. There is usually pleomorphism of the epithelial cells, and the nuclei and nucleoli are often prominent. Mitotic figures are rarely seen. A characteristic feature within the sheets of epithelial cells is circular areas filled with a homogeneous substance resembling amyloid-like material, which stains positively with Congo red. Some of these cells are also filled by calcified material in the form of concentric Liesegang's rings, which are pathognomonic of this tumor.[3,8-10,12]

Recently, variants of CEOT, which may have a bearing on the prognosis and management, have been described. Three such variants reported in the English literature are the noncalcifying CEOT with Langerhans' cells, the CEOT displaying cementum-like and bone-like material, and the clear-cell CEOT.[12-17] The former variant of noncalcifying epithelial odontogenic tumor is histologically similar to the peripheral type of

[a]Department of Maxillofacial and Oral Surgery, Medical University of Southern Africa, Republic of South Africa.
[b]Department of Oral Pathology, Medical University of Southern Africa, Republic of South Africa.
Received for publication June 24, 1999; returned for revision Oct 18, 1999; accepted for publication Jan 20, 2000.

1079-2104/2000/$12.00 + 0 7/16/106577
doi:10.1067/moe.2000.106577

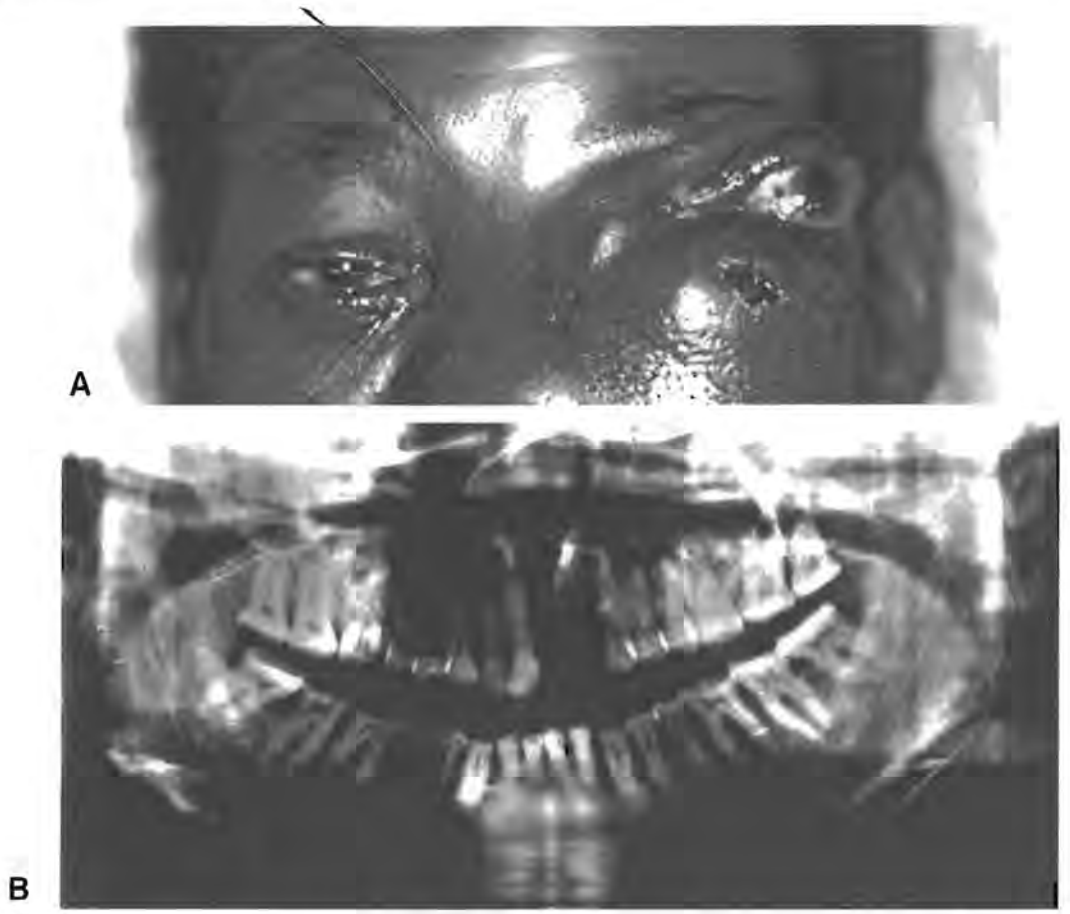


Fig 1. **A**. Large swelling of left face causing severe left orbital dystopia. Note fistula below left eye. **B**, Panoramic view of patient showing large, poorly demarcated lytic lesion with missing left central and lateral incisors.

CEOT but is devoid of calcifications, and one may speculate that this variant's clinical behavior would be less aggressive than the peripheral lesion.[12,13] It has been proposed that CEOTs with more amyloid and calcifications could be treated less aggressively.[8,18] CEOTs with large amounts of bone-like or cementum-like material probably indicate a higher level of differentiation and thus may account for their more self-limiting behavior, unlike the ameloblastoma.[19] The clear-cell CEOT variant is more aggressive with a higher recurrence rate (22%), and some would consider this form to be a low-grade odontogenic carcinoma.[20]

In 1984, Basu et al[3] reported a malignant CEOT that showed evidence of local tissue invasion and regional lymph node metastasis.[8,20] There have also been reports of various other odontogenic lesions occurring in association or in combination with CEOT. These include dentigerous cysts[5] and adenomatoid odontogenic tumors,[6,13] as well as presentation of CEOT as an intramural lesion of the dental sac.[7,8]

The purpose of this article is to report an unusual CEOT arising in the maxilla that has expanded into the cranial cavity, causing orbital dystopia and severe intracranial complications.

## CASE REPORT

A 54-year-old black man was referred to the Department of Maxillofacial and Oral Surgery by a rural clinic for assessment of a large swelling, causing severe left orbital dystopia and gross facial asymmetry (Fig 1, *A*). His family had noticed that he struggled to maintain his balance, and he presented with urinary incontinence. He had noticed this slow-growing lesion for a number of years, but had neglected to report it to his clinic because it was asymptomatic. His medical history was completely unremarkable, with no evidence of systemic diseases. The patient had no vision in his left eye. Below this eye was evidence of a pus-draining fistula. No regional nerve paresthesia or lymphadenopathy was present. Intraorally, there was a firm, expansile lesion, involving the left maxilla, with obliteration of the left maxillary buccal vestibule. There was no palatal expansion. The oral mucosa was intact and normal in color. The left maxillary central and lateral incisors were extracted many years ago. The patient had very poor oral hygiene. A panoramic radiograph showed a large, poorly demarcated lyric lesion with irregular areas of opacities involving the left maxillary sinus and orbit (Fig 1, *B*). The differential diagnosis included cemento-

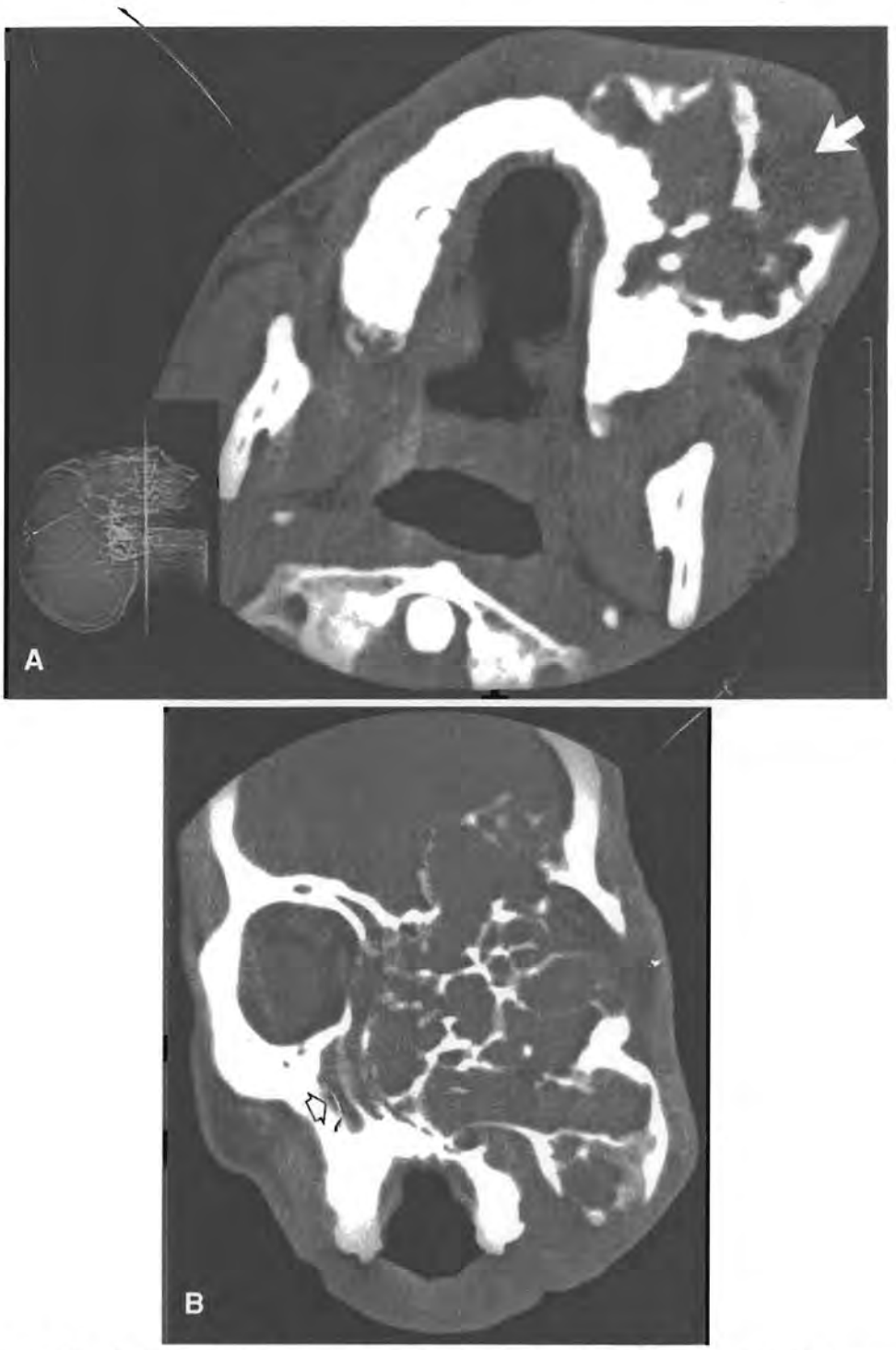


Fig 2. **A**, Axial CT scan at level of maxilla showing buccal expansion and cortical perforation *(arrow)*. **B**. Coronal CT scan through orbits showing tumor expanding intracranially, obliterating left maxillary antrum, left orbit, nasal cavities, ethmoidal sinus, left frontal sinus, and displacing medial wall of right antrum *(arrow)* and of right orbit. Note lack of palatal expansion.

ossifying fibroma, ameloblastic odontoma, and CEOT. Computed tomography (CT) scans of the maxilla and orbits were obtained to show axial and coronal sections of the soft tissues and facial bones. A well-circumscribed isodense mass with expanding radiopaque margins containing areas of irreg stellate opacities was seen (Fig 2. *A* and *B*).

Magnetic resonance imaging showed a massive tu destroying the left maxilla through to the anterior cra

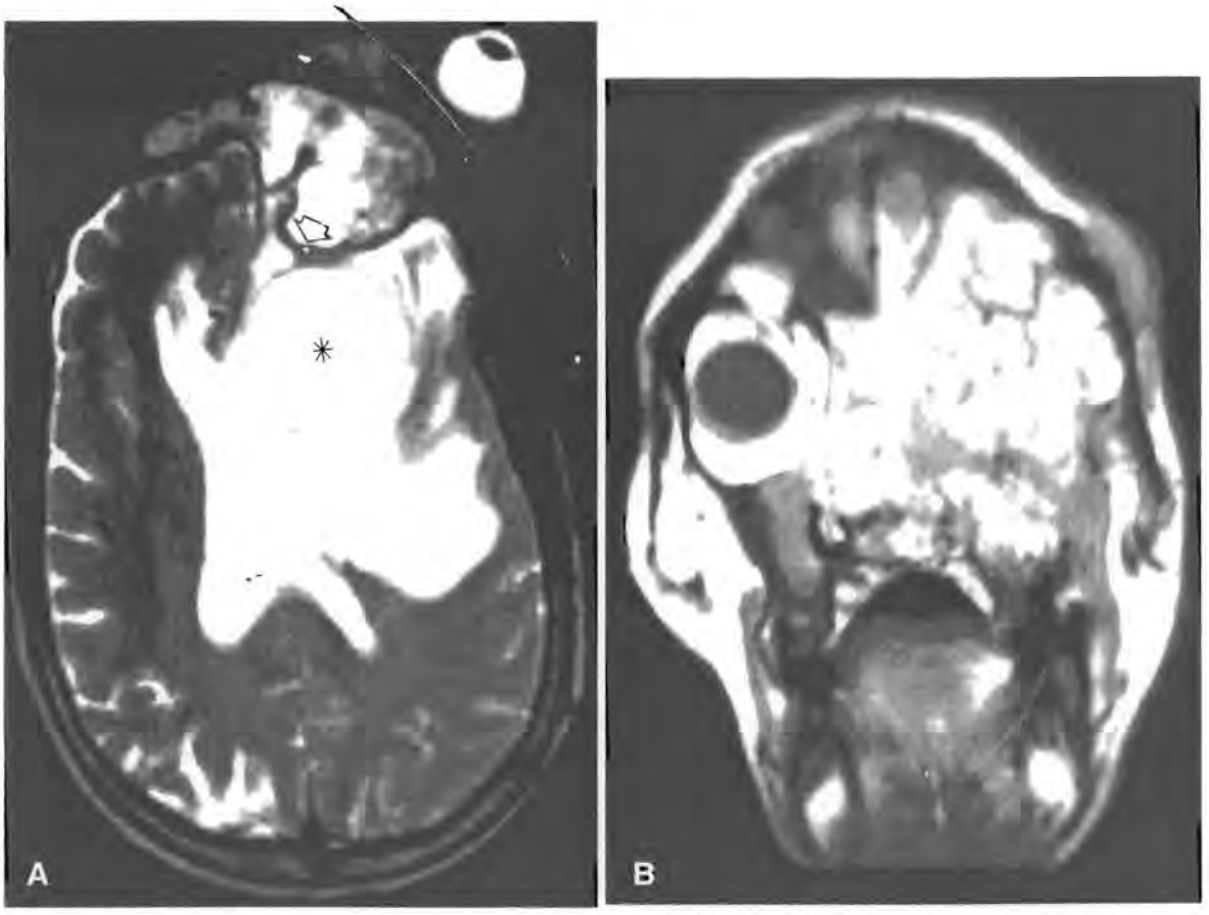


Fig 3. **A**. Axial magnetic resonance scan ($T^2$ series) showing displaced left eye and tumor extending into frontal area *(arrow)*. Note well-circumscribed mass *(asterisk)* posterior to tumor. **B**, Coronal magnetic resonance scan ($T_1$ series) showing massive infiltration into frontal area of brain.

fossa. The tumor invaded the left orbit and displaced the left eye anterosuperolaterally (Fig 3, *A*). The left eye showed no infiltration by tumor.

There was invasion of the right orbit and the right antrum. The tumor infiltrated through the ethmoid sinuses and the cribiform plate into the frontal area (Fig 3, *B*). There was also a large, well-circumscribed fluid-retained area in the frontal lobe, which may have been an abscess with surrounding brain edema. The midline of the brain was displaced to the right with compression of the adjacent right ventricle (Fig 4).

An angiogram of the left internal and external carotid artery was done with the Seldinger technique. The intracranial extension of the tumor showed displacement of the middle cerebral artery laterally and the anterior cerebral artery medially (Fig 5). An incisional biopsy of the left maxillary vestibule was performed with the patient under local anesthesia. The patient was admitted to the academic hospital for further preoperative workup. Histologic examination showed a fibrous connective tissue capsule surrounding sheets of pleomorphic polyhedral epithelial cells, containing nuclei of varying forms and sizes and lacking mitotic activity. An extracellular eosinophilic material resembling amyloid was focally present. There were concentric calcifications with Liesegang rings (Fig 6). The histologic diagnosis was CEOT.

The Department of Neurosurgery was consulted, and the patient was prescribed methylprednisolone to alleviate brain edema. He showed dramatic recovery of neurologic symptoms and requested to be discharged. At his follow-up visit a month later, the patient had noticed a large amount of pus draining from below the left eye. His condition further improved over the next few days. A CT scan showed a significant reduction in the size of the fluid-filled space in the frontal area of the brain. Several treatment options were explained to the patient and his family. The patient requested a temporary discharge and was then lost to follow up.

## DISCUSSION

CEOT is a rare benign epithelial odontogenic neoplasm that was first described by Pindborg in an abstract in 1955 and again as an article in 1958.[1,2] Though this tumor is benign, a few cases have been reported as locally aggressive, invading surrounding

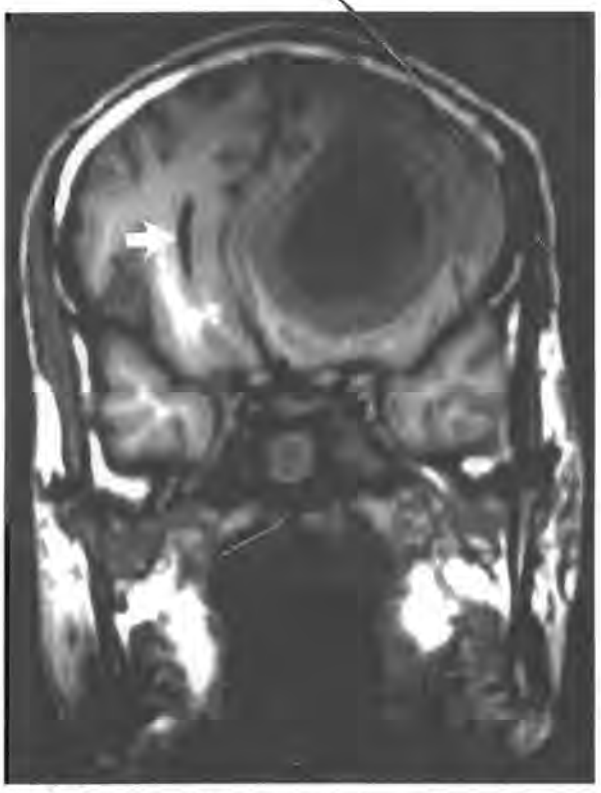

Fig 4. Magnetic resonance imaging (coronal view) showing large, well-circumscribed area causing midline shift, obliteration of left ventricle, and compression of right ventricle *(arrow)*.

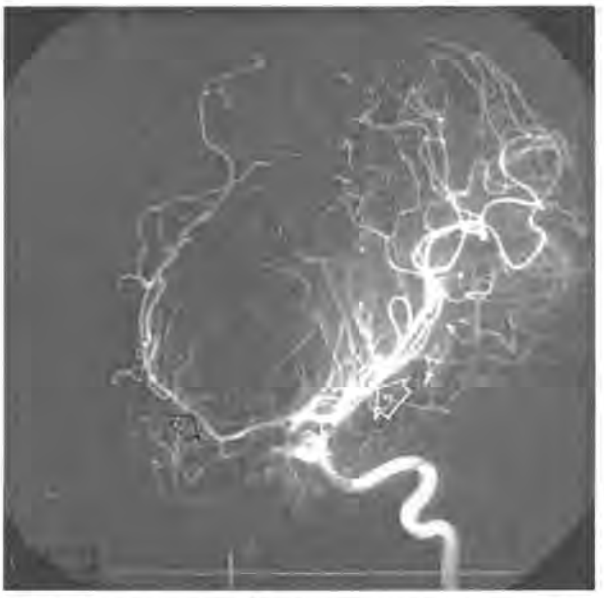

Fig 5. Angiogram of left internal carotid artery, showing lateral displacement of middle cerebral artery *(white arrow)* and medial displacement of anterior cerebral artery *(black arrow)*.

soft tissues and bone.[21] CEOTs account for less than 1% of all odontogenic tumors.[1,2]

Ficarra et al[7] suggested that the neoplasm arises from cell remnants frequently seen in the wall of the dental sac that resemble the reduced enamel epithelium. Regarding the extraosseous-type lesions, the origin is less certain,[8] but Ai Ru et al[22] suggested that the peripheral type arises from oral epithelium. The prevalence in the molar region is 3 times that of the premolar area. Fifty-two percent of cases are associated with an unerupted tooth.[1] It would appear that our case also arose from the anterior maxilla or from the wall of the maxillary sinus and then expanded over the years by the path of least resistance through the maxillary sinus to the ethmoid sinus, eroding the cribiform plates into the frontal area. No palatal expansion was evident, despite extensive orbital and intracranial involvement. CEOT arising in the maxillary sinus is extremely rare.[23] Three other cases have been described in the English literature of CEOT that possibly originated in the maxillary sinus wall.[21,24,25]

The clinical features are usually those of a painless, slow-growing intraosseous mass. However, a tumor in the maxilla may cause pain, nasal obstruction, epistaxis, headaches, and proptosis.[1,19] Our patient gave no history of any of the above symptoms, and only when neurologic symptoms occurred did he seek help. Although intracranial extension was demonstrated beyond doubt, the large fluid-filled space in the frontoparietal area of the brain was probably not part of the tumor. The pus that drained from below the left eye was followed by a reduction in size of the fluid-filled space, making it likely to be a brain abscess. It is proposed that distortion of the paranasal sinuses may have resulted in blockage of drainage and sinus infection, which extended into the brain.

Treatment options for CEOT have ranged from simple enucleation to radical and extensive resection.[8] Several authors initially advocated aggressive treatment, but increasingly, histologic information shows that this tumor does not appear to extend into the intertrabecular bony spaces as does an ameloblastoma[1,19]; therefore, a more conservative approach is warranted.[10] Sadeghi and Hopper[26] believe the surgical treatment of CEOT should be guided by the site, size, and the histologic features of the lesion. Thus, maxillary neoplasms would be treated more aggressively because of their close proximity to vital and important structures,[23] whereas mandibular lesions could be approached more conservatively. Our intended treatment plan was primarily to debulk the tumor and then later, with reconstructive procedures, to repair soft and hard tissue defects. A modified Weber incision, which would continue superi-

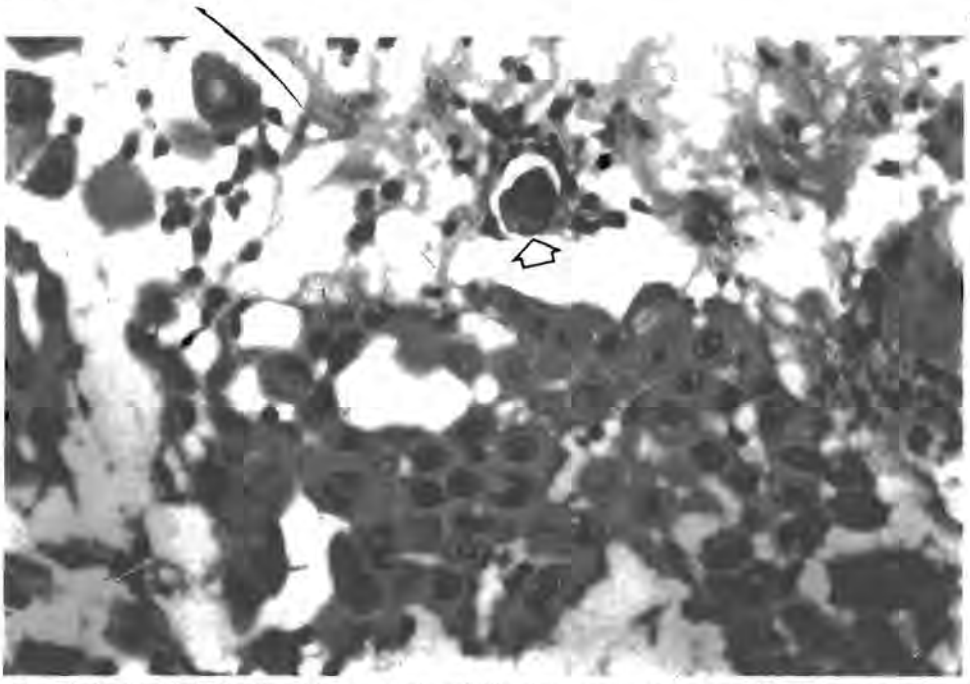

Fig 6. Polyhedral epithelial cells with concentric calcification *(arrow)* (hematoxylin-eosin, original magnification ×200).

orly as a paranasal incision that extends onto the forehead vertically to join the superior limb of a left temporal flap, would have allowed the whole facial skin to reflect laterally, giving direct access to the maxilla, cribriform plate, and ethmoid area. The patient unfortunately declined surgery and was lost to follow-up.

Our case demonstrates that, although CEOTs are benign, neglect of a maxillary lesion can lead to serious intracranial involvement, which could severely complicate patient management.

## REFERENCES

1. Franklin CD, Pindborg JJ. The calcifying epithelial odontogenic tumor: a review and analysis of 113 cases. Oral Surg Oral Med Oral Pathol 1976;42:753-65.
2. Pindborg JJ. A calcifying odontogenic tumor. Cancer 1958;11:838-43.
3. Basu MK, Matthews JB, Sear AJ, Browne RM. Calcifying epithelial odontogenic tumor: a case showing features of malignancy. J Oral Pathol 1984;15:310-9.
4. Siar CH, Ng KH. The combined epithelial odontogenic tumor in Malaysians. Br J Oral Maxillofac Surg 1991;29:106-9.
5. Ismail IM, Al-Talabani NG. Calcifying epithelial odontogenic tumor associated with dentigerous cyst. Int J Oral Maxillofac Surg 1986;15:108-11.
6. Bingham RA, Adrian JC. Combined epithelial odontogenic tumor-adenomatoid odontogenic tumor and calcifying epithelial odontogenic tumor: report of a case. J Oral Maxillofac Surg 1986;44:574-7.
7. Ficarra G, Hansen LS, Stiesmeyer EH. Intramural calcifying epithelial odontogenic tumor. Int J Oral Maxillofac Surg 1987;16:217-21.
8. Nelson SR, Schow SR, Read LA, Svane TJ. Treatment of an extensive calcifying epithelial odontogenic tumor of the mandible. J Oral Maxillofac Surg 1992;50:1126-31.
9. Maranda G, Gourgi M. Calcifying epithelial odontogenic tumor (Pindborg tumor). Review of the literature and case report. J Can Dent Assoc 1986;52:1009-12.
10. Leipzig B, Yau PC. Pindborg tumor of the mandible. Otolaryngol Head Neck Surg 1982;90:69-74.
11. Sharer WG, Hine MK, Levy BM. A Textbook of oral pathology. 4th ed. Philadelphia: WB Saunders; 1983. p. 286-9.
12. Asano M, Takahashi T, Kusama K, Iwase T, Hori M, Yamanoi H, et al. A variant of calcifying epithelial odontogenic tumor with Langerhans cells. J Oral Pathol Med 1990;19:430-4.
13. Takata T, Ogawa I, Miyauchi M, Ijuhin N, Nikai H, Fujita M. Non-calcifying Pindborg tumor with Langerhans cells. J Oral Pathol Med 1993;22:378-83.
14. El-Labban NG. Cementum-like material in a case of Pindborg tumor. J Oral Pathol Med 1990;19:166-9.
15. Slootweg PJ. Bone and cementum as stromal features in Pindborg tumor. J Oral Pathol Med 1991;20:93-5.
16. Hicks M J, Flaitz C, Batsakis JG. Adenomatoid and calcifying epithelial tumor. Ann Otol Rhinol Laryngol 1993;102:159-61.
17. Schmidt-Westhausen A, Philipsen HP, Reichart PA. Clear cell calcifying epithelial odontogenic tumor: a case report. Int J Oral Maxillofac Surg 1992;21:47-9.
18. Andrade M, Medeiros PJ, Prado R, Sampaio R. Calcifying epithelial odontogenic tumor (Pindborg tumor): report of case. J Oral Maxillofac Surg 1992;50:1324-6.
19. Krolls SO, Pindborg JJ. Calcifying epithelial odontogenic tumor. A survey of 23 cases and discussion of histomorphologic variations. Arch Pathol 1974;98:206-10.
20. Hicks MJ, Flaitz CM, Wong MEK, McDaniel RK, Cagle PT. Clear cell variant of odontogenic tumor: case report and review of the literature. Head Neck 1994;16:272-7.
21. Baunsgaard P, Løntoft E, Serensen M. Calcifying epithelial odontogenic tumor (Pindborg tumor): an unusual case. Laryngoscope 1983;93:635-8.
22. Ai Ru L, Zhen L, Jian S. Calcifying epithelial odontogenic tumors: Clinicopathologic study of nine cases. J Oral Pathol 1982;11:399-406.
23. Lee CYS, Mohammadi H, Mostofi R, Hadidi A. Calcifying epithelial odontogenic tumor of the maxillary sinus. J Oral Maxillofac Surg 1992;50:1326-8.

24. Gon F. The calcifying epithelial odontogenic tumor: report of a case and study of its histogenesis. Br J Cancer 1964;19:39-50.
25. Stinson PG, Luna MA, Butler JJ. Seventeen year history of a calcifying epithelial odontogenic (Pindborg) tumor. J Oral Surg 1968;25:204-8.
26. Sadeghi EM, Hopper TL. Calcifying epithelial odontogenic tumor. J Oral Maxillofac Surg 1982;40:225-9.

*Reprint requests:*

Professor M. M. R. Bouckaert
Department of Maxillofacial and Oral Surgery
Box D23
PO Medunsa, 0204
South Africa

# Hodgkin's disease presenting in the maxilla

## A case report

**Glenn E. Lello[1] and Erich Raubenheimer[2]**

[1]Departments of Maxillofacial and Oral Surgery, and [2]Oral Pathology and Oral Biology Medical University of Southern Africa, Medunsa 0204, South Africa

*G. E. Lello and E. Raubenheimer: Hodgkin's disease presenting in the maxilla. A case report. Int. J. Oral Maxillofac. Surg. 1989; 18: 7–9.*

*Abstract.* A rare case of intra-oral, extra nodal, maxillary Hodgkin's disease (Stage I), with no other discernible tissue involvement is described and discussed. The pertinent literature is reviewed.

Key words: Hodgkin's disease.

Accepted for publication 10 August 1988

Hodgkin's disease, a malignant lymphoma first described by Thomas Hodgkin in 1832[12], occurs most commonly in the 20- to 30-year age group, with a second peak in incidence after the age of 55 years. Males are said to be affected more frequently.

Presentation is most commonly in the form of a painless but progressive enlargement of lymph nodes in the neck. Extra nodal presentation with involvement of the spleen, bone marrow, skin, intestines and liver is less common. Malaise, fever, weight loss and pruritus are among the more frequently associated signs and symptoms.

Histologically, the disease is characterized by the presence of malignant lymphoid cells and inflammatory cells including lymphocytes, histiocytes, eosinophils and plasma cells; however Reed-Sternberg cells: large, multinucleated cells with very large 'owl-eye' neucleoli and 'mirror-image' nuclei, must be identified within this cellular background for the histological diagnosis to be made.

Classification of the disease is in accordance with the abundance of lymphocytes observed within the infiltrate. The Rye classification[15] is made following histological examination of an involved excised lymph node, and is based on the nature and pattern of lymphocytic infiltration of the node.

Prognostication of survival times must, however, take into account the staging of the disease, for which the Ann Arbor classification[5], based on the anatomical location of the lesion, is most widely followed.

Hodgkin's disease uncommonly involves bone clinically, and rarely involves the jawbone; primary involvement of the maxilla has only been reported once previously[20].

### Case report

In January 1987, a 51-year-old black female attended her dentist complaining of mobile and painful 11 and 21 teeth. Both teeth were extracted.

Approximately 2 months later, the mucosa covering the crest of the alveolus at the extraction site ulcerated, with extension onto the palate and into the buccal sulcus. The ulcer was painful, and the patient reported a putrid taste. 2 months later, the patient consulted our unit.

On presentation, the patient's medical history revealed that despite a good appetite, she had recently lost weight. Clinically, the patient appeared anaemic; however a general physical examination failed to detect any other abnormalities. No lymphadenopathy was present.

Intra-orally, the mucosa overlying the alveolus between the 14 and the 23 had ulcerated with a similar area of palatal involvement (Fig. 1). The 14, 13, 12, 22 and 23 teeth were mobile, vital and protruded from the denuded, grey/black discoloured alveolar bone. The upper lip was oedematous and painful to the touch. A diagnosis of cancrum oris was made, with underlying anaemia, malnutrition and the trauma of tooth extraction being considered as precipitating causes.

Swabs for bacteriological investigation were taken from the area; haematological, electrolyte, serological, immunological and certain spesific tests were conducted; as chest radiographs and electrocardiographs were also taken, in order to exclude tuberculosis, syphilis and bilharzia amoungst other conditions. Abnormal findings included a haemoglobin level of 9 gm%, and a Klebsiella pneumoniae culture from the lesion.

*Fig. 1.* Necrosis and sloughing of the maxillary alveolar and sulcus mucosa with exposure of alveolar bone (arrow).

The patient was transfused 2 units of fresh, whole blood, placed on a high protein died, and administered appropriate antibiotics; debridement of the lesion with extraction of 12 was undertaken before covering the area with bismuth-iodoform paste and petroleum jelly gauze.

11 days following admission, the haemoglobin level was 14.5 gm%, and the exposed bone had been largely covered with granulation tissue, although swelling of the upper lip persisted. The patient reported night sweats. Pruritus was not present. Increased weight loss had not occurred.

Biopsy of the alveolus and lip in the region of 24 revealed a Hodgkin's lymphoma infiltrate consisting of Reed-Sternberg cells, mononuclear Hodgkin cells and a mixed inflammatory infiltrate (Fig. 2). Biopsies of a neck and groin lymphnode and bone marrow of the iliac crest and sternum revealed reactive changes only, with no evidence of lymphoma. Gastroscopy and gastric and duodenal biopsy were normal. Bone marrow needle biopsies of the iliac crest and sternum revealed hyperplastic changes only.

The patient was classified as having an extra nodal Stage I Hodgkins Lymphoma. Treatment with nitrogen mustard, vincristine, vinblastine, procarbazine, prednisone and oxhetazine, administered in a series of 8 cycles, was instituted. Following the first cycle of treatment, the response was dramatic, with complete clinical reversal of the lip and alveolar lesion occurring. The remaining cycles were administered. 1 year post-treatment, the patient has gained weight, reports an absence of clinical symptoms, and the oral lesion has healed (Fig. 3).

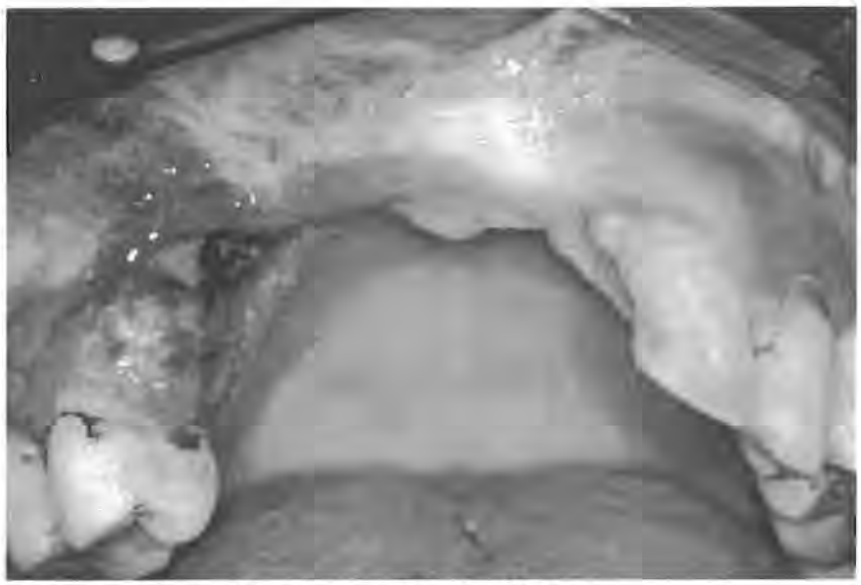

*Fig. 3.* 1-year post-operative, at the time of extraction of 13.

## Discussion

The case described here is extremely unusual in that the patient presented with a Hodgkin's lymphoma lesion involving only extra nodal tissue. WOOD & COLTMAN[26] reported that Hodgkin's disease limited to the extra nodal sites had an incidence of 0.25%. Only 6 cases appear to have been reported to involve the oral mucosa[3,7,8,14,19,24].

Bone involvement in Hodgkin's disease was reported to have occured in only 269 of 2006 cases by STEINER[21], while JACKSON & PARKER[13] and GRANGER & WHITAKER[11] report the incidence of bone involvement to be 23% and 9.6%, respectively. BEARMAN *et al.*[4] report the range of bone involvement to be between 5% and 15%; however STEINER[21] cautions that bone biopsies at post-mortem are likely to reveal about a 78% bone involvement.

Hodgkin's lymphoma presenting as a primary bone lesion was said by MIRRA[17] to be in the region of 0.3% of all cases. Furthermore, of the 12 reported cases of Hodgkin's lymphoma affecting the jawbones[1,2,6,9,10,16,22,25], only 1 case has hitherto been reported as having presented as a primary lesion of the maxilla[20].

In our patient, the infected, cancrum oris-like lesion developing on the maxilla is in accordance with the findings of COHEN *et al.*[6], who suggest that the severe infection accompanying Hodgkin's lymphomatous involvement of the mandible in their reported case is probably a manifestation of the presumed T-cell dysfunction thought to underlie Hodgkin's disease[23].

Of interest is the comment of FORMAN & WESSON[9] that primary bone origin is unlikely, since no case existed on record at that time of Hodgkin's disease being confined to the skeleton alone. In the present case, clinical examination of the liver, spleen, skin, and histological examination of neck and groin lymph nodes, as well as of biopsies of gastric and duodenal mucosa, iliac crest and

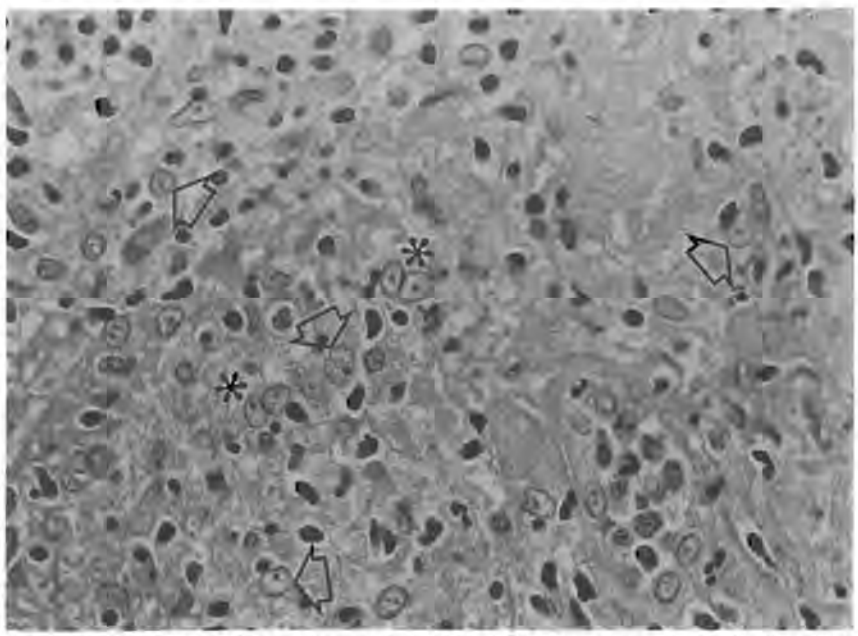

*Fig. 2.* Mixed cellular infiltrate characteristic of Hodgkin's lymphoma. Note the Hodgkin's cells (arrows) and Reed-Sternberg cells (asterisks).

sternum, failed to detect Hodgkin's disease. Liver, spleen and mediastinal scanning or a staging laparotomy with biopsies of the liver, spleen and lymph nodes would be necessary to support or refute the likelihood of this case having only maxillary and oral mucosal involvement.

Although biopsy of the deeper portions of the alveolus as part of the debridement procedure histologically revealed the Hodgkin infiltrate to be widespread and deep within the alveolus, the possibility cannot be entirely ruled out that bone involvement was secondary to primary alveolar mucosal involvement.

Prognosis for stage I Hodgkin's disease would appear to be fair[15,18,23]. Bone involvement indicates a grave prognosis according to FORMAN & WESSON[9], with an overall survival rate when all cases of Hodgkin's disease are taken into account of 41%, dropping to 4% for those in whom bone lesions are detected clinically[11]. Despite this, our patient with Stage I extra nodal bone involvement, responded excellently to chemotherapy.

Prognosis following involvement of the jawbones has not been specifically reported; however 3 patients with Hodgkin's disease of the mandible[6,9,22] are reported to have died 15, 6 and 7 months following diagnosis, respectively.

*Acknowledgements* – We wish to thank Mrs. M. M. Barnard for secretarial services.

## References


1. Ames, M. I.: Oral manifestation of Hodgkin's disease. Report of a case. *Oral Surg.* 1958: **11**: 155–157.
2. Bailey, B. J. & Brindley, P. C.: Manifestations of malignant lymphomas in the head and neck. *Trans. Am. Acad. Ophthal. Otolaryng.* 1979: **74**: 283–286.
3. Bathard-Smith, P. J., Coonar, H. S. & Markus, A. F.: Hodgkin's disease presenting intra-orally. *Br. J. Oral Surg.* 1078: **16**: 64–69.
4. Bearman, R. M., Pongolis, G. A. & Rappaport, H.: Hodgkin's disease, lymphocyte depletion type: a clinicopathologic study of 39 patients. *Cancer* 1978: **41**: 293–302.
5. Carbone, P. P., Kaplan, H. S., Musshoff, K., Smithers, D. W. & Tubiana, M.: Report of the committee on Hodgkin's disease; staging classification symposium. *Cancer Res.* 1971: **31**: 1860–1866.
6. Cohen, M. A., Bender, S. & Struthers, P. J.: Hodgkin's disease of the jaws, review of the literature and report of a case. *Oral Surg.* 1984: **57**: 413–417.
7. Cook, H. P.: Oral Lymphomas. *Oral Surg.* 1961: **14**: 690–694.
8. Eisenbud, L. & Kotch, R.: Hodgkin's 'sarcoma' of the cheek. Report of a case. *Oral Surg.* 1954: **7**: 213–215.
9. Forman, G. H. & Wesson, C. H.: Hodgkin's disease of the mandible. *Br. J. Oral Surg.* 1970: **7**: 146–152.
10. Fucilla, I. S. & Hamann, A.: Hodgkin's disease in bone. *Radiol.* 1961: **77**: 53–60.
11. Granger, W. & Whitaker, P.: Hodgkin's disease in bone with special reference to periosteal reaction. *Br. J. Radiol.* 1967: **40**: 939–948.
12. Hodgkin, T.: On some morbid appearances of the absorbent glands and spleen. *Med.-Chir. Trans. London.* 1932: **17**: 68–32.
13. Jackson, H. S. & Parker, F.: Hodgkin's disease: Involvement of certain other organs. *New Eng. J. Med.* 1945: **233**: 369–373.
14. Kinnman, J., Shin, H. I. & Wetteland, P.: Hodgkin's disease of the tongue. Report of a case in a Korean male. *Laryngoscope* 1969: **79**: 446–457.
15. Lukes, R. J. & Butler, J. J.: The pathology and nomenclature of Hodgkin's disease. *Cancer Res.* 1966: **26**: 1063–1083.
16. Meyer, G., Roswit, B. & Unger, S. M.: Hodgkin's disease of the oral cavity. *Am. J. Roentgenolog. Radium Thermal Nuclear Med.* 1959: **81**: 430–434.
17. Mirra, J. M.: *Bone tumours: diagnosis and treatment.* Lippincott, Philadelphia 1980, pp 407–410.
18. Newcomer, L. N., Silverstein, M. B., Cadman, E. C., Farber, L. R., Bertino, J. R. & Prosnitz, L. R.: Bone involvement in Hodgkin's disease. *Cancer Res.* 1982: **49**: 338–342.
19. Peters, R. A., Beltaos, E., Graanlaw, R. W. & Schloesser, L. L.: Intraoral extranodal Hodgkin's disease. *J. Oral Surg.* 1977: **35**: 311–314.
20. Steg, R. F., Dahlin, D. C. & Gores, R. J.: Malignant lymphoma of the mandible and maxillary region. *Oral Surg.* 1959: **12**: 128–141.
21. Steiner, P. E.: Hodgkin's disease. The incidence, distribution, nature and possible significance of the lymphogranulomatous lesions in the bone marrow. A review with original data. *Arch Path.* 1943: **36**: 627–637.
22. Stern, N. S. & Shensa, D. R.: Hodgkin's disease of the mandible: report of a case. *J. Oral Surg.* 1973: **31**: 628–631.
23. Thomas, L. B. & Berard, C. W.: Hodgkin's disease: relationship and histopathological type at diagnosis of clinical parameters and to histological progression and anatomical distribution at autopsy. *Cancer Res.* 1973: **15**: 253–273.
24. Tillman, H. H.: Malignant lymphomas involving the oral cavity and surrounding structures. Report of 12 cases. *Oral Surg.* 1965: **19**: 60–65.
25. Tiwari R. M.: Hodgkin's disease of the maxilla. *J. Laryngol. and Otol.* 1973: **87**: 85–89.
26. Wood, N. L. & Coltman, C. A.: Localized primary extra-nodal Hodgkin's disease. *Annals Int. Med.* 1973: **78**: 113–118.


Address:
*Professor E. J. Raubenheimer*
*Department of Oral Pathology and Oral Biology*
*P. O. Box D24*
*Medunsa 0204*
*Republic of South Africa*

# Low-grade intraosseous osteosarcoma of the jaws

Erich J. Raubenheimer, MChD,[a] and Claudia E. Noffke, MSc,[b] Pretoria, South Africa
MEDICAL UNIVERSITY OF SOUTHERN AFRICA

Two cases of low-grade intraosseous osteosarcomas are reported, bringing the total number of such osteosarcomas in the jawbones documented in recent literature to six. Our first case involved the maxilla of a 69-year-old man and the second involved the mandible of an 18-year-old girl. In clinical and microscopic appearance, these neoplasms resemble benign proliferations in many respects. Subtle differences include cortical bone destruction, soft tissue infiltration, irregular bone production with foci of abundant osteoid, and mild cellular atypia. Complete removal at the first attempt is of paramount importance, inasmuch as a significant percentage of these neoplasms recur as high-grade osteosarcomas if they are inadequately treated.
**(Oral Surg Oral Med Oral Pathol Oral Radiol Endod 1998;86:82-5)**

Low-grade intraosseous osteosarcomas are rare, and they are often inappropriately diagnosed as benign neoplasms. They represented 1.9% of all osteosarcomas in the files of the Mayo Clinic[1] and 1% of osteosarcomas in a study conducted in Italy.[2] The lesion has an equal gender distribution and commonly affects a patient in the third decade of life.[3] Low-grade intraosseous osteosarcomas are of endosteal origin, and most occur in the metaphysis of the femur and tibia. In the Mayo Clinic series of 80 cases, 12 low-grade intraosseous osteosarcomas occurred in flat bones; 2 of these were in the mandible and 1 was in the maxilla.[3]

Microscopically, low-grade intraosseous osteosarcomas show an infiltrative growth pattern despite a low mitotic index and lack of significant cellular atypia. They are frequently misdiagnosed as fibrous dysplasia[4,5] or other benign fibro-osseous proliferations.[2,6]

The purpose of this study was to highlight the diagnosis of low-grade osteosarcoma and to emphasize its distinction from other benign proliferations of central bony origin.

## CASE REPORTS

The files of the Department of Oral Pathology at Medunsa, which serves a mainly rural and periurban black African population, were searched for low-grade intraosseous osteosarcomas. Between 1985 and 1997, 36 cases of osteosarcoma were diagnosed. Of these, two were reported as low-grade intraosseous osteosarcomas.

[a]Professor and Head, Department of Oral Pathology, Medunsa Oral Health Centre.
[b]Lecturer, Department of Oral Pathology, Medunsa Oral Health Centre.
Received for publication Oct. 14, 1997; returned for revision Jan. 21, 1998; accepted for publication Mar. 31, 1998.

1079-2104/98/$5.00 + 0 **7/14/90847**

### Case 1

A 69-year-old man appeared for treatment with a complaint of a painless and rapidly enlarging swelling of the premaxilla of less than 4 months duration. On external examination, a tumor measuring 4 × 3 cm was seen to be elevating the upper lip (Fig. 1). The mucosal surface was ulcerated and the lesion was bony-hard. The maxillary incisors were absent. Radiographic examination showed both loss of the cortical plate and a bone-forming lesion, the posterior margin of which was well demarcated (Fig. 2). A clinical diagnosis of a benign osseous proliferation was made, and a biopsy was performed. Microscopic examination showed sheets and plates of mature bone with excessive osteoid formation focally. Mitotic activity was below 1 mitosis per 10 high-power fields. The lesion infiltrated through the labial cortical plate of the maxilla around groups of submucosal minor salivary glands (Fig. 3) and extended into the base of the ulcer on the labial mucosa. A diagnosis of a low-grade intraosseous osteosarcoma was made, and the tumor was removed with wide excision.

### Case 2

The second case involved the right mandible of an 18-year-old girl. She appeared for treatment with a 7-month history of slow expansion of the inferior border of the mandible. The swelling, which did not cause buccal or lingual enlargement, was painful on palpation. Paresthesia of the inferior alveolar nerve was not present. Radiographic examination showed a well-defined lytic lesion extending from the right mandibular canine to the second molar tooth. Erosion of the inferior border of the mandible was present (Fig. 4). An intraoral incisional biopsy was performed. Microscopic examination showed the presence of giant cells irregularly arranged in a mitotically inactive cellular stroma, foci of bone formation, and cystic spaces filled with blood. A diagnosis of a central giant cell granuloma with aneurysmal bone cyst formation was made, and the lesion was enucleated. In addition to the changes observed in the biopsy, microscopic examination of the enucleated specimen showed mildly cellular spindle-shaped areas with atypical osteoblasts that were associated with osteoid production (Fig. 5). The diagnosis was changed to that of a low-grade osteosarcoma and the affected segment of the mandible was resected.

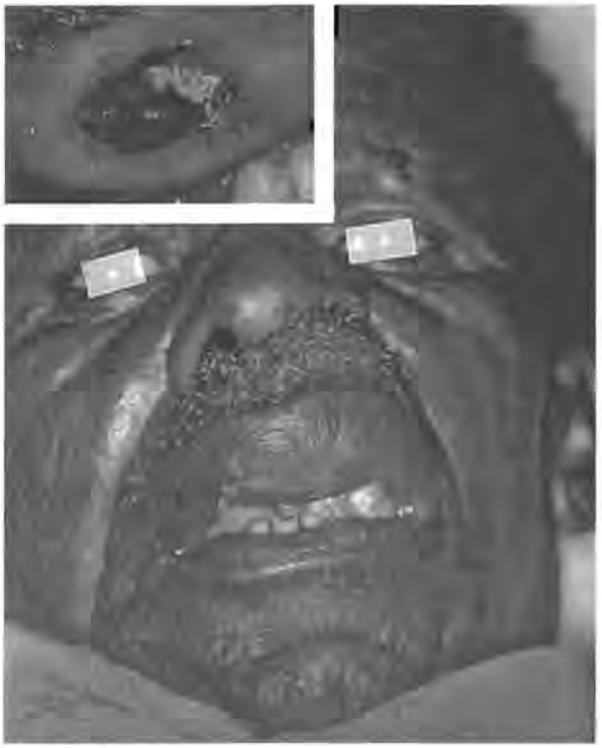

Fig. 1. Elevation with infiltration of upper lip in case 1. Note ulcer on labial mucosa *(inset)*.

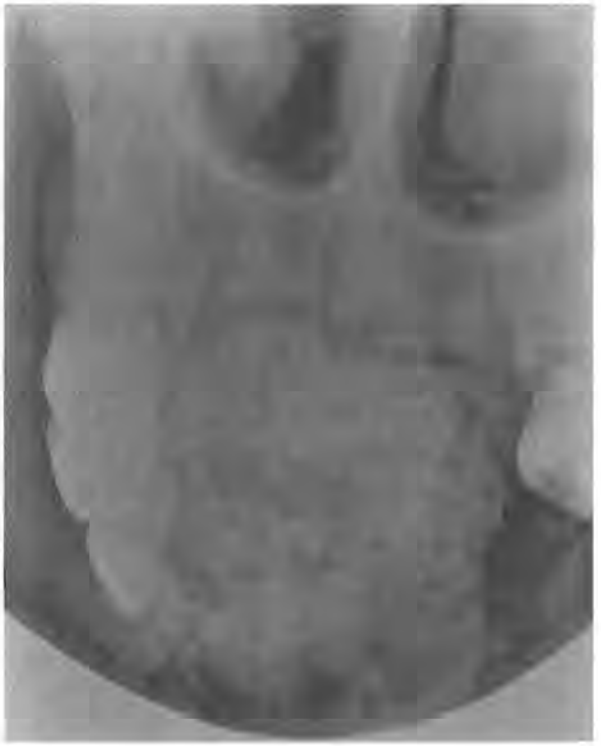

Fig. 2. Radiographic view of case 1 shows demarcation of lesion posteriorly.

## DISCUSSION

Intraosseous low-grade osteosarcoma is a rare variety of osteosarcoma. It warrants separate recognition because its prognosis, unlike that of classical osteosarcoma, is excellent. Parosteal osteosarcomas, which develop outside bone, share this excellent prognosis. Low-grade intraosseous osteosarcomas are, however, less common than the latter variety and distinguished by development within bone.[1]

Low-grade intraosseous osteosarcomas affecting the jaws are infrequently reported. Kurt et al.[3] documented two cases in the mandible and one in the maxilla; another case, with chondromyxoid fibroma-like features, was reported in the maxilla.[7] The latter case affected the right maxilla of a 24-year-old male patient who died 1 year after local excision of the neoplasm with pulmonary metastasis. The 10 low-grade intraosseous osteosarcomas reported by Bertoni et al.[2] in 1992 all involved extragnathic sites. No mention was made of low-grade neoplasms in a series of 34 osteosarcomas affecting craniofacial bones.[8] A low-grade osteosarcoma of the sphenoid bone that mimicked fibrous dysplasia was recently reported.[5] An osteosarcoma involving the mandible that was microscopically interpreted as fibrous dysplasia on both the incisional biopsy and excised specimen[4] probably represented another example of low-grade intraosseous osteosarcoma of the jawbones. It is our contention that some of the earlier cases in which malignant change was reported in fibrous dysplasia[9] in fact represented low-grade intraosseous osteosarcoma from the onset.

The great pitfall in the diagnosis of low-grade osteosarcoma lies in the fact that it is clinically, radiographically, and microscopically distinct from benign conditions affecting bone. Accurate diagnosis is primarily based on the clinical, radiographic, or microscopic identification of an infiltrative growth pattern. In a series of 80 low-grade intraosseous osteosarcomas, poor margination was present in two thirds of cases and there was extension into soft tissue in one half of cases.[3] Seven of the 10 cases reported by Bertoni et al.[2] showed cortical violation with soft tissue invasion. Both of our cases demonstrate that although the histopathologic features favor a benign process in many microscopic fields, cortical destruction with dermal and mucosal infiltration are the most important criteria in establishing the final diagnosis. Microscopically, the infiltrative growth pattern in case 1 was reflected by the loss of the buccal bone plate and by the bone-forming lesion infiltrating the mucosa, growing around minor salivary glands rather than displacing them. Our second case, however, was well demarcated, and it exhibited sharp

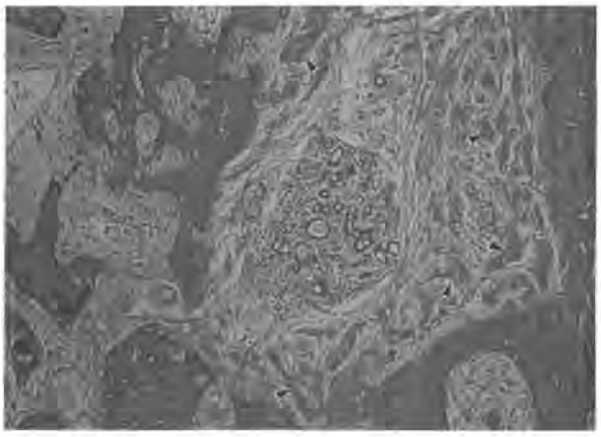

Fig. 3. Infiltration of well-differentiated bone-forming tumor around minor salivary gland in case 1; abundance of osteoid *(arrows)* can also be seen (hematoxylin-eosin, original magnification ×100).

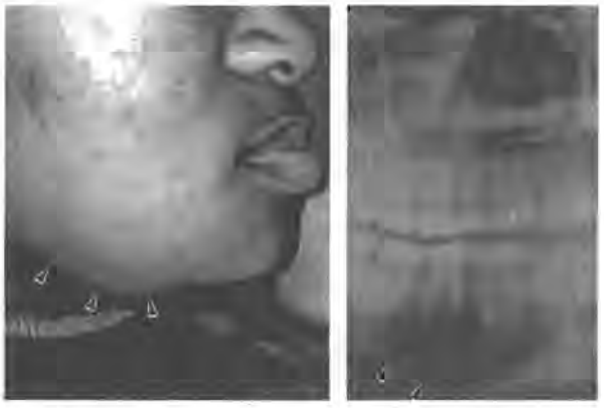

Fig. 4. Expansion of inferior border of mandible in case 2 *(left, arrows)*. Panoramic radiograph *(right)* shows well-defined lytic lesion with destruction of inferior border *(arrows)*.

margins, which were featured in 20% of the cases reported by Kurt et al.[3] and 3 of 10 cases in the series of Bertoni et al.[2] Violation of the inferior border of the mandible with infiltration of the dermis was present, however.

Microscopically, low-grade intraosseous osteosarcoma is essentially a spindle-cell tumor with irregular bone production, low cellularity, fewer than 4 mitoses per 10 high-power fields, and an absence of pronounced atypia. In most cases, heavy seams of irregular calcified osteoid or scattered seams of osteoid embedded in a collagen stroma with multiple vascular spaces are seen.[3] Abundant osteoid with osteoblastic rimming may mimic an osteoblastoma.[3,10] Other growth patterns include areas resembling fibrous dysplasia, desmoplastic fibroma, or fibromyxoid change.[2,7] Our second case focally showed changes compatible with a central giant cell granuloma with aneurysmal bone cyst formation on initial biopsy.

From a differential diagnostic point of view, distinction from fibrous dysplasia poses the most important problem. It is frequently not possible to make the distinction microscopically alone, and although low-grade intraosseous osteosarcomas may appear benign on radiographs, fibrous dysplasia never shows the infiltrative characteristics of a malignancy.[3] The solid areas in aneurysmal bone cysts are sometimes mistaken for low-grade intraosseous osteosarcoma. The latter is hypocellular with little mitotic activity whereas aneurysmal bone cyst shows increased cellularity and brisk mitotic activity.[1,3] The scarcity of mitotic figures in the stroma of the initial biopsy of our case 1 is an indication that the proliferation is not entirely compatible with that found in a giant cell granuloma.

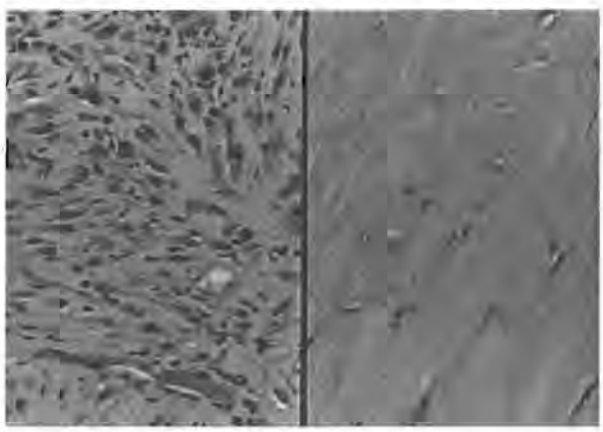

Fig. 5. Microscopic appearance of excision specimen of case 2. Note spindle-shaped growth pattern (*left;* hematoxy lin-eosin, original magnification ×100). Abundant osteoid and mildly atypical osteoblasts can also be seen (*right*; hematoxylin-eosin, original magnification ×200).

Histologically there may be an overlap in the features of low-grade osteosarcoma and parosteal osteosarcoma. The latter is distinguished by its location on the surface of the bone rather than centrally and within bone.[2]

Although our cases have not been followed for a sufficient period of time, the literature makes it clear that complete removal at the first attempt is important. The transformation of low-grade intraosseous osteosarcoma into high-grade osteosarcoma at recurrence occurred in 15% of patients in the Mayo Clinic series. The course of cases with recurrent growths is reported to be similar to that of cases of high-grade osteosarcoma, and the development of metastasis correlated

with this transformation.[3] The treatment of choice is therefore wide excision with amputation if technically feasible. Lesional curettage or marginal excision should be considered to be inadequate therapy.[2,3]

We thank Mrs. C. S. Begemann for secretarial assistance.

## REFERENCES

1. Dahlin DC, Unni KK. Bone tumors: general aspects and data on 8452 cases. 4th ed. Springfield, Ill: Charles C. Thomas; 1986. p. 297-300.
2. Bertoni F, Bacchini P, Fabbri N, Merouri M, Picci P, Ruagieri P, et al. Osteosarcoma: low-grade intraosseous-type osteosarcoma, histologically resembling parosteal osteosarcoma, fibrous dysplasia and desmoplastic fibroma. Cancer 1993;71:338-45.
3. Kurt AM, Unni KK, McLeod RA, Pritchard DJ. Low-grade intraosseous osteosarcoma. Cancer 1990;65:1418-28.
4. Yamashiro M, Komori A. Osteosarcoma mimicking fibrous dysplasia of the jaw. Int J Oral Maxillofac Surg 1987;16:112-5.
5. Paric YK, Yang MH, Choi WS, Lim YJ. Well differentiated low-grade osteosarcoma of the clivus. Skeletal Radiol 1995;24:386-8.
6. Koury ME, Regezi JA, Perrott DH, Kaban LB. "Atypical" fibro-osseous lesions: diagnostic challenges and treatment concepts. Int J Oral Maxillofac Surg 1995;24:162-9.
7. Chow LTC, Lin J, Yip KMH, Kununa SM, Ahuja AT, Kings WWK, et al. Chondromyxoid fibroma-like osteosarcoma: a distinct variant of low-grade osteosarconoma. Histopathology 1996;29:429-36.
8. Vege DS, Borges AM, Aggrawal K, Balasubramaniam G, Parikh DM, Bhaser B. Osteosarcoma of the craniofacial bones: a clinico-pathological study. J Craniomaxillofac Surg 1991;19:90-3.
9. Riddel DM. Malignant change in fibrous dysplasia: report of a case. J Bone Joint Surg 1964;46B:251-5.
10. Nojima T, Yamaguchi H, Nagashima K, Nagai Y, Kanda M. Osteosarcoma resembling osteoblastoma and its heterotransplantation into nude mice. Acta Pathol Jpn 1992;42:75-81.

*Reprint requests:*
Erich J. Raubenheimer, MChD
Department of Oral Pathology
Medical University of Southern Africa, Box D24
P.O. MEDUNSA 0204
South Africa

Dentomaxillofacial Radiology (2000) 29, 128-130

www.nature.com/dmfr

CASE REPORT

# Tumoral calcinosis of the temporomandibular joint region

C Nolffke*[1], E Raubenheimer[1] and E Fischer[1]

[1]*Department of Oral Pathology, Medical University of Southern Africa, South Africa*

A rare case of tumoral calcinosis, discovered in the medial pterygoid muscle and around the temporomandibular joint on a routine panoramic radiograph is presented. CT was found to be ideal for the determination of the exact location of the calcifications. The differential diagnosis of tumoral calcinosis is discussed.

**Keywords:** tumoral calcinosis; calcification, pathologic; temporomandibular joint; facial muscles

## Case report

A 29-year-old Caucasian female presented for routine dental examination. A panoramic radiograph revealed a calcified mass superimposed on the upper third of the ramus of the left side of the mandible (Figure 1a). The dental practitioner interpreted the mass as an ectopic tooth which was outside the focal trough of the panoramic radiograph. The patient was referred to an oral and maxillofacial surgeon for further management. CT (Figure 1b) showed a large area of calcification, measuring 1 cm in diameter in the left medial pterygoid muscle as well as multiple smaller calcifications in both the muscle and the soft tissue medial to the temporomandibular joint. No other clinical signs or symptoms were associated with the lesions. No history of trauma could be obtained. A clinical diagnosis of metastatic soft tissue calcification was made. Normal kidney function and serum calcium, phosphate, 1,25-$(OH)_2$-vitamin D and parathyroid hormone concentrations, however, failed to confirm this diagnosis. The large calcification was removed using an intra-oral approach and submitted for pathological examination. On sectioning, the mass was found to consist of a friable, amorphous, chalky white material enclosed in a fibrous capsule. Microscopy showed the calcification to be composed of a concentric amorphous deposit of calcified material exhibiting bony metaplasia peripherally (Figure 2). A final diagnosis of tumoral calcinosis was made. No familial history of the condition could be obtained.

## Discussion

Tumoral calcinosis is a rare disorder of unknown cause first described by Duret in 1899.[1] Ghormley and McCrary[2] described a similar condition in three sisters in 1942, but the term 'tumoral calcinosis' was only introduced by Inclan in 1943,[3] who diagnosed the disorder in three Black women. The condition most frequently occurs in Black people,[4] particularly those of African descent,[3-5] and shows a slight predominance in females in the first or second decades of life. Development is rare in patients over 50 years of age.[6] Tumoral calcinosis presents with multiple calcified masses ('tumors') commonly located in periarticular regions without being connected to the associated joint.[7] Hips, elbows and shoulders are most frequently affected, the two latter areas being more prone to recurrence and aggressive behaviour. The face, fingers and knees are rarely involved.[6] Three cases have been documented in the region of the temporomandibular joint[6, 8] and one in the premaxillary area.[9]

In one-third of cases tumoral calcinosis manifests as a component of an heritable metabolic disease, transmitted either as an autosomal recessive or, more likely, as an autosomal dominant with variable clinical expressivity.[10] A congenital defect in phosphate metabolism has also been suggested following a report of an associated increase in serum phosphate in siblings with the condition.[11] In our case the serum phosphate was normal. In order to avoid confusion with

*Correspondence to: CEE Nolffke, Department of Pathology, Box D24, Medunsa, P.O. Medunsa, 0204, South Africa
Received 28 June 1999; accepted 24 November 1999

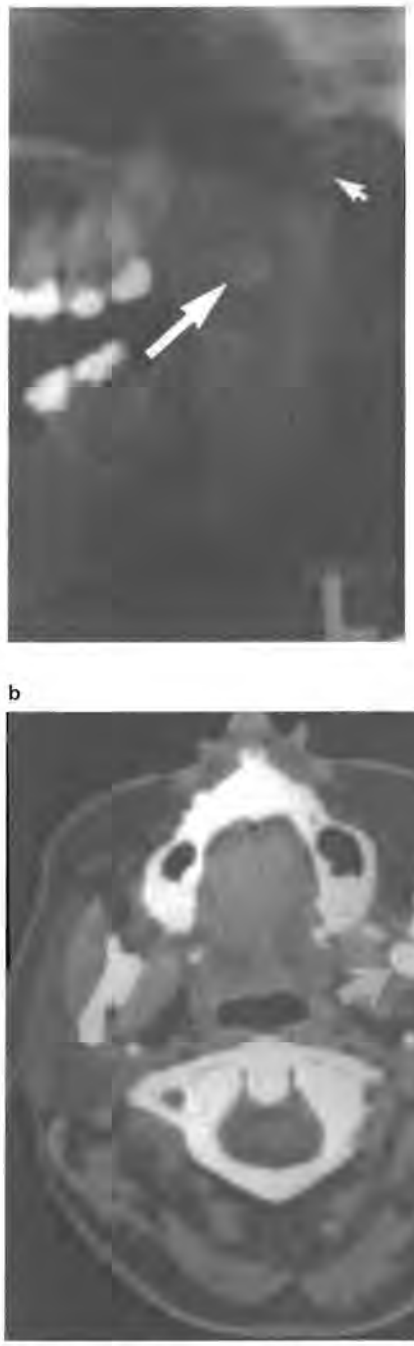


**Figure 1** (a) Part of a panoramic radiograph showing calcified masses superimposed on the upper third of the left mandibular ramus (large arrow) and temporomandibular joint (small arrows). (b) Axial CT scan through the left mandibular ramus showing the location of the largest calcification (arrow) and the smaller lesions both anterior and posterior to it

metastatic calcification, we agree with Zanetti[6] that the term tumoral calcinosis should be restricted to those cases in which both serum calcium and phosphate are normal. The role of local trauma with inflammation has been considered in the pathogenesis of tumoral

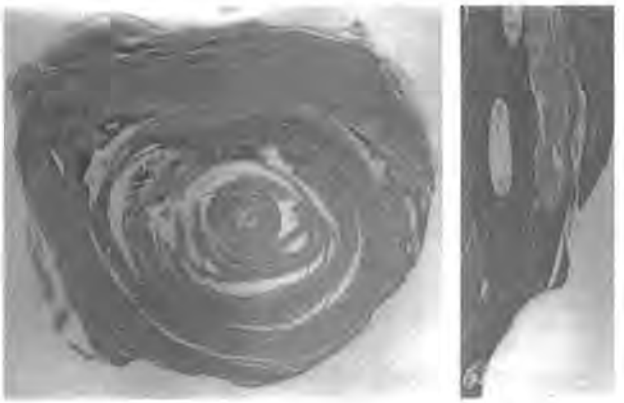

**Figure 2** Microscopic appearance of the calcified mass (left) (H&E section, magnification ×80). Bony metaplasia was present in the peripheral part of the lesion (right) (H&E section, magnification ×200)

calcinosis since a history of trauma and degeneration of the articular capsule was reported in a number of cases.[1,6,12] No history of trauma could be obtained in our case. Dystrophic calcification is a more appropriate term for calcified deposits secondary to tissue damage and we would discourage the use of the term tumoral calcinosis in association with a history of trauma. Gal *et al*[13] reported facial or intra-oral pathological changes associated with tumoral calcinosis at a very young age. These initial findings included erythematous patches and a maculopapular rash on the face and extremities, hoarseness and angular cheilitis. None of these findings were present in our case.

Tumoral calcinosis grows rapidly, sometimes appearing in a matter of months. The masses may be huge and are usually painless although pain may result during joint movement.[4] Radiographically, the lesions present as nodular peri-articular and soft tissue masses. Surgical excision is recommended in cases presenting with large lesions associated with deformities or symptoms. Incomplete excision can lead to multiple recurrences.[14]

The differential radiological diagnosis of tumoral calcinosis should include implanted foreign material, dystrophic or metastatic calcification, phlebolith, calcified haemangioma, fibrodysplasia ossificans progressiva, calcinosis cutis, gout and synovial osteochondromatosis. Implanted foreign material will be associated with a history of trauma. Dystrophic calcifications present as irregular foci of mineralization within areas of tissue degeneration in necrotising infections, malignant tumours or haemorrhage. Metastatic calcifications are associated with derangements in mineral metabolism, most notably acute hyperparathyroidism and renal failure and present as diffuse mineral deposits which have an affinity for the elastic tissue of blood vessel walls. The calcifications in phleboliths and calcified haemangiomas are associated with thrombosed vascular spaces. Fibrodysplasia ossificans progressiva is characterised by bony dyspla-

sia of connective tissue and skeletal muscle and the mineralised deposits of calcinosis cutis are localised close to the surface of the skin. In gout, deposits of monosodium urate form within and around various joints, leading to chronic arthritis and a foreign body giant cell reaction. Synovial osteochondromatosis is an uncommon benign lesion, characterised by multiple osteocartilaginous nodules in the synovium of joints.

## References

1. Duret MH. Tumeurs multiples et singularires des bourses sereuses. *Bull Mem Soc Anat Paris* 1899; **74:** 725–731.
2. Ghormley RK, McGrary W. Multiple calcified bursae and calcified cysts in soft tissues. *Trans West SA* 1942; **51:** 292–296.
3. Inclan A. Tumoral calcinosis. *JAMA* 1943; **121:** 490–495.
4. Spjut HJ, Dorfman HD, Fechner RE, Ackerman LV (eds). Miscellaneous lesions. In: *Tumours of Bone and Cartilage*, Fasicle 5. Washington D.C.: Armed Forces Institute of Pathology, 1970: pp 423–428.
5. Smit GG, Schoeman A. Tumoral calcinosis. *J Bone Joint Surg Br* 1967; **49B:** 698–703.
6. Zanetti U, Derada W, Troletti G, Burlini D, Rossi D. Tumoral calcinosis: a case report. *Int J Oral Maxillofac Surg* 1994; **23:** 271–272.
7. Shirasuna K, Sugiyama M, Yasui Y. Tumoral calcinosis around the mandibular condyle. *Int J Oral Maxillofac Surg* 1991; **20:** 36–37.
8. Sledz K, Ortiz O, Wax M, Bouquot J. Tumoural calcinosis of the temporomandibular joint: CT and MRI findings. *AJNR Am J Neuroradiol* 1995; **16:** 782–785.
9. Marinho RO, Anderson GP, Warren AY. Tumoral calcinosis in the premaxillary region. *Oral Surg Oral Med Oral Pathol Oral Radiol Endod* 1999; **87:** 725–729.
10. Slavin RE, Wen J, Kumar D, Evans EB. Familial tumoral calcinosis. *J Am Surg Pathol* 1993; **17:** 788–802.
11. Lafferty FW, Reynolds ES, Pearson OH. Tumoral calcinosis. A metabolic disease of obscure etiology. *Am J Med* 1965; **38:** 105–118.
12. Barton DL, Reeves RJ. Tumoral calcinosis. Report of three cases and review of the literature. *AJR Am J Roentgenol* 1961; **86:** 351–358.
13. Gal G, Metzker A, Garlick J, Gold Y, Calderon S. Head and neck manifestations of tumoral calcinosis. *Oral Surg Oral Med Oral Path Oral Radiol Endod* 1994; **77:** 158–166.
14. Noyez JF, Murphree SM, Chen K. Tumoral calcinosis, a clinical report of eleven cases. *Acta Orthop Belg* 1993; **59:** 249–254.